UNIVERSIDADE FEDERAL DA BAHIA
INSTITUTO DE QUÍMICA
PROGRAMA DE PÓS-GRADUAÇÃO EM QUÍMICA

RAÍZA LOPES BORGES ANDRADE

ELEMENTOS TERRAS RARAS E εNd COMO TRAÇADORES DE PROCESSOS NATURAIS EM AMBIENTES COSTEIRO E OCEÂNICO

Salvador - BA

2024

RAÍZA LOPES BORGES ANDRADE

ELEMENTOS TERRAS RARAS E εNd COMO TRAÇADORES DE PROCESSOS NATURAIS EM AMBIENTES COSTEIRO E OCEÂNICO

Tese apresentada ao Programa de Pós Graduação em Química do Instituto de Química da Universidade Federal da Bahia, como requisito para obtenção do grau de Doutora em Química.

Orientadora: Profa. Dra. Vanessa Hatje

Salvador - BA

2024

TERMO DE APROVAÇÃO

RAÍZA LOPES BORGES ANDRADE

"ELEMENTOS TERRAS RARAS E εNd COMO TRAÇADORES DE PROCESSOS NATURAIS EM AMBIENTES COSTEIRO E OCEÂNICO"

Defesa de Tese aprovada como requisito parcial para obtenção do grau de Doutora em Química, Universidade Federal da Bahia, pela seguinte banca examinadora:

gov.br Documento assinado digitalmente
VANESSA HATJE
Data: 03/09/2024 12:13:48-0300
Verifique em https://validar.iti.gov.br

Profa. Dra. Vanessa Hatje _____
Doutorado em Oceanografia Química pela The University of Sydney (Austrália)
Universidade Federal da Bahia

Tristan C. C. Rousseau
SIAPE 2329503
LABOMAR
Universidade Federal do Ceará

Prof. Dr. Tristan Charles Clitandre Rousseau _____
Doutorado em SDU2E pelo Geosciences Environnement Toulouse (GET)- Université Paul sabatier, França
Universidade Federal do Ceará

gov.br Documento assinado digitalmente
RODRIGO KERR DUARTE PEREIRA
Data: 29/08/2024 17:00:56-0300
Verifique em https://validar.iti.gov.br

Prof. Dr. Rodrigo Kerr Duarte Pereira _____
Doutorado em Oceanografia Física, Química e Geológica pela Universidade Federal do Rio Grande (FURG)
Universidade Federal do Rio Grande

gov.br Documento assinado digitalmente
MONICA WALLNER KERSANACH
Data: 30/08/2024 11:55:19-0300
Verifique em https://validar.iti.gov.br

Profa. Dra. Mônica Wallner-Kersanach _____
Doutorado em Ciências Naturais (especialidade Biologia/Química) pelo Universität Bremen (Alemanha)
Universidade Federal do Rio Grande

gov.br Documento assinado digitalmente
CARLOS EDUARDO DE REZENDE
Data: 29/08/2024 17:28:03-0300
Verifique em https://validar.iti.gov.br

Prof. Dr. Carlos Eduardo de Rezende
Doutorado em Ciências Biológicas (Biofísica) pela Universidade Federal do Rio de Janeiro (UFRJ)
Universidade Estadual do Norte Fluminense

Salvador, 29 de agosto de 2024.

AGRADECIMENTOS

Aos meus pais e familiares queridos,

Não há palavras suficientes para agradecer pelo apoio incondicional em cada fase desta jornada. Cada conquista é também fruto do apoio e suporte inabaláveis que sempre me proporcionaram. Vocês foram minha âncora nos momentos difíceis e minha inspiração para seguir em frente. Obrigada pelo amor incondicional e por encorajarem a perseguir meus sonhos.

Aos meus amigos e colegas de laboratório,

Vocês foram mais do que parceiros de estudo, foram cúmplices de risadas, conspiradores de ideias malucas e o suporte que me fez acreditar que tudo era possível. Obrigado por cada debate acalorado, cada risada compartilhada, pelas conversas que geraram ideias novas e por transformar a pesquisa em uma aventura compartilhada. Juntos, transformamos desafios em oportunidades e construímos memórias que levarei para sempre.

À minha orientadora Vanessa Hatje,

Pelo seu suporte constante, por acreditar no meu potencial e por me guiar com paciência e sabedoria ao longo desta jornada acadêmica, sou profundamente grata. Ao longo dos anos, você me ensinou como fazer ciência de qualidade e abriu meus horizontes para esse universo de possibilidades. Sua amizade e compreensão foram fundamentais para que eu pudesse alcançar este momento tão significativo. Este trabalho é um reflexo do seu apoio constante e confiança em mim.

A todos que fizeram parte desta jornada, o meu mais sincero OBRIGADA! Vocês são parte essencial deste capítulo da minha vida.

APRESENTAÇÃO

Esta tese de doutorado tem como objetivo a aplicação de elementos terras raras (REE) e εNd[1] como traçadores de processos naturais em ambientes oceânico e costeiro. Para o seu primeiro capítulo, foi realizada uma revisão bibliográfica sobre o ciclo biogeoquímico dos REE, considerando também os fatores antrópicos emergentes, na forma de um artigo científico publicado na revista Global Biogeochemical Cycles. Este primeiro capítulo foi resultado de uma colaboração entre cientistas com experiencia no estudo da distribuição de REE em diversos ambientes e tem potencial para vir a se tornar uma referência em estudos de REE no meio ambiente nos próximos anos. O segundo capítulo da tese foi escrito na forma de artigo científico, já publicado na revista Chemical Geology. Nele, foi realizado um estudo ao longo do estuário do rio Paraguaçu e da Baía de Todos os Santos para avaliar o fracionamento dos REE em águas tropicais costeiras. O terceiro capítulo da tese é composto pela aplicação de εNd para o estudo de processos que ocorrem no continuo continente oceano e de circulação e formação de massas de água tendo como áreas de estudo alguns pontos da costa do Brasil, bem como do oceano Atlântico tropical e sul e da península Antártica. As amostras já foram coletadas durante 4 cruzeiros PIRATA/GEOTRACES, SAMBAR/GEOTRACES e PROANTAR/GEOTRACES realizados em 2017 e 2018 a bordo do Navio Hidroceanográfico Vital de Oliveira, 2019 a bordo do Navio Hidroceanográfico Alphacrucis e a bordo do Navio Hidroceanográfico Almirante Maximiano entre as latitudes 15N e 65S. Esses resultados escritos na forma de artigo científico serão submetidos à revista Earth and Planetary Science Letters. O quarto capítulo é resultado da minha atuação enquanto jovem embaixadora de todo o Atlântico durante o meu doutorado. Nesse período, participei de diversas discussões sobre a implementação da Década da Ciência Oceânica pelo Desenvolvimento Sustentável da Organização das Nações Unidas. Esse trabalho resultou na escrita de um artigo de revisão publicado na revista Frontiers in Marine Science sobre as fontes, lacunas de conhecimento e perspectivas futuras no que diz respeito à poluentes no oceano Atlântico Sul.

[1] εNd é uma notação que compara a razão Nd^{143}/Nd^{144} de uma determinada amostra com a razão Nd^{143}/Nd^{144}=0.512638 do reservatório uniforme condrítico (CHUR) representativo do valor médio da Terra (Wasserburg et al., 1981) e é definido pela equação:

$$\varepsilon Nd = \left[\frac{\left({}^{143}Nd/{}^{144}Nd \right)_{Amostra}}{\left({}^{143}Nd/{}^{144}Nd \right)_{CHUR}} - 1 \right] \times 10000$$

RESUMO

Os Elementos Terras Raras (REE) são um grupo de 17 elementos cujas propriedades químicas permitem sua utilização como excelentes traçadores geoquímicos. Além disso, esses elementos, essenciais em diversas aplicações tecnológicas, médicas e agropecuárias, estão gerando preocupações ambientais devido ao aumento de seu uso antrópico que gera impactos ainda pouco conhecidos. A compreensão do ciclo biogeoquímico dos REE é crucial para avaliar e mitigar seus impactos e melhorar sua utilização como traçadores em estudos geoquímicos. Neste trabalho os REE são estudados tanto por meio de revisão bibliográfica, quanto estudos de caso. Inicialmente, é apresentada uma revisão do conhecimento atual sobre os REE e as lacunas que precisam ser preenchidas para um uso sustentável nas aplicações humanas e eficaz como traçadores geoquímicos. No intuito de preencher essas lacunas, o estudo sobre a distribuição e fracionamento dos REEs na Baía de Todos os Santos evidencia como fatores naturais e antropogênicos, como gradientes de salinidade, estrutura geológica e as marés afetam as concentrações desses elementos em regiões costeiras. As anomalias de gadolínio no estuário do Paraguaçu demonstram que a contaminação pode se espalhar além das áreas mais próximas da fonte original, apontando o ser o humano como um vetor de disseminação. Já nas análises em águas dos oceanos Antártico e Atlântico, a composição isotópica do Nd foi utilizada para investigar a ocorrência de processos como o Boundary Exchange e a mistura de massas d'água. Em ambas as regiões, foram observadas influências geológicas e de massas d'água na composição isotópica do Nd. O estudo sugeriu a necessidade de complementação da pesquisa com dados de concentração de REEs para aprofundar a compreensão do Boundary Exchange e outros processos. Por fim, tendo em vista a Década da Ciência Oceânica para o Desenvolvimento Sustentável da ONU, foi realido um estudo indicando as principais fontes de contaminação no Atlântico Sul e as lacunas de conhecimento, propondo uma colaboração mais estreita entre pesquisadores, comunidades tradicionais e o setor privado dos países ao redor do Atlântico Sul para promover um ambiente oceânico mais saudável e sustentável.

Palavras-chave: Elementos Terras Raras; Isótopos de Neodímio; Oceano Atlântico; Península Antártica; Boundary Exchange; Contaminação; Gd Antropogênico; GEOTRACES

ABSTRACT

The Rare Earth Elements (REE) are a group of 17 elements whose chemical properties allow their use as excellent geochemical tracers. These elements are essential in several technological, medical, and agricultural applications. The increase in their anthropogenic use is causing environmental concerns, especially because their impacts are still little known. Understanding the REE biogeochemical cycle is crucial to evaluate and mitigate their impacts and improve their usage as tracers in geochemical studies. In this work, REE are studied both through bibliographical review and case studies. Initially, a review of current knowledge about REE and the gaps that need to be filled for sustainable use in human applications and effective use as geochemical tracers is presented. In order to fill these gaps, the study on the distribution and fractionation of REEs in Todos os Santos Bay highlights how natural and anthropogenic factors, such as salinity gradients, geological structure, and tides, affect the concentrations of these elements in coastal regions. The gadolinium anomalies in the Paraguaçu estuary demonstrate that contamination can spread beyond the areas closest to the original source, pointing to humans as vectors of dissemination. In the Antarctic and Atlantic oceans, the isotopic composition of Nd of seawater was used to investigate the occurrence of processes such as Boundary Exchange and the mixing of water masses. In both regions, geological and water mass influences on the isotopic composition of Nd were observed. The study suggested the need to complement research with REE concentration data to deepen the understanding of the Boundary Exchange and other processes. Finally, in view of the UN Decade of Ocean Science for Sustainable Development, a study was carried out indicating the main sources of contamination in the South Atlantic and the gaps in knowledge, proposing closer collaboration between researchers, traditional communities and the private sector in countries around the South Atlantic to promote a healthier and more sustainable ocean environment.

Keywords: Rare Earth Elements; Neodymium Isotopes; Atlantic Ocean; Antarctic Peninsula; Boundary Exchange; Contamination; Anthropogenic Gd; GEOTRACES

ÍNDICE

1 Introdução 10

1.1 Elementos Terras Raras 10

1.2 Isótopos de Neodímio como traçadores 19

1.3 Referências 26

2 Objetivos 38

2.1 Objetivo geral 38

2.2 Objetivos específicos 38

3 Capítulo 1: The Global Biogeochemical Cycle of the Rare Earth Elements 39

4 Capítulo 2: REE fractionation and human Gd footprint along the continuum between Paraguaçu River to coastal South Atlantic waters 106

5 Capítulo 3: Neodymium isotopes across Antarctic and South and Central western Atlantic 131

6 Capítulo 4: Pollutants in the South Atlantic Ocean: Sources, Knowledge Gaps and Perspectives for the Decade of Ocean Science 171

7 Conclusão 189

1. INTRODUÇÃO

1.1 Elementos Terras Raras

Os elementos terras raras (REE) são, de acordo com a classificação da International Union of Pure and Applied Chemistry (IUPAC), um grupo de 17 elementos químicos, dos quais 15 pertencem na tabela periódica ao grupo dos lantanídeos, composto por lantânio (La, Z=57); cério (Ce, Z=58); praseodímio (Pr, Z=59); neodímio (Nd, Z=60); promécio (Pm, Z=61); samário (Sm, Z=62); európio (Eu, Z=63); gadolínio (Gd, Z=64); térbio (Tb, Z=65); disprósio (Dy, Z=66); hólmio (Ho, Z=67); érbio (Er, Z=68); túlio (Tm, Z=69); itérbio (Yb, Z=70) e lutécio (Lu, Z=71), aos quais se juntam o escândio (Sc, Z=21) e o ítrio (Y, Z=39). Em seus estudos, muitos cientistas excluem o Sc deste grupo devido ao seu raio iônico pequeno e comportamento químico diferenciado (Till et al., 2017).

Os REE não são raros em termos de abundância crustal média, no entanto os seus depósitos minerais de interesse econômico são numericamente limitados e, atualmente 97% da produção mundial de REE é proveniente da China (Migaszewski & Gałuszka, 2015). Essa é provavelmente uma das razões pelas quais foram considerados raros quando descobertos e isolados pela primeira vez na forma de óxidos (terras). Esses elementos são, na verdade, relativamente abundantes na crosta terrestre. O Ce, por exemplo, é o 25º elemento mais abundante na crosta terrestre com 60 ppm, enquanto Lu, o REE menos abundante, está na faixa de 0,5 ppm (Barbalace, 2023).

Todos os REE apresentam estado de oxidação trivalente, apesar de Ce^{4+} e Eu^{2+} também ocorrerem. Dentre os REE, o Pm é o único elemento do grupo que não forma isótopos estáveis. Uma característica marcante nos REE é a variação sutil e gradual no comportamento químico observada ao longo da série dos lantanídeos (Haskin & Frey, 1966). Esse atributo permite que os REE sofram fracionamento, i.e. durante uma transição de fase os REE são redistribuídos em parcelas menores cujas composições variam de acordo com o gradiente das suas propriedades químicas. O fracionamento, bem como outras propriedades, dos lantanídeos é majoritariamente explicado por sua configuração eletrônica (Migaszewski & Gałuszka, 2015). Começando pelo La, a subcamada 4*f* começa a ser preenchida, antes da camada 5*d* (Laveuf & Cornu, 2009). Esse fenômeno acontece devido ao fraco efeito de blindagem dos elétrons 4*f*. A blindagem é a redução da carga nuclear efetiva na nuvem eletrônica resultante das forças de repulsão eletromagnéticas que os elétrons exercem uns

sobre os outros (Menezes & Santos, 2021). O orbital *f* possui blindagem mais fraca e, quanto mais fraca a blindagem, maior é a atração do núcleo sobre a camada de valência. Assim, com o aumento do número de prótons (Z maior), ocorre a redução gradual do raio atômico dos elementos ao longo da série (contração lantanídica) (Laveuf & Cornu, 2009). Outra consequência da contração lantanídica é o aumento da energia de ionização ao longo da série, uma vez que o núcleo com uma maior carga efetiva atrai mais fortemente os elétrons e dificulta sua remoção do átomo (Menezes & Santos, 2021).

De uma forma geral, os REE são um grupo muito coeso, apresentando propriedades físico-químicas previsíveis que variam de forma sistemática e gradual ao longo da série. Essas propriedades servem de base para subdivisões dos REE. Os REE são geralmente separados em dois ou três grupos: leves (LREE), incluindo os elementos do La ao Eu e as vezes o Gd, e pesados (HREE), do Gd ou Tb até Lu (J. Huang et al., 2021; Sanematsu et al., 2015); ou leves (LREE), incluindo os elementos do La ao Pm, médios (MREE), do Sm ao Ho, e pesados (HREE), do Er ao Lu (Baudouin et al., 2020; Chapela Lara et al., 2018; Munemoto et al., 2020). Já o Y, apesar de ser o REE de menor massa atômica, é geralmente classificado junto aos HREE devido ao raio iônico e as similaridades físico-químicas com esse grupo (Haskin & Frey, 1966). Em geral, os LREE são mais abundantes que os HREE e, como um todo, os REE são considerados litófilos, já que substituem outros cátions de raio e carga comparável nas estruturas de minerais (Migaszewski & Gałuszka, 2015).

Devido a suas características e capacidade de fracionamento, os REE são bons traçadores geoquímicos de processos naturais e até antrópicos, permitindo inferir sobre processos complexos que outros elementos traçadores (e.g., Pb, Ra, Rn, Sr) não permitem (Andrade et al., 2017; Andrews et al., 2016; Hatje et al., 2017). Esse grupo de elementos é utilizado para caracterização de rochas ígneas de vários tipos, determinação de fontes de sedimentos, além de entendimento de processos de remoção de elementos da coluna d'água por adsorção em partículas (scavenging), padrões de circulação oceânicos e massas d'água, reconstruir condições climáticas passadas, entre outros (Chaillou et al., 2006a; Garcia-Solsona et al., 2014a; Haley et al., 2014; Mercadier et al., 2011a; Shynu et al., 2013a; Sotto Alibo & Nozaki, 2004; Zheng et al., 2016a). Os REE também são bons traçadores de impactos antrópicos, já tendo sido empregados para identificar contaminação proveniente de atividades de mineração, industrial e domestica/hospitalar (Bau & Dulski, 1996; Hatje et al., 2014a; Kulaksiz & Bau, 2013a; Mirlean et al., 2020a).

A distribuição dos REE segue o padrão Oddo-Harkins (Harkins, 1917; Haskin & Frey, 1966; Nikanorov, 2009), onde os elementos de número atômico par são cerca de uma ordem de magnitude mais abundantes que os elementos de número atômico impar adjacentes. Isso gera um padrão de “zigue zague” nas concentrações desses elementos quando plotados frente a seu número atômico. Na década de 1960, Akimasa Masuda e Larry Coryell propuseram uma forma simples de representar os REE de forma a facilitar sua interpretação. A proposta consistia em normalizar as concentrações de REE frente a um padrão de referência natural (Coryell et al., 1963). Assim, agentes normalizadores (AN) começaram a ser usados para eliminar o “zigue zague” nas distribuições de REE, além de possibilitar a identificação de fracionamento e possíveis anomalias em materiais geológicos e ambientais, facilitando a interpretação de resultados (Anenburg & Williams, 2022). Isso porque, uma vez normalizadas, as concentrações de REE na amostra devem apresentar um padrão suave tendendo a linearidade e qualquer desvio é indicativo de um fracionamento geoquímico em relação aquele agente normalizador ou o que ele representa. A seguir, será discutido um pouco mais sobre a questão dos agentes normalizadores, porém, esse assunto será abordado com mais detalhes no capítulo 1.

O agente normalizador é uma referência do que é considerado natural para uma área ou matriz. Atualmente, existe uma grande variedade de ANs e sua aplicação em um estudo depende de diversos fatores como: o objetivo do estudo; a matriz sendo analisada; quais aspectos se deseja enfatizar; quais dados estão disponíveis etc. Geralmente, é interessante o emprego de um AN similar a matriz da amostra, assim especificidades da amostra serão acentuadas pelo procedimento, enquanto similaridades entre as matrizes serão desacentuadas (Rétif et al., 2023).

Em estudos com REE, os ANs geralmente aplicados podem ser classificados como globais ou locais. As referencias globais mais aplicadas são xistos (Bau et al., 2018; Rétif et al., 2023), representando a composição da porção superior da crosta continental (uma vez eles representam razoavelmente bem a composição média de oligoelementos da crosta terrestre superior pós-arqueana, independente da origem), e os condritos, representando a composição inicial da Terra (Barrat et al., 2012; McLennan, 1989; Nance & Taylor, 1976). Os condritos são geralmente aplicados em estudos de cosmoquímica e geoquímica ígnea, devido a sua característica de enfatizar as diferenças entre a amostra e a Terra (Anders & Grevesse, 1989;

Barrat et al., 2012). Enquanto isso, os xistos são mais aplicados em estudos de geoquímica ambiental, sedimentar e aquosa, acentuando características da matiz/amostra e especificidades que diferenciam-na da composição da superfície terrestre (Bau et al., 2018). Vários exemplos de xistos e condritos podem ser encontrados na literatura (Bau et al., 2018; Gromet et al., 1984; Hans Wedepohl, 1995; Kamber et al., 2005; Rudnick & Gao, 2003; Taylor & McLennan, 1985), porém o Post-Archean Australian Shale (PAAS) é o que tem sido mais aplicado e, de uma forma geral, a aplicação de outros xistos não causaria alterações significativas na interpretação e conclusões obtidas (Bau et al., 2018; Rétif et al., 2023). De uma forma geral, emprego de um AN amplamente usado é uma vantagem, já que isso facilita comparações entre estudos. Ainda assim, existem casos em que os objetivos do trabalho ou até a matriz sendo estudada podem exigir a aplicação de um AN menos comumente aplicado e isso não é um problema, desde que a escolha seja realizada de forma consciente.

Existem alguns AN considerados globais, mas que apresentam especificidades de matriz e, por isso, tem aplicações mais restritas. É o caso do MORB (Mid-Ocean Ridge Basalt; Taylor & Mclennan, 2001), que é um representante da composição da crosta oceânica, divergindo de outros representantes da crosta continental. Esse também é o caso de média mundial de argila ribeirinha (WRAC - World River Average Clay) e a media mundial de siltes ribeirinhos (WRAS - World River Average Silts) propostas por (Bayon et al., 2015a), que podem ser de interesse em estudos de REE em amostras de origem fluvial (i.e., sedimentos e água).

Em algumas situações, pode ser interessante normalizar as concentrações de REE de uma amostra usando um AN local, que pode ser até mesmo outra amostra ou um valor conhecido para o local do estudo (Hatje et al., 2014a; Pedreira et al., 2018; Rousseau et al., 2015a). Esse é o caso quando se deseja demonstrar as diferenças e similaridades entre os dois. Muitas vezes, mesmo quando um AN local é aplicado, é importante fazer a normalização também com um AN global para comparação com resultados produzidos em outros lugares.

Os REE também apresentam propriedades eletroquímicas, magnéticas, espectroscópicas e térmicas que os permitem ser empregados em uma gama de aplicações, especialmente em novas tecnologias, tais como lasers, baterias, super-ímãs, supercondutores, painéis solares, lentes oftálmicas, fibra óptica, catalizadores, computadores, celulares, carros elétricos, turbinas eólicas, marcadores em imunologia, agente de contraste em exames de ressonância magnética, entre outras (Balaram, 2019). Além disso, eles também são empregados para melhorar a produção na agricultura e pecuária (Tariq et al., 2020; Tommasi et al., 2021, 2023;

Tyler, 2004). Devido ao aumento no uso dos REE em atividades antrópicas, tem crescido também a preocupação em relação aos possíveis impactos do lançamento de resíduos contendo esses elementos nos mais diversos ecossistemas, especialmente aqueles em que os REE existem em concentrações naturalmente mais baixas, como é o caso do ambiente marinho e costeiro (Hatje et al., 2016; Lerat-Hardy et al., 2019; Ma & Wang, 2023; Pedreira et al., 2018).

Estudos que indicam que os REE causam fitotoxicidade, neurotoxicidade, genotoxicidade, citotoxicidade, estresse oxidativo e interferem no sistema endócrino, apesar disso, a avaliação de seu risco ecológico como um todo depende de vários fatores como rota de administração, concentração, tempo de exposição, sensibilidade da espécie, entre outros (Badri et al., 2017; Gonzalez et al., 2014; Guo et al., 2020; Gwenzi et al., 2018; Tommasi et al., 2023; Zhang et al., 2022). Como outras características, a toxicidade dos REE não é uniforme e alguns estudos indicam que a toxicidade de formas livres de REE varia com o peso atômico, sendo os LREE mais tóxicos que os HREE, possivelmente devido a estes últimos apresentarem maiores constantes de estabilidade (Blaise et al., 2018; Gonzalez et al., 2014; Lin et al., 2022).

As aplicações dos REE acabam se tornando fonte de contaminação para o ambiente. Nas ultimas décadas, os processos de mineração, produção industrial e rural, reciclagem e destinação de resíduos acabaram se tornando fontes locais de REE para solos, água e ar (Işıldar et al., 2018; Tan et al., 2015). Ainda assim, avanços tecnológicos podem ajudar a reduzir essas emissões, como foi o caso da região norte da Europa após implementação de diversas políticas controle de emissões de poeira pela queima de combustíveis fósseis e por industrias locais (metalúrgica e produção de cal e derivados) (Rühling & Tyler, 2004).

No ambiente aquático existem diversos registros de anomalias antrópicas de REE. Kulaksiz e Bau (2013), por exemplo, encontraram contaminação por La e Sm nas águas do rio Reno, Alemanha, devido ao lançamento de efluentes industriais da produção de catalizadores para craqueamento de petróleo. Já no rio Pérola, China, foi identificada contaminação por Sm, Pr, Nd, Dy e Ho derivada do processo de reciclagem de REE e outras atividades industriais na região (Ma et al., 2019; Ma & Wang, 2023). Já o Gd, cuja forma complexada é usada como agente de contraste em exames de ressonância magnética foi identificado pela primeira vez em águas de rios na Alemanha (Bau & Dulski, 1996) e desde então diversos estudos reportaram Gd antropogênico em outros rios, além de lagos, água subterrânea, água de torneira e água marinha costeira em diversas partes do mundo (Brünjes & Hofmann, 2020;

Johannesson et al., 2017a; Kulaksiz & Bau, 2011; Lawrence et al., 2009; Y. Liu et al., 2022; Merschel et al., 2015; Pedreira et al., 2018). No capítulo 2 deste trabalho foi identificada contaminação por gadolínio antropogênico mesmo distante de locais em que ele é empregado como agente de contraste. Estudos avaliando séries temporais em rios na França (séries de 15 anos) e EUA (série de 20 anos) identificaram crescimento de duas a treze vezes nas concentrações de Gd antropogênico, respectivamente, indicando a tendência de aumento nas emissões desse contaminante (Hatje et al., 2016; Lerat-Hardy et al., 2019).

O Brasil já foi o maior produtor mundial de REE, mas atualmente essa posição pertence a China (De Sousa Filho & Serra, 2014). Existem registros de contaminação por REE no Brasil devido a mineração, produção industrial, produção agrícola, efluentes residenciais/hospitalares (Amorim et al., 2019; Braz et al., 2022; de Freitas et al., 2023; Miekeley et al., 1992; Pedreira et al., 2018; Silva et al., 2019). Foi estimado que aplicações biomédicas geraram uma emissão entre 530kg e 5.3 toneladas de Gd antropogênico no Brasil em 2016, dos quais, até ~ 2kg Gd d^{-1} foram descartados no oceano Atlântico (Pedreira et al., 2018). Além disso, Silva et al. (2019) estimou que cerca de 13.000 toneladas de REE são anualmente adicionadas aos solos brasileiros através de fertilizantes.

Considerando o aumento no uso de REE nas últimas décadas e o fato de suas concentrações naturais no ambiente serem baixas, eles são tidos como microcontaminantes e a diferenciação entre ambientes contaminados e naturalmente enriquecidos (não contaminados) ainda é um desafio (Kulaksiz & Bau, 2007; Nigro et al., 2018).

As características dos REE enquanto grupo (i.e., tendência geral de comportamento gradualmente diferenciado frente a processos físico-químicos e desvios da concentração dos elementos normalizados em relação aos seus vizinhos) os permite ser usados para identificar perfis anômalos de elementos individuais. Estes desvios, também chamados de anomalias, são claramente distinguíveis e podem ser quantificados, uma vez que o valor normalizado "não anômalo" pode ser interpolado ou extrapolado a partir do padrão definido pelos outros REE (Hissler et al., 2015; Kulaksiz & Bau, 2013a; Möller et al., 2002; Sotto Alibo & Nozaki, 2004). Isso é especialmente relevante para amostras ambientais, já que permite distinguir entre as contribuições antropogênicas e naturais referente a concentração total de um REE e quantificar o componente antrópico.

Não existe um consenso sobre qual o melhor método para aplicar quando se deseja calcular

anomalias de REE. Rétif et al. (2023) identificou o uso de 82 equações diferentes para cálculos de anomalias de REE. No geral, os métodos de extrapolação são geralmente usados nos casos em que a aplicação de métodos de interpolação, de menor incerteza, não é possível. Isso é muito comum no caso de elementos na extremidade do grupo, caso do La (Alibo & Nozaki, 1999; Kulaksiz & Bau, 2013a), ou quando há suspeita de anomalia também no elemento vizinho ao de interesse, caso do Ce, se houver suspeita de anomalia de La (Lawrence & Kamber, 2006). (Barrat et al., 2023) demonstraram que o uso de extrapolações lineares pode resultar em valores tendenciosos para as anomalias, que vão depender até mesmo do tipo de normalização empregada. Nesse mesmo trabalho, também ficou claro que a extrapolação geométrica é confiável para o cálculo de anomalias de La e Ce em diversas amostras geológicas e ambientais, sem alterações devido a normalização aplicada.

É comum que os autores prefiram usar a interpolação para cálculo de anomalias devido a sua menor incerteza, porém ainda existem diversos métodos dentro da interpolação. Os métodos de interpolação mais simples (lineares e geométricos) vão se basear na ideia de uma certa linearidade entre os REE como um todo ou, pelo menos, na parte do grupo usada para determinar a anomalia (Hissler et al., 2015; Kulaksiz & Bau, 2013a). Porém, a forma da curva normalizada dos REE nem sempre é linear, podendo apresentar, por exemplo, formato sinusoidal, em U ou de colher (Anenburg & Williams, 2022). Alguns métodos de interpolação levam em consideração o chamado “efeito tétrade”, que seria uma quebra nas tendências de distribuição dos REE em quatro grupos (1: La-Nd, 2: Pm-Gd, 3: Gd-Ho e 4:Er-Lu), sendo um efeito mais aparente em águas naturais e rochas que interagiram com fluidos (Bau, 1997). Para evitar a questão da possível não linearidade dos REE como um todo, alguns autores aplicam métodos de modelagem, como ajustes polinomiais (Anenburg & Williams, 2022; Möller et al., 2002).

De uma forma geral, a quantificação de metais em matrizes ambientais pode ser considerada um desafio analítico devido aos interferentes e as diminutas concentrações de REE em matrizes ambientais. Ao longo dos anos, várias técnicas foram usadas para a quantificação de REE em água do mar. Alguns exemplos são análise de ativação de nêutrons (INAA, Instrumental Neutron Activation Analysis), espectrometria de massas por ionização térmica com diluição isotópica (ID-TIMS, *Isotopic Dilution - Thermal Ionisation Mass Spectrometry*) e espectrometria de emissão atômica com plasma indutivamente acoplado (ICP AES, *Inductively Coupled Plasma Atomic Emission Spectrometry*). Porém essas técnicas

apresentam limitações como limites de detecção elevados, grande tempo de preparo e necessidade de grandes volumes de amostra (De Baar et al., 1985; Greaves et al., 1989; Liang et al., 2005). Atualmente a espectrometria de massas com plasma indutivamente acoplado (ICP-MS) é o instrumento preferencialmente usado para a medida de REE em amostras ambientais como a água do mar. O emprego do ICP-MS oferece vantagens, como a análise elementar e isotópica sequencial rápida e de alta sensibilidade, o que permite a obtenção de resultados rápidos, com boa precisão e baixos limites de detecção usando volumes razoavelmente baixos de amostras (Zheng et al., 2015).

A análise de REE em matrizes ambientais, em muitos casos, exige pré-tratamento das amostras, seja através de digestão ácida, para amostras biológicas e geológicas, ou processos de remoção de interferentes e pré-concentração. A análise de REE exige aplicação de métodos de alta precisão analítica para permitir a identificação de pequenas alterações no fracionamento entre os REE, porém alguns procedimentos químicos podem gerar fracionamento durante o processo de pré-tratamento e algumas interferências poliatômicas e isobáricas podem dificultar as análises (Chung et al., 2009; Field & Sherrell, 1998). Por isso, a escolha criteriosa de um procedimento analítico adequado é crucial para a qualidade dos resultados nessas análises. Em águas estuarinas e marinhas, especificamente, o sal é um fator que pode causar danos aos equipamentos usados na quantificação dos REE, podendo chegar a representar mais de 3% da matriz (Loáiciga, 2006). Por isso, é essencial a remoção do sal dessas amostras antes da análise. Além disso, as concentrações de REE em águas oceânicas geralmente se encontram em níveis sub $pg.L^{-1}$, gerando a necessidade de preconcentração.

Diversas técnicas tem sido empregadas para a preconcentração e separação dos REE da matriz marinha, incluindo extração líquido-líquido (Chandrasekaran et al., 2012; Shabani et al., 1990), co-precipitação com Fe ou Mg (Bayon et al., 2011; Freslon et al., 2011; Greaves et al., 1989), extração em fase sólida (De Baar et al., 1985; Fu et al., 2007; Hatje et al., 2014a; Rahmi et al., 2007; Willie & Sturgeon, 2001; Zhu et al., 2006) e cromatografia iônica (Haley & Klinkhammer, 2003). A aplicação da extração em fase sólida associada com a análise em ICP-MS tem se tornado uma metodologia mais aplicada por ser relativamente barata e permitir fatores de enriquecimento elevados e oferecendo boas recuperações. Ao longo dos anos, várias substâncias foram testadas para preconcentração e extração de REE de água marinha, como nanotubos de carbono (Liang et al., 2005), fibras quelantes (Wen et al., 1999; Zhang et

al., 1998) e resinas quelantes, como Toyopearl AF Chelate 650M iminodiacetate® (Willie & Sturgeon, 2001), Chelex 100® (Rahmi et al., 2007) e mais recentemente NOBIAS-chelate PA-1® (Hatje et al., 2014a). Esta última contém em sua composição ácido etilenodiaminotriacético (EDTA) e ácido iminodiacético (IDA), apresentando elevada afinidade para extração de REE da água marinha.

Algumas das metodologias propostas para o preparo das amostras envolviam o uso de sistemas em linha ou acoplados (Fu et al., 2007; Haley & Klinkhammer, 2003; Zhu et al., 2009), no intuito de reduzir o tempo de trabalho no pré-tratamento e aumentar a produtividade. Dentre as opções de sistemas online existe o seaFAST-pico® (Elemental Scientific Inc, USA). Esse sistema, que utiliza a NOBIAS-chelate PA-1®, permite a purificação e pré-concentração de todos os REE (dentre outros elementos) de forma rápida, automatizada e direta a partir de pequenos volumes de água marinha (~ 12mL). Ele pode ser utilizado tanto de forma em linha, diretamente conectada a um ICP-MS, quanto preconcentrando as amostras em pequenos frascos. A grande desvantagem do utilização do seaFAST-pico® em linha é que o preparo de uma amostra leva cerca de 17min, enquanto a leitura em um ICP-MS leva um período muitas vezes menor, o que acarretaria em um aumento desnecessário de custos com gás. Ainda assim, a utilização do seaFAST-pico® de forma offline para a determinação de REE em água do mar é vantajosa por ser uma forma de eliminar a matriz salina, pré-concentrar os analitos a concentrações de interesse usando volumes pequenos de amostras, minimizar a manipulação pelo analista e consequentemente as chances de contaminação, além de diminuir o tempo de preparo das amostras (Behrens et al., 2016).

Para além do preparo da amostra, a obtenção de resultados de qualidade para a quantificação de REE usando ICP-MS depende de uma série de cuidados para minimizar interferentes. As interferências isobáricas podem ser evitadas fazendo uma seleção criteriosa dos isótopos para análise. Já as interferências poliatômicas (como o óxido de Ba no Eu e óxidos de LREE em HREE) são mais complicadas de serem evitadas e precisam ser consideradas e corrigidas (Chung et al., 2009). Uma forma comum de lidar com essa questão é a leitura de soluções de padrões dos elementos formadores de óxidos e hidróxidos para calcular as taxas de formação desses interferentes e realizar a correção (Field & Sherrell, 1998). Uma outra possibilidade é a utilização das câmaras de dessolvatação como sistema de introdução de amostra, e.g. Aridus (CETAC) e Apex (Elemental Scientific inc). Elas convertem as amostras líquidas em aerossóis secos através de um dispositivo com uma membrana aquecida antes de introduzi-

las no plasma e conseguem reduzir a formação de óxidos a níveis desprezíveis, além de um aumento da sensibilidade e um menor consumo de amostras (Chung et al., 2009; Field & Sherrell, 1998; Zheng et al., 2015).

Outro fator que deve ser considerado nas análises de REE é a que a recuperação desses elementos pode não ser completa e por isso, a utilização de métodos que permitam avaliar o rendimento das etapas de preconcentração se faz necessário. Um dos métodos já utilizados envolve a adição de Túlio nas amostras e cálculo desse rendimento a partir da anomalia positiva criada artificialmente para esse elemento (Bayon et al., 2011; Freslon et al., 2011). Outra opção muito amplamente aplicada é a diluição isotópica, que permite a medida da concentração das amostras independente do rendimento dos pré-tratamentos, sendo um método bastante robusto (Behrens et al., 2016; Field & Sherrell, 1998; Shaw et al., 2003).

1.2 Isótopos de Neodímio como traçadores

O neodímio possui sete isótopos de ocorrência natural, sendo cinco estáveis (^{142}Nd, ^{143}Nd, ^{145}Nd, ^{146}Nd e ^{148}Nd) e dois radioisótopos de meia-vida longa (^{144}Nd e ^{150}Nd). Dentre eles, o ^{143}Nd se destaca por ser o produto do decaimento radioativo do ^{147}Sm. Essa característica faz com que a abundância natural do ^{143}Nd varie de acordo com o tempo e a razão Sm/Nd da rocha de origem (Gioia & Pimentel, 2000). Assim, a razão ^{143}Nd/^{144}Nd (expressa como εNd) pode ser usada como uma assinatura para a rocha e refletir a natureza e material de origem da amostra. Regiões de atividade vulcânica recente apresentam valores de εNd mais radiogênicos (maiores), enquanto rochas mais antigas apresentam valores menos radiogênicos (menores) (Bayon et al., 2015a; Phan et al., 2018; Tachikawa et al., 2003a). Dessa forma, o εNd pode ser usado para identificar origem de material litogênico, bem como caminho advectivo e mistura de massas d'água no oceano, sendo considerado um traçador quasi-conservativo, nesse caso (Lacan & Jeandel, 2005a; Tachikawa et al., 2017a; Wu et al., 2022a). No capítulo 3 deste trabalho é um exemplo de aplicação de εNd como traçador, tendo sido empregado ao longo do oceano Atlântico oeste e na península Antártica.

De uma forma geral, para a aplicação de REE como traçadores de processos nos oceanos é essencial o conhecimento de suas fontes e sumidouros, além de sua mobilidade depois de depositados no assoalho oceânico. Para tal, além das distribuições das concentrações dos REE, é relevante entender também a sua composição isotópica. Desde o final da década de 1980 já se sabia que a composição isotópica do Nd (expressa como εNd) variava de -13 no

oceano Atlântico Norte até -5 no oceano Pacífico e que quando distante de fontes de material litogênico, o εNd se comporta como um traçador conservativo da mistura de massas d'água (Bertram & Elderfield, 1993; Jeandel, 1993a; Jeandel et al., 1998; D. J. Piepgras et al., 1979; D. J. Piepgras & Wasserburg, 1987a; D. Piepgras & Wasserburg, 1982). Desde então, vários estudos enfatizaram que as estimativas de Nd provenientes apenas dos aportes atmosférico e de rios não eram suficientes para explicar as concentrações de Nd e as variações no εNd entre os oceanos (Bertram & Elderfield, 1993; Jeandel, 1993a; Jeandel & Zindler, 1995; Lacan & Jeandel, 2001a; Tachikawa et al., 1999a). Isso se deve ao fato que, considerando apenas as estimativas desses aportes (i.e., rio e atmosfera), o tempo de residência do Nd nos oceanos seria da ordem de 5000 anos (Bertram & Elderfield, 1993), e, portanto grandes diferenças isotópicas entre as massas d'água não seriam possíveis já que a circulação de revolvimento[2] (~1000 anos) causaria mistura e homogeneização desses isótopos. Dessa forma, o tempo de residência[3] do Nd nos oceanos deveria ser menor que ou da mesma ordem de grandeza que a circulação de revolvimento para a manutenção das diferenças isotópicas entre as regiões.

Alguns autores começaram a chamar esse impasse no balanço de massa como "Paradoxo do Nd" (Bertram & Elderfield, 1993; Jeandel & Zindler, 1995; Tachikawa et al., 1999a). Uma definição alternativa para esse paradoxo é dada pela desconexão entre as distribuições das concentrações de Nd e sua composição isotópica. Isso se dá devido ao fato das razões isotópicas do Nd variarem entre os diferentes oceanos e, dentro de um mesmo oceano, dependendo do caminho advectivo das massas d'água, já as concentrações de Nd, assim como outros REE de forma geral, se distribuem de forma similar ao silicato (De Baar et al., 1985), i.e. apresentando aumento progressivo de concentrações com o aumento da profundidade e no decorrer do caminho advectivo das massas d´água. A conclusão lógica para o Paradoxo do Nd, independente de qual definição for usada, é de que apesar das fontes de Nd para o oceano serem espacialmente variáveis, gerando εNd entre -25 e 0 (Lacan & Jeandel, 2005a), o aporte de fluxos atmosféricos e de rios não são suficientes para explicar essa variabilidade. Consequentemente, fontes, sumidouros e/ou processos importantes para o ciclo oceânico do Nd não estavam sendo considerados ou foram subestimados.

[2] **Circulação de revolvimento** é a circulação oceânica global movida pelas diferenças de densidade entre as massas de água no oceano (Talley, 2013).

[3] **Tempo de residência** (algumas vezes tratado como *tempo de remoção*) é a quantidade média de tempo definido como a razão entre a quantidade deste elemento em um determinado reservatório e o fluxo de entrada (ou saída) total deste elemento para este reservatório (Roy-Barman & Jeandel, 2016).

Desde então, surgiram diversas teorias para explicar a diferença entre o fluxo de Nd total encontrado no oceano e o fluxo que efetivamente chegava até ele através das fontes já consideradas como importantes. Algumas das teorias foram: (i) a liberação de Nd do material particulado de rios em função do aumento da força iônica na região estuarina (Sholkovitz, 1993; Tachikawa et al., 2004); (ii) uma maior taxa de dissolução (>2%) do Nd proveniente de poeira atmosférica (Jeandel & Zindler, 1995; Tachikawa et al., 1999a); (iii) interação oceano-sedimento nas margens continentais (Lacan & Jeandel, 2001a; Tachikawa et al., 2003a); (iv) água subterrânea, que já era considerada como importante fonte de Ra e Ba (Johannesson & Burdige, 2007a).

Nos anos que se seguiram, diversos estudos usando modelagem foram realizados numa tentativa de resolver o paradoxo. Vários desses estudos concluíram que o Paradoxo do Nd só poderia ser solucionado se trocas entre as frações particulada-dissolvida fossem levadas em consideração (Arsouze et al., 2007, 2009a; Rempfer et al., 2011a; Siddall et al., 2008a), o que já havia sido previamente indicado em estudos anteriores (Bertram & Elderfield, 1993; Lacan & Jeandel, 2005a; Tachikawa et al., 1999a, 2003a). Tachikawa et al. (2003) suspeitaram que as potenciais fontes de Nd poderiam ser as margens continentais. Posteriormente, Lacan e Jeandel (2005) evidenciaram que ocorreu uma troca significativa entre material particulado e dissolvido nas margens continentais e quantificaram essa troca, em 4 locais nas três bacias oceânicas e ao longo das margens basáltica e granítica (Groelândia, Ilha de Java, Papua Nova Guiné e Mar da China). Essa troca chamada entre os sedimentos e a água nas margens continentais é chamada de "*Boundary Exchange*" (BE, i.e., processo de remoção compensado por aportes de sedimentos ao longo a margem continental) e modificaria a assinatura isotópica de uma massa de água sem afetar significativamente sua concentração. O princípio do BE é que a dissolução e precipitação de partículas e/ou dessorção e adsorção de elementos associados a elas pode levar ao processo de remoção reversível (*reversible scavenging*, Bacon e Anderson, 1982). A remoção reversível se baseia na ideia de uma troca contínua entre os elementos existentes na água e na superfície de partículas, presumindo trocas reversíveis. Quando a velocidade dessas trocas fosse rápida o suficiente, seria possível alcançar um equilíbrio entre as partículas participantes da troca e a água marinha no seu entorno.

Inicialmente, os primeiros autores a mencionar o BE não descreveram a fonte ou o mecanismo

do funcionamento. Estudos posteriores indicaram que era possível que uma fração do material litogênico se dissolvesse, liberando uma fração dos elementos (Abbott et al., 2019; Jones, Pearce, & Oelkers, 2012; Jones, Pearce, Jeandel, et al., 2012; Pearce et al., 2013). Esse processo de remoção reversível se daria principalmente em regiões de margens continentais e deltas de rios devido ao fato da dissolução de material particulado nos oceanos ser fortemente ligada a precipitação de fases secundárias, em função da concentração da maioria dos elementos na água do mar ser saturada ou supersaturada em relação às fases secundárias (Jeandel, 2016a; Jeandel & Oelkers, 2015). Considerando que essas trocas ocorram de forma simultânea ou em escalas de tempo curtas, os elementos liberados pela dissolução de partículas ficariam disponíveis localmente, i.e. na interface água-partícula, predominantemente nas margens oceânicas. Ainda assim, é importante salientar que BE poderia ocorrer em qualquer camada da coluna d'água, não se limitando ao fundo (Jeandel, 2016a; Lacan & Jeandel, 2005a). Dessa forma, o BE seria um processo chave para resolver o Paradoxo do Nd, pois poderia representar uma fonte importante. Neste contexto, o emprego do εNd torna-se uma ferramenta importante para elucidar o Paradoxo do Nd e também rastrear fontes, processos e o caminho advectivo de massas d'água no oceano (Jeandel, 1993; Molina-Kescher et al., 2014; Paffrath et al., 2021; D. J. Piepgras & Wasserburg, 1987).

A avaliação do efeito geral da dissolução do material particulado na química da água do mar a partir da concentração e/ou distribuições dos REE é um desafio já que mesmo quando não são observadas mudanças nas concentrações desses elementos, as mudanças no εNd indicam a ocorrência de trocas. Uma possível explicação para a manutenção das concentrações dos REE dissolvidos é o fato de que a concentração do rabdofano ($REEPO_4 \cdot nH_2O$) na água do mar é próxima da saturação e esse mineral precipita facilmente a partir de fluidos aquosos em temperatura ambiente (Roncal-Herrero et al., 2011). Isso indica que o rabdofano pode atuar como um tampão para as concentrações de REE nos oceanos, já que grande parte desses elementos liberados na dissolução do material particulado pode ser rapidamente reprecipitado como uma fase mais estável, i.e. o rabdofano compensaria as trocas de REE, mantendo suas concentrações constantes. Assim, seria possível a ocorrência de mudança nos valores de εNd, devido a dissolução do material particulado, sem que houvessem grandes mudanças nas concentrações de REE, em função do processo de reprecipitação.

De acordo com os experimentos de modelagem realizados por Rempfer et al. (2011a), o aporte de Nd proveniente de rios (6%) e partículas atmosféricas (4%) é de mínima importância. Em vez disso, seus experimentos indicaram que a maior parte do Nd dissolvido (cerca de 90%) chega aos oceanos pela interface sedimento-água do mar, particularmente nas margens continentais, corroborando com trabalhos anteriores (Arsouze et al., 2007, 2009a, 2010; Tachikawa et al., 2003a). No entanto, Rempfer et al. (2011a) ressalva que os resultados experimentais indicam que apesar do baixo percentual total de contribuição de rios e poeira atmosférica no total de Nd que chega aos oceanos (cerca de 10%), esses aportes ainda são contribuições importantes para o ciclo do Nd, particularmente nos 500m superiores da coluna d'água, onde a consistência entre o modelo experimental usado e a realidade é maior. Estudos mais recentes também indicam que os impactos do processo de BE vão variar a depender de fatores como a diferença isotópica entre a água do mar e os sedimentos, além da própria composição mineralógica desses sedimentos (Adebayo et al., 2022a; Y. Huang et al., 2023).

Depois que diversos estudos começaram a corroborar com a ocorrência do *BE* como explicação para o Paradoxo do Nd, começaram a surgir suspeitas de que processos parecidos pudessem estar afetando as distribuições de outros elementos nos oceanos. Notou-se que a massa de elementos que chega aos oceanos através de partículas terrígenas (material em suspensão em rios, transporte aéreo, etc.) domina o transporte de elementos pouco solúveis (e.g.: REE, Fe, Al) e excede a massa transportada pela fração dissolvida para a maioria dos elementos por um fator de 17 a 30 vezes, incluindo os mais solúveis (e.g.: Ca, K, Sr e Mg) (Jeandel, 2016a; Jeandel & Oelkers, 2015; Oelkers et al., 2011, 2012). Além disso, sabe-se que o grau de importância do material particulado transportado pelos rios para os oceanos nos ciclos dos elementos depende intimamente da reatividade, solubilidade de cada elemento (Oelkers et al., 2011, 2012). Dessa forma, fluxos bentônicos, incluindo a dissolução do material particulado no oceano pode ser um mecanismo importante, contribuindo com numerosos elementos para os oceanos e as estimativas baseadas no transporte pela fração dissolvida dos rios sozinha podem subestimar significativamente os fluxos globais de elementos para os oceanos (Jeandel & Oelkers, 2015). De fato, Jeandel (2016) propôs que existem 5 principais fontes de material solido para os oceanos, sendo elas: aporte atmosférico; aporte de rios (nas formas de sólidos em suspensão, dissolvidos ou coloidal); remobilização de sedimentos; aporte submarino de água subterrânea; e fluidos hidrotermais provenientes das dorsais meso-oceânicas e arcos vulcânicos.

No oceano aberto o principal efeito do desse processo será nas composições isotópicas dos elementos. Para elementos menos solúveis como Fe e Nd uma pequena interação entre as frações dissolvida-particulada poderia gerar grandes mudanças isotópicas, enquanto para elementos mais solúveis, como o Br, essa alteração poderia ser negligenciável (Oelkers et al., 2012). Ainda assim, o efeito da dissolução do material particulado será mais importante nas margens do oceano, uma vez que uma grande fração dos produtos desse processo são re-precipitadas localmente por meio de *BE* (Jeandel & Oelkers, 2015). Alguns estudos já evidenciaram o efeito significativo da dissolução de partículas na composição isotópica de Sr e Nd nos oceanos (Jones, Pearce, Jeandel, et al., 2012; Pearce et al., 2013). Também existem evidências da importância das trocas na interface oceano-partículas no ciclo de elementos como Pb, Th, Fe, Mo, Zn, Cu e Ni (Archer & Vance, 2008; Cameron & Vance, 2014; Charette et al., 2016; Chen et al., 2023; Homoky et al., 2013; Little et al., 2014; Radic et al., 2011; Roy-Barman et al., 2002).

Como alguns elementos afetados por processos de remoção reversível atuam como micronutrientes importantes, a exemplo do Fe, a remoção reversível de partículas pode afetar o seu ciclo e, consequentemente, a produtividade primária marinha (Jeandel & Oelkers, 2015; Roshan et al., 2020). Uma importante consequência desse processo leva em consideração o fato de que o transporte de material particulado para o oceano é mais sensível a variações de temperatura e escoamento do que o transporte da fração dissolvida. O aumento no número de barragens, além da utilização de ambientes costeiros para o desenvolvimento urbano e industrial, tem causado importantes mudanças na morfologia da zona costeira, em particular os estuários (Li et al., 2017; B. Xu et al., 2016).

Estuários são zonas de transição entre o continente e o oceano, os quais atuam como importantes reatores químicos. O gradiente de salinidade, a elevada quantidade de material inorgânico e orgânico, entre outros, facilitam o aprisionamento de elementos-traço nos sistemas costeiros, tanto em estuários e baías, como na plataforma continental (Andrade et al., 2020; Jickells et al., 2016; Lawrence & Kamber, 2006; Sholkovitz, 1993; Shynu et al., 2013a). Ademais, é de se esperar que as atividades antrópicas causem impactos na distribuição global dos elementos-traço nos oceanos, com possíveis consequências climáticas (Jeandel, 2016a; Jeandel & Oelkers, 2015; Jickells et al., 2016). Portanto, é imprescindível novos estudos para esclarecer o mecanismo por detrás do BE, i.e. entender como ocorre o fracionamento dos elementos durante a dissolução e precipitação mineral, além de processos

bióticos, e assim quantificar os fluxos de REE para o oceano. Dessa forma, será possível compreender melhor a biogeoquímica dos REE nos oceanos e prever seu comportamento, especialmente considerando a influência das atividades antrópicas e mudanças climáticas. Porém, esse é o tipo de resultado que exige um esforço de cooperação internacional para ser alcançado (Hatje et al., 2022).

O oceano é vital para a vida na Terra. Ele não apenas regula o clima, mas também abriga uma variedade de ecossistemas, muitos dos quais fornecem alimento e sustento para os seres humanos. Porém diversas atividades antrópicas tem colocado em risco a capacidade do oceano de fornecer esses serviços. O aumento das emissões antrópicas de dióxido de carbono que leva ao aquecimento do planeta e à acidificação dos oceanos, a pesca excessiva, a eutrofização de ambientes costeiros a partir de rejeitos não tratados, a contaminação das águas com poluentes emergentes, a destruição de ambientes costeiros que servem de berçários para diversas espécies marinhas, a poluição sonora no ambiente marinho, entre outros feitos da humanidade podem acabar causando prejuízos irreversíveis em diversos ecossistemas, gerando efeitos negativos para a própria humanidade (Brauko et al., 2020; Forney et al., 2017; Hall-Spencer & Harvey, 2019; Hatje et al., 2016; Issifu et al., 2022; Malik et al., 2017; Miranda et al., 2021). Por isso, partindo da necessidade da humanidade de atuar em prol da saúde oceânica, em 2017 a Organização das Nações Unidas (ONU) resolveu instituir o período de 2021 a 2030 como a Década das Nações Unidas de Ciência Oceânica para o Desenvolvimento Sustentável, também chamada de Década do Oceano (UNESCO, 2019). Propondo assim, que a comunidade internacional cooperasse em busca do desenvolvimento científico, da promoção de parcerias e da construção de infraestruturas para alcançar um oceano saudável e sustentável. Uma das metas da Década é alcançar um oceano limpo, onde as fontes de poluição sejam identificadas e mitigadas ou minimizadas. Para tal, será necessário o envolvimento de cientistas, mas também de várias parcelas da sociedade, como governos, empresas, indústria e sociedade civil. A Década se faz uma oportunidade única para utilização da interface ciência-política em prol de conectar a ciência oceânica com as necessidades da sociedade.

Nesse contexto, o presente trabalho tem como objetivo principal avaliar a ocorrência, distribuição e potencial de aplicação de REE como traçadores de processos naturais e antrópicos em água estuarina e marinha. Este projeto se insere no contexto da Década dos Oceanos como produção de conhecimento científico a partir da colaboração de diversas

instituições para suprir lacunas de conhecimento e servir de base para novas pesquisas e políticas que promovam a saúde do Oceano e subsidie o alcance dos objetivos de desenvolvimento sustentável (ODS) da Agenda 2030.

1.3 REFERÊNCIAS

Abbott, A. N., Löhr, S., & Trethewy, M. (2019). Are clay minerals the primary control on the oceanic rare earth element budget? Frontiers in Marine Science, 6(AUG). https://doi.org/10.3389/fmars.2019.00504

Adebayo, S. B., Cui, M., Williams, T. J., Martin, E., & Johannesson, K. H. (2022). Evolution of rare earth element and εNd compositions of Gulf of Mexico seawater during interaction with Mississippi River sediment. Geochimica et Cosmochimica Acta, 335, 231–242. https://doi.org/10.1016/j.gca.2022.08.024

Alibo, D. S., & Nozaki, Y. (1999). Rare earth elements in seawater: Particle association, shale-normalization, and Ce oxidation. Geochimica et Cosmochimica Acta, 63(3–4), 363–372.

Amorim, A. M., Sodré, F. F., Rousseau, T. C. C., & Maia, P. D. (2019). Assessing rare-earth elements and anthropogenic gadolinium in water samples from an urban artificial lake and its tributaries in the Brazilian Federal District. Microchemical Journal, 148, 27–34. https://doi.org/10.1016/j.microc.2019.04.055

Anders, E., & Grevesse, N. (1989). Abundances of the elements: Meteoritic and solar. Geochimica et Cosmochimica Acta, 53, 197–214.

Andrade, R. L. B., Hatje, V., Masqué, P., Zurbrick, C. M., Boyle, E. A., & Santos, W. P. C. (2017). Chronology of anthropogenic impacts reconstructed from sediment records of trace metals and Pb isotopes in Todos os Santos Bay (NE Brazil). Marine Pollution Bulletin, 125(1–2), 459–471. https://doi.org/10.1016/j.marpolbul.2017.07.053

Andrade, R. L. B., Hatje, V., Pedreira, R. M. A., Böning, P., & Pahnke, K. (2020). REE fractionation and human Gd footprint along the continuum between Paraguaçu River to coastal South Atlantic waters. Chemical Geology, 532. https://doi.org/10.1016/j.chemgeo.2019.119303

Andrews, M. G., Jacobson, A. D., Lehn, G. O., Horton, T. W., & Craw, D. (2016). Radiogenic and stable Sr isotope ratios (87Sr/86Sr, δ88/86Sr) as tracers of riverine cation sources and biogeochemical cycling in the Milford Sound region of Fiordland, New Zealand. Geochimica et Cosmochimica Acta, 173, 284–303. https://doi.org/10.1016/j.gca.2015.10.005

Anenburg, M., & Williams, M. J. (2022). Quantifying the Tetrad Effect, Shape Components, and Ce–Eu–Gd Anomalies in Rare Earth Element Patterns. Mathematical Geosciences, 54(1), 47–70. https://doi.org/10.1007/s11004-021-09959-5

Archer, C., & Vance, D. (2008). The isotopic signature of the global riverine molybdenum flux and anoxia in the ancient oceans. Nature Geoscience, 1(9), 597–600. https://doi.org/10.1038/ngeo282

Arsouze, T., Dutay, J. C., Lacan, F., & Jeandel, C. (2007). Modeling the neodymium isotopic composition with a global ocean circulation model. Chemical Geology, 239(1–2), 165–177. https://doi.org/10.1016/j.chemgeo.2006.12.006

Arsouze, T., Dutay, J.-C., Lacan, F., & Jeandel, C. (2009). Reconstructing the Nd oceanic cycle using a coupled dynamical-biogeochemical model. In Biogeosciences (Vol. 6). www.biogeosciences.net/6/2829/2009/

Arsouze, T., Treguier, A. M., Peronne, S., Dutay, J. C., Lacan, F., & Jeandel, C. (2010). Modeling the Nd isotopic composition in the North Atlantic basin using an eddy-permitting model. Ocean Science, 6(3), 789–797. https://doi.org/10.5194/os-6-789-2010

Bacon, M. P., & Anderson, R. F. (1982). Distribution of thorium isotopes between dissolved and particulate forms in the deep sea. Journal of Geophysical Research: Oceans, 87(C3), 2045–2056. https://doi.org/10.1029/jc087ic03p02045

Badri, N., Florea, A., Mhamdi, M., Matei, H., Tekaya, W. H., Bâati, R., Maghraoui, S., & Tekaya, L. (2017). Toxicological effects and ultrastructural changes induced by lanthanum and cerium in ovary and uterus of Wistar rats. Journal of Trace Elements in Medicine and Biology, 44, 349–355. https://doi.org/10.1016/j.jtemb.2017.09.011

Balaram, V. (2019). Rare earth elements: A review of applications, occurrence, exploration, analysis, recycling, and environmental impact. Geoscience Frontiers, 10(4), 1285–1303. https://doi.org/10.1016/j.gsf.2018.12.005

Barbalace, K. (2023). Periodic Table of Elements. Environmental Chemistry. https://EnvironmentalChemistry.com/yogi/periodic/

Barrat, J. A., Bayon, G., & Lalonde, S. (2023). Calculation of cerium and lanthanum anomalies in geological and environmental samples. Chemical Geology, 615. https://doi.org/10.1016/j.chemgeo.2022.121202

Barrat, J. A., Zanda, B., Moynier, F., Bollinger, C., Liorzou, C., & Bayon, G. (2012). Geochemistry of CI chondrites: Major and trace elements, and Cu and Zn Isotopes. Geochimica et Cosmochimica Acta, 83, 79–92. https://doi.org/10.1016/j.gca.2011.12.011

Bau, M. (1997). The lanthanide tetrad effect in highly evolved felsic igneous rocks - a reply to the comment by Y. Pan. Contributions to Mineralogy and Petrology, 128, 409–412.

Bau, M., & Dulski, P. (1996). Anthropogenic origin of positive gadolinium anomalies in river waters. Earth and Planetary Science Letters, 143, 245–255.

Bau, M., Schmidt, K., Pack, A., Bendel, V., & Kraemer, D. (2018). The European Shale: An improved data set for normalisation of rare earth element and yttrium concentrations in environmental and biological samples from Europe. Applied Geochemistry, 90, 142–149. https://doi.org/10.1016/j.apgeochem.2018.01.008

Baudouin, C., France, L., Boulanger, M., Dalou, C., & Devidal, J. L. (2020). Trace element partitioning between clinopyroxene and alkaline magmas: parametrization and role of M1 site on HREE enrichment in clinopyroxenes. Contributions to Mineralogy and Petrology, 175(5). https://doi.org/10.1007/s00410-020-01680-6

Bayon, G., Birot, D., Bollinger, C., & Barrat, J. A. (2011). Multi-Element Determination of Trace Elements in Natural Water Reference Materials by ICP-SFMS after Tm Addition and Iron Co-precipitation. Geostandards and Geoanalytical Research, 35(1), 145–153. https://doi.org/10.1111/j.1751-908X.2010.00064.x

Bayon, G., Toucanne, S., Skonieczny, C., André, L., Bermell, S., Cheron, S., Dennielou, B., Etoubleau, J., Freslon, N., Gauchery, T., Germain, Y., Jorry, S. J., Ménot, G., Monin, L., Ponzevera, E., Rouget, M. L., Tachikawa, K., & Barrat, J. A. (2015). Rare earth elements and neodymium isotopes in world river sediments revisited. Geochimica et Cosmochimica Acta, 170, 17–38. https://doi.org/10.1016/j.gca.2015.08.001

Behrens, M. K., Muratli, J., Pradoux, C., Wu, Y., Böning, P., Brumsack, H. J., Goldstein, S. L., Haley, B., Jeandel, C., Paffrath, R., Pena, L. D., Schnetger, B., & Pahnke, K. (2016). Rapid and precise analysis of rare earth elements in small volumes of seawater - Method and intercomparison. Marine Chemistry, 186, 110–120. https://doi.org/10.1016/j.marchem.2016.08.006

Bertram, C. J., & Elderfield, H. (1993). The geochemical balance of the rare earth elements and neodymium isotopes in the oceans. Geochimica et Cosmochimica Acta, 57, 1957–1986.

Blaise, C., Gagné, F., Harwood, M., Quinn, B., & Hanana, H. (2018). Ecotoxicity responses of the freshwater cnidarian Hydra attenuata to 11 rare earth elements. Ecotoxicology and Environmental Safety, 163, 486–491. https://doi.org/10.1016/j.ecoenv.2018.07.033

Brauko, K. M., Cabral, A., Costa, N. V., Hayden, J., Dias, C. E. P., Leite, E. S., Westphal, R. D., Mueller, C. M., Hall-Spencer, J. M., Rodrigues, R. R., Rörig, L. R., Pagliosa, P. R., Fonseca, A. L., Alarcon, O. E., & Horta, P. A. (2020). Marine Heatwaves, Sewage and Eutrophication Combine to Trigger Deoxygenation and Biodiversity Loss: A SW Atlantic Case Study. Frontiers in Marine Science, 7. https://doi.org/10.3389/fmars.2020.590258

Braz, A. M. de S., da Costa, M. L., Ramos, S. J., Pereira, W. V. da S., Rizzo, R., & Fernandes, A. R. (2022). Effects of long-term phosphate fertilization on potential risks of emerging contaminants in agroecosystems of the eastern Amazon, Brazil. Environmental Pollutants and Bioavailability, 34(1), 74–87. https://doi.org/10.1080/26395940.2022.2046506

Brünjes, R., & Hofmann, T. (2020). Anthropogenic gadolinium in freshwater and drinking water systems. In Water Research (Vol. 182). Elsevier Ltd. https://doi.org/10.1016/j.watres.2020.115966

Cameron, V., & Vance, D. (2014). Heavy nickel isotope compositions in rivers and the oceans. Geochimica et Cosmochimica Acta, 128, 195–211. https://doi.org/10.1016/j.gca.2013.12.007

Chaillou, G., Anschutz, P., Lavaux, G., & Blanc, G. (2006). Rare earth elements in the modern sediments of the Bay of Biscay (France). Marine Chemistry, 100(1–2), 39–52. https://doi.org/10.1016/j.marchem.2005.09.007

Chandrasekaran, K., Karunasagar, D., & Arunachalam, J. (2012). Dispersive liquid-liquid micro-extraction for simultaneous preconcentration of 14 lanthanides at parts per trillion levels from groundwater and determination using a micro-flow nebulizer in inductively coupled plasma-quadrupole mass spectrometry. Journal of Analytical Atomic Spectrometry, 27(6), 1024–1031. https://doi.org/10.1039/c2ja30066d

Chapela Lara, M., Buss, H. L., & Pett-Ridge, J. C. (2018). The effects of lithology on trace element and REE behavior during tropical weathering. Chemical Geology, 500, 88–102. https://doi.org/10.1016/j.chemgeo.2018.09.024

Charette, M. A., Lam, P. J., Lohan, M. C., Kwon, E. Y., Hatje, V., Jeandel, C., Shiller, A. M., Cutter, G. A., Thomas, A., Boyd, P. W., Homoky, W. B., Milne, A., Thomas, H., Andersson, P. S., Porcelli, D., Tanaka, T., Geibert, W., Dehairs, F., & Garcia-Orellana, J. (2016). Coastal ocean and shelf-sea biogeochemical cycling of trace elements and isotopes: Lessons learned from GEOTRACES. In Philosophical Transactions of the Royal Society A: Mathematical, Physical and Engineering Sciences (Vol. 374, Issue 2081). Royal Society of London. https://doi.org/10.1098/rsta.2016.0076

Chen, M., Carrasco, G., Zhao, N., Wang, X., Lee, J. N., Tanzil, J. T. I., Annammala, K. V., Poh, S. C., Lauro, F. M., Ziegler, A. D., Duangnamon, D., & Boyle, E. A. (2023). Boundary exchange completes the marine Pb cycle jigsaw. Proceedings of the National Academy of Sciences of the United States of America, 120(6). https://doi.org/10.1073/pnas.2213163120

Chung, C. H., Brenner, I., & You, C. F. (2009). Comparison of microconcentric and membrane-desolvation sample introduction systems for determination of low rare earth element concentrations in surface and subsurface waters using sector field inductively coupled plasma mass spectrometry. Spectrochimica Acta - Part B Atomic Spectroscopy, 64(9), 849–856. https://doi.org/10.1016/j.sab.2009.06.013

Coryell, C. D., Chase, J. W., & Winchester, J. W. (1963). A Procedure for Geochemical Interpretation of Terrestrial Rare-Earth Abundance Patterns. Journal of Geophysical Research, 68(2), 559–566.

De Baar, H. J. w, Bacon, Mi. P., Brewer, P. G., & Bruland, K. W. (1985). Rare earth elements in the Pacific and Atlantic Oceans. Genchrmrca CI Cosmochrmrca Acra, 49, 1943–1959.
de Freitas, A. da S., Pompermayer, L. L. de O., Santos, A. D. de O., do Nascimento, M. T. L., Saint'Pierre, T. D., Hauser-Davis, R. A., Baptista Neto, J. A., & da Fonseca, E. M. (2023). Rare earth elements as sediment contamination tracers in a coastal lagoon in the state of Rio de Janeiro, Brazil. Journal of Trace Elements and Minerals, 4, 100068. https://doi.org/10.1016/j.jtemin.2023.100068
De Sousa Filho, P. C., & Serra, O. A. (2014). Terras raras no brasil: Histórico, produção e perspectivas. In Quimica Nova (Vol. 37, Issue 4, pp. 753–760). Sociedade Brasileira de Quimica. https://doi.org/10.5935/0100-4042.20140121
Field, M. P., & Sherrell, R. M. (1998). Magnetic sector ICPMS with desolvating micronebulization: Interference-free subpicogram determination of rare earth elements in natural samples. Analytical Chemistry, 70(21), 4480–4486. https://doi.org/10.1021/ac980455v
Forney, K. A., Southall, B. L., Slooten, E., Dawson, S., Read, A. J., Baird, R. W., & Brownell, R. L. (2017). Nowhere to go: Noise impact assessments for marine mammal populations with high site fidelity. Endangered Species Research, 32(1), 391–413. https://doi.org/10.3354/esr00820
Freslon, N., Bayon, G., Birot, D., Bollinger, C., & Barrat, J. A. (2011). Determination of rare earth elements and other trace elements (Y, Mn, Co, Cr) in seawater using Tm addition and Mg(OH)2 co-precipitation. Talanta, 85(1), 582–587. https://doi.org/10.1016/j.talanta.2011.04.023
Fu, Q., Yang, L., & Wang, Q. (2007). On-line preconcentration with a novel alkyl phosphinic acid extraction resin coupled with inductively coupled plasma mass spectrometry for determination of trace rare earth elements in seawater. Talanta, 72(4), 1248–1254. https://doi.org/10.1016/j.talanta.2007.01.015
Garcia-Solsona, E., Jeandel, C., Labatut, M., Lacan, F., Vance, D., Chavagnac, V., & Pradoux, C. (2014). Rare earth elements and Nd isotopes tracing water mass mixing and particle-seawater interactions in the SE Atlantic. Geochimica et Cosmochimica Acta, 125, 351–372. https://doi.org/10.1016/j.gca.2013.10.009
Gioia, S. M. C. L., & Pimentel, M. M. (2000). The Sm-Nd Isotopic Method in the Geochronology Laboratory of the University of Brasília. Anais Da Academia Brasileira de Ciências, 72(2), 219–245.
Gonzalez, V., Vignati, D. A. L., Leyval, C., & Giamberini, L. (2014). Environmental fate and ecotoxicity of lanthanides: Are they a uniform group beyond chemistry? In Environment International (Vol. 71, pp. 148–157). Elsevier Ltd. https://doi.org/10.1016/j.envint.2014.06.019
Greaves, M. J., Elderfield, H., & Klinkhammer, G. P. (1989). DETERMINATION OF THE RARE EARTH ELEMENTS IN NATURAL WATERS BY ISOTOPE-DILUTION MASS SPECTROMETRY. In Analytica Chimica Actu (Vol. 218). Elsevier Science Publishers B.V.
Gromet, L. P., Dymek, R. F., Haskin, L. A., & Korotev, R. L. (1984). The "North American shale composite": Its compilation, major and trace element characteristics. Geochimica et Cosmochimica Acta, 48, 2469–2482.
Guo, C., Wei, Y., Yan, L., Li, Z., Qian, Y., Liu, H., Li, Z., Li, X., Wang, Z., & Wang, J. (2020). Rare earth elements exposure and the alteration of the hormones in the hypothalamic-pituitary-thyroid (HPT) axis of the residents in an e-waste site: A cross-sectional study. Chemosphere, 252. https://doi.org/10.1016/j.chemosphere.2020.126488
Gwenzi, W., Mangori, L., Danha, C., Chaukura, N., Dunjana, N., & Sanganyado, E. (2018). Sources, behaviour, and environmental and human health risks of high-technology rare

earth elements as emerging contaminants. In Science of the Total Environment (Vol. 636, pp. 299–313). Elsevier B.V. https://doi.org/10.1016/j.scitotenv.2018.04.235
Haley, B. A., Frank, M., Hathorne, E., & Pisias, N. (2014). Biogeochemical implications from dissolved rare earth element and Nd isotope distributions in the Gulf of Alaska. Geochimica et Cosmochimica Acta, 126, 455–474. https://doi.org/10.1016/j.gca.2013.11.012
Haley, B. A., & Klinkhammer, G. P. (2003). Complete separation of rare earth elements from small volume seawater samples by automated ion chromatography: Method development and application to benthic flux. Marine Chemistry, 82(3–4), 197–220. https://doi.org/10.1016/S0304-4203(03)00070-7
Hall-Spencer, J. M., & Harvey, B. P. (2019). Ocean acidification impacts on coastal ecosystem services due to habitat degradation. In Emerging Topics in Life Sciences (Vol. 3, Issue 2, pp. 197–206). Portland Press Ltd. https://doi.org/10.1042/ETLS20180117
Hans Wedepohl, K. (1995). The composition of the continental crust. Geochimica et Cosmochimica Acta, 59(7), 1217–1232. https://doi.org/10.1016/0016-7037(95)00038-2
Harkins, W. D. (1917). The evolution of the elements and the stability of complex atoms. Journal of the American Chemical Society, 39(5), 856–879.
Haskin, L. A., & Frey, F. A. (1966). Dispersed and Not-So-Rare Earths. Science, 152(3720), 299–314. https://www.science.org
Hatje, V., Attisano, K. K., de Souza, M. F. L., Mazzilli, B., de Oliveira, J., de Araújo Mora, T., & Burnett, W. C. (2017). Applications of radon and radium isotopes to determine submarine groundwater discharge and flushing times in Todos os Santos Bay, Brazil. Journal of Environmental Radioactivity, 178–179, 136–146. https://doi.org/10.1016/j.jenvrad.2017.08.004
Hatje, V., Bruland, K. W., & Flegal, A. R. (2014). Determination of rare earth elements after pre-concentration using NOBIAS-chelate PA-1®resin: Method development and application in the San Francisco Bay plume. Marine Chemistry, 160, 34–41. https://doi.org/10.1016/j.marchem.2014.01.006
Hatje, V., Bruland, K. W., & Flegal, A. R. (2016). Increases in Anthropogenic Gadolinium Anomalies and Rare Earth Element Concentrations in San Francisco Bay over a 20 Year Record. Environmental Science and Technology, 50(8), 4159–4168. https://doi.org/10.1021/acs.est.5b04322
Hatje, V., Sarin, M., Sander, S. G., Omanović, D., Ramachandran, P., Völker, C., Barra, R. O., & Tagliabue, A. (2022). Emergent interactive effects of climate change and contaminants in coastal and ocean ecosystems. Frontiers in Marine Science, 9. https://doi.org/10.3389/fmars.2022.936109
Hissler, C., Hostache, R., Iffly, J. F., Pfister, L., & Stille, P. (2015). Anthropogenic rare earth element fluxes into floodplains: Coupling between geochemical monitoring and hydrodynamic sediment transport modelling. Comptes Rendus - Geoscience, 347(5–6), 294–303. https://doi.org/10.1016/j.crte.2015.01.003
Homoky, W. B., John, S. G., Conway, T. M., & Mills, R. A. (2013). Distinct iron isotopic signatures and supply from marine sediment dissolution. Nature Communications, 4. https://doi.org/10.1038/ncomms3143
Huang, J., Tan, W., Liang, X., He, H., Ma, L., Bao, Z., & Zhu, J. (2021). REE fractionation controlled by REE speciation during formation of the Renju regolith-hosted REE deposits in Guangdong Province, South China. Ore Geology Reviews, 134. https://doi.org/10.1016/j.oregeorev.2021.104172
Huang, Y., Colin, C., Liu, Z., Douville, E., Dapoigny, A., Haurine, F., Wu, Q., & Tien-Shun Lin, A. (2023). Impacts of nepheloid layers and mineralogical compositions of oceanic margin

sediments on REE concentrations and Nd isotopic compositions of seawater. Geochimica et Cosmochimica Acta, 359, 57–70. https://doi.org/10.1016/j.gca.2023.08.026
Işıldar, A., Rene, E. R., van Hullebusch, E. D., & Lens, P. N. L. (2018). Electronic waste as a secondary source of critical metals: Management and recovery technologies. Resources, Conservation and Recycling, 135, 296–312. https://doi.org/10.1016/j.resconrec.2017.07.031
Issifu, I., Alava, J. J., Lam, V. W. Y., & Sumaila, U. R. (2022). Impact of Ocean Warming, Overfishing and Mercury on European Fisheries: A Risk Assessment and Policy Solution Framework. Frontiers in Marine Science, 8. https://doi.org/10.3389/fmars.2021.770805
Jeandel, C. (1993). Concentration and isotopic composition of Nd in the South Atlantic Ocean. Earth and Planetary Science Letters, 117, 581–591.
Jeandel, C. (2016). Overview of the mechanisms that could explain the “Boundary Exchange” at the land-ocean contact. In Philosophical Transactions of the Royal Society A: Mathematical, Physical and Engineering Sciences (Vol. 374, Issue 2081). Royal Society of London. https://doi.org/10.1098/rsta.2015.0287
Jeandel, C., & Oelkers, E. H. (2015). The influence of terrigenous particulate material dissolution on ocean chemistry and global element cycles. In Chemical Geology (Vol. 395, pp. 50–66). Elsevier. https://doi.org/10.1016/j.chemgeo.2014.12.001
Jeandel, C., Thouron, D., & Fieux, M. (1998). Concentrations and isotopic compositions of neodymium in the eastern Indian Ocean and Indonesian straits. Geochimica et Cosmochimica Acta, 62(15), 2597–2607.
Jeandel, C., & Zindler, A. (1995). Exchange of neodymium and its isotopes between seawater and small and large particles in the Sargasso Sea. In Geochimica et Cosmochimica Acta (Vol. 59, Issue 3).
Jickells, T. D., Andrews, J. E., & Parkes, D. J. (2016). Direct and Indirect Effects of Estuarine Reclamation on Nutrient and Metal Fluxes in the Global Coastal Zone. Aquatic Geochemistry, 22(4), 337–348. https://doi.org/10.1007/s10498-015-9278-7
Johannesson, K. H., & Burdige, D. J. (2007). Balancing the global oceanic neodymium budget: Evaluating the role of groundwater. Earth and Planetary Science Letters, 253(1–2), 129–142. https://doi.org/10.1016/j.epsl.2006.10.021
Johannesson, K. H., Palmore, C. D., Fackrell, J., Prouty, N. G., Swarzenski, P. W., Chevis, D. A., Telfeyan, K., White, C. D., & Burdige, D. J. (2017). Rare earth element behavior during groundwater–seawater mixing along the Kona Coast of Hawaii. Geochimica et Cosmochimica Acta, 198, 229–258. https://doi.org/10.1016/j.gca.2016.11.009
Jones, M. T., Pearce, C. R., Jeandel, C., Gislason, S. R., Eiriksdottir, E. S., Mavromatis, V., & Oelkers, E. H. (2012). Riverine particulate material dissolution as a significant flux of strontium to the oceans. Earth and Planetary Science Letters, 355–356, 51–59. https://doi.org/10.1016/j.epsl.2012.08.040
Jones, M. T., Pearce, C. R., & Oelkers, E. H. (2012). An experimental study of the interaction of basaltic riverine particulate material and seawater. Geochimica et Cosmochimica Acta, 77, 108–120. https://doi.org/10.1016/j.gca.2011.10.044
Kamber, B. S., Greig, A., & Collerson, K. D. (2005). A new estimate for the composition of weathered young upper continental crust from alluvial sediments, Queensland, Australia. Geochimica et Cosmochimica Acta, 69(4), 1041–1058. https://doi.org/10.1016/j.gca.2004.08.020
Kulaksiz, S., & Bau, M. (2007). Contrasting behaviour of anthropogenic gadolinium and natural rare earth elements in estuaries and the gadolinium input into the North Sea. Earth and Planetary Science Letters, 260(1–2), 361–371. https://doi.org/10.1016/j.epsl.2007.06.016

Kulaksiz, S., & Bau, M. (2011). Anthropogenic gadolinium as a microcontaminant in tap water used as drinking water in urban areas and megacities. Applied Geochemistry, 26(11), 1877–1885. https://doi.org/10.1016/j.apgeochem.2011.06.011
Kulaksiz, S., & Bau, M. (2013). Anthropogenic dissolved and colloid/nanoparticle-bound samarium, lanthanum and gadolinium in the Rhine River and the impending destruction of the natural rare earth element distribution in rivers. Earth and Planetary Science Letters, 362, 43–50. https://doi.org/10.1016/j.epsl.2012.11.033
Lacan, F., & Jeandel, C. (2001). Tracing Papua New Guinea imprint on the central Equatorial Paci¢c Ocean using neodymium isotopic compositions and Rare Earth Element patterns. Earth and Planetary Science Letters, 186, 497–512. www.elsevier.com/locate/epsl
Lacan, F., & Jeandel, C. (2005). Neodymium isotopes as a new tool for quantifying exchange fluxes at the continent-ocean interface. Earth and Planetary Science Letters, 232(3–4), 245–257. https://doi.org/10.1016/j.epsl.2005.01.004
Laveuf, C., & Cornu, S. (2009). A review on the potentiality of Rare Earth Elements to trace pedogenetic processes. In Geoderma (Vol. 154, Issues 1–2, pp. 1–12). https://doi.org/10.1016/j.geoderma.2009.10.002
Lawrence, M. G., & Kamber, B. S. (2006). The behaviour of the rare earth elements during estuarine mixing-revisited. Marine Chemistry, 100(1–2), 147–161. https://doi.org/10.1016/j.marchem.2005.11.007
Lawrence, M. G., Ort, C., & Keller, J. (2009). Detection of anthropogenic gadolinium in treated wastewater in South East Queensland, Australia. Water Research, 43(14), 3534–3540. https://doi.org/10.1016/j.watres.2009.04.033
Lerat-Hardy, A., Coynel, A., Dutruch, L., Pereto, C., Bossy, C., Gil-Diaz, T., Capdeville, M. J., Blanc, G., & Schäfer, J. (2019). Rare Earth Element fluxes over 15 years into a major European Estuary (Garonne-Gironde, SW France): Hospital effluents as a source of increasing gadolinium anomalies. Science of the Total Environment, 656, 409–420. https://doi.org/10.1016/j.scitotenv.2018.11.343
Li, X., Chen, H., Jiang, X., Yu, Z., & Yao, Q. (2017). Impacts of human activities on nutrient transport in the Yellow River: The role of the Water-Sediment Regulation Scheme. Science of the Total Environment, 592, 161–170. https://doi.org/10.1016/j.scitotenv.2017.03.098
Liang, P., Liu, Y., & Guo, L. (2005). Determination of trace rare earth elements by inductively coupled plasma atomic emission spectrometry after preconcentration with multiwalled carbon nanotubes. Spectrochimica Acta - Part B Atomic Spectroscopy, 60(1), 125–129. https://doi.org/10.1016/j.sab.2004.11.010
Lin, Y. T., Liu, R. X., Audira, G., Suryanto, M. E., Roldan, M. J. M., Lee, J., Ger, T. R., & Hsiao, C. Der. (2022). Lanthanides Toxicity in Zebrafish Embryos Are Correlated to Their Atomic Number. Toxics, 10(6). https://doi.org/10.3390/toxics10060336
Little, S. H., Vance, D., Walker-Brown, C., & Landing, W. M. (2014). The oceanic mass balance of copper and zinc isotopes, investigated by analysis of their inputs, and outputs to ferromanganese oxide sediments. Geochimica et Cosmochimica Acta, 125, 673–693. https://doi.org/10.1016/j.gca.2013.07.046
Liu, Y., Wu, Q., Jia, H., Wang, Z., Gao, S., & Zeng, J. (2022). Anthropogenic rare earth elements in urban lakes: Their spatial distributions and tracing application. Chemosphere, 300. https://doi.org/10.1016/j.chemosphere.2022.134534
Loáiciga, H. A. (2006). Modern-age buildup of CO2 and its effects on seawater acidity and salinity. Geophysical Research Letters, 33(10). https://doi.org/10.1029/2006GL026305
Ma, L., Dang, D. H., Wang, W., Evans, R. D., & Wang, W. X. (2019). Rare earth elements in the Pearl River Delta of China: Potential impacts of the REE industry on water,

suspended particles and oysters. Environmental Pollution, 244, 190–201. https://doi.org/10.1016/j.envpol.2018.10.015
Ma, L., & Wang, W. X. (2023). Dissolved rare earth elements in the Pearl River Delta: Using Gd as a tracer of anthropogenic activity from river towards the sea. Science of the Total Environment, 856. https://doi.org/10.1016/j.scitotenv.2022.159241
Malik, A., Mertz, O., & Fensholt, R. (2017). Mangrove forest decline: consequences for livelihoods and environment in South Sulawesi. Regional Environmental Change, 17(1), 157–169. https://doi.org/10.1007/s10113-016-0989-0
McLennan, S. M. (1989). Rare earth elements in sedimentary rocks: influence of provenance and sedimentary processes. In Geochemistry and Mineralogy of Rare Earth Elements (pp. 169–200).
Menezes, J. F. S. de, & Santos, R. G. dos. (2021). QUÍMICA DE LANTANÍDEOS. In O ensino e a pesquisa em química 2 (pp. 160–191). Atena Editora. https://doi.org/10.22533/at.ed.23521310815
Mercadier, J., Cuney, M., Lach, P., Boiron, M. C., Bonhoure, J., Richard, A., Leisen, M., & Kister, P. (2011). Origin of uranium deposits revealed by their rare earth element signature. Terra Nova, 23(4), 264–269. https://doi.org/10.1111/j.1365-3121.2011.01008.x
Merschel, G., Bau, M., Baldewein, L., Dantas, E. L., Walde, D., & Bühn, B. (2015). Tracing and tracking wastewater-derived substances in freshwater lakes and reservoirs: Anthropogenic gadolinium and geogenic REEs in Lake Paranoá, Brasilia. Comptes Rendus - Geoscience, 347(5–6), 284–293. https://doi.org/10.1016/j.crte.2015.01.004
Miekeley, N., Coutinho De Jesus, H., Porto Da Silveira, C. L., Linsalata, P., & Morse, R. (1992). Rare-earth elements in groundwaters from the Osamu Utsumi mine and Morro do Ferro analogue study sites, Poços de Caldas, Brazil. Journal of GeochemicalExploration, 45, 365–387.
Migaszewski, Z. M., & Gałuszka, A. (2015). The Characteristics, Occurrence, and Geochemical Behavior of Rare Earth Elements in the Environment: A Review. Critical Reviews in Environmental Science and Technology, 45(5), 429–471. https://doi.org/10.1080/10643389.2013.866622
Miranda, D. de A., Leonel, J., Benskin, J. P., Johansson, J., & Hatje, V. (2021). Perfluoroalkyl Substances in the Western Tropical Atlantic Ocean. Environmental Science and Technology, 55(20), 13749–13758. https://doi.org/10.1021/acs.est.1c01794
Mirlean, N., Calliari, L., & Johannesson, K. (2020). Dredging in an estuary causes contamination by fluid mud on a tourist ocean beach. Evidence via REE ratios. Marine Pollution Bulletin, 159. https://doi.org/10.1016/j.marpolbul.2020.111495
Molina-Kescher, M., Frank, M., & Hathorne, E. (2014). South Pacific dissolved Nd isotope compositions and rare earth element distributions: Water mass mixing versus biogeochemical cycling. Geochimica et Cosmochimica Acta, 127, 171–189. https://doi.org/10.1016/j.gca.2013.11.038
Möller, P., Paces, T., Dulski, P., & Morteani, G. (2002). Anthropogenic Gd in surface water, drainage system, and the water supply of the City of Prague, Czech Republic. Environmental Science and Technology, 36(11), 2387–2394. https://doi.org/10.1021/es010235q
Munemoto, T., Solongo, T., Okuyama, A., Fukushi, K., Yunden, A., Batbold, T., Altansukh, O., Takahashi, Y., Iwai, H., & Nagao, S. (2020). Rare earth element distributions in rivers and sediments from the Erdenet Cu–Mo mining area, Mongolia. Applied Geochemistry, 123. https://doi.org/10.1016/j.apgeochem.2020.104800

Nance, W. B., & Taylor, S. R. (1976). Rare earth element patterns and crustal evolution-I. Australian post-Archean sedimentary rocks. Geochimica et Cosmochimica Acta, 40, 1539–1551.
Nigro, A., Sappa, G., & Barbieri, M. (2018). Boron isotopes and rare earth elements in the groundwater of a landfill site. Journal of Geochemical Exploration, 190, 200–206. https://doi.org/10.1016/j.gexplo.2018.02.019
Nikanorov, A. M. (2009). The Oddo-Harkins rule and distribution of chemical elements in freshwater ecosystems. Doklady Earth Sciences, 426(1), 600–604. https://doi.org/10.1134/S1028334X09040205
Oelkers, E. H., Gislason, S. R., Eiriksdottir, E. S., Jones, M., Pearce, C. R., & Jeandel, C. (2011). The role of riverine particulate material on the global cycles of the elements. Applied Geochemistry, 26(SUPPL.). https://doi.org/10.1016/j.apgeochem.2011.03.062
Oelkers, E. H., Jones, M. T., Pearce, C. R., Jeandel, C., Eiriksdottir, E. S., & Gislason, S. R. (2012). Riverine particulate material dissolution in seawater and its implications for the global cycles of the elements. In Comptes Rendus - Geoscience (Vol. 344, Issues 11–12, pp. 646–651). https://doi.org/10.1016/j.crte.2012.08.005
Paffrath, R., Pahnke, K., Böning, P., Rutgers van der Loeff, M., Valk, O., Gdaniec, S., & Planquette, H. (2021). Seawater-Particle Interactions of Rare Earth Elements and Neodymium Isotopes in the Deep Central Arctic Ocean. Journal of Geophysical Research: Oceans, 126(8). https://doi.org/10.1029/2021JC017423
Pearce, C. R., Jones, M. T., Oelkers, E. H., Pradoux, C., & Jeandel, C. (2013). The effect of particulate dissolution on the neodymium (Nd) isotope and Rare Earth Element (REE) composition of seawater. Earth and Planetary Science Letters, 369–370, 138–147. https://doi.org/10.1016/j.epsl.2013.03.023
Pedreira, R. M. A., Pahnke, K., Böning, P., & Hatje, V. (2018). Tracking hospital effluent-derived gadolinium in Atlantic coastal waters off Brazil. Water Research, 145, 62–72. https://doi.org/10.1016/j.watres.2018.08.005
Phan, T. T., Gardiner, J. B., Capo, R. C., & Stewart, B. W. (2018). Geochemical and multi-isotopic (87Sr/86Sr, 143Nd/144Nd, 238U/235U) perspectives of sediment sources, depositional conditions, and diagenesis of the Marcellus Shale, Appalachian Basin, USA. Geochimica et Cosmochimica Acta, 222, 187–211. https://doi.org/10.1016/j.gca.2017.10.021
Piepgras, D. J., & Wasserburg, G. J. (1987). Rare earth element transport in the western North Atlantic inferred from Nd isotopic observations. Geochimica et Cosmochimica Acta, 51, 1257–1271.
Piepgras, D. J., Wasserburg, G. J., & Dasch, E. J. (1979). THE ISOTOPIC COMPOSITION OF Nd IN DIFFERENT OCEAN MASSES. In Earth and Planetary Science Letters (Vol. 45).
Piepgras, D., & Wasserburg, G. (1982). Isotopic Composition of Neodymium in Waters from the Drake Passage. Science, 217, 207–217.
Radic, A., Lacan, F., & Murray, J. W. (2011). Iron isotopes in the seawater of the equatorial Pacific Ocean: New constraints for the oceanic iron cycle. Earth and Planetary Science Letters, 306(1–2), 1–10. https://doi.org/10.1016/j.epsl.2011.03.015
Rahmi, D., Zhu, Y., Fujimori, E., Umemura, T., & Haraguchi, H. (2007). Multielement determination of trace metals in seawater by ICP-MS with aid of down-sized chelating resin-packed minicolumn for preconcentration. Talanta, 72(2), 600–606. https://doi.org/10.1016/j.talanta.2006.11.023
Rempfer, J., Stocker, T. F., Joos, F., Dutay, J. C., & Siddall, M. (2011). Modelling Nd-isotopes with a coarse resolution ocean circulation model: Sensitivities to model

parameters and source/sink distributions. Geochimica et Cosmochimica Acta, 75(20), 5927–5950. https://doi.org/10.1016/j.gca.2011.07.044
Rétif, J., Zalouk-Vergnoux, A., Briant, N., & Poirier, L. (2023). From geochemistry to ecotoxicology of rare earth elements in aquatic environments: Diversity and uses of normalization reference materials and anomaly calculation methods. In Science of the Total Environment (Vol. 856). Elsevier B.V. https://doi.org/10.1016/j.scitotenv.2022.158890
Roncal-Herrero, T., Rodríguez-Blanco, J. D., Oelkers, E. H., & Benning, L. G. (2011). The direct precipitation of rhabdophane (REEPO4 · H 2O) nano-rods from acidic aqueous solutions at 5-100 °c. Journal of Nanoparticle Research, 13(9), 4049–4062. https://doi.org/10.1007/s11051-011-0347-6
Roshan, S., DeVries, T., Wu, J., John, S., & Weber, T. (2020). Reversible scavenging traps hydrothermal iron in the deep ocean. Earth and Planetary Science Letters, 542. https://doi.org/10.1016/j.epsl.2020.116297
Rousseau, T. C. C., Sonke, J. E., Chmeleff, J., Van Beek, P., Souhaut, M., Boaventura, G., Seyler, P., & Jeandel, C. (2015). Rapid neodymium release to marine waters from lithogenic sediments in the Amazon estuary. Nature Communications, 6. https://doi.org/10.1038/ncomms8592
Roy-Barman, M., Coppola, L., & Souhaut, M. (2002). Thorium isotopes in the western Mediterranean Sea: an insight into the marine particle dynamics. Earth and Planetary Science Letters, 196, 161–174. www.elsevier.com/locate/epsl
Roy-Barman, M., & Jeandel, C. (2016). MARINE GEOCHEMISTRY. Oxford University Press.
Rudnick, R. L., & Gao, S. (2003). Composition of the Continental Crust. In Treatise on Geochemistry (pp. 1–64). Elsevier. https://doi.org/10.1016/B0-08-043751-6/03016-4
Rühling, Å., & Tyler, G. (2004). Changes in the atmospheric deposition of minor and rare elements between 1975 and 2000 in south Sweden, as measured by moss analysis. Environmental Pollution, 131(3), 417–423. https://doi.org/10.1016/j.envpol.2004.03.005
Sanematsu, K., Kon, Y., & Imai, A. (2015). Influence of phosphate on mobility and adsorption of REEs during weathering of granites in Thailand. Journal of Asian Earth Sciences, 111, 14–30. https://doi.org/10.1016/j.jseaes.2015.05.018
Shabani, M. B., Akagi, T., Shimizu, H., & Masuda, A. (1990). Determination of Trace Lanthanides and Yttrium in Seawater by Indutively Coupled Plama Mass Spectrometry after Preconcentration with Solvent Extraction and Back-Extraction. Analytical Chemistry, 62, 2709–2014. https://pubs.acs.org/sharingguidelines
Shaw, T. J., Duncan, T., & Schnetger, B. (2003). A preconcentration/matrix reduction method for the analysis of rare earth elements in seawater and groundwaters by isotope dilution ICPMS. Analytical Chemistry, 75(14), 3396–3403. https://doi.org/10.1021/ac026158e
Sholkovitz, E. R. (1993). The geochemistry of rare earth elements in the Amazon River estuary. Geochimica et Cosmochimica Acta, 57, 2181–2190.
Shynu, R., Rao, V. P., Parthiban, G., Balakrishnan, S., Narvekar, T., & Kessarkar, P. M. (2013). REE in suspended particulate matter and sediment of the Zuari estuary and adjacent shelf, western India: Influence of mining and estuarine turbidity. Marine Geology, 346, 326–342. https://doi.org/10.1016/j.margeo.2013.10.004
Siddall, M., Khatiwala, S., van de Flierdt, T., Jones, K., Goldstein, S. L., Hemming, S., & Anderson, R. F. (2008). Towards explaining the Nd paradox using reversible scavenging in an ocean general circulation model. Earth and Planetary Science Letters, 274(3–4), 448–461. https://doi.org/10.1016/j.epsl.2008.07.044
Silva, F. B. V., Nascimento, C. W. A., Alvarez, A. M., & Araújo, P. R. M. (2019). Inputs of rare earth elements in Brazilian agricultural soils via P-containing fertilizers and soil

correctives. Journal of Environmental Management, 232, 90–96. https://doi.org/10.1016/j.jenvman.2018.11.031
Sotto Alibo, D., & Nozaki, Y. (2004). Dissolved rare earth elements in the eastern Indian Ocean: Chemical tracers of the water masses. Deep-Sea Research Part I: Oceanographic Research Papers, 51(4), 559–576. https://doi.org/10.1016/j.dsr.2003.11.004
Tachikawa, K., Arsouze, T., Bayon, G., Bory, A., Colin, C., Dutay, J. C., Frank, N., Giraud, X., Gourlan, A. T., Jeandel, C., Lacan, F., Meynadier, L., Montagna, P., Piotrowski, A. M., Plancherel, Y., Pucéat, E., Roy-Barman, M., & Waelbroeck, C. (2017). The large-scale evolution of neodymium isotopic composition in the global modern and Holocene ocean revealed from seawater and archive data. Chemical Geology, 457, 131–148. https://doi.org/10.1016/j.chemgeo.2017.03.018
Tachikawa, K., Athias, V., & Jeandel, C. (2003). Neodymium budget in the modern ocean and paleo-oceanographic implications. Journal of Geophysical Research: Oceans, 108(8). https://doi.org/10.1029/1999jc000285
Tachikawa, K., Jeandel, C., & Roy-Barman, M. (1999). A new approach to the Nd residence time in the ocean: the role of atmospheric inputs. Earth and Planetary Science Letters, 170, 433–446. www.elsevier.com/locate/epsl
Tachikawa, K., Roy-Barman, M., Michard, A., Thouron, D., Yeghicheyan, D., & Jeandel, C. (2004). Neodymium isotopes in the Mediterranean Sea: Comparison between seawater and sediment signals. Geochimica et Cosmochimica Acta, 68(14), 3095–3106. https://doi.org/10.1016/j.gca.2004.01.024
Talley, L. (2013). Closure of the Global Overturning Circulation Through the Indian, Pacific, and Southern Oceans: Schematics and Transports. Oceanography, 26(1), 80–97. https://doi.org/10.5670/oceanog.2013.07
Tan, Q., Li, J., & Zeng, X. (2015). Rare Earth Elements Recovery from Waste Fluorescent Lamps: A Review. In Critical Reviews in Environmental Science and Technology (Vol. 45, Issue 7, pp. 749–776). Taylor and Francis Inc. https://doi.org/10.1080/10643389.2014.900240
Tariq, H., Sharma, A., Sarkar, S., Ojha, L., Pal, R. P., & Mani, V. (2020). Perspectives for rare earth elements as feed additive in livestock - A review. In Asian-Australasian Journal of Animal Sciences (Vol. 33, Issue 3, pp. 373–381). Asian-Australasian Association of Animal Production Societies. https://doi.org/10.5713/ajas.19.0242
Taylor, S. R., & Mclennan, S. M. (2001). Chemical Composition and Element Distribution in the Earth's Crust. Encyclopedia of Physical Science and Technology, 312, 697–719.
Taylor, S. Ross., & McLennan, S. M. . (1985). The Continental Crust: its Composition and Evolution. Blackwell Scientific.
Till, C. P., Shelley, R. U., Landing, W. M., & Bruland, K. W. (2017). Dissolved scandium, yttrium, and lanthanum in the surface waters of the North Atlantic: Potential use as an indicator of scavenging intensity. Journal of Geophysical Research: Oceans, 122(8), 6684–6697. https://doi.org/10.1002/2017JC012696
Tommasi, F., Thomas, P. J., Lyons, D. M., Pagano, G., Oral, R., Siciliano, A., Toscanesi, M., Guida, M., & Trifuoggi, M. (2023). Evaluation of Rare Earth Element-Associated Hormetic Effects in Candidate Fertilizers and Livestock Feed Additives. In Biological Trace Element Research (Vol. 201, Issue 5, pp. 2573–2581). Springer. https://doi.org/10.1007/s12011-022-03331-2
Tommasi, F., Thomas, P. J., Pagano, G., Perono, G. A., Oral, R., Lyons, D. M., Toscanesi, M., & Trifuoggi, M. (2021). Review of Rare Earth Elements as Fertilizers and Feed Additives: A Knowledge Gap Analysis. In Archives of Environmental Contamination and

Toxicology (Vol. 81, Issue 4, pp. 531–540). Springer. https://doi.org/10.1007/s00244-020-00773-4
Tyler, G. (2004). Rare earth elements in soil and plant systems-A review. In Plant and Soil (Vol. 267).
UNESCO. (2019). A ciência que precisamos para o oceano que queremos: a Década das Nações Unidas da Ciência Oceânica para o Desenvolvimento Sustentável (2021-2030). https://ciencianomar.mctic.gov.br/wp-content/uploads/2020/06/265198por.pdf
Wasserburg, G. J., Jacobsen, S. B., DePaolo, D. J., McCulloch, M. T., & Wen, T. (1981). Precise determination of Sm/Nd ratios, Sm and Nd isotopic abundances in standard solutions*. Geochimica et Cosmochimica Acta, 45, 2311–2323.
Willie, S. N., & Sturgeon, R. E. (2001). Determination of transition and rare earth elements in seawater by flow injection inductively coupled plasma time-of-flight mass spectrometry. In Spectrochimica Acta Part B (Vol. 56).
Wu, Y., Pena, L. D., Anderson, R. F., Hartman, A. E., Bolge, L. L., Basak, C., Kim, J., Rijkenberg, M. J. A., de Baar, H. J. W., & Goldstein, S. L. (2022). Assessing neodymium isotopes as an ocean circulation tracer in the Southwest Atlantic. Earth and Planetary Science Letters, 599. https://doi.org/10.1016/j.epsl.2022.117846
Xu, B., Yang, D., Burnett, W. C., Ran, X., Yu, Z., Gao, M., Diao, S., & Jiang, X. (2016). Artificial water sediment regulation scheme influences morphology, hydrodynamics and nutrient behavior in the Yellow River estuary. Journal of Hydrology, 539, 102–112. https://doi.org/10.1016/j.jhydrol.2016.05.024
Zhang, X., Hu, Z., Pan, H., Bai, Y., Hu, Y., & Jin, S. (2022). Effects of rare earth elements on bacteria in rhizosphere, root, phyllosphere and leaf of soil–rice ecosystem. Scientific Reports, 12(1). https://doi.org/10.1038/s41598-022-06003-2
Zheng, X. Y., Plancherel, Y., Saito, M. A., Scott, P. M., & Henderson, G. M. (2016). Rare earth elements (REEs) in the tropical South Atlantic and quantitative deconvolution of their non-conservative behavior. Geochimica et Cosmochimica Acta, 177, 217–237. https://doi.org/10.1016/j.gca.2016.01.018
Zheng, X. Y., Yang, J., & Henderson, G. M. (2015). A Robust Procedure for High-Precision Determination of Rare Earth Element Concentrations in Seawater. Geostandards and Geoanalytical Research, 39(3), 277–292. https://doi.org/10.1111/j.1751-908X.2014.00307.x
Zhu, Y., Itoh, A., Fujimori, E., Umemura, T., & Haraguchi, H. (2006). Determination of rare earth elements in seawater by ICP-MS after preconcentration with a chelating resin-packed minicolumn. Journal of Alloys and Compounds, 408–412, 985–988. https://doi.org/10.1016/j.jallcom.2004.12.092
Zhu, Y., Umemura, T., Haraguchi, H., Inagaki, K., & Chiba, K. (2009). Determination of REEs in seawater by ICP-MS after on-line preconcentration using a syringe-driven chelating column. Talanta, 78(3), 891–895. https://doi.org/10.1016/j.talanta.2008.12.072

2. OBJETIVOS

2.1. OBJETIVO GERAL

O objetivo geral desta tese é estudar a ocorrência e distribuição dos REE no meio ambiente visando entender o seu potencial de aplicação como traçadores de processos naturais e antrópicos em águas estuarina e marinha.

2.2. OBJETIVOS ESPECÍFICOS

2.2.1. Realizar uma revisão bibliográfica sobre os REE e seus ciclos biogeoquímicos identificando as principais lacunas de conhecimento;

2.2.2.Identificar os padrões de distribuição, fracionamento dos elementos REE e processos controladores em amostras de águas da Baía de Todos os Santos e plataforma continental adjacente;

2.2.3.Estudar as potenciais fontes de REE para região e o potencial uso do εNd como traçador de circulação de massas d'água e processos de BE em amostras de água do Atlântico oeste e da Península Antártica

2.2.5. Identificar as principais lacunas de conhecimento e áreas estratégicas de investimento para avanços nos estudos no que diz respeito à poluição no oceano Atlântico Sul no intuito de direcionar esforços na Década da Ciência Oceânica para o Desenvolvimento Sustentável.

Capítulo 1:

The Global Biogeochemical Cycle of the Rare Earth Elements

Global Biogeochemical Cycles

REVIEW ARTICLE
10.1029/2024GB008125

Special Collection:
The Elements Collection

The Global Biogeochemical Cycle of the Rare Earth Elements

V. Hatje[1,2], J. Schijf[3], K. H. Johannesson[4,5], R. Andrade[1], M. Caetano[6], P. Brito[6], B. A. Haley[7], M. Lagarde[8], and C. Jeandel[8]

[1]Centro Interdisciplinar de Energia e Ambiente (CIEnAm) & Department of Analytical Chemistry, Universidade Federal da Bahia, Salvador, Brazil, [2]Marine Environment Laboratories, International Atomic Energy Agency (IAEA), Monaco, Principality of Monaco, [3]Chesapeake Biological Laboratory, University of Maryland Center for Environmental Science, Solomons, MD, USA, [4]School for the Environment, University of Massachusetts Boston, Boston, MA, USA, [5]Intercampus Marine Science Graduate Program, University of Massachusetts System, Boston, MA, USA, [6]Portuguese Institute for Sea and Atmosphere (IPMA), Lisboa, Portugal, [7]College of Earth, Ocean, and Atmospheric Sciences (CEOAS), Oregon State University, Corvallis, OR, USA, [8]Laboratoire d'études en Géophysique et Océanographie Spatiales (LEGOS), CNRS, CNES, UT3, IRD, Université de Toulouse, Toulouse, France

Key Points:

- Rare earth elements (REE) are powerful tracers of both natural and anthropogenic processes within terrestrial and ocean environments
- REE are controlled by absorption, adsorption/desorption, co-precipitation, remineralization, and particle dissolution
- REE are technology-critical metals with broad applications in the future low-carbon global economy

Supporting Information:

Supporting Information may be found in the online version of this article.

Correspondence to:

V. Hatje,
vhatje@ufba.br;
v.hatje@iaea.org

Citation:

Hatje, V., Schijf, J., Johannesson, K. H., Andrade, R., Caetano, M., Brito, P., et al. (2024). The global biogeochemical cycle of the rare earth elements. *Global Biogeochemical Cycles*, *38*, e2024GB008125. https://doi.org/10.1029/2024GB008125

Received 16 FEB 2024
Accepted 14 MAY 2024

Author Contributions:

Conceptualization: V. Hatje, J. Schijf, K. H. Johannesson
Formal analysis: V. Hatje, J. Schijf, K. H. Johannesson, B. A. Haley, M. Lagarde
Methodology: V. Hatje
Project administration: V. Hatje
Supervision: V. Hatje
Visualization: V. Hatje, J. Schijf
Writing – original draft: V. Hatje, J. Schijf, K. H. Johannesson, M. Caetano, B. A. Haley, M. Lagarde, C. Jeandel

Abstract To improve our understanding and guide future studies and applications, we review the biogeochemistry of the rare earth elements (REE). The REEs, which form a chemically uniform group due to their nearly identical physicochemical properties, include the lanthanide series elements plus scandium (Sc) and yttrium (Y). These elements, in conjunction with the neodymium isotopes, are powerful tools for understanding key oceanic, terrestrial, biological and even anthropogenic processes. Furthermore, their unique properties render them essential for various technological processes and products. Here, we delve into the characteristics of REE biogeochemistry and discuss normalization procedures and REE anomalies. We also examine the aqueous speciation of REEs, contributing to a better understanding of their behavior in aquatic settings, including the role of neodymium isotopes. We then focus on their environmental distribution, fractionation, and controlling processes in different environmental systems across the land-ocean continuum. In addition, we analyze sinks, sources, and the mobility of REEs, providing insights into their behavior in these environments. We further investigate the sources of anthropogenic REEs and their bioavailability, bioaccumulation, and transfer along food webs. We also explore the potential effects of climate change on the cycling, mobility and bioavailability of REEs, underlining the importance of current research in this evolving field. In summary, we provide a comprehensive review of REE behavior in the environment, from their properties and roles to their distribution and anthropogenic impacts, offering valuable insights and pinpointing key knowledge gaps.

1. Introduction

1.1. Definition, Classification, and Physicochemical Properties

Rare earth elements (REE) are a group of chemical elements that consist of the 15 lanthanides (La, lanthanum; Ce, cerium; Pr, praseodymium; Nd, neodymium; Pm, promethium; Sm, samarium; Eu, europium; Gd, gadolinium; Tb, terbium; Dy, dysprosium; Ho, holmium; Er, erbium; Tm, thulium; Yb, ytterbium; Lu, lutetium), as well as scandium (Sc) and yttrium (Y). Scandium and Y are included as REEs because they share similar properties and are found in the same column (III) of the periodic table. Notably, Pm is a lanthanide that is produced only through nuclear reactions and is virtually absent in nature.

REEs are commonly classified into two or three groups. According to the International Union for Pure and Applied Chemistry (IUPAC), the light rare earth elements (LREE) include La through Eu, whereas the heavy rare earth elements (HREE) consist of Gd through Lu. Another classification divides them based on their atomic weight into three groups: LREE (La to Pm), middle rare earth elements (MREE) (Sm to Gd), and HREE (Tb to Lu) (e.g., Johannesson & Lyons, 1995; Nakamura et al., 1997). Yttrium (Y) mimics the HREE, particularly Ho, because of the similarity in their ionic radii. On the other hand, Sc is a much smaller cation with a chemical behavior that differs from other REEs (Till et al., 2017) and is generally treated separately.

REEs exhibit unique properties such as magnetism, luminescence, electrochemical activity, and thermal characteristics. They are primarily found in the trivalent oxidation state in Earth surface systems (although other REE, for instance Ce can also occur in the tetravalent state, and Eu in the divalent state, as will be discussed later) and

Writing – review & editing: J. Schijf, K. H. Johannesson, R. Andrade, M. Caetano, P. Brito, B. A. Haley, M. Lagarde, C. Jeandel

demonstrate similar physicochemical properties that systematically and gradually vary across the series. These similarities are the result of their electron configurations.

A progressive filling of the inner 4f electron shell throughout the series accompanies the gradual decrease in their ionic radii with increasing atomic number (i.e., the lanthanide contraction). This phenomenon happens due to the poor shielding effect of the 4f electrons. The poorer the shielding, the stronger the nuclear attraction to the electrons, causing decreased atomic radius with increased proton numbers, as observed in the lanthanide contraction. Another consequence of the lanthanide contraction is a general increase in ionization potential across the series. Therefore, REEs exhibit strong fractionation due to size and charge and significant "within-group" fractionation resulting from the lanthanide contraction.

The term "rare earth" can be misleading as some REEs (e.g., La and Ce) have a crustal abundance comparable to copper (Cu) and lead (Pb), and are more abundant than mercury (Hg) and platinum (Pt) (Lide & Haynes, 2009). Even the scarcest REEs (Lu and Tm) are more abundant in the Earth's crust than elements such as cadmium (Cd) and selenium (Se). However, REEs are widely dispersed in the Earth's crust, occurring in multiple mineral sources but with limited occurrences in economically viable ore deposits. Indeed, the similarity in the ionic radius and oxidation state among the REEs allows for their substitution within various crystal lattices. The slight differences in ionic radius across the series commonly result in the segregation of REEs into deposits enriched in either LREE or HREE, the latter including yttrium (Castor & Hedrick, 2006).

The growing interest in the REE cycle can be attributed to substantial advancements in analytical instrumentation, with inductively coupled plasma mass spectrometry (ICP-MS) playing a prominent role. This highly sensitive technique has revolutionized the field by enabling the accurate quantification of all REEs, even at extremely low concentrations ranging from nanomolar to picomolar levels, in complex environmental matrices such as seawater and groundwater. These analytical advancements have provided the means for laboratories around the world to conduct high-quality measurements of REEs in a wide variety of samples, including ocean, surface and groundwaters, rocks, and biological tissues, which has led to important discoveries of the biogeochemical processes that control REE concentrations and fractionation in the environment.

1.2. Roles—Micronutrients, Contaminants, Tracers, and Proxies

Since the last decades of the twentieth century, the REE's unique properties have made them essential tools for understanding key oceanic, terrestrial, and biological processes. Like other trace elements, such as Cu and zinc (Zn) (e.g., Anderson, 2020; Anderson et al., 2014), REEs may play multiple roles.

REEs were once believed to lack biological activity in organisms. However, despite their diminishing concentrations, in some cases REEs are preferably used over other more abundant elements. For example, despite the billion-fold greater concentrations of calcium (Ca) in natural environments compared to REEs, due to their similar ionic radius, they can likely displace Ca at Ca-binding sites in biological systems (Thomas et al., 2014). At low concentrations, REEs may act as micronutrients, enhancing crop yield (e.g., wheat, rice, maize) and livestock production (Pang et al., 2002; Tariq et al., 2020; Tommasi et al., 2021, 2023; M. Q. Wang & Xu, 2003). The concentration-dependent positive effects of REEs are grounded in hormesis, where mild environmental stressors, such as low doses of REE-based substances, yield beneficial outcomes. These applications have seen extensive use in China for more than three decades and have also been adopted in other countries including Japan, Australia, Switzerland, and Korea (Abdelnour et al., 2019; Turra, 2018; Tyler, 2004; M. Q. Wang & Xu, 2003).

Over the last 10 years, studies have revealed the evolving roles of REEs in organic carbon metabolism (Keltjens et al., 2014; Nakagawa et al., 2012; Picone & den Camp, 2019; Reitz & Medema, 2022; Shiller et al., 2017). Analysis of a global ocean metagenomic/metatranscriptomic data set indicates the widespread presence of lanthanide (Ln)-dependent methanol-, ethanol-, sorbose-, and glucose-dehydrogenases across all metagenomes, with numerous individual organisms hosting dozens of unique Ln-dependent genes (Voutsinos et al., 2023). This data set also suggests that biological methanol oxidation in the majority of surface ocean areas is predominantly Ln-dependent. Nonetheless, the mechanisms governing REE acquisition and transport as well as the global distribution and biogeochemical significance of lanthanide-dependent metabolism remain largely unknown (Shiller et al., 2017; Takahashi et al., 2007; Voutsinos et al., 2023).

Similar to other trace elements, REEs are influenced by anthropogenic activities. They are crucial components of high-tech products, including "smartphone" miniaturized speakers, contrast agents for magnetic resonance

imaging in medicine, and components of low-carbon energy and transportation systems such as electric vehicles, solar panels, and wind turbines (Balaram, 2019; Castor & Hedrick, 2006; Haxel, 2002). Consequently, the fast-growing demand for REE has led to an increase in global mining and REE inputs that can disrupt natural biogeochemical cycles and cause REE contamination in water, sediments, and biota (R. L. Andrade et al., 2020; Bau & Dulski, 1996a; Delgado et al., 2012; Hatje et al., 2016; Merschel & Bau, 2015; Pedreira et al., 2018; Pinto et al., 2019). Therefore, depending on their concentration, REE can act as both micronutrients and contaminants, exhibiting various toxic effects, as will be discussed further.

Due to their chemically coherent behavior, REEs provide valuable insights into petrogenic, geochemical, and oceanic processes that other single or multiple element tracers cannot distinguish. In addition, the isotopic composition (IC) of Nd is used as a tool in reconstructing ocean circulation in the modern as in the past ocean (Abbott, Haley, McManus et al., 2015; Hathorne et al., 2015; Jeandel, 1993; Lacan & Jeandel, 2005; Piepgras & Wasserburg, 1982, 1987; van de Flierdt et al., 2016). Nd composition is typically expressed in the epsilon notation:

$$\varepsilon\mathrm{Nd} = \left[\left(\frac{^{143}\mathrm{Nd}_{\mathrm{sample}}/^{144}\mathrm{Nd}_{\mathrm{sample}}}{^{143}\mathrm{Nd}_{\mathrm{CHUR}}/^{144}\mathrm{Nd}_{\mathrm{CHUR}}}\right) - 1\right] \times 10^4 \quad (1)$$

where CHUR is the chondritic uniform reservoir used as an average Earth value ($^{143}Nd/^{144}Nd = 0.512638$) (Jacobsen & Wasserburg, 1980).

The most important scientific step forward obtained by coupling the analysis of Nd isotopes to that of the REE (and mostly Nd) concentrations in the ocean was to reveal what was called the "Nd paradox." The "Nd paradox" is the term used to name the partial decoupling between Nd concentrations and isotopic compositions in the ocean (Goldstein & Hemming, 2003; Jeandel et al., 1995, 1998; Johannesson & Burdige, 2007; Tachikawa et al., 2003; van der Flierdt et al., 2004). The isotopic constraint revealed that the Nd oceanic budget was not balanced and that an important "missing source" was required to balance both the Nd isotopic signature and concentration along the Atlantic-Pacific conveyor belt (Goldstein & Hemming, 2003; Tachikawa et al., 2003). This missing source, required to modify the isotopic signatures while the concentration was barely changing, was called "Boundary Exchange" (or BE) by Lacan and Jeandel (2005) since these authors strongly suggested that the main mechanism explaining the paradox was occurring along the oceanic margins. However, these authors could not identify the mechanisms leading to this "exchange," which will be discussed in the next sections.

The REE abundance pattern, along with the redox-sensitive element Ce, and Nd isotopic composition, can be used for reconstructing past environmental conditions and studying weathering, sediment provenance, and climate change that occurred on the continents in the past (Frank, 2002; X. Liu et al., 2019; Sousa et al., 2022; Taylor & McLennan, 1985; Tachikawa et al., 2017). REE serve as powerful geochemical tracers for the characterization of igneous rock formation conditions, water mass origin and fate while transported by ocean currents, and determination of sediment sources, in addition to helping characterize scavenging processes, particle-solution exchange, present and past oceanic circulation patterns, and changes in submarine groundwater discharge and mixing (Alibo & Nozaki, 2004; Bigot et al., 1984; Elderfield, 1988; Haley et al., 2014; Johannesson et al., 2011; Johannesson, Stetzenbach, & Hodge, 1997; Jeandel, 1993; Piepgras & Wasserburg, 1982, 1987; X. Y. Zheng et al., 2016). Furthermore, they are effective tracers for identifying anthropogenic REE inputs and dispersion in the environment, helping to identify contamination from mining, industrial activities, agriculture, as well as hospital and domestic wastewater (Bau & Dulski, 1996a; Hatje et al., 2014; Kulaksiz & Bau, 2013; Mirlean et al., 2020; Romero et al., 2010, among many others). In addition, because of the similar valence and ionic radii of the REE and trivalent actinides (e.g., Am^{3+}-americium, Cm^{3+}-curium, and Cf^{3+}-californium), the REEs are analogs for these radioactive transuranics and may be used to safely study their behavior in the environment (Choppin, 1983; R. Silva & Nitsche, 1995).

1.3. Presentation and Normalization Procedures

The Oddo-Harkins rule states that elements with even atomic numbers are more abundant in the solar system compared to those with odd atomic numbers. As a result, when plotting the abundance of REEs against their

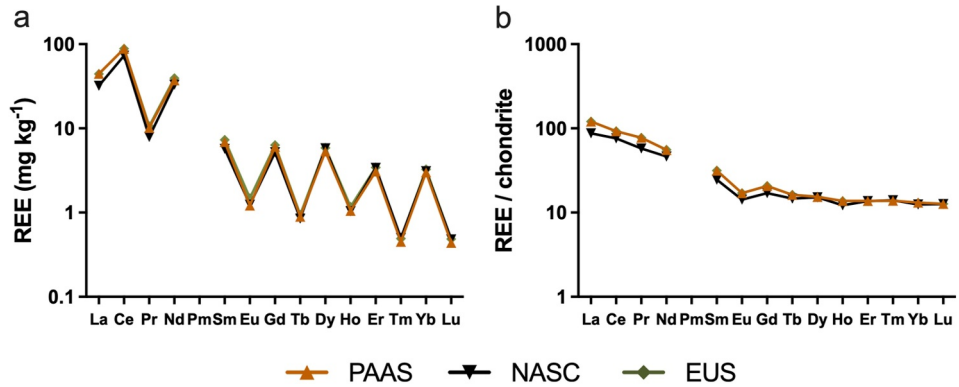

Figure 1. Abundances of Rare Earth Elements (REE) in various shales used for normalization. (a) logarithmic plot of abundances of REE in Post-Archean Australian Shale (PAAS; Pourmand et al., 2012), North American Shale Composite (NASC; McLennan, 1989), and European Shale (EUS; Bau et al., 2018) and (b) the same data after normalization to chondrite (Taylor & McLennan, 1985).

atomic number or ionic radius, a zig-zag pattern emerges (Figure 1a), making data interpretation complex. To address this issue, REE concentration data are normalized against a natural reference standard, such as water or rock (e.g., Masuda, 1962). This smooths out the natural Oddo-Harkins distribution of REEs (Figure 1b), simplifying data interpretation and enabling comparisons among different environmental matrices. Normalization also facilitates the identification and quantification of REE anomalies, which are deviations from the smooth normalized pattern. Anomalies may indicate either REE enrichment or depletion. By having a normalized baseline, expected REE concentrations can be interpolated or extrapolated from the smooth REE pattern, making it easier to detect and analyze anomalous behavior (e.g., Bau et al., 2018; Rétif et al., 2023). Furthermore, the smoothness of the normalized pattern allows for a qualitative assessment of the analytical quality of the data (Bau et al., 2018).

There is a multitude of normalizing agents in the literature (Table 1). The selection of the most suitable normalizing agent depends on several factors including the research objectives, the specific matrix being studied, the geographical location, and the specific aspects that need to be emphasized. In addition, the normalizing agent should represent the source of the REE in the sample, enabling the examination of fractionation across the lanthanide series compared to the REE pattern in the source. Detailed criteria whereby reference standards are (or should be) chosen have recently been reviewed (Rétif et al., 2023).

Among the various options, two materials are commonly employed for REE normalization: shales and chondrites. Shales represent the average composition of the upper continental crust and are used in studies related to environmental geochemistry and ocean research. On the other hand, chondrites are representative of the bulk composition of the Earth and find application in studies focused on igneous geochemistry and cosmochemistry. The choice between shales and chondrites depends on the specific field of study and the research context.

In surface Earth sciences, the most widely used normalizing agent is the Post-Archean Australian Shale (PAAS), proposed in 1976 (Nance & Taylor, 1976) and refined in 1989 (McLennan, 1989). A more recent study conducted in Australia utilized a distinct set of shale samples and directly measured all REEs, unlike earlier studies that had estimated the concentrations of Tm and Lu. The findings of this study align closely with previous research, with slightly elevated concentrations of LREE due to improved accuracy in REE measurements and the resulting smoother normalized REE patterns (Pourmand et al., 2012). PAAS has been used for several matrices, including sediments, soils, fresh and marine waters, and biological samples.

Another shale standard commonly utilized for normalization is the North American Shale Composite (NASC) (M. A. Haskin & Haskin, 1966). NASC consists of a compilation of 40 samples, with 20 sourced from the United States and the remaining 20 collected from Zimbabwe, Antarctica, and unknown locations.

The European Shale (EUS) originally described in 1935 (Minami, 1935) and revised in 1966 (L. A. Haskin et al., 1966; M. A. Haskin & Haskin, 1966) has recently been improved and although it was recommended for normalizing shale samples originating from Europe (Bau et al., 2018), it is preferable to use a more widely applied

Table 1
REE and Y Concentrations (mg kg^{-1}) in Different Shale Reference Materials Used for REE Normalization

	PAAS[a]	PAAS[b]	PAAS[c]	NASC[d,e]	NASC[b]	UCC[f]	UCC[g]	EUS[e]	EUS[h]	MUQ[i]	WRAS[j]	WRAC[j]
Y	28	27	27.31	27	27	20.7	21	31.8	31.9	31.85	29.40	29.84
La	38	38.2	44.56	32	32	32.3	31	41.1	44.3	32.51	37.80	44.61
Ce	80	79.6	88.25	70	73	65.7	63	81.3	88.5	71.09	77.7	89.2
Pr	8.9	8.83	10.15	7.9	7.9	6.3	7.1	10.4	10.6	8.46	8.77	9.69
Nd	32	33.9	37.32	31	33	25.9	27	40.1	39.5	32.91	32.69	35.6
Sm	5.6	5.55	6.884	5.7	5.7	4.7	4.7	7.30	7.30	6.88	6.15	6.70
Eu	1.1	1.08	1.215	1.24	1.24	0.95	1	1.52	1.48	1.57	1.188	1.383
Gd	4.2	4.66	6.043	5.21	5.2	2.8	4	6.03	6.34	6.36	5.19	5.37
Tb	0.77	0.774	0.8914	0.85	0.85	0.5	0.7	1.05	0.944	0.99	0.819	0.831
Dy	4.4	4.68	5.325	5	5.8	2.9	3.9	-	5.86	5.89	4.95	4.87
Ho	1	0.991	1.053	1.04	1.04	0.62	0.83	1.20	1.17	1.22	1.019	0.980
Er	2.9	2.85	3.075	3.4	3.4	-	2.3	3.35	3.43	3.37	2.97	2.78
Tm	0.5	0.405	0.451	0.5	0.5	-	0.3	0.56	0.492	0.51	-	-
Yb	2.8	2.82	3.012	3.1	3.1	1.5	2	3.29	3.26	3.25	3.01	2.72
Lu	0.5	0.433	0.4386	0.48	0.48	0.27	0.31	0.58	0.485	0.49	0.456	0.406

Note. PAAS, Post-Archean Australian Shale; NASC, North American Shale Composite; UCC, Upper Continental Crust; EUS, European Shale; MUQ, Mud from Queensland; WRAS, World River Average Silts and WRAC, World River Average Clays. [a]Nance & Taylor (1976), [b]McLennan (1989), [c]Pourmand et al. (2012), [d]L. A. Haskin et al. (1966), [e]M. A. Haskin & Haskin (1966), [f]Wedepohl (1995), [g]Rudnick & Gao (2003), [h]Bau et al. (2018), [i]Kamber et al. (2005), [j]Bayon et al. (2015).

standard, such as PAAS, to ensure that all REE data are comparable. Despite the different source materials, all these shale standards exhibit similar concentration values (Table 1) and remove the zig-zag pattern. Consequently, the REE normalized pattern derived from the use of PAAS, NASC, and EUS does not significantly impact their interpretation (Bau et al., 2018; Rétif et al., 2023).

Similar to shales, there are also several chondrite reference materials (Masuda, 1975; McDonough & Sun, 1995; Taylor & McLennan, 1985) and other standards less commonly employed for normalizing REEs. One example is the Mid-Ocean Ridge Basalt (MORB; Taylor & McLennan, 2002), which represents the composition of the upper mantle, differing from other representatives of the continental crust that might be of interest in marine geochemical research. Likewise, the World River Average Silts (WRAS) and Word River Average Clay (WRAC; Bayon et al., 2015) serve as representative samples of the average composition of the weathered and eroded upper continental crust from rivers around the world. These references are suitable for investigating REEs in freshwater systems. For unconsolidated sediments there is the Mud from Queensland (MUQ), a composite of alluvial fine-grained sediment samples from Australia (Kamber et al., 2005). Another reference is the Upper Continental Crust (UCC), originally proposed in 1985 (Taylor & McLennan, 1985), revised in 1995 (Wedepohl, 1995) and further revised in 2003 (Rudnick & Gao, 2003). UCC represents sedimentary rocks and glacial deposits of the upper continental crust.

Shales and chondrites differ greatly from biological matrices regarding REE composition and nature, although both have been previously used to normalize biological samples (de Sena et al., 2022; Santos et al., 2023; Squadrone et al., 2017). Because of the differences among matrices, it is challenging to identify inter-sample deviations when using shales and chondrites for biological sample normalization. Consequently, it is recommended to employ matrix-matched samples (i.e., organisms from the same order) for normalization, enabling the identification of fractionation, geogenic anomalies, and anthropogenic influences on REE concentrations in biological samples (Rétif et al., 2023). However, so far no reference material specific to biological samples has been proposed.

In many cases, it is preferable to normalize REE concentrations using a local and/or a matrix-matched normalizing agent. This local or matrix-matched reference sample may present inter-element concentrations

much closer to those of the study sites than the shales and chondrite references usually employed. Local normalization permits the assessment of subtle variations between samples that might otherwise go unnoticed. Besides, this normalization is essential to distinguish contributions to the total REE concentration derived from natural processes (i.e., background REE concentrations) from anthropogenic ones (Bau et al., 2018). This approach has been used, for instance, in marine studies, where local seawater is used in combination with PAAS normalization to enhance data interpretation (Haley & Klinkhammer, 2003; Hatje et al., 2016; Nozaki et al., 1999).

1.4. REE Anomalies From Redox Chemistry and Complexation

REEs generally exist in nature in the +III oxidation state and they form M^{3+} cations in aqueous solution. Under conditions that occur in and on the Earth's crust, only cerium can be oxidized to Ce(IV) and europium reduced to Eu(II), which are, respectively, more and less particle-reactive than their trivalent REE neighbors. The different geochemical behavior that results from such transformations leads to inter-element fractionation that can be observed as anomalies in the normalized REE pattern.

The quantification of anomalies required to compare different samples and studies remains one of the most debated and confounding topics in REE geochemistry. Rétif et al. (2023) extracted 15–20 different equations from the literature for each of the anomalies of Ce, Eu, and Gd. Although simple inter-element ratios can be used (e.g., Ce/Nd), more commonly the abundance of an anomalous element is compared to what it is expected to be from the behavior of its neighbors in the REE pattern. The latter is written as Ln_x*, where Ln_x indicates an REE (lanthanide) with atomic number x and the anomaly is calculated as $[Ln_x]/[Ln_x^*]$, with all abundances normalized to a suitable standard. The value of $[Ln_x^*]$ can be calculated as a simple interpolation between its immediate neighbors on either side (Alibo & Nozaki, 1999):

$$[Ln_x{}^*] = \frac{([Ln_{x-1}] + [Ln_{x+1}])}{2} \tag{2a}$$

or for more distant neighbors:

$$[Ln_x{}^*] = \frac{(j \times [Ln_{x-i}] + i \times [Ln_{x+j}])}{(i+j)} \tag{2b}$$

with i, $j > 0$, which is also valid for extrapolations, that is, if both neighbors are on the same side of Ln_x ($i < 0$ or $j < 0$). If the REE pattern is exactly linear, that is, of the form $[Ln_x^*] = ax + b$, the two equations are equivalent. However, if the pattern is curved, Equation 2b will increasingly underestimate or overestimate the anomaly for larger values of i and j depending on whether the curvature is convex or concave. In that case, it is more appropriate to use a geometric mean (Lawrence & Kamber, 2006):

$$[Ln_x{}^*] = [Ln_{x-i}]^{j/(i+j)} \times [Ln_{x+j}]^{i/(i+j)} \tag{3a}$$

or, equivalently:

$$log[Ln_x{}^*] = \frac{(j \times log[Ln_{x-i}] + i \times log[Ln_{x+j}])}{(i+j)} \tag{3b}$$

The REE patterns are commonly displayed on a log scale, which tends to linearize them and provoke the use of Equation 2b, even when Equation 3b is the better choice (note their similarity, except for the log conversion). This is exacerbated by the fact that the ratio $[Ln_x]/[Ln_x^*]$ is typically expressed on a log scale to more easily distinguish enrichment ($[Ln_x]/[Ln_x^*] > 1$, hence $\log([Ln_x]/[Ln_x^*]) > 0$) from depletion ($[Ln_x]/[Ln_x^*] < 1$ thus $\log([Ln_x]/[Ln_x^*]) < 0$), which is why these are referred to as positive and negative anomalies, respectively (e.g., Elderfield & Greaves, 1981). A recent review and rigorous mathematical treatment recommends that Equation 3a should always be used as it is more robust and makes the anomaly calculation less dependent on the type of normalization (Barrat et al., 2023). With any of the equations above, the uncertainty of the anomaly can be estimated by suitable mathematical propagation of analytical errors for the REE concentrations (Beers, 1957). It may be noted that,

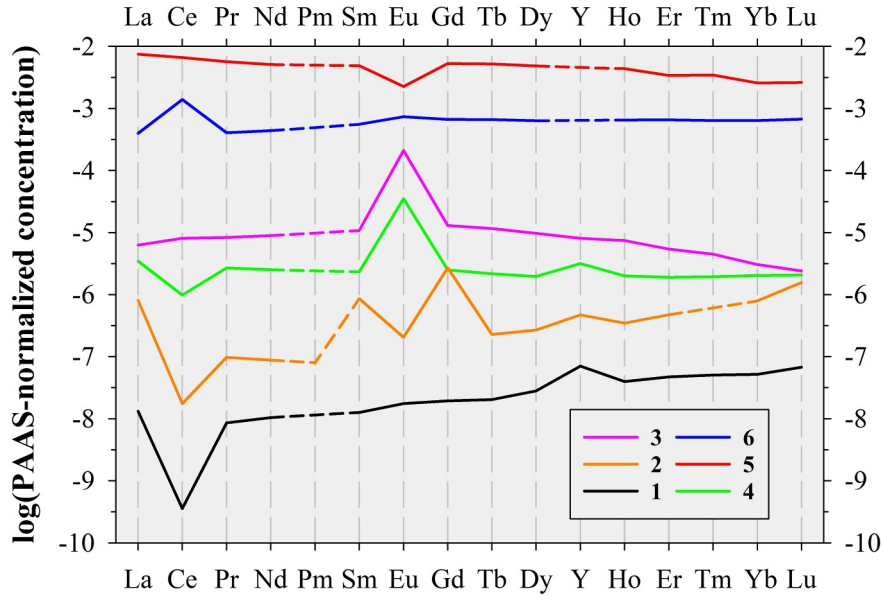

Figure 2. Examples of Rare Earth Elements (REE) patterns with distinctive single-element anomalies. Anomalies of Y are emphasized by placing it between Dy and Ho; the three elements have similar ionic radii, but Y has more ionic properties due to its lack of *f*-electrons. Non-reported elements were interpolated between immediate neighbors, except Pm in pattern 2, which was extrapolated from Pr and Nd to emphasize the Sm anomaly. All patterns were normalized to the revised PAAS values of Pourmand et al. (2012). Patterns 1, 5, and 6 were vertically shifted by −1, −4 and −3 log units, respectively, for clarity. (1) South-Pacific seawater (station SO225-21-1, 3,992 m) with characteristic negative Ce and positive Y anomalies (Molina-Kescher et al., 2018). (2) River Rhine at Leverkusen (Germany) during low-flow conditions (7 Nov 2011). Positive anomalies are due to contaminants from medical facilities (Gd) and a cracking catalyst plant (La and Sm) upstream (Kulaksiz & Bau, 2013). (3) Hydrothermal fluid (sample BS-13-4/2) from the Mid-Atlantic Ridge with a strong positive Eu anomaly (Bau & Dulski, 1999). (4) Discharge from the SWS diffuse vent site on the Juan de Fuca Ridge. The presence of both a negative Ce and positive Eu anomaly indicates extensive mixing of the hydrothermal fluid with ambient seawater (Bao et al., 2008). (5) Fluid inclusion in granophyre (sample CPU-2). The negative Eu anomaly is a host signature of the granitic magma with which it was at equilibrium (Banks et al., 1994). (6) Manganese nodule (sample D535) from the South Pacific Ocean with a positive Ce anomaly due to oxidation on the δ-MnO_2 surface (Takahashi et al., 2000).

whereas the majority of natural Ce anomalies are negative, common laboratory contaminants like dust tend to have a shale-like REE pattern. Usually, blanks and hence analytical errors are thus proportionally larger for Ce than for the other LREEs.

More subtle REE anomalies (e.g., for Y, La, Gd) may be due to the tetrad effect (Kawabe et al., 1998; McLennan, 1994; Takahashi, Yoshida, et al., 2002) which, for example, makes Y less covalently bound in complexes and thus less particle-reactive than Ho (Bau, 1999; Nozaki et al., 1997) (Figure 2, pattern 1). This phenomenon is caused by spin-pairing effects in REE binding to different anions (Kawabe, 1992) and is most prominent when REEs are fractionated in precipitation-dissolution systems (Takahashi, Yoshida, et al., 2002). It is less pronounced for REE sorption, where the similar REE fractionations of opposing surfaces and solution complexation are canceled out (Tao et al., 2004).

Some anomalies (Figure 2, pattern 2) indicate the input of a single REE as contaminants (Kulaksiz & Bau, 2013; Rogowska et al., 2018). Different approaches have been proposed to quantify these and other REE fractionation effects, including multi-element ratios (Monecke et al., 2002; Osborne et al., 2015) and polynomial fits (Möller et al., 2002).

The reduction of Eu(III) in aqueous solutions only proceeds readily at temperatures above ∼250°C and high pressure (Sverjensky, 1984). Such conditions are uncommon in natural waters and mostly occur in underground hydrothermal systems. As Eu^{3+} is reduced to the much larger Eu^{2+} cation, it becomes less compatible with its crystal lattice sites in the host rock and is preferentially leached into the hydrothermal fluid, leading to a strong relative Eu enrichment, that is, a positive anomaly (Klinkhammer et al., 1994). Very large (>10) positive Eu anomalies have been found in hot fluids emanating from vents along submarine spreading ridges (Bao et al., 2008;

Hongo et al., 2007; Klinkhammer et al., 1994; Michard, 1989; Olivarez & Owen, 1991), as exemplified by pattern 3 in Figure 2. As the fluid is rapidly diluted by cold, oxygenated seawater, Eu is re-oxidized and scavenged by ferromanganese oxides that copiously precipitate within the buoyant plume (Klinkhammer et al., 1983; Olivarez & Owen, 1989). As mixing and scavenging progress, the solution rapidly loses the hydrothermal REE signature and acquires the characteristic REE signature of seawater (Figure 2, pattern 1), whereby intermediate patterns with both a negative Ce and positive Y and Eu anomalies have been observed in both the solution (Figure 2, pattern 4) and plume particles (German & Elderfield, 1990; Grenier et al., 2013; Klinkhammer et al., 1994).

Positive Eu anomalies in natural waters do not always reflect in situ reduction as they can be inherited as a source signature of rocks with which the solution is at equilibrium. The larger Eu^{2+} cation more readily partitions into minerals such as plagioclase and orthoclase feldspar, a major component of, for example, North-African dust (Pourmand et al., 2014). Similarly, negative Eu anomalies in solution, which are not readily explained in terms of in situ redox processes, can be inherited from previously Eu-depleted minerals or melts (Figure 2, pattern 5).

Unfortunately, polyatomic interferences during ICP-MS analyses of environmental samples can lead to spurious (typically positive) Eu anomalies (Jiang et al., 2007) that are relatively widespread in the literature and often unrecognized, leading to erroneous conclusions. Indeed, both isotopes, ^{151}Eu and ^{153}Eu, overlap with oxide ions of Ba ($Ba^{16}O^{+}$) that form in the argon plasma (Dulski, 1994; Smirnova et al., 2006). Whereas it is commonly argued that Ba can be removed by preparatory chromatography, many natural samples have Ba/Eu ratios over 1000, so removing >99% may still leave analyte and interferent signals of comparable size. Any residual interference is moreover challenging to discern because the ratio of the interfering Ba isotopes (^{135}Ba/^{137}Ba ~0.59) is similar in magnitude to that of the Eu isotopes (^{151}Eu/^{153}Eu ~0.92), that is, even if the total BaO and Eu signals are of equal size, the Eu isotope ratio will change by no more than a few percent, whereas the apparent Eu concentration would double. Although the introduction of new techniques such as in-line sample preparation and desolvating nebulization systems have greatly improved the suppression of interferences in ICP-MS analyses of environmental REE samples (Wysocka, 2021), these innovations are not yet routinely implemented.

The oxidation of Ce(III) to Ce(IV) is commonly taken to proceed in the presence of free oxygen, for example, as follows:

$$Ce^{3+}_{(aq)} + \frac{1}{4}O_{2(aq)} + \frac{3}{2}H_2O_{(l)} \rightarrow CeO_{2(s)} + 3H^{+}_{(aq)} \quad (4)$$

with a half-reaction potential falling between the equivalent oxidations of Mn^{2+} to $Mn(IV)O_2$ and Fe^{2+} to $Fe(III)(OH)_3$. Whether the product is assumed to be CeO_2 or $Ce(OH)_4$, it is clear that the oxidation is strongly pH-dependent and suppressed at low pH. At elevated pH, the oxidation is more likely to involve hydrolyzed Ce (III) species such as $CeOH^{2+}$ (Yu et al., 2006). A speciation model (de Baar et al., 1988) showed that the seawater concentration of total dissolved Ce in equilibrium with CeO_2(s) should be exceedingly low ($<10^{-15}$ M). It is therefore more likely that Ce oxidation occurs at the surface of particles upon sorption of Ce^{3+} (Figure 2, pattern 6). The resulting Ce^{4+} ion is much more strongly bound, causing enhanced retention of Ce relative to the trivalent REE and a negative Ce anomaly in the solution (Figure 2, pattern 1). In suboxic to anoxic waters, Ce(IV) is reduced and released from particles, causing the Ce anomaly to disappear or sometimes become modestly positive (de Baar et al., 1988; German et al., 1991; German & Elderfield, 1989; Schijf et al., 1994, 1995; Tachikawa, Jeandel, & Roy-Barman, 1999; Tachikawa, Jeandel, Vangriesheim, & Dupré, 1999).

The ostensibly direct relationship between the presence of free oxygen and the Ce anomaly gave rise to the idea that the latter might be used as a proxy of the redox status of the paleo-ocean, provided that the seawater Ce anomaly signal is transferred to and permanently preserved in the marine sedimentary record (Hodel et al., 2021). The seawater signal is believed to be most reliably recorded by authigenic phases such as carbonates, phosphates, ferromanganese oxides, and chert. Sedimentary phosphates display a bewildering range of REE patterns that largely appear to be post-depositional (Bright et al., 2009; Reynard et al., 1999; Shields & Stille, 2001) and suitable samples must be selected with the utmost care (Jiang et al., 2007; Morad & Felitsyn, 2001). Studies on carbonates and chert are more promising (Ding et al., 2022; Q. Guo et al., 2007; MacLeod & Irving, 1996; Tostevin et al., 2016) as their REE patterns may be less prone to alteration (X. Liu et al., 2019). A notable advance has been recognizing the need for careful sample preparation to avoid interference from REE-rich contaminant

phases (Cao et al., 2020). Unfortunately, whereas it was found early on that foraminiferal REE signals are primarily contained in external ferromanganese oxide coatings (Palmer & Elderfield, 1986), it appears that these are commonly microscopically intercalated with the sample to a level where they cannot be effectively removed (Tachikawa et al., 2013).

Despite ongoing progress, the interpretation of sedimentary Ce anomalies remains a source of controversy and confusion due to uncertainty about what signal is actually recorded and where (Osborne et al., 2017; Skinner et al., 2019). Whereas a particle at equilibrium may acquire a seawater REE pattern directly, the negative Ce anomaly of seawater presumably arises because Ce is more efficiently scavenged than the trivalent REE. One might therefore argue that oxidizing conditions should leave bulk particulates with a positive Ce anomaly (Tachikawa, Jeandel, & Roy-Barman, 1999; Wilde et al., 1996). Besides redox conditions, the Ce anomaly may be sensitive to other influences, such as water depth and depositional setting (Murray et al., 1991) or freshwater inputs (Johannesson et al., 2006; Y. Zhao et al., 2021). Whereas it is known that Ce oxidation can be catalyzed on the surface of Mn oxides (Lagarde et al., 2020; Moffett, 1990; Takahashi et al., 2007; Tanaka et al., 2010), there is also a growing realization that it can be promoted by a variety of inorganic (Riglet-Martial et al., 1998; Yu et al., 2006) and especially organic ligands (Cervini-Silva et al., 2008; Deng et al., 2020; Seto & Akagi, 2008; Yoshida et al., 2004), even under anoxic conditions (Kraemer & Bau, 2022). This level of complexity is not yet adequately captured by either thermodynamic (Cao et al., 2022) or steady-state (Bellefroid et al., 2018) oxidation models. On the other hand, analytical developments, such as the ability of synchrotron X-rays to probe the Ce oxidation state in situ (Takahashi, Sakami, & Nomura, 2002), have sparked a recent resurgence of the field. Initially, gloomy assessments of its potential (Holser, 1997; Pattan et al., 2005) are lately sounding a more hopeful note (Skinner et al., 2019; K. Zhang & Shields, 2022). Along its predictable trajectory in the Elderfield Paleoceanographic Proxy Confidence Factor Phase Chart (PPCPP) (Elderfield, 2002), the Ce paleo redox proxy may finally be moving from the “pessimism phase" into the “realism phase."

1.5. Aqueous Speciation of Yttrium and the REE

The term aqueous speciation refers to the distribution of a metal among its dissolved species including complexes with all available organic and inorganic ligands. A key variable is the relative contribution of the free hydrated or uncomplexed cation, expressed as a fraction of the total metal concentration, which controls solubility, reactivity toward particles, and possibly uptake by organisms (Weltje et al., 2004). Interactions with individual ligands are also important, as some complexes have been found to intensify metal sorption on certain particle surfaces (Davranche et al., 2004), whereas specific organic ligands may promote bioavailability and thereby facilitate microbial acquisition of essential metals (Butler, 1998).

Speciation modeling involves solving a system of equations comprising mass balances for all relevant metals and ligands as well as mass action expressions for the pertinent complexation reactions (F. Morel & Morgan, 1972). The latter requires thermodynamic equilibrium constants for each reaction at conditions appropriate to the solution at hand. These so-called stability constants are functions of temperature, pressure, and solution composition, that is, ionic strength. The relative contribution of a complex to the speciation depends only on the stability constant and the free-ligand concentration, but not on the concentration of the metal, provided it is much smaller than that of the ligand (Bruno, 1997; Christenson & Schijf, 2011; Millero, 1992). It follows that this contribution may be significant either when the complex is very stable, the ligand very abundant, or both.

The complexation of yttrium and the REEs with numerous organic and inorganic ligands has been studied over a wide range of conditions. The evolving database of stability constants has been reviewed or critically evaluated multiple times (Byrne & Sholkovitz, 1996; Millero, 1992; Schijf & Byrne, 2021; Wood, 1990a). REEs are classified as hard acid cations with a particular affinity for ligands that contain oxygen functional groups (Turner et al., 1981). However, unlike metals that are extensively hydrolyzed, such as Be and Th, or that greatly favor a single ligand, such as chloride for Ag and Cd (Byrne, 2002), the REEs form a variety of species. The most stable inorganic ones are the first- and second-order complexes with, respectively, one and two carbonate anions. The current consensus has REE speciation dominated by these carbonate complexes in most alkaline waters, notably in seawater. Nevertheless, the REEs also form stable complexes with phosphate, silicate, and fluoride, which may prevail in situations where carbonate complexation is suppressed. Even the comparatively weak REE ligands sulfate and chloride may be prominent in waters of unusual composition. Whereas the REEs have a substantial tendency to hydrolyze, hydrolysis is typically minor in the presence of stronger ligands. Turner et al. (1981) have

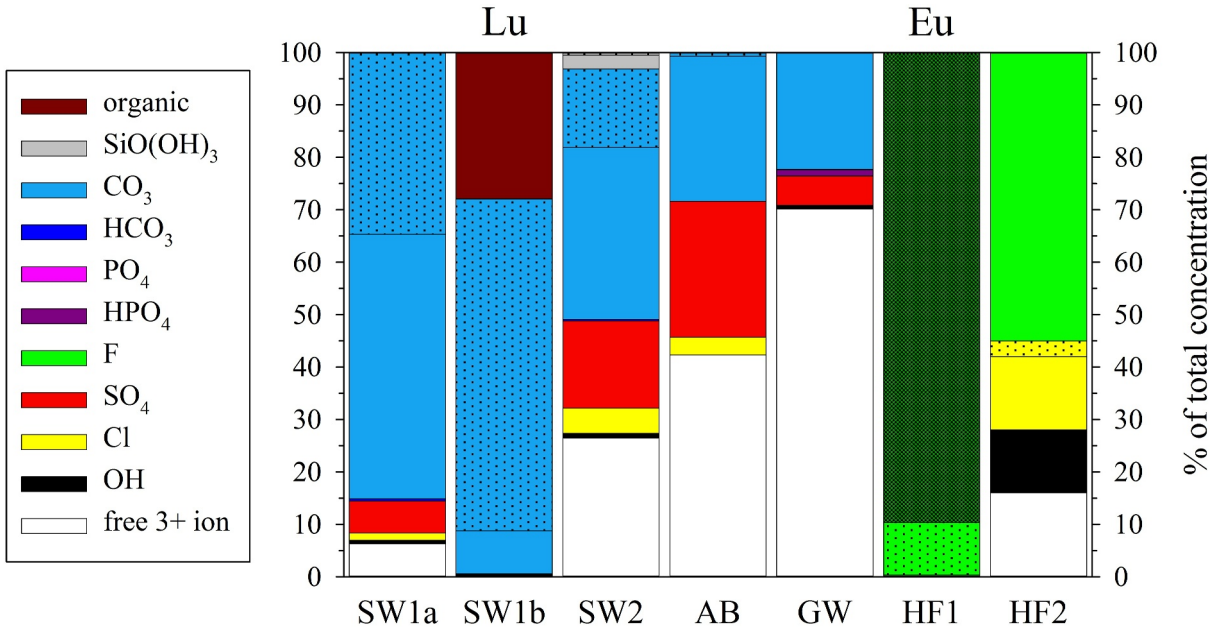

Figure 3. Modeled speciation of lanthanum (La), except as labeled above the columns, in various natural waters. Species contributions are shown as fractions of the total rare earth elements (REE) concentration. Bars in each column are stacked as shown in the legend. Contributions less than 0.5% cannot be resolved in the graph. Second-order (e.g., EuF^{+}_{2}) and third-order (e.g., EuF^{0}_{3}) complexes are indicated with light and heavy stippling, respectively. SW1a is standard surface seawater ($S = 35$) at $T = 25$°C. Speciation of the heaviest REE (Lu) is shown for comparison (SW1b). Organic complexation is modeled as a single strong ligand (trihydroxamate siderophore desferrioxamine B) at a fixed free concentration of 10^{-13} M (Christenson & Schijf, 2011). SW2 is adjusted for deep ocean conditions ($T = 2$°C, $P = 500$ atm) (Schijf & Byrne, 2021). AB is the anoxic, hypersaline lower brine of the Bannock Basin in the eastern Mediterranean (Schijf et al., 1995). GW is the model groundwater of Wood (1990a), recalculated with new stability constants by Johannesson, Stetzenbach, et al. (1996), at pH 7. HF1 is the model hydrothermal fluid of Wood (1990b) at $T = 100$°C and P_{sat} with a total fluoride concentration of 10^{-4} m; Eu speciation is shown (his Figure 18b). HF2 is the model hydrothermal fluid of Haas et al. (1995) at $T = 300$°C and P_{sat} (their Fig. 8). The composition of HF2 is similar to that of HF1, except for tenfold higher concentrations of fluoride and sulfate; both are shown at pH 5.

argued that their affinity for both carbonate and hydroxide also gives the REE a propensity for organic complexation. The marine geochemistry of metals with this preference, such as Fe and Cu, can be completely governed by organic complexes. Although some biogenic and anthropogenic REE ligands have been identified (Christenson & Schijf, 2011; Cotruvo Jr. et al., 2018; Schijf & Byrne, 2001), the extent of organic REE complexation in natural waters remains unknown to some degree.

The next paragraphs provide a summary of our present understanding of REE speciation in seawater and other alkaline waters, in waters where carbonate is not the primary ligand, and in hydrothermal fluids. Examples are shown in Figure 3 for surface and deep seawater, a brine, a model groundwater, and two model hydrothermal fluids, focusing on the lightest element, La. For seawater, the speciation of Lu, the heaviest element, is added for comparison to illustrate the full range of REE behaviors. Critical knowledge gaps are emphasized, for instance, ligands that have been inadequately studied and the influence of pressure at low temperatures.

Seawater is by far the most common natural solution, yet it is rather unique because of its high ionic strength (I ~0.7 M) and almost constant composition throughout the ocean at all depths; its elevated pH (~8), which increases the fraction of free carbonate; and its high concentrations of the weaker ligands, chloride and sulfate. Marine REE speciation was recently summarized by Schijf and Byrne (2021) and is shown in Figure 3 (columns SW1a, b) for the ocean surface. It is dominated by carbonate for all REEs, ranging from ~85% to 99% of total concentrations, in the absence of organic complexes. From La to Lu, the fraction of second-order complex increases to gradually match and then exceed that of the first-order complex. Contributions of the free cation and the sulfate complex (each ~6%) and of the chloride and hydroxide complexes (0.5%–1.5%) are significant for La yet decline across the series to negligible levels. The dominance of carbonate, especially the contribution of higher-order complexes, can be even greater in solutions more alkaline than seawater. Möller and Bau (1993) observed REE patterns with an unusual positive Ce anomaly in the waters of Turkish Lake Van (pH ~ 9.6), which they attributed to the intriguing possibility of dissolved Ce(IV) being stabilized as a highly anionic fifth-order carbonate complex. Smaller positive

Ce anomalies have been observed in Mono Lake, California (pH ∼ 9.8), where the second-order carbonate complex comprises >99% of each dissolved REE (Johannesson & Lyons, 1994). Conversely, REE carbonate complexation may be strongly suppressed in the hypersaline submarine brine of Bannock Basin (Schijf et al., 1995), leading to free-cation fractions of up to >40%, as shown in Figure 3 (column AB). In addition to lower pH (∼7.6), this is caused by competition for the carbonate ligand by excess Mg^{2+} and Ca^{2+}.

The importance of organic REE complexation is uncertain, although their chemical properties suggest that it may be considerable (Turner et al., 1981). Metals whose marine geochemistry is controlled by organic complexes seem to have an overwhelming affinity for a small number of extremely strong and highly specific ligands (Vraspir & Butler, 2009). That may also apply to the REE as well is indicated by recent evidence that some are a ubiquitous component of key microbial enzymes (Cotruvo Jr. et al., 2018; Shiller et al., 2017). Christenson and Schijf (2011) measured the stability of REE complexes with the model siderophore DFOB and proposed that they may constitute up to 30% of the total Lu concentration at a free ligand concentration of only 10^{-13} M, mostly at the expense of its carbonate species. However, their importance diminishes with decreasing atomic number, becoming minor around Gd (Figure 3, columns SW1a,b). Unless biogenic REE ligands can be explicitly identified and investigated or the speciation model verified by direct analysis (Pižeta et al., 2015), the role of organic REE complexation in seawater remains speculative and may well be underestimated.

Another potentially important but largely neglected ligand in seawater is silicate. Until recently, only one group had determined stability constants for REE complexation with silicate and only for Eu (Jensen & Choppin, 1996; Pathak & Choppin, 2006; Thakur et al., 2007). It appears that Eu forms a first- and second-order complex similar to but substantially more stable than the corresponding carbonate complexes. Based on their results, Akagi (2013) argued that (inorganic) REE speciation is dominated by silicate throughout the ocean. That would be a remarkable conclusion, upending the paradigm that carbonate is the primary inorganic REE ligand, with potentially far-reaching implications for our understanding of REE marine geochemistry. Patten and Byrne (2017) measured the stability constant ($_{sil}\beta_1$) for the first-order silicate complex of Fe(III) and used a linear free-energy relation as well as a reanalysis of the data of Jensen (1994) to show that $_{sil}\beta_1$ for Eu was too high by 1–2 orders of magnitude, which was later confirmed (Soli & Byrne, 2017). Employing a novel titration method that is much faster and able to determine both constants, the first measurements of $_{sil}\beta_1$ and $_{sil}\beta_1$ are now in progress for yttrium and all REEs (Schijf & Byrne, 2021). Preliminary results suggest that silicate complexation is of minor importance in seawater and does not surpass carbonate complexation even in the nutrient-rich deep Pacific Ocean (Figure 3, column SW2), although this conclusion may need to be amended for the HREE if both reactions are proportionately impeded at high pressure (Schijf & Byrne, 2021).

Terrestrial waters of low ionic strength, characteristic of rivers, lakes, and shallow aquifers, are less strongly buffered than seawater and thus have a wider range of generally more acidic pH (4–9). While the concentrations of inorganic ligands are lower than in seawater, those of metals that are strong competitors for REE complexation, including Fe, Mn, and Al, can be much higher. In addition, rivers and lakes generally contain elevated levels of dissolved organic matter (DOM), yet with very different characteristics. Finally, the main controlling variables, pH and PCO_2, can show enormous temporal variation on short timescales caused by diel photosynthesis/respiration cycles (Gammons et al., 2005). Under these conditions, carbonate complexation of the REE is commonly suppressed to various degrees, especially in waters draining silicate rocks, allowing for enhanced complexation with other ligands, such as phosphate, possibly silicate, sulfate, or even small carboxylic acids that occur in root exudates (Schijf & Byrne, 2001).

Freshwaters can have a nearly infinite variety of compositions; hence, constraining REE speciation requires direct measurement of many chemical parameters. Perhaps consequently, it has received much less attention in the literature than seawater and most of the work has focused on groundwater. Only a single example is presented here (Figure 3, column GW) (Johannesson, Stetzenbach, et al., 1996). Carbonate complexation is suppressed by the lower pH of 7 and restricted to the first-order complex. Because the concentrations of competing ligands like sulfate and phosphate are low, REE speciation is largely shifted to the free cation, comprising more than half of the total. Johannesson, Stetzenbach, et al. (1996) also present results for pH 8 and 9, with the contribution of carbonate increasing accordingly and becoming more seawater-like, although organic complexation was not considered. The influence of low pH is shown by Turner et al. (1981), who calculated REE speciation in a model river water at pH 6, where La exists as about 75% free cation and 25% complexed with sulfate, with the contribution of the carbonate complex reduced to less than 1%. In sulfate-rich waters, the contribution of the

REE–sulfate complex can become even more pronounced, as predicted by Schijf and Byrne (2004) and modeled for the acidic Canadian Colour Lake (Johannesson & Lyons, 1995), where dissolved REEs appear to be about equally divided between the free cation and the first-order sulfate complex, with a minor but significant contribution from the first-order fluoride complex, particularly for the HREEs.

Organic REE complexation has been studied much more extensively in freshwater than in seawater. In DOM-rich waters (Adebayo et al., 2018; Dia et al., 2000; Pourret et al., 2007; Tang & Johannesson, 2003), the influence of organic ligands should be quite substantial, although it is lessened below pH 5 as most of their functional groups become protonated. Contrary to the ocean, where the organic speciation of many metals appears to be controlled by a few very strong but relatively small ligands (Vraspir & Butler, 2009), the most important organic molecules in freshwater may be a diverse class of humic and fulvic acids containing myriad functional groups. More effort has been devoted to the parameterization of these polyanionic multidentate ligands in advanced speciation computer codes (Marsac et al., 2011, 2021; Milne et al., 2003; Pourret & Martinez, 2009) than to their detailed characterization or an exact determination of their stability constants. Although humic compounds are thought to affect marine metal speciation (Whitby & van den Berg, 2015), they have a different origin and structure. Terrestrial humic ligands are so large that they cross into the realm of colloids, which play a complicated part in REE behavior as they bridge the gap between dissolved and particulate species (Schijf & Zoll, 2011). One exception to the predominance of humic and fulvic acids may be the role of certain exceedingly strong manmade ligands. The polycarboxylic acid DTPA and similar compounds are used as contrast agents (CA) for magnetic resonance imaging (MRI) and discharged in large quantities bound to Gd, which, despite its stability, may be exchanged for other REEs in so-called transmetallation processes (Idée et al., 2006), globally leading to positive Gd anomalies in rivers (Rogowska et al., 2018). These contaminants are emerging in rivers, estuaries, and coastal waters (e.g., R. L. Andrade et al., 2020; Bau & Dulski, 1996a; Hatje et al., 2014, 2016; Pedreira et al., 2018), as will be discussed later on.

Hydrothermal fluids, found in the subsurface and emitted from seafloor vent systems where pressures are very high, are characterized by temperatures of 50–400°C (at P_{sat}) or above. Their compositions are commonly very different from surface waters due to contact with ambient minerals and can be markedly enriched in weaker inorganic ligands and competing metal cations. Hydrothermal fluids generally have low levels of organic ligands and phosphate due to a lack of biological activity. Concentrations of the REEs may be quite high and saturated with regard to insoluble salts such as fluorides (Migdisov & Williams-Jones, 2007), showing unusual distribution patterns. Relevant thermodynamic data are lacking due to the experimental challenges of measuring stability constants at high temperatures and pressures. Several studies have focused on REE complexation with chloride, fluoride, and sulfate (Gammons et al., 1996; Gammons, 2002; Migdisov et al., 2008; Migdisov & Williams-Jones, 2006, 2007; Ragnarsdottir et al., 1998). These reactions are endothermic and thus strongly favored at high temperature, particularly for the high-order complexes. Wood (1990b) critically reviewed stability constants up to 350°C and P_{sat}. Haas et al. (1995) invoked a comprehensive, self-consistent data set of enthalpies and entropies to model stability constants out to 1000°C and 5 kbar. The latter paper emphasizes broad trends and may be less accurate at specific temperatures. Both use the resulting constants to calculate REE speciation as a function of pH in model hydrothermal fluids of somewhat similar composition (Figure 3, columns HF1 and HF2).

The Eu speciation of Wood (1990b) in hydrothermal fluids is entirely dominated by fluoride, consisting of about 90% of the third-order complex. Despite a higher temperature and tenfold more fluoride, only half of the La concentration of Haas et al. (1995) consists of the first-order fluoride complex, the rest being nearly equally divided among the free cation and the hydroxide and two chloride complexes. These discrepancies illustrate the troublesome sensitivity of REE speciation calculations to minor differences in conditions and solution composition, considering the present uncertainties in the thermodynamic data.

It is important to bear in mind that the examples of REE speciation presented here are only models based on thermodynamic data and not on any kind of in situ measurement. Unlike other trace metals (e.g., Pižeta et al., 2015), it is not yet feasible to measure the concentrations of free REE cations or their complexes directly. Besides a general agreement between calculated speciation diagrams and REE geochemical behavior in natural systems, we have no independent analytical confirmation of their accuracy. In other words, a speciation diagram is only as good as the model employed to derive it. The main problems that may cause speciation diagrams to be flawed are (a) inaccurate or (b) missing thermodynamic data and (c) the exclusion of important ligands or competing metals. The example of REE–silicate complexation demonstrates how inaccurate data can lead to

erroneous conclusions. Thermodynamic data are sorely lacking at high temperatures and pressures, particularly solubility products that are crucial wherever waters are in close contact with rocks, soils, and sediments. Most experiments are performed at standard state conditions and whereas complexation enthalpies are known for many reactions, these are commonly measured over a limited range of temperature, preventing an accurate determination of molar heat capacities (Schijf & Byrne, 2008). This hampers speciation modeling not only in hydrothermal fluids but notably at high pressure and *low* temperature (Lee & Byrne, 1994), reflecting conditions throughout the deep ocean. Finally, many ligands and other metals are omitted from REE speciation models because their relevance cannot be assessed from available data. This has been true for silicate and phosphate, for which stability constants have not been directly measured for most REEs. For organic compounds, key ligands in many natural waters have not even been identified. It is also true for metals in hydrothermal fluids, which can be competitive and present at high concentrations. In summary, model results should be interpreted with caution and published stability constants and speciation diagrams not always accepted at face value.

2. Environmental Distribution and Controlling Processes—Elements and Isotopes

2.1. Rivers, Lakes, and Groundwater

One of the earliest investigations of REEs in groundwaters showed that because REEs formed strong and stable aqueous complexes with chelators, they were potentially powerful tracers of groundwater-rock reactions and groundwater flow (Bigot et al., 1984). These authors reported that the adsorption and desorption behavior of the REEs was proportional to their stability constants with aqueous ligands, and that these features of REEs would lead to fractionation of the REE series during their transport along the groundwater flow paths, similar to what is observed for rivers and estuaries. Following on the study by Bigot et al. (1984), Smedley (1991) quantified the concentrations of the REEs in mildly acidic groundwaters from a granitic rock aquifer and from a metasedimentary (chiefly slate) rock aquifer in Cornwall from the southwestern United Kingdom. She demonstrated that the REE signatures of these groundwaters closely resembled the REE signatures of the specific rock types through which they flowed, further emphasizing their utility as tracers of water-rock reactions (Smedley, 1991). Moreover, she showed that characterizing the REE signature of groundwaters can provide a means of tracing groundwater flow based on aquifer composition, which has since been the theme of several later studies (Johannesson, Stetzenbach, & Hodge, 1997; Johannesson, Stetzenbach, Hodge, Kreamer, & Zhou, 1997; Tweed et al., 2006). Such an approach is essentially identical to the use of strontium isotope ratios in groundwaters (Lyons et al., 1995; Ojiambo et al., 2003).

To a first approximation, the input-normalized REE signature of groundwaters and river waters appears to reflect the results of biogeochemical reactions between the waters and REE bearing minerals in the aquifer rocks or source rocks during chemical weathering, as well as clay minerals and Fe-Mn oxides/oxyhydroxides coating these and other minerals (Chevis, Johannesson, Burdige, Tang, et al., 2015; Goldstein & Jacobsen, 1988b; Smedley, 1991; Tang & Johannesson, 2005; Willis & Johannesson, 2011). Here, weak acids such as carbonic acid and organic acids, some likely produced by microbes, appear to be responsible for mobilizing REEs during chemical weathering reactions (Banfield & Eggleton, 1989; Brantley et al., 2001; Cervini-Silva et al., 2005; Nesbitt, 1979; Taunton et al., 2000; Voutsinos et al., 2022). The relative distributions of the REE mobilized by these biogeochemical reactions can then be further fractionated by the combined impacts of aqueous solution and surface complexation (Byrne & Liu, 1998; Elderfield et al., 1990; Goldstein & Jacobsen, 1988b; Johannesson et al., 2005; Sholkovitz, 1978; Willis & Johannesson, 2011). Specifically, aqueous complexation of REE with dissolved ligands like carbonate anions and natural organic ligands preferentially stabilize the HREE in solution by lowering the aquo ion activity, for example, $a_{Yb^{3+}}$, thus impeding surface complexation reactions of the HREE compared to the LREE (Byrne & Kim, 1990; Cantrell & Byrne, 1987; Marsac et al., 2010; Pourret et al., 2007). These same solution and surface complexation reactions are also thought to be responsible for the fractionation of the REEs in rivers, estuaries, and the ocean (Byrne & Liu, 1998; Elderfield et al., 1990; Goldstein & Jacobsen, 1988a, 1988b; Hoyle et al., 1984; Schijf et al., 2015). Moreover, the dissolved inorganic and organic ligands in weathering solutions preferentially complex with the HREEs, effectively removing them from the site of active weathering, whereas the LREEs are preferentially retained by adsorption or incorporation in secondary clay minerals or phosphate minerals formed during incongruent chemical weathering (Banfield & Eggleton, 1989; Duddy, 1980; Schau & Henderson, 1983). Colloids are also likely to be important in elevating LREE

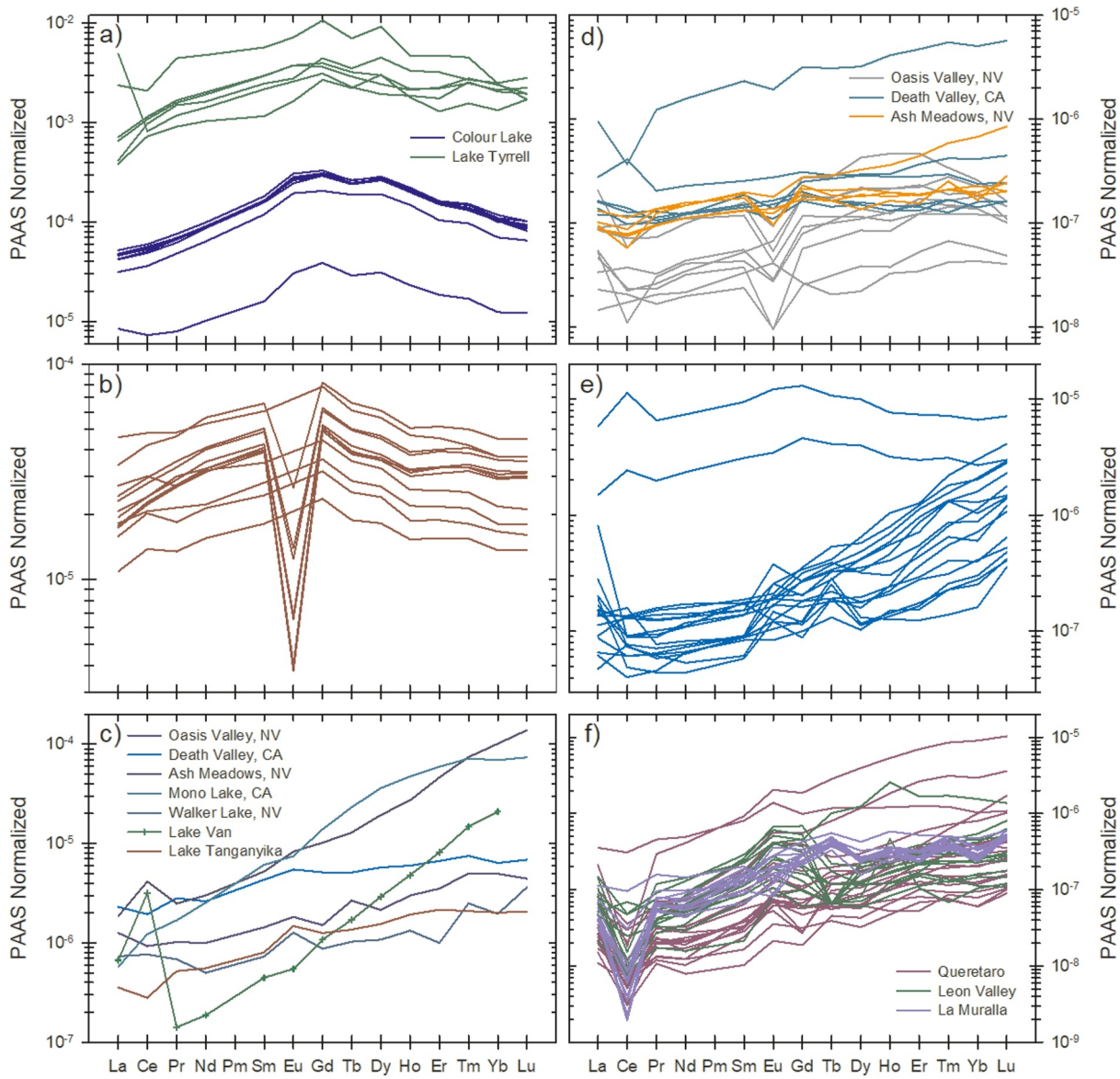

Figure 4. Rare Earth Elements (REE) patterns of lake and groundwater samples normalized to PAAS. (a) acid waters ($3.6 \leq pH \leq 4.7$) from Colour Lake (Nunavut, Canada) and acid groundwaters (pH 3.1) beneath Lake Tyrrell, Victoria, Australia; (b) acidic, organic-rich blackwaters of the Great Dismal Swamp in Virginia, USA; (c) alkaline lake waters from the western Great Basin of the USA (Goose, Summer, Abert, Mono, and Walker Lakes; ($9 \leq pH \leq 10$) as well as from Lake Van in Turkey (pH 9.6) and Lake Tanganyika (pH 8.75) in East Africa; (d) groundwaters from Oasis Valley, Ash Meadows, and Death Valley in southern Nevada and eastern California, USA; (e) groundwaters from southern Saskatchewan, Canada; (f) groundwaters from the states of Guanajuato and Querétaro in México. Note that the ordinate varies between panels owing to the large differences in REE concentrations as a function of pH. Data from Fee et al. (1992), Möller and Bau (1993), Johannesson and Lyons (1994, 1995), Johannesson, Stetzenbach, Hodge, Kreamer and Zhou (1997), Johannesson et al. (1994, 1999, 2000, 2005, 2006), Barrat et al. (2000), and Johannesson and Hendry (2000).

concentrations in rivers (Merschel et al., 2017) and some groundwaters (Brewer et al., 2022; Goldstein & Jacobsen, 1988b; Ingri et al., 2000; Smedley, 1991; Stolpe et al., 2013).

Following Smedley (1991), Fee et al. (1992) investigated the REEs in acid, hypersaline groundwaters from Victoria, Australia, and Gosselin et al. (1992) studied the REEs in chloride-rich acid groundwater from Texas, USA. Both investigations further illustrated the utility of the REE to trace different groundwater sources and identify possible water-rock reactions. For example, Fee et al. (1992) used differences in the shale-normalized REE patterns to distinguish between three different types of groundwaters beneath an Australian dry lake (Figure 4a) that included: (a) regional groundwaters exhibiting the highest REE concentrations, (b) an

intermediate "transitional" groundwater with lower REE concentrations, and (c) a reflux brine located beneath both the regional and "transitional" groundwaters. In contrast, Gosselin et al. (1992) showed that acid groundwaters that flowed through arkosic rocks had flat, shale-normalized patterns that closely resembled the REE patterns of these rocks, whereas groundwaters that flowed through carbonate rocks and had reacted with MREE-enriched Fe-Mn oxides/oxyhydroxide coatings on the carbonate minerals and/or secondary vug-filling minerals had MREE enriched patterns. Similar MREE-enriched shale-normalized patterns of acid waters were observed in the Canadian High Arctic (Figure 4a) that also appear to reflect water-rock reactions with MREE enriched Fe(III)/Mn(IV) oxides/oxyhydroxides within the local bedrock and associated sediments (Johannesson & Lyons, 1995; Johannesson & Zhou, 1999). In contrast, the shale-normalized MREE-enriched patterns of surface waters from the Great Dismal Swamp in Virginia likely reflect preferential complexation of MREE with natural organic matter (Johannesson et al., 2014; Marsac et al., 2010; Tang & Johannesson, 2010) (Figure 4b).

Following these earlier studies, the REEs were successfully employed to trace groundwater flow, mixing, and mineral dissolution reactions in aquifers from Tennessee, southern Nevada, and Massachusetts in the USA as well as in Victoria, Australia (Bau et al., 2004; Johannesson et al., 1999; McCarthy et al., 1996; Tweed et al., 2006, among many others). In a series of papers from the mid-to late 1990s, Johannesson and colleagues reported that the input-normalized REE patterns of groundwaters discharging from regional carbonate aquifers in southern Nevada and eastern California differed from those abstracted from felsic volcanic rock aquifers from the same geographic region (Johannesson, Lyons et al., 1996; Johannesson, Stetzenbach et al., 1996; Johannesson, Stetzenbach, Hodge, Kreamer, & Zhou, 1997; Stetzenbach et al., 2001; Figure 4d). The REE fractionation patterns were consistent with groundwaters issuing from carbonate springs in Death Valley National Park, California, having originated by mixing of locally recharged groundwaters with groundwaters from the Pahranagat Valley ~150 km to the north (Johannesson, Stetzenbach, & Hodge, 1997; Johannesson, Stetzenbach, Hodge, Kreamer, & Zhou, 1997). These conclusions were supported by stable water isotope ratios (i.e., $\delta^{18}O$, δD) and uranium-series isotopes (i.e., $^{234}U/^{238}U$) of regional groundwaters and hydrologic head levels as well as the orientation of several major faults in southern Nevada and eastern California (Farmer, 1996; Johannesson, Stetzenbach, & Hodge et al., 1997; Laczniak et al., 1996).

Although the application of the particle-reactive REE to trace groundwater flow seems counterintuitive, the inclusion of aqueous complexation modeling helped facilitate a more mechanistic understanding of how the REE could exhibit pseudo-conservative behavior over groundwater flow paths of several tens of kilometers. Specifically, aqueous complexation modeling suggests that the REEs are chiefly complexed with carbonate ions in circumneutral pH groundwaters, and further that the dicarbonato complex (i.e., $Ln(CO_3)_2^-$) accounted for substantial fractions of dissolved HREEs, especially when pH exceeded ~7.5 (Johannesson et al., 2005; Johannesson, Stetzenbach, et al., 1996). The dicarbonato complex is not as strongly adsorbed as other REE species onto surface sites within the local aquifer, preferring instead to remain in solution relative to the LREE, which primarily formed positively charged carbonato complexes (i.e., $LnCO_3^+$) (Johannesson, Stetzenbach, & Hodge, 1997; Tang & Johannesson, 2005) (Figure 4f). These findings are reminiscent of the early work by Bigot et al. (1984). Hence, these and other investigations underscored the importance of controls that aqueous complexation, and hence solution composition, place on the fate and transport of REEs in groundwater flow systems (Rönnback et al., 2008; Tweed et al., 2006).

As with other reactive metals, the geochemistry of the REEs in natural terrestrial waters is closely coupled to pH, exhibiting an inverse relationship such that REE concentrations increase with decreasing pH (Elderfield et al., 1990; Goldstein & Jacobsen, 1987, 1988b). Hence, some of the lowest measured REE concentrations have been reported for circumneutral pH groundwaters where individual REEs such as Yb can be 5- to 10-fold lower than in seawater (Kreamer et al., 1996; Stetzenbach et al., 1994) (Figures 4d–4f). At higher pH values REE concentrations tend to increase such that alkaline, saline lakes with pH ≈ 10 like Mono Lake in eastern California, Lake Abert in eastern Oregon, Lake Van in Turkey (Figure 4c), and Lakes Aha and Hongfeng in China (data not shown) are strongly enriched in the REE, and especially the HREE (Barrat et al., 2000; Johannesson et al., 1994; Johannesson & Lyons, 1994; Möller & Bau, 1993; Z. L. Wang et al., 2013). Indeed, not only are the input-normalized fractionation patterns enriched in HREE over the LREE in Mono and Abert Lakes, but the measured concentrations of individual HREE are also higher than those for individual LREE (Johannesson et al., 1994; Johannesson & Lyons, 1994) (Figure 4c). The increase in HREE concentrations is thought to reflect stabilization of HREE in these lake waters owing to the formation of strong carbonate complexes, particularly dicarbonato complexes (Johannesson & Lyons, 1994; Möller & Bau, 1993).

Terrestrial waters with pH ≥ 10 appear to be rare and largely confined to regions where low-temperature serpentinization is ongoing (e.g., Bruni et al., 2002; Chavagnac et al., 2013; Leong & Shock, 2020, and references therein). To the best of our knowledge, only one study reports REE concentrations in hyperalkaline, high pH groundwaters (pH ≥ 11), which do not exhibit enrichment in the HREE like those reported for alkaline, saline lake waters, and instead have flat to mildly LREE enriched, shale normalized REE patterns (Zwicker et al., 2022). The lack of strong, HREE enrichment in these hyperalkaline groundwaters likely reflects the low dissolved inorganic carbon concentrations in which alkalinity is dominated by hydroxyl ions and not carbonate ions.

Therefore, although some terrestrial waters have REE distributions that closely reflect the REE distributions of local rocks/sediments/minerals (e.g., Banner et al., 1988; Gosselin et al., 1992; Smedley, 1991), others such as alkaline, saline lakes and circumneutral pH groundwaters commonly have highly fractionated, input-normalized REE patterns compared to both shale composites and local rocks (Figures 4c–4f). In many instances, the input normalized REE fractionation patterns of circumneutral pH groundwaters resemble those of seawater, namely middle to HREE enrichments relative to the LREE, negative Ce anomalies, and even superchondritic Y/Ho ratios (Bau et al., 2004; Chevis, Johannesson, Burdige, Cable, et al., 2015; Johannesson et al., 2005, 2006; Johannesson et al., 2011) (Figure 4f). These observations are consistent with a model that REE fractionation patterns evolve along groundwater flow paths as groundwaters react with the aquifer rocks/sediments and biogeochemical processes such as anaerobic microbial respiration and chemical weathering modify the groundwater chemistry and pH.

A conceptual model advanced by Johannesson and collaborators (Johannesson et al., 1999, 2005) and further supported by other researchers (Alibo & Nozaki, 1999; Tang & Johannesson, 2005; Tweed et al., 2006) is that REEs are initially mobilized in groundwater systems near the recharge area (e.g., Nesbitt, 1979). These infiltrating waters are commonly saturated with respect to atmospheric CO_2 and become even more acidic as they pass through the soil zone owing to CO_2 generated by respiring plants (e.g., roots) and soil microbes. As a result, infiltrating soil waters with pH values as low as 4 are not uncommon. Such acidic aqueous fluids can mobilize REEs in relative distributions that closely mimic the most environmentally labile mineral fractions, including coatings on the aquifer minerals and/or organic matter phases within the soil zone of the recharge area (Duvert et al., 2015; Omonona & Okogbue, 2017; Pédrot et al., 2015; Tang & Johannesson, 2005). As the initially acidic groundwater flows down a gradient along the flow path, it continues to react with minerals within the aquifer materials generating HCO_3^-, as silicate and carbonate minerals dissolve, and raising the groundwater pH. Increases in pH are partly buffered by CO_2 produced within the aquifer by respiring bacteria that use terminal electron acceptors such as Fe(III)/Mn(IV) oxides/oxyhydroxides and SO_4^{2-} to oxidize organic carbon and other reductants. However, because many groundwater flow systems are highly oligotrophic, chemical weathering of minerals within these flow systems commonly plays a dominant role, driving pH increases to values that can exceed 9 (Chapelle & Knobel, 1983; Flynn et al., 2012; Lovley & Chapelle, 1995; Park et al., 2006). As groundwater pH rises above 7, the combination of aqueous and surface complexation further fractionates the REEs by preferentially stabilizing HREEs in solution as $Ln(CO_3)_2^-$ complexes, contrary to the LREEs, which are preferentially adsorbed onto mineral surface sites (Biddau et al., 2009; Carr et al., 2016; Johannesson et al., 2005; Tang & Johannesson, 2006; Willis & Johannesson, 2011). These processes act to enrich the input-normalized HREE values in groundwaters and deplete the input-normalized values of the LREE, leading to HREE enriched input-normalized fractionation patterns. Similar competition between aqueous complexation and surface complexation also modifies river water REE distributions, commonly leading to HREE-enriched shale-normalized patterns (Byrne & Liu, 1998; Elderfield et al., 1990; Hoyle et al., 1984; Sholkovitz, 1995).

Submarine groundwater discharge (SGD) has been recognized as an important source of REEs to the coastal ocean (Duncan & Shaw, 2003; Johannesson & Burdige, 2007). Diagenetic REE flux to coastal waters appears to be related to the biogeochemical degradation of organic carbon of terrestrial origin (Duncan & Shaw, 2003). Moreover, it was hypothesized that SGD may be an important component of the missing Nd flux to the ocean necessary to balance the ocean Nd budget and address the "Nd paradox" (Goldstein & Hemming, 2003; Johannesson & Burdige, 2007). Because SGD occurs along ocean margins, it is likely to be part of the "Boundary Exchange" process.

Several site-specific investigations of the REE and Nd isotopes revealed substantial terrestrial SGD fluxes to coastal waters that ranged from 1 to 3 mmol Nd day^{-1} along the Kona Coast of Hawaii up to 26 mmol Nd day^{-1} within the Pettaquamscutt River estuary in Rhode Island (Chevis et al., 2021; Chevis, Johannesson, Burdige,

Tang, et al., 2015; Johannesson et al., 2011, 2017). At the Florida and Rhode Island sites, the terrestrial SGD REE flux was of the same magnitude as local stream water fluxes. The magnitude of the terrestrial SGD Nd fluxes reported for the Indian River Lagoon (Florida), the Pettaquamscutt River estuary, and the Kona Coast are comparable to those for a barrier island along the coast of Germany (5.03 mmol Nd day^{-1}; Paffrath et al., 2020) and the Bay of Bengal near the Sankarabarini River in southern India (25.7 mmol Nd day^{-1}; Ponnumani et al., 2022), but several orders of magnitude lower than found along the coast of Jeju Island, South Korea (57.5–219 mol Nd day^{-1}; I. Kim & Kim 2011, 2014). Molina-Kescher et al. (2018) estimated SGD fluxes from Tahiti, another basaltic island in the South Pacific, which were also similar in magnitude to those reported for the Kona Coast of Hawaii (Johannesson et al., 2017). Hence, the substantially higher SGD fluxes of Nd reported from Jeju Island are perplexing but appear to reflect the remarkably high REE concentrations measured in coastal groundwaters from this basaltic island.

To the best of our knowledge, the first SGD Nd isotope compositions and fluxes were reported by Chevis et al. (2021) for the Indian River Lagoon system of Florida's Atlantic coast. These authors concluded that biogeochemical reactions occurring in the subterranean estuary, namely microbially facilitated reductive dissolution of Fe(III) oxides/oxyhydroxides coating the sandy, quartz-rich sediments, was the chief source of Nd and hence REE to these coastal waters. More specifically, labile marine-sourced organic matter that circulates through the subterranean estuary fuels microbial respiration of the Fe(III) oxides/oxyhydroxides, which releases both Fe (II) and adsorbed REEs into solution (Roy et al., 2010, 2011, 2013). Once mobilized, Fe(II) and REEs flow upward with advecting groundwater. Ferrous iron precipitates as Fe sulfide minerals in the shallow sediments directly below the seafloor, whereas the REEs are discharged into the overlying coastal surface waters of the Indian River Lagoon (Chevis et al., 2021). These researchers estimated that the total SGD flux of Nd (i.e., terrestrial and recirculated marine flux) was on the order of 200 mmol day^{-1} and had an εNd value of −6.5. Hence, the SGD flux accounts for about half of the total surface water flux of Nd to the coastal ocean (i.e., ca. 400 mmol Nd day^{-1}) from the studied portion of the Indian River Lagoon, and furthermore, the Nd isotope composition of this total surface flux was identical to the total SGD flux, that is, $\varepsilon Nd(0) = -6.47 \pm 0.16$ (Chevis et al., 2021).

In summary, research into the REE in terrestrial waters over the past 30 years has helped illuminate the mechanisms that mobilize these trace elements from geological materials as well as the biogeochemical processes that fractionate the REE in natural waters. Some of the important processes that have been identified include differential or incongruent weathering of minerals, aqueous complexation with inorganic and natural organic ligands, solubility constraints set by sparingly soluble REE phosphate, carbonate, and hydroxide minerals, and sorption of REE onto metal oxide/oxyhydroxides and clay minerals. Future research is still required to more quantitatively understand the origins of the myriad of input-normalized REE fractionation patterns observed for terrestrial waters (Figure 4), develop models that can simulate the fate and transport of REEs in aquifers, and how recently identified methanotrophs that can use or even require lanthanides in an alternative methanol dehydrogenase to metabolize methane (e.g., Daumann, 2019) may also influence REEs in terrestrial waters.

2.2. Land-Ocean Interfaces

2.2.1. Estuaries

Estuarine processes have long been recognized as of high importance in modifying the input of dissolved and particulate riverine loads of inorganic and organic matter to coastal waters and ultimately the ocean (Eckert & Sholkovitz, 1976; Lawrence & Kamber, 2006; Sholkovitz, 1978). The study of REE and Nd isotope composition in river-suspended material has shown that the general assumption that they are not fractionated during Earth surface processes may be overstated (Bayon et al., 2015). Nd isotopic analysis on different grain-size fractions may display distinct compositions, attributed to the preferential breakdown of young volcanic material, while high REE mobility could occur during weathering under all types of climate, leading to significant decoupling of Nd isotopes between parent rocks, soils, and river waters (Bayon et al., 2015 and references therein).

It is important to understand the physico-chemical processes governing the behavior of trace metals during estuarine mixing of river and seawater to estimate the impact of estuarine removal on the trace element budget of the world's oceans. Following the removal of iron and other trace elements through the flocculation of inorganic and organic nanoparticles and colloids, dissolved REEs experience substantial removal in the estuarine zone, exhibiting non-conservative behavior along the salinity gradient (e.g., R. L. Andrade et al., 2020; Elderfield

et al., 1990; Goldstein & Jacobsen, 1988a, 1988b; Rousseau et al., 2015; Sholkovitz et al., 1978, 1995; Sholkovitz & Szymczak, 2000; Sholkovitz, 1993). Hoyle et al. (1984) demonstrated a significant removal of estuarine REEs from solution, mainly in the low salinity range (0–5 salinity), concluding that REEs are strongly associated with organic matter and that REE removal occurs due to the flocculation of iron-organic matter colloids. These authors also noted that Ce behaved coherently with La and Nd, implying that the Ce anomaly is not generated due to estuarine mixing. Similarly, Sholkovitz (1993) observed over 90% removal of REEs in the Amazon estuary within a salinity range of 0–6.6, attributing this phenomenon to the coagulation of riverine colloids. However, in the same study, a slight increase in REE concentrations was observed within the salinity range of 6.6–34, resulting from the release of REEs from sediments and suspended particles or the heterogeneous distribution of REE concentrations within the Amazon River plume. Conversely, Merschel et al. (2017) found REE conservative behavior in Rio Negro, Brazil. According to the authors, in this system, the nanoparticles and colloids are mainly humic and fulvic acids that during estuarine mixing precipitate removing trace elements including REE from the solution (Fox, 1983; Sholkovitz, 1978; Zhou et al., 1994). Other studies have also indicated a slight increase in REE concentrations at high salinities (Elderfield et al., 1990; Sholkovitz & Szymczak, 2000). Additionally, a pattern of HREE (heavy REE) > MREE (medium REE) > LREE (light REE) release has been observed at higher salinities, which is the reverse of the order observed at lower salinities (e.g., R. L. Andrade et al., 2020; Rousseau et al., 2015; Sholkovitz, 1993). Figure 5 illustrates this variability pattern, showcasing the differential fractionation of REEs along the salinity gradient in various estuarine systems. The increase in REE concentrations from mid to high salinity starts at lower salinities for the HREE (between 10 and 15) than for the MREE (between 10 and 25) and the LREE (between 15 and 25) (Figure 5). Sholkovitz (1995) reported that REE fractionation accompanies the removal of the dissolved phase during the coagulation of organic iron oxide colloids, to which REEs are strongly associated, and is also a result of the release of REEs from river and estuarine particles with increasing salinity. Several dominant factors of REE speciation and fractionation in estuaries have been identified, considering total organic carbon (TOC) as the most important factor for REE speciation and bioavailability in estuarine sediments (Chakraborty et al., 2011). Although more than half of REEs were bound to inert complexes and were not bioaccessible, about 20%–30% were associated with TOC. Furthermore, C. Zhang et al. (1998) considered that REEs were fractionated as iron and manganese compounds (9%–16%), carbonates (3%–6%), and water-soluble (1%–11%) fractions. In the Rhine-Meuse estuary, Moermond et al. (2001) report that dissolved REEs are mainly complexed with carbonates and dissolved organic matter, pointing to a decrease in the relative abundance of the ionic form $LnCO_3^+$ from La to Lu, while the relative abundance of $Ln(CO_3)_2^-$ increases.

Fluvial and groundwater inputs are important sources of terrestrial REEs to the ocean, although other sources (e.g., dust deposition and deep-sea benthic flux) likely play a significant role (e.g., Abbott, 2019; Abbott, Haley, & McManus, 2015; Byrne & Sholkovitz, 1996; Duncan & Shaw, 2003; Haley et al., 2017; Johannesson & Burdige, 2007; Sholkovitz, 1993), as will be discussed. Globally, the riverine shale-normalized patterns of REEs are diverse, evidencing light, medium, and heavy REE enrichments, with concentrations ranging across three orders of magnitude. In contrast, the normalized marine REE pattern is globally more consistent and characterized by a depletion of LREE relative to HREE, an enrichment of La, and a depletion of Ce (Byrne & Liu, 1998; Elderfield & Greaves, 1981; Elderfield,et al., 1988, 1990; Garcia-Solsona & Jeandel, 2020; Lawrence & Kamber, 2006; Molina-Kescher et al., 2014; Molina-Kescher et al., 2018; Osborne et al., 2015; Pham et al., 2019; Siddall et al., 2008; X. Y. Zheng et al., 2016).

The distribution of REEs in estuarine sediments is influenced by various early diagenetic processes, particularly co-precipitation into Fe-Mn oxides/oxyhydroxides, redox conditions in the water column, the composition of terrigenous sources, and anthropogenic inputs (Brito, Prego et al., 2018). Several authors have studied the geochemical cycling of the REEs in estuaries, which can be used as geochemical indicators associated with the origin of the sediments (Babu et al., 2021; Censi et al., 2005; de Chanvalon et al., 2016; de Freitas et al., 2021; Hannigan et al., 2010; Merschel et al., 2017; Munksgaard et al., 2003; Prego et al., 2009; Silva-Filho et al., 2011). Bayon et al. (2015) confirmed earlier assumptions that river sediments do not generally exhibit significant grain-size dependent Nd isotopic variability, although, a subtle decoupling of Nd isotopes between clays and silts was identified in a few major river systems, suggesting that preferential weathering of volcanic and/or sedimentary rocks relative to more resistant lithologies may occur in river basins, possibly leading locally to Nd isotopic decoupling between different size fractions. Bayon, Douglas, et al. (2020) also examine REE and neodymium isotopic compositions in grain-size fractions from river-suspended matter in the Murray-Darling Basin and a marine sediment core off the coast of Australia, showing that significant size-dependent geochemical decoupling

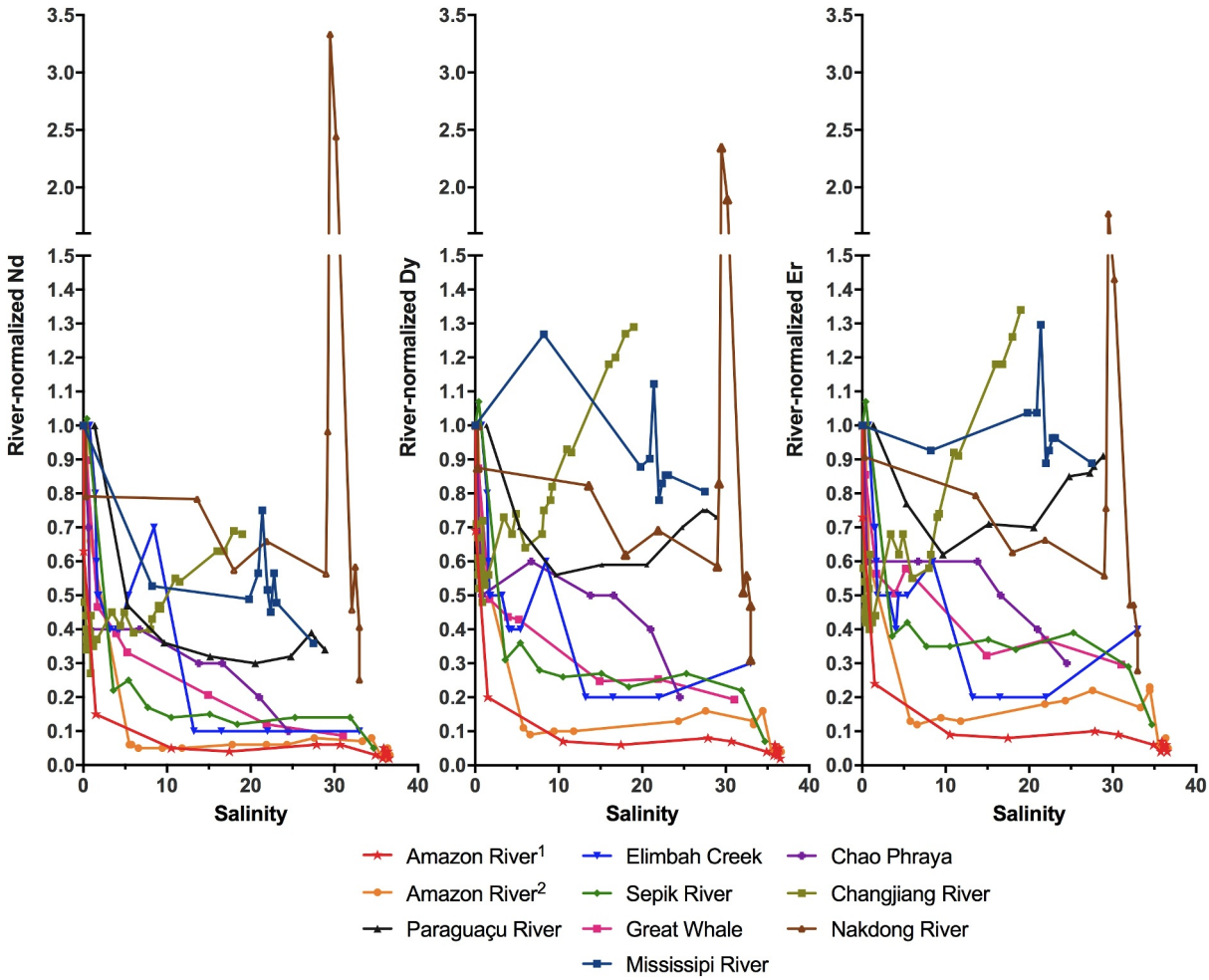

Figure 5. Concentrations of Nd (LREE), Dy (MREE), and Er (HREE) normalized to the REE concentrations of the freshwater endmember along the salinity gradient in several estuarine systems (adapted from R. L. Andrade et al., 2020). Data from: Amazon River[1] (Rousseau et al., 2015), Amazon River[2] (Sholkovitz, 1993), Paraguaçu River (R. L. Andrade et al., 2020), Elimbah Creek (Lawrence & Kamber, 2006), Sepik River (Sholkovitz & Szymczak, 2000), Great Whale River (Goldstein & Jacobsen, 1988a), Mississippi River (Adebayo et al., 2018), Chao Phraya River (Nozaki et al., 2000), Changjiang River (Z. L. Wang & Liu, 2008), and Nakdong River (T. Kim et al., 2020). The Nakdong River presents a sharp rise in REE normalized concentrations around salinity 30 due to the influence of wastewater discharge from a wastewater treatment plant.

can occur in river systems, with a preference for volcanic origin for fine-grained inorganic particles transported by river systems and suggesting that river sediment discharge is accompanied by the export of fine-grained volcanogenic particles to the ocean, potentially impacting marine productivity.

Furthermore, numerous studies have focused on the mobility of REEs between dissolved and particulate fractions in estuaries impacted by acid mine drainage (AMD) inputs (Brito, Cesário et al., 2020 and references therein). AMD is characterized by low pH and high concentrations of dissolved elements, including trace metals such as REEs, which can alter the fractionation of REEs in the receiving environment. Because estuaries act as transition zones, acidic REE-rich waters interact with alkaline ocean waters, leading to complex processes that control the geochemical characteristics of dissolved and particulate REEs. Lecomte et al. (2017) found that REE are retained in minerals formed from the interaction of AMD with seawater (pH > 6), resulting in increased concentrations of REE in estuarine sediments. Conversely, at low pH values (3–3.5), REEs are released into the solution. In the case of the Huelva estuary (southwestern Spain), a study revealed higher REE concentrations at low pH values in the river, whereas as pH increased in the estuary, these metals were reabsorbed onto insoluble salts and Fe oxide/oxyhydroxides (Lecomte et al., 2017). Similar behavior has been observed in other AMD-related estuarine systems (Ayora et al., 2015; Bonnail et al., 2017; Pérez-López et al., 2010; Prudêncio et al., 2015; Sharifi et al., 2013; Soyol-Erdene et al., 2018).

Estuarine sediments associated with salt marshes (Brito, Prego et al., 2018; López-González et al., 2012; Morgan et al., 2016; S. Wang et al., 2015), mangroves (de Freitas et al., 2021; Kumar et al., 2014; Morgan et al., 2016; Sappal et al., 2014; Silva-Filho et al., 2011), and seagrasses (de Sena et al., 2022) accumulate high amounts of fine-grained particles rich in metals, including REE. The chemical zonation of sediments plays a crucial role in the distribution of these elements between solid particles and pore waters (e.g., Berner, 1980). Because permeable sediments are a major feature in estuaries due to the presence of benthic organisms, plants, and different particles in nature, these sedimentary environments may act as a source of solutes (e.g., metals, nutrients, and organic complexes). Rivers were once thought to be the main source of REEs (Goldstein & Jacobsen, 1988b) to coastal zones, but recent studies have suggested that submarine groundwater discharges (SGD) also act as an additional source of LREE and MREE, but a sink for HREE (Chevis, Johannesson, Burdige, Tang, et al., 2015; Johannesson & Burdige, 2007; Johannesson et al., 2011; Tachikawa et al., 2003). High REE concentrations in SGD are suggested to be linked to the degradation of REE-rich relict terrestrial organic carbon and the reduction of Fe-oxides under anoxic conditions in sediments (Chevis, Johannesson, Burdige, Tang, et al., 2015; Johannessen et al., 2011; Duncan & Shaw, 2003).

In sandy subtidal areas, advection and diffusion are the main processes that transport solutes across the sediment-water interface. Otherwise, in muddy or muddy-sandy submerged sediments, diffusion becomes the primary transport mechanism across this interface, leading to vertical fluxes. The intricate interplay of biogeochemical cycles involving iron (Fe) and manganese (Mn) governs the fluxes of REEs from sediments to the water column (Adebayo et al., 2020; Schijf et al., 1995). Adebayo et al. (2020) showed that the strong concentration gradient between pore waters and the overlying waters results in an upward diffusive flux of REEs into the estuarine water column. Similar findings were reported by Sholkovitz (1992) in the Chesapeake Bay, USA; and Weltje et al. (2002) in the catchment area of the Rhine and Meuse rivers (The Netherlands). The upward flux of REEs from pore waters is accompanied by fractionation along the REE series and a preferential input of Ce relative to other trivalent REE neighbors (Sholkovitz, 1992).

In summary, estuarine processes are vital in altering the input of dissolved and particulate riverine loads into coastal and oceanic waters. Specifically, dissolved REEs display non-conservative behavior along the salinity gradient, reflecting the influence of factors such as salinity, organic carbon and particle nature on REE distribution and fractionation within estuaries. Additionally, the transport mechanisms of REE across sediment-water interfaces and the fluxes of REE from sediments to the water column underscore the intricate interplay of biogeochemical cycles involving iron and manganese.

2.2.2. Vegetated Coastal Ecosystems: The Plant-Soil System

During the process of weathering, REEs, together with other trace elements, are gradually released from mineral structures and can take various forms. They may enter solution, become retained on the surfaces of soil particles, or form complexes with organic matter, carbonates, phosphates, and/or other sedimentary phases (such as oxides/oxyhydroxides of Fe and Mn) (Gonzalez et al., 2014; Khan et al., 2017).

In vegetated coastal ecosystems (VCE) like saltmarshes, seagrasses, and mangroves, plants thrive in waterlogged and anoxic soil conditions. The root systems of these plants disrupt the chemical zonation of the soil (Vale & Sundby, 1998), leading to heterogeneous patterns of redox conditions (Sundby et al., 2003). The chemistry of the waterlogged anoxic soils is primarily influenced by Fe, Mn and S, which change with plant activity and the annual cycle of root growth and decay. This is significant because the speciation of sedimentary Fe and Mn is known to influence the cycling of REEs (Quinn et al., 2006), including their labile forms (Brioschi et al., 2013; Z. Huang et al., 2023; Ramos et al., 2016).

During tidal cycles, the excursion of water in VCE with the ebb and flood periods facilitates the exchange of solutes between the soil and the overlying water (e.g., Caetano et al., 1997; Huettel et al., 1998). Several studies have demonstrated upward advection fluxes of solutes from intertidal flat sediments to the water column, including nutrients (Ospina-Alvarez et al., 2014; Rocha, 1998) and redox-sensitive elements and trace metals (Caetano et al., 1997; Taillefert et al., 2007). Similar observations have been made in saltmarsh soils (Santos-Echeandía et al., 2010). Bioturbation of saltmarsh soils may promote the formation of Fe and Mn oxides/oxyhydroxides, which scavenge REEs through adsorption and/or coprecipitation. In saltmarshes of South Brazil, it seems that bioturbation plays a role in Ce redox chemistry, leading to positive Ce anomalies in core soils (L. Costa, Johannesson, et al., 2021). Although physical processes such as bioturbation and dredging can also

influence the exchange of REEs across the sediment-water interface (L. Costa, Johannesson, et al., 2021; Johannesson et al., 2011; Mirlean et al., 2020; Schaller, 2014), this topic has been understudied.

In VCE, the water column height is typically low, and episodes of wind can lead to sediment resuspension in shallow areas. This resuspension process can induce changes in the sorption equilibrium of solutes (Simon, 1989). The estuarine environment, with its dynamic nature, has a substantial impact on the speciation, solubility, distribution, and fluxes of various metal species including REEs. However, there is a lack of comprehensive studies that assess the spatial and temporal distribution of REEs and their sources and cycling within the complex estuarine—vegetated coastal ecosystems (de Freitas et al., 2021).

In many of these vegetated environments, the salinity gradient plays a role in promoting flocculation and precipitation reactions, similar to what is observed in estuaries and groundwaters. These processes facilitate the exchange of REEs between dissolved and particulate forms. During these processes, dissolved REEs are often removed, particularly in low salinity waters, due to salt-induced coagulation of colloids. This leads to fractionation, with a preferential removal of LREE over MREE and HREE (L. Costa, Johannesson, et al., 2021; Hoyle et al., 1984). L. Costa, Johannesson, et al. (2021) demonstrated an enrichment of LREE over HREE in sediments from the freshwater and brackish sections of the Patos lagoon system (Brazil), compared to sediments influenced by seawater, which exhibited a flatter REE profile.

Marshes, mangroves, and seagrass plants have the ability to mobilize and store metals within the sediments, surrounding roots, and belowground tissues (Caetano et al., 2008; L. Costa, Johannesson, et al., 2021; L. Costa, Mirlean, et al., 2021; de Sena et al., 2022). Although extensive research has been conducted on the mobilization and storage of first row transition metals and other traditional "toxic metals" such as Cu, Cd, and Hg (see Weis & Weis, 2004 for a review), investigations focusing on REEs have only recently gained attention due to their technological importance and growing environmental implications (Brito, Malvar et al., 2018; Brito, Mil-Homens et al., 2020; Mandal et al., 2019; Prasad & Ramanathan, 2008; Sappal et al., 2014). A comprehensive review study conducted by Khan et al. (2017) shed light on the speciation and bioavailability of REEs in soil, plant, and aquatic ecosystems, emphasizing their environmental impacts. The increased research interest in REEs in recent years is closely linked to their potential detrimental effects on living organisms, highlighting the importance of understanding their speciation, and bioavailability to evaluate associated health risks (M. Andrade et al., 2021; Henríquez-Hernández et al., 2017; Y. Ma et al., 2016; H. Zhang et al., 2010).

Studies conducted in mangroves along the Ganges River in India have revealed that plant activity does not substantially influence the retention of REEs in vegetated sediments (Mandal et al., 2019; Prasad & Ramanathan, 2008; Sappal et al., 2014). Instead, these studies suggest that the primary source of REEs in mangrove sediments is likely associated with the weathering of aluminosilicate materials from crustal sources, transported by fluvial processes. L. Costa, Johannesson, et al. (2021) have also observed that the presence of clay-silt sediment components plays a role in the accumulation of REEs by enhancing their adsorption onto mineral surfaces or through complexation with organic matter associated with these particles.

On the other hand, other studies have reported increased accumulation of REEs in mangrove-vegetated sediments from the Zhangjiang estuary in China (R. Zhang et al., 2013), Sepetiba Bay in Brazil (Silva-Filho et al., 2011), and Red Sea Mangroves in Saudi Arabia (Aljahdali & Alhassan, 2022). In these cases, the observed patterns were attributed to the variability of particle nature and the influence of anthropogenic inputs rather than the direct impact of plant activity.

A contrasting accumulation pattern was observed in the Jaguaripe estuary in Brazil (de Freitas et al., 2021), where mangrove-vegetated sediments exhibited lower REE content compared to adjacent estuarine sediments. This difference was also attributed to the characteristics of the sediment particles (grain size, organic matter and carbonate contents). The authors further investigated the depth profile variability of these elements in mangrove-vegetated sediments and found that the distribution of REEs is primarily controlled by post-depositional early diagenesis processes, mainly precipitation of Fe and Mn oxide/oxyhydroxides. In sites where redox-sensitive Fe and Mn showed minor variability with depth, substantial REE accumulation is not expected.

Sappal et al. (2014) proposed that fractionation of REEs in mangrove sediments is controlled by alkaline and reducing conditions, which lead to the removal of MREEs and LREEs through processes such as adsorption and precipitation onto Fe/Mn oxides/oxyhydroxides. Changes in ionic strength and REE-particle interactions also contribute to the REE fractionation (de Freitas et al., 2021; Mandal et al., 2019; Prasad & Ramanathan, 2008).

The redox status of the sediments plays a substantial role in the fractionation of Ce (Sholkovitz et al., 1992). Because these elements are redox-sensitive, and the redox status of mangrove sediments may change seasonally due to root oxygen input and Fe/Mn and S cycles, data on Ce anomalies are highly variable. Differences in anomaly patterns between plant organs and their surrounding rhizosediments (sedimentary environment that surrounds the root system) indicate that redox-driven biological processes influence the fractionation of Ce within the plant (de Sena et al., 2022). Additionally, the bioavailable fraction of these elements in the sediment also affects the anomalies observed in plant tissues.

L. Costa, Johannesson, et al. (2021) emphasize that Ce anomalies are influenced by early diagenetic processes and bioturbation. In Patos Lagoon (Brazil), Ce anomalies increase at sediment depths where oxic conditions are facilitated by burrowing crabs and saltmarsh plants, which enhance oxygen penetration. At greater sediment depths, the suboxic environment leads to lower Ce anomalies due to the reduction of Mn(IV) and Ce(IV), which mobilizes Ce(III) into the pore waters, resulting in decreased Ce content in the particulate fraction (de Sena et al., 2022).

The bioavailability of REEs plays a critical role in their transfer from soil to plants and their subsequent bioaccumulation in different plant tissues (Khan et al., 2017). However, most studies have focused on terrestrial plants, primarily in the context of plant-soil interactions in agriculture. The bioaccumulation of REEs depends on the availability of soluble and exchangeable fractions, which is influenced by various physicochemical environmental conditions such as ionic strength, dissolved organic carbon, total organic carbon, pH, redox status, cation exchange capacity, particle nature, and metal speciation (Arciszewska et al., 2022; Brito et al., 2021; Macmillan et al., 2019; Tyler, 2004; Weltje et al., 2004). These conditions exhibit wide variability in saltmarshes, seagrasses, and mangroves (de Sena et al., 2022).

Mandal et al. (2019) demonstrated that mangrove plants exhibit higher uptake of REE in belowground parts compared to aboveground plant tissues, although the total concentration of REE in the plants is lower than in the rhizosediment. The bioaccumulation and translocation factors show species-specific variability, indicating different partitioning of REEs and varying levels of efficiency in mangrove uptake (Alhassan & Aljahdali, 2021; Aljahdali & Alhassan, 2022; Mandal et al., 2019).

De Sena et al. (2022) conducted a study on seagrass meadows in Todos os Santos Bay (Brazil) to investigate the impact of environmental conditions that is, the proximity of reefs, mangroves, and sandy beaches, on sedimentary REE distribution. Similar to findings in mangroves, the retention of REEs in vegetated sediment is primarily influenced by particle nature and environmental settings. Seagrass roots were found to accumulate higher levels of REE compared to aboveground plant organs, although the overall accumulation was lower than in the sediment (de Sena et al., 2022; Komar et al., 2014). Interestingly, de Sena et al. (2022) noted that the low accumulation of REE in seagrass *Halodule wrightii*, along with limited translocation to aboveground plant parts, suggests a relatively low phytoaccumulation potential. In contrast, a different pattern was observed in *Cymodocea nodosa* in Makirina Bay (Croatia), with a translocation factor greater than 1, indicating the upward transfer of REEs through sediment-to-rhizome and/or water-to-leaf/epiphyte pathways (Komar et al., 2014). This suggests a preferential retention of REEs within the photosynthetic tissues of seagrass rather than in belowground plant parts. This could also be the result of the direct sorption from seawater (Zoll & Schijf, 2012). Notably, the uptake of REE by plants results in fractionation, with a preferential accumulation of HREE (de Sena et al., 2022). Organic ligands such as citric acid may play an important role in the transport of REEs in the xylem, leading to the enrichment of HREEs in aerial plant parts (Yuan et al., 2017).

Saltmarshes, colonized by halophyte plants, present increased sediment-root interaction compared with mangroves and seagrasses. In a study conducted by Brito, Prego et al. (2018) in the Rosário's saltmarsh in the Tagus estuary (southwest Europe), higher concentrations of REE were found in sediments colonized by *Sarcocornia fruticosa* and *Spartina maritima* compared to non-colonized sediments. This suggests that these plants may contribute to the enrichment of REEs in rhizosediments. The authors also observed higher REE concentrations in the roots compared with the aboveground parts of the plants, but no evidence of REE translocation within the plants. Additionally, distinct fractionation patterns were observed in the aboveground plant parts, with a clear enrichment of LREE relative to HREE, as well as an enrichment of MREE relative to LREE and HREE. A similar pattern was observed in another halophyte species, *Halimione portulacoides*, suggesting limited translocation of REEs to the upper organs or low retention of these elements in stems and leaves (Brito, Mil-Homens et al., 2020). In the marsh area, the authors identified specific layers of REE accumulation in the roots of *H. portulacoides*,

particularly for Y and MREE, indicating scavenging and accumulation in belowground organs, depending on the bioavailability rather than the total concentrations. Although salt marshes along with other vegetated coastal ecosystems are generally considered sinks for metals, including REEs, they can also act as a source of these elements (Caçador et al., 2009). This occurs through the uptake of metals from sediments by roots, translocation to the aboveground parts of plants, and subsequent return to the soil following senescence and the fall of aerial plant parts. Caçador et al. (2009) found that a sizeable fraction of metal-containing detritus is exported from the marsh, releasing substantial amounts of Zn, Cu, Co, and Cd (68, 8.2, 13 and 0.4 kg, respectively) per growing season. Although REEs exhibited low translocation factors from roots to aerial plant parts, further investigation is needed to evaluate the significance of this process in the REE cycle within estuaries and bays containing vegetated coastal ecosystems.

In summary, research has revealed various trends in REE accumulation within coastal vegetated ecosystems, influenced by factors such as sediment composition, environmental conditions, and human activities. The availability of REEs in sediments significantly impacts their uptake by plants, with studies highlighting species-specific differences in uptake and distribution among mangroves, saltmarshes, and seagrasses. Despite advancements, this field of study remains relatively novel, prompting further exploration into the role of vegetated coastal environments in the REE cycle and their potential as indicators for biogeochemical processes. Several hypotheses concerning REE dynamics within plant-soil systems require further investigation, along with the largely unexplored potential of REEs as tracers for both natural and anthropogenic processes.

2.3. Marine Sediments and Pore Water

The first dedicated investigation into marine pore water REE was conducted by Elderfield and Sholkovitz (1987) in 15 m deep water of Buzzard's Bay, MA, USA. Several studies followed this trend, all focusing on shallow waters (<300 m) (German & Elderfield, 1989; Sholkovitz et al., 1989, 1992). These studies alluded to the strong geochemical cycling of the REEs in the uppermost sediments. However, it was only more recent technological advances, in both sampling and analytical tools, that have enabled scientists to investigate REE behavior in open ocean sediments (Haley et al., 2004). As such, the potential importance of the sediment-water interface was not fully recognized until documentation of Nd isotopic alteration in bottom water near the sea floor (Lacan & Jeandel, 2004). Discovery of these deep water column isotopic anomalies offered an alternative, benthic explanation for the "Nd Paradox" (Goldstein & Hemming, 2003; Siddall et al., 2008); that is, an explanation that was not directly a function of water column processes (Lacan & Jeandel, 2005). While interest in these benthic processes is increasing, to date only <500 data exist for the REEs in pore water, a smaller subset of these having co-analyzed the sediment (for leachable phases and for the total sediment digest), and only a very small number of Nd isotope analyses of pore water (<30). About half of these pore water REE data are from samples >300 m deep in the oceans. A compilation of these data (Abbott, Haley, & McManus, 2015; Abbott, Haley, McManus & Reimers, 2015; Bayon et al., 2011; Deng et al., 2022; Deng et al., 2017; Elderfield & Sholkovitz, 1987; German & Elderfield, 1989; Haley et al., 2004; Patton et al., 2021; Sholkovitz et al., 1989; Sholkovitz et al., 1992) is tabulated in Supporting Information (Table S1).

Given the potential range in geochemical settings and the relative scarcity of pore water studies, much remains to be understood about the mechanisms involved in REE cycling in upper marine sediments. However, four overarching observations can be made with the data currently available. First, concentrations of REE in pore water in the upper sediments appear to be always elevated over bottom water (typically the maximum concentration in the water column). The implication of elevated pore water concentrations is that there is a ubiquitous benthic flux of REEs to the oceans. However, there are only a few attempts to estimate this flux (Abbott et al., 2019; Deng et al., 2017). Although much more data are required to make accurate global budgetary assessments, these order-of-magnitude estimates indicate that the benthic flux far exceeds surface ocean-sourced fluxes (such as rivers and dust). Moreover, it appears on par with the "missing flux" required to reconcile "Nd Paradox" (Abbott et al., 2019; Arsouze et al., 2007; Deng et al., 2017; Haley et al., 2017; Tachikawa et al., 2003). Estimates of SGD fluxes surpass these estimates, although both are benthic sources of REEs (Johannesson et al., 2011). Thus, there is good evidence to suggest that the benthic flux occurring within SGD, along the margins or at the bottom of the abyss is a critical, if not dominant, flux term in the global marine budget of REEs.

The second overarching observation is that whereas pore water supports a benthic source of REE to the ocean, the sediments remain the predominant sink for REE in the environment. Solid (e.g., biogenic fluorapatites, apatites,

phosphates, metal oxides minerals) and semi-solid phases (metal oxides, POM) are enriched in REE either through incorporation into the crystal lattice or via surface adsorption (e.g., Bayon et al., 2004; Bayon et al., 2011; Byrne & Sholkovitz, 1996; Du et al., 2022; Klinkhammer, 1980; Martin & Haley, 2000; Piper, 1974; Quadros et al., 2019; Schijf & Byrne, 2021; Schijf et al., 2015; Shaw & Wasserburg, 1985). Thus, the sediments act as a (dissolved) source and (particulate) sink of marine REEs, somewhat analogous to a capacitor (Haley et al., 2017). The largest sinks of REE appear to be Mn-oxides due to the ubiquity of this phase, and post-depositional phosphates (especially biogenic) due to their extreme REE enrichment (Abbott et al., 2016; Du et al., 2022; Takahashi et al., 2015; Toyoda & Tokonami, 1990). Whereas the latter is ostensibly a fairly inert sink term (although Du et al., 2022 indicate this may be otherwise), the former is certainly prone to changes in environmental redox state. That is, reduction of Mn-oxides that occurs in marine sediments can lead to release/cycling of REE (e.g., Froelich et al., 1979).

The fact that REEs are tightly coupled to Mn cycling appears to be a third generality of sedimentary REE geochemistry (Takahashi et al., 2015). Because Mn undergoes dynamic redox cycling between oxic and anoxic environments, the REEs also tend to show dynamic behavior in these sediments. In addition, the REEs have intricate complexation and readsorption behavior, which seems to make the association with Mn redox cycling unclear (Abbott et al., 2016; Du et al., 2022).

A fourth overarching observation is that pore water REEs also reflect input delivered by particulate organic matter (POM), but the details are more ambiguous. There is both laboratory and field evidence for strong association of REE with organic matter (OM) (Bau, 1996; Byrne & Kim, 1990; de Baar et al., 1988; Haley et al., 2004; Koeppenkastrop & De Carlo, 1992; Schijf et al., 1995; Sholkovitz, 1992; Stanley & Byrne, 1990; Tachikawa, Jeandel, Vangriesheim, & Dupré, 1999). Generally, the data all indicate that POM carries a LREE-enriched pattern (normalized to PAAS), whereas dissolved organic carbon (DOC) tends to complex and keep the HREE in solution. Unfortunately, there are very few direct analyses of REE in POM (Byrne & Kim, 1990; Davranche et al., 2005, 2011; Freslon et al., 2014; Pourret & Tuduri, 2017; Stanley & Byrne, 1990; Tachikawa, Jeandel, Vangriesheim, & Dupré, 1999). Furthermore, like Mn in the sediments, the tendency of REE to adsorb to surfaces (particularly OM surfaces), while the POM itself is undergoing remineralization, makes the relationship between POM and REE observationally abstruse. Sedimentary-based observations further suggest that Mn-oxides and POM are the predominant scavenging agents of REEs in the water column.

In addition to the four generalities mentioned above, marine sediment REEs exhibit distinct behaviors in oxic and anoxic conditions, although the mechanisms underlying each are still not fully understood. The inherent complexity arises from the kinetics of sedimentary processes, which are influenced by the temporal variability of inputs and the timescales of the chemical processes involved. In general, the REEs in oxic pore water are only moderately elevated over bottom water (Haley et al., 2004), with differences between the two most likely arising from changes in carbonate chemistry, and the resulting impact on dissolved REEs. The shale-normalized REE pattern of oxic pore water (Figure 6) is similar to the water column but commonly more pronounced (e.g., greater HREE/LREE; Haley et al., 2004). The amplification of the pattern could result from sedimentary processes mirroring those observed in the water column but compressed within the upper pore water. For instance, the organic complexing agents of the HREE could be more concentrated in the pore water compared to the water column.

In reducing pore water, dissolved REE abundances are generally far greater than in seawater, presumably reflecting an in situ input from metal oxides (Mn-oxides more likely than Fe-oxides) that are being reduced (as described above). The REE pattern of reducing pore water has a characteristic MREE enrichment when normalized to shale (Figure 6), which mirrors that of solid phase Mn-Fe oxides and some phosphates. However, there is nuance to these REE patterns beyond simple enrichment in MREE, which is likely crucial for understanding the ongoing processes. The cause for MREE enrichment in Mn-oxides is as yet uncertain; there is no evincing reason why the MREE would be relatively more incorporated over other REEs (Auer et al., 2017; Byrne & Sholkovitz, 1996; Hannigan & Sholkovitz, 2001; Koeppenkastrop & De Carlo, 1992; Lumiste et al., 2019; Reynard et al., 1999). It is possible that the MREE enrichment stems from relatively less available LREE (already adsorbed onto particles) and HREE (complexed) (Haley et al., 2021).

Cerium in pore water appears straightforward but is likely to be otherwise. There is clearly an Eh threshold that is reached whereby Ce(IV) is reduced to Ce(III), and [Ce] then acts like any other LREE in pore water (Haley et al., 2004). This can best be seen in reducing sediment cores, where the Ce-anomaly reaches a value of ~1.

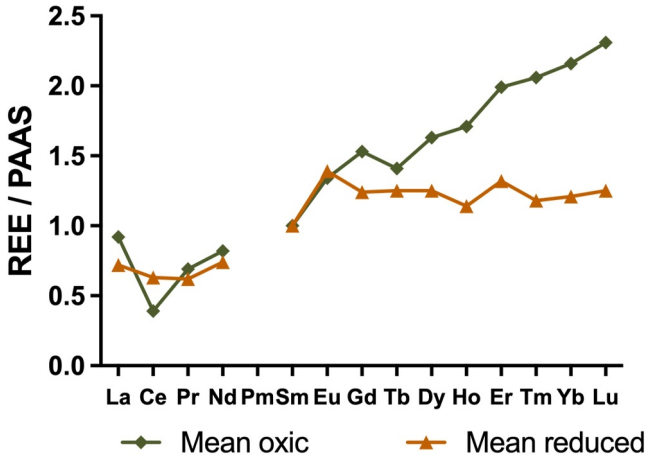

Figure 6. Mean shale-normalized REE pattern of oxic (Abbott, Haley, McManus et al., 2015; Bayon et al., 2011; Deng et al., 2017, 2022; Haley et al., 2004) and reduced pore waters (Abbott, Haley, McManus et al., 2015; Deng et al., 2022; Elderfield & Sholkovitz, 1987; German & Elderfield, 1989; Himmler et al., 2013; J. Kim et al., 2012; Patton et al., 2021; Sholkovitz et al., 1989).

However, in many reducing pore waters, and overlapping oxic pore waters, the Ce-anomaly varies to values <0.2. Cerium concentration appears to be positively correlated to the Ce-anomaly in these oxic and sub-oxic pore waters, which implies that the relative release of solid Ce(IV) phases into pore water is not a true threshold, but a more complex interaction of solid phase Ce (IV), and reduced [Ce(III)] that is reacting and complexing like the other strictly trivalent LREE in solution. This complexity is consistent with observations of microbial mediation (Moffett, 1990) and/or an active role of organic ligands in Ce redox cycling (Kraemer & Bau, 2022). Moreover, as with all relational parameterizations, the Ce-anomaly is a function of its neighboring REE. The geochemical transformations of other LREE will cause the Ce-anomaly to vary even with static [Ce].

Use of neodymium isotopes in pore water offers a means to better determine the mechanisms involved in the source and sink functions of REEs in marine sediments. To date, there are very few observations ($n \sim 30$) on the Nd isotopic composition of pore waters, largely due to the analytical hurdles associated with making these measurements. Pacific margin and slope pore water ε_{Nd} appear to differ from the local bottom water, implying that there is a sedimentary source of "new" REEs in pore water (beyond that which is derived from the water column) (Abbott, Haley, McManus et al., 2015; Du et al., 2022). Mineral dissolution and secondary precipitation have been observed in low-temperature settings on relatively short timescales (R. L. Andrade et al., 2020; Du et al., 2022; Jeandel & Oelkers, 2015; Lacan & Jeandel, 2005; Rousseau et al., 2015; Wilson et al., 2012, 2013). Thus, an immediate suggestion is that dissolution of the more reactive volcanic minerals drives the source of this "new" REE component, which is consistent with the more radiogenic ε_{Nd} of the available data (Abbott et al., 2016; Abbott, Haley, McManus et al., 2015). The North Atlantic, however, shows evidence for the input of less-radiogenic benthic Nd (Du et al., 2022). How extensive this "new" REE source is and what it consists of are active questions that will have important implications for interpretations of both modern and past ocean REE and ε_{Nd} compositions.

Deep sediment (>1 m) pore water REE data are few, but indicate that REEs continue to react/fractionate during late stage diagenesis, at the sulfate:sulfide and methane fronts for instance (J. H. Kim et al., 2016). The dissolved REE will certainly reflect concomitant changes in the solid phase REE, which in turn may be preserved in sedimentary rock records and thus used as tools to understand depositional histories. Curiously, no pore water has as yet been found showing a relative MREE depletion (normalized to shale), one that might indicate loss to solid phases.

There are clearly many outstanding questions regarding marine sediment REEs, even fundamental questions such as: what are the relative roles of Mn-Oxides and phosphates—perhaps barites as well (Guichard et al., 1979; Haley & Klinkhammer, 2003; Martin et al., 1995)—as either sink or source terms to the ocean? What is the source of "new" REEs observed in sedimentary pore water? Is water column scavenging of REEs reversible or irreversible? Further emerging questions have yet to be properly posed, such as the possible effects of low-temperature recrystallization of minerals on the REE (especially that of the transition of the Mn-oxides birnessite to todorokite) (Atkins et al., 2014, 2016). Resolving these processes will also help us better understand the alteration of original signals to enable the use of REEs as tracers of past oceans (Bayon et al., 2004; Cao et al., 2022; Elderfield & Sholkovitz, 1987; Osborne et al., 2017; Palmer & Elderfield, 1986).

In summary, the sediment-water interface is a dynamic exchange interface for REEs. More than a simple sink, marine sediments seem to act also as a source for recycled water column REEs and a source of "new" REEs to the oceans. The magnitude of the source from all sediments appears to be greater than other estimates for terrestrial REE inputs and is especially significant in reducing sediments. The mechanisms for the recycling of water-column-scavenged and the generation of "new" REEs in marine sediments are still uncertain but appear in part to have strong ties to Mn-oxide redox cycling and POM remineralization. Improving our understanding of marine sediment REEs will help better define the budget of REEs in the ocean, likely helping to resolve the "Nd paradox" and provide better constraints on interpretations of modern and past marine REE and ε_{Nd} data, as well as

informing us on the economic/societal potential of deep sea sediment-hosted REEs (Hein et al., 2020; Ijiri et al., 2018; Kato et al., 2011; Ohta et al., 2016; Takaya et al., 2018).

2.4. Ocean

REE distributions in the ocean result from inputs from various sources previously detailed (i.e., rivers, SGD, sediment remobilization at the margins and bottom of the ocean, atmospheric deposits, and hydrothermal sources), advection by water masses and transformations in the water column (i.e., internal cycle). The processes influencing the internal cycle of REEs in the ocean encompass exchanges between dissolved and particulate phases: absorption, adsorption co-precipitation with authigenic minerals, desorption, remineralization, and particle dissolution. As particles represent the only oceanic sink for chemical elements, it is essential to identify and quantify these processes to estimate the oceanic mass balance of not only REE, but of all elements.

In the ocean, absorption occurs when REEs are incorporated into particles during their formation, particularly during primary production. There are two proposed pathways for REE incorporation: one involving methanotrophic bacteria and the other in diatom frustules. Methanotrophs can use REEs to replace calcium for catalyzing methane transformation (Keltjens et al., 2014), resulting in REE depletion in surface waters, which has a more pronounced effect on LREE (Bayon, Lemaitre, et al., 2020; Meyer et al., 2021; Shiller et al., 2017). Regarding frustules, Akagi et al. (2011) and Lagarde et al. (2020) have observed a HREE enrichment in comparison to LREE in particles that are significantly enriched in siliceous material. Akagi et al. (2011) made this observation with the siliceous fraction of settling particles in the Bering Sea and North Pacific Ocean corrected for the dominant terrigenous fraction, whereas Lagarde et al. (2020) conducted similar analysis on total particles in the Irminger and Labrador Seas during a declining diatom bloom. Akagi (2013) suggested a preferential incorporation of HREE driven by the fact that REE-H_3SiO_4 complexes are stronger for HREE than LREE. This calculation is based on formation constants established by Thakur et al. (2007) and Jensen and Choppin (1996), which have been significantly reassessed at a lower level by Soli and Byrne (2017) and Patten and Byrne (2017). Thus, the proportion of REE-H_3SiO_4 complexes established by Akagi (2013) appears to be greatly overestimated. To date, the connection between REEs and silica remains unclear, and a subject of debate.

Adsorption can occur on various constituents, including organic matter (Byrne & Kim, 1990; Zoll & Schijf, 2012), calcium carbonate (Palmer, 1985), opal, and Fe-Mn oxides/oxyhydroxides (Bau & Koschinsky, 2009; Ohta & Kawabe, 2001; Palmer & Elderfield, 1986). Even though Fe-Mn oxides/oxyhydroxides are recognized as major players in REE scavenging (Bau, 1999; Bau et al., 1996; Palmer & Elderfield, 1986; Schijf et al., 2015; Tachikawa, Jeandel, Vangriesheim, & Dupré, 1999), their role in the fractionation of REEs is not yet clearly established. There is evidence of a preferential adsorption of LREE by Fe hydroxides (Bau, 1999; Koeppenkastrop & De Carlo, 1993; Kuss et al., 2001; Schijf & Marshall, 2011) and by Mn oxides, which correlates with Particulate Organic Carbon (POC) concentrations and may result from bacterial activity (Kuss et al., 2001; Ohnuki et al., 2008). Conversely, Ohta and Kawabe (2001) found significant preferential adsorption of LREE on Mn oxides, which was not observed for Fe hydroxides in laboratory experiments. Among the REEs, Ce exhibits distinct behavior due to its additional oxidation state. In the ocean, its redox cycle is strongly linked to the Mn cycle (Bau & Dulski, 1996b; Elderfield, 1988; Moffett, 1990, 1994). Cerium oxidation can occur through abiotic processes, catalyzed by manganese oxides (Bau, 1999; Byrne & Kim, 1990; Koeppenkastrop & De Carlo, 1992) or through biotic processes, where microbial activity catalyzes it at the surface of particles (Moffett, 1990, 1994). The resulting Ce(IV) is sparingly soluble, leading to a Ce enrichment in particles compared to other REEs and a Ce depletion in seawater (Elderfield, 1988; Tachikawa, Jeandel, Vangriesheim, & Dupré, 1999). The role of Fe hydroxides in Ce scavenging is less clear. Bau and Koschinsky (2009) observed pronounced scavenging of Ce by both MnO_2 and $Fe(OH)_3$ in ferromanganese crusts. However, experiments involving the addition of REEs during Mn oxide and Fe hydroxide precipitation showed little (Davranche et al., 2004) or no evidence of preferential Ce scavenging by Fe hydroxides (De Carlo et al., 1997; Koeppenkastrop & De Carlo, 1992; Ohta & Kawabe, 2001; Quinn et al., 2006; Schijf & Marshall, 2011).

Organic matter displays slightly negatively charged sites that can adsorb REEs. Adsorption on plants has been reported in several studies (M. Costa et al., 2020; de Sena et al., 2022; Pinto et al., 2020; Ramasamy et al., 2019; Santos et al., 2023), revealing a preferential LREE adsorption. Additionally, preferential HREE adsorption has been observed on bacterial cells (Moriwaki et al., 2013; Moriwaki & Yamamoto, 2013; Takahashi et al., 2005; Tsuruta, 2006). Haley et al. (2014) used the term "bio-active pool" to describe the influence of biological

processes observed in the distribution of dissolved REEs, which is attributed to bacterial activity. Sutorius et al. (2022) demonstrated, by incubation experiment, that the development of phytoplanktonic and associated bacterial development significantly impacts REE distribution through sorption processes and complexation with organic matter, although this effect is only observed during bloom periods.

REEs can also be transferred to the particulate phase via co-precipitation with authigenic minerals such as rhabdophane (Pearce et al., 2013). Besides, there is also the possibility of co-precipitation of Ce with Mn oxides with different kinetics (Moffett, 1990, 1994).

The processes responsible for transferring REE from the particulate to the dissolved phase include: (a) desorption from particles (R. L. Andrade et al., 2020; Elderfield, 1988; Hara et al., 2009; Nozaki & Alibo, 2003; Sholkovitz et al., 1994), resulting in the enrichment of LREE in the dissolved phase due to their preferential adsorption; (b) particle disaggregation and dissolution (Byrne & Kim, 1990; Elderfield, 1988; Nozaki & Alibo, 2003; Sholkovitz et al., 1994; Stichel et al., 2015), and (c) remineralization of organic matter (Hara et al., 2009). As previously mentioned, the overall balance favors the preferential adsorption of LREE to HREE on particles, due to a competition between surface and solution complexation processes which each favor the HREE (Byrne & Kim, 1990; Elderfield, 1988; Elderfield et al., 1990; Elderfield & Greaves, 1982; Sholkovitz et al., 1994; Tachikawa, Jeandel, Vangriesheim, & Dupré, 1999), that are in higher proportion as free cations (Koeppenkastrop et al., 1991; Schijf et al., 2015; Sholkovitz et al., 1994). This scavenging effect is particularly pronounced for Ce as detailed above.

The particle-solution dynamics result in the nutrient-like distribution of REEs, which is strongly influenced by particle dynamics and explained by scavenging (Alibo & Nozaki, 1999; Garcia-Solsona et al., 2014; Haley et al., 2017; Nozaki & Alibo, 2003; Oka et al., 2021; R. Wang et al., 2021). There is currently active discussion on the nature of this scavenging, whether it is reversible or not (Haley et al., 2017; Siddall et al., 2008), a distinction that has a critical bearing on how REE and ε_{Nd} are distributed in the oceans. For example, POM will remineralize in the water column, which has a different geochemical imprint on dissolved REE than Mn-oxide, which should not be prone to dissolution in oxygenated seawater. This results in a correlation between REE and nutrient distributions, observed with dissolved silica (de Baar et al., 1983; Elderfield, 1988; Garcia-Solsona et al., 2014; Hathorne et al., 2015; Pham et al., 2019; van de Flierdt et al., 2016; X. Y. Zheng et al., 2016), and to a lesser extent with phosphate and nitrate anions (de Baar et al., 2018; Garcia-Solsona et al., 2014; Hathorne et al., 2015). This correlation with silica is not observed everywhere in the ocean (de Baar et al., 2018; X. Y. Zheng et al., 2016), and suggests that REE and nutrient cycles are not coupled but are influenced by particle dynamics according to different processes, namely production and remineralization for nutrients, and reversible scavenging dependent on particle concentrations for REE (de Baar et al., 2018; Elderfield et al., 1988). At depth, distributions of re-generated nutrients and REEs released from particles would be correlated, mainly depending on the mixing of water masses (Osborne et al., 2017; van de Flierdt et al., 2016; X. Y. Zheng et al., 2016). The better correlation with silica compared to other nutrients could be explained by its better preservation in particles (de Baar et al., 2018), phosphate and nitrate remineralization being faster than REE enrichment by reversible scavenging. So far, the impact of phytoplankton and bacteria on the REE cycle remains unclear at a global scale, and the mechanisms behind it are far from being understood.

In addition to reversible scavenging and lithogenic/benthic inputs, the distributions of REEs depend on circulation, making them valuable tracers for these processes (de Baar et al., 2018; X. Y. Zheng et al., 2016). While REEs are suitable tracers for dissolved-particle exchanges, their optimal utilization requires either analyzing them in both phases or extracting the non-conservative fraction of the dissolved signal (X. Y. Zheng et al., 2016) in addition to analyzing dissolved normalized patterns.

Among the REEs, Nd is studied more broadly through its isotopic composition (εNd). Figure 7 shows a compilation of Nd concentration and IC in the global ocean (van de Flierdt et al., 2016). The clear variation in Nd isotopic composition between the 3 major ocean basins is not reflected in dissolved concentrations, which are more evenly distributed between the basins. This observation led to the "Nd Paradox", missing term and "BE" concepts. Indeed, the recognition of the Nd paradox challenged the idea that rivers and atmospheric inputs are the main sources of REEs to the ocean, as these inputs are not sufficient to reconstruct the isotopic gradient observed between the Atlantic and the Pacific (Albarède et al., 1997; Jeandel & Peng, 1989; Tachikawa et al., 2003). Indeed, most large rivers and dust-reaching the Pacific have negative εNd values, approximately −10, poor in ^{143}Nd (Goldstein et al., 1984; Goldstein & Jacobsen, 1988b; Jones et al., 1994; Nakai et al., 1993). It is important

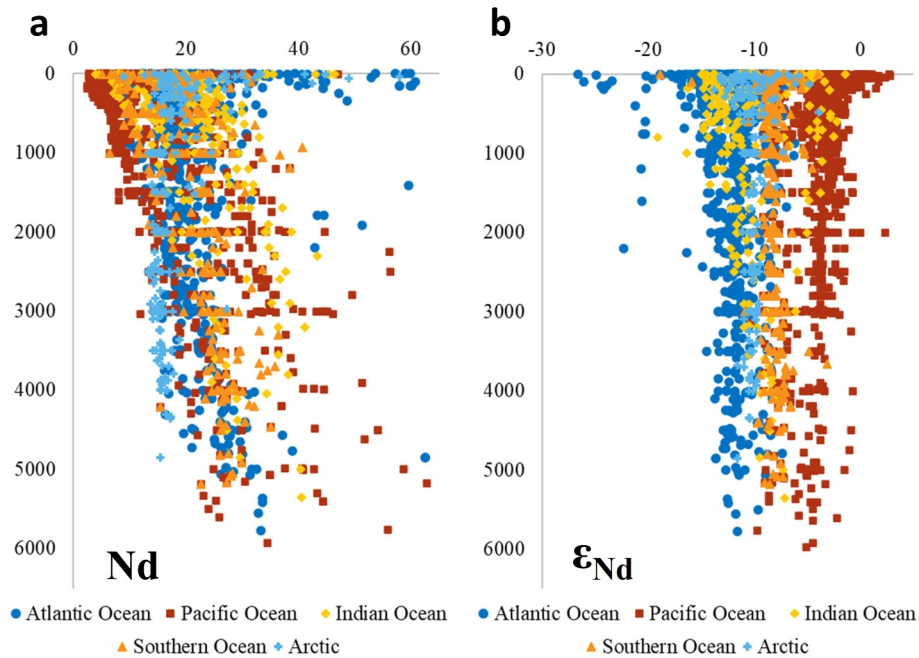

Figure 7. Global ocean compilation of (a) dissolved Nd concentrations and (b) corresponding Nd isotopic composition (εNd). Data extracted from van de Flierdt et al. (2016), Filippova et al. (2017), Crocket et al. (2018), Paffrath et al. (2021) and Pham et al. (2022).

to note that changing the isotopic composition of water masses along their paths requires large inputs of elements, that is, doubling the variation in Nd concentration between the Atlantic and Pacific did not reflect the sheer number of inputs required to change the Nd isotopic composition. Researchers then began to suspect that ocean margins, whose significance was often mentioned but not quantified in terms of element mass balance calculations in the ocean, could play an important role in the observed variations of isotopic signatures (Jeandel et al., 1998; Lacan & Jeandel, 2001; Tachikawa et al., 2003). They believed that by using isotopes, they could quantify this role. Figure 8 presents a compilation of the margin Nd isotopic composition. A comparison with Figure 7 reveals that seawater tends to imprint the Nd isotopic composition of the surrounding continents, with the least and most radiogenic values in the Atlantic and in the Pacific, respectively (Garcia-Solsona et al., 2014; Grenier et al., 2013; Jendeal et al., 1998; Lacan & Jeandel, 2001, 2005; Lambelet et al., 2016; Tachikawa et al., 2003; Wilson et al., 2012). In addition, REEs are about 6 orders of magnitude more concentrated in rocks (μmol/kg, Rudnick & Gao, 2003) than in seawater (pmol/kg, Figure 7). Thus, margin inputs are a good candidate to explain Nd isotopic composition variation along the thermohaline circulation. This was confirmed by measurements conducted in hydrographically invariant water masses that showed Nd isotopic composition variations together with rather constant Nd concentrations (Lacan & Jeandel, 2001, 2005; Tachikawa et al., 2003). Away from the margins and the sources they represent, εNd behaves as a conservative tracer and its value is only influenced by the mixing of water masses (Jeandel, 1993; Piepgras & Wasserburg, 1982; von Blanckenburg, 1999). Consequently, it becomes a tracer of the mixing of water masses, with its evolution linked to the thermohaline circulation (Figure 7).

To explain this, one must pose that there is an input of Nd with a sufficiently different isotopic composition compared to seawater to significantly modify the latter. This input is likely to be quickly followed by the removal of Nd through adsorption onto marine particles. This process will decrease the Nd concentration in the water while retaining the isotopic signature resulting from the recent Nd addition. The element exchanges at the margins lead to the "Boundary Exchange" concept (Lacan & Jeandel, 2005), which involves the transfer of elements/isotopes across the interface separating seawater from sediments and rocks. Margin boundary processes include SGD inputs, partial dissolution of lithogenic sediments and benthic flux. This assumption was supported by observations of at least six continental margins (Lacan & Jeandel, 2005), then discussed and confirmed by more recent studies (Basak et al., 2015; Garcia-Solsona et al., 2014; Grenier et al., 2013; Lambelet et al., 2016; Rickli et al., 2014; Wilson et al., 2012). So far, the "Boundary Exchange" flux is not well constrained, and could

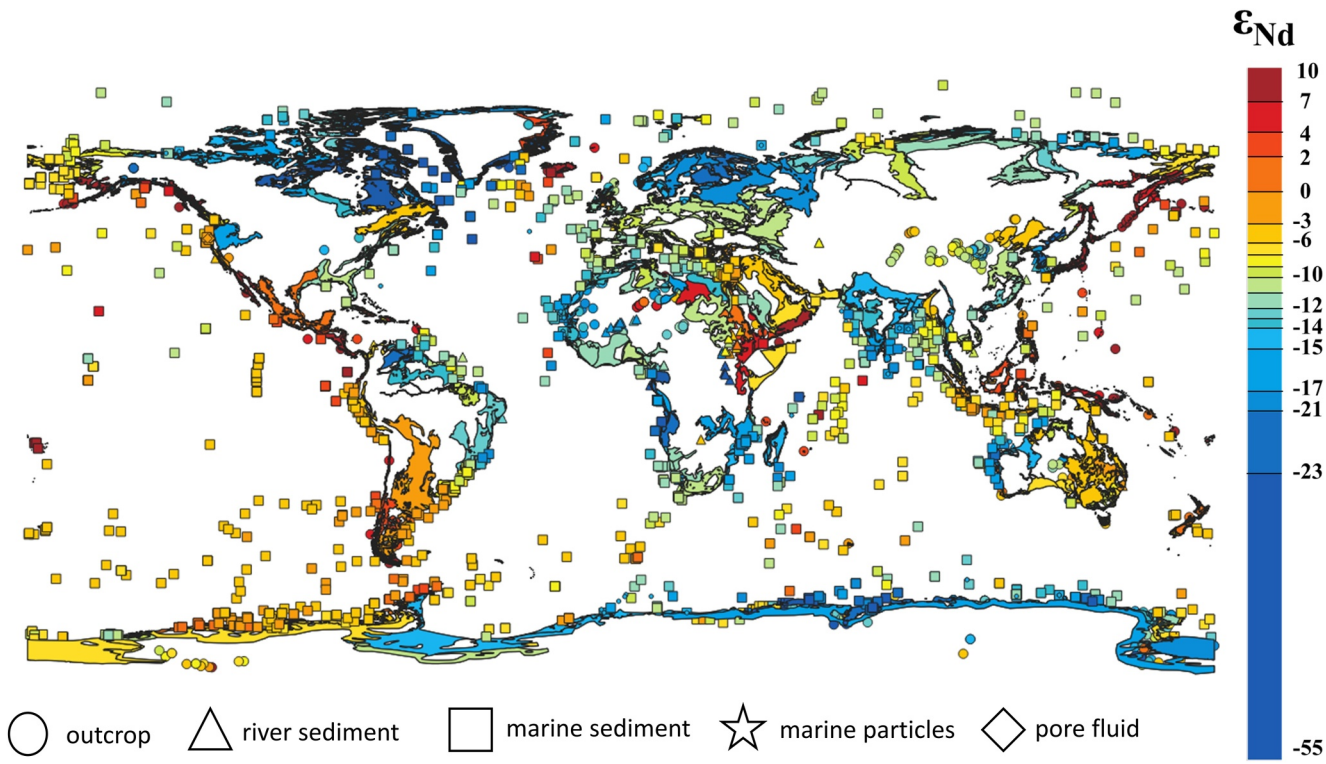

Figure 8. εNd in geological outcrops (dots), river sediment (triangles), marine sediment (squares), marine particles (stars), pore fluids (diamond), and interpolated continental εNd from the measured data. Data and interpolation method from Robinson et al. (2021).

contribute to offset the missing flux to balance the Nd oceanic budget, estimated at 8×10^9 g/y (Tachikawa et al., 2003).

The Nd isotopic composition also appears to trace the influence of hydrothermal vents in mid-oceanic ridges, as indicated by changes in isotopic composition without changes in concentration (Chavagnac et al., 2018; Jeandel et al., 2013; Stichel et al., 2018). However, these results are still to be confirmed. Atmospheric dust also influences the isotopic composition of surface waters by dissolution (van de Flierdt et al., 2016). Their role has been demonstrated by modeling in the Mediterranean, where the atmospheric flux is high (Ayache et al., 2023).

In addition to field observations and mass balance calculations, the impact of "Boundary Exchange" on the global balance of Nd has been tested by coupling the assumed exchanges at margins into various general ocean circulation models (Gu et al., 2017; Rempfer et al., 2011; Siddall et al., 2008; Tachikawa et al., 2003) and regional models (Ayache et al., 2023). These models demonstrate that "Boundary Exchange" plays a dominant role in supplying Nd to the ocean, surpassing rivers and dust inputs by an order of magnitude (10^9 vs. 10^8 g Nd.yr^{-1}) (Rempfer et al., 2011; Tachikawa et al., 2003). Ayache et al. (2023) estimated that the marginal inputs represent ~80% of total Nd supply to the Mediterranean Sea. By dissolving only a small fraction (~0.1% to 3%, required by the model), substantial Nd inputs can be generated (Tachikawa et al., 2003). These models better simulate dissolved Nd concentrations when scavenging is reversible rather than irreversible, and also underscore the sensitivity of the models to the parametrized distribution of Nd between dissolved and particulate phases (Arsouze et al., 2009; Gu et al., 2017; Rempfer et al., 2011; Siddall et al., 2008).

"Boundary Exchange" processes are likely more intense in the first 500 m along the margins than in the abysses. It is probable that, due to the dynamics of more violent surface currents and internal tides, greater fluxes of particles together with faster and more efficient exchange processes occur in the upper 500 m than at depth (Barbot et al., 2022). Thus, the occurrence of clouds of suspended particles created by currents and undersea storms may also generate exchanges in deep water. If the processes responsible for generating "Boundary Exchange" (including their kinetics) are not explicitly described by field balances or models, the presumed dissolution of the lithogenic material implies that submarine alteration has occurred. Singh et al. (2012) demonstrated in the Bay of

Bengal that inputs of dissolved Nd released from sediments deposited by the river affect intermediate and deep waters. Similarly, the dissolution of labile phases of river-borne lithogenic sediments from the Mississippi River likely controls the Nd isotopic composition of the Gulf of Mexico (Adebayo et al., 2022). In the South China Sea, Y. Huang, Wu, and Hseu (2023) found that the seawater Nd isotopic composition was more effectively altered by pedogenic minerals from Chinese tropical soils, whereas the sediment from the Taiwan margin, consisting of fresh detrital material resulting from intense physical erosion of the Taiwan Island, had no significant impact. The relative influence of the different sediment and mineral-associated phases and their alteration still need to be understood.

In short, the study of REEs in the ocean reveals a complex interaction of various sources and processes influencing their distribution. From rivers to hydrothermal vents, these elements undergo absorption, desorption, co-precipitation, and remineralization, shaping their partitioning between dissolved and particulate phases. Conversely, this distribution can be traced back to the processes that determined it. The use of Nd isotopic composition (εNd) emerges as a crucial tracer, allowing the disentanglement of the relative importance of different sources of REE to the ocean: sediment deposited on ocean margins, hydrothermal activity, and atmospheric inputs. The concept of 'Boundary Exchange' underscores significant fluxes of REE across the seawater-sediment interface, with profound implications for oceanic budgets (not just REE) and circulation models. Both modeling efforts and empirical observations emphasize the dominant role of "Boundary Exchange" in supplying REEs to the ocean, with notable contributions from processes such as the dissolution of lithogenic material from rivers and submarine alteration, which significantly impact seawater Nd isotopic composition.

3. Anthropogenic Impacts on REE Distribution

Due to their remarkable catalytic, phosphorescent, and magnetic properties, REEs can significantly enhance a number of products and find applications in a wide range of fields, including industry, technology, agriculture, and medicine (Balaram, 2019; Gwenzi et al., 2018; Yuksekdag et al., 2022). Because of the increasing utilization of REEs over the past few decades, they are now considered emerging contaminants. Differentiating between contaminated and naturally enriched sites poses a substantial challenge (Kulaksiz & Bau, 2007; Nigro et al., 2018).

3.1. Sources of Anthropogenic REE

Solid wastes, wastewaters, and air emissions from mining and mineral processing are substantial anthropogenic sources of REE (Gomes et al., 2022; Gwenzi et al., 2018; Ladonin, 2017; Lai et al., 2023; Lima & Ottosen, 2021; W. Liu et al., 2019; Massari & Ruberti, 2013; Schüler et al., 2011; Zapp et al., 2022). REE mining can also produce radioactive pollution, primarily from thorium and uranium (Kotelnikova et al., 2021; Massari & Ruberti, 2013). Another problem associated with the mining that is, acid mine drainage (AMD), known for releasing sulfuric acid, potentially toxic elements such as zinc (Zn), nickel (Ni), and copper (Cu), also increases the total content of REEs as well as the content of acid-soluble REEs (Ladonin, 2017). AMD-contaminated waters can have REE concentrations exceeding that of neutral freshwaters by 2–3 orders of magnitude and enrichment in MREEs (Gomes et al., 2022).

Certain industries have been applying REEs in their processes for decades when environmental contamination by REEs was still not a concern. For instance, sediments along the California coast have been contaminated with REEs since the 1960s due to petroleum-cracking catalysts and related by-products (Olmez et al., 1991). More recently, Kulaksiz and Bau (2013) also reported river water contamination with La and Sm due to industrial cracking catalyst production effluents. Fossil-fuel combustion and waste incineration have caused REE input to the soil, water, and air in the past several decades (Işıldar et al., 2018; Tan et al., 2015).

A recent study detailed the influence of historical steel-making processes on the REE composition and mobility in river sediment cores (Hissler et al., 2023). The disposal of industrial waste from steel production led to alterations in the shale normalized ratios of La/Lu and Y/Ho, as well as the enrichment of Eu, Yb, Sm, Ce, and Tm. Additionally, Hissler et al. (2023) demonstrated that REEs in contaminated sediments are more mobile compared to particles originating from soil erosion. Regions near steel plants can also be relatively enriched in Nd compared with other areas (Geagea et al., 2007; Hissler et al., 2008, 2016).

Recent applications of REEs in the technology industry, including superconductivity products, batteries, wind turbines, nuclear reactors, solar panels, permanent magnets, and cathode ray tubes, also contribute to contamination (L. Ma et al., 2019; L. Ma & Wang, 2023). For example, L. Ma & Wang (2023) identified Sm anomalies close to a permanent magnet industry. L. Ma et al. (2019) earlier found positive anomalies of Pr, Nd, Dy, and Ho in the same river, indicating the impact of REE recycling and other industrial activities in the area.

REEs possess exceptional properties useful for medical applications, including exhibiting potential antimicrobial activities comparable to copper (Cu) (Wakabayashi et al., 2016). Gadolinium is widely used as a contrast agent (Gd-CA) for magnetic resonance imaging (Bau & Dulski, 1996a; Raymond & Pierre, 2005; Telgmann et al., 2013). Gd-CAs, being stable and non-reactive, can pass through wastewater treatment and enter natural aquatic environments, leading to increased Gd concentrations in waters nearby densely populated areas with advanced healthcare systems, as shown in the pioneering work by Bau and Dulski (1996a). Temporal studies have reported 2 to 13-fold increases in anthropogenic Gd concentrations in the last decades in the Garonne River in France (Lerat-Hardy et al., 2019), and in coastal waters of California, USA, respectively (Hatje et al., 2016). Pedreira et al. (2018) estimated that biomedical applications in Brazil in 2016 discharged up to 2 kg Gd d^{-1} into the Atlantic Ocean. Anthropogenic Gd has also been detected in lakes, groundwater, and tap water all around the world (e.g., Brünjes & Hofmann, 2020; Johannesson et al., 2017; Kulaksiz & Bau, 2011; Y. Liu et al., 2022; Merschel et al., 2015).

The REE-based fertilizers are a source of REE to soils (e.g., Bispo et al., 2021; Hu et al., 2006; F. B. V. Silva et al., 2019). However, data about the REE content in agricultural supplies worldwide are still limited, with most studies focusing on La, Ce, or REE mixtures and their effects on a few plant species (Tommasi et al., 2021). The amount of REE in fertilizers depends on the phosphorus content and source and the industrial process involved in the fertilizer manufacture (F. B. V. Silva et al., 2019; Turra et al., 2011). China, the largest REE-fertilizer consumer, employs between 50 and 100 million tons of REE oxides in agroecosystems, whereas Brazil, the world's fourth consumer of fertilizers, applies ∼13,000 tons of REE annually to soils (F. B. V. Silva et al., 2019). Considering that the REE supplied by fertilizers is much more soluble and reactive than the regular soil pool (Tyler, 2004), this continuous practice may pose a risk to agricultural sustainability. Additionally, the production of phosphate fertilizers emits anthropogenic REEs into the environment, with phosphate plants contributing to substantial REE discharges (El Zrelli et al., 2021; Volokh et al., 1990). El Zrelli et al. (2021) estimated that a single phosphate fertilizer plant on the coast of Tunisia discharges annually up to 1,500 tons of REEs into the marine environment. The negative impacts of substantial REE inputs to soils extend beyond plants, as evidenced by correlated Sm anomalies ranging from 6 to 20 in the lakes of Wuhan due to agricultural activities (Y. Liu et al., 2022). Furthermore, positive Pr anomalies reported in estuarine sediments from Brazil were attributed to the manufacturing of monoammonium phosphate, a fertilizer product largely commercialized in Brazil (L. Costa, Mirlean. et al., 2021).

As the world continues to address the urgent need for decarbonization and transition to renewable energy sources, REEs have emerged as critical components in various technologies, such as electric vehicles, magnetic refrigeration, fluorescent lamps, nuclear reactors, and wind turbines (Evans et al., 2022; Pavel et al., 2017; Zhou et al., 2016). Although these alternatives offer substantial environmental benefits, their widespread adoption raises concerns about the potential pollution problems associated with the extraction, production, and disposal of REE products. In the scientific community, there are concerns about the future disposal of electric vehicle batteries and Nd-based permanent magnets when they reach the end of their life cycle. Although efforts are being made to develop efficient recycling systems (e.g., Binnemans et al., 2013, 2015; Nancharaiah et al., 2016), the sheer volume of these materials expected to reach the end of their life cycle in the coming decades poses a significant challenge. Improper disposal and dismissal of the entire lifecycle of these products could result in REEs and other metals leaching into the environment. Further research is still needed to understand the pathways and consequences of the anthropogenic inputs of REEs, as well as their large-scale and long-term implications for the environment and human health (F. Silva et al., 2019; Tariq et al., 2020; Tommasi et al., 2021).

3.2. Bioavailability, Bioaccumulation and Biomagnification

REE are found in organisms across various kingdoms, including Animalia, Plantae, Fungi, Protista, Bacteria, and Monera (Barrat et al., 2022; Brito et al., 2021; Chistoserdova, 2016; de Sena et al., 2022; Espejo et al., 2023; Liang & Shen, 2022; Marginson et al., 2023; Merschel & Bau, 2015; Ponnurangam et al., 2016; Santos et al., 2023;

Zocher et al., 2018). With the increase in anthropogenic activities, the input of REEs into the environment has risen, making it crucial to understand the processes that regulate their uptake by organisms and transfer across the food web. Additionally, it is crucial to understand the impact of their presence on biological systems, considering both individual and community levels.

REE toxicity within the lanthanide group is not uniform. Some studies indicate that free REE toxic levels vary with atomic weight, and LREE promote higher toxicity than HREE, possibly due to the higher stability constants of the heavier elements (Blaise et al., 2018; Gonzalez et al., 2014; Lin et al., 2022). REE may cause various adverse effects, such as phytotoxicity, neurotoxicity, genotoxicity, cytotoxicity, endocrine disruption, and oxidative stress (Blaise et al., 2018; Y. Liu et al., 2019; Pagano et al., 2016; Xu et al., 2017). However, the ecological and human risks of REEs depend on their concentrations, chemical form, species sensitivity, age of the organism, route and duration of exposure, and interaction with other environmental factors (Badri et al., 2017; Gonzalez et al., 2014; C. Guo et al., 2020; Gwenzi et al., 2018; Souza et al., 2021; Tommasi et al., 2023; X. Zhang et al., 2022).

The toxicity of an element or its potential to have an adverse effect on organisms or ecosystems largely depends on its bioavailability. Bioavailability refers to the fraction of an element present in an environmental compartment that is available to cross an organism's cellular membrane (Luoma, 1983, 1989). After crossing the membrane, storage, transformation, degradation, and assimilation can occur within the organism. If a net accumulation of a contaminant in an organism from all possible intake routes, including water, air, and diet, occurs, the contaminant bioaccumulates in the organism (Chapman et al., 1996). In recent years, some studies have assessed the bioavailability and bioaccumulation of REEs, yielding variable results (Brito et al., 2021; Espejo et al., 2023; Orani et al., 2022; Paper et al., 2023; P. Zhao et al., 2022). Many factors influence the observed variability, and it is important to consider that each study compares the REE content in a specific group of organisms to a different environmental compartment, such as water or sediments/soils. Sediments, freshwater, and seawater, for instance, present very different REE concentrations and fractionation patterns, which influence the results and make direct comparisons between toxicological studies challenging.

Human exposure to REEs may also be a problem. Contamination of tap water by Gd contrast agents (Gd-CAs) has been observed in cities with highly developed healthcare systems, such as Berlin (Bau & Dulski, 1996a; Kulaksiz & Bau, 2011; Schmidt et al., 2019; Tepe et al., 2014), Düsseldorf and München (Schmidt et al., 2019), in Germany, London (UK) (Kulaksiz & Bau, 2011), and Prague (Czech Republic) (Möller et al., 2002). Gd contamination has also been observed in tap water-based popular carbonated soft drinks (Schmidt et al., 2019). Souza et al. (2021) identified high human bioaccessibility of Gd-CAs in tap water (i.e., >77% of Gd released in the gastrointestinal tract, therefore available for absorption), raising concerns about the potential toxicity of these contaminants to the human body when ingested above a certain threshold. On the other hand, Zocher et al. (2022) identified high REE bioaccumulation factors in duckweeds (i.e., three to five orders of magnitude), whereas Gd-CAs were considered unavailable. These contrasting results might exemplify how different biological systems deal with anthropogenic-derived REE species and how the route of intake may influence the bioavailability of these emerging contaminants.

REE bioavailability is specific to each element (Brito et al., 2021; de Sena et al., 2022). Furthermore, a mixture of REEs might show interactions that cause different impacts than individual REEs. Both antagonistic and additive effects have been reported for REE mixtures (Lachaux et al., 2022; E. Morel et al., 2021). Speciation, similar to other metals, plays a key role in REE bioavailability and toxicity. Arciszewska et al. (2022) indicated that bioavailability of dissolved species in aquatic systems decreases from free ions to inorganic complexes and to organic complexes. de Sena et al. (2022) also suggested that speciation of REEs in soils was a determining factor for the bioavailability and REE uptake by seagrasses.

Interactions between soil, plant roots, and microorganisms may increase REE bioavailability (Tyler, 2004; Zaharescu et al., 2017), which could become a concern, especially in areas fertilized with REE minerals or contaminated regions. X. Zhang et al. (2022) observed that REE affect bacterial communities causing reductions in biodiversity and abundance, along with the dominance of bacteria resistant to REE stress and capable of degrading the organic complexes formed by REE mining. Thus, bioavailable REEs exert an impact on the ecosystem and are reciprocally influenced by it.

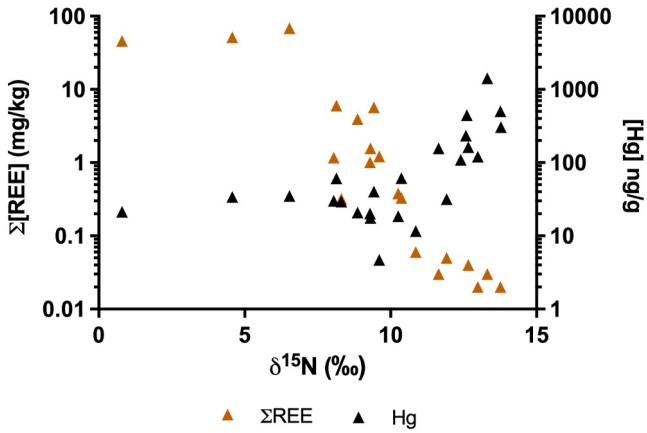

Figure 9. Decrease in the concentration of the total REE and mercury along a trophic web, illustrated by the $\delta^{15}N$. The data indicate that REEs experienced trophic dilution, while Hg illustrates biomagnification. Adapted from Santos et al., 2023.

Some studies have shown species-specific and tissue-specific variations in the bioaccumulation of REEs, both in terms of total concentrations and fractionation patterns (MacMillan et al., 2017; Marginson et al., 2023; Santos et al., 2023; Squadrone et al., 2020). These studies suggest that detoxifying organs, such as the liver and kidneys, may serve as monitoring tissues, given their tendency to accumulate higher concentrations of REE compared to muscle tissue. Furthermore, observations in humans indicate that factors such as gender, age, alcohol consumption, and smoking habits can influence the concentrations and fractionation of REEs (Hao et al., 2015; Wei et al., 2013). These findings highlight the significance of considering ecological, environmental, physiological, and even social factors in the evaluation of REE transfer, accumulation, and distribution for risk assessments and food safety evaluations.

The transfer of REEs across the soil-plant system has been extensively studied, mainly because of its significant application in agriculture. Current findings indicate that the transfer of REEs from the environment to organisms is generally low, although some species (e.g., *Dicranopteris linearis*; H. Zheng et al., 2023) exhibit hyperaccumulation, making them potential candidates for REE mining and bioremediation of polluted sites (Chour et al., 2020; Liang & Shen, 2022; Orani et al., 2022; Paper et al., 2023).

The uptake of REEs from soils depends on various factors such as plant species as well as their growing conditions and the REE content in the substrate (Brioschi et al., 2013; Brito et al., 2021). Total concentrations of REE in soils typically do not serve as reliable predictors of concentrations in plants (Santos et al., 2023). However, uptake is positively correlated with soil acidity, soluble REE soil fractions, and organic matter content (Tyler, 2004). A study by Thomas et al. (2014) indicated that under more acidic conditions, the uptake and toxicity of REEs to terrestrial plants increased. In aquatic environments, REE bioaccumulation has been linked to lower pH levels and higher ratios of REE to dissolved organic carbon and free ion REE concentrations (Macmillan et al., 2019).

An important aspect that must be investigated when dealing with emerging contaminants like the REE is their trophic transfer capacity, which could lead to biomagnification or biodilution. However, this topic has been insufficiently studied thus far with regards to the REEs. The few available reports in the literature for aquatic and terrestrial ecosystems suggest not only a low potential for biomagnification of REEs but also a trend of biodilution across food webs (Amyot et al., 2017; MacMillan et al., 2017; Marginson et al., 2023; Santos et al., 2023; Squadrone et al., 2018). Biodilution is characterized by the decline in the concentration of REEs along the food web due to intake and elimination processes, resulting in a net loss of REEs from prey to predators, as illustrated in Figure 9. This behavior is opposite to that experienced by mercury (Hg) within the same trophic chain. From a human perspective, this finding is positive. However, given that REEs are emerging contaminants (Gwenzi et al., 2018; Hatje et al., 2014; Souza et al., 2021; Tepe et al., 2014), there are still knowledge gaps concerning their behavior and toxicity that need to be addressed to establish environmental and food safety thresholds for these elements.

3.3. REE and Anthropogenic Environmental Changes

The toxicity, bioavailability, bioaccumulation, reactivity, and fate of the REE are sensitive to environmental physico-chemical conditions. Co-occurrence of trace contaminants and other anthropogenic stressors such as climate change (CC) drivers (e.g., warming, altered precipitation patterns, deoxygenation, acidification, extreme events, changes in ocean circulation and mixing) can amplify the effects of contaminants on the ecosystem health, services, and functions (Hatje et al., 2022). These stressors may alter bioaccumulation and toxicity patterns, thereby influencing organism's responses (Boukadida et al., 2016; Leite et al., 2020, 2023) and potentially compromising food security.

Recent attention has been given to the effect of CC drivers on trace elements (Cabral et al., 2019; Gwynn et al., 2024; Hatje et al., 2022; Jin et al., 2021; Pan et al., 2023). However, studies specifically concerning the effects of CC drivers on REEs are scarce. Additionally, the impacts of temperature, pH, and salinity shifts on REE

geochemistry have received more attention than other drivers such as sea-level rise, acidification, deoxygenation, and extreme events. For example, an increase in temperature from 17 to 21°C has been observed to increase Nd accumulation in *Mytilus galloprovincialis*, possibly associated with a slight decrease in detoxification capacity (GSTs activity; Leite et al., 2023). A recent study involving the same species found that the interaction between Pr and elevated temperatures resulted in histopathological injuries, redox imbalance, and cellular damage (Leite et al., 2024). These findings align with the results observed for mussels exposed to Ce oxide nanoparticles and mercury at increased temperatures (Morosetti et al., 2020). However, the warmer temperatures did not cause more damage to mussel gills than Nd and temperature acting separately (Leite et al., 2023). On the other hand, Nd and temperature had a higher impact on mussel digestive tracts (Leite et al., 2023). The impact on organisms may not only depend on the emerging interactions between contaminants and CC drivers (e.g., temperature rise during a heat wave) but also on the exposure duration (Leite et al., 2020, 2023). Higher temperatures may facilitate the elimination of certain contaminants (Figueiredo et al., 2022; Maulvault et al., 2018). For example, La elimination by *Spisula solida* was more efficient under higher temperatures than under control conditions (Figueiredo et al., 2022).

Salinity, which can vary under changing precipitation, evaporation scenarios, or ice melting due to CC, is another important factor. Salinity influences metal speciation, metal bioavailability, and organism metabolism. Higher salinity has been shown to increase metal uptake in marine mussels due to a decrease in chloride complexation, leading to increased free metal ions (Campbell, 1995). Low salinity may also cause higher metabolism, favoring contaminant accumulation (Freitas et al., 2020). A recent study showed that higher metabolism of bivalves at salinity 20 enhanced the accumulation of La and was closely related to the organisms' biochemical performance (i.e., antioxidant activity and biotransformation defenses activation) and cellular damage (M. Andrade et al., 2021). The dual stress from increased salinity and La concentrations may overwhelm the defense mechanisms and this combination may also cause neurotoxicity (Andrade et al., 2021).

Climate-induced events, such as drying of tailing piles, drier soils, and lowering of the water table, may expose sulfidic minerals to oxic conditions, resulting in prolonged periods of baseflow with lower pH and higher solute concentrations (Rue & McKnight, 2021). In such conditions, REEs may be mobilized through primary weathering of sulfide and silicate minerals. Rue and McKnight (2021) showed that REE concentrations and fluxes increased with increasing air temperature over the past 30 years. This new contribution of REEs raises concerns for aquatic ecosystems and the quality of drinking water sources. However, no drinking water quality standards exist for REEs, and questions remain regarding exposure thresholds for impacts on aquatic life and human health.

Although there are significant knowledge gaps, it is expected that the CC drivers of concern for radionuclides (Gwynn et al., 2024) and toxic metals will impact REEs in similar ways. For instance, the surface pH of seawater will decrease by 0.1–0.4 units (Cooley et al., 2022) and will impact the speciation, bioavailability, and overall biogeochemical behavior of trace elements. Metals that form strong complexes with carbonates, phosphates, and silicates, such as REEs, will be strongly affected by changes in pH, resulting in an increase in their free ionic forms. The free form of REEs will increase by 15%–24% under more acidic conditions (Millero et al., 2009).

The interaction of REEs with CC and other anthropogenic drivers could lead to significant impacts at high biological levels. A better understanding of the emerging interactions between CC and REEs is crucial for predicting future changes across the land-ocean continuum. This comprehension will be instrumental in developing effective measures to protect ecosystems.

4. Conclusions

There is substantial evidence supporting the significant contribution and usefulness of REEs as tracers or proxies in comprehending geochemical processes in both oceanic and terrestrial environments. Although the application of REEs to assess biological processes is still in its early stages, preliminary studies show promising potential. Additionally, REEs can function as micronutrients and contaminants.

Although the sources and sinks of these elements are relatively well understood, the REE mass balance in the ocean is not completely resolved; for instance, the impact of boundary exchange and inputs from SGD need more studies. Besides, it is essential to consider the potential impact of anthropogenic activities and global climate change. Such factors could significantly alter the concentrations, speciation, distribution patterns, and residence time of REEs in environmental compartments.

Moreover, there is a crucial need to investigate the potential health effects of anthropogenic REEs on ecosystems and human health. Therefore, investments aimed at improving our understanding of the life cycle of REEs, from mining and ore processing to the final disposition and recycling of REE products, should be encouraged. This becomes particularly relevant as society transitions to low-carbon energy, where REEs play a key role in electronics production.

In conclusion, further research and awareness are essential to effectively harness the benefits of REEs while mitigating any potential negative consequences. A comprehensive understanding of their behavior and impact is crucial for sustainable and responsible usage of these valuable elements in various sectors.

Data Availability Statement

Data were not used or created for this research.

Acknowledgments
The authors were sponsored by CAPES (RA, Finance Code 001) and CNPq (VH 302477/2022-5). The IAEA is grateful for the support provided to its Marine Environment Laboratories by the Government of the Principality of Monaco. This is UMCES contribution #6374. This work was supported by Fundação para a Ciência e Tecnologia (FTC), through the project EMINENT (2022.08285.PTDC).

References

Abbott, A. N. (2019). A benthic flux from calcareous sediments results in non-conservative neodymium behavior during lateral transport: A study from the Tasman man Sea. *Geology*, *47*(4), 363–366. https://doi.org/10.1130/G45904.1

Abbott, A. N., Haley, B. A., & McManus, J. (2015). Bottoms up: Sedimentary control of the deep North Pacific Ocean's εNd signature. *Geology*, *43*(11), 1035–1038. https://doi.org/10.1130/G37114.1

Abbott, A. N., Haley, B. A., & McManus, J. (2016). The impact of sedimentary coatings on the diagenetic Nd flux. *Earth and Planetary Science Letters*, *449*, 217–227. https://doi.org/10.1016/j.epsl.2016.06.001

Abbott, A. N., Haley, B. A., McManus, J., & Reimers, C. E. (2015). The sedimentary flux of dissolved rare earth elements to the ocean. *Geochimica et Cosmochimica Acta*, *154*, 186–200. https://doi.org/10.1016/j.gca.2015.01.010

Abbott, A. N., Löhr, S., & Trethewy, M. (2019). Are clay minerals the primary control on the oceanic rare earth element budget? *Frontiers in Marine Science*, *6*(AUG), 1–19. https://doi.org/10.3389/fmars.2019.00504

Abdelnour, S. A., Abd El-Hack, M. E., Khafaga, A. F., Noreldin, A. E., Arif, M., Chaudhry, M. T., et al. (2019). Impacts of rare earth elements on animal health and production: Highlights of cerium and lanthanum. *Science of the Total Environment*, *672*, 1021–1032. https://doi.org/10.1016/j.scitotenv.2019.02.270

Adebayo, S. B., Cui, M., Hong, T., Akintomide, O., Kelly, R. P., & Johannesson, K. H. (2020). Rare earth element cycling and reaction path modeling across the chemocline of the Pettaquamscutt River estuary, Rhode Island. *Geochimica et Cosmochimica Acta*, *284*, 21–42. https://doi.org/10.1016/j.gca.2020.06.001

Adebayo, S. B., Cui, M., Hong, T., White, C. D., Johannesson, K. H., & Martin, E. E. (2018). Rare earth elements geochemistry and Nd isotopes in the Mississippi river and Gulf of Mexico mixing zone. *Frontiers in Marine Science*, *5*(May), 1–18. https://doi.org/10.3389/fmars.2018.00166

Adebayo, S. B., Cui, M., Williams, T. J., Martin, E., & Johannesson, K. H. (2022). Evolution of rare earth element and εNd compositions of Gulf of Mexico seawater during interaction with Mississippi River sediment. *Geochimica et Cosmochimica Acta*, *335*, 231–242. https://doi.org/10.1016/j.gca.2022.08.024

Akagi, T. (2013). Rare earth element (REE)–silicic acid complexes in seawater to explain the incorporation of REEs in opal and the "leftover" REEs in surface water: New interpretation of dissolved REE distribution profiles. *Geochimica et Cosmochimica Acta*, *113*, 174–192. https://doi.org/10.1016/j.gca.2013.03.014

Akagi, T., Fu, F., Hongo, Y., & Takahashi, K. (2011). Composition of rare earth elements in settling particles collected in the highly productive North Pacific Ocean and Bering Sea: Implications for siliceous-matter dissolution kinetics and formation of two REE-enriched phases. *Geochimica et Cosmochimica Acta*, *75*(17), 4857–4876. https://doi.org/10.1016/j.gca.2011.06.001

Albarède, F., Goldstein, S. L., & Dautel, D. (1997). The neodymium isotopic composition of manganese nodules from the Southern and Indian oceans, the global oceanic neodymium budget, and their bearing on deep ocean circulation. *Geochimica et Cosmochimica Acta*, *61*(6), 1277–1291. https://doi.org/10.1016/S0016-7037(96)00404-8

Alhassan, A. B., & Aljahdali, M. O. (2021). Fractionation and distribution of rare earth elements in marine sediment and bioavailability in avicennia marina in central red sea mangrove ecosystems. *Plants*, *10*(6), 1233. https://doi.org/10.3390/plants10061233

Alibo, D. S., & Nozaki, Y. (1999). Rare earth elements in seawater: Particle association, shale-normalization, and Ce oxidation. *Geochimica et Cosmochimica Acta*, *63*(3/4), 363–372. https://doi.org/10.1016/S0016-7037(98)00279-8

Alibo, D. S., & Nozaki, Y. (2004). Dissolved rare earth elements in the eastern Indian Ocean: Chemical tracers of the water masses. *Deep-Sea Research Part I Oceanographic Research Papers*, *51*(4), 559–576. https://doi.org/10.1016/j.dsr.2003.11.004

Aljahdali, M. O., & Alhassan, A. B. (2022). Rare earth elements and bioavailability in northern and southern Central Red Sea Mangroves, Saudi Arabia. *Molecules*, *27*(14), 4335. https://doi.org/10.3390/molecules27144335

Amyot, M., Clayden, M. G., Macmillan, G. A., Perron, T., & Arscott-Gauvin, A. (2017). Fate and trophic transfer of rare earth elements in temperate lake food webs. *Environmental Science and Technology*, *51*(11), 6009–6017. https://doi.org/10.1021/acs.est.7b00739

Anderson, R. (2020). GEOTRACES: Accelerating research on the marine biogeochemical cycles of trace elements and their isotopes robert. *Annual Review of Marine Science*, *12*(1), 49–85. https://doi.org/10.1146/annurev-marine-010318-095123

Anderson, R., Mawji, E., Cutter, G. A., Measures, C. I., & Jeandel, C. (2014). GEOTRACES: Changing the way we explore ocean chemistry. *Oceanography*, *27*(1), 50–61. https://doi.org/10.5670/oceanog.2014.07

Andrade, M., Soares, A. M. V. M., Solé, M., Pereira, E., & Freitas, R. (2021). Salinity influences on the response of Mytilus galloprovincialis to the rare-earth element lanthanum. *Science of the Total Environment*, *794*, 148512. https://doi.org/10.1016/j.scitotenv.2021.148512

Andrade, R. L., Hatje, V., Pedreira, R. M., Boening, P., & Pahnke, K. (2020). REE fractionation and human Gd footprint along the continuum between Paraguaçu River to coastal South Atlantic waters. *Chemical Geology*, *532*, 119303. https://doi.org/10.1016/j.chemgeo.2019.119303

Arciszewska, Ż., Gama, S., Leśniewska, B., Malejko, J., Nalewajko-Sieliwoniuk, E., Zambrzycka-Szelewa, E., & Godlewska-Żyłkiewicz, B. (2022). The translocation pathways of rare earth elements from the environment to the food chain and their impact on human health. *Process Safety and Environmental Protection*, *168*, 205–223. https://doi.org/10.1016/j.psep.2022.09.056

Arsouze, T., Dutay, J. C., Lacan, F., & Jeandel, C. (2007). Modeling the neodymium isotopic composition with a global ocean circulation model. *Chemical Geology*, *239*(1–2), 165–177. https://doi.org/10.1016/j.chemgeo.2006.12.006

Arsouze, T., Dutay, J.-C., Lacan, F., & Jeandel, C. (2009). Reconstructing the Nd oceanic cycle using a coupled dynamical – Biogeochemical model. *Biogeosciences Discussions*, *6*(3), 5549–5588. https://doi.org/10.5194/bgd-6-5549-2009

Atkins, A. L., Shaw, S., & Peacock, C. L. (2014). Nucleation and growth of todorokite from birnessite: Implications for trace-metal cycling in marine sediments. *Geochimica et Cosmochimica Acta*, *144*, 109–125. https://doi.org/10.1016/j.gca.2014.08.014

Atkins, A. L., Shaw, S., & Peacock, C. L. (2016). Release of Ni from birnessite during transformation of birnessite to todorokite: Implications for Ni cycling in marine sediments. *Geochimica et Cosmochimica Acta*, *189*, 158–183. https://doi.org/10.1016/j.gca.2016.06.007

Auer, G., Reuter, M., Hauzenberger, C. A., & Piller, W. E. (2017). The impact of transport processes on rare earth element patterns in marine authigenic and biogenic phosphates. *Geochimica et Cosmochimica Acta*, *203*, 140–156. https://doi.org/10.1016/j.gca.2017.01.001

Ayache, M., Dutay, J. C., Tachikawa, K., Arsouze, T., & Jeandel, C. (2023). Neodymium budget in the Mediterranean Sea: Evaluating the role of atmospheric dusts using a high-resolution dynamical-biogeochemical model. *Biogeosciences*, *20*(1), 205–227. https://doi.org/10.5194/bg-20-205-2023

Ayora, C., Macías, F., Torres, E., & Nieto, J. M. (2015). Rare earth elements in acid mine drainage. *XXXV Reunión de la Sociedad Española de Mineralogía; Sociedad Espanola de Mineralogia: Huelva, Spain*, 1–22.

Babu, S. S., Venkata Ramana, R., Purnachandra Rao, V., Ram Mohan, M., Sawant, S., Satyasree, N., & Keshav Krishna, A. (2021). Rare earth elements of sediments in rivers and estuaries of the East Coast of India. *Current Science*, *120*(3), 519. https://doi.org/10.18520/cs/v120/i3/519-537

Badri, N., Florea, A., Mhamdi, M., Matei, H., Tekaya, W. H., Bâati, R., et al. (2017). Toxicological effects and ultrastructural changes induced by lanthanum and cerium in ovary and uterus of Wistar rats. *Journal of Trace Elements in Medicine & Biology*, *44*(August), 349–355. https://doi.org/10.1016/j.jtemb.2017.09.011

Balaram, V. (2019). Rare earth elements: A review of applications, occurrence, exploration, analysis, recycling, and environmental impact. *Geoscience Frontiers*, *10*(4), 1285–1303. https://doi.org/10.1016/j.gsf.2018.12.005

Banfield, J. F., & Eggleton, R. A. (1989). Apatite replacement and rare earth mobilization, fractionation, and fixation during weathering. *Clays and Clay Minerals*, *37*(2), 113–127. https://doi.org/10.1346/CCMN.1989.0370202

Banks, D. A., Yardley, B. W. D., Campbell, A. R., & Jarvis, K. E. (1994). REE composition of an aqueous magmatic fluid: A fluid inclusion study from the Capitan Pluton, New Mexico, U.S.A. *Chemical Geology*, *113*(3–4), 259–272. https://doi.org/10.1016/0009-2541(94)90070-1

Banner, J. L., Hanson, G. N., & Meyers, W. J. (1988). Rare earth element and Nd isotope variations in regionally extensive dolomites from the Burlington-Keokuk Formation (Mississippian): Implications for REE mobility during carbonate diagenesis. *Journal of Sedimentary Petrology*, *58*, 415–432.

Bao, S.-X., Zhou, H.-Y., Peng, X.-T., Ji, F.-W., & Yao, H.-Q. (2008). Geochemistry of REE and yttrium in hydrothermal fluids from the Endeavour segment, Juan de Fuca Ridge. *Geochemical Journal*, *42*(4), 359–370. https://doi.org/10.2343/geochemj.42.359

Barbot, S., Lagarde, M., Lyard, F., Marsaleix, P., Lherminier, P., & Jeandel, C. (2022). Internal tides responsible for lithogenic inputs along the Iberian continental slope. *Journal of Geophysical Research: Oceans*, *127*(10). https://doi.org/10.1029/2022JC018816

Barrat, J. A., Bayon, G., & Lalonde, S. (2023). Calculation of cerium and lanthanum anomalies in geological and environmental samples. *Chemical Geology*, *615*, 121202. https://doi.org/10.1016/j.chemgeo.2022.121202

Barrat, J. A., Boulègue, J., Tiercelin, J. J., & Lesourd, M. (2000). Strontium isotopes and rare-earth element geochemistry of hydrothermal carbonate deposits from Lake Tanganyika, east Africa. *Geochimica et Cosmochimica Acta*, *64*(2), 287–298. https://doi.org/10.1016/S0016-7037(99)00294-X

Barrat, J. A., Chauvaud, L., Olivier, F., Poitevin, P., Bayon, G., & Ben Salem, D. (2022). Rare earth elements and yttrium in suspension-feeding bivalves (dog cockle, Glycymeris glycymeris L.): Accumulation, vital effects and pollution. *Geochimica et Cosmochimica Acta*, *339*, 12–21. https://doi.org/10.1016/j.gca.2022.10.033

Basak, C., Pahnke, K., Frank, M., Lamy, F., & Gersonde, R. (2015). Neodymium isotopic characterization of Ross Sea Bottom Water and its advection through the southern South Pacific. *Earth and Planetary Science Letters*, *419*, 211–221. https://doi.org/10.1016/j.epsl.2015.03.011

Bau, M. (1996). Controls on the fractionation of isovalent trace elements in magmatic and aqueous systems: Evidence from Y/Ho, Zr/Hf, and lanthanide tetrad effect. *Contributions to Mineralogy and Petrology*, *123*(3), 323–333. https://doi.org/10.1007/s004100050159

Bau, M. (1999). Scavenging of dissolved yttrium and rare earths by precipitating iron oxyhydroxide: Experimental evidence for Ce oxidation, Y-Ho fractionation, and lanthanide tetrad effect. *Geochimica et Cosmochimica Acta*, *63*(1), 67–77. https://doi.org/10.1016/S0016-7037(99)00014-9

Bau, M., Alexander, B., Chesley, J. T., Dulski, P., & Brantley, S. L. (2004). Mineral dissolution in the Cape Cod aquifer, Massachusetts, USA: I. Reaction stoichiometry and impact of accessory feldspar and glauconite on strontium isotopes, solute concentrations, and REY distribution. *Geochimica et Cosmochimica Acta*, *68*(6), 1199–1216. https://doi.org/10.1016/j.gca.2003.08.015

Bau, M., & Dulski, P. (1996a). Anthropogenic origin of positive gadolinium anomalies in river waters. *Earth and Planetary Science Letters*, *143*(1–4), 245–255. https://doi.org/10.1016/0012-821X(96)00127-6

Bau, M., & Dulski, P. (1996b). Distribution of yttrium and rare-earth elements in the Penge and Kuruman iron-formations, Transvaal Supergroup, South Africa. *Precambrian Research*, *79*(1–2), 37–55. https://doi.org/10.1016/0301-9268(95)00087-9

Bau, M., & Dulski, P. (1999). Comparing yttrium and rare earths in hydrothermal fluids from the Mid-Atlantic Ridge: Implications for Y and REE behaviour during near-vent mixing and for the Y/Ho ratio of Proterozoic seawater. *Chemical Geology*, *155*(1–2), 77–90. https://doi.org/10.1016/S0009-2541(98)00142-9

Bau, M., & Koschinsky, A. (2009). Oxidative scavenging of cerium on hydrous Fe oxide: Evidence from the distribution of rare earth elements and yttrium between Fe oxides and Mn oxides in hydrogenetic ferromanganese crusts. *Geochemical Journal*, *43*(1), 37–47. https://doi.org/10.2343/geochemj.1.0005

Bau, M., Koschinsky, A., Dulski, P., & Hein, J. R. (1996). Comparison of the partitioning behaviours of yttrium, rare earth elements, and titanium between hydrogenetic marine ferromanganese crusts and seawater. *Geochimica et Cosmochimica Acta*, *60*(10), 1709–1725. https://doi.org/10.1016/0016-7037(96)00063-4

Bau, M., Schmidt, K., Pack, A., Bendel, V., & Kraemer, D. (2018). The European Shale: An improved data set for normalisation of rare earth element and yttrium concentrations in environmental and biological samples from Europe. *Applied Geochemistry*, *90*(January), 142–149. https://doi.org/10.1016/j.apgeochem.2018.01.008

Bayon, G., Birot, D., Ruffine, L., Caprais, J., Ponzevera, E., Bollinger, C., et al. (2011). Evidence for intense REE scavenging at cold seeps from the Niger Delta margin. *Earth and Planetary Science Letters*, *312*(3–4), 443–452. https://doi.org/10.1016/j.epsl.2011.10.008

Bayon, G., Douglas, G. B., Denton, G. J., Monin, L., & De Deckker, P. (2020). Preferential riverine export of fine volcanogenic particles to the southeast Australian margin. *Frontiers in Marine Science*, *7*, 89. https://doi.org/10.3389/fmars.2020.00089

Bayon, G., German, C. R., Burton, K. W., Nesbitt, R. W., & Rogers, N. (2004). Sedimentary Fe-Mn oxyhydroxides as paleoceanographic archives and the role of aeolian flux in regulating oceanic dissolved REE. *Earth and Planetary Science Letters*, *224*(3–4), 477–492. https://doi.org/10.1016/j.epsl.2004.05.033

Bayon, G., Lemaitre, N., Barrat, J.-A., Wang, X., Feng, D., & Duperron, S. (2020). Microbial utilization of rare earth elements at cold seeps related to aerobic methane oxidation. *Chemical Geology*, *555*, 119832. https://doi.org/10.1016/j.chemgeo.2020.119832

Bayon, G., Toucanne, S., Skonieczny, C., André, L., Bermell, S., Cheron, S., et al. (2015). Rare earth elements and neodymium isotopes in world river sediments revisited. *Geochimica et Cosmochimica Acta*, *170*, 17–38. https://doi.org/10.1016/j.gca.2015.08.001

Beers, Y. (1957). *Introduction to the theory of error* (2nd ed.). Addison-Wesley Publishing Co.

Bellefroid, E. J., Hood, A. V. S., Hoffman, P. F., Thomas, M. D., Reinhard, C. T., & Planavsky, N. (2018). Constraints on Paleoproterozoic atmospheric oxygen levels. *Proceedings of the National Academy of Sciences*, *115*(32), 8104–8109. https://doi.org/10.1073/pnas.1806216115

Berner, R. A. (1980). *Early diagenesis: A theoretical approach*. Princeton University Press.

Biddau, R., Bensimon, M., Cidu, R., & Parriaux, A. (2009). Rare earth elements in groundwater from different Alpine aquifers. *Chemie der Erde*, *69*(4), 327–339. https://doi.org/10.1016/j.chemer.2009.05.002

Bigot, S., Treuil, M., Dumonceau, J., & Fromage, F. (1984). Couplage des équations de transfert de masse et des lois d'interactions solution-solide par l'utilisation des lanthanides comme traceurs — Approche expérimentale. *Journal of Hydrology*, *70*(1–4), 133–148. https://doi.org/10.1016/0022-1694(84)90118-5

Binnemans, K., Jones, P. T., Blanpain, B., Van Gerven, T., & Pontikes, Y. (2015). Towards zero-waste valorisation of rare-earth-containing industrial process residues: A critical review. *Journal of Cleaner Production*, *99*, 17–38. https://doi.org/10.1016/j.jclepro.2015.02.089

Binnemans, K., Jones, P. T., Blanpain, B., Van Gerven, T., Yang, Y., Walton, A., & Buchert, M. (2013). Recycling of rare earths: A critical review. *Journal of Cleaner Production*, *51*, 1–22. https://doi.org/10.1016/j.jclepro.2012.12.037

Bispo, F., Menezes, M., Fontana, A., Sarkis, J. S., Gonçalves, C., Carvalho, T., et al. (2021). Rare earth elements (REEs) geochemical patterns and contamination aspects in Brazilian benchmark soils. *Environmental Pollution*, *289*, 11792. https://doi.org/10.1016/j.envpol.2021.117972

Blaise, C., Gagné, F., Harwood, M., Quinn, B., & Hanana, H. (2018). Ecotoxicity responses of the freshwater cnidarian Hydra attenuata to 11 rare earth elements. *Ecotoxicology and Environmental Safety*, *163*(July), 486–491. https://doi.org/10.1016/j.ecoenv.2018.07.033

Bonnail, E., Pérez-López, R., Sarmiento, A. M., Nieto, J. M., & DelValls, T. Á. (2017). A novel approach for acid mine drainage pollution biomonitoring using rare earth elements bioaccumulated in the freshwater clam Corbicula fluminea. *Journal of Hazardous Materials*, *338*, 466–471. https://doi.org/10.1016/j.jhazmat.2017.05.052

Boukadida, K., Banni, M., Gourves, P. Y., & Cachot, J. (2016). High sensitivity of embryo-larval stage of the Mediterranean mussel, Mytilus galloprovincialis to metal pollution in combination with temperature increase. *Marine Environmental Research*, *122*, 59–66. https://doi.org/10.1016/j.marenvres.2016.09.007

Brantley, S. L., Liermann, L. J., Bau, M., & Wu, S. (2001). Uptake of trace metals and rare earth elements from hornblende by a soil bacterium. *Geomicrobiology Journal*, *18*(1), 37–61. https://doi.org/10.1080/01490450151079770

Brewer, A., Dror, I., & Berkowitz, B. (2022). Electronic waste as a source of rare earth element pollution: Leaching, transport in porous media, and the effects of nanoparticles. *Chemosphere*, *287*, 132217. https://doi.org/10.1016/j.chemosphere.2021.132217

Bright, C. A., Cruse, A. M., Lyons, T. W., MacLeod, K. G., Glascock, M. D., & Ethington, R. L. (2009). Seawater rare-earth element patterns preserved in apatite of Pennsylvanian conodonts? *Geochimica et Cosmochimica Acta*, *73*(6), 1609–1624. https://doi.org/10.1016/j.gca.2008.12.014

Brioschi, L., Steinmann, M., Lucot, E., Pierret, M. C., Stille, P., Prunier, J., & Badot, P. M. (2013). Transfer of rare earth elements (REE) from natural soil to plant systems: Implications for the environmental availability of anthropogenic REE. *Plant and Soil*, *366*(1–2), 143–163. https://doi.org/10.1007/s11104-012-1407-0

Brito, P., Caetano, M., Martins, M. D., & Caçador, I. (2021). Effects of salt marsh plants on mobility and bioavailability of REE in estuarine sediments. *Science of the Total Environment*, *759*, 144314. https://doi.org/10.1016/j.scitotenv.2020.144314

Brito, P., Cesário, R., & Monteiro, C. E. S. (2020). Lesser-known metals with potential impacts in the marine environment. In *Coastal and deep ocean pollution* (pp. 215–247). CRC Press. https://doi.org/10.1201/9780203704271-10

Brito, P., Malvar, M., Galinha, C., Caçador, I., Canário, J., Araújo, M. F., & Raimundo, J. (2018). Yttrium and rare earth elements fractionation in salt marsh halophyte plants. *Science of the Total Environment*, *643*, 1117–1126. https://doi.org/10.1016/j.scitotenv.2018.06.291

Brito, P., Mil-Homens, M., Caçador, I., & Caetano, M. (2020). Changes in REE fractionation induced by the halophyte plant Halimione portulacoides, from SW European salt marshes. *Marine Chemistry*, *223*(November 2019), 103805. https://doi.org/10.1016/j.marchem.2020.103805

Brito, P., Prego, R., Mil-homens, M., Caçador, I., & Caetano, M. (2018). Sources and distribution of yttrium and rare earth elements in surface sediments from Tagus estuary, Portugal. *Science of the Total Environment*, *621*, 317–325. https://doi.org/10.1016/j.scitotenv.2017.11.245

Bruni, J., Canepa, M., Chiodini, G., Cioni, R., Cipolli, F., Longinelli, A., et al. (2002). Irreversible water-rock mass transfer accompanying the generation of the neutral, Mg-HCO_3 and high-pH, Ca-OC spring waters of the Genova province, Italy. *Applied Geochemistry*, *17*(4), 455–474. https://doi.org/10.1016/S0883-2927(01)00113-5

Brünjes, R., & Hofmann, T. (2020). Anthropogenic gadolinium in freshwater and drinking water systems. *Water Research*, *182*, 115966. https://doi.org/10.1016/j.watres.2020.115966

Bruno, J. (1997). Trace element modelling. In I. Grenthe & I. Puidomenech (Eds.), *Modelling in aquatic chemistry*, *Modelling in aquatic chemistry* (pp. 593–621).

Butler, A. (1998). Acquisition and utilization of transition metal ions by marine organisms. *Science*, *281*(5374), 207–209. https://doi.org/10.1126/science.281.5374.207

Byrne, R. H. (2002). Speciation in seawater. In A. M. Ure & C. M. Davidson (Eds.), *Chemical speciation in the environment* (2nd ed., pp. 322–357). Blackwell Science.

Byrne, R. H., & Kim, K. H. (1990). Rare earth element scavenging in seawater. *Geochimica et Cosmochimica Acta*, *54*(10), 2645–2656. https://doi.org/10.1016/0016-7037(90)90002-3

Byrne, R. H., & Liu, X. (1998). A coupled riverine-marine fractionation model for dissolved rare earths and yttrium. *Aquatic Geochemistry*, *4*(1), 103–121. https://doi.org/10.1023/A:1009651919911

Byrne, R. H., & Sholkovitz, E. R. (1996). Marine chemistry and geochemistry of the lanthanides. In K. A. GschneidnerJr, & L. Eyring (Eds.), *Handbook on the physics and chemistry of rare earths* (Vol. 23, pp. 497–593). Elsevier. https://doi.org/10.1016/s0168-1273(96)23009-0

Cabral, H., Fonseca, V., Sousa, T., & Leal, M. C. (2019). Synergistic effects of climate change and marine pollution: An overlooked interaction in coastal and estuarine areas. *International Journal of Environmental Research and Public Health*, *16*(15), 1–17. https://doi.org/10.3390/ijerph16152737

Caçador, I., Caetano, M., Duarte, B., & Vale, C. (2009). Stock and losses of trace metals from salt marsh plants. *Marine Environmental Research*, *67*(2), 75–82. https://doi.org/10.1016/j.marenvres.2008.11.004

Caetano, M., Falcão, M., Vale, C., & Bebianno, M. J. (1997). Tidal flushing of ammonium, iron and manganese from inter-tidal sediment pore waters. *Marine Chemistry*, *58*(1–2), 203–211. https://doi.org/10.1016/S0304-4203(97)00035-2

Caetano, M., Vale, C., Cesário, R., & Fonseca, N. (2008). Evidence for preferential depths of metal retention in roots of salt marsh plants. *Science of the Total Environment*, *390*(2–3), 466–474. https://doi.org/10.1016/j.scitotenv.2007.10.015

Campbell, P. (1995). Interactions between trace metals and organisms: Critique of the free-ion activity model. In Willey (Ed.), *Metal speciation and bioavailability in aquatic systems*. (pp. 45–102).

Cantrell, K. J., & Byrne, R. H. (1987). Rare earth element complexation by carbonate and oxalate ions. *Geochimica et Cosmochimica Acta*, *51*(3), 597–605. https://doi.org/10.1016/0016-7037(87)90072-X

Cao, C., Liu, X.-M., Bataille, C. P., & Liu, C. (2020). What do Ce anomalies in marine carbonates really mean? A perspective from leaching experiments. *Chemical Geology*, *532*, 119413. https://doi.org/10.1016/j.chemgeo.2019.119413

Cao, C., Liu, X.-M., & Chen, J. (2022). Cerium anomaly as a tracer for paleo-oceanic redox conditions: A thermodynamics-based Ce oxidation modeling approach. *Frontiers in Earth Science*, *10*, 927826. https://doi.org/10.3389/feart.2022.927826

Carr, S. A., Liu, J., & Tesoro, A. G. (2016). Transport and fate of microplastic particles in wastewater treatment plants. *Water Research*, *91*, 174–182. https://doi.org/10.1016/j.watres.2016.01.002

Castor, S. B., & Hedrick, J. B. (2006). Rare earth elements. *Industrial Minerals and Rocks*, *7*, 769–792.

Censi, P., Spoto, S. E., Nardone, G., Saiano, F., Punturo, R., Di Geronimo, S. I., et al. (2005). Rare-earth elements and yttrium distributions in mangrove coastal water systems: The western Gulf of Thailand. *Chemistry and Ecology*, *21*(4), 255–277. https://doi.org/10.1080/02757540500213216

Cervini-Silva, J., Fowle, D. A., & Banfield, J. (2005). Biogenic dissolution of a soil cerium-phosphate mineral. *American Journal of Science*, *305*(6–8 SPEC. ISS.), 711–726. https://doi.org/10.2475/ajs.305.6-8.711

Cervini-Silva, J., Gilbert, B., Fakra, S., Friedlich, S., & Banfield, J. (2008). Coupled redox transformations of catechol and cerium at the surface of a cerium(III) phosphate mineral. *Geochimica et Cosmochimica Acta*, *72*(10), 2454–2464. https://doi.org/10.1016/j.gca.2008.02.017

Chakraborty, P., Babu, P. R., & Sarma, V. V. (2011). A multi-method approach for the study of lanthanum speciation in coastal and estuarine sediments. *Journal of Geochemical Exploration*, *110*(2), 225–231. https://doi.org/10.1016/j.gexplo.2011.05.013

Chapelle, F., & Knobel, L. (1983). Aqueous geochemistry and exchangeable cation composition of glauconite in the Aquia aquifer, Maryland. *Ground Water*, *21*(3), 343–352. https://doi.org/10.1111/j.1745-6584.1983.tb00734.x

Chapman, P. M., Allen, H. E., Godtfredsen, K., & Z'Graggen, M. N. (1996). Policy analysis, peer reviewed: Evaluation of bioaccumulation factors in regulating metals. *Environmental Science & Technology*, *30*(10), 448A–452A. https://doi.org/10.1021/es962436d

Chavagnac, V., Monnin, C., Ceuleneer, G., Boulart, C., & Hoareau, G. (2013). Characterization of hyperalkaline fluids produced by low-temperature serpentinization of mantle peridotites in the Oman and Ligurian ophiolites. *Geochemistry, Geophysics, Geosystems*, *14*(7), 2496–2522. https://doi.org/10.1002/ggge.20147

Chavagnac, V., Saleban Ali, H., Jeandel, C., Leleu, T., Destrigneville, C., Castillo, A., et al. (2018). Sulfate minerals control dissolved rare earth element flux and Nd isotope signature of buoyant hydrothermal plume (EMSO-Azores, 37°N Mid-Atlantic Ridge). *Chemical Geology*, *499*, 111–125. https://doi.org/10.1016/j.chemgeo.2018.09.021

Chevis, D. A., Johannesson, K. H., Burdige, D. J., Cable, J. E., Martin, J. B., & Roy, M. (2015). Rare earth element cycling in a sandy subterranean estuary in Florida, USA. *Marine Chemistry*, *176*, 34–50. https://doi.org/10.1016/j.marchem.2015.07.003

Chevis, D. A., Johannesson, K. H., Burdige, D. J., Tang, J., Bradley Moran, S., & Kelly, R. P. (2015). Submarine groundwater discharge of rare earth elements to a tidally-mixed estuary in Southern Rhode Island. *Chemical Geology*, *397*, 128–142. https://doi.org/10.1016/j.chemgeo.2015.01.013

Chevis, D. A., Mohajerin, T. J., Yang, N., Cable, J. E., Rasbury, E. T., Hemming, S. R., et al. (2021). Neodymium Isotope Geochemistry of a Subterranean Estuary. *Frontiers in Water*, *3*(November), 1–21. https://doi.org/10.3389/frwa.2021.778344

Chistoserdova, L. (2016). Lanthanides: New life metals? *World Journal of Microbiology and Biotechnology*, *32*(8), 1–7. https://doi.org/10.1007/s11274-016-2088-2

Choppin, G. R. (1983). Comparison of the solution chemistry of the actinides and lanthanides. *Journal of the Less-Common Metals*, *93*(2), 323–330. https://doi.org/10.1016/0022-5088(83)90177-7

Chour, Z., Laubie, B., Morel, J. L., Tang, Y. T., Simonnot, M. O., & Muhr, L. (2020). Basis for a new process for producing REE oxides from Dicranopteris linearis. *Journal of Environmental Chemical Engineering*, *8*(4), 103961. https://doi.org/10.1016/j.jece.2020.103961

Christenson, E. A., & Schijf, J. (2011). Stability of YREE complexes with the trihydroxamate siderophore desferrioxamine B at seawater ionic strength. *Geochimica et Cosmochimica Acta*, *75*(22), 7047–7062. https://doi.org/10.1016/j.gca.2011.09.022

Cooley, S., Schoeman, D., Bopp, L., Boyd, P., Donner, S., Ghebrehiwet, Y., et al. (2022). Oceans and coastal ecosystems and their services supplementary material. climate change 2022: Impacts, adaptation and vulnerability. contribution of working group II. In H. O. Pörtner, D. Roberts, M. Tignor, et al. (Eds.), *Sixth assessment report of the*. Intergovernmental Panel on Climate Change.

Costa, L., Johannesson, K., Mirlean, N., & Quintana, G. (2021). Rare earth element distributions in salt marsh sediment cores reveal evidence of environmental lability during bioturbation and diagenetic processes. *Chemical Geology*, *584*, 120503. https://doi.org/10.1016/j.chemgeo.2021.120503

Costa, L., Mirlean, N., & Johannesson, K. (2021). Rare earth elements as tracers of sediment contamination by fertilizer industries in Southern Brazil, Patos Lagoon Estuary. *Applied Geochemistry*, *129*(February), 104965. https://doi.org/10.1016/j.apgeochem.2021.104965

Costa, M., Henriques, B., Pinto, J., Fabre, E., Dias, M., Soares, J., et al. (2020). Influence of toxic elements on the simultaneous uptake of rare earth elements from contaminated waters by estuarine macroalgae. *Chemosphere*, *252*, 126562. https://doi.org/10.1016/j.chemosphere.2020.126562

Cotruvo, J. A., Jr., Featherston, E. R., Mattocks, J. A., Ho, J. V., & Laremore, T. N. (2018). Lanmodulin: A highly selective lanthanide-binding protein from a lanthanide-utilizing bacterium. *Journal of the American Chemical Society*, *140*(44), 15056–15061. https://doi.org/10.1021/jacs.8b09842

Crocket, K. C., Hill, E., Abell, R. E., Johnson, C., Gary, S. F., Brand, T., & Hathorne, E. C. (2018). Rare earth element distribution in the NE Atlantic: Evidence for benthic sources, longevity of the seawater signal, and biogeochemical cycling. *Frontiers in Marine Science*, *5*, 147. https://doi.org/10.3389/fmars.2018.00147

Daumann, L. J. (2019). Essential and ubiquitous: The emergence of lanthanide metallobiochemistry. *Angewandte Chemie International Edition*, *58*(37), 12795–12802. https://doi.org/10.1002/anie.201904090

Davranche, M., Grybos, M., Gruau, G., Pédrot, M., Dia, A., & Marsac, R. (2011). Rare earth element patterns: A tool for identifying trace metal sources during wetland soil reduction. *Chemical Geology*, *284*(1–2), 127–137. https://doi.org/10.1016/j.chemgeo.2011.02.014

Davranche, M., Pourret, O., Gruau, G., & Dia, A. (2004). Impact of humate complexation on the adsorption of REE onto Fe oxyhydroxide. *Journal of Colloid and Interface Science*, *277*(2), 271–279. https://doi.org/10.1016/j.jcis.2004.04.007

Davranche, M., Pourret, O., Gruau, G., Dia, A., & Le Coz-Bouhnik, M. (2005). Adsorption of REE (III)-humate complexes onto MnO2: Experimental evidence for cerium anomaly and lanthanide tetrad effect suppression. *Geochimica et Cosmochimica Acta*, *69*(20), 4825–4835. https://doi.org/10.1016/j.gca.2005.06.005

de Baar, H. J. W., Bacon, M. P., & Brewer, P. G. (1983). Rare-earth distributions with a positive Ce anomaly in the Western North Atlantic Ocean. *Nature*, *301*, 324–328. https://doi.org/10.1038/301324a0

de Baar, H. J. W., Bruland, K. W., Schijf, J., van Heuven, S. M. A. C., & Behrens, M. K. (2018). Low cerium among the dissolved rare earth elements in the central North Pacific Ocean. *Geochimica et Cosmochimica Acta*, *236*, 5–40. https://doi.org/10.1016/j.gca.2018.03.003

de Baar, H. J. W., German, C. R., Elderfield, H., & van Gaans, P. (1988). Rare earth element distributions in anoxic waters of the Cariaco Trench. *Geochimica et Cosmochimica Acta*, *52*(5), 1203–1219. https://doi.org/10.1016/0016-7037(88)90275-X

De Carlo, E. H., Wen, X. Y., & Irving, M. (1997). The influence of redox reactions on the uptake of dissolved Ce by suspended Fe and Mn oxide particles. *Aquatic Geochemistry*, *3*(4), 357–389. https://doi.org/10.1023/A:1009664626181

de Chanvalon, A. T., Metzger, E., Mouret, A., Knoery, J., Chiffoleau, J., & Brach-papa, C. (2016). Particles transformation in estuaries: Fe, Mn and REE signatures through the Loire Estuary. *Journal of Sea Research*, *118*, 103–112. https://doi.org/10.1016/j.seares.2016.11.004

de Freitas, T. O. P., Pedreira, R. M. A., & Hatje, V. (2021). Distribution and fractionation of rare earth elements in sediments and mangrove soil profiles across an estuarine gradient. *Chemosphere*, *264*, 128431. https://doi.org/10.1016/j.chemosphere.2020.128431

Delgado, J., Pérez-López, R., Galván, L., Nieto, J. M., & Boski, T. (2012). Enrichment of rare earth elements as environmental tracers of contamination by acid mine drainage in salt marshes: A new perspective. *Marine Pollution Bulletin*, *64*(9), 1799–1808. https://doi.org/10.1016/j.marpolbul.2012.06.001

Deng, G., Ma, T., Tanaka, K., Ohnuki, T., Qiu, X., & Yu, Q. (2020). Saccharide-mediated transformation of Ce during the formation of manganese (hydr)oxide. *Geochimica et Cosmochimica Acta*, *286*, 143–158. https://doi.org/10.1016/j.gca.2020.07.028

Deng, K., Yang, S., Du, J., Lian, E., & Vance, D. (2022). Dominance of benthic flux of REEs on continental shelves: Implications for oceanic budgets. *Geochemical Perspectives Letters*, *22*, 26–30. https://doi.org/10.7185/geochemlet.2223

Deng, Y., Ren, J., Guo, Q., Cao, J., Wang, H., & Liu, C. (2017). Rare earth element geochemistry characteristics of seawater and porewater from deep sea in western Pacific. *Scientific Reports*, *7*(1), 1–13. https://doi.org/10.1038/s41598-017-16379-1

de Sena, I. M., Souza, L. A., Patire, V. F., Arias-Ortiz, A., Creed, J. C., Cruz, I., & Hatje, V. (2022). Environmental Settings of Seagrass Meadows Control Rare Earth Element Distribution and Transfer from Soil to Plant Compartments. *SSRN Electronic Journal*, *843*(June). https://doi.org/10.2139/ssrn.4081360

Dia, A., Gruau, G., Olivié-Lauquet, G., Riou, C., Molénat, J., & Curmi, P. (2000). The distribution of rare earth elements in groundwaters: Assessing the role of source-rock composition, redox changes and colloidal particles. *Geochimica et Cosmochimica Acta*, *64*(24), 4131–4151. https://doi.org/10.1016/S0016-7037(00)00494-4

Ding, Y., Sun, W., Liu, S., Xie, J., Tang, D., Zhou, X., et al. (2022). Low oxygen levels with high redox heterogeneity in the late Ediacaran shallow ocean: Constraints from I/(Ca + Mg) and Ce/Ce* of the Dengying Formation, South China. *Geobiology*, *20*(6), 790–809. https://doi.org/10.1111/gbi/12520

Du, J., Haley, B. A., Mix, A. C., Abbott, A. N., McManus, J., & Vance, D. (2022). Reactive-transport modeling of neodymium and its radiogenic isotope in deep-sea sediments: The roles of authigenesis, marine silicate weathering and reverse weathering. *Earth and Planetary Science Letters*, *596*, 117792. https://doi.org/10.1016/j.epsl.2022.117792

Duddy, I. R. (1980). Redistribution and fractionation of rare-earth and other elements in a weathering profile. *Chemical Geology*, *30*(4), 363–381. https://doi.org/10.1016/0009-2541(80)90102-3

Dulski, P. (1994). Interferences of oxide, hydroxide and chloride analyte species in the determination of rare earth elements in geological samples by inductively coupled plasma-mass spectrometry. *Fresenius' Journal of Analytical Chemistry*, *350*(4–5), 194–203. https://doi.org/10.1007/BF00322470

Duncan, T., & Shaw, T. J. (2003). The mobility of rare earth elements and redox sensitive elements in the groundwater/seawater mixing zone of a shallow coastal aquifer. *Aquatic Geochemistry*, *9*(3), 233–255. https://doi.org/10.1023/B:AQUA.0000022956.20338.26

Duvert, C., Cendón, D. I., Raiber, M., Seidel, J. L., & Cox, M. E. (2015). Seasonal and spatial variations in rare earth elements to identify inter-aquifer linkages and recharge processes in an Australian catchment. *Chemical Geology*, *396*, 83–97. https://doi.org/10.1016/j.chemgeo.2014.12.022

Eckert, J. M., & Sholkovitz, E. R. (1976). The flocculation of iron, aluminium and humates from river water by electrolytes. *Geochimica et Cosmochimica Acta*, *40*(7), 847–848. https://doi.org/10.1016/0016-7037(76)90036-3

Elderfield, H. (1988). The oceanic chemistry of the rare-earth elements. *Philosophical Transactions of the Royal Society of London*, *325*(1583), 105–126. https://doi.org/10.1098/rsta.1988.0046

Elderfield, H. (2002). Foraminiferal Mg/Ca paleothermometry: Expected advances and unexpected consequences. *12th Annual V.M. Goldschmidt Conference*, *66*, A213.

Elderfield, H., & Greaves, M. J. (1981). Negative cerium anomalies in the rare earth element patterns of oceanic ferromanganese nodules. *Earth and Planetary Science Letters*, *55*(1), 163–170. https://doi.org/10.1016/0012-821X(81)90095-9

Elderfield, H., & Greaves, M. J. (1982). The rare earth elements in seawater. *Nature*, *296*(5854), 214–219. https://doi.org/10.1038/296214a0

Elderfield, H., & Sholkovitz, E. R. (1987). Rare earth elements in the pore waters of reducing nearshore sediments. *Earth and Planetary Science Letters*, *82*(3–4), 280–288. https://doi.org/10.1016/0012-821X(87)90202-0

Elderfield, H., Upstill-Goddard, R., & Sholkovitz, E. R. (1990). The rare earth elements in rivers, estuaries, and coastal seas and their significance to the composition of ocean waters. *Geochimica et Cosmochimica Acta*, *54*(4), 971–991. https://doi.org/10.1016/0016-7037(90)90432-K

Elderfield, H., Whitfield, M., Burton, J. D., Bacon, M. P., & Liss, P. S. (1988). The oceanic chemistry of the rare-earth elements. *Philosophical Transactions of the Royal Society of London - Series A: Mathematical and Physical Sciences*, *325*, 105–126. https://doi.org/10.1098/rsta.1988.0046

El Zrelli, R., Baliteau, J. Y., Yacoubi, L., Castet, S., Grégoire, M., Fabre, S., et al. (2021). Rare earth elements characterization associated to the phosphate fertilizer plants of Gabes (Tunisia, Central Mediterranean Sea): Geochemical properties and behavior, related economic losses, and potential hazards. *Science of the Total Environment*, *791*, 148268. https://doi.org/10.1016/j.scitotenv.2021.148268

Espejo, W., Chiang, G., Kitamura, D., Kashiwada, S., O'Driscoll, N. J., & Celis, J. E. (2023). Occurrence of rare earth elements (REEs) and trace elements (TEs) in feathers of adult and young Gentoo penguins from King George Island, Antarctica. *Marine Pollution Bulletin*, *187*(January), 1–6. https://doi.org/10.1016/j.marpolbul.2023.114575

Evans, J., DeHart, M., Weaver, K., & Keiser, D., Jr. (2022). Burnable absorbers in nuclear reactors – A review. *Nuclear Engeneering and Design*, *391*, 111726. https://doi.org/10.1016/j.nucengdes.2022.111726

Farmer, D. (1996). *Investigation of regional flow patterns in the Ash Meadows ground-water basin of southern Nevada using uranium isotope ratios*. University of Nevada, Las Vegas.

Fee, J. A., Gaudette, H. E., Lyons, W. B., & Long, D. T. (1992). Rare-earth element distribution in Lake Tyrrell groundwaters, Victoria, Australia. *Chemical Geology*, *96*(1–2), 67–93. https://doi.org/10.1016/0009-2541(92)90122-L

Figueiredo, C., Grilo, T., Oliveira, R., Ferreira, I., Gil, F., Lopes, C., et al. (2022). Single and combined ecotoxicological effects of ocean warming, acidification and lanthanum exposure on the surf clam (Spisula solida). *Chemosphere*, *303*, 134850. https://doi.org/10.1016/j.chemosphere.2022.134850

Filippova, A., Frank, M., Kienast, M., Rickli, J., Hathorne, E., Yashayaev, I. M., & Pahnke, K. (2017). Water mass circulation and weathering inputs in the Labrador Sea based on coupled Hf–Nd isotope compositions and rare earth element distributions. *Geochimica et Cosmochimica Acta*, *199*, 164–184. https://doi.org/10.1016/j.gca.2016.11.024

Flynn, T. M., Sanford, R. A., Santo Domingo, J. W., Ashbolt, N. J., Levine, A. D., & Bethke, C. M. (2012). The active bacterial community in a pristine confined aquifer. *Water Resources Research*, *48*(9), 1–10. https://doi.org/10.1029/2011WR011568

Fox, L. E. (1983). The removal of dissolved humic acid during estuarine mixing. *Estuarine, Coastal and Shelf Science*, *16*(4), 431–440. https://doi.org/10.1016/0272-7714(83)90104-X

Frank, M. (2002). Radiogenic isotopes: Tracers of past ocean circulation and erosional input. *Reviews of Geophysics*, *40*(1), 1. https://doi.org/10.1029/2000RG000094

Freitas, R., Costa, S., Cardoso, C. E., Morais, T., Moleiro, P., Matias, A. C., et al. (2020). Toxicological effects of the rare earth element neodymium in Mytilus galloprovincialis. *Chemosphere*, *244*, 125457. https://doi.org/10.1016/j.chemosphere.2019.125457

Freslon, N., Bayon, G., Toucanne, S., Bermell, S., Bollinger, C., Chéron, S., et al. (2014). Rare earth elements and neodymium isotopes in sedimentary organic matter. *Geochimica et Cosmochimica Acta*, *140*, 177–198. https://doi.org/10.1016/j.gca.2014.05.016

Froelich, P. N., Klinkhammer, G. P., Bender, M. L., Luedtke, N. A., Heath, G. R., Cullen, D., et al. (1979). Early oxidation of organic matter in pelagic sediments of the eastern equatorial Atlantic: Suboxic diagenesis. *Geochimica et Cosmochimica Acta*, *43*(7), 1075–1090. https://doi.org/10.1016/0016-7037(79)90095-4

Gammons, C. H. (2002). Complexation of the rare earth elements with aqueous chloride at 200°C and 300°C and saturated water vapor pressure. *Water-Rock Interaction, Ore Deposits, Environmental Geochemistry*, *7*, 191–207.

Gammons, C. H., Nimick, D. A., Parker, S. R., Cleasby, T. E., & McCleskey, R. B. (2005). Diel behavior of iron and other heavy metals in a mountain stream with acidic to neutral pH: Fisher Creek, Montana, USA. *Geochimica et Cosmochimica Acta*, *69*(10), 2505–2516. https://doi.org/10.1016/j.gca.2004.11.020

Gammons, C. H., Wood, S. A., & Williams-Jones, A. E. (1996). The aqueous geochemistry of the rare earth elements and yttrium: VI. Stability of neodymium chloride complexes from 25 to 300°C. *Geochimica et Cosmochimica Acta*, *60*(23), 4615–4630. https://doi.org/10.1016/S0016-7037(96)00262-1

Garcia-Solsona, E., & Jeandel, C. (2020). Balancing rare earth element distributions in the Northwestern Mediterranean Sea. *Chemical Geology*, *532*, 119372. https://doi.org/10.1016/j.chemgeo.2019.119372

Garcia-Solsona, E., Jeandel, C., Labatut, M., Lacan, F., Vance, D., Chavagnac, V., & Pradoux, C. (2014). Rare earth elements and Nd isotopes tracing water mass mixing and particle-seawater interactions in the SE Atlantic. *Geochimica et Cosmochimica Acta*, *125*, 351–372. https://doi.org/10.1016/j.gca.2013.10.009

Geagea, M. L., Stille, P., Gauthier-Lafaye, F., & Millet, M. (2007). Tracing of industrial emissions in an urban environment using Pb, Sr, Nd, and C isotopes (tree bark biomonitoring and aerosol sampling). *Geochimica et Cosmochimica Acta*, *71*(15, S), A537. https://doi.org/10.1021/es071704c

German, C. R., & Elderfield, H. (1989). Rare earth elements in Saanich Inlet, British Columbia, a seasonally anoxic basin. *Geochimica et Cosmochimica Acta*, *53*(10), 2561–2571. https://doi.org/10.1016/0016-7037(89)90128-2

German, C. R., & Elderfield, H. (1990). Application of the Ce anomaly as a paleoredox indicator: The ground rules. *Paleoceanography*, *5*(5), 823–833. https://doi.org/10.1029/PA005i005p00823

German, C. R., Holliday, B. P., & Elderfield, H. (1991). Redox cycling of rare earth elements in the suboxic zone of the Black Sea. *Geochimica et Cosmochimica Acta*, *55*(12), 3553–3558. https://doi.org/10.1016/0016-7037(91)90055-A

Goldstein, S. J., & Jacobsen, S. (1987). The Nd and Sr isotopic systematics of river-water dissolved material: Implications for the sources of Nd and Sr in seawater. *Chemical Geology*, *66*(3–4), 245–272. https://doi.org/10.1016/0168-9622(87)90045-5

Goldstein, S. J., & Jacobsen, S. (1988a). REE in the Great Whale River estuary, northwest Quebec. *Earth and Planetary Science Letters*, *88*(3–4), 241–252. https://doi.org/10.1016/0012-821X(88)90081-7

Goldstein, S. J., & Jacobsen, S. B. (1988b). Rare earth elements in river waters. *Earth and Planetary Science Letters*, *89*(1), 35–47. https://doi.org/10.1016/0012-821X(88)90031-3

Goldstein, S. L., & Hemming, S. R. (2003). Long-lived isotopic tracers in oceanography, paleoceanography, and ice-sheet dynamics. *Treatise on geochemistry*, *6*, 453–483. https://doi.org/10.1016/B978-0-08-095975-7.00617-3

Goldstein, S. L., O'nions, R. K., & Hamilton, P. J. (1984). A Sm-Nd isotopic study of atmospheric dusts and particulates from major river systems. *Earth and Planetary Science Letters*, *70*(2), 221–236. https://doi.org/10.1016/0012-821X(84)90007-4

Gomes, P., Valente, T., Marques, R., Prudêncio, M. I., & Pamplona, J. (2022). Rare earth elements - Source and evolution in an aquatic system dominated by mine-Influenced waters. *Journal of Environmental Management*, *322*(July), 116125. https://doi.org/10.1016/j.jenvman.2022.116125

Gonzalez, V., Vignati, D. A. L., Leyval, C., & Giamberini, L. (2014). Environmental fate and ecotoxicity of lanthanides: Are they a uniform group beyond chemistry? *Environment International*, *71*, 148–157. https://doi.org/10.1016/j.envint.2014.06.019

Gosselin, D. C., Smith, M. R., Lepel, E. A., & Laul, J. C. (1992). Rare earth elements in chloride-rich groundwater, Palo Duro Basin, Texas, USA. *Geochimica et Cosmochimica Acta*, *56*(4), 1495–1505. https://doi.org/10.1016/0016-7037(92)90219-9

Grenier, M., Jeandel, C., Lacan, F., Vance, D., Venchiarutti, C., Cros, A., & Cravatte, S. (2013). From the subtropics to the central equatorial Pacific Ocean: Neodymium isotopic composition and rare earth element concentration variations. *Journal of Geophysical Research: Oceans*, *118*(2), 592–618. https://doi.org/10.1029/2012JC008239

Gu, S., Liu, Z., Jahn, A., Rempfer, J., Zhang, J., & Joos, F. (2017). Neodymium isotopes in the ocean model of the Community Earth System 2 Model (CESM1.3). *Geoscientific Model Development Discussions*, *2*, 1–41. https://doi.org/10.5194/gmd-2017-40

Guichard, F., Church, T. M., Treuil, M., & Jaffrezic, H. (1979). Rare earths in barites: Distribution and effects on aqueous partitioning. *Geochimica et Cosmochimica Acta*, *43*(7), 983–997. https://doi.org/10.1016/0016-7037(79)90088-7

Guo, C., Wei, Y., Yan, L., Li, Z., Qian, Y., Liu, H., et al. (2020). Rare earth elements exposure and the alteration of the hormones in the hypothalamic-pituitary-thyroid (HPT) axis of the residents in an e-waste site: A cross-sectional study. *Chemosphere*, *252*, 126488. https://doi.org/10.1016/j.chemosphere.2020.126488

Guo, Q., Shields, G. A., Liu, C., Strauss, H., Zhu, M., Pi, D., et al. (2007). Trace element chemostratigraphy of two Ediacaran-Cambrian successions in South China: Implications for organosedimentary metal enrichment and silicification in the early Cambrian. *Palaeoceanography, Palaeoclimatology, Palaeoecology*, *254*(1–2), 194–216. https://doi.org/10.1016/j.palaeo.2007.03.016

Gwenzi, W., Mangori, L., Danha, C., Chaukura, N., Dunjana, N., & Sanganyado, E. (2018). Sources, behaviour, and environmental and human health risks of high-technology rare earth elements as emerging contaminants. *Science of the Total Environment*, *636*, 299–313. https://doi.org/10.1016/j.scitotenv.2018.04.235

Gwynn, J. P., Hatje, V., Casacuberta, N., Sarin, M., & Osvath, I. (2024). The effect of climate change on sources of radionuclides to the marine environment. *Communications Earth & Environment*, *5*(1), 135. https://doi.org/10.1038/s43247-024-01241-w

Haas, J. R., Shock, E. L., & Sassani, D. C. (1995). Rare earth elements in hydrothermal systems: Estimates of standard partial molal thermodynamic properties of aqueous complexes of the rare earth elements at high pressures and temperatures. *Geochimica et Cosmochimica Acta*, *59*(21), 4329–4350. https://doi.org/10.1016/0016-7037(95)00314-P

Haley, B. A., Du, J., Abbott, A. N., & McManus, J. (2017). The Impact of Benthic Processes on Rare Earth Element and Neodymium Isotope Distributions in the Oceans. *Frontiers in Marine Science*, *4*(December), 1–12. https://doi.org/10.3389/fmars.2017.00426

Haley, B. A., Frank, M., Hathorne, E., & Pisias, N. (2014). Biogeochemical implications from dissolved rare earth element and Nd isotope distributions in the Gulf of Alaska. *Geochimica et Cosmochimica Acta*, *126*, 455–474. https://doi.org/10.1016/j.gca.2013.11.012

Haley, B. A., & Klinkhammer, G. P. (2003). Complete separation of rare earth elements from small volume seawater samples by automated ion chromatography: Method development and application to benthic flux. *Marine Chemistry*, *82*(3–4), 197–220. https://doi.org/10.1016/S0304-4203(03)00070-7

Haley, B. A., Klinkhammer, G. P., & McManus, J. (2004). Rare earth elements in pore waters of marine sediments. *Geochimica et Cosmochimica Acta*, *68*(6), 1265–1279. https://doi.org/10.1016/j.gca.2003.09.012

Haley, B. A., Wu, Y., Muratli, J. M., Basak, C., Pena, L. D., & Goldstein, S. L. (2021). Rare earth element and neodymium isotopes of the eastern US GEOTRACES Equatorial Pacific Zonal Transect (GP16). *Earth and Planetary Science Letters*, *576*, 117233. https://doi.org/10.1016/j.epsl.2021.117233

Hannigan, R., Dorval, E., & Jones, C. (2010). The rare earth element chemistry of estuarine surface sediments in the Chesapeake Bay. *Chemical Geology*, *272*(1–4), 20–30. https://doi.org/10.1016/j.chemgeo.2010.01.009

Hannigan, R. E., & Sholkovitz, E. R. (2001). The development of middle rare earth element enrichments in freshwaters: Weathering of phosphate minerals. *Chemical Geology*, *175*(3–4), 495–508. https://doi.org/10.1016/S0009-2541(00)00355-7

Hao, Z., Li, Y., Li, H., Wei, B., Liao, X., Liang, T., & Yu, J. (2015). Levels of rare earth elements, heavy metals and uranium in a population living in Baiyun Obo, Inner Mongolia, China: A pilot study. *Chemosphere*, *128*, 161–170. https://doi.org/10.1016/j.chemosphere.2015.01.057

Hara, Y., Obata, H., Doi, T., Hongo, Y., Gamo, T., Takeda, S., & Tsuda, A. (2009). Rare earth elements in seawater during an iron-induced phytoplankton bloom of the western subarctic Pacific (SEEDS-II). *Deep Sea Research Part II: Topical Studies in Oceanography*, *56*(26), 2839–2851. https://doi.org/10.1016/j.dsr2.2009.06.009

Haskin, L. A., Wideman, T. R., Frey, A. F., Collins, K. A., Keedy, C. R., & Haskin, M. A. (1966). Rare earths in sediments. *Journal of Geophysical Research*, *71*(24), 6091–6105. https://doi.org/10.1029/jz071i024p06091

Haskin, M. A., & Haskin, L. A. (1966). Rare earths in European shale: A redetermination. *Science*, *154*(3748), 507–509. https://doi.org/10.1126/science.154.3748.507

Hathorne, E. C., Stichel, T., Brück, B., & Frank, M. (2015). Rare earth element distribution in the Atlantic sector of the Southern Ocean: The balance between particle scavenging and vertical supply. *Marine Chemistry*, *177*, 157–171. https://doi.org/10.1016/j.marchem.2015.03.011

Hatje, V., Bruland, K. W., & Flegal, A. R. (2014). Determination of rare earth elements after pre-concentration using NOBIAS-chelate PA-1 resin: Method development and application in the San Francisco Bay plume. *Marine Chemistry*, *160*, 34–41. https://doi.org/10.1016/j.marchem.2014.01.006

Hatje, V., Bruland, K. W., & Flegal, A. R. (2016). Increases in Anthropogenic Gadolinium Anomalies and Rare Earth Element Concentrations in San Francisco Bay over a 20 Year Record. *Environmental Science and Technology*, *50*(8), 4159–4168. https://doi.org/10.1021/acs.est.5b04322

Hatje, V., Sarin, M., Sander, S. G., Ramachandran, P., Völker, C., Barra, R. O., & Tagliabue, A. (2022). Emergent interactive effects of climate change and contaminants in coastal and ocean ecosystems. *Frontiers in Marine Science*, *9*(July), 1–8. https://doi.org/10.3389/fmars.2022.936109

Haxel, G., Hedrick, J. B., Orris, G. J., Stauffer, P. H., & Hendley, J. W. (2002). Rare earth elements: Critical resources for high technology. *US Department of the Interior, US Geological Survey*, *87*(2). https://doi.org/10.3133/fs08702

Hein, J., Koschinsky, A., & Kuhn, T. (2020). Deep-ocean polymetallic nodules as a resource for critical materials. *Nature Reviews Earth & Environment*, *1*(3), 158–169. https://doi.org/10.1038/s43017-020-0027-0

Henríquez-hernández, L. A., Boada, L. D., Carranza, C., Pérez-arellano, J. L., González-antuña, A., Camacho, M., et al. (2017). Blood levels of toxic metals and rare earth elements commonly found in e-waste may exert subtle e ff ects on hemoglobin concentration in sub-Saharan immigrants. *Environment International*, *109*, 20–28. https://doi.org/10.1016/j.envint.2017.08.023

Himmler, T., Haley, B. A., Torres, M. E., Klinkhammer, G. P., Bohrmann, G., & Peckmann, J. (2013). Rare earth element geochemistry in cold-seep pore waters of Hydrate Ridge, northeast Pacific Ocean. *Geo-Marine Letters*, *33*(5), 369–379. https://doi.org/10.1007/s00367-013-0334-2

Hissler, C., Montarges-Pelletier, E., Kanbar, H. J., Le Meur, M., & Gauthier, C. (2023). Impact of past steel-making activities on lanthanides and Y (REY) fractionation and potential mobility in riverbank sediments. *Frontiers in Earth Science*, *10*, 1–12. https://doi.org/10.3389/feart.2022.1056919

Hissler, C., Stille, P., Franc, J., Laurent, P., Chabaux, F., & Pfister, L. (2016). Origin and Dynamics of Rare Earth Elements during Flood Events in Contaminated River Basins: Sr − Nd − Pb Isotopic Evidence. *Environmental Science & Technology*, *50*(9), 4624–4631. https://doi.org/10.1021/acs.est.5b03660

Hissler, C., Stille, P., Krein, A., Geagea, M. L., Perrone, T., Probst, J. L., & Hoffmann, L. (2008). Identifying the origins of local atmospheric deposition in the steel industry basin of Luxembourg using the chemical and isotopic composition of the lichen Xanthoria parietina. *Science of the Total Environment*, *405*(1–3), 338–344. https://doi.org/10.1016/j.scitotenv.2008.05.029

Hodel, F., Grespan, R., de Rafélis, M., Dera, G., Lezin, C., Nardin, E., et al. (2021). Drake Passage gateway opening and Antarctic Circumpolar Current onset 31 Ma ago: The message of foraminifera and reconsideration of the Neodymium isotope record. *Chemical Geology*, *570*(November 2020), 120171. https://doi.org/10.1016/j.chemgeo.2021.120171

Holser, W. T. (1997). Evaluation of the application of rare-earth elements to paleoceanography. *Palaeogeography, Palaeoclimatology, Palaeoecology*, *132*(1–4), 309–323. https://doi.org/10.1016/S0031-0182(97)00069-2

Hongo, Y., Obata, H., Gamo, T., Nakaseama, M., Ishibashi, J., Konno, U., et al. (2007). Rare earth elements in the hydrothermal system at Okinawa Trough back-arc basin. *Geochemical Journal*, *41*, 1–15. https://doi.org/10.2343/geochemj.41.1

Hoyle, J., Elderfield, H., Gledhill, A., & Greaves, M. (1984). The behaviour of the rare earth elements during mixing of river and sea waters. *Geochimica et Cosmochimica Acta*, *48*(1), 143–149. https://doi.org/10.1016/0016-7037(84)90356-9

Hu, Z., Haneklaus, S., Sparovek, G., & Schnug, E. (2006). Rare earth elements in soils. *Communications in Soil Science and Plant Analysis*, *37*(9–10), 1381–1420. https://doi.org/10.1080/00103620600628680

Huang, Y., Colin, C., Liu, Z., Douville, E., Dapoigny, A., Haurine, F., et al. (2023). Impacts of nepheloid layers and mineralogical compositions of oceanic margin sediments on REE concentrations and Nd isotopic compositions of seawater. *Geochimica et Cosmochimica Acta*, *359*, 57–70. https://doi.org/10.1016/j.gca.2023.08.026

Huang, Z. Y., Wu, C. Y., & Hseu, Z. Y. (2023). Rare earth elements in tea garden soils and their bioavailability to tea buds in Taiwan. *Science of the Total Environment*, *893*, 164895. https://doi.org/10.1016/j.scitotenv.2023.164895

Huettel, M., Ziebis, W., Forster, S., & Luther, G. W. (1998). Advective Transport Affecting Metal and Nutrient Distributions and Interfacial Fluxes in Permeable Sediments. *Geochimica et Cosmochimica Acta*, *62*(4), 613–631. https://doi.org/10.1016/S0016-7037(97)00371-2

Idée, J. M., Port, M., Raynal, I., Schaefer, M., Le Greneur, S., & Corot, C. (2006). Clinical and biological consequences of transmetallation induced by contrast agents for magnetic resonance imaging: A review. *Fundamental & Clinical Pharmacology*, *20*(6), 563–576. https://doi.org/10.1111/j.1472-8206.2006.00447.x

Ijiri, A., Okamura, K., Ohta, J., Nishio, Y., Hamada, Y., Iijima, K., & Inagaki, F. (2018). Uptake of porewater phosphate by REY-rich mud in the western North Pacific Ocean. *Geochemical Journal*, *52*(4), 373–387. https://doi.org/10.2343/geochemj.2.0522

Ingri, J., Widerlund, A., Land, M., Gustafsson, Ö., Andersson, P., & Öhlander, B. (2000). Temporal variations in the fractionation of the rare earth elements in a Boreal river; the role of colloidal particles. *Chemical Geology*, *166*(1–2), 23–45. https://doi.org/10.1016/S0009-2541(99)00178-3

Işıldar, A., Rene, E. R., van Hullebusch, E. D., & Lens, P. N. L. (2018). Electronic waste as a secondary source of critical metals: Management and recovery technologies. *Resources, Conservation and Recycling*, *135*(December 2016), 296–312. https://doi.org/10.1016/j.resconrec.2017.07.031

Jacobsen, S. B., & Wasserburg, G. J. (1980). Sm-Nd isotopic evolution of chondrites. *Earth and Planetary Science Letters*, *50*(1), 139–155. https://doi.org/10.1016/0012-821X(80)90125-9

Jeandel, C. (1993). Concentration and isotopic composition of Nd in the South Atlantic Ocean. *Earth and Planetary Science Letters*, *117*(3–4), 581–591. https://doi.org/10.1016/0012-821X(93)90104-H

Jeandel, C., Bishop, J., & Zindler, A. (1995). Exchange of neodymium and its isotopes between seawater and small and large particles in the Sargasso Sea. *Geochimica et Cosmochimica Acta*, *59*(3), 535–547. https://doi.org/10.1016/0016-7037(94)00367-U

Jeandel, C., Delattre, H., Grenier, M., Pradoux, C., & Lacan, F. (2013). Rare earth element concentrations and Nd isotopes in the Southeast Pacific Ocean. *Geochemistry, Geophysics, Geosystems*, *14*(2), 328–341. https://doi.org/10.1029/2012GC004309

Jeandel, C., & Oelkers, E. H. (2015). The influence of terrigenous particulate material dissolution on ocean chemistry and global element cycles. *Chemical Geology*, *395*, 50–66. https://doi.org/10.1016/j.chemgeo.2014.12.001

Jeandel, C., & Peng, T. (1989). Isotopic composition of Nd in Atlantic surface water may signal water flow from the Pacific and Indian Oceans. *Transactions - American Geophysical Union*, *70*(1132). https://doi.org/10.1029/2001GB001635

Jeandel, C., Thouron, D., & Fieux, M. (1998). Concentrations and isotopic compositions of neodymium in the eastern Indian Ocean and Indonesian straits. *Geochimica et Cosmochimica Acta*, *62*(15), 2597–2607. https://doi.org/10.1016/S0016-7037(98)00169-0

Jensen, M., & Choppin, G. (1996). Complexation of europium(III) by aqueous orthosilicic acid. *Radiochimica Acta*, *72*, 143–1150. https://doi.org/10.1524/ract.1996.72.3.143

Jensen, M. P. (1994). *Competitive complexation Studies of Europium(III) and Uranium(VI) Complexation by aqueous orthosilicic acid, College of Arts and Sciences* (p. 198). Florida State University.

Jiang, S. Y., Zhao, H. X., Chen, Y. Q., Yang, T., Yang, J. H., & Ling, H. F. (2007). Trace and rare earth element geochemistry of phosphate nodules from the lower Cambrian black shale sequence in the Mufu Mountain of Nanjing, Jiangsu province, China. *Chemical Geology*, *244*(3–4), 584–604. https://doi.org/10.1016/j.chemgeo.2007.07.010

Jin, P., Zhang, J., Wan, J., Overmans, S., Gao, G., Ye, M., et al. (2021). The Combined Effects of Ocean Acidification and Heavy Metals on Marine Organisms: A Meta-Analysis. *Frontiers in Marine Science*, *8*, 1–14. https://doi.org/10.3389/fmars.2021.801889

Johannesson, K. H., & Burdige, D. J. (2007). Balancing the global oceanic neodymium budget: Evaluating the role of groundwater. *Earth and Planetary Science Letters*, *253*(1–2), 129–142. https://doi.org/10.1016/j.epsl.2006.10.021

Johannesson, K. H., Chevis, D. A., Burdige, D. J., Cable, J. E., Martin, J. B., & Roy, M. (2011). Submarine groundwater discharge is an important net source of light and middle REEs to coastal waters of the Indian River Lagoon, Florida, USA. *Geochimica et Cosmochimica Acta*, *75*(3), 825–843. https://doi.org/10.1016/j.gca.2010.11.005

Johannesson, K. H., Cortés, A., Ramos Leal, J. A., Ramírez, A. G., & Durazo, J. (2005). Geochemistry of rare earth elements in groundwaters from a rhyolite aquifer, central México. *Rare earth elements in groundwater flow systems*, 187–222. https://doi.org/10.1007/1-4020-3234-X_8

Johannesson, K. H., Farnham, I. M., Guo, C., & Stetzenbach, K. J. (1999). Rare earth element fractionation and concentration variations along a groundwater flow path within a shallow, basin-fill aquifer, southern Nevada, USA. *Geochimica et Cosmochimica Acta*, *63*(18), 2697–2708. https://doi.org/10.1016/S0016-7037(99)00184-2

Johannesson, K. H., Hawkins, D. L., & Cortés, A. (2006). Do Archean chemical sediments record ancient seawater rare earth element patterns? *Geochimica et Cosmochimica Acta*, *70*(4), 871–890. https://doi.org/10.1016/j.gca.2005.10.013

Johannesson, K. H., & Hendry, M. J. (2000). Rare earth element geochemistry of groundwaters from a thick till and clay-rich aquitard sequence, Saskatchewan, Canada. *Geochimica et Cosmochimica Acta*, *64*(9), 1493–1509. https://doi.org/10.1016/S0016-7037(99)00402-0

Johannesson, K. H., Lyons, W., & Bird, D. (1994). Rare earth element concentrations and speciation in alkaline lakes from the western U.S.A. *Geophysical Research Letters*, *21*(9), 773–776. https://doi.org/10.1029/94GL00005

Johannesson, K. H., & Lyons, W. B. (1995). Rare-earth element geochemistry of Colour Lake, an acidic freshwater lake on Axel Heiberg Island, Northwest Territories, Canada. *Chemical Geology*, *119*(1–4), 209–223. https://doi.org/10.1016/0009-2541(94)00099-T

Johannesson, K. H., Lyons, W. B., Yelken, M. A., Gaudette, H. E., & Stetzenbach, K. J. (1996). Geochemistry of the rare-earth elements in hypersaline and dilute acidic natural terrestrial waters: Complexation behavior and middle rare-earth element enrichments. *Chemical Geology*, *133*(1–4), 125–144. https://doi.org/10.1016/S0009-2541(96)00072-1

Johannesson, K. H., & Lyons, W. J. (1994). The rare earth element geochemistry of Mono Lake water and the importance of carbonate complexing. *Limnology & Oceanography*, *39*(5), 1141–1154. https://doi.org/10.4319/lo.1994.39.5.1141

Johannesson, K. H., Palmore, C. D., Fackrell, J., Prouty, N. G., Swarzenski, P. W., Chevis, D. A., et al. (2017). Rare earth element behavior during groundwater–seawater mixing along the Kona Coast of Hawaii. *Geochimica et Cosmochimica Acta*, *198*, 229–258. https://doi.org/10.1016/j.gca.2016.11.009

Johannesson, K. H., Stetzenbach, K. J., & Hodge, V. F. (1997). Rare earth elements as geochemical tracers of regional groundwater mixing. *Geochimica et Cosmochimica Acta*, *61*(17), 3605–3618. https://doi.org/10.1016/S0016-7037(97)00177-4

Johannesson, K. H., Stetzenbach, K. J., Hodge, V. F., Kreamer, D. K., & Zhou, X. (1997). Delineation of groundwater flow systems in the southern Great Basin using aqueous rare earth element distributions. *Ground Water*, *35*(5), 807–819. https://doi.org/10.1111/j.1745-6584.1997.tb00149.x

Johannesson, K. H., Stetzenbach, K. J., Hodge, V. F., & Lyons, W. B. (1996). Rare earth element complexation behavior in circumneutral pH groundwaters: Assessing the role of carbonate and phosphate ions. *Earth and Planetary Science Letters*, *139*, 305–319. https://doi.org/10.1016/0012-821X(96)00016-7

Johannesson, K. H., Telfeyan, K., Chevis, D. A., Rosenheim, B. E., & Leybourne, M. (2014). Rare earth elements in stromatolites—1. Evidence that modern terrestrial stromatolites fractionate rare earth elements during incorporation from ambient waters. *Evolution of Archean Crust and Early Life*, 385–411. https://doi.org/10.1007/978-94-007-7615-9_14

Johannesson, K. H., & Zhou, X. (1999). Origin of middle rare earth element enrichments in acid waters of a Canadian High Arctic lake. *Geochimica et Cosmochimica Acta*, *63*(1), 153–165. https://doi.org/10.1016/S0016-7037(98)00291-9

Johannesson, K. H., Zhou, X., Guo, C., Stetzenbach, K. J., & Hodge, V. F. (2000). Origin of rare earth element signatures in groundwaters of circumneutral pH from southern Nevada and eastern California, USA. *Chemical Geology*, *164*(3–4), 239–257. https://doi.org/10.1016/S0009-2541(99)00152-7

Jones, C. E., Halliday, A. N., Rea, D. K., & Owen, R. M. (1994). Neodymium isotopic variations in North Pacific modern silicate sediment and the insignificance of detrital REE contributions to seawater. *Earth and Planetary Science Letters*, *127*(1–4), 55–66. https://doi.org/10.1016/0012-821X(94)90197-X

Kamber, B. S., Greig, A., & Collerson, K. D. (2005). A new estimate for the composition of weathered young upper continental crust from alluvial sediments, Queensland, Australia. *Geochimica et Cosmochimica Acta*, *69*(4), 1041–1058. https://doi.org/10.1016/j.gca.2004.08.020

Kato, Y., Fujinaga, K., Nakamura, K., Takaya, Y., Kitamura, K., Ohta, J., et al. (2011). Deep-sea mud in the Pacific Ocean as a potential resource for rare-earth elements. *Nature Geoscience*, *4*(8), 535–539. https://doi.org/10.1038/ngeo1185

Kawabe, I. (1992). Lanthanide tetrad effect in the Ln3+ ionic radii and refined spin-pairing energy theory. *Geochemical Journal*, *26*(6), 309–335. https://doi.org/10.2343/geochemj.26.309

Kawabe, I., Toriumi, T., Ohta, A., & Miura, N. (1998). Monoisotopic REE abundances in seawater and the origin of seawater tetrad effect. *Geochemical Journal*, *32*(4), 213–229. https://doi.org/10.2343/geochemj.32.213

Keltjens, J., Pol, A., Reimann, J., & Op den Camp, H. (2014). PQQ-dependent methanol dehydrogenases: Rare-earth elements make a difference. *Applied Microbiology and Biotechnology*, *98*(14), 6163–6183. https://doi.org/10.1007/s00253-014-5766-8

Khan, A. M., Bakar, N. K. A., Bakar, A. F. A., & Ashraf, M. A. (2017). Chemical speciation and bioavailability of rare earth elements (REEs) in the ecosystem: A review. *Environmental Science and Pollution Research*, *24*(29), 22764–22789. https://doi.org/10.1007/s11356-016-7427-1

Kim, I., & Kim, G. (2011). Large fluxes of rare earth elements through submarine groundwater discharge (SGD) from a volcanic island, Jeju, Korea. *Marine Chemistry*, *127*(1–4), 12–19. https://doi.org/10.1016/j.marchem.2011.07.006

Kim, I., & Kim, G. (2014). Submarine groundwater discharge as a main source of rare earth elements in coastal waters. *Marine Chemistry*, *160*, 11–17. https://doi.org/10.1016/j.marchem.2014.01.003

Kim, J., Torres, M. E., Haley, B. A., Kastner, M., Pohlman, J. W., Riedel, M., & Lee, Y. (2012). The effect of diagenesis and fluid migration on rare earth element distribution in pore fluids of the northern Cascadia accretionary margin. *Chemical Geology*, *291*, 152–165. https://doi.org/10.1016/j.chemgeo.2011.10.010

Kim, J. H., Torres, M. E., Haley, B. A., Ryu, J. S., Park, M. H., Hong, W. L., & Choi, J. (2016). Marine silicate weathering in the anoxic sediment of the Ulleung Basin: Evidence and consequences. *Geochemistry, Geophysics, Geosystems*, *17*(8), 3437–3453. https://doi.org/10.1002/2016GC006356

Kim, T., Kim, H., & Kim, G. (2020). Tracing river water versus wastewater sources of trace elements using rare earth elements in the Nakdong River estuarine waters. *Marine Pollution Bulletin*, *160*, 111589. https://doi.org/10.1016/j.marpolbul.2020.111589

Klinkhammer, G. (1980). Early diagenesis in sediments from the eastern equatorial Pacific, II. Pore water metal results. *Earth and Planetary Science Letters*, *49*(1), 81–101. https://doi.org/10.1016/0012-821X(80)90151-X

Klinkhammer, G., Elderfield, H., & Hudson, A. (1983). Rare earth elements in seawater near hydrothermal vents. *Nature*, *305*(5931), 185–188. https://doi.org/10.1038/305185a0

Klinkhammer, G., German, C. R., Elderfield, H., Greaves, M. J., & Mitra, A. (1994). Rare earth elements in hydrothermal fluids and plume particulates by inductively coupled plasma mass spectrometry. *Marine Chemistry*, *45*(3), 179–186. https://doi.org/10.1016/0304-4203(94)90001-9

Koeppenkastrop, D., & De Carlo, E. H. (1992). Sorption of rare-earth elements from seawater onto synthetic mineral particles: An experimental approach. *Chemical Geology*, *95*(3–4), 251–263. https://doi.org/10.1016/0009-2541(92)90015-W

Koeppenkastrop, D., & De Carlo, E. H. (1993). Uptake of Rare Earth Elements from Solution by Metal Oxides. *Environmental Science and Technology*, *27*(9), 1796–1802. https://doi.org/10.1021/es00046a006

Koeppenkastrop, D., Decarlo, E. H., & Roth, M. (1991). A method to investigate the interaction of rare earth elements in aqueous solution with metal oxides. *Journal of Radioanalytical and Nuclear Chemistry*, *152*(2), 337–346. https://doi.org/10.1007/BF02104687

Komar, D., Rogan Šmuc, N., Lambaša Belak, Ž., Slavica Matešić, S., Lojen, S., Kniewald, G., et al. (2014). Geochemical Characteristics and Distribution of Rare Earth Elements in Makirina Bay Sediments (N. Dalmatia, Republic of Croatia). *Geologica Macedonica*, *28*(2), 127–137.

Kotelnikova, A. D., Rogova, O. B., & Stolbova, V. V. (2021). Lanthanides in the Soil: Routes of Entry, Content, Effect on Plants, and Genotoxicity (a Review). *Eurasian Soil Science*, *54*(1), 117–134. https://doi.org/10.1134/S1064229321010051

Kraemer, D., & Bau, M. (2022). Siderophores and the formation of cerium anomalies in anoxic environments. *Geochemical Perspectives Letters*, *22*, 50–55.| https://doi.org/10.7185/geochemlet.2227

Kreamer, D. K., Hodge, V. F., Rabinowitz, I., Johannesson, K. H., & Stetzenbach, K. J. (1996). Trace Element Geochemistry in Water from Selected Springs in Death Valley National Park, California. *Ground Water*, *34*(1), 95–103. https://doi.org/10.1111/j.1745-6584.1996.tb01869.x

Kulaksiz, S., & Bau, M. (2007). Contrasting behaviour of anthropogenic gadolinium and natural rare earth elements in estuaries and the gadolinium input into the North Sea. *Earth and Planetary Science Letters*, *260*(1–2), 361–371. https://doi.org/10.1016/j.epsl.2007.06.016

Kulaksiz, S., & Bau, M. (2011). Anthropogenic gadolinium as a microcontaminant in tap water used as drinking water in urban areas and megacities. *Applied Geochemistry*, *26*(11), 1877–1885. https://doi.org/10.1016/j.apgeochem.2011.06.011

Kulaksiz, S., & Bau, M. (2013). Anthropogenic dissolved and colloid/nanoparticle-bound samarium, lanthanum and gadolinium in the Rhine River and the impending destruction of the natural rare earth element distribution in rivers. *Earth and Planetary Science Letters*, *362*, 43–50. https://doi.org/10.1016/j.epsl.2012.11.033

Kumar, K., Saion, E., Halimah, M. K., Ck, Y., & Hamzah, M. S. (2014). Rare earth element (REE) in surface mangrove sediment by instrumental neutron activation analysis. *Journal of Radioanalytical and Nuclear Chemistry*, *301*(3), 667–676. https://doi.org/10.1007/s10967-014-3221-z

Kuss, J., Garbe-Schönberg, C. D., & Kremling, K. (2001). Rare earth elements in suspended particulate material of North Atlantic surface waters. *Geochimica et Cosmochimica Acta*, *65*(2), 187–199. https://doi.org/10.1016/S0016-7037(00)00518-4

Lacan, F., & Jeandel, C. (2001). Tracing Papua New Guinea imprint on the central Equatorial Pacific Ocean using neodymium isotopic compositions and Rare Earth Element patterns. *Earth and Planetary Science Letters*, *186*(3–4), 497–512. https://doi.org/10.1016/S0012-821X(01)00263-1

Lacan, F., & Jeandel, C. (2004). Denmark Strait water circulation traced by heterogeneity in neodymium isotopic compositions. *Deep-Sea Research Part I Oceanographic Research Papers*, *51*(1), 71–82. https://doi.org/10.1016/j.dsr.2003.09.006

Lacan, F., & Jeandel, C. (2005). Neodymium isotopes as a new tool for quantifying exchange fluxes at the continent – Ocean interface. *Earth and Planetary Science Letters*, *232*(3–4), 245–257. https://doi.org/10.1016/j.epsl.2005.01.004

Lachaux, N., Cossu-Leguille, C., Poirier, L., Gross, E. M., & Giamberini, L. (2022). Integrated environmental risk assessment of rare earth elements mixture on aquatic ecosystems. *Frontiers in Environmental Science*, *10*(September). https://doi.org/10.3389/fenvs.2022.974191

Laczniak, R. J., Cole, J. C., Sawyer, D. A., & Trudeau, D. A. (1996). *Summary of hydrogeological controls on ground-water flow at the Nevada test site, Nye county, Nevada*. U. S. Geol. Surv. Water Resour. Investigations Report.

Ladonin, D. V. (2017). Lanthanides in soils of the Cherepovets steel mill impact zone. *Eurasian Soil Science*, *50*(6), 672–680. https://doi.org/10.1134/S1064229317060047

Lagarde, M., Lemaitre, N., Planquette, H., Grenier, M., Belhadj, M., Lherminier, P., & Jeandel, C. (2020). Particulate rare earth element behavior in the North Atlantic (GEOVIDE cruise). *Biogeosciences*, *17*(22), 5539–5561. https://doi.org/10.5194/bg-17-5539-2020

Lai, J., Liu, J., Wu, D., & Xu, J. (2023). Pollution and health risk assessment of rare earth elements in Citrus sinensis growing soil in mining area of southern China. *PeerJ*, *11*, e15470. https://doi.org/10.7717/peerj.15470

Lambelet, M., van de Flierdt, T., Crocket, K., Rehkämper, M., Kreissig, K., Coles, B., et al. (2016). Neodymium isotopic composition and concentration in the western North Atlantic Ocean: Results from the GEOTRACES GA02 section. *Geochimica et Cosmochimica Acta*, *177*, 1–29. https://doi.org/10.1016/j.gca.2015.12.019

Lawrence, M. G., & Kamber, B. S. (2006). The behaviour of the rare earth elements during estuarine mixing-revisited. *Marine Chemistry*, *100*(1–2), 147–161. https://doi.org/10.1016/j.marchem.2005.11.007

Lecomte, K. L., Sarmiento, A. M., Borrego, J., & Nieto, J. M. (2017). Rare earth elements mobility processes in an AMD-affected estuary: Huelva Estuary (SW Spain). *Marine Pollution Bulletin*, *121*(1–2), 282–291. https://doi.org/10.1016/j.marpolbul.2017.06.030

Lee, J. H., & Byrne, R. H. (1994). Pressure dependence of gadolinium carbonate complexation in seawater. *Geochimica et Cosmochimica Acta*, *58*(19), 4009–4016. https://doi.org/10.1016/0016-7037(94)90263-1

Leite, C., Coppola, F., Monteiro, R., Russo, T., Polese, G., Silva, M. R. F., et al. (2020). Toxic impacts of rutile titanium dioxide in Mytilus galloprovincialis exposed to warming conditions. *Chemosphere*, *252*, 126563. https://doi.org/10.1016/j.chemosphere.2020.126563

Leite, C., Coppola, F., Queirós, V., Russo, T., Gianluca, P., Pretti, C., et al. (2023). Can temperature influence the impacts in Mytillus galloprovincialis bt neodymium? Comparison between exposure and recovery periods. *Environmental Toxicology and Pharmacology*, *97*, 104029. https://doi.org/10.1016/j.etap.2022.104029

Leite, C., Russo, T., Cuccaro, A., Pinto, J., Polese, G., Soares, A. M. V. M., et al. (2024). Praseodymium and warming interactions in mussels: Comparison between observed and predicted results. *Science of the Total Environment*, *29*(April 2024), 172893. https://doi.org/10.1016/j.scitotenv.2024.172893

Leong, J. A. M., & Shock, E. L. (2020). Thermodynamic constraints on the geochemistry of low-temperature, continental, serpentinization-generated fluids. *American Journal of Science*, *320*(3), 185–325. https://doi.org/10.2475/03.2020.01

Lerat-Hardy, A., Coynel, A., Dutruch, L., Pereto, C., Bossy, C., Gil-Diaz, T., et al. (2019). Rare Earth Element fluxes over 15 years into a major European Estuary (Garonne-Gironde, SW France): Hospital effluents as a source of increasing gadolinium anomalies. *Science of the Total Environment*, *656*, 409–420. https://doi.org/10.1016/j.scitotenv.2018.11.343

Liang, C., & Shen, J. (2022). Removal of yttrium from rare-earth wastewater by Serratia marcescens: Biosorption optimization and mechanisms studies. *Scientific Reports*, *12*(1), 1–14. https://doi.org/10.1038/s41598-022-08542-0

Lide, D. R., & Haynes, W. M. (2009). *Handbook of chemistry and Physics* (90th ed.). CRC Press.

Lima, A. T., & Ottosen, L. (2021). Recovering rare earth elements from contaminated soils: Critical overview of current remediation technologies. *Chemosphere*, *265*, 129163. https://doi.org/10.1016/j.chemosphere.2020.129163

Lin, Y. T., Liu, R. X., Audira, G., Suryanto, M., Roldan, M., Lee, J.-S., et al. (2022). Lanthanides Toxicity in Zebrafish Embryos Are Correlated to Their Atomic Number. *Toxics*, *10*(6), 336–350. https://doi.org/10.3390/toxics10060336

Liu, W. S., Guo, M. N., Liu, C., Yuan, M., Chen, X. T., Huot, H., et al. (2019a). Water, sediment and agricultural soil contamination from an ion-adsorption rare earth mining area. *Chemosphere*, *216*, 75–83. https://doi.org/10.1016/j.chemosphere.2018.10.109

Liu, X., Hardisty, D. S., Lyons, T. W., & Swart, P. K. (2019). Evaluating the fidelity of the cerium paleoredox tracer during variable carbonate diagenesis on the Great Bahamas Bank. *Geochimica et Cosmochimica Acta*, *248*, 25–42. https://doi.org/10.1016/j.gca.2018.12.028

Liu, Y., Wu, M., Zhang, L., Bi, J., Song, L., Wang, L., et al. (2019). Prenatal exposure of rare earth elements cerium and ytterbium and neonatal thyroid stimulating hormone levels: Findings from a birth cohort study. *Environment International*, *133*(September), 105222. https://doi.org/10.1016/j.envint.2019.105222

Liu, Y., Wu, Q., Jia, H., Wang, Z., Gao, S., & Zeng, J. (2022). Anthropogenic rare earth elements in urban lakes: Their spatial distributions and tracing application. *Chemosphere*, *300*(November 2021), 134534. https://doi.org/10.1016/j.chemosphere.2022.134534

López-González, N., Borrego, J., Carro, B., Grande, J. A., de la Torre, M. L., & Valente, T. (2012). Rare-earth-element fractionation patterns in estuarine sediments as a consequence of acid mine drainage: A case study in SW Spain. *Boletin Geologico y Minero*, *123*(1), 55–64.

Lovley, D. R., & Chapelle, F. H. (1995). Deep subsurface microbial processes. *Reviews of Geophysics*, *33*(3), 365–381. https://doi.org/10.1029/95RG01305

Lumiste, K., Mänd, K., Bailey, J., Paiste, P., Lang, L., Lepland, A., & Kirsimäe, K. (2019). REE+Y uptake and diagenesis in Recent sedimentary apatites. *Chemical Geology*, *525*(May), 268–281. https://doi.org/10.1016/j.chemgeo.2019.07.034

Luoma, S. N. (1983). Bioavailability of trace metals to aquatic organisms—A review. *Science of the Total Environment*, *28*(1–3), 1–22. https://doi.org/10.1016/S0048-9697(83)80004-7

Luoma, S. N. (1989). Can we determine the biological availability of sediment-bound trace elements? *Hydrobiologia*, *176*(1), 379–396. https://doi.org/10.1007/BF00026572

Lyons, W., Tyler, S., Gaudette, H., & Long, D. (1995). The use of strontium isotopes in determining groundwater mixing and brine fingering in a playa spring zone, Lake Tyrrell, Australia. *Journal of Hydrology*, *167*(1–4), 225–239. https://doi.org/10.1016/0022-1694(94)02601-7

Ma, L., Dang, D. H., Wang, W., Evans, R. D., & Wang, W. X. (2019). Rare earth elements in the Pearl River Delta of China: Potential impacts of the REE industry on water, suspended particles and oysters. *Environmental Pollution*, *244*, 190–201. https://doi.org/10.1016/j.envpol.2018.10.015

Ma, L., & Wang, W. (2023). Dissolved rare earth elements in the Pearl River Delta: Using Gd as a tracer of anthropogenic activity from river towards the sea. *Science of the Total Environment*, *856*(May 2022), 159241. https://doi.org/10.1016/j.scitotenv.2022.159241

Ma, Y., Wang, J., Peng, C., Ding, Y., He, X., Zhang, P., et al. (2016). Toxicity of cerium and thorium on Daphnia magna. *Ecotoxicology and Environmental Safety*, *134*, 226–232. https://doi.org/10.1016/j.ecoenv.2016.09.006

MacLeod, K. G., & Irving, A. J. (1996). Correlation of cerium anomalies with indicators of paleoenvironment. *Journal of Sedimentary Research*, *66*(5), 948–955. https://doi.org/10.1306/D426844B-2B26-11D7-8648000102C1865D

MacMillan, G. A., Chételat, J., Heath, J. P., Mickpegak, R., & Amyot, M. (2017). Rare earth elements in freshwater, marine, and terrestrial ecosystems in the eastern Canadian Arctic. *Environmental Sciences: Processes & Impacts*, *19*(10), 1336–1345. https://doi.org/10.1039/c7em00082k

Macmillan, G. A., Clayden, M. G., Chételat, J., Richardson, M. C., Ponton, D. E., Perron, T., & Amyot, M. (2019). Environmental Drivers of Rare Earth Element Bioaccumulation in Freshwater Zooplankton. *Environmental Science and Technology*, *53*(3), 1650–1660. https://doi.org/10.1021/acs.est.8b05547

Mandal, S. K., Ray, R., González, A. G., Mavromatis, V., Pokrovsky, O. S., & Jana, T. K. (2019). State of rare earth elements in the sediment and their bioaccumulation by mangroves: A case study in pristine islands of Indian Sundarban. *Environmental Science and Pollution Research*, *26*(9), 9146–9160. https://doi.org/10.1007/s11356-019-04222-1

Marginson, H., MacMillan, G. A., Grant, E., Gérin-Lajoie, J., & Amyot, M. (2023). Rare earth element bioaccumulation and cerium anomalies in biota from the Eastern Canadian subarctic (Nunavik). *Science of the Total Environment*, *879*, 163024. https://doi.org/10.1016/j.scitotenv.2023.163024

Marsac, R., Catrouillet, C., Davranche, M., Bouhnik-Le Coz, M., Briant, N., Janot, N., et al. (2021). Modeling rare earth elements binding to humic acids with model VII. *Chemical Geology*, *567*, 120099. https://doi.org/10.1016/j.chemgeo.2021.120099

Marsac, R., Davranche, M., Gruau, G., Bouhni-Le Coz, M., & Dia, A. (2011). An improved description of the interactions between rare earth elements and humic acids by modeling: PHREEQC-Model VI coupling. *Geochimica et Cosmochimica Acta*, *75*(19), 5625–5637. https://doi.org/10.1016/j.gca.2011.07.009

Marsac, R., Davranche, M., Gruau, G., & Dia, A. (2010). Metal loading effect on rare earth element binding to humic acid: Experimental and modelling evidence. *Geochimica et Cosmochimica Acta*, *74*(6), 1749–1761. https://doi.org/10.1016/j.gca.2009.12.006

Martin, E., & Haley, B. A. (2000). Fossil fish teeth as proxies for seawater Sr and Nd isotopes. *Geochimica et Cosmochimica Acta*, *64*(5), 835–847. https://doi.org/10.1016/S0016-7037(99)00376-2

Martin, E., Macdougall, J., Herbert, T., Paytan, A., & Kastner, M. (1995). Strontium and neodymium isotopic analyses of marine barite separates. *Geochimica et Cosmochimica Acta*, *59*(7), 1353–1361. https://doi.org/10.1016/0016-7037(95)00049-6

Massari, S., & Ruberti, M. (2013). Rare earth elements as critical raw materials: Focus on international markets and future strategies. *Resources Policy*, *38*(1), 36–43. https://doi.org/10.1016/j.resourpol.2012.07.001

Masuda, A. (1962). Regularities in variation of relative abundances of lanthanide elements and an attempt to analyse separation-index patterns of some minerals. *Journal of Earth Sciences*, *10*, 173–187.

Masuda, A. (1975). Abundances of monoisotopic REE, consistent with the Leedey chondrite values. *Geochemical Journal*, *9*(3), 183–184. https://doi.org/10.2343/geochemj.9.183

Maulvault, A. L., Camacho, C., Barbosa, V., Alves, R., Anacleto, P., Fogaça, F., et al. (2018). Assessing the effects of seawater temperature and pH on the bioaccumulation of emerging chemical contaminants in marine bivalves. *Environmental Research*, *161*(July 2017), 236–247. https://doi.org/10.1016/j.envres.2017.11.017

McCarthy, J. F., Stafford, P. L., & Toran, L. E. (1996). Colloid-facilitated field-scale transport of lanthanides and actinides in fractured saprolite. *Eos*, *77*, F212.

McDonough, W. F., & Sun, S. s. (1995). The composition of the Earth. *Chemical Geology*, *120*(3–4), 223–253. https://doi.org/10.1016/0009-2541(94)00140-4

McLennan, S. M. (1989). Rare earth elements in sedimentary rocks: Influence of provenance and sedimentary processes. In B. Lipin & G. McKay (Eds.), *Geochemistry and mineralogy of rare Earth elements*, *Reviews in mineralogy* (pp. 169–200).

McLennan, S. M. (1994). Rare earth element geochemistry and the "tetrad" effect. *Geochimica et Cosmochimica Acta*, *58*(9), 2025–2033. https://doi.org/10.1007/s11004-021-09959-5

Merschel, G., & Bau, M. (2015). Rare earth elements in the aragonitic shell of freshwater mussel Corbicula fluminea and the bioavailability of anthropogenic lanthanum, samarium and gadolinium in river water. *Science of the Total Environment*, *533*, 91–101. https://doi.org/10.1016/j.scitotenv.2015.06.042

Merschel, G., Bau, M., Baldewein, L., Dantas, E. L., Walde, D., & Bühn, B. (2015). Tracing and tracking wastewater-derived substances in freshwater lakes and reservoirs: Anthropogenic gadolinium and geogenic REEs in Lake Paranoá, Brasilia. *Comptes Rendus Geoscience*, *347*(5–6), 284–293. https://doi.org/10.1016/j.crte.2015.01.004

Merschel, G., Bau, M., & Dantas, E. L. (2017). Contrasting impact of organic and inorganic nanoparticles and colloids on the behavior of particle-reactive elements in tropical estuaries: An experimental study. *Geochimica et Cosmochimica Acta*, *197*, 1–13. https://doi.org/10.1016/j.gca.2016.09.041

Meyer, A. C. S., Grundle, D., & Cullen, J. T. (2021). Selective uptake of rare earth elements in marine systems as an indicator of and control on aerobic bacterial methanotrophy. *Earth and Planetary Science Letters*, *558*, 116756. https://doi.org/10.1016/j.epsl.2021.116756

Michard, A. (1989). Rare earth element systematics in hydrothermal fluids. *Geochimica et Cosmochimica Acta*, *53*(3), 745–750. https://doi.org/10.1016/0016-7037(89)90017-3

Migdisov, A. A., & Williams-Jones, A. E. (2006). A spectrophotometric study of erbium (III) speciation in chloride solutions at elevated temperatures. *Chemical Geology*, *234*(1–2), 17–27. https://doi.org/10.1016/j.chemgeo.2006.04.002

Migdisov, A. A., & Williams-Jones, A. E. (2007). An experimental study of the solubility and speciation of neodymium (III) fluoride in F-bearing aqueous solutions. *Geochimica et Cosmochimica Acta*, *71*(12), 3056–3069. https://doi.org/10.1016/j.gca.2007.04.004

Migdisov, A. A., Williams-Jones, A. E., Normand, C., & Wood, S. A. (2008). A spectrophotometric study of samarium (III) speciation in chloride solutions at elevated temperatures. *Geochimica et Cosmochimica Acta*, *72*(6), 1611–1625. https://doi.org/10.1016/j.gca.2008.01.007

Millero, F., Woosley, R., DiTrolio, B., & Waters, J. (2009). Effect of Ocean Acidification on the Speciation of Metals in Seawater. *Oceanography*, *22*(4), 72–85. https://doi.org/10.5670/oceanog.2009.98

Millero, F. J. (1992). Stability constants for the formation of rare earth-inorganic complexes as a function of ionic strength. *Geochimica et Cosmochimica Acta*, *56*(8), 3123–3132. https://doi.org/10.1016/0016-7037(92)90293-R

Milne, C. J., Kinniburgh, D. G., van Riemsdijk, W. H., & Tipping, E. (2003). Generic NICA-Donnan model parameters for metal-ion binding by humic substances. *Environmental Science & Technology*, *37*(5), 958–971. https://doi.org/10.1021/es0258879

Minami, E. (1935). Gehalte an seltenenErden in europaischen und japanischen. *Nach. Ges. Wiss. Goettingen*, *1*, 155–170.

Mirlean, N., Calliari, L., & Johannesson, K. (2020). Dredging in an estuary causes contamination by fluid mud on a tourist ocean beach. Evidence via REE ratios. *Marine Pollution Bulletin*, *159*(May), 111495. https://doi.org/10.1016/j.marpolbul.2020.111495
Moermond, C. T. A., Tijink, J., van Wezel, A. P., & Koelmans, A. a. (2001). Distribution, speciation, and bioavailability of lanthanides in the Rhine-Meuse estuary, The Netherlands. *Environmental Toxicology and Chemistry*, *20*(9), 1916–1926. https://doi.org/10.1002/etc.5620200909
Moffett, J. W. (1990). Microbially mediated cerium oxidation in sea water. *Nature*, *345*(6274), 421–423. https://doi.org/10.1038/345421a0
Moffett, J. W. (1994). The relationship between cerium and manganese oxidation in the marine environment. *Limnology & Oceanography*, *39*(6), 1309–1318. https://doi.org/10.4319/lo.1994.39.6.1309
Molina-kescher, M., Frank, M., & Hathorne, E. (2014). South Pacific dissolved Nd isotope compositions and rare earth element distributions: Water mass mixing versus biogeochemical cycling. *Geochimica et Cosmochimica Acta*, *127*, 171–189. https://doi.org/10.1016/j.gca.2013.11.038
Molina-Kescher, M., Hathorne, E. C., Osborne, A. H., Behrens, M. K., Kölling, M., Pahnke, K., & Frank, M. (2018). The influence of Basaltic Islands on the Oceanic REE Distribution: A case study from the tropical South Pacific. *Frontiers in Marine Science*, *5*. https://doi.org/10.3389/fmars.2018.00050
Möller, P., & Bau, M. (1993). Rare-earth patterns with positive cerium anomaly in alkaline waters from Lake Van, Turkey. *Earth and Planetary Science Letters*, *117*(3–4), 671–676. https://doi.org/10.1016/0012-821X(93)90110-U
Möller, P., Paces, T., Dulski, P., & Morteani, G. (2002). Anthropogenic Gd in surface water, drainage system, and the water supply of the city of Prague, Czech Republic. *Environmental Science & Technology*, *36*(11), 2387–2394. https://doi.org/10.1021/es010235q
Monecke, T., Kempe, U., Monecke, J., Sala, M., & Wolf, D. (2002). Tetrad effect in rare earth element distribution patterns: A method of quantification with application to rock and mineral samples from granite-related rare metal deposits. *Geochimica et Cosmochimica Acta*, *66*(7), 1185–1196. https://doi.org/10.1016/S0016-7037(01)00849-3
Morad, S., & Felitsyn, S. (2001). Identification of primary Ce-anomaly signatures in fossil biogenic apatite: Implication for the Cambrian oceanic anoxia and phosphogenesis. *Sedimentary Geology*, *143*(3–4), 259–264. https://doi.org/10.1016/S0037-0738(01)00093-8
Morel, E., Cui, L., Zerges, W., & Wilkinson, K. J. (2021). Mixtures of rare earth elements show antagonistic interactions in Chlamydomonas reinhardtii. *Environmental Pollution*, *287*, 117594. https://doi.org/10.1016/j.envpol.2021.117594
Morel, F., & Morgan, J. (1972). A numerical method for computing equilibria in aqueous chemical systems. *Environmental Science & Technology*, *6*(1), 58–67. https://doi.org/10.1021/es60060a006
Morgan, B., Johnston, S. G., Burton, E. D., & Hagan, R. E. (2016). Acidic drainage drives anomalous rare earth element signatures in intertidal mangrove sediments. *Science of the Total Environment*, *573*, 831–840. https://doi.org/10.1016/j.scitotenv.2016.08.172
Moriwaki, H., Koide, R., Yoshikawa, R., Warabino, Y., & Yamamoto, H. (2013). Adsorption of rare earth ions onto the cell walls of wild-type and lipoteichoic acid-defective strains of Bacillus subtilis. *Applied Microbiology and Biotechnology*, *97*(8), 3721–3728. https://doi.org/10.1007/s00253-012-4200-3
Moriwaki, H., & Yamamoto, H. (2013). Interactions of microorganisms with rare earth ions and their utilization for separation and environmental technology. *Applied Microbiology and Biotechnology*, *97*(1), 1–8. https://doi.org/10.1007/s00253-012-4519-9
Morosetti, B., Freitas, R., Pereira, E., Hamza, H., Andrade, M., Coppola, F., et al. (2020). Will temperature rise change the biochemical alterations induced in Mytilus galloprovincialis by cerium oxide nanoparticles and mercury? *Environmental Research*, *188*, 109778. https://doi.org/10.1016/j.envres.2020.109778
Munksgaard, N. C., Lim, K., & Parry, D. L. (2003). Rare earth elements as provenance indicators in North Australian estuarine and coastal marine sediments. *Estuarine, Coastal and Shelf Science*, *57*(3), 399–409. https://doi.org/10.1016/S0272-7714(02)00368-2
Murray, R. W., Buchholtz ten Brink, M. R., Brumsack, H. J., Gerlach, D. C., & RussIII, G. P. (1991). Rare earth elements in Japan Sea sediments and diagenetic behavior of Ce/Ce*: Results from ODP Leg 127. *Geochimica et Cosmochimica Acta*, *55*(9), 2453–2466. https://doi.org/10.1016/0016-7037(91)90365-C
Nakagawa, T., Mitsui, R., Tani, A., Sasa, K., Tashiro, S., Iwama, T., et al. (2012). A Catalytic Role of XoxF1 as La3+-Dependent Methanol Dehydrogenase in Methylobacterium extorquens Strain AM1. *PLoS One*, *7*(11), 1–7. https://doi.org/10.1371/journal.pone.0050480
Nakai, S., Halliday, A., & Rea, D. (1993). Trace element abundance, and Sr and Nd isotope ratios of dust samples in the Pacific Ocean (Table 2). *Pangea*.
Nakamura, Y., Tsumura, Y., Tonogai, Y., Shibata, T., & Ito, Y. (1997). Differences in behavior among the chlorides of seven rare earth elements administered intravenously to rats. *Fundamental and Applied Toxicology*, *37*(2), 106–116. https://doi.org/10.1006/faat.1997.2322
Nance, W. B., & Taylor, S. R. (1976). Rare earth element patterns and crustal sedimentary rocks. *Geochimica et Cosmochimica Acta*, *40*(12), 1539–1551. https://doi.org/10.1016/0016-7037(76)90093-4
Nancharaiah, Y. V., Mohan, S. V., & Lens, P. N. L. (2016). Biological and Bioelectrochemical Recovery of Critical and Scarce Metals. *Trends in Biotechnology*, *34*(2), 137–155. https://doi.org/10.1016/j.tibtech.2015.11.003
Nesbitt, H. (1979). Mobility and fractionation of rare earth elements during weathering of a granodiorite. *Nature*, *279*(5710), 206–210. https://doi.org/10.1038/279206a0
Nigro, A., Sappa, G., & Barbieri, M. (2018). Boron isotopes and rare earth elements in the groundwater of a landfill site. *Journal of Geochemical Exploration*, *190*(September 2017), 200–206. https://doi.org/10.1016/j.gexplo.2018.02.019
Nozaki, Y., & Alibo, D. S. (2003). Importance of vertical geochemical processes in controlling the oceanic profiles of dissolved rare earth elements in the northeastern Indian Ocean. *Earth and Planetary Science Letters*, *205*(3–4), 155–172. https://doi.org/10.1016/S0012-821X(02)01027-0
Nozaki, Y., Alibo, D. S., Amakawa, H., Gamo, T., & Hasumoto, H. (1999). Dissolved rare earth elements and hydrography in the Sulu Sea. *Geochimica et Cosmochimica Acta*, *63*(15), 2171–2181. https://doi.org/10.1016/S0016-7037(99)00142-8
Nozaki, Y., Lerche, D., Alibo, D. S., & Snidvongs, A. (2000). The estuarine geochemistry of rare earth elements and indium in the Chao Phraya River, Thailand. *Geochimica et Cosmochimica Acta*, *64*(23), 3983–3994. https://doi.org/10.1016/S0016-7037(00)00473-7
Nozaki, Y., Zhang, J., & Amakawa, H. (1997). The fractionation between Y and Ho in the marine environment. *Earth and Planetary Science Letters*, *148*(1–2), 329–340. https://doi.org/10.1016/S0012-821X(97)00034-4
Ohnuki, T., Ozaki, T., Kozai, N., Nankawa, T., Sakamoto, F., Sakai, T., et al. (2008). Concurrent transformation of Ce(III) and formation of biogenic manganese oxides. *Chemical Geology*, *253*(1–2), 23–29. https://doi.org/10.1016/j.chemgeo.2008.03.013
Ohta, A., & Kawabe, I. (2001). REE (III) adsorption onto Mn dioxide (δ-MnO 2) and Fe oxyhydroxide. *Geochimica et Cosmochimica Acta*, *65*(5), 695–703. https://doi.org/10.1016/S0016-7037(00)00578-0
Ohta, J., Yasukawa, K., Machida, S., Fujinaga, K., Nakamura, K., Takaya, Y., et al. (2016). Geological factors responsible for REY-rich mud in the western North Pacific Ocean: Implications from mineralogical and grain size distributions. *Geochemical Journal*, *50*(6), 591–603. https://doi.org/10.2343/geochemj.2.0435

Ojiambo, S. B., Lyons, W. B., Welch, K. A., Poreda, R. J., & Johannesson, K. H. (2003). Strontium isotopes and rare earth elements as tracers of groundwater-lake water interactions, Lake Naivasha, Kenya. *Applied Geochemistry*, *18*(11), 1789–1805. https://doi.org/10.1016/S0883-2927(03)00104-5

Oka, A., Tazoe, H., & Obata, H. (2021). Simulation of global distribution of rare earth elements in the ocean using an ocean general circulation model. *Journal of Oceanography*, *77*(3), 413–430. https://doi.org/10.1007/s10872-021-00600-x

Olivarez, A. M., & Owen, R. M. (1989). REE/Fe variations in hydrothermal sediments: Implications for the REE content of seawater. *Geochimica et Cosmochimica Acta*, *53*(3), 757–762. https://doi.org/10.1016/0016-7037(89)90019-7

Olivarez, A. M., & Owen, R. M. (1991). The europium anomaly of seawater: Implications for fluvial versus hydrothermal REE inputs to the oceans. *Chemical Geology*, *92*(4), 317–328. https://doi.org/10.1016/0009-2541(91)90076-4

Olmez, I., Sholkovltz, E. R., Hermann, D., & Eganhouse, R. P. (1991). Rare Earth Elements in Sediments off Southern California: A New Anthropogenic Indicator. *Environmental Science and Technology*, *25*(2), 310–316. https://doi.org/10.1021/es00014a015

Omonona, O. V., & Okogbue, C. O. (2017). Geochemistry of rare earth elements in groundwater from different aquifers in the Gboko area, central Benue Trough, Nigeria. *Environmental Earth Sciences*, *76*(1), 1–19. https://doi.org/10.1007/s12665-016-6329-3

Orani, A. M., Vassileva, E., & Thomas, O. P. (2022). Marine sponges as coastal bioindicators of rare earth elements bioaccumulation in the French Mediterranean Sea. *Environmental Pollution*, *304*(March), 119172. https://doi.org/10.1016/j.envpol.2022.119172

Osborne, A. H., Haley, B. A., Hathorne, E. C., Plancherel, Y., & Frank, M. (2015). Rare earth element distribution in Caribbean seawater: Continental inputs versus lateral transport of distinct REE compositions in subsurface water masses. *Marine Chemistry*, *177*, 172–183. https://doi.org/10.1016/j.marchem.2015.03.013

Osborne, A. H., Hathorne, E. C., Schijf, J., Plancherel, Y., Böning, P., & Frank, M. (2017). The potential of sedimentary foraminiferal rare earth element patterns to trace water masses in the past. *Geochemistry, Geophysics, Geosystems*, *18*(4), 1550–1568. https://doi.org/10.1002/2016GC006782

Ospina-Álvarez, N., Caetano, M., Vale, C., Santos-Echeandía, J., Bernárdez, P., & Prego, R. (2014). Exchange of nutrients across the sediment–water interface in intertidal ria systems (SW Europe). *Journal of Sea Research*, *85*, 349–358. https://doi.org/10.1016/j.seares.2013.07.002

Paffrath, R., Pahnke, K., Behrens, M. K., Reckhardt, A., Ehlert, C., Schnetger, B., & Brumsack, H. J. (2020). Rare Earth Element Behavior in a Sandy Subterranean Estuary of the Southern North Sea. *Frontiers in Marine Science*, *7*(June). https://doi.org/10.3389/fmars.2020.00424

Paffrath, R., Pahnke, K., Böning, P., Rutgers van der Loeff, M., Valk, O., Gdaniec, S., & Planquette, H. (2021). Seawater-Particle Interactions of Rare Earth Elements and Neodymium Isotopes in the Deep Central Arctic Ocean. *Journal of Geophysical Research: Oceans*, *126*(8), e2021JC017423. https://doi.org/10.1029/2021JC017423

Pagano, G., Guida, M., Siciliano, A., Oral, R., Koçbaş, F., Palumbo, A., et al. (2016). Comparative toxicities of selected rare earth elements: Sea urchin embryogenesis and fertilization damage with redox and cytogenetic effects. *Environmental Research*, *147*, 453–460. https://doi.org/10.1016/j.envres.2016.02.031

Palmer, M. R. (1985). Rare earth elements in foraminifera tests. *Earth and Planetary Science Letters*, *73*(2–4), 285–298. https://doi.org/10.1016/0012-821X(85)90077-9

Palmer, M. R., & Elderfield, H. (1986). Rare earth elements and neodymium isotopes in ferromanganese oxide coatings of Cenozoic foraminifera from the Atlantic Ocean. *Geochimica et Cosmochimica Acta*, *50*(3), 409–417. https://doi.org/10.1016/0016-7037(86)90194-8

Pan, F., Xiao, K., Cai, Y., Li, H., Guo, Z., Wang, X., et al. (2023). Integrated effects of bioturbation, warming and sea-level rise on mobility of sulfide and metalloids in sediment porewater of mangrove wetlands. *Water Research*, *233*, 119788. https://doi.org/10.1016/j.watres.2023.119788

Pang, X., Li, D., & Peng, A. (2002). Application of rare-earth elements in the agriculture of china and its environmental behavior in soil. *Environmental Science & Pollution Research*, *9*(2), 143–148. https://doi.org/10.1007/BF02987462

Paper, M., Koch, M., Jung, P., Lakatos, M., Nilges, T., & Brück, T. B. (2023). Rare earths stick to rare cyanobacteria: Future potential for bioremediation and recovery of rare earth elements. *Frontiers in Bioengineering and Biotechnology*, *11*, 1–14. https://doi.org/10.3389/fbioe.2023.1130939

Park, J., Sanford, R. A., & Bethke, C. M. (2006). Geochemical and microbiological zonation of the Middendorf aquifer, South Carolina. *Chemical Geology*, *230*(1–2), 88–104. https://doi.org/10.1016/j.chemgeo.2005.12.001

Pathak, P. N., & Choppin, G. R. (2006). Thermodynamic study of metal silicate complexation in perchlorate media. *Radiochimica Acta*, *94*(2), 81–86. https://doi.org/10.1524/ract.2006.94.2.81

Pattan, J. N., Pearce, N. J. G., & Mislankar, P. G. (2005). Constraints in using Cerium-anomaly of bulk sediments as an indicator of paleo bottom water redox environment: A case study from the Central Indian Ocean Basin. *Chemical Geology*, *221*(3–4), 260–278. https://doi.org/10.1016/j.chemgeo.2005.06.009

Patten, J. T., & Byrne, R. H. (2017). Assessment of Fe(III) and Eu(III) complexation by silicate in aqueous solutions. *Geochimica et Cosmochimica Acta*, *202*, 361–373. https://doi.org/10.1016/j.gca.2016.12.004

Patton, G. M., Francois, R., Weis, D., Hathorne, E., Gutjahr, M., Frank, M., & Gordon, K. (2021). An experimental investigation of the acquisition of Nd by authigenic phases of marine sediments. *Geochimica et Cosmochimica Acta*, *301*, 1–29. https://doi.org/10.1016/j.gca.2021.02.010

Pavel, C. C., Lacal-Arántegui, R., Marmier, A., Schüler, D., Tzimas, E., Buchert, M., et al. (2017). Substitution strategies for reducing the use of rare earths in wind turbines. *Resources Policy*, *52*(May), 349–357. https://doi.org/10.1016/j.resourpol.2017.04.010

Pearce, C. R., Jones, M. T., Oelkers, E. H., Pradoux, C., & Jeandel, C. (2013). The effect of particulate dissolution on the neodymium (Nd) isotope and Rare Earth Element (REE) composition of seawater. *Earth and Planetary Science Letters*, *369–370*, 138–147. https://doi.org/10.1016/j.epsl.2013.03.023

Pedreira, R. M. A., Pahnke, K., Böning, P., & Hatje, V. (2018). Tracking hospital effluent-derived gadolinium in Atlantic coastal waters off Brazil. *Water Research*, *145*, 62–72. https://doi.org/10.1016/j.watres.2018.08.005

Pédrot, M., Dia, A., Davranche, M., & Gruau, G. (2015). Upper soil horizons control the rare earth element patterns in shallow groundwater. *Geoderma*, *239*, 84–96. https://doi.org/10.1016/j.geoderma.2014.09.023

Pérez-López, R., Delgado, J., Nieto, J. M., & Márquez-García, B. (2010). Rare earth element geochemistry of sulphide weathering in the São Domingos mine area (Iberian Pyrite Belt): A proxy for fluid–rock interaction and ancient mining pollution. *Chemical Geology*, *276*(1), 29–40. https://doi.org/10.1016/j.chemgeo.2010.05.018

Pham, V. Q., Grenier, M., Cravatte, S., Michael, S., Jacquet, S., Belhadj, M., et al. (2019). Dissolved rare earth elements distribution in the Solomon Sea. *Chemical Geology*, *524*, 11–36. https://doi.org/10.1016/j.chemgeo.2019.05.012

Pham, V. Q., Jeandel, C., Grenier, M., Cravatte, S., Eldin, G., Belhadj, M., et al. (2022). Neodymium Isotopic Composition and Rare Earth Element Concentration Variations in the Coral and Solomon Seas. *Frontiers in Environmental Chemistry*, *3*. https://doi.org/10.3389/fenvc.2022.803944

Picone, N., & den Camp, H. J. O. (2019). Role of rare earth elements in methanol oxidation. *Current Opinion in Chemical Biology*, *49*, 39–44. https://doi.org/10.1016/j.cbpa.2018.09.019

Piepgras, D. J., & Wasserburg, G. J. (1982). Isotopic composition of neodymium in waters from the Drake Passage. *Science*, *217*(4556), 207–217. https://doi.org/10.1126/science.217.4556.207

Piepgras, D. J., & Wasserburg, G. J. (1987). Rare earth element transport in the western North Atlantic inferred from Nd isotopic observations. *Geochimica et Cosmochimica Acta*, *51*(5), 1257–1271. https://doi.org/10.1016/0016-7037(87)90217-1

Pinto, J., Costa, M., Leite, C., Borges, C., Coppola, F., Henriques, B., et al. (2019). Ecotoxicological effects of lanthanum in Mytilus galloprovincialis: Biochemical and histopathological impacts. *Aquatic Toxicology*, *211*, 181–192. https://doi.org/10.1016/j.aquatox.2019.03.017

Pinto, J., Henriques, B., Soares, J., Costa, M., Dias, M., Fabre, E., et al. (2020). A green method based on living macroalgae for the removal of rare-earth elements from contaminated waters. *Journal of Environmental Management*, *263*, 110376. https://doi.org/10.1016/j.jenvman.2020.110376

Piper, D. Z. (1974). Rare earth elements in the sedimentary cycle: A summary. *Chemical Geology*, *14*(4), 285–304. https://doi.org/10.1016/0009-2541(74)90066-7

Pižeta, I., Sander, S. G., Hudson, R. J. M., Omanović, D., Baars, O., Barbeau, K. A., et al. (2015). Interpretation of complexometric titration data: An intercomparison of methods for estimating models of trace metal complexation by natural organic ligands. *Marine Chemistry*, *173*, 3–24. https://doi.org/10.1016/j.marchem.2015.03.006

Ponnumani, G., Prakash, R., Srinivasamoorthy, K., & Rajesh Kanna, A. (2022). No title. In V. Senapathi, S. Sekar, P. Viswanathan, & C. Sabarathinam (Eds.), *Groundwater contamination in coastal aquifers: Assessment and management* (pp. 35–54). Elsevier.

Ponnurangam, A., Bau, M., Brenner, M., & Koschinsky, A. (2016). Mussel shells of Mytilus edulis as bioarchives of the distribution of rare earth elements and yttrium in seawater and the potential impact of pH and temperature on their partitioning behavior. *Biogeosciences*, *13*(3), 751–760. https://doi.org/10.5194/bg-13-751-2016

Pourmand, A., Dauphas, N., & Ireland, T. J. (2012). A novel extraction chromatography and MC-ICP-MS technique for rapid analysis of REE, Y and Sc: Revising CI-chondrite and Post-Archean Australian Shale (PAAS) abundances. *Chemical Geology*, *291*(38–54), 38–54. https://doi.org/10.1016/j.chemgeo.2011.08.011

Pourmand, A., Prospero, J. M., & Sharifi, A. (2014). Geochemical fingerprinting of trans-Atlantic African dust based on radiogenic Sr-Nd-Hf isotopes and rare earth element anomalies. *Geology*, *42*(8), 675–678. https://doi.org/10.1130/G35624.1

Pourret, O., Davranche, M., Gruau, G., & Dia, A. (2007). Organic complexation of rare earth elements in natural waters: Evaluating model calculations from ultrafiltration data. *Geochimica et Cosmochimica Acta*, *71*(11), 2718–2735. https://doi.org/10.1016/j.gca.2007.04.001

Pourret, O., & Martinez, R. E. (2009). Modeling lanthanide series binding sites on humic acid. *Journal of Colloid and Interface Science*, *330*(1), 45–50. https://doi.org/10.1016/j.jcis.2008.10.048

Pourret, O., & Tuduri, J. (2017). Continental shelves as potential resource of rare earth elements. *Scientific Reports*, *7*(1), 1–6. https://doi.org/10.1038/s41598-017-06380-z

Prasad, M. B. K., & Ramanathan, A. L. (2008). Distribution of rare earth elements in the Pichavaram mangrove sediments of the southeast coast of India. *Journal of Coastal Research*, *1*(24), 126–134. https://doi.org/10.2112/05-0533.1

Prego, R., Caetano, M., Vale, C., & Marmolejo-rodrıguez, J. (2009). Rare earth elements in sediments of the Vigo Ria, NW Iberian Peninsula. *Continental Shelf Research*, *29*(7), 896–902. https://doi.org/10.1016/j.csr.2009.01.009

Prudêncio, M. I., Valente, T., Marques, R., Sequeira Braga, M. A., & Pamplona, J. (2015). Geochemistry of rare earth elements in a passive treatment system built for acid mine drainage remediation. *Chemosphere*, *138*, 691–700. https://doi.org/10.1016/j.chemosphere.2015.07.064

Quadros, A. F., Nordhaus, I., Reuter, H., & Zimmer, M. (2019). Modelling of mangrove annual leaf litterfall with emphasis on the role of vegetation structure. *Estuarine, Coastal and Shelf Science*, *218*, 292–299. https://doi.org/10.1016/j.ecss.2018.12.012

Quinn, K. A., Byrne, R. H., & Schijf, J. (2006). Sorption of yttrium and rare earth elements by amorphous ferric hydroxide: Influence of solution complexation with carbonate. *Geochimica et Cosmochimica Acta*, *70*(16), 4151–4165. https://doi.org/10.1016/j.gca.2006.06.014

Ragnarsdottir, K. V., Oelkers, E. H., Sherman, D. M., & Collins, C. R. (1998). Aqueous speciation of yttrium at temperatures from 25 to 340°C at Psat: An situ EXAFS study. *Chemical Geology*, *151*(1–4), 29–39. https://doi.org/10.1016/S0009-2541(98)00068-0

Ramasamy, D. L., Porada, S., & Sillanpää, M. (2019). Marine algae: A promising resource for the selective recovery of scandium and rare earth elements from aqueous systems. *Chemical Engineering Journal*, *371*(April), 759–768. https://doi.org/10.1016/j.cej.2019.04.106

Ramos, S. J., Dinali, G. S., Oliveira, C., Martins, G. C., Moreira, C. G., Siqueira, J. O., & Guilherme, L. R. G. (2016). Rare Earth Elements in the Soil Environment. *Current Pollution Reports*, *2*(1), 28–50. https://doi.org/10.1007/s40726-016-0026-4

Raymond, K. N., & Pierre, V. C. (2005). Next generation, high relaxivity gadolinium MRI agents. *Bioconjugate Chemistry*, *16*(1), 3–8. https://doi.org/10.1021/bc049817y

Reitz, Z. L., & Medema, M. H. (2022). Genome mining strategies for metallophore discovery. *Current Opinion in Biotechnology*, *77*(Iii), 102757. https://doi.org/10.1016/j.copbio.2022.102757

Rempfer, J., Stocker, T. F., Joos, F., Dutay, J., & Siddall, M. (2011). Modelling Nd-isotopes with a coarse resolution ocean circulation model: Sensitivities to model parameters and source/sink distributions. *Geochimica et Cosmochimica Acta*, *75*(20), 5927–5950. https://doi.org/10.1016/j.gca.2011.07.044

Rétif, J., Zalouk-Vergnoux, A., Briant, N., & Poirier, L. (2023). From geochemistry to ecotoxicology of rare earth elements in aquatic environments: Diversity and uses of normalization reference materials and anomaly calculation methods. *Science of the Total Environment*, *856*, 158890. https://doi.org/10.1016/j.scitotenv.2022.158890

Reynard, B., Lécuyer, C., & Grandjean, P. (1999). Crystal-chemical controls on rare-earth element concentrations in fossil biogenic apatites and implications for paleoenvironmental reconstructions. *Chemical Geology*, *155*(3–4), 233–241. https://doi.org/10.1016/S0009-2541(98)00169-7

Rickli, J., Gutjahr, M., Vance, D., Fischer-Gödde, M., Hillenbrand, C. D., & Kuhn, G. (2014). Neodymium and hafnium boundary contributions to seawater along the West Antarctic continental margin. *Earth and Planetary Science Letters*, *394*, 99–110. https://doi.org/10.1016/j.epsl.2014.03.008

Riglet-Martial, C., Vitorge, P., & Calmon, V. (1998). Electrochemical characterisation of the Ce(IV) limiting carbonate complex. *Radiochimica Acta*, *82*(special-issue.69), 69–76. https://doi.org/10.1524/ract.1998.82

Robinson, S., Ivanovic, R., van de Flierdt, T., Blanchet, C. L., Tachikawa, K., Martin, E. E., et al. (2021). Global continental and marine detrital εNd: An updated compilation for use in understanding marine Nd cycling. *Chemical Geology*, *567*, 120119. https://doi.org/10.1016/j.chemgeo.2021.120119

Rocha, C. (1998). Rhythmic ammonium regeneration and flushing in intertidal sediments of the Sado estuary. *Limnology & Oceanography*, *43*(5), 823–831. https://doi.org/10.4319/lo.1998.43.5.0823

Rogowska, J., Olkowska, E., Ratajczyk, W., & Wolska, L. (2018). Gadolinium as a New Emerging Contaminant of Aquatic Environments. *Environmental Toxicology and Chemistry*, *37*(6), 1523–1534. https://doi.org/10.1002/etc.4116

Romero, F. M., Prol-Ledesma, R. M., Canet, C., Alvares, L. N., & Pérez-Vázquez, R. (2010). Acid drainage at the inactive Santa Lucia mine, western Cuba: Natural attenuation of arsenic, barium and lead, and geochemical behavior of rare earth elements. *Applied Geochemistry*, *25*(5), 716–727. https://doi.org/10.1016/j.apgeochem.2010.02.004

Rönnback, P., Åström, M., & Gustafsson, J. P. (2008). Comparison of the behaviour of rare earth elements in surface waters, overburden groundwaters and bedrock groundwaters in two granitoidic settings, Eastern Sweden. *Applied Geochemistry*, *23*(7), 1862–1880. https://doi.org/10.1016/j.apgeochem.2008.02.008

Rousseau, T., Sonke, J., Chmeleff, J., Van Beek, P., Souhaut, M., Boaventura, G., et al. (2015). Rapid neodymium release to marine waters from lithogenic sediments in the Amazon estuary. *Nature Communications*, *6*(May), 7592. https://doi.org/10.1038/ncomms8592

Roy, M., Martin, J. B., Cable, J. E., & Smith, C. G. (2013). Variations of iron flux and organic carbon remineralization in a subterranean estuary caused by inter-annual variations in recharge. *Geochimica et Cosmochimica Acta*, *103*, 301–315. https://doi.org/10.1016/j.gca.2012.10.055

Roy, M., Martin, J. B., Cherrier, J., Cable, J. E., & Smith, C. G. (2010). Influence of sea level rise on iron diagenesis in an east Florida subterranean estuary. *Geochimica et Cosmochimica Acta*, *74*(19), 5560–5573. https://doi.org/10.1016/j.gca.2010.07.007

Roy, M., Martin, J. B., Smith, C. G., & Cable, J. E. (2011). Reactive-transport modeling of iron diagenesis and associated organic carbon remineralization in a Florida (USA) subterranean estuary. *Earth and Planetary Science Letters*, *304*(1–2), 191–201. https://doi.org/10.1016/j.epsl.2011.02.002

Rudnick, R., & Gao, S. (2003). 3.1 Composition of the Continental Crust. In H. D. Holland & K. K. Turekian (Eds.), *Treatise on geochemistry* (Fisrt Edition, Vol. 3: The Cru, pp. 1–64). : Elsevier-Pergamon. https://doi.org/10.1016/B0-08-043751-6/03016-4

Rue, G., & McKnight, D. (2021). Enhanced rare earth element mobilization in a mountain watershed of the Colorado Mineral Belt with concomitant detection in aquatic biota: Increasing climate change-driven degradation to water quality. *Environmental Science and Technology*, *55*(21), 14378–14388. https://doi.org/10.1021/acs.est.1c02958

Santos, A. C. S. S., Souza, L. A., Araujo, T. G., de Rezende, C. E., & Hatje, V. (2023). Fate and trophic transfer of rare earth elements in a tropical estuarine food web. *Environmental Science and Technology*, *57*(6), 2404–2414. https://doi.org/10.1021/acs.est.2c07726

Santos-Echeandía, J., Vale, C., Caetano, M., Pereira, P., & Prego, R. (2010). Effect of tidal flooding on metal distribution in pore waters of marsh sediments and its transport to water column (Tagus estuary, Portugal). *Marine Environmental Research*, *70*(5), 358–367. https://doi.org/10.1016/j.marenvres.2010.07.003

Sappal, S. M., Ramanathan, A., Ranjan, R. K., Singh, G., & Kumar, A. (2014). Rare Earth Elements As Biogeochemical Indicators In Mangrove Ecosystems (Pichavaram, Tamilnadu, India). *Journal of Sedimentary Research*, *84*(9), 781–791. https://doi.org/10.2110/jsr.2014.63

Schaller, J. (2014). Bioturbation/bioirrigation by Chironomus plumosus as main factor controlling elemental remobilization from aquatic sediments? *Chemosphere*, *107*, 336–343. https://doi.org/10.1016/j.chemosphere.2013.12.086

Schau, M., & Henderson, J. B. (1983). Archean chemical weathering at three localities on the canadian shield. *Precambrian Research*, *20*(C), 189–224. https://doi.org/10.1016/S0166-2635(08)70243-3

Schijf, J., & Byrne, R. H. (2001). Stability constants for mono- and dioxalato-complexes of Y and the REE, potentially important species in groundwaters and surface freshwaters. *Geochimica et Cosmochimica Acta*, *65*(7), 1037–1046. https://doi.org/10.1016/S0016-7037(00)00591-3

Schijf, J., & Byrne, R. H. (2004). Determination of SO4β1 for yttrium and the rare earth elements at I = 0.66 m and t = 25°C—Implications for YREE solution speciation in sulfate-rich waters. *Geochimica et Cosmochimica Acta*, *68*(13), 2825–2837. https://doi.org/10.1016/j.gca.2003.12.003

Schijf, J., & Byrne, R. H. (2008). Comment on "An experimental study of the solubility and speciation of neodymium (III) fluoride in F-bearing aqueous solutions" by A.A. Migdisov and A.E. Williams-Jones. *Geochimica et Cosmochimica Acta*, *72*(22), 5574–5577. https://doi.org/10.1016/j.gca.2008.06.032

Schijf, J., & Byrne, R. H. (2021). Speciation of yttrium and the rare earth elements in seawater: Review of a 20-year analytical journey. *Chemical Geology*, *585*, 120479. https://doi.org/10.1016/j.chemgeo.2021.120479

Schijf, J., Christenson, E. A., & Byrne, R. H. (2015). YREE scavenging in seawater: A new look at an old model. *Marine Chemistry*, *177*, 460–471. https://doi.org/10.1016/j.marchem.2015.06.010

Schijf, J., de Baar, H. J. W., & Millero, F. J. (1994). Kinetics of Ce and Nd scavenging in Black Sea waters. *Marine Chemistry*, *46*(4), 345–359. https://doi.org/10.1016/0304-4203(94)90031-0

Schijf, J., de Baar, H. J. W., & Millero, F. J. (1995). Vertical distributions and speciation of dissolved rare earth elements in the anoxic brines of Bannock Basin, eastern Mediterranean Sea. *Geochimica et Cosmochimica Acta*, *59*(16), 3285–3299. https://doi.org/10.1016/0016-7037(95)00219-P

Schijf, J., & Marshall, K. S. (2011). YREE sorption on hydrous ferric oxide in 0.5M NaCl solutions: A model extension. *Marine Chemistry*, *123*(1–4), 32–43. https://doi.org/10.1016/j.marchem.2010.09.003

Schijf, J., & Zoll, A. M. (2011). When dissolved is not truly dissolved——The importance of colloids in studies of metal sorption on organic matter. *Journal of Colloid and Interface Science*, *361*(1), 137–147. https://doi.org/10.1016/j.jcis.2011.05.029

Schmidt, K., Bau, M., Merschel, G., & Tepe, N. (2019). Anthropogenic gadolinium in tap water and in tap water-based beverages from fast-food franchises in six major cities in Germany. *Science of the Total Environment*, *687*, 1401–1408. https://doi.org/10.1016/j.scitotenv.2019.07.075

Schüler, D., Buchert, M., Liu, R., Dittrich, S., & Merz, C. (2011). Study on rare earths and their recycling. *Öko-Institut eV Darmstadt*, *49*, 30–40.

Seto, M., & Akagi, T. (2008). Chemical conditions for the appearance of a negative Ce anomaly in stream waters and groundwaters. *Geochemical Journal*, *42*(4), 371–380. https://doi.org/10.2343/geochemj.42.371

Sharifi, R., Moore, F., & Keshavarzi, B. (2013). Geochemical behavior and speciation modeling of rare earth elements in acid drainages at Sarcheshmeh porphyry copper deposit, Kerman Province, Iran. *Chemie der Erde*, *73*(4), 509–517. https://doi.org/10.1016/j.chemer.2013.03.001

Shaw, H. F., & Wasserburg, G. J. (1985). Sm-Nd in marine carbonates and phosphates: Implications for Nd isotopes in seawater and crustal ages. *Geochimica et Cosmochimica Acta*, *49*(2), 503–518. https://doi.org/10.1016/0016-7037(85)90042-0

Shields, G., & Stille, P. (2001). Diagenetic constraints on the use of cerium anomalies as palaeoseawater redox proxies: An isotopic and REE study of Cambrian phosphorites. *Chemical Geology*, *175*(1–2), 29–48. https://doi.org/10.1016/S0009-2541(00)00362-4

Shiller, A. M., Chan, E., Joung, D., Redmond, M., & Kessler, J. (2017). Light rare earth element depletion during Deepwater Horizon blowout methanotrophy. *Scientific Reports*, *7*, 1–9. https://doi.org/10.1038/s41598-017-11060-z

Sholkovitz, E. R. (1978). The flocculation of dissolved Fe, Mn, Al, Cu, Ni, Co and Cd during estuarine mixing. *Earth and Planetary Science Letters*, *41*(1), 77–86. https://doi.org/10.1016/0012-821X(78)90043-2

Sholkovitz, E. R. (1992). Chemical evolution of rare earth elements: Fractionation between colloidal and solution phases of filtered river water. *Earth and Planetary Science Letters*, *114*(1), 77–84. https://doi.org/10.1016/0012-821X(92)90152-L

Sholkovitz, E. R. (1993). The geochemistry of rare earth elements in the Amazon River estuary. *Geochimica et Cosmochimica Acta*, *57*(10), 2181–2190. https://doi.org/10.1016/0016-7037(93)90559-F

Sholkovitz, E. R. (1995). The aquatic chemistry of rare earth elements in rivers and estuaries. *Aquatic Geochemistry*, *1*(1), 1–34. https://doi.org/10.1007/BF01025229

Sholkovitz, E. R., Boyle, E. A., & Price, N. B. (1978). The removal of dissolved humic acids and iron during estuarine mixing. *Earth and Planetary Science Letters*, *40*(1), 130–136. https://doi.org/10.1016/0012-821X(78)90082-1

Sholkovitz, E. R., Landing, W. M., & Lewis, B. L. (1994). Ocean particle chemistry: The fractionation of rare earth elements between suspended particles and seawater. *Geochimica et Cosmochimica Acta*, *58*(6), 1567–1579. https://doi.org/10.1016/0016-7037(94)90559-2

Sholkovitz, E. R., Piepgras, D. J., & Jacobsen, S. B. (1989). The pore water chemistry of rare earth elements in Buzzard Bay sediments. *Geochimica et Cosmochimica Acta*, *53*(11), 2847–2856. https://doi.org/10.1016/0016-7037(89)90162-2

Sholkovitz, E. R., Shaw, T. J., & Schneider, D. L. (1992). The geochemistry of rare earth elements in the seasonally anoxic water column and porewaters of Chesapeake Bay. *Geochimica et Cosmochimica Acta*, *56*(9), 3389–3402. https://doi.org/10.1016/0016-7037(92)90386-W

Sholkovitz, E. R., & Szymczak, R. (2000). The estuarine chemistry of rare earth elements: Comparison of the Amazon, Fly, Sepik and the Gulf of Papua systems. *Earth and Planetary Science Letters*, *179*(2), 299–309. https://doi.org/10.1016/S0012-821X(00)00112-6

Siddall, M., Khatiwala, S., van de Flierdt, T., Jones, K., Goldstein, S. L., Hemming, S., & Anderson, R. F. (2008). Towards explaining the Nd paradox using reversible scavenging in an ocean general circulation model. *Earth and Planetary Science Letters*, *274*(3–4), 448–461. https://doi.org/10.1016/j.epsl.2008.07.044

Silva, F. B. V., Nascimento, C. W. A., Alvarez, A. M., & Araújo, P. R. M. (2019). Inputs of rare earth elements in Brazilian agricultural soils via P-containing fertilizers and soil correctives. *Journal of Environmental Management*, *232*, 90–96. https://doi.org/10.1016/j.jenvman.2018.11.031

Silva, R., & Nitsche, H. (1995). Actinide Environmental Chemistry. *Radiochimica Acta*, *70–77*(Supplement), 377–396. https://doi.org/10.1524/ract.1995.7071.special-issue.377

Silva-Filho, E. V., Sanders, C. J., Bernat, M., Figueiredo, A. M. G., Sella, S. M., & Wasserman, J. (2011). Origin of rare earth element anomalies in mangrove sediments, Sepetiba Bay, SE Brazil: Used as geochemical tracers of sediment sources. *Environmental Earth Sciences*, *64*(5), 1257–1267. https://doi.org/10.1007/s12665-011-0942-y

Simon, N. S. (1989). Nitrogen cycling between sediment and the shallow-water column in the transition zone of the Potomac River and Estuary. II. The role of wind-driven resuspension and adsorbed ammonium. *Estuarine, Coastal and Shelf Science*, *28*(5), 531–547. https://doi.org/10.1016/0272-7714(89)90028-0

Singh, S. P., Singh, S. K., Goswami, V., Bhushan, R., & Rai, V. K. (2012). Spatial distribution of dissolved neodymium and εNd in the Bay of Bengal: Role of particulate matter and mixing of water masses. *Geochimica et Cosmochimica Acta*, *94*, 38–56. https://doi.org/10.1016/j.gca.2012.07.017

Skinner, L. C., Sadekov, A., Brandon, M., Greaves, M., Plancherel, Y., de la Fuente, M., et al. (2019). Rare Earth Elements in early-diagenetic foraminifer 'coatings': Pore-water controls and potential palaeoceanographic applications. *Geochimica et Cosmochimica Acta*, *245*, 118–132. https://doi.org/10.1016/j.gca.2018.10.027

Smedley, P. L. (1991). The geochemistry of rare earth elements in groundwater from the Carnmenellis area, southwest England. *Geochimica et Cosmochimica Acta*, *55*(10), 2767–2779. https://doi.org/10.1016/0016-7037(91)90443-9

Smirnova, E. V., Mysovskaya, I. N., Lozhkin, V. I., Sandimirova, G. P., Pakhomova, N. N., & Smagunova, A. A. (2006). Spectral interferences from polyatomic barium ions in inductively coupled plasma mass spectrometry. *Journal of Applied Spectroscopy*, *73*(6), 911–917. https://doi.org/10.1007/s10812-006-0175-0

Soli, A. L., & Byrne, R. H. (2017). Europium silicate complexation at 25°C and 0.7 molar ionic strength. *Marine Chemistry*, *195*, 138–142. https://doi.org/10.1016/j.marchem.2017.02.006

Sousa, T. A., Venancio, I. M., Marques, E. D., Figueiredo, T. S., Nascimento, R. A., Smoak, J. M., et al. (2022). REE anomalies changes in bottom sediments applied in the western equatorial Atlantic since the last interglacial. *Frontiers in Marine Science*, *9*, 1–14. https://doi.org/10.3389/fmars.2022.846976

Souza, L. A., Pedreira, R. M. A., Miró, M., & Hatje, V. (2021). Evidence of high bioaccessibility of gadolinium-contrast agents in natural waters after human oral uptake. *Science of the Total Environment*, *793*, 148506. https://doi.org/10.1016/j.scitotenv.2021.148506

Soyol-Erdene, T. O., Valente, T., Grande, J. A., & de la Torre, M. L. (2018). Mineralogical controls on mobility of rare earth elements in acid mine drainage environments. *Chemosphere*, *205*, 317–327. https://doi.org/10.1016/j.chemosphere.2018.04.095

Squadrone, S., Brizio, P., Battuello, M., Nurra, N., Sartor, R. M., Benedetto, A., et al. (2017). A first report of rare earth elements in northwestern Mediterranean seaweeds. *Marine Pollution Bulletin*, *122*(1–2), 236–242. https://doi.org/10.1016/j.marpolbul.2017.06.048

Squadrone, S., Brizio, P., Stella, C., Mantia, M., Favaro, L., Biancani, B., et al. (2020). Differential bioaccumulation of trace elements and rare earth elements in the muscle, kidneys, and liver of the invasive Indo-Pacific Lionfish (Pterois spp.) from Cuba. *Biological Trace Element Research*, *196*(1), 262–271. https://doi.org/10.1007/s12011-019-01918-w

Squadrone, S., Nurra, N., Battuello, M., Mussat Sartor, R., Stella, C., Brizio, P., et al. (2018). Trace elements, rare earth elements and inorganic arsenic in seaweeds from Giglio Island (Thyrrenian Sea) after the Costa Concordia shipwreck and removal. *Marine Pollution Bulletin*, *133*, 88–95. https://doi.org/10.1016/j.marpolbul.2018.05.028

Stanley, J., & Byrne, R. (1990). The influence of solution chemistry on REE uptake by Ulva Lactuca L. in seawater. *Geochimica et Cosmochimica Acta*, *54*(6), 1587–1595. https://doi.org/10.1016/0016-7037(90)90393-Y

Stetzenbach, K. J., Amano, M., Kreamer, D. K., & Hodge, V. F. (1994). Testing the limits of ICP-MS determination of trace elements in ground water at the parts-per-trillion level. *Ground Water*, *32*(6), 976–985. https://doi.org/10.1111/j.1745-6584.1994.tb00937.x

Stetzenbach, K. J., Hodge, V. F., Guo, C., Farnham, I. M., & Johannesson, K. H. (2001). Geochemical and statistical evidence of deep carbonate groundwater within overlying volcanic rock aquifers/aquitards of southern Nevada, USA. *Journal of Hydrology*, *243*(3–4), 254–271. https://doi.org/10.1016/S0022-1694(00)00418-2

Stichel, T., Hartman, A. E., Duggan, B., Goldstein, S. L., Scher, H., & Pahnke, K. (2015). Separating biogeochemical cycling of neodymium from water mass mixing in the Eastern North Atlantic. *Earth and Planetary Science Letters*, *412*, 245–260. https://doi.org/10.1016/j.epsl.2014.12.008

Stichel, T., Pahnke, K., Duggan, B., Goldstein, S. L., Hartman, A. E., Paffrath, R., & Scher, H. D. (2018). TAG plume: Revisiting the hydrothermal neodymium contribution to seawater. *Frontiers in Marine Science*, *5*, 96. https://doi.org/10.3389/fmars.2018.00096

Stolpe, B., Guo, L., & Shiller, A. M. (2013). Binding and transport of rare earth elements by organic and iron-rich nanocolloids in alaskan rivers, as revealed by field-flow fractionation and ICP-MS. *Geochimica et Cosmochimica Acta*, *106*, 446–462. https://doi.org/10.1016/j.gca.2012.12.033

Sundby, B., Vale, C., Caetano, M., & LutherIII, G. W. (2003). Redox Chemistry in the Root Zone of a Salt Marsh Sediment in the Tagus Estuary, Portugal. *Aquatic Geochemistry*, *9*(3), 257–271. https://doi.org/10.1023/B:AQUA.0000022957.42522.9a

Sutorius, M., Mori, C., Greskowiak, J., Boettcher, L., Bunse, C., Dittmar, T., et al. (2022). Rare earth element behaviour in seawater under the influence of organic matter cycling during a phytoplankton spring bloom – A mesocosm study. *Frontiers in Marine Science*, *9*, 1–20. https://doi.org/10.3389/fmars.2022.895723

Sverjensky, D. A. (1984). Europium redox equilibria in aqueous solution. *Earth and Planetary Science Letters*, *67*(1), 70–78. https://doi.org/10.1016/0012-821X(84)90039-6

Tachikawa, K., Arsouze, T., Bayon, G., Bory, A., Colin, C., Dutay, J. C., et al. (2017). The large-scale evolution of neodymium isotopic composition in the global modern and Holocene ocean revealed from seawater and archive data. *Chemical Geology*, *457*, 131–148. https://doi.org/10.1016/j.chemgeo.2017.03.018

Tachikawa, K., Athias, V., & Jeandel, C. (2003). Neodymium budget in the modern ocean and paleo-oceanographic implications. *Journal of Geophysical Research*, *108*(C8), 3254. https://doi.org/10.1029/1999JC000285

Tachikawa, K., Jeandel, C., & Roy-Barman, M. (1999). A new approach to the Nd residence time in the ocean: The role of atmospheric inputs. *Earth and Planetary Science Letters*, *170*(4), 433–446. https://doi.org/10.1016/S0012-821X(99)00127-2

Tachikawa, K., Jeandel, C., Vangriesheim, A., & Dupré, B. (1999). Distribution of rare earth elements and neodymium isotopes in suspended particles of the tropical Atlantic Ocean (EUMELI site). *Deep-Sea Research Part I Oceanographic Research Papers*, *46*(5), 733–755. https://doi.org/10.1016/S0967-0637(98)00089-2

Tachikawa, K., Toyofuku, T., Basile-Doelsch, I., & Delhaye, T. (2013). Microscale neodymium distribution in sedimentary planktonic foraminiferal tests and associated mineral phases. *Geochimica et Cosmochimica Acta*, *100*, 11–23. https://doi.org/10.1016/j.gca.2012.10.010

Taillefert, M., Neuhuber, S., & Bristow, G. (2007). The effect of tidal forcing on biogeochemical processes in intertidal salt marsh sediments. *Geochemical Transactions*, *8*, 1–15. https://doi.org/10.1186/1467-4866-8-6

Takahashi, Y., Châtellier, X., Hattori, K. H., Kato, K., & Fortin, D. (2005). Adsorption of rare earth elements onto bacterial cell walls and its implication for REE sorption onto natural microbial mats. *Chemical Geology*, *219*(1–4), 53–67. https://doi.org/10.1016/j.chemgeo.2005.02.009

Takahashi, Y., Hayasaka, Y., Morita, K., Kashiwabara, T., Nakada, R., Marcus, M. A., et al. (2015). Transfer of rare earth elements (REE) from manganese oxides to phosphates during early diagenesis in pelagic sediments inferred from REE patterns, X-ray absorption spectroscopy, and chemical leaching method. *Geochemical Journal*, *49*(6), 653–674. https://doi.org/10.2343/geochemj.2.0393

Takahashi, Y., Manceau, A., Geoffroy, N., Marcus, M. A., & Usui, A. (2007). Chemical and structural control of the partitioning of Co, Ce, and Pb in marine ferromanganese oxides. *Geochimica et Cosmochimica Acta*, *71*(4), 984–1008. https://doi.org/10.1016/j.gca.2006.11.016

Takahashi, Y., Sakami, H., & Nomura, M. (2002). Determination of the oxidation state of cerium in rocks by Ce LIII-edge X-ray absorption near-edge structure spectroscopy. *Analytica Chimica Acta*, *468*(2), 345–354. https://doi.org/10.1016/S0003-2670(02)00709-2

Takahashi, Y., Shimizu, H., Usui, A., Kagi, H., & Nomura, M. (2000). Direct observation of tetravalent cerium in ferromanganese nodules and crusts by X-ray-absorption near-edge structure (XANES). *Geochimica et Cosmochimica Acta*, *64*(17), 2929–2935. https://doi.org/10.1016/S0016-7037(00)00403-8

Takahashi, Y., Yoshida, H., Sato, N., Hama, K., Yusa, Y., & Shimizu, H. (2002). W- and M-type tetrad effects in REE patterns for water-rock systems in the Tono uranium deposit, central Japan. *Chemical Geology*, *184*(3–4), 311–335. https://doi.org/10.1016/S0009-2541(01)00388-6

Takaya, Y., Yasukawa, K., Kawasaki, T., FujiTakaya, Y., Yasukawa, K., Kawasaki, T., et al. (2018). The tremendous potential of deep-sea mud as a source of rare-earth elements. *Scientific Reports*, *8*(1), 5763. https://doi.org/10.1038/s41598-018-23948-5

Tan, Q., Li, J., & Zeng, X. (2015). Rare Earth Elements Recovery from Waste Fluorescent Lamps: A Review. *Critical Reviews in Environmental Science and Technology*, *45*(7), 749–776. https://doi.org/10.1080/10643389.2014.900240

Tanaka, K., Tani, Y., Takahashi, Y., Tanimizu, M., Suzuki, Y., Kozai, N., & Ohnuki, T. (2010). A specific Ce oxidation process during sorption of rare earth elements on biogenic Mn oxide produced by Acremonium sp. strain KR21-2. *Geochimica et Cosmochimica Acta*, *74*(19), 5463–5477. https://doi.org/10.1016/j.gca.2010.07.010

Tang, J., & Johannesson, K. H. (2003). Speciation of rare earth elements in natural terrestrial waters: Assessing the role of dissolved organic matter from the modeling approach. *Geochimica et Cosmochimica Acta*, *67*(13), 2321–2339. https://doi.org/10.1016/S0016-7037(02)01413-8

Tang, J., & Johannesson, K. H. (2005). Adsorption of rare earth elements onto Carrizo sand: Experimental investigations and modeling with surface complexation. *Geochimica et Cosmochimica Acta*, *69*(22), 5247–5261. https://doi.org/10.1016/j.gca.2005.06.021

Tang, J., & Johannesson, K. H. (2006). Controls on the geochemistry of rare earth elements along a groundwater flow path in the Carrizo Sand aquifer, Texas, USA. *Chemical Geology*, *225*(1–2), 156–171. https://doi.org/10.1016/j.chemgeo.2005.09.007

Tang, J., & Johannesson, K. H. (2010). Ligand extraction of rare earth elements from aquifer sediments: Implications for rare earth element complexation with organic matter in natural waters. *Geochimica et Cosmochimica Acta*, *74*(23), 6690–6705. https://doi.org/10.1016/j.gca.2010.08.028

Tao, Z., Wang, X., Guo, Z., & Chu, T. (2004). Is there a tetrad effect in the adsorption of lanthanides (III) at solid-water interfaces? *Colloids and Surfaces A: Physicochemical and Engineering Aspects*, *251*(1–3), 19–25. https://doi.org/10.1016/j.colsurfa.2004.08.078

Tariq, H., Sharma, A., Sarkar, S., Ojha, L., Pal, R. P., & Mani, V. (2020). Perspectives for rare earth elements as feed additive in livestock - A review. *Asian-Australasian Journal of Animal Sciences*, *33*(3), 373–381. https://doi.org/10.5713/ajas.19.0242

Taunton, A. E., Welch, S. A., & Banfield, J. F. (2000). Geomicrobiological controls on light rare earth element, Y and Ba distributions during granite weathering and soil formation. *Journal of Alloys and Compounds*, *303–304*, 30–36. https://doi.org/10.1016/S0925-8388(00)00597-1

Taylor, S. R., & McLennan, S. M. (1985). The continental crust: Its composition and evolution.

Taylor, S. R., & McLennan, S. M. (2002). Chemical composition and element distribution in the Earth's crust. In *Encyclopedia of physical science and technology* (3rd ed., pp. 697–719). Academic Press. https://doi.org/10.1016/b0-12-227410-5/00097-1

Telgmann, L., Sperling, M., & Karst, U. (2013). Determination of gadolinium-based MRI contrast agents in biological and environmental samples: A review. *Analytica Chimica Acta*, *764*, 1–16. https://doi.org/10.1016/j.aca.2012.12.007

Tepe, N., Romero, M., & Bau, M. (2014). High-technology metals as emerging contaminants: Strong increase of anthropogenic gadolinium levels in tap water of Berlin, Germany, from 2009 to 2012. *Applied Geochemistry*, *45*, 191–197. https://doi.org/10.1016/j.apgeochem.2014.04.006

Thakur, P., Singh, D. K., & Choppin, G. R. (2007). Polymerization study of o-Si(OH)4 and complexation with Am(III), Eu(III) and Cm(III). *Inorganica Chimica Acta*, *360*(12), 3705–3711. https://doi.org/10.1016/j.ica.2007.04.051

Thomas, P. J., Carpenter, D., Boutin, C., & Allison, J. E. (2014). Rare earth elements (REEs): Effects on germination and growth of selected crop and native plant species. *Chemosphere*, *96*, 57–66. https://doi.org/10.1016/j.chemosphere.2013.07.020

Till, C. P., Shelley, R. U., Landing, W. M., & Bruland, K. W. (2017). Dissolved scandium, yttrium, and lanthanum in the surface waters of the North Atlantic: Potential use as an indicator of scavenging intensity. *Journal of Geophysical Research: Oceans*, *122*(8), 6684–6697. https://doi.org/10.1002/2017JC012696

Tommasi, F., Thomas, P. J., Lyons, D. M., Pagano, G., Oral, R., Siciliano, A., et al. (2023). Evaluation of Rare Earth Element-Associated Hormetic Effects in Candidate Fertilizers and Livestock Feed Additives. *Biological Trace Element Research*, *201*(5), 2573–2581. https://doi.org/10.1007/s12011-022-03331-2

Tommasi, F., Thomas, P. J., Pagano, G., Perono, G. A., Oral, R., Lyons, D. M., et al. (2021). Review of Rare Earth Elements as Fertilizers and Feed Additives: A Knowledge Gap Analysis. *Archives of Environmental Contamination and Toxicology*, *81*(4), 531–540. https://doi.org/10.1007/s00244-020-00773-4

Tostevin, R., Shields, G. A., Tarbuck, G. M., He, T., Clarkson, M. O., & Wood, R. A. (2016). Effective use of cerium anomalies as a redox proxy in carbonate-dominated marine settings. *Chemical Geology*, *438*, 146–162. https://doi.org/10.1016/j.chemgeo.2016.06.027

Toyoda, K., & Tokonami, M. (1990). Diffusion of rare-earth elements in fish teeth from deep-sea sediments. *Nature*, *345*(6276), 607–609. https://doi.org/10.1038/345607a0

Tsuruta, T. (2006). Selective accumulation of light or heavy rare earth elements using gram-positive bacteria. *Colloids and Surfaces B: Biointerfaces*, *52*(2), 117–122. https://doi.org/10.1016/j.colsurfb.2006.04.014

Turner, D. R., Whitfield, M., & Dickson, A. G. (1981). The equilibrium speciation of dissolved components in freshwater and sea water at 25°C and 1 atm pressure. *Geochimica et Cosmochimica Acta*, *45*(6), 855–881. https://doi.org/10.1016/0016-7037(81)90115-0

Turra, C. (2018). Sustainability of rare earth elements chain: From production to food–a review. *International Journal of Environmental Health Research*, *28*(1), 23–42. https://doi.org/10.1080/09603123.2017.1415307

Turra, C., Fernandes, E. A. D. N., & Bacchi, M. A. (2011). Evaluation on rare earth elements of Brazilian agricultural supplies. *Journal of Environmental Chemistry and Ecotoxicology*, *3*(4), 86–92.

Tweed, S. O., Weaver, T. R., Cartwright, I., & Schaefer, B. (2006). Behavior of rare earth elements in groundwater during flow and mixing in fractured rock aquifers: An example from the Dandenong Ranges, southeast Australia. *Chemical Geology*, *234*(3–4), 291–307. https://doi.org/10.1016/j.chemgeo.2006.05.006

Tyler, G. (2004). Rare earth elements in soil and plant systems - A review. *Plant and Soil*, *267*(1–2), 191–206. https://doi.org/10.1007/s11104-005-4888-2

Vale, C., & Sundby, B. (1998). The interactions between living organisms and metals in intertidal and subtidal sediments. In *Metal metabolism in aquatic environments* (pp. 19–29). Springer US. https://doi.org/10.1007/978-1-4757-2761-6_2

van de Flierdt, T., Franck, M., Lee, D., Halliday, A., Reynolds, B., & Hein, J. (2004). New constraints on the sources and behavior of neodymium and hafnium in seawater from Pacific Ocean ferromanganese crusts. *Geochimica et Cosmochimica Acta*, *68*(19), 3827–3843. https://doi.org/10.1016/j.gca.2004.03.009

van de Flierdt, T., Griffths, A. M., Lambelet, M., Little, S. H., Stichel, T., & Wilson, D. J. (2016). Neodymium in the oceans: A global database, a regional comparison and implications for palaeoceanographic research. *Philosophical Transactions of the Royal Society A: Mathematical, Physical & Engineering Sciences*, *374*(2081), 20150293. https://doi.org/10.1098/rsta.2015.0293

Volokh, A. A., Gorbunov, A. V., Gundorina, S. F., Revich, B. A., Frontasyeva, M. V., & Chen, S. P. (1990). Phosphorus fertilizer production as a source of rare-earth elements pollution of the environment. *Science of the Total Environment*, *95*(C), 141–148. https://doi.org/10.1016/0048-9697(90)90059-4

von Blanckenburg, F. (1999). Tracing Past Ocean Circulation? *Science*, *286*(5446), 1862–1863. https://doi.org/10.1126/science.286.5446.1862

Voutsinos, M., Banfield, J. F., & Mcclelland, H. O. (2023). Extensive and diverse lanthanide-dependent metabolism in the ocean. https://doi.org/10.1101/2023.07.25.550467

Voutsinos, M. Y., West-Roberts, J. A., Sachdeva, R., Moreau, J. W., & Banfield, J. F. (2022). Do lanthanide-dependent microbial metabolisms drive the release of REEs from weathered granites? *bioRxiv*, 2022–2103. https://doi.org/10.1101/2022.03.08.483559

Vraspir, J. M., & Butler, A. (2009). Chemistry of marine ligands and siderophores. *Annual Review of Marine Science*, *1*, 43–63. https://doi.org/10.1146/annurev.marine.010908.163712

Wakabayashi, T., Ymamoto, A., Kazaana, A., Nakano, Y., Nojiri, Y., & Kashiwazaki, M. (2016). Antibacterial, Antifungal and Nematicidal Activities of Rare Earth Ions. *Biological Trace Element Research*, *174*(2), 464–470. https://doi.org/10.1007/s12011-016-0727-y

Wang, M. Q., & Xu, Z. R. (2003). Effect of supplemental lanthanum on the growth performance of pigs. *Asian-Australasian Journal of Animal Sciences*, *16*(9), 1360–1363. https://doi.org/10.5713/ajas.2003.1360

Wang, R., Clegg, J., Scott, P., Larkin, C., Deng, F., Thomas, A., et al. (2021). Reversible scavenging and advection – Resolving the neodymium paradox in the South Atlantic. *Geochimica et Cosmochimica Acta*, *314*, 121–139. https://doi.org/10.1016/j.gca.2021.09.015

Wang, S., Wu, S., Yan, W., Huang, W., Miao, L., Lu, J., et al. (2015). Rare metal elements in surface sediment from five bays on the northeastern coast of the South China Sea. *Environmental Earth Sciences*, *74*(6), 4961–4971. https://doi.org/10.1007/s12665-015-4504-6

Wang, Z. L., & Liu, C. Q. (2008). Geochemistry of rare earth elements in the dissolved, acid-soluble and residual phases in surface waters of the Changjiang Estuary. *Journal of Oceanography*, *64*(3), 407–416. https://doi.org/10.1007/s10872-008-0034-0

Wang, Z. L., Zhu, Z. Z., Wang, Z. L., & Liu, C. Q. (2013). Rare earth element geochemistry of waters and suspended particles in alkaline lakes using extraction and sequential chemical methods. *Geochemical Journal*, *47*(6), 639–649. https://doi.org/10.2343/geochemj.2.0290

Wedepohl, K. H. (1995). The composition of the continental crust. *Geochimica et Cosmochimica Acta*, *59*(7), 1217–1232. https://doi.org/10.1016/0016-7037(95)00038-2

Wei, B., Li, Y., Li, H., Yu, J., Ye, B., & Liang, T. (2013). Rare earth elements in human hair from a mining area of China. *Ecotoxicology and Environmental Safety*, *96*, 118–123. https://doi.org/10.1016/j.ecoenv.2013.05.031

Weis, J. S., & Weis, P. (2004). Metal uptake, transport and release by wetland plants: Implications for phytoremediation and restoration. *Environment International*, *30*(5), 685–700. https://doi.org/10.1016/j.envint.2003.11.002

Weltje, L., Heidenreich, H., Zhu, W., Wolterbeek, H. T., Korhammer, S., Goeij, J. J. M., & Markert, B. (2002). Lanthanide concentrations in freshwater plants and molluscs, related to those in surface water, pore water and sediment. A case study in The Netherlands. *Science of the Total Environment*, *286*(1–3), 191–214. https://doi.org/10.1016/S0048-9697(01)00978-0

Weltje, L., Verhoof, L. R. C. W., Verweij, W., & Hamers, T. (2004). Lutetium speciation and toxicity in a microbial bioassay: Testing the free-ion model for lanthanides. *Environmental Science and Technology*, *38*(24), 6597–6604. https://doi.org/10.1021/es049916m

Whitby, H., & van den Berg, C. M. G. (2015). Evidence for copper-binding humic substances in seawater. *Marine Chemistry*, *173*, 282–290. https://doi.org/10.1016/j.marchem.2014.09.011

Wilde, P., Quinby-Hunt, M. S., & Erdtmann, B.-D. (1996). The whole-rock cerium anomaly: A potential indicator of eustatic sea-level changes in shales of the anoxic facies. *Sedimentary Geology*, *101*(1–2), 43–53. https://doi.org/10.1016/0037-0738(95)00020-8

Willis, S. S., & Johannesson, K. H. (2011). Controls on the geochemistry of rare earth elements in sediments and groundwaters of the Aquia aquifer, Maryland, USA. *Chemical Geology*, *285*(1–4), 32–49. https://doi.org/10.1016/j.chemgeo.2011.02.020

Wilson, D. J., Piotrowski, A. M., Galy, A., & Clegg, J. A. (2013). Reactivity of neodymium carriers in deep sea sediments: Implications for boundary exchange and paleoceanography. *Geochimica et Cosmochimica Acta*, *109*, 197–221. https://doi.org/10.1016/j.gca.2013.01.042

Wilson, D. J., Piotrowski, A. M., Galy, A., & McCave, I. N. (2012). A boundary exchange influence on deglacial neodymium isotope records from the deep western Indian Ocean. *Earth and Planetary Science Letters*, *341–344*, 35–47. https://doi.org/10.1016/j.epsl.2012.06.009

Wood, S. A. (1990a). The aqueous geochemistry of the rare-earth elements and yttrium. 1. Review of available low-temperature data for inorganic complexes and the inorganic REE speciation of natural waters. *Chemical Geology*, *82*, 159–186. https://doi.org/10.1016/0009-2541(90)90080-Q

Wood, S. A. (1990b). The aqueous geochemistry of the rare-earth elements and yttrium. 2. Theoretical predictions of speciation in hydrothermal solutions to 350°C at saturation water vapor pressure. *Chemical Geology*, *88*(1–2), 99–125. https://doi.org/10.1016/0009-2541(90)90106-H

Wysocka, I. (2021). Determination of rare earth element concentrations in natural waters - A review of ICP-MS measurement approaches. *Talanta*, *221*, 121636. https://doi.org/10.1016/j.talanta.2020.121636

Xu, T., Zhang, M., Hu, J., Li, Z., Wu, T., Bao, J., et al. (2017). Behavioral deficits and neural damage of Caenorhabditis elegans induced by three rare earth elements. *Chemosphere*, *181*, 55–62. https://doi.org/10.1016/j.chemosphere.2017.04.068

Yoshida, T., Ozaki, T., Ohnuki, T., & Francis, A. J. (2004). Adsorption of rare earth elements by g-Al2O3 and Pseudomonas fluorescens cells in the presence of desferrioxamine B: Implication of siderophores for the Ce anomaly. *Chemical Geology*, *212*(3–4), 239–246. https://doi.org/10.1016/j.chemgeo.2004.08.046

Yu, P., Hayes, S. A., O'Keefe, T. J., O'Keefe, M. J., & Stoffer, J. O. (2006). The phase stability of cerium species in aqueous systems. II. The Ce (III/IV)-H_2O-H_2O_2/O_2 systems. Equilibrium considerations and Pourbaix diagram calculations. *Journal of the Electrochemical Society*, *153*(1), C74–C79. https://doi.org/10.1149/1.2130572

Yuan, M., Guo, M.-N., Liu, W.-S., Liu, C., van der Ent, A., Morel, J. L., et al. (2017). The accumulation and fractionation of rare earth elements in hydroponically grown *Phytolacca americana L. Plant and Soil*, *421*(1–2), 67–82. https://doi.org/10.1007/s11104-017-3426-3

Yuksekdag, A., Kose-Mutlu, B., Siddiqui, A. F., Wiesner, M. R., & Koyuncu, I. (2022). A holistic approach for the recovery of rare earth elements and scandium from secondary sources under a circular economy framework – A review. *Chemosphere*, *293*(October 2021), 133620. https://doi.org/10.1016/j.chemosphere.2022.133620

Zaharescu, D. G., Burghelea, C. I., Dontsova, K., Presler, J. K., Maier, R. M., Huxman, T., et al. (2017). Ecosystem Composition Controls the Fate of Rare Earth Elements during Incipient Soil Genesis. *Scientific Reports*, *7*, 1–15. https://doi.org/10.1038/srep43208

Zapp, P., Schreiber, A., Marx, J., & Kuckshinrichs, W. (2022). Environmental impacts of rare earth production. *MRS Bulletin*, *47*(3), 267–275. https://doi.org/10.1557/s43577-022-00286-6

Zhang, C., Wang, L., Zhang, S., & Li, X. (1998). Geochemistry of rare earth elements in the mainstream of the Yangtze River, China. *Applied Geochemistry*, *13*(4), 451–462. https://doi.org/10.1016/S0883-2927(97)00079-6

Zhang, H., He, X., Bai, W., Guo, X., Zhang, Z., Chaia, Z., & Zhao, Y. (2010). Ecotoxicological assessment of lanthanum with Caenorhabditis elegans in liquid medium. *Metallomics*, *2*(12), 806–810. https://doi.org/10.1039/c0mt00059k

Zhang, K., & Shields, G. A. (2022). Sedimentary Ce anomalies: Secular change and implications for paleoenvironmental evolution. *Earth-Science Reviews*, *229*, 104015. https://doi.org/10.1016/j.earscirev.2022.104015

Zhang, R., Yan, C., & Liu, J. (2013). Effect of Mangroves on the Horizontal and Vertical Distributions of Rare Earth Elements in Sediments of the Zhangjiang Estuary in Fujian Province, Southeastern China. *Journal of Coastal Research*, *29*(2005), 1341–1350. https://doi.org/10.2112/JCOASTRES-D-11-00215.1

Zhang, X., Hu, Z., Pan, H., Bai, Y., Hu, Y., & Jin, S. (2022). Effects of rare earth elements on bacteria in rhizosphere, root, phyllosphere and leaf of soil–rice ecosystem. *Scientific Reports*, *12*(1), 1–17. https://doi.org/10.1038/s41598-022-06003-2

Zhao, P., Bi, R., Sanganyado, E., Zeng, X., Li, W., Lyu, Z., et al. (2022). Rare earth elements in oysters and mussels collected from the Chinese coast: Bioaccumulation and human health risks. *Marine Pollution Bulletin*, *184*(July), 114127. https://doi.org/10.1016/j.marpolbul.2022.114127

Zhao, Y., Wei, W., Li, S., Yang, T., Zhang, R., Somerville, I., et al. (2021). Rare earth element geochemistry of carbonates as a proxy for deep-time environmental reconstruction. *Palaeogeography, Palaeoclimatology, Palaeoecology*, *574*, 110443. https://doi.org/10.1016/j.palaeo.2021.110443

Zheng, H., Yang, Y., Liu, W., Zhong, Y., Cao, Y., Qiu, R. L., et al. (2023). Rare earth elements detoxification mechanism in the hyperaccumulator Dicranopteris linearis: [silicon-pectin] matrix fixation. *Journal of Hazardous Materials*, *452*(November 2022), 131254. https://doi.org/10.1016/j.jhazmat.2023.131254

Zheng, X. Y., Plancherel, Y., Saito, M. A., Scott, P. M., & Henderson, G. M. (2016). Rare earth elements (REEs) in the tropical South Atlantic and quantitative deconvolution of their non-conservative behavior. *Geochimica et Cosmochimica Acta*, *177*, 217–237. https://doi.org/10.1016/j.gca.2016.01.018

Zhou, B., Li, Z., Zhao, Y., Zhang, C., & Wei, Y. (2016). Rare earth elements supply vs. clean energy technologies: New problems to be solve. *Mineral Resources Management*, *32*(4), 29–44. https://doi.org/10.1515/gospo-2016-0039

Zhou, J. L., Rowland, S., Fauzi, R., Mantoura, C., & Braven, J. (1994). The formation of humic coatings on mineral particles under simulated estuarine conditions—A mechanistic study. *Water Research*, *28*(3), 571–579. https://doi.org/10.1016/0043-1354(94)90008-6

Zocher, A. L., Klimpel, F., Kraemer, D., & Bau, M. (2022). Naturally grown duckweeds as quasi-hyperaccumulators of rare earth elements and yttrium in aquatic systems and the biounavailability of gadolinium-based MRI contrast agents. *Science of the Total Environment*, *838*(5), 155909. https://doi.org/10.1016/j.scitotenv.2022.155909

Zocher, A. L., Kraemer, D., Merschel, G., & Bau, M. (2018). Distribution of major and trace elements in the bolete mushroom Suillus luteus and the bioavailability of rare earth elements. *Chemical Geology*, *483*(2), 491–500. https://doi.org/10.1016/j.chemgeo.2018.03.019

Zoll, A. M., & Schijf, J. (2012). A surface complexation model of YREE sorption on Ulva lactuca in 0.05-5.0M NaCl solutions. *Geochimica et Cosmochimica Acta*, *97*, 183–199. https://doi.org/10.1016/j.gca.2012.08.022

Zwicker, J., Smrzka, D., Vadillo, I., Jiménez-Gavilán, P., Giampouras, M., Peckmann, J., & Bach, W. (2022). Trace and rare earth element distribution in hyperalkaline serpentinite-hosted spring waters and associated authigenic carbonates from the Ronda peridotite. *Applied Geochemistry*, *147*(June), 105492. https://doi.org/10.1016/j.apgeochem.2022.105492

Supporting Information

A very limited number of published studies have addressed Rare Earth Elements (REE) content in porewaters and even less have performed Nd isotopic analyses. Table S1 is a compilation of all data available to date of REE and εNd in porewaters.

Table S1. Data of REE in porewater from previous studies.

Ref. nº	Station Name	Latitude Longitude	Water depth (m)	Depth (cm)	La	Ce	Pr	Nd	Sm	Eu	Gd	Tb	Dy	Ho	Er	Tm	Yb	Lu	εNd
1	Sta.J		15	-5.00		91.90		27.20	4.70	1.04			6.83		5.71		6.26	1.07	
1	Sta.J		15	-5.00	42.50	106.00		27.20	4.13	0.92			7.39		5.56		6.04		
1	Sta.J		15	0.50	51.80	130.00		65.20	15.00	3.38	19.50		26.90		19.70		22.70	3.70	
1	Sta.J		15	0.50		320.00		62.90	14.80	3.20	20.30		25.10		21.20		23.70	4.00	
1	Sta.J		15	2.00		757.00		245.00	40.00	8.46			41.90		29.30		32.30	5.17	
1	Sta.J		15	4.00	106.00	227.00		107.00	23.40	4.97	26.50		29.20		21.90		23.20	3.97	
1	Sta.J	41°32.3'N 70°44.3'W	15	6.00	44.60	98.60		49.00	11.00	2.02			16.20		13.70		15.70	2.67	
1	Sta.J		15	8.00	151.00	264.00		121.00	24.70	5.06			26.30		18.00		18.80	3.07	
1	Sta.J		15	10.00	137.00	268.00		114.00	23.40	4.84	27.10		25.30		17.80		18.60		
1	Sta.J		15	12.00		608.00		274.00	52.50	10.40							28.60		
1	Sta.J		15	14.00		912.00		356.00	69.80	13.60	59.80		61.40		35.90		34.20	5.49	
1	Sta.J		15	18.00	444.00	898.00		358.00		13.20	66.20		62.20		36.10		32.10	5.50	
1	Sta.J		15	24.00		1162.00		486.00	98.10	19.70	87.30		83.40		48.80		48.50	7.77	
1	Sta.J		15	28.00		1910.00		815.00	164.00	30.80			127.0		73.00		68.60	10.80	
2	Sta.J		15	-5.00	61.80	145.00		38.30	6.50	1.40	8.76		10.50		8.72			1.43	
2	Sta.J		15	1.50	117.00	428.00		93.10	19.00	3.87	20.00								
2	Sta.J	41°32.3'N 70°44.3'W	15	4.50	269.00	693.00		266.00	51.90	9.60	49.10		46.40		27.30		25.10		
2	Sta.J		15	7.50	379.00	1248.00		306.00	55.80	14.50	51.40		47.40		27.70		27.30		
2	Sta.J		15	10.50	631.00	1531.00		595.00	115.00	21.00	104.00								
2	Sta.J		15	13.50	842.00	2070.00		788.00	152.00	27.70	140.00								

2	Sta.J		15	19.50	950.00	2359.00		892.00	175.0	32.80	150.00		132.0		73.40		67.90	10.50
2	Sta.J		15	25.50	1095.00	2673.00		1041	204.0	37.70	190.00		155.0		85.40		77.80	12.30
2	Sta.J		15	31.50	1059.00	2448.00		1031	201.0	31.20	192.00		159.0		87.00		80.00	12.60
2	Sta.J		15	34.50	927.00	2263.00		895.00	176.0	32.90	159.00				80.00			12.00
2	Sta.J		15	37.50	1764.00	4104.00		1733	344.00	63.10	311.00							
2	Sta.J		15	40.50	1216.00	2915.00		1214	245.00	45.50	229.00		194.00		109.00		104.00	16.20
2	Sta.J		15	42.50	1300.00	3308.00		1245	251.00	47.30	229.00		201.00		116.00		113.00	18.00
2	Sta.J		15	46.50	913.00	2271.00		888.00	178.00	33.70	169.00		151.00		91.40		91.00	14.90
2	Sta.J		15	52.50	1057.00	2508.00		1040	210.00	39.20	198.00		172.00		102.00		103.00	16.70
2	Sta.J		15	63.00	896.00	2361.00		830.00	167.00	32.40	160.00		152.00		97.10		103.00	17.50
2	Sta.J		15	69.00	551.00	1768.00		512.00	102.00	19.80	102.00		104.00		75.40		85.30	
3	SaanichInlet		219	-5.00	55.00	61.00		33.00	6.20	1.70			6.80		4.80			
3	SaanichInlet		219	1.50	1217.00	649.00		344.00	84.90									
3	SaanichInlet		219	4.50	479.00	193.00		127.00	40.30	12.30			96.90		82.30			
3	SaanichInlet	48°36.6'N 123°30.0'W	219	7.50		244.00		171.00	46.20				135.00		163.00			
3	SaanichInlet		219	10.50	533.00	168.00		113.00	35.70				119.00					
3	SaanichInlet		219	13.50	49.00	48.00		31.00	8.60	3.25					68.10			
3	SaanichInlet		219	16.50	28.00	18.00		13.00	3.40	1.25					11.70			
5	MC64		2930	-5.00	45.40	3.30	6.08	23.60	4.52	1.67	6.31	1.04	8.17	2.38	8.30	1.29	8.85	1.87
5	MC64		2930	0.00	49.80	9.20	6.56	28.20	4.23	1.58	5.88	1.10	9.11	2.29	8.93	1.28	10.69	1.81
5	MC64		2930	0.21	125.00	27.40	24.06	93.30	21.65	6.20	30.85	5.70	42.71	9.53	34.62	6.33	48.34	10.32
5	MC64		2930	0.63	131.90	58.50	17.76	100.00	19.61	5.88	31.10	3.98	35.03	8.33	29.45	5.17	41.43	9.52
5	MC64		2930	1.18	128.70	42.60	19.16	90.90	20.07	5.97	31.90	4.47	40.02	10.30	36.70	6.11	51.23	10.87
5	MC64	17°02.12'S 78°06.53W	2930	1.18	122.60	36.90	16.24	77.80	14.83	4.08	27.82	4.05	33.18	8.02	34.63	5.32	44.95	10.28
5	MC64		2930	1.88	128.40	24.40	18.57	87.50	19.59	5.22	23.94	4.07	27.18	7.01	24.24	3.21	26.01	5.16
5	MC64		2930	1.88	118.20	35.70	19.54	73.80	17.64	3.73	23.93	2.79	25.24	6.07	20.74	2.87	22.44	4.90
5	MC64		2930	2.57	77.10	25.00	9.17	37.90	9.32	2.54	11.20	1.60	13.35	3.36	12.67	1.69	14.45	2.83
5	MC64		2930	2.57	57.10	10.30	7.64	32.00	7.60	-0.02	8.38	0.59	11.76	2.14	8.53	0.95	11.53	2.19
5	MC64		2930	3.26	206.90	67.50	33.37	155.80	32.22	8.09	40.51	5.70	41.47	9.83	31.13	4.45	31.57	5.73
5	MC64		2930	3.26	166.60	59.40	24.56	112.70	16.96	4.56	28.69	3.11	31.67	6.93	23.43	3.05	23.24	4.12

5	MC64		2930	4.96	103.20	62.70	13.98	62.00	13.37	3.24	16.96	2.30	16.92	4.41	13.99	1.85	14.00	2.63
5	MC64		2930	5.65	193.30	74.20	29.70	130.00	25.74	8.12	33.00	5.43	33.38	7.58	25.70	3.60	24.52	4.56
5	MC64		2930	8.69	127.70	51.00	15.54	75.70	14.73	4.11	17.45	2.78	17.85	4.38	15.30	2.07	13.05	2.59
5	MC64		2930	12.08	97.60	53.10	15.67	69.20	13.18	4.18	16.06	2.68	18.12	4.53	14.48	2.33	12.84	2.60
5	MC64		2930	15.47	90.50	187.30	9.59	40.40	6.39	2.06	8.20	1.06	8.84	2.28	8.03	1.16	8.79	1.46
5	MC64		2930	15.47	90.20	199.40	8.05	34.10	6.25	0.99	7.07	0.11	9.65	2.18	8.19	1.06	8.56	1.09
5	MC64		2930	18.86	70.00	66.40	11.32	43.20	7.52	2.01	10.59	1.20	11.41	2.10	8.22	1.11	7.45	1.16
5	Stn.10		3400	-5.00	46.90	3.83	4.42	19.50	4.31	0.02	5.53	0.57	7.09	1.81	7.58	0.80	5.77	1.14
5	Stn.10		3400	-5.00	42.20	1.82	4.67	23.10	3.74	0.69	5.19	0.63	6.38	1.87	6.62	1.00	6.33	1.14
5	Stn.10		3400	0.00	221.20	69.10	36.60	140.10	31.30	7.94	38.90	5.07	36.00	8.34	26.30	3.36	25.90	3.62
5	Stn.10		3400	0.21	418.70	400.00	91.10	367.40	79.80	20.10	76.30	13.70	92.50	17.60	60.90	8.37	53.60	9.16
5	Stn.10		3400	0.63	538.00	580.00	104.40	435.20	93.10	22.20	96.40	14.50	91.40	22.10	67.70	9.34	64.00	12.10
5	Stn.10		3400	1.33	896.60	1288.90	214.40	945.30	201.70	44.50	179.80	31.00	192.30	32.20	98.60	12.60	78.90	10.40
5	Stn.10		3400	2.33	1325.70	2482.30	307.20	1279.9	245.60	64.70	231.10	37.50	223.90	40.90	118.80	15.00	96.70	15.40
5	Stn.10		3400	3.33	1181.40	2239.60	299.60	1275.4	275.70	63.00	219.50	36.90	240.80	43.40	115.90	15.70	96.30	15.00
5	Stn.10		3400	4.33	1091.20	2552.00	277.00	1113.0	247.40	55.70	220.00	34.20	196.90	35.50	104.30	14.10	89.40	14.10
5	Stn.10	36°06.11'N 122°35.23'W	3400	5.33	900.80	1848.30	232.20	941.90	201.20	45.50	182.40	29.80	182.50	31.70	89.50	11.60	74.70	11.20
5	Stn.10		3400	6.33	437.80	879.10	101.50	412.90	84.40	19.30	83.90	12.50	81.80	16.00	43.20	6.03	44.40	6.41
5	Stn.10		3400	7.83														
5	Stn.10		3400	9.83	402.60	911.60	86.20	355.20	76.20	19.70	83.00	11.60	75.50	16.20	45.20	6.35	42.00	7.84
5	Stn.10		3400	11.83	274.20	480.80	57.90	261.90	52.70	14.10	50.80	9.00	70.00	13.50	40.40	5.76	40.10	7.36
5	Stn.10		3400	13.83	421.10	763.60	83.80	481.70	82.10	21.50	87.30	13.20	84.30	17.40	51.90	7.70	48.40	8.51
5	Stn.10		3400	15.83	357.70	770.60	78.40	318.70	71.30	18.90	74.60	10.70	69.10	15.30	43.70	6.75	49.10	8.55
5	Stn.10		3400	19.83	367.20	620.00	83.90	378.90	80.90	20.90	76.50	11.90	86.10	15.20	50.70	6.99	52.60	8.90
5	Stn.10		3400	21.53	296.80	633.70	66.20	284.10	51.30	14.60	60.40	9.25	62.30	13.40	44.80	6.81	53.80	9.59
5	Stn.10		3400	22.92	536.10	999.60	107.30	647.80	108.10	29.40	105.30	16.20	108.30	21.50	61.80	9.44	60.30	11.00
5	Stn.8		800	-5.00	40.80	2.49	3.85	21.50	3.66	1.25	4.93	0.93	6.73	1.88	7.09	1.06	6.79	1.42
5	Stn.8	35°26.24'N 121°26.98'W	800	0.00	51.90	32.80	5.62	25.40	4.29	0.35	5.28	0.64	7.05	1.68	7.91	0.57	4.91	0.88
5	Stn.8		800	0.00	45.20	14.20	6.32	33.00	5.03	1.13	5.89	0.88	7.20	1.90	6.76	0.91	6.12	1.05
5	Stn.8		800	0.21	262.20	437.40	51.20	210.30	40.70	8.50	43.60	6.04	37.40	6.94	24.00	2.93	17.90	2.52

5	Stn.8		800	0.63	314.70	567.60	63.70	274.70	53.40	10.20	56.60	8.10	53.70	10.30	30.10	3.32	24.00	3.23
5	Stn.8		800	1.33	1060.70	1994.10	230.40	926.00	179.8	40.10	170.7	25.30	142.80	29.80	81.30	11.20	63.90	10.20
5	Stn.8		800	2.33	1040.20	1971.40	239.70	998.60	177.0	40.20	166.7	25.50	166.00	32.20	88.30	11.10	71.80	11.00
5	Stn.8		800	3.33	1063.00	2169.10	239.40	986.60	186.7	45.00	181.5	26.90	161.60	29.90	89.60	12.40	66.90	10.00
5	Stn.8		800	4.33	*6650.6*	*12834.5*	*1161.0*	*3660.9*	*95.90*	*22.80*	*93.10*	*15.10*	*82.00*	*16.40*	*44.10*	*5.74*	*38.10*	*6.20*
5	Stn.8		800	5.33	311.70	664.00	69.90	266.30	49.80	10.80	50.30	7.65	46.20	10.40	29.50	3.17	22.10	2.91
5	Stn.8		800	6.33	494.60	951.60	105.20	581.10	96.70	22.60	87.10	14.10	86.70	17.10	44.30	6.33	39.40	5.75
5	Stn.8		800	7.83	767.10	1468.70	201.30	763.50	162.3	36.10	155.9	23.80	135.50	26.10	79.40	9.96	59.80	9.93
5	Stn.8		800	9.83	754.00	1411.60	171.40	694.00	136.5	31.30	125.9	17.70	118.80	22.60	63.10	8.66	52.50	8.45
5	Stn.8		800	11.83	817.00	1534.60	208.80	812.90	163.6	35.80	158.4	23.00	144.10	30.60	77.90	11.30	66.00	10.70
5	Stn.8		800	13.83	784.30	1414.20	199.30	760.20	161.0	35.30	157.7	22.60	140.90	26.80	77.50	11.10	59.70	10.40
5	Stn.8		800	15.83	911.30	2006.80	197.10	857.80	173.9	34.80	155.9	24.10	138.40	27.30	81.20	10.30	63.10	10.30
5	Stn.8		800	17.83	1204.70	2296.80	267.70	1088.30	210.9	48.70	210.6	29.60	187.30	36.30	97.40	13.20	81.50	11.80
5	Stn.8		800	19.83	908.20	2029.50	206.40	836.80	178.5	35.80	157.5	24.40	139.40	28.70	78.10	11.50	63.10	9.27
5	Stn.8		800	21.83	721.30	1323.00	166.3	669.90	146.2	32.10	137.7	21.30	127.90	25.20	74.40	10.50	57.00	9.17
5	Stn.9		1600	-5.00	33.70	10.50	4.59	19.00	3.06	0.54	5.88	0.42	6.18	1.51	5.29	0.55	5.03	0.62
5	Stn.9		1600	-5.00	25.50	6.95	4.79	24.30	3.85	0.95	4.75	0.68	6.29	1.61	6.07	0.72	4.89	0.97
5	Stn.9		1600	0.00	62.90	24.60	6.35	32.30	6.70	1.04	7.99	0.98	10.40	2.88	11.00	1.13	10.00	1.72
5	Stn.9		1600	0.21	181.30	240.30	28.00	143.00	26.90	5.85	31.20	4.74	27.50	6.74	22.10	3.33	24.90	4.54
5	Stn.9		1600	0.69	173.50	210.90	31.80	140.00	28.00	6.50	34.20	5.41	35.10	8.06	29.60	4.27	28.60	5.05
5	Stn.9	35°33.93'N 122°03.38'W	1600	1.47	329.30	489.00	58.80	250.20	50.00	11.30	53.50	8.13	52.60	11.60	34.40	5.27	34.40	6.29
5	Stn.9		1600	2.47	266.00	430.20	54.20	241.10	47.40	9.28	59.20	8.51	46.90	11.20	33.10	5.60	36.50	5.26
5	Stn.9		1600	7.97														
5	Stn.9		1600	9.97	186.20	251.80	33.40	146.10	28.20	4.22	25.90	5.02	27.60	6.76	23.60	3.17	16.40	3.75
5	Stn.9		1600	11.97	229.20	339.50	38.80	168.20	33.80	8.15	37.80	5.61	36.60	7.31	24.60	3.76	22.30	4.32
5	Stn.9		1600	13.97	164.10	260.00	31.10	122.40	27.10	5.99	31.90	4.40	29.30	6.66	24.20	3.29	23.50	4.26
5	Stn.9		1600	16.47	206.00	305.90	36.00	157.90	35.50	6.50	35.40	6.25	35.10	9.21	23.70	4.19	26.80	4.37
6	ER CS40 (Mud Volcano)		680	1.00	185.00	563.00	65.90	266.00	49.90	9.30	39.10	62.00	38.50	7.90	23.80		19.00	2.60

6	N2-Kl--41 (Pockmarks)		540	1.25	485.00	1439.00	133.00	518.00	95.10	22.00	745.00	10.00	52.60	10.10	26.70		23.90	3.70
6	N2-Kl--41 (Pockmarks)		540	17.50	382.00	1117.00	103.00	388.00	68.50	15.50	67.60	9.00	47.30	9.90	28.20		25.40	4.30
6	N2-Kl-20 (Pockmarks)		540	1.25	723.00	2177.00	193.00	746.00	139.00	30.70	111.60	153.00	81.50	15.80	40.80		33.30	4.80
6	N2-Kl-20 (Pockmarks)		540	7.50	472.00	1386.00	124.00	486.00	90.70	19.90	*739.00*	102.00	56.70	11.60	32.60		26.50	4.00
6	N2-Kl-20 (Pockmarks)		540	77.50	326.00	870.00	79.20	319.00	62.50	16.80	685.00	*99.00*	59.60	13.20	38.00		31.60	4.90
7	U1325		2194	73.00	113.32	250.97	29.24	124.69	41.11	12.32	64.29	12.97	105.60	32.10	126.40	24.12	176.42	36.40
7	U1325		2194	293.00	132.88	231.56	23.81	123.23	35.07	11.66	56.82	7.93	69.25	15.16	68.27	9.04	96.80	15.38
7	U1325		2194	443.00	152.74	361.01	44.97	217.75	64.20	18.98	104.11	12.54	97.38	23.34	79.28	11.53	87.11	13.51
7	U1325		2194	523.00	187.83	410.06	44.60	217.47	49.45	12.99	77.11	10.95	69.70	21.73	68.82	13.31	112.20	19.28
7	U1325		2194	593.00	125.48	293.80	35.24	147.75	37.27	13.03	75.85	13.79	107.47	25.26	102.12	15.32	159.63	26.17
7	U1325		2194	673.00	152.36	291.28	28.77	179.44	48.93	13.34	88.76	11.52	102.46	22.68	99.56	16.90	121.72	22.75
7	U1325		2194	743.00	172.19	407.93	51.25	273.12	84.50	21.82	99.94	19.14	151.51	36.23	117.90	24.87	172.62	32.17
7	U1325		2194	2675.00	41.73	101.87	12.48	69.68	13.54	5.61	29.91	7.51	97.44	42.43	187.96	40.75	359.31	77.34
7	U1325	48.6450°N 126.9830°W	2194	3635.00	324.38	767.79	91.29	365.15	86.61	28.17	129.86	19.72	140.17	38.52	141.54	26.07	229.39	46.24
7	U1325		2194	4593.00	117.34	240.26	29.35	145.66	40.32	11.31	69.83	12.14	99.86	38.15	152.41	30.25	272.79	54.06
7	U1325		2194	5043.00	269.66	428.28	44.11	158.20	32.44	1.77	28.07	7.06	81.56	28.07	153.00	31.47	250.67	59.26
7	U1325		2194	5543.00	74.12	183.31	29.51	127.20	28.17	8.58	53.49	13.43	92.49	22.26	80.74	16.74	113.90	19.85
7	U1325		2194	6913.00	112.99	212.80	29.26	133.77	34.78	6.31	47.17	10.97	95.58	22.92	93.58	19.02	132.41	28.40
7	U1325		2194	10976.00	98.56	203.54	35.62	144.47	33.84	7.20	55.77	12.68	113.23	29.93	135.04	25.32	201.66	39.15
7	U1325		2194	11455.00	205.63	431.49	65.17	279.86	73.89	19.11	87.61	21.39	165.56	39.48	151.96	31.25	219.14	46.86
7	U1325		2194	24925.00	96.79	74.76	13.71	60.89	22.73	11.62	53.89	4.08	43.75	12.59	43.06	7.62	60.01	10.24
7	U1325		2194	26890.00	187.63	156.64	44.77	169.01	49.44	23.25	63.32	11.09	74.88	21.87	59.42	9.16	77.71	16.54
7	U1325		2194	29780.00	200.62	211.23	50.97	205.33	48.38	12.82	68.28	13.26	101.84	23.25	79.48	13.47	89.32	14.48
7	U1329	48.7890°N 126.6780°W	946	145.00	71.16	147.74	14.81	57.13	12.16	3.78	23.19	5.33	30.46	9.85	29.55	6.22	42.47	8.83
7	U1329		946	295.00	29.85	64.69	7.13	33.42	2.82	1.68	4.00	2.76	6.23	3.81	13.94	3.20	17.02	4.62

7	U1329		946	445.00	14.84	26.82	2.60	11.97	2.60	0.59	2.43	1.01	4.34	2.70	10.59	3.17	22.31	4.63
7	U1329		946	643.00	16.84	37.11	3.00	19.86	4.41	1.12	0.70	1.87	7.18	3.42	14.54	2.53	22.22	5.83
7	U1329		946	793.00	43.03	96.08	17.84	66.99	17.48	5.94	28.60	5.82	50.29	16.82	54.57	9.45	77.29	15.61
7	U1329		946	943.00	55.68	126.49	21.40	90.33	25.52	8.40	33.33	7.60	57.29	15.23	61.53	10.15	85.18	17.79
7	U1329		946	1093.00	63.42	139.36	19.91	74.21	27.92	8.35	34.90	10.14	80.59	27.60	119.06	22.66	193.19	45.10
7	U1329		946	1243.00	78.21	144.97	22.74	81.09	18.53	7.51	38.14	9.57	72.33	21.63	91.60	18.81	156.59	37.21
7	U1329		946	1393.00	93.83	196.56	28.83	115.30	35.71	14.98	56.67	13.50	111.83	30.51	116.04	20.98	157.76	33.08
7	U1329		946	2421.00	21.90	42.56	6.65	24.27	4.45	3.87	10.98	2.89	19.83	6.58	23.62	5.48	40.20	7.69
7	U1329		946	5353.00	66.74	70.07	8.29	50.63	10.62	6.59	35.82	6.19	41.94	14.42	50.55	10.01	67.18	15.00
7	U1329		946	7450.00	10.77	28.54	1.31	11.23	3.93	0.83	4.17	0.51	0.55	1.29	4.13	0.78	6.94	2.20
7	U1329		946	8900.00	50.96	80.06	8.98	51.69	13.81	3.90	20.60	3.44	19.44	7.95	22.88	5.13	39.41	8.20
7	U1329		946	10298.00	57.75	200.21	15.03	63.70	13.81	7.86	17.70	5.97	28.65	9.74	29.60	6.97	49.51	11.41
7	U1329		946	11250.00	69.85	97.34	13.53	59.92	13.06	7.76	12.82	5.28	19.23	7.71	24.25	4.20	33.30	6.67
7	U1329		946	12900.00	88.75	165.73	22.12	88.17	23.34	13.27	31.12	9.14	43.59	13.49	40.85	6.52	50.41	11.25
7	U1329		946	13995.00	118.18	148.38	18.66	92.31	15.40	11.97	16.26	6.23	37.15	11.13	34.49	4.36	52.57	7.97
7	U1329		946	15275.00	110.09	193.22	23.96	120.62	27.74	10.95	41.51	8.64	50.82	14.43	44.56	6.66	55.62	9.35
7	U1329		946	17645.00	99.25	153.00	20.87	97.94	19.65	9.43	25.30	7.66	53.02	14.99	43.99	7.91	56.44	9.71
8	HRN (A99-11-AD3423)		600	0.00	43.20			11.50	5.06	2.27	3.45	0.87		2.00	1.17	0.48	2.67	0.67
8	HRN (A99-11-AD3423)		600	0.75	117.00	236.00	37.20	93.30	24.80	6.57	20.80	4.00		5.87	13.00	2.06	14.30	2.58
8	HRN (A99-11-AD3423)		600	2.26	171.00	616.00	69.70	251.00	59.70	14.10	47.70	8.22		11.20	29.90	5.24	36.60	6.56
8	HRN (A99-11-AD3423)	44°40.03'N 125°06.01'W	600	3.77	98.60	160.00	18.20	44.70	21.40	3.76	12.90	2.80		4.79	6.99	1.56	7.03	1.73
8	HRN (A99-11-AD3423)		600	5.27	99.10	90.70	9.13	46.20	8.61	3.33	14.50	4.58			2.63		4.02	1.68
8	HRN (A99-11-AD3423)		600	6.78	161.00	96.40	22.20	26.60	15.80	8.47	14.80	8.43		5.19	7.17	4.83	12.10	7.23
8	HRN (A99-11-AD3423)		600	8.28	115.00	57.30	6.05	25.30	8.35	2.82	5.82	2.73			1.96		2.54	2.50

8	HRS (A99-37-AD3430)		768	0.00	35.70		1.64	6.40	2.70		1.10	0.62		0.78	3.26	0.14	2.43	0.49
8	HRS (A99-37-AD3430)		768	0.71	120.00	193.00	30.90	87.40	35.70	5.81	36.10	5.40		9.70	30.50	4.46	24.00	5.99
8	HRS (A99-37-AD3430)		768	2.12	207.00	928.00	101.00	386.00	110.00	26.70	105.00	16.20		19.70	48.50	8.35	53.30	8.48
8	HRS (A99-37-AD3430)		768	3.53	245.00	397.00	52.90	269.00	49.40	12.30	57.00	9.49		15.40	52.30	6.36	42.20	8.16
8	HRS (A99-37-AD3430)	44°34.20'N 125°08.82'W	768	4.94	269.00	502.00	68.30	203.00	42.60	8.87	39.00	5.88		10.30	28.00	3.61	25.50	2.55
8	HRS (A99-37-AD3430)		768	6.35	83.20	232.00	35.40	147.00	38.20	7.06	29.30	3.86		3.32	9.18	1.22	8.61	1.47
8	HRS (A99-37-AD3430)		768	7.76	65.80		3.99	19.50	15.30	1.27	13.40	1.21		0.65	7.26	0.48	4.71	1.52
8	HRS (A99-37-AD3430)		768	9.17	95.50	85.60	14.70	43.00	10.50	1.08	12.10	1.66		1.67	11.00	0.44	5.70	1.79
8	HRS (A99-37-AD3430)		768	10.59	82.20	50.70	8.48	22.00	11.80	1.96	11.10	2.11		2.00	3.48	1.32	5.68	1.70
9	BIFII Stn.1		105	1.20	132.54	282.04	35.35	140.34	38.62	9.69	33.37	5.47	29.53	6.32	15.25	2.04	14.18	1.93
9	BIFII Stn.1		105	2.40	143.10	306.67	38.12	163.58	40.83	9.01	36.93	5.27	30.80	5.55	16.08	1.94	15.31	1.93
9	BIFII Stn.1		105	3.50	159.05	341.65	41.20	176.50	35.31	9.28	42.27	6.28	29.79	5.97	17.40	2.24	14.63	2.02
9	BIFII Stn.1		105	4.70	115.35	233.60	26.73	120.97	29.24	7.78	30.25	4.19	27.50	5.49	14.42	1.99	10.80	1.93
9	BIFII Stn.1		105	5.90	54.07	103.29	13.52	62.42	13.79	4.23	14.24	3.11	15.28	2.92	8.78	1.27	6.53	1.08
9	BIFII Stn.1	43°56'N 124°19'W	105	7.10	221.09	466.19	56.46	235.91	48.55	12.01	46.71	6.48	33.10	6.15	18.07	2.55	15.31	1.98
9	BIFII Stn.1		105	8.30	136.19	304.29	36.61	138.19	34.76	9.96	36.93	5.13	29.53	5.67	15.91	2.34	12.38	1.79
9	BIFII Stn.1		105	9.40	251.44	586.42	74.02	295.31	73.38	22.79	69.41	9.59	53.46	9.61	27.18	3.31	25.66	3.25
9	BIFII Stn.1		105	10.60	187.07	433.03	53.60	215.24	51.50	16.22	47.95	7.43	39.60	7.62	22.10	3.40	17.51	2.72
9	BIFII Stn.1		105	11.80	69.68	140.21	18.01	76.53	20.23	7.43	17.80	3.53	19.52	3.91	11.42	1.64	10.25	1.57
9	BIFII Stn.1		105	13.00	86.68	190.81	24.81	113.00	26.90	9.04	28.92	5.40	23.55	4.47	14.09	1.98	12.94	2.24
9	BIFII Stn.1		105	14.20	54.74	114.74	14.15	65.86	16.55	4.64	15.57	3.04	19.60	3.70	10.44	1.63	8.33	1.36

9	BIFII Stn.2		192	1.18	289.89	682.02	82.53	308.39	75.40	82.33	70.20	10.54	56.20	10.66	29.60	4.67	24.09	4.25
9	BIFII Stn.2		192	1.20	220.14	452.89	75.02	274.80	59.69	18.42	70.67	8.68	50.01	10.60	24.53	3.29	19.97	2.94
9	BIFII Stn.2		192	2.36	759.96	1884.90	220.15	893.39	200.27	223.04	183.27	24.35	126.81	22.61	61.66	7.45	44.33	6.47
9	BIFII Stn.2		192	3.50	367.92	818.69	97.06	414.16	100.10		90.90	12.47	74.27	13.41	36.99	4.79	27.89	3.91
9	BIFII Stn.2		192	3.54	335.12	807.87	97.68	373.75	100.94	212.60	88.09	12.12	53.16	11.21	32.94	4.35	22.47	3.95
9	BIFII Stn.2		192	4.70	875.88	1921.10	332.01	1151.42	297.98	81.39	285.60	35.50	189.71	34.63	86.27	11.10	63.53	9.77
9	BIFII Stn.2	43°55'N 124°41'W	192	4.72	1016.30	2514.43	302.61	1181.56	262.70	285.24	245.37	32.67	160.28	28.96	75.74	10.13	59.51	7.82
9	BIFII Stn.2		192	5.90	973.13	2403.56	286.13	1102.83	244.46	301.01	220.40	30.12	143.44	25.44	71.96	9.20	56.48	8.16
9	BIFII Stn.2		192	7.08	1009.01	2497.15	298.28	1175.06	263.10	285.35	236.94	31.29	152.17	27.82	72.98	9.16	54.05	8.08
9	BIFII Stn.2		192	8.26	960.70	2436.29	292.49	1135.33	254.59	234.97	221.75	28.91	146.29	28.06	68.77	9.71	53.44	8.68
9	BIFII Stn.2		192	10.60	1801.12	4547.89	540.29	2117.92	458.51	195.13	397.59	53.42	256.86	44.62	118.10	15.40	87.04	12.50
9	BIFII Stn.2		192	10.60	1917.81	4553.23	549.53	2248.01	514.38		437.22	56.20	311.42	52.80	139.78	18.23	97.96	12.51
9	BIFII Stn.2		192	13.00	1024.53	2562.88	308.34	1250.17	247.70	118.87	216.69	30.71	147.50	26.13	72.25	9.57	54.66	7.99
9	BIFII Stn.3		95	1.18	404.43	656.19	87.69	374.72	88.12	24.22	91.09	11.91	68.77	12.15	30.82	3.90	24.86	4.29
9	BIFII Stn.3		95	2.36	718.99	1323.02	178.21	802.27	176.25	45.96	194.03	26.96	135.91	27.53	66.91	7.93	47.60	7.64
9	BIFII Stn.3		95	3.54	564.88	1108.15	147.85	640.12	154.93	40.62	159.09	22.24	115.48	24.07	58.68	7.55	43.37	6.94
9	BIFII Stn.3		95	4.72	635.89	1365.89	182.34	788.91	167.01	44.63	174.69	24.16	117.75	24.15	60.79	6.78	42.05	6.41
9	BIFII Stn.3		95	5.90	738.72	1565.90	197.79	847.21	185.48	50.35	184.05	25.13	131.05	24.84	62.06	8.00	47.87	7.35
9	BIFII Stn.3		95	7.08	666.28	1455.97	178.64	727.57	170.56	42.53	171.57	23.81	120.67	23.92	58.47	6.84	41.25	7.29
9	BIFII Stn.3	40°57'N 124°18'W	95	8.26	412.79	851.07	109.88	460.96	99.49	32.80	119.16	16.37	83.69	16.77	46.65	5.12	32.53	5.00
9	BIFII Stn.3		95	9.44	572.66	1254.64	143.72	616.43	136.45	37.19	143.49	19.26	101.53	19.30	53.19	6.27	39.67	5.94
9	BIFII Stn.3		95	10.63	165.49	361.49	42.10	197.38	44.77	12.78	49.91	7.97	40.22	7.92	22.16	3.01	16.92	2.59
9	BIFII Stn.3		95	11.81	341.35	754.68	91.28	398.40	98.07	24.03	98.57	12.96	74.60	14.92	38.84	4.29	27.77	3.88
9	BIFII Stn.3		95	13.00	325.94	708.65	89.54	402.65	95.94	24.98	92.96	12.96	77.52	15.46	39.26	4.41	28.03	4.53
9	BIFII Stn.3		95	14.20	164.34	323.36	42.97	182.20	45.48	12.02	46.79	7.00	43.47	8.61	22.80	3.01	19.04	3.35
9	BIFII Stn.6		125	1.20	535.50	1135.63	144.04	587.89	110.86	29.18	107.93	15.23	71.69	13.00	37.36	4.48	26.45	4.76
9	BIFII Stn.6		125	2.40	540.82	1270.92	161.56	675.86	158.35	36.43	139.26	19.79	92.41	18.61	45.08	6.12	40.52	6.87
9	BIFII Stn.6	41°00'N 124°20'W	125	3.50	922.79	2096.37	272.20	1168.49	245.18	70.00	244.56	28.89	148.24	25.23	69.87	9.40	57.91	8.58
9	BIFII Stn.6		125	4.70	448.91	1039.61	133.64	569.96	127.45	51.85	121.01	16.08	80.45	15.81	43.92	5.51	32.64	5.37

9	BIFII Stn.6		125	6.90	207.98	422.77	54.72	242.93	55.43	19.07	65.51	9.19	42.49	8.54	20.69	2.69	16.92	2.76	
9	BIFII Stn.6		125	9.10	300.27	551.49	93.17	362.10	95.41	37.22	95.34	12.14	67.33	13.01	33.04	3.90	26.87	3.34	
9	BIFII Stn.6		125	11.30	207.98	337.03	42.32	160.94	33.40	20.41	43.05	5.95	30.82	6.46	19.63	2.24	13.22	2.41	
9	BIFII Stn.6		125	13.40	161.38	313.66	51.74	206.81	49.82	13.50	55.20	7.03	46.06	8.71	22.61	3.07	16.52	2.13	
9	BIFII Stn.6		125	15.60	120.12	214.08	25.46	109.32	26.29	9.35	29.95	4.11	27.25	5.61	13.09	2.11	12.69	2.00	
9	BIFII Stn.6		125	18.80	50.42	86.17	15.89	60.83	17.86	5.17	23.83	3.63	22.37	5.09	11.77	1.67	11.44	1.69	
9	BIFII Stn.6		125	22.00	255.22	473.66	56.79	217.42	52.59	19.84	46.17	8.23	44.11	9.54	26.60	3.71	22.21	4.23	
9	BIFII Stn.6		125	25.20	144.67	274.60	37.27	145.83	39.31	16.71	30.59	6.42	34.69	7.91	22.17	3.12	18.85	2.41	
9	BIFII Stn.6		125	28.30	197.96	430.88	50.29	215.94	50.54	15.89	51.99	8.17	46.85	9.83	22.98	3.55	20.27	3.14	
9	BIFII Stn.6		125	31.50	149.57	286.25	46.85	188.21	49.82	20.44	55.20	7.80	43.86	9.65	27.66	3.77	21.42	3.30	
9	HH1200		1216	0.00	31.24	11.35	5.80	17.53	4.23	1.14	7.53	0.93	8.11	2.10	7.80	1.27	7.45	1.25	
9	HH1200		1216	0.00	107.16	124.25	26.29	87.30	19.27	5.17	25.51	2.58	18.42	4.20	13.56	2.19	13.62	1.89	
9	HH1200		1216	0.00	33.67	10.41	5.50	19.32	4.23	1.26	7.94	0.93	7.90	2.05	7.52	1.36	9.26	1.29	
9	HH1200		1216	0.00	54.94	38.07	10.24	43.29	8.58	3.04	9.61	1.83	11.96	3.00	8.77	1.39	9.36	1.53	
9	HH1200		1216	1.23	245.64	551.12	65.31	289.01	56.31	14.61	55.52	9.84	40.58	10.25	26.24	4.33	23.35	4.52	-3.5
9	HH1200		1216	2.47	472.40	1084.94	127.44	491.50	95.62	26.58	104.33	15.09	73.91	13.56	39.20	6.06	35.03	5.28	-2.9
9	HH1200	43°50'N 124°59'W	1216	3.70	435.80	1031.42	117.94	496.10	91.37	23.08	96.68	11.94	65.70	13.44	34.78	5.29	31.81	5.03	-1.2
9	HH1200		1216	4.93	429.12	983.75	116.53	450.08	79.68	19.28	89.98	11.94	64.25	12.64	37.31	5.86	33.82	4.52	-1.3
9	HH1200		1216	6.17	353.61	824.55	93.30	357.12	69.06	17.23	79.45	8.66	52.17	10.59	28.46	3.84	25.37	3.92	-1.5
9	HH1200		1216	7.40	281.32	664.45	74.46	328.59	67.99	16.36	63.18	8.00	42.99	9.23	25.93	4.13	21.74	4.01	-1.5
9	HH1200		1216	8.63	257.38	587.10	67.95	280.73	57.37	13.44	61.26	7.87	46.86	8.66	27.51	3.17	22.95	3.15	-2.3
9	HH1200		1216	9.87	224.23	499.18	58.79	242.99	49.93	11.10	45.95	7.61	40.10	8.32	22.45	3.46	22.55	3.84	-1.6
9	HH1200		1216	11.10	206.50	448.37	51.05	205.25	47.81	11.98	50.73	6.95	35.26	6.38	20.23	3.56	22.15	3.15	-1.2
9	HH200		202	1.23	175.87	433.47	53.17	202.52	45.04	10.97	45.36	5.79	29.43	5.36	14.30	2.00	11.35	1.71	-0.10
9	HH200		202	2.47	147.57	381.93	46.60	181.16	42.95	9.47	38.98	5.35	25.86	4.71	14.14	1.84	10.62	1.61	-0.2
9	HH200		202	3.70	196.57	502.28	60.88	240.92	58.01	12.61	53.84	6.78	33.98	6.23	17.25	2.46	14.03	2.13	-0.2
9	HH200	43°44'N 124°41'W	202	4.93	210.62	540.39	67.16	263.96	60.93	14.09	56.36	7.56	38.48	7.12	18.65	2.50	15.05	2.31	-0.5
9	HH200		202	6.17	235.31	597.83	74.65	291.05	65.53	14.64	60.48	8.79	45.67	7.46	22.88	2.87	16.63	2.63	0.0
9	HH200		202	7.40	222.58	571.50	69.76	274.67	62.92	15.35	58.21	8.04	41.40	7.78	21.85	2.77	15.25	2.40	-0.1
9	HH200		202	8.63	137.64	346.57	42.31	162.51	41.07	8.52	37.30	5.25	25.72	4.76	14.55	1.94	10.79	1.83	-0.1

9	HH200		202	9.87	134.99	339.66	40.53	165.89	38.98	8.54	35.11	4.94	25.35	4.75	13.77	1.73	10.54	1.77	0.0
9	HH200		202	11.10	192.16	512.73	61.08	245.47	57.59	12.48	52.50	7.31	37.74	6.70	19.43	2.48	14.60	2.20	-0.2
9	HH200		202	13.30	236.35	619.62	77.47	312.99	73.06	17.51	70.14	9.60	48.83	9.03	23.22	3.17	17.97	2.56	n/a
9	HH200		202	15.50	303.90	817.41	100.47	397.81	99.10	21.44	90.30	12.26	60.38	11.23	32.74	3.62	22.11	3.15	n/a
9	HH200		202	17.70	208.81	565.06	68.18	277.04	65.53	14.80	60.06	8.33	39.22	7.94	21.17	2.50	16.63	2.45	n/a
9	HH3000		3060	0.00	63.29	24.31	11.45	44.37	11.75	2.78	13.80	1.48	13.38	3.94	11.91	2.11	13.62	2.25	
9	HH3000		3060	0.00	68.22	13.24	10.61	46.15	7.15	3.04	10.57	2.11	15.44	4.19	13.29	2.49	13.70	2.23	
9	HH3000		3060	0.00	74.71	14.56	11.35	50.64	9.06	3.51	11.85	2.44	17.61	3.89	14.39	2.20	15.37	2.20	
9	HH3000		3060	1.23	337.04	428.58	85.20	337.79	76.49	21.03	89.02	12.33	69.56	14.47	47.43	7.02	49.93	8.01	-1.8
9	HH3000		3060	2.47	554.13	936.53	142.94	563.29	120.05	30.38	125.39	18.76	103.38	18.57	60.07	9.23	61.61	9.29	-1.8
9	HH3000	43°52'N 125°38'W	3060	3.70	736.69	1479.34	184.83	726.20	152.99	39.14	174.21	21.91	118.84	23.81	61.65	8.94	57.98	9.80	-1.6
9	HH3000		3060	4.93	768.69	1638.98	187.82	724.36	150.86	34.76	157.94	21.38	119.32	23.69	63.55	9.61	59.19	9.54	-1.8
9	HH3000		3060	6.17	807.60	1741.07	198.91	787.87	157.24	36.51	169.42	23.62	124.63	25.86	70.19	10.28	61.20	9.72	-2.4
9	HH3000		3060	7.40	526.50	1106.07	122.34	512.67	96.68	23.37	113.91	15.22	86.47	18.34	54.38	7.79	44.70	7.24	-1.9
9	HH3000		3060	8.63	358.22	741.35	85.20	339.63	72.24	17.82	85.19	10.76	65.70	14.01	39.52	5.77	39.86	6.05	-1.8
9	HH3000		3060	9.87	243.34	482.77	52.63	211.69	47.81	13.73	52.65	7.48	48.79	10.82	32.88	5.00	32.21	5.62	-1.8
9	HH3000		3060	11.10	210.42	423.63	45.06	208.01	41.43	10.22	45.95	7.74	42.03	9.57	27.82	4.13	28.99	4.35	-1.7
9	HH500		500	0.00	32.46	25.93	6.18	21.83	4.23	1.39	6.69	1.10	7.02	1.78	5.74	0.88	5.63	1.05	
9	HH500		500	0.00	26.95	16.46	4.59	18.96	4.70	2.02	6.69	0.77	6.80	1.78	5.46	0.83	6.17	1.05	
9	HH500		500	0.00	28.25	13.43	4.37	15.74	3.76	1.01	5.44	0.82	5.04	1.52	5.60	0.83	5.45	0.88	
9	HH500		500	1.23	189.87	378.94	65.60	224.34	52.17	13.00	53.94	6.37	36.63	7.08	19.73	2.90	14.34	2.37	
9	HH500		500	2.47	432.35	1066.05	126.74	474.01	108.36	23.95	101.46	13.12	73.91	12.42	33.51	4.42	24.16	4.94	
9	HH500	43°52'N 124°54'W	500	3.70	326.33	675.61	114.18	398.24	105.75	23.60	97.01	12.69	68.43	12.64	32.76	4.74	24.51	4.06	
9	HH500		500	4.93	108.29	225.34	37.73	134.18	33.84	8.08	34.71	4.67	27.85	5.09	14.11	1.89	11.44	1.69	
9	HH500		500	4.93	175.92	377.51	46.87	195.03	49.85	11.72	32.99	6.17	32.58	5.69	15.41	2.28	12.32	2.08	
9	HH500		500	6.17	253.73	533.55	88.65	332.04	81.31	19.81	81.54	10.11	53.08	10.18	27.41	3.64	21.24	3.14	
9	HH500		500	7.40	110.88	225.74	38.64	137.40	31.96	8.58	35.54	4.23	28.07	5.77	13.28	2.28	11.98	1.97	
9	HH500		500	0.0*	55.85	69.12	11.64	53.91	10.49	3.63	12.49	1.78	10.22	2.71	7.40	1.14	6.85	1.01	
11	MABC25	17°N	5322	0.50	1670.00	3059.00	384.00	1654.00	362.00	92.50	395.00	63.80	351.00	72.10	203.00	29.00	170.00	27.40	

11	MABC25	162°E	5322	1.50	167.00	236.00	43.90	190.00	46.70	12.30	53.20	9.73	44.50	11.30	26.70	3.86	22.40	3.84
11	MABC25		5322	2.50	57.00	65.80	8.61	36.80	7.78	3.59	10.40	1.36	12.10	2.44	7.25	0.94	7.67	1.21
11	MABC25		5322	3.50	49.50	84.70	10.80	46.10	9.28	3.42	11.30	1.64	14.50	2.52	8.01	0.97	7.54	1.45
11	MABC25		5322	4.50	275.00	502.00	70.40	311.00	65.90	17.70	75.10	11.20	64.70	15.90	42.00	5.53	39.40	6.29
11	MABC25		5322	6.50	148.00	253.00	38.70	174.00	42.80	8.88	36.60	5.98	40.90	7.82	24.60	3.39	19.90	3.08
11	MABC25		5322	10.00	41.50	49.10	7.65	33.30	4.69	2.37	9.61	1.12	9.63	1.56	6.84	0.83	6.30	0.93
11	MABC25		5322	16.00	119.00	63.50	31.60	139.00	26.30	8.78	39.10	5.55	32.40	6.97	21.00	2.60	17.80	2.28
11	MABC25		5322	22.50	22.30	27.80	8.94	34.00	3.76	2.71	9.31	0.75	3.34	0.86	3.40	0.38	2.85	0.27
11	MABC25		5322	28.50	39.70	55.50	6.27	23.60	3.07	3.21	5.10	0.69	5.55	1.24	4.17	0.74	5.51	0.91
12	SoG		251	0.50	79.19	71.38	13.48	69.33	12.64	4.61	18.44	2.45	16.62	3.52	10.76	1.42	10.98	1.37
12	SoG		251	1.50	64.79	121.34	15.61	83.19	15.30	5.26	19.71	2.64	19.08	4.00	12.56	1.66	13.87	1.94
12	SoG		251	2.50	122.39	271.23	36.91	201.05	46.55	13.82	69.95	9.44	55.38	12.13	36.47	5.33	35.25	5.14
12	SoG		251	3.50	122.39	256.96	35.49	221.85	53.21	18.43	69.95	10.07	67.69	13.95	43.05	5.92	41.61	5.72
12	SoG		251	4.50	136.79	285.51	42.58	256.52	66.51	19.08	95.39	13.22	86.15	18.80	57.40	7.70	52.01	8.00
12	SoG		251	5.50	129.59	221.27	42.58	249.58	59.86	17.77	82.67	11.33	80.00	17.59	53.81	7.70	52.01	7.43
12	SoG		251	6.50	115.19	199.86	42.58	249.58	59.86	18.43	89.03	11.96	86.15	18.80	57.99	8.29	57.79	8.00
12	SoG		251	7.50	143.99	285.51	49.68	291.18	73.16	23.03	101.75	15.10	98.46	20.62	63.37	8.88	63.57	9.14
12	SoG		251	8.50	151.19	278.37	49.68	263.45	66.51	21.72	95.39	13.85	92.31	19.41	59.19	8.29	57.79	8.00
12	SoG	49°12.986'N	251	9.50	136.79	264.10	49.68	298.11	79.81	25.01	108.11	16.36	104.62	23.04	69.35	9.47	69.35	10.29
12	SoG	123°32.085'W	251	11.00	179.99	499.64	63.88	318.91	66.51	19.74	95.39	15.10	92.31	19.41	60.98	8.29	63.57	9.14
12	SoG		251	13.00	323.97	642.40	99.36	526.90	133.01	40.80	178.06	25.17	160.00	33.96	107.62	14.21	98.24	13.72
12	SoG		251	15.00	316.77	685.22	92.26	457.57	106.41	32.90	133.55	18.88	123.08	26.68	77.72	11.25	80.90	10.86
12	SoG		251	17.00	316.77	706.64	78.07	381.31	79.81	24.35	120.83	17.62	98.46	21.22	66.36	9.47	63.57	9.14
12	SoG		251	19.00	331.17	699.50	85.17	422.91	99.76	33.56	127.19	18.25	110.77	24.26	69.95	10.06	75.12	9.72
12	SoG		251	21.00	338.37	706.64	85.17	436.77	99.76	33.56	127.19	17.62	116.92	23.65	66.36	9.47	69.35	8.57
12	SoG		251	23.00	424.77	877.94	99.36	471.44	99.76	28.95	146.26	22.03	123.08	26.08	83.70	10.66	69.35	10.29
12	SoG		251	25.00	273.58	571.02	70.97	381.31	86.46	28.95	101.75	15.10	98.46	21.22	58.59	8.29	63.57	7.43
12	SoG		251	27.00	388.77	863.67	106.46	499.17	106.41	33.56	120.83	16.99	104.62	21.22	62.18	8.29	63.57	7.43
12	SoG		251	29.00	388.77	856.53	106.46	526.90	113.06	41.46	152.62	22.66	135.38	28.50	83.70	11.25	80.90	10.29
13	B14	30.101°N	46	0.00	68.54	30.84	10.65	46.59	9.78	2.50	13.86	2.14	15.57	3.82	11.96	1.66	10.29	1.66

13	B14	122.868°E	46	1.00	141.18	160.89	21.43	94.36	19.35	4.94	27.47	4.09	27.75	6.49	19.85	2.72	16.87	2.80
13	B14		46	2.00	167.82	203.14	17.89	78.20	14.63	3.55	21.05	2.96	20.00	4.91	15.31	2.13	13.46	2.34
13	B14		46	5.00	72.57	99.71	9.44	43.54	9.04	2.37	14.44	2.20	16.00	4.06	13.39	1.95	12.89	2.29
13	B14		46	6.00	206.55	250.46	21.43	93.46	16.49	4.08	24.10	3.27	22.77	5.58	17.64	2.43	15.31	2.74
13	B14		46	7.00	57.96	83.51	7.81	36.19	7.91	2.04	12.53	1.89	13.72	3.58	11.84	1.72	11.67	2.17
13	B14		46	11.00	69.62	110.28	10.50	48.46	10.77	2.76	15.96	2.45	17.35	4.31	13.75	1.95	12.94	2.29
13	B14		46	15.00	41.25	61.96	5.96	27.52	6.38	1.65	9.54	1.51	10.95	2.85	9.45	1.36	9.19	1.71
13	B14		46	19.00	51.19	72.45	6.67	30.99	6.98	1.78	10.68	1.64	12.12	3.15	10.28	1.54	10.58	1.89
13	C1-11[b]	31.766°N 121.102°E	13		49.68	65.88	11.85	52.62	12.17	2.90	18.76	2.08	13.91	3.21	10.16	1.42	9.13	1.54
13	C1-1[b]		13		56.66	75.73	13.20	59.21	13.04	3.03	19.14	2.14	14.52	3.40	10.46	1.48	9.48	1.60
13	C10	30.968°N 122.45°E	12	0.00	44.42	26.20	8.16	35.57	7.98	2.04	11.96	1.83	13.29	3.34	10.94	1.54	10.06	1.71
13	C10		12	1.00	95.32	154.18	17.39	77.44	17.89	4.67	29.32	4.22	30.34	7.58	23.86	3.37	22.08	3.43
13	C10		12	3.00	120.01	174.30	20.09	87.91	19.62	5.00	31.48	4.34	30.71	7.58	23.26	3.26	21.38	3.31
13	C10		12	4.00	115.62	186.37	20.09	88.88	20.09	5.26	29.51	4.47	30.71	7.34	22.96	3.20	20.11	3.31
13	C10		12	6.00	151.55	242.18	25.34	111.27	24.41	6.25	38.35	5.22	36.12	8.79	26.49	3.73	24.16	3.77
13	C10		12	7.00	164.22	243.40	22.71	99.00	20.42	5.13	32.24	4.28	29.85	7.46	23.14	3.26	21.73	3.49
13	C10		12	9.00	76.96	107.49	8.94	40.56	9.38	2.24	15.45	2.14	15.51	4.12	13.45	1.95	13.98	2.46
13	C10		12	12.00	63.79	76.23	6.81	32.93	7.32	2.04	13.48	2.20	15.20	4.06	13.87	2.07	14.68	2.69
13	C10		12	16.00	32.90	37.33	3.97	20.17	6.45	1.45	10.56	1.64	11.63	3.52	12.38	1.89	13.75	2.51
13	C10		12	25.00	35.35	47.75	4.97	22.95	7.18	1.51	10.24	1.64	13.11	3.70	12.56	1.89	13.75	2.40
13	C13	30.803°N 122.886°E	33	0.00	60.26	18.49	9.30	40.35	8.78	2.24	13.35	2.08	15.26	3.82	12.38	1.72	11.27	1.83
13	C13		33	1.00	116.70	169.45	17.81	77.09	16.89	4.08	25.25	3.59	24.68	5.82	18.12	2.49	16.47	2.63
13	C13		33	2.00	119.22	150.96	12.28	54.42	10.31	2.43	16.22	2.27	15.51	3.88	12.26	1.72	11.96	2.11
13	C13		33	3.00	120.66	176.23	14.83	65.52	13.23	3.22	20.03	2.83	18.83	4.61	14.35	2.07	14.16	2.40
13	C13		33	4.00	155.72	232.26	22.07	93.52	18.36	4.54	24.10	3.52	23.88	5.64	17.88	2.49	16.07	2.80
13	C13		33	7.00	96.33	129.84	11.36	50.96	9.91	2.50	15.77	2.33	15.88	4.00	12.79	1.84	12.31	2.23
13	C13		33	9.00	61.99	64.38	5.46	24.61	5.39	1.18	8.01	1.26	8.86	2.43	8.37	1.24	8.67	1.66
13	C13		33	11.00	62.49	75.09	6.74	31.41	6.05	1.51	9.79	1.38	10.03	2.67	8.97	1.30	8.67	1.60
13	C13		33	17.00	35.28	40.61	3.69	17.26	3.99	0.92	5.98	0.88	6.77	1.88	6.40	0.95	6.99	1.31

13	C13		33	21.00	51.69	65.31	6.46	29.33	6.98	1.58	9.35	1.51	11.08	2.97	10.10	1.48	10.52	1.89
13	C6-1		6	0.00	76.89	53.03	10.01	44.93	9.98	2.57	18.51	2.20	16.00	4.06	13.57	1.95	12.83	2.23
13	C6-1		6	1.00	53.06	54.89	9.16	41.18	9.04	2.30	17.87	2.08	14.34	3.76	12.20	1.78	11.79	1.94
13	C6-1		6	2.00	61.92	84.51	11.21	50.47	11.64	3.03	22.19	2.52	17.54	4.49	14.35	2.07	13.41	2.23
13	C6-1		6	4.00	61.27	91.58	12.14	54.08	13.30	3.42	26.33	2.89	20.00	5.03	16.26	2.37	16.01	2.51
13	C6-1	31.068°N 122.042°E	6	7.00	95.68	149.75	17.18	75.98	15.90	4.54	29.76	3.02	20.25	4.91	15.54	2.19	14.50	2.40
13	C6-1		6	9.00	130.31	212.56	24.13	104.69	22.48	6.12	36.12	4.28	28.43	6.85	20.45	2.90	18.95	3.09
13	C6-1		6	11.00	96.62	139.61	18.17	83.96	19.55		31.99	3.96	27.57	6.55	20.39	2.84	18.95	3.03
13	C6-1		6	17.00	180.42	296.15	32.43	144.20	31.86	8.16	50.30	6.67	45.42	11.10	33.42	4.68	30.34	4.80
13	C6-1		6	21.00	125.99	194.22	23.14	110.30	26.47	6.91	41.08	5.85	41.85	10.49	33.42	4.79	32.07	5.20

Reference 1 is (Elderfield & Sholkovitz, 1987); 2 is (Sholkovitz et al., 1989); 3 is (German & Elderfield, 1989); 4 is (Sholkovitz et al., 1992); 5 is (Haley et al., 2004); 6 is (Bayon et al., 2011); 7 is (Kim et al., 2012); 8 is (Himmler et al., 2013); 9 is (Abbott, Haley, McManus, et al., 2015); 10 is (Abbott, Haley, & McManus, 2015); 11 is (Deng et al., 2017); 12 is (Patton et al., 2021); 13 is (Deng et al., 2022).

Capítulo 2:

REE fractionation and human Gd footprint along the continuum between Paraguaçu River to coastal South Atlantic waters

Chemical Geology 532 (2020) 119303

Contents lists available at ScienceDirect

Chemical Geology

journal homepage: www.elsevier.com/locate/chemgeo

REE fractionation and human Gd footprint along the continuum between Paraguaçu River to coastal South Atlantic waters

Raíza L.B. Andrade[a,*], Vanessa Hatje[a], Rodrigo M.A. Pedreira[a], Philipp Böning[b], Katharina Pahnke[b]

[a] Centro Interdisciplinar de Energia e Ambiente, CIENAM, Universidade Federal da Bahia, Ondina, Salvador, Bahia, 40170-115, Brazil
[b] Marine Isotope Geochemistry, Institute for Chemistry and Biology of the Marine Environment (ICBM), University of Oldenburg, Oldenburg, Germany

ARTICLE INFO

Editor: Catherine Chauvel

Keywords:
REE
Tidal cycle
GEOTRACES
Anthropogenic Gd
Todos os Santos Bay
Estuarine mixing

ABSTRACT

In this study, we evaluated the fractionation of dissolved Rare Earth Elements (REE) from the continuum between the Paraguaçu Estuary through Todos os Santos Bay (BTS), Bahia, Brazil and during a 12 h tidal cycle in a pier station. The results show that REE were scavenged in the estuarine low salinity region (< 5) following the order Light > Medium > Heavy (LREE > MREE > HREE), likely due to colloids coagulation/precipitation. At mid to high salinities, REE concentrations gradually increased, starting with HREE, followed by MREE and LREE. Within Todos os Santos Bay, a clear difference between the eastern and western sides was observed: 1) The western side presented very similar REE patterns, clearly influenced by the fluvial input (Paraguaçu and Subaé Rivers), 2) the eastern side of the bay showed more scattered REE patterns, possibly due to the influence of different sources, such as submarine groundwater discharge (SGD) and the mixing with coastal seawater. The salinity at a pier station did not vary throughout the tidal cycle experiment (S≅33.4), but the REE pattern changed from a terrigenous (flat) at low tide to a marine-like (HREE enriched) pattern at the flood tide. Anthropogenic Gd anomalies (Gd/Gd* > 1.4) were observed at the estuary and also at high tide and during ebb tide along the tidal cycle experiment. Taken together, these observations show that the REE behavior along the continent-ocean continuum is quite variable. Moreover, the occurrence of anthropogenic Gd indicates that anthropogenic inputs of REE may complicate their use as a tracer for natural processes in the future.

1. Introduction

The rare earth elements (REE) are a coherent group of elements that share chemical properties due to their uniform trivalent charge (with the exception of Ce^{4+} and Eu^{2+}), and the gradual decrease in their ionic radii with increasing atomic number (i.e., the lanthanide contraction) that accompanies the progressive filling of the 4*f*-electron shell across the REE series. These element abundances are fractionated during environmental processes in a subtle and predictable manner (e.g., Elderfield, 1988). This fractionation across the REE series can be used to trace and provide insight into biogeochemical processes, atmospheric-driven particles, water mass pathway, and mixing of the modern ocean that single element tracers cannot discriminate (Elderfield and Greaves, 1982; Elderfield, 1988; Elderfield et al., 1990; Sholkovitz et al., 1994; Johannesson et al., 2005; Haley et al., 2014, Censi et al., 2017). Understanding the REE chemical behavior is thus essential for their successful application as tracers of natural processes.

The fluvial inputs of dissolved and particulate REE (Elderfield et al., 1990; Sholkovitz, 1995; Sholkovitz et al., 1999; Osborne et al., 2014), dissolution of atmospheric (Greaves et al., 1994; Aubert et al., 2002), lithogenic sediments (Abbott et al., 2015; Rousseau et al., 2015), and submarine groundwater discharge (SGD) (Kim and Kim, 2011, 2014; Chevis et al., 2015; Johannesson et al., 2017) were recognized as potentially important sources of REE for the coastal and ocean waters.

Along the continuum continent-ocean, several processes cause REE abundances and normalized patterns to evolve. Estuaries play an important role in this scenario; they are important biogeochemical reactors where river fluxes of inorganic and organic matter affect the chemistry and fluxes of elements to the ocean waters. The geochemistry of REE in estuarine waters and its implications to the ocean chemistry has mostly been studied between the 1980 and late 1990. These studies revealed that the flocculation of river-dissolved organic matter by sea salt drives the non-conservative behavior of REE in estuaries. Removal of dissolved REE during mixing with seawater along the salinity gradient, especially in low salinity waters, reflects the salt-induced coagulation of Fe-rich organic colloids that scavenge REE promoting their

* Corresponding author.
E-mail address: raiza.lopes@ufba.com (R.L.B. Andrade).

https://doi.org/10.1016/j.chemgeo.2019.119303
Received 19 March 2019; Received in revised form 30 August 2019; Accepted 11 September 2019
Available online 13 September 2019

fractionation (Hoyle et al., 1984; Goldstein and Jacobsen, 1988b; Sholkovitz, 1992, 1993; Sholkovitz and Szymczak, 2000; Rousseau et al., 2015). Among the REE, the light REE (LREE) tend to be more reactive than the middle (MREE) and the heavy REE (HREE) (Sholkovitz, 1995). Studies have reported that at high salinities, the concentrations may increase again as the result of REE being released from sediments and suspended particles (Sholkovitz and Szymczak, 2000; Rousseau et al., 2015).

More recently, the geochemistry of REE in estuarine and coastal waters has regained attention. The use of REE in medical applications and as technology critical elements, key for the transition towards a low-carbon energy economy, is growing (Vidal et al., 2013) and anthropogenic REE inputs to the aquatic systems are expected to grow accordingly.

Among the REE, the most widespread contaminant in marine waters is the anthropogenically-derived Gd (Zhu et al., 2004; Ogata and Terakado, 2006; Kulaksiz and Bau, 2007; Hatje et al., 2014, 2016; Pedreira et al., 2018). Gd-complexes are commonly used as magnetic resonance imaging (MRI) contrast agents since the late 1980s. The free Gd^{3+} can bind to Ca^{2+} binding enzymes and, therefore, lead to adverse biological effects. To prevent toxicity, the Gd can only be used as a contrast agent after being chelated to a ligand. Because of their high stability and chemically inert nature, the Gd-complexes are very resistant to decomposition, thus they have been thought to be mostly excreted from the body into domestic sewage systems within few hours of application. On the contrary of the natural REE, the anthropogenic Gd is not affected by the removal or release processes that may fractionate the natural REE and behave conservatively during mixture in estuarine waters (Kulaksiz and Bau, 2007). Due to this contrasting behavior, anthropogenic Gd emissions result in positive anthropogenic Gd anomalies. Whereas anthropogenic Gd can be used as a new tracer in marine waters for sewage discharge, it also may soon complicate the use of REE as tracers for natural processes and, therefore, it needs further investigations.

In order to assess (i) the importance of anthropogenic Gd inputs, (ii) the impact of exchanges between freshwater systems, submarine groundwater discharge (SGD) and marine waters on REE fractionation and controlling dynamics and also (iii) to expand the database for the as yet poorly studied tropical coastal waters, we present REE concentrations from water samples across the continuum between the Paraguaçu estuary through Todos os Santos Bay to the coastal waters of Northeastern Brazil.

2. Study site

Todos os Santos Bay (BTS, Fig. 1) is the second largest bay (1223 km^2) in Brazil. It presents tropical climate characteristics and diverse ecosystems (coral reefs, estuaries, mangroves, islands, and tidal flats) (Cirano and Lessa, 2007; Hatje and de Andrade, 2009). The bay's water depth is shallower than 25 m in 94% of its area, presenting an average depth of 9.8 m. The sediments in the southern section of the bay are predominantly sand, while mud composes most of the sediments in the northern section (Lessa and Dias, 2009). Sixty percent of the annual precipitation in BTS is concentrated during the wet season, between March and July, while the dry season dominates the rest of the year (Cirano and Lessa, 2007).

BTS is considered a fluvial-marine depositional environment with semidiurnal tides (max. range 2.7 m) and tide-driven currents (Lessa et al., 2001). There are three main tributaries for the bay, the Paraguaçu (Drainage Area (DA): 56,300 km^2 and Average Riverine Discharge (ARD): 112 m^3s^{-1}), Jaguaripe (DA: 2200 km^2 ARD: 0.32 m^3s^{-1}), and Subaé (DA: 600 km^2 ARD: 7.7 m^3s^{-1}) Rivers. The Paraguaçu River presents the largest drainage area among all tributaries of the BTS, representing 95% of the catchment, draining most of the geological formations in the BTS basin and, consecutively, yielding a broad representation of the composition of the fluvial inputs to BTS. The Paraguaçu River has had its hydrological regime artificially controlled since the construction of the Pedra do Cavalo dam (PC dam) in 1985. From 1986 onwards, Paraguaçu River's average discharge has dropped from 91 $m^3\ s^{-1}$ to 64 $m^3\ s^{-1}$ (Cirano and Lessa, 2007). In general, BTS waters display marine characteristics throughout the year (salinity > 28), albeit in the winter freshwater fluxes increase greatly. In a recent study, the total submarine groundwater discharge (SGD) input to BTS, i.e. the fresh and the recirculated marine groundwater inputs to the bay, has been estimated to be 300 m^3s^{-1} by using Ra and Rn as proxies (Hatje et al., 2017). This value is similar to the maximum monthly average freshwater discharge, which includes the fluvial and the precipitation-evaporation discharges to the bay, which are estimated to be 277 m^3s^{-1} (Cirano and Lessa, 2007; Lessa et al., 2009).

Todos os Santos Bay is also influenced by anthropogenic activities (e.g. industrial and domestic effluents, shrimp farming, mining, intense harbor activities) that take place in its surrounds (Hatje and Barros, 2012; Andrade et al., 2017 and references therein).

3. Methods

3.1. Sampling preparation and sample collection

Prior to sampling, sample bottles were immersed in detergent (Extran®, Merck, Germany), and then soaked in 6 N HCl solution (reagent grade), followed by a 6 N HNO_3 solution (reagent grade), for a week each. The bottles were subsequently rinsed and stored in a weak HNO_3 solution (~pH 2; trace metal grade).

Surficial water samples were collected through the Paraguaçu River (P0; right after the PC river dam) and estuary (stations P1 to P9) and Todos os Santos Bay (stations B1 to B13). Sampling strategy (Fig. 1) considered the discharge of rivers, as well as the water circulation, sediment characteristics, and tidal influence, in a way to include all main features of the bay. To evaluate the inputs of SGD, surficial water samples were collected hourly over a tidal cycle (12 h) at the end of a 140 m long pier at Marina do Bonfim (station TS) at a location known to have SGD.

All samples were collected with a trace-metal clean surface pump system that included a peristaltic pump (Masterflex, Cole Parmer Instrument Company, USA) and PFA Teflon tubing connected to capsule filters (0.2 μm Supor Acropak® with Fluorodyne II membrane) following Pedreira et al. (2018). Sample bottles were rinsed three times with sample prior to bottle filling. Afterward, the samples were taken to the laboratory, acidified to pH 1.8 (HCl 30% Suprapur®, Merck), and stored in plastic bags at ambient temperature. Water ancillary parameters (pH, O_2, and salinity) were measured using a pre-calibrated multi-probe (YSI 6600 V, USA), except at the pier station were a calibrated water quality analyzer (Datasonda Hydrolab 4 A) was employed. Long-lived (^{226}Ra, ^{228}Ra) and short-lived (^{223}Ra, ^{224}Ra) radium isotopes, as well as phosphate, ammoniacal nitrogen, nitrite, nitrate, and dissolved silicate concentrations for the studied sites are reported in Hatje et al. (2017).

3.2. Analytical methods

The REE analyses were carried out by isotope dilution (ID) ICP-MS following procedures previously described in Behrens et al. (2016). Aliquots of samples were weighted and spiked with a multi-element REE isotope spike (DKM), then they were left to homogenize for at least 48 h. The samples were pre-concentrated using the automated seaFAST system (Elemental Scientific Inc. Omaha, Nebraska, USA).

The REE measurements were carried out using an HR ICP-MS (Element, Thermo Finnigan, Germany) coupled to a desolvation introduction system (Aridus 2, Teledyne CETAC, Omaha, USA), and set using a 100 ng l^{-1} tune solution of Ba, Ce, and Lu to obtain higher sensitivity and lower oxide formation (< 0.03% for Ce oxide). That way, corrections for oxide interferences were not necessary. Blanks and

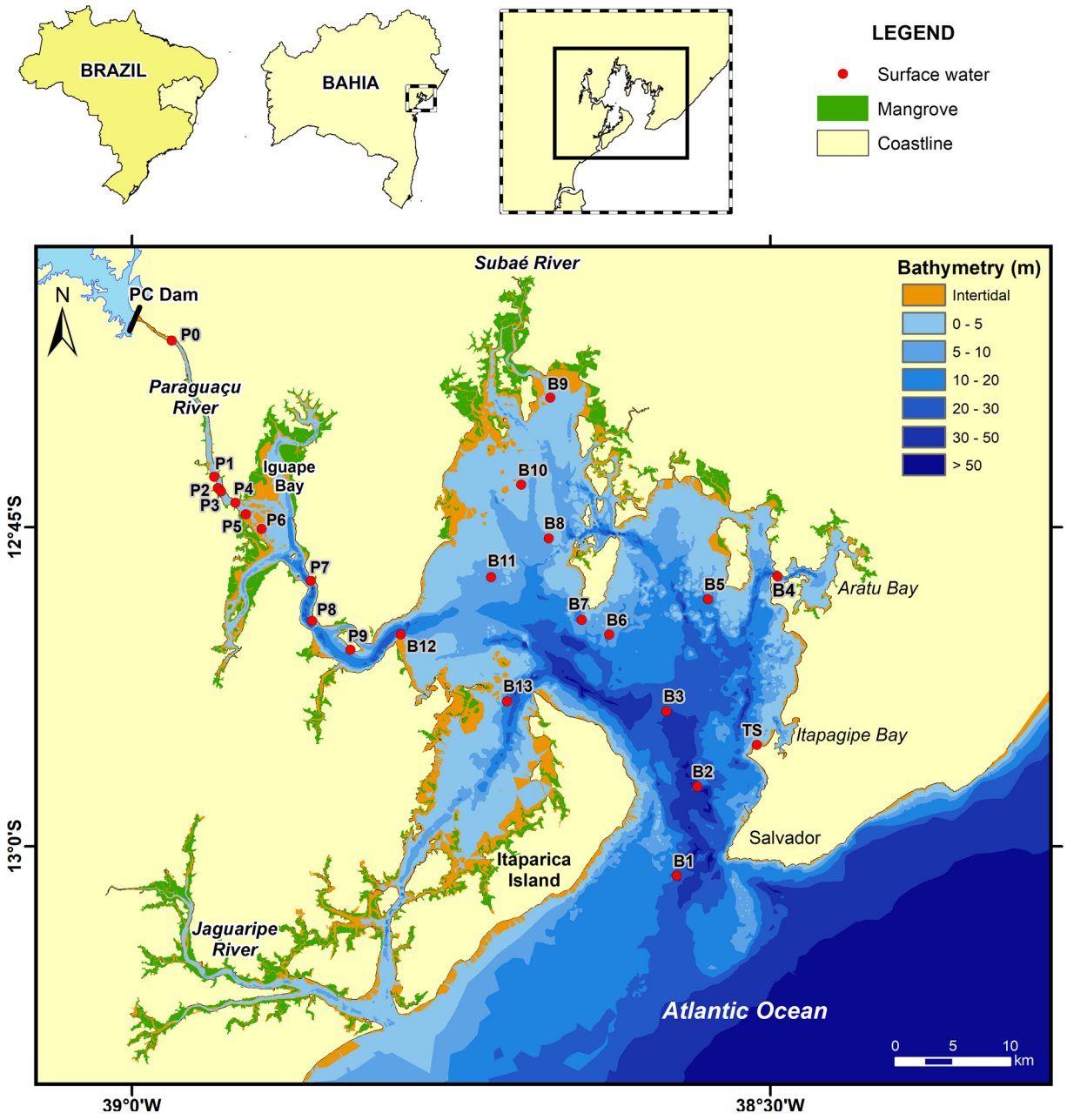

Fig. 1. Sampling stations along the continuum between the Paraguaçu River, through the Todos os Santos Bay, to the continental shelf, Bahia, Brazil. Stations P1-P9 were collected throughout the estuary, stations B1-B13 in the Todos os Santos Bay and TS represents the site used for the tidal cycle study.

replicates were included in each batch. Blanks contributed to less than 1% of the sample signal. Furthermore, spiked and unspiked standards were analyzed to check the sensitivity for mono-isotope elements and correction of the equipment mass bias. Accuracy was checked using GEOTRACES reference samples (North Pacific SAFe 3000 m and GEOTRACES Santa Barbara Coastal water, GSC) (Table S1). Replicate analyses of samples were within 5% (1 s).

4. Results

4.1. REE spatial patterns

The results obtained for surficial waters from Paraguaçu Estuary and Todos os Santos Bay are given in Table 1. For the samples of Paraguaçu Estuary, the salinity varied from 1.35 to 28.87, whereas inside the bay salinity varied from 28.63 to 33.40. Freshwater (P0) can only be found at the Paraguaçu River right after the PC dam. In the Paraguaçu Estuary, pH ranged from 7.55 (P8) to 8.25 (P3), while pH in the bay fluctuated between 8.00 (B1) and 8.42 (B11) (Table S2). Water temperatures extended from 25.45 °C at P1 to 27.50 °C at B9.

The sum of REE varied from 106 (B4) to 707 pmol kg^{-1} (P1), with the largest variability found within the Paraguaçu Estuary. Differences in the abundance of REE were also observed between the western and the eastern side of the bay. Clearly, the western side of the bay, which is more influenced by freshwater inputs, presents less variability among sites and slightly more abundant REE than the eastern side.

The PAAS-normalized REE patterns (for numerical procedures see supplementary material) are shown in Fig. 2. To facilitate the presentation of results and discussion, data from the western and eastern sides of the bay were presented separately. In general, all REE presented a decrease in concentrations from low (S = 1.35; minimum salinity measured in the estuary) to high salinities (S = 28.87). The removal

Table 1
Concentrations of REE (pmol kg^{-1}) and salinity of surface waters from the continuum between Paraguaçu Estuary through Todos os Santos Bay, Bahia, Brazil.

Station	Salinity	La	Ce	Pr	Nd	Sm	Eu	Gd	Tb	Dy	Ho	Er	Tm	Yb	Lu
		(pmol kg^{-1})													
P0		122	152	29	124	24	5.5	27	3.2	20	4.0	12.8	1.8	12.4	2.3
P1	1.35	155	215	40	151	32	7.7	38	4.1	24	5.4	15.2	2.3	14.9	2.7
P2	5.29	67	102	17.6	71	16.0	4.0	21	2.5	16.6	3.4	11.6	1.6	11.4	1.9
P3	9.68	58	72	11.4	54	10.9	3.0	15.6	1.9	13.4	2.9	9.5	1.4	9.0	1.6
P4	15.15	57	64	12.3	48	10.8	2.8	16.8	2.0	13.9	3.4	10.7	1.6	10.4	1.8
P5	20.55	61	52	11.1	45	10.0	2.8	15.5	1.9	14.0	3.4	10.7	1.6	10.5	1.9
P6	24.78	64	60	12.0	49	10.5	2.9	15.3	2.2	16.7	3.7	12.8	1.8	11.7	1.9
P7	27.26	78	69	13.6	58	11.3	3.3	16.5	2.2	17.6	3.9	13.1	1.8	12.0	2.0
P8	27.76	74	62	12.3	55	10.8	3.2	15.4	2.2	17.9	4.0	13.3	1.8	11.8	2.0
P9	28.87	68	54	12.3	52	10.8	3.0	15.3	2.3	17.3	4.1	13.7	1.9	12.2	2.0
B1	33.4	56	88	11.9	50	9.3	2.4	11.2	1.5	10.0	2.1	6.8	0.92	5.9	1.0
B2	32.93	34	41	8.3	30	6.9	1.8	10.1	1.3	8.9	2.1	6.8	1.0	6.3	1.0
B3	32.55	38	38	8.0	35	7.1	1.9	10.1	1.5	11.5	2.5	8.5	1.1	7.3	1.2
B4	32.52	19	25	4.3	20	4.2	1.2	7.1	1.0	8.1	2.0	6.4	0.94	5.8	1.1
B5	32.06	31	27	7.2	28	6.8	1.8	11.0	1.6	11.1	2.8	8.8	1.3	7.9	1.3
B6	30.92	52	34	9.2	40	8.5	2.5	12.9	1.9	13.7	3.4	10.4	1.6	9.5	1.6
B7	30.42	49	38	10.8	41	9.6	2.7	14.1	2.2	15.3	3.8	12.1	1.8	10.8	1.7
B8	29.73	54	41	11.0	47	10.2	2.8	15.0	2.4	17.8	4.0	13.8	1.8	11.6	1.8
B9	28.63	59	42	11.1	53	11.9	3.8	19.1	3.0	22	5.2	15.8	2.2	13.3	2.2
B10	29.69	51	34	11.3	44	11.3	3.1	17.6	2.8	19.5	4.8	14.9	2.1	12.8	2.0
B11	28.92	60	44	10.9	50	10.3	3.0	14.6	2.4	18.5	4.0	13.3	1.8	11.4	1.8
B12	29.33	58	40	12.0	45	10.5	2.9	15.4	2.3	16.5	4.2	13.1	1.9	12.1	2.0
B13	30.89	52	39	10.1	43	9.2	2.7	13.6	2.1	15.5	3.6	11.7	1.6	10.5	1.7

process was more intense in the estuarine low salinity region (< 5). As the observed reduction in abundances varied from element to element and was gradually less intense as the atomic number increased, a fractionation process was observed. Thus, the LREE were more efficiently removed than the MREE, and the HREE were the least affected group among them. As a result, there was a gradual change in the PAAS-normalized REE patterns from relatively flat, for the fluvial endmembers (P1, S = 1.35, and P0, freshwater collected right after the PC river dam) to HREE enriched ones in the bay (Fig. 2). At mid to high salinities (> 10), MREE and HREE concentrations started to increase, however, this process was not intense enough to overcome the general decreasing tendency of LREE in comparison to the fluvial endmember (P1). To illustrate that, the sample with lowest salinity (P1) in the estuary was applied as a normalizing agent (Figs. 3, S1) to evidence the differential gradual fractioning of REE along the salinity gradient within the estuary. The fluvial endmember (i.e., S ≈ 0, station P0) is located right after the PC dam. Due to the low freshwater flow down the dam the waters at the head of the estuary are generally under the influence of tides and so, salinities are usually over 1. As such, the percentages of removal calculated for each REE (taking P1 as reference) through the estuary evidence that the maximum REE removal from the dissolved phase is the smallest for HREE, varying from 38% (Er) up to 46% (Ho), followed by MREE (44% (Dy) to 64% for (Eu)), and LREE (63% (La) to 76% (Ce)) (Table S4). Besides, Fig. 3 also illustrates that an increase in REE concentrations from mid to high salinities starts at lower salinities for the HREE (between 10 and 15) than for the MREE (between 10 and 25) and the LREE (between 15 and 25). Data from estuaries elsewhere around the world are also plotted in Fig. 3 for comparison.

Fig. 4 shows the variations in Ce/Ce* and Gd/Gd* throughout the salinity gradient for samples from both the estuary and the bay. The estuarine samples presented a decreasing tendency for the values of Ce/Ce* from 0.69 at P2 to 0.43 at P9. In the bay, Ce/Ce* varied from 0.33 (B10) to 0.79 (B1). The western side of the bay presented more preeminent negative anomalies, ranging from 0.33 to 0.40 at B11, while the eastern side of the bay showed higher variability in Ce/Ce* values, from 0.42 up to 0.79.

Gadolinium anomalies were always positive and varied from 1.1 at B07 to 1.6 at P1. The upper reaches of Paraguaçu (P1-P5) presented higher Gd/Gd* than other areas and stations P1 and P5 presented Gd/Gd* values slightly above 1.4, considered here as the limit for the natural Gd anomaly (Song et al., 2017).

4.2. REE variations during tidal cycle

The results obtained for surficial waters collected hourly during a 12-h time period at a pier station (station TS, Fig. 1) are shown in Table 2. Sampling started at low tide (T1) and reached high tide after 6.5 h of elapsed time (~T7). During the sampling period, salinity varied only slightly from 33.26 to 33.60. Similarly, the pH also varied

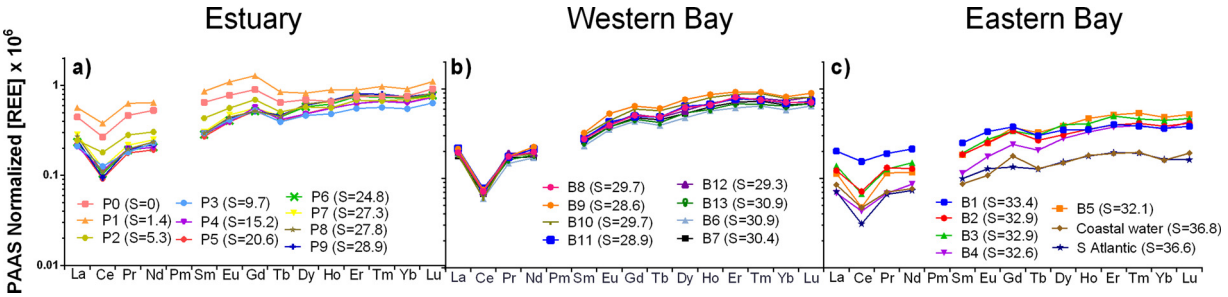

Fig. 2. PAAS-normalized REE patterns for stations from Paraguaçu Estuary (a) western (b) and eastern (c) sides of Todos os Santos Bay. P0 represents a fluvial station located right after the Pedra do Cavalo dam at the Paraguaçu River. South Atlantic water (CoFeMUG, station 1, 10 m deep (Zheng et al., 2016)) and Coastal water (E01S, off the coast of Salvador (Pedreira et al., 2018)) are plotted for comparison.

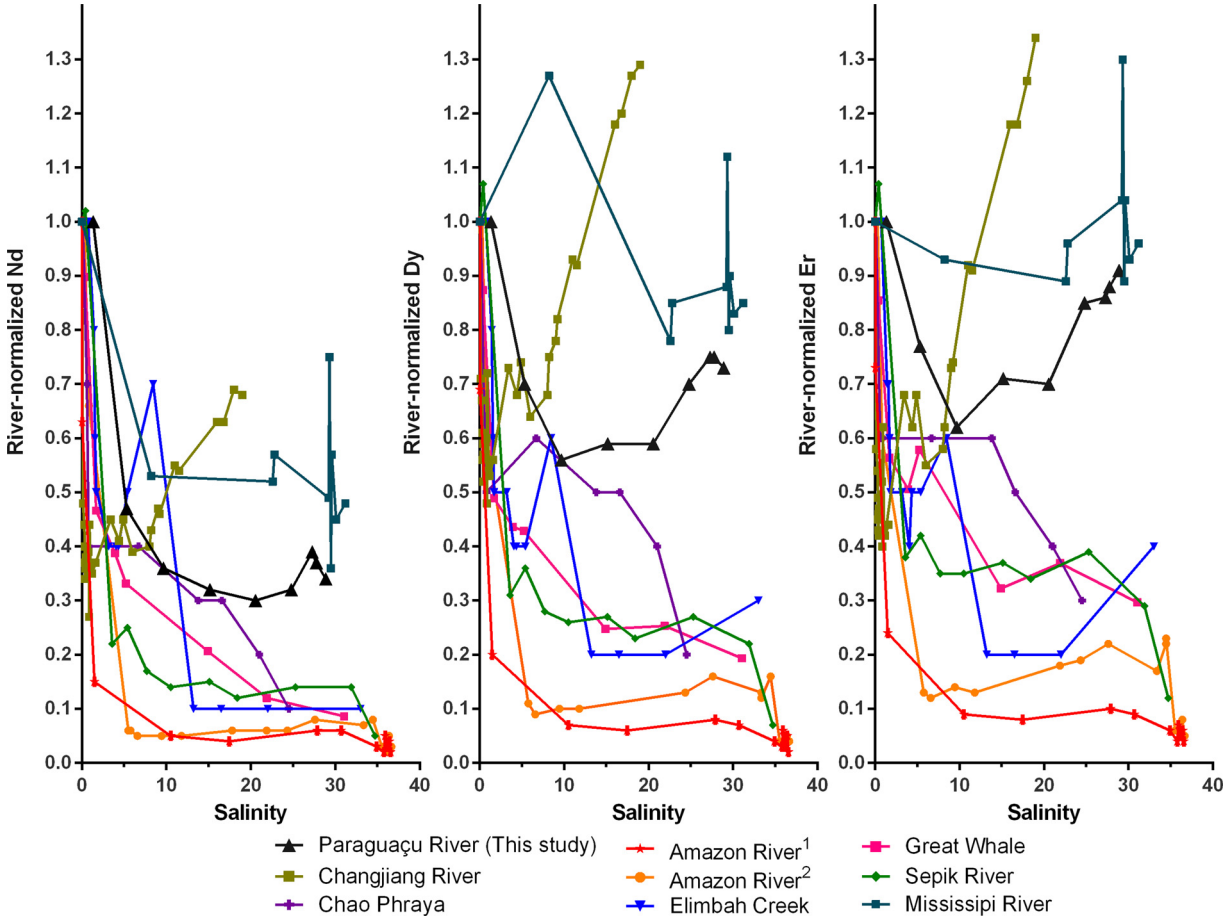

Fig. 3. Estuarine concentrations of Nd (LREE), Dy (MREE), and Er (HREE) normalized to the REE concentrations of the freshwater endmember (P1, S = 1.35). Chanhgjiang River (Wang and Liu, 2008), Sepik River (Sholkovitz and Szymczak, 2000), Elimbah Creek (Lawrence and Kamber, 2006), Chao Phraya River (Nozaki et al., 2000), Great Whale River (Goldstein and Jacobsen, 1988b), Amazon River1 (Rousseau et al., 2015), Amazon River2 (Sholkovitz, 1993), Mississipi River (Adebayo et al., 2018) data normalized by their respective fluvial endmember are plotted for comparison.

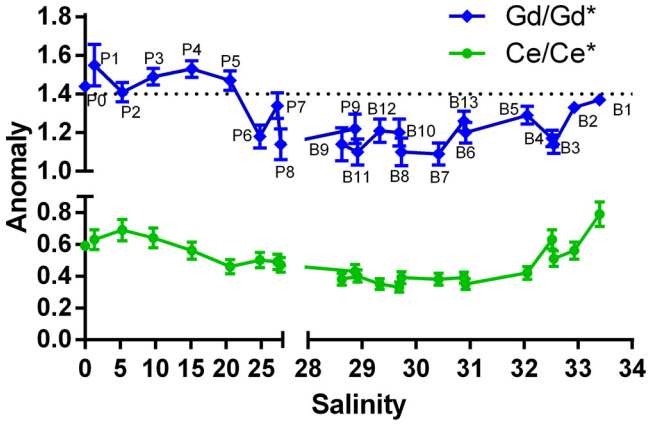

Fig. 4. Variations in Gd/Gd* (blue line) and Ce/Ce* (green line) through the salinity gradient at stations in the Paraguaçu Estuary and Todos os Santos Bay. The dashed black line is the maximum limit (1.4) adopted in this study as the natural Gd/Gd*; values above this line are considered anthropogenic anomalies. (For interpretation of the references to colour in this figure legend, the reader is referred to the web version of this article).

in a narrow interval, from 8.60 to 8.73, except for T1 (low tide), which exhibited a notably different pH of 7.67 (Table S3). Temperature varied from 24.58 to 26.04 °C, at low tide (T1) and high tide (T7) respectively.

The concentrations of REE varied from 0.57 pmol kg^{-1} (Tm at T13) to 273pmol kg^{-1} (Ce at T1). The sum of REE decreased one order of magnitude during the 6 h period of the incoming tide, from 658 pmol kg^{-1} (T1) at low tide to 70 pmol kg^{-1} (T7) at high tide. The largest change was observed for the LREE (60–94%) followed by the MREE (40–88%) and HREE (24–65%) (Fig. S1; Table S4).

During flood tide, PAAS-normalized REE patterns gradually changed from flat (T1) to HREE enriched (T7) (Fig. 5b; Figure S3). They also remained HREE-enriched throughout the following ebb tide.

Similarly to what has been observed through the Paraguaçu Estuary and at Todos os Santos Bay, negative Ce anomalies were present in all samples and ranged from 0.55 to 0.97, at T11 and T1 respectively (Fig. 5c). Generally, Ce/Ce* decreased with time, i.e., the negative Ce anomalies strengthened. The gadolinium anomaly varied between 1.3 and 2.3. There were two peaks of Gd/Gd* through time, at high tide (T7; 2.3) and during ebb tide (T11; 2.3). During most of the 12 -h sampling, Gd/Gd* was above 1.4, the only exceptions were T1, T9, and T10.

5. Discussion

5.1. Paraguaçu estuary REE

Usually river waters present relatively flat REE patterns without a Ce anomaly, though some rivers show an HREE, MREE, or LREE enriched pattern (e.g. Goldstein and Jacobsen, 1988a; Elderfield et al., 1990; Sholkovitz, 1993, 1995; Tepe et al., 2014; Rousseau et al., 2015). However, through the estuarine zone, the mixing of freshwater with seawater promotes several processes leading to the removal of many

Table 2
Concentrations of REEs (pmol kg^{-1}) and salinity of surface waters collected hourly during a 12 h period at station TS (12°55′14.4″ S, 38°30′37.9″ W), Todos os Santos Bay, Bahia, Brazil.

Sample	Local time	Salinity	La (pmol kg^{-1})	Ce	Pr	Nd	Sm	Eu	Gd	Tb	Dy	Ho	Er	Tm	Yb	Lu
T1	**9:00**	**33.53**	**139**	**273**	**31**	**121**	**22**	**5.3**	**23**	**2.9**	**17.5**	**3.3**	**9.8**	**1.3**	**7.8**	**1.3**
T2	10:00	33.41	55	92	12.0	49	9.7	2.5	13.7	1.6	9.8	2.2	6.3	0.91	5.4	1.0
T3	11:00	33.31	42	68	9.2	39	7.8	2.1	11.7	1.3	8.4	1.9	5.5	0.80	5.2	0.90
T4	12:00	33.34	35	58	8.6	32	7.4	1.8	11.4	1.2	7.6	1.8	5.3	0.79	5.0	0.88
T5	13:00	33.28	30	55	7.4	30	6.5	1.6	10.4	1.1	7.9	1.6	5.5	0.73	5.0	0.85
T6	14:00	33.26	31	48	6.9	28	5.9	1.6	10.7	1.0	7.2	1.6	5.0	0.72	4.5	0.81
T7	**15:00**	**33.3**	**12.6**	**16.6**	**2.8**	**10.8**	**2.8**	**0.72**	**7.2**	**0.65**	**4.8**	**1.3**	**4.1**	**0.61**	**4.0**	**0.72**
T8	16:00	33.45	13.7	17.0	3.0	12.2	2.7	0.70	6.0	0.64	5.0	1.2	4.3	0.61	4.1	0.72
T9	17:00	33.6	16.0	17.1	3.0	13.7	2.8	0.75	5.3	0.65	5.1	1.3	4.3	0.61	4.0	0.71
T10	18:00	33.52	19.1	26	5.5	24	5.3	1.4	7.8	1.0	7.1	1.6	5.3	0.69	4.6	0.77
T11	19:00	33.4	15.4	17.6	3.5	15.2	3.3	0.90	7.0	0.67	4.8	1.3	4.1	0.62	3.8	0.71
T12	20:00	33.45	14.0	17.3	3.4	13.3	3.1	0.82	6.7	0.68	4.8	1.2	4.2	0.62	4.0	0.70
T13	**21:00**	**33.48**	**13.9**	**18.1**	**3.0**	**13.4**	**2.9**	**0.80**	**6.1**	**0.65**	**5.1**	**1.2**	**4.0**	**0.57**	**3.8**	**0.65**

Where T1 and T13 (bold) represent the low tide (1.60 m and 1.70 m, respectively) and T7 (bold) corresponds to the high tide (3.40 m).

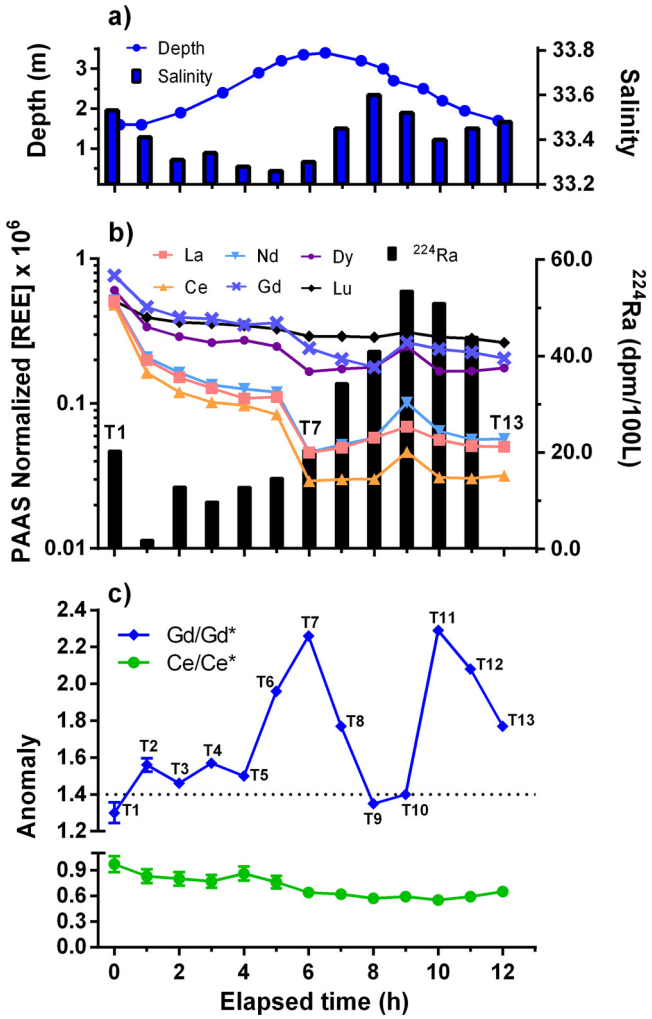

Fig. 5. Tidal cycle trend of (a) water column depth (left Y-axis) and salinity (right Y-axis); (b) selected PAAS-normalized REEs (left Y-axis; La, Ce, Nd, Gd, Dy, and Lu) and ^{224}Ra (right Y-axis; data from Hatje et al. (2017)); and (c) variations in Gd/Gd* (blue line) and Ce/Ce* (green line) at station TS, where the dashed line is the maximum limit (1.4) adopted in this work for the natural Gd/Gd*. Samples T1 (0 h) and T13 (12 h) represent low tides, while sample T7 (6 h) represents a high tide. Between each sampling there is 1 h difference, completing a 12 h cycle. (For interpretation of the references to colour in this figure legend, the reader is referred to the web version of this article).

constituents of the river dissolved/colloidal load, such as Fe, dissolved organic matter, and REE (Boyle et al., 1977; Sholkovitz and Copland, 1981; Sholkovitz et al., 1983; Elderfield, 1988; Elderfield et al., 1990; Merschel et al., 2017). The total dissolved REE flux of a river is a result of the balance between the rate of river input and estuarine removal and release processes. For the Paraguaçu River, as well, conservative mixing is not sufficient to explain the changes in REE concentrations through the salinity gradient (Figure S2).

Although no measurements of REE concentrations in the colloidal or particulate fractions were made in this study, the salt-induced coagulation and flocculation of Fe-rich organic colloids in low salinities is a well-documented process (Sholkovitz, 1993, 1995; Lawrence and Kamber, 2006; Rousseau et al., 2015). Colloids present gradually higher abundance of REE from HREE to LREE when compared to the dissolved composition (Sholkovitz, 1992; Rousseau et al., 2015). In a recent study, Mershel et al. (2017) have shown experimentally that during estuarine mixing, river waters rich in inorganic nanoparticles and colloids have their LREE preferentially partitioned onto solid phase due to their more pronounced complexation with ligands on particles and colloid surfaces while HREE tend to stay in solution due to stronger complexation to dissolved ligands. Such a process is most likely causing the removal and fractionation of REE in the Paraguaçu estuary, similarly to what has been reported in other estuaries such as Amazon, Fly, Sepik, and Connecticut (Rousseau et al., 2015, Sholkovitz, 1993, 1992).

From mid to high salinities, the removal process is generally overcome by release processes due to desorption and/or dissolution from particles (Rousseau et al., 2015; Sholkovitz and Szymczak, 2000; Sholkovitz, 1993, 1995). At the Paraguaçu estuary, the combination of the different intensities of both release and removal processes throughout the lanthanide series caused a fractionation in their normalized abundances towards a more marine-like pattern as salinity increased. As a result, at the mouth of the estuary (P9, S = 28.9) the waters present the classical HREE enriched pattern with a Ce anomaly (Fig. 2), although some fractionation towards an even more marine-like pattern was still observed within the bay. That fractionation pattern has been reported in other estuaries around the world (Martin et al., 1976; Goldstein and Jacobsen, 1988a; Sholkovitz, 1995; Sholkovitz and Szymczak, 2000; Lawrence and Kamber, 2006; Rousseau et al., 2015).

Compared to other estuaries, the data for the Paraguaçu Estuary stands out by presenting limited removal (up to 70% for LREE and 38% for HREE) in the low salinity region and remarkable release starting at salinities > 10 (Fig. 3). The increase in REE abundances was particularly intense for the HREE, and gradually less noticeable towards LREE (Figs. 3, S1). For HREE (as well as Dy and Tb) the increase in concentrations surpassed the values expected considering conservative mixing (Figure S2). A similar pattern with even more pronounced HREE

release has been reported for the Changjiang River (Wang and Liu, 2008), the Fly River-Gulf of Papua (1997 data; (Sholkovitz and Szymczak, 2000)), and the Mississipi River (Adebayo et al., 2018). In the case of these rivers, the increases in REE concentrations at mid to high salinities were attributed to sediment-water interactions, caused by friction in shallow water environments and/or high amounts of suspended particulate material. It needs to be noted that the low removal and high release percentages observed in this work are possibly less intense since a large proportion of removal is usually observed in the very low salinity region and the salinity of the endmember used for normalization was 1.35 (sample P1). Previous studies have reported removal rates of 30% up to 85% between salinities 0 and 1.5 (Lawrence et al., 2006; Rousseau et al., 2015,). However, in the case of Paraguaçu River, the dam that controls the river water flux reduces the input of freshwater significantly and salinities at the estuary head, below the dam, are generally under tidal influence (Lessa et al., 2001). The water sample P0 from right after the dam was collected for comparison, however, considering the estimated ~2.5 years water residence time within the dam (considering PC dam volume = 4.64 10^9 m^3) and that the REE concentrations in P0 were below the one observed at the head of the estuary (P1), we considered P0 not to be a representative freshwater endmember. To corroborate our choice of P1 as a normalizing agent, the Nd removal of 70% obtained for this work is the value generally used in marine models, based on empirical values obtained for estuaries around the world (Tachikawa et al., 2003; Arsouze et al., 2009; Rempfer et al., 2011; Rousseau et al., 2015).

Nonetheless, even with underestimated values, the general tendency for changes in the REE pattern through the salinity gradient would not be affected. Considering that, it is important to highlight some notorious characteristics. Lanthanum presented lower removal and larger desorption/remineralization rates than its LREE neighbors (Table S4). It also started to show increased concentrations at lower salinities (S = 20.6) than the other LREE (S = 24.8). This tendency has been previously reported and attributed to a greater chemical stability of La complexes due to its available 4*f*-electron shell (Lawrence and Kamber, 2006), suggesting that La might rather behave as a MREE.

Another distinct characteristic for the Paraguaçu Estuary is its removal/release pattern. Though many studies have reported the LREE > MREE > HREE removal pattern (Elderfield et al., 1990; Sholkovitz, 1993, 1995; Sholkovitz and Szymczak, 2000; Lawrence and Kamber, 2006; Rousseau et al., 2015; Merschel et al., 2017), little has been said about preferential release of HREE in mid to high salinities. Most studies have also supported the LREE > MREE > HREE preferential release (Sholkovitz, 1995; Lawrence and Kamber, 2006; Rousseau et al., 2015). However, the preferential release of HREE has also been previously observed on the Amazon River and Fly River/Gulf of Papua (Sholkovitz, 1993; Sholkovitz and Szymczak, 2000). In the Paraguaçu River, the order of preferential release is HREE > MREE ~ La > LREE. This is evidenced both by the fact that the HREE displayed increased concentrations at lower salinities and that HREE presented a larger percentage increase in concentrations after reaching a minimum value than the LREE. Sholkovitz (1993) suggested that the release of REE from bottom sediments in high salinity regions of the estuary could be the cause of this fractionation. Sholkovitz and Szymczak (2000) also indicated the shallow environment and lower than usual river discharge as a possible cause for the increased physical coupling between sediments and surface waters of the Fly River, producing the large REE increases detected. The latter proposed that the most likely mechanism controlling the release of these elements would be desorption of REE lightly bound to the surfaces of bottom sediments and particles in suspension at shallow estuarine environments.

The shallow waters of the upper reaches of the Paraguaçu Estuary (ranging from 1.5 m to 6.9 m at P2 and P5, respectively) and the artificially controlled water flux suggest that similar processes may control the release and fractionation of dissolved REE in the upper estuary. The stations upstream the Iguape Bay (Fig. 1), an area that may act as a buffer for sedimentation processes along the estuarine gradient, may have lower dynamics favoring particle-water interactions. The Paraguaçu River presents a fluvial delta prograding into Iguape Bay, which might enhance the friction between sediments and water especially during very low tide levels (Lessa et al., 2001). This might be one factor influencing the intensity of REE release in the area, since the increase in HREE from station P4 to P5 (upstream of Iguape Bay) was much lower than the one observed from P5 to P6 (inside Iguape Bay). Once at the lower course of the river (Paraguaçu Channel, which connects the Iguape Bay to Todos os Santos Bay) the water depth reaches 25 m and stronger flows are observed (Genz et al., 2006). Therefore, sample P7, still under Iguape Bay influence and presenting the lowest turbidity in the estuary, shows the highest concentrations (after P1) for most elements (table S4), while samples P8 and P9 are under a very different dynamic setting, which might be a reason for the decrease in REE concentrations, particularly LREE.

Recent studies have proposed that particle dissolution may also have an important role in controlling the dissolved REE load of estuarine and ocean waters. Pearce et al. (2013) experimentally demonstrated that the interaction of basaltic particles with marine water causes REE release through a dissolution mechanism, even though that dissolution might be compensated by removal processes resulting in the net reduction of REE concentrations in the dissolved pool. Corroborating that, Rousseau et al., 2015 verified the occurrence of the dissolution of lithogenic suspended particles as the main mechanism causing the change in εNd at the Amazon Estuary. That study showed that within a 3 weeks period the Amazon dissolved pool reached εNd equivalent to that of suspended particles. Data from both studies suggest that isotopic Nd composition changes due to the dissolution of particles can be observed within short periods. For the Amazon (Rousseau et al., 2015), non-conservative εNd changes have been observed within a week period. That means that even for an estuary with a short water residence time, such as Paraguaçu (residence time < 1 week, Hatje et al., 2017), dissolution mechanisms could occur at a measurable scale. However, how significant that process would be for the net flux of REE to the bay would depend on other factors, such as the intensity of removal processes and particle surface area and origin. Regardless of the mechanism, the HREE form stronger complexes with dissolved ligands compared to LREE, therefore they would not only present lower particle adsorption factors but also preferential release to the dissolved pool.

It is important to highlight that even with evidence supporting the dissolution mechanism, it does not mean that the desorption mechanism does not happen or that it is not significant. Both mechanisms could happen simultaneously and present diverse levels of importance in different estuaries. More studies on both are still needed to quantify their relevance for the continental flux of REE to the ocean and provide better insights on how anthropogenic activities, such as river damming or siltation, might influence that flux and in a larger scale the natural cycles of REE, as well as other elements.

5.2. Todos os Santos bay REE

The REE patterns in the eastern part of the bay are more scattered than those of the western part (Fig. 2b and c), especially for the LREE. The western part of the bay presents a relatively higher content of REE, reflecting the direct contribution of the fluvial systems, compared to those retrieved from the eastern part that has an open connection and thus a more dynamic water exchange with coastal Atlantic waters.

In order to potentially identify sources of REE and reveal their contributions, the HREE/LREE versus MREE/MREE* ratios are shown in Fig. 6. The surface waters of the estuary exhibit a clear gradient for the HREE/LREE versus MREE/MREE* ratios that roughly follows the salinity gradient (i.e., P1-P9), ranging from 1.42 to 3.40 and from 1.16 and 1.35, respectively indicating the Paraguaçu River as one of the main sources of REE for the bay waters. Samples B12 and B13 seem to

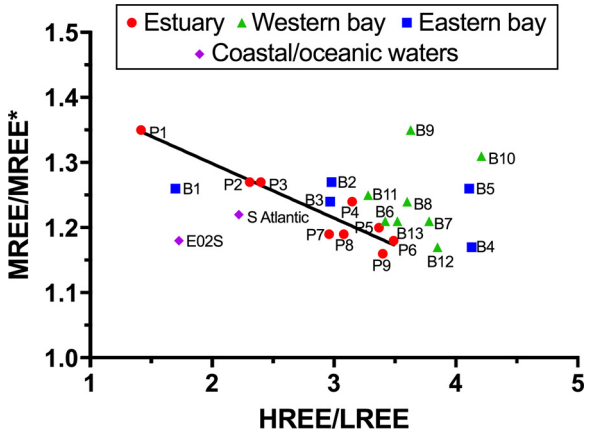

Fig. 6. HREE/LREE versus MREE/MREE* for samples from the Paraguaçu Estuary and Todos os Santos Bay. Where HREE/LREE is represented by Yb_{SN}/Nd_{SN} and MREE/MREE* is the ratio between the average of Gd_{SN} and Dy_{SN} and the average of Yb_{SN} and Nd_{SN}, where SN means the element has been PAAS-normalized. Red circles represent Paraguaçu Estuary samples, green triangles and blue squares are samples from the western and eastern sides of Todos os Santos Bay, respectively, and purple diamonds are samples from the adjacent continental shelf (E02S, Pedreira et al., 2018) and S Atlantic (station 1, 10 m deep, Zheng et al., 2016). The black line is the linear relationship that characterizes the Paraguaçu estuary data ($r = 0.94$; $p < 0.05$). (For interpretation of the references to colour in this figure legend, the reader is referred to the web version of this article).

follow the same gradient reflecting the mixture between estuarine and bay waters. The MREE/MREE* ratios in the estuarine waters together with B12 and B13 were negatively correlated to salinity ($r = 0.92$; $p < 0.05$; Figure S4), implying that the high values mainly reflect the freshwater dissolved inputs from Paraguaçu River. Though B6 and B11 seemed to follow the same trend, they did not present a significant correlation.

Fig. 6 also shows that there is a difference between samples from the northwestern and southwestern sides of the bay, probably due to the geological settings of the Paraguaçu River that runs through crystalline basement (southwest, stations B12 and B13) and the Subaé Basin, consisting of shales (northwest, stations B9 and B10) (Dominguez and Bittencourt, 2009). Stations B9 and B10 in the northwestern-most section of BTS, under the influence of Subaé River, have higher HREE/LREE and MREE/MREE* ratios than all the other samples.

On the other side, it has been previously reported that the eastern part of the bay, where B4 (near the entrance of Aratu Bay) and B5 (close to Mare Island) were sampled (Fig. 1), presents higher activities for all 4 Ra isotopes than the rest of the bay and estuarine waters, suggesting additional sources, potentially SGD (Hatje et al., 2017) influencing the water composition. The BTS is part of the sedimentary Recôncavo-Tucano-Jatobá Rift formed during the South Atlantic rifting (Magnavita et al., 1994). The geomorphology, determined by tectonic alignments could favor groundwater flow.

Meanwhile, samples B1, B2, and B3, collected closer to the mouth of the bay fall between the western bay samples and the coastal/oceanic ones (E02S and S Atlantic, respectively; Pedreira et al., 2018 and Zheng et al., 2016), reflecting the mixture of these waters at the bay entrance.

The processes that generate the seawater REE patterns observed at BTS occur within the estuarine zone of Paraguaçu river and at the bay itself (Fig. 2). Relatively flat REE patterns gradually evolve towards HREE-enriched patterns that are similar to the Atlantic Ocean water (Zheng et al., 2016). The detected REE patterns are thus a combination of estuarine and intra-bay processes (i.e. river input + seawater mixture + water particle interaction + SGD).

5.3. REE variations during a tidal cycle

At the pier station, REE samples were collected hourly over a 12 h period. During flood tide, the PAAS Normalized REE patterns changed from terrigenous to marine like (Fig. 5). This change was anticipated due to the increased marine influence caused by the tidal cycle. Interestingly, not only the fractionation, causing HREE enrichment, but also the reduction in ΣREE (almost 90%) was similar to what is normally observed in estuaries, despite the high salinity ($S > 33$) throughout the tidal cycle. At low tide (T1), the pH (7.67) and the REE patterns were different from all other measurements during the temporal series (Fig. 5 and Table S3). The flat REE pattern associated with the lower pH of this sample may indicate inputs from a source, although this is not shown in the salinity. One possible reason is that groundwater discharge was located close to shore and the sampling was off a 140 m long pier. This hypothesis is supported by the existence of a well supplying freshwater to the marina near the pier, however, it needs to be tested.

On the other hand, during ebbing tide, the expected change to a terrigenous REE pattern was not observed, although there is some indication of a more terrigenous pattern at T10. During low tide, the degree of marine influence at the sampling site was not reduced compared to SGD flux. One possible explanation for this unexpected temporal behavior is input of recirculated submarine groundwater or marine SGD that would not carry a strong terrigenous signal, but would still retain a high Ra signal due to Ra isotopes preferential desorption to waters with high ionic strength. Recently Hatje et al. (2017) estimated the total (saline and fresh) SGD input to Todos os Santos Bay ($300\ m^3\ s^{-1}$) and used radon/salinity measurements to indicate that some areas, including areas off Itapagipe Bay (location of the pier station), might have enhanced SGD inputs. That study also emphasized that bay water that is tidally driven into the subsurface (recirculated), can return to the bay as the tide turns and that in many tidal environments this type of SGD forcing is volumetrically more important than freshwater SGD input (Burnett et al., 2003; Moore, 2010; Hatje et al., 2017). In fact, the ^{224}Ra increase during ebb tide (Fig. 5) provides strong evidence of SGD input even though the REE pattern is indicating a marine influence. Therefore, marine SGD changes the temporal REE pattern. It was expected that as soon as the recirculated marine water left the aquifer during low tide, the REE would return to its flat terrestrial pattern, as observed in T1, due to freshwater SGD influence. However, the sampling period ended with a low tide and no such change was observed. It is possible that the recirculated water might take longer than the ebb tide period (considering BTS has a semidiurnal tide) to leave the subsurface, as gravity is the only force driving it out. In fact, previous studies have reported that semi-diurnal changes of tidal height drive temporal fluctuations in marine SGD and that maximum discharge is often reported a few hours after the low tide (Taniguchi et al., 2006; Taniguchi et al., 2008; Nakajima et al., 2018). Thus, a longer sampling period comprising the whole tidal cycle (24 h) would be necessary to better evaluate the influences SGD has on REE and other geochemical patterns.

Though not so evident, T10 (ebbing tide) also presents higher REE concentrations and lower HREE enrichment than samples collected right after and before it. These characteristics are probably related to the slightly lower pH of this sample, which might reflect a similar mixing to a different water mass, in accordance with what was observed at low tide (T1), though in reduced proportion. In both cases, pH is a key factor to understand the REE behavior and consequently the processes occurring at the site. Firstly, because it is indicating the mixing of different water masses. In addition, pH is known to influence the sorption of REE to particle surfaces and samples with higher pH have been reported with lower concentrations and more fractionated REE compositions relative to the composition of Earth's crust (Sholkovitz, 1995; Johannesson et al., 2017).

Overall, there was a co-variation trend between pH and REE

concentrations (i.e. for pHxΣREE: $r = 0.79$ $p < 0.05$, excluding T1, to avoid bias due to data distribution on X-axis). Considering the lack of substantial changes in ionic strength in such a high salinity environment, one can infer that the pH could act as a major factor controlling the REE fractionation, mainly because the pH can alter the carbonate equilibrium, as well as destabilize the oxi-hydroxides, causing precipitation, and therefore modify the dominant form of REE in solution by changing its ligands. Further studies are necessary to better constrain the effects of pH variation on REE distribution in high salinity environments, especially in light of changes in pH expected in the next years for the oceans worldwide.

5.4. REE anomalies

5.4.1. Ce

As expected, the negative anomaly increased with the salinity, either due to the coagulation of river colloids or biological activity associated with high productivity (Sholkovitz, 1993; Merschel et al., 2017; Moffett 1990). Cerium is also the element with the largest removal factor (76%), however, its removal was not especially larger when compared to its LREE neighbor Pr (72%).

In the Bay, Ce/Ce* was more negative at the western side (Fig. 4) that receives more influence of the fluvial inputs from Paraguaçu and Subaé estuaries. On the other side of the bay, however, less negative values were observed. These stations are closer to the entry of the bay and to areas with enhanced SGD input (Hatje et al., 2017), therefore, the mixing of these waters within the bay might also influence the Ce distributions.

The observation of a negative Ce anomaly in all samples collected during the tidal cycle was not surprising considering their high salinity ($S > 33$). Even so, sample T1 exhibited almost no anomaly ($Ce/Ce^* = 0.97$), probably reflecting the influence of the freshwater SGD input. During flood tide and most of the ebb tide, the samples collected after T1 presented gradually more negative Ce/Ce*, reaching 0.55 at T11. Associated with the observed fractionation and decrease in REE concentrations, it indicates a gradual increase of the seawater influence in the dissolved REE at the site. With the proximity to low tide, the Ce anomaly started to decrease possibly indicating that the freshwater SGD started to increase its influence over the REE behavior. As that slight change of influence was not observed in the normalized REE pattern, it might imply that Ce/Ce* might be a more sensitive indicator for the mixing.

5.4.2. Gd

Inside the bay, Gd anomalies were generally within a range considered natural, from 1 to 1.4 (Fig. 4). However, in the estuary, stations P1, P3, P4, and P5 presented Gd anomalies above natural levels, indicating the presence of an additional source of Gd. Since the 1990s, Gd anomalies have been reported in rivers, lakes, groundwater, seawater, wastewater and even tap water (Bau and Dulski, 1996a; Rabiet et al., 2009; Kulaksiz and Bau, 2011; Merschel et al., 2015; Brünjes et al., 2016; Hatje et al., 2016; Johannesson et al., 2017; Song et al., 2017; Pedreira et al., 2018) as a result of anthropogenic activities, mostly the application of Gd as a contrasting agent used in magnetic resonance imaging (MRI).

In the case of Paraguaçu Estuary, there are no known MRI machines being operated in the catchment area. Even so, there were detectable anthropogenic Gd anomalies in the estuary, mainly at mid to low salinity regions ($S < 20$). Brünjes et al. (2016) showed that even in urban areas where there were no MRI facilities, anthropogenic Gadolinium was released through the sewage treatment plant into rivers. Over 90% of the elimination of Gd complexes generally occurs through the urine within the first 48 h of injection of the contrast in healthy patients (Schumann-Giampieri and Krestin, 1991). In individuals with renal insufficiency, it might take longer and Gd complexes may not be completely eliminated (Schumann-Giampieri and Krestin, 1991; Joffe et al., 1998).

In the case of cities alongside the Paraguaçu Estuary, the proximity to larger urban centers (25–125 km), where Gd-based contrast agents are applied could allow the MRI patients to be examined there and eliminate the Gd complexes, or at least part of it, after returning home. Therefore, when the wastewaters from these cities are discharged to the river, they may be carrying anthropogenic Gd, leading to the observed anomalies. The Gd complexes applied as contrast agents are highly stable and the general wastewater treatments processes cause little if any removal of these composts (Bau and Dulski, 1996; Bau et al., 2006; Morteani et al., 2006; Lawrence et al., 2009). However, more than 99% of anthropogenic Gd removal has been reported in plants that employ reverse osmosis as part of the wastewater treatment processes (Lawrence et al., 2010), though that is not the case of any Brazilian treatment plant up to date.

In a recent study, Pedreira et al. (2018) observed Gd anomalies up to 3.4 in the waters off the coast of Salvador under the influence of two submarine sewage outfalls. That study also identified the decrease of these anomalies with the distance from the sources (sewage outfalls) and that all the stations at the entry of the bay presented natural Gd/Gd* values (i.e. $Gd/Gd^* < 1.4$). These results corroborate the observed Gd/Gd* distributions throughout Todos os Santos Bay (Fig. 4), indicating that inputs of the submarine outfalls are not significantly influencing the Gd concentrations inside the bay.

However, the data for the time-series (Fig. 6) imply a source of anthropogenic Gd inside Todos os Santos Bay. The most likely source of the high Gd anomalies is the water of Itapagipe Bay, which is highly contaminated by domestic sewage (CRA, 2004; Hatje et al., 2009). Due to its proximity and tidal forcing, the waters from Itapagipe Bay might reach the TS station. Also, the Gd/Gd* lowered between T7 and T10, even with increasing ^{224}Ra, reinforcing the hypothesis that the recirculated groundwater was not the main source of anthropic Gd to the samples. It was unexpected that some anomalies observed during the tidal cycle were higher than the ones observed in the Paraguaçu estuary. That might be a consequence of proximity to the source or possibly due to the lower ΣREE in the TS samples, since low natural REE concentrations highlight the presence of small amounts of anthropogenic Gd. As the ΣREE varied up to an order of magnitude with time, the high ΣREE in sample T1 (low tide) might be masking a similar amount of anthropogenic Gd. The Gd complex is very stable and soluble even in estuary and seawater conditions (Kulaksiz and Bau, 2007), then it is evident that seawater REE patterns will be a lot more sensitive to any anthropogenic Gd input. Also, Schijf and Christy (2018) suggested that the presence of high amounts of Mg and Ca in saline waters may cause instability to the Gd complex, causing the release of part of this contaminant and making it even harder to differentiate natural from anthropogenic Gd. This might be extremely concerning, considering the toxicological potential of free Gd and its still unknown impacts in marine ecosystems.

6. Conclusions

The concentrations of dissolved REE across the continuum continent – oceans are controlled by several processes that combined have a major effect on the biogeochemistry of REE in the marine environment. Here we showed that the salinity gradient, the tidal cycle, and potentially SGD inputs, water-particle interactions (sorption, desorption, and dissolution), and anthropogenic inputs play a role in the fractionation and concentrations of REE. At the Paraguaçu Estuary, in mid to high salinities the HREE presented dissolved concentration increases at lower salinities, followed by MREE and LREE. The observed REE order of release in these salinities follows HREE > MREE > LREE, which is the reverse of the order of removal observed in low salinities.

During the tidal cycle, the variations in REE concentrations and patterns were attributed to the variable influence of the tides and its interaction with other coastal relevant factors, such as SGD inputs and

anthropogenic influence. As for BTS, river inputs and water circulation, as well as open connection to the sea and, possibly, geological setting, presented major importance on the observed REE distribution.

The observation of anthropogenic Gd at the Paraguaçu Estuary evidenced human beings as transporting agents, carrying the Gd complex in the body for enough time to contaminate areas distant from the point sources. Therefore, the results suggest that the increase of high technology wastes in coastal areas may complicate the use of REE as tracers of natural processes.

Despite all previous efforts, there are still uncertainties on how and to which extent each of these factors influences the REE fractionation in coastal waters. The use of Nd isotopes and the evaluation of REE associated to the particulate phase could help to solve the hypothesis presented here.

Acknowledgments

The authors are thankful to A. Passos and the Laboratório de Oceanografia Química (Federal University of Bahia) colleagues for helping during the sampling campaign and the Marine Isotope Geochemistry Group of ICBM (University of Oldenburg), especially R. Paffrath and M. Schulz, for helping R. Pedreira during the sample analyses. We also thank W. Burnett, the reviewers and C Chauvel for their constructive comments on the text. This project was financially supported by FAPESB (PET0034/2012; PAM Nº. 0020/2014) and CNPq (441829/2014-7). The authors were sponsored by CAPES (R. Andrade and R. Pedreira), SCOR (R. Pedreira) and CNPq (V. Hatje - 239977/2012-2).

Appendix A. Supplementary data

Supplementary material related to this article can be found, in the online version, at doi:https://doi.org/10.1016/j.chemgeo.2019.119303.

References

Abbott, A.N., Haley, B.A., McManus, J., Reimers, C.E., 2015. The sedimentary flux of dissolved rare earth elements to the ocean. Geochim. Cosmochim. Acta 154, 186–200. https://doi.org/10.1016/j.gca.2015.01.010. Available at:.

Adebayo, S.B., Cui, M., Hong, T., White, C.D., Martin, E.E., Johannesson, K.H., 2018. Rare earth elements geochemistry and Nd isotopes in the Mississippi River and Gulf of Mexico mixing Zone. Front. Mar. Sci. 5, 1–18.

Andrade, R.L.B., Hatje, V., Masqué, P., Zurbrick, C.M., Boyle, E.A., Santos, W.P.C., 2017. Chronology of anthropogenic impacts reconstructed from sediment records of trace metals and Pb isotopes in Todos os Santos Bay (NE Brazil). Mar. Pollut. Bull. 125, 459–471.

Arsouze, T., Dutay, J.-C., Lacan, F., Jeandel, C., 2009. Reconstructing the Nd oceanic cycle using a coupled dynamical – biogeochemical model. Biogeosci. Discuss. 6, 5549–5588.

Aubert, D., Stille, P., Probst, A., Gauthier-lafaye, F., Pourcelot, L., Del nero, M., 2002. Characterization and migration of atmospheric REE in soils and surface waters. Geochim. Cosmochim. Acta 66, 3339–3350.

Bau, M., Dulski, P., 1996. Anthropogenic origin of positive gadolinium anomalies in river waters. Earth Planet. Sci. Lett. 143, 245–255. Available at: http://linkinghub.elsevier.com/retrieve/pii/0012821X96001276.

Bau, M., Knappe, A., Dulski, P., 2006. Anthropogenic gadolinium as a micropollutant in river waters in Pennsylvania and in Lake Erie, northeastern United States. Chemie Der Erde - Geochem. 66, 143–152.

Behrens, M.K., Muratli, J., Pradoux, C., Wu, Y., Böning, P., Brumsack, H., Goldstein, S.L., Haley, B., Jeandel, C., Paffrath, R., Pena, L.D., Schnetger, B., Pahnke, K., 2016. Rapid and precise analysis of rare earth elements in small volumes of seawater - Method and intercomparison. Mar. Chem. 186, 110–120. https://doi.org/10.1016/j.marchem.2016.08.006. Available at:.

Boyle, Ea., Edmond, J.M., Sholkovitz, E.R., 1977. The mechanism of iron removal in estuaries. Geochim. Cosmochim. Acta 41, 1313–1324.

Brünjes, R., Bichler, A., Hoehn, P., Lange, F.T., Brauch, H.J., Hofmann, T., 2016. Anthropogenic gadolinium as a transient tracer for investigating river bank filtration. Sci. Total Environ. 571, 1432–1440. https://doi.org/10.1016/j.scitotenv.2016.06.105. Available at:.

Burnett, W.C., Bokuniewicz, H., Huettel, M., Moore, W., Taniguchi, M., 2003. Groundwater and pore water inpunts to the coastal zone. Biogeochemistry 66, 3–33.

Censi, P., Cibella, F., Falcone, E.E., Cuttitta, G., Saiano, F., Inguaggiato, C., Latteo, V., 2017. Rare earths and trace elements contents in leaves: A new indicator of the composition of atmospheric dust. Chemosphere 169, 342–350. https://doi.org/10.1016/j.chemosphere.2016.11.085.

Chevis, Da., Johannesson, K.H., Burdige, D.J., Tang, J., Bradley Moran, S., Kelly, R.P., 2015. Submarine groundwater discharge of rare earth elements to a tidally-mixed estuary in Southern Rhode island. Chem. Geol. 397, 128–142. Available at: http://linkinghub.elsevier.com/retrieve/pii/S0009254115000182.

Cirano, M., Lessa, G.C., 2007. Oceanographic characteristics of báia de todas Os santos, Brazil. Rev. Bras. Geofísica 25, 363–387.

CRA, 2004. Diagnóstico Da Concentração De Metais Pesados E Hidrocarbonetos De Petróleo Nos Sedimentos E Biota Da Baía De Todos Os Santos. Volume I -Caracterização Geral Da Baía De Todos Os Santos. Salvador, Bahia, Brazil.

Dominguez, J.M.L., Bittencourt, A.C.S.P., 2009. Geologia. In: De, A.J.B., Hatje, V. (Eds.), Baía De Todos Os Santos: Aspectos Oceanográficos. EDUFBA, Salvador, pp. 25–66.

Elderfield, H., 1988. The oceanic chemistry of the rare-earth elements. Philos. Trans. R. Soc. London. 325, 105–126.

Elderfield, H., Greaves, M.J., 1982. The rare earth elements in seawater. Nature 296, 214–219.

Elderfield, H., Upstill-Goddard, R., Sholkovitz, E.R., 1990. The rare earth elements in rivers, estuaries, and coastal seas and their significance to the composition of ocean waters. Geochim. Cosmochim. Acta 54, 971–991. Available at: http://linkinghub.elsevier.com/retrieve/pii/001670379090432K.

Goldstein, S.J., Jacobsen, S.B., 1988a. Rare earth elements in river waters. Earth Planet. Sci. Lett. 89, 35–47.

Goldstein, S.J., Jacobsen, S.B., 1988b. REE in the Great Whale River estuary, northwest quebec. Earth Planet. Sci. Lett. 88, 241–252.

Greaves, M.J., Statham, P.J., Elderfield, H., 1994. Rare earth element mobilization from marine atmospheric dust into seawater. Mar. Chem. 46, 255–260.

Haley, B.A., Frank, M., Hathorne, E., Pisias, N., 2014. Biogeochemical implications from dissolved rare earth element and Nd isotope distributions in the Gulf of Alaska. Geochim. Cosmochim. Acta 126, 455–474. https://doi.org/10.1016/j.gca.2013.11.012. Available at:.

Hatje, V., de Andrade, J.B., 2009. In: Hatje, V., de Andrade, J.B. (Eds.), Baía De Todos Os Santos: Aspectos Oceanográficos. EDUFBA, Salvador, pp. 302.

Hatje, V., Barros, F., 2012. Overview of the 20th century impact of trace metal contamination in the estuaries of Todos os Santos Bay: past, present and future scenarios. Mar. Pollut. Bull. 64, 2603–2614. Available at: http://www.ncbi.nlm.nih.gov/pubmed/22841387.

Hatje, V., Bícego, M.C., de Carvalho, G.C., de Andrade, J.B., 2009. Contaminação química. In: Hatje, V., de Andrade, J.B. (Eds.), Baía De Todos Os Santos: Aspectos Oceanográficos. EDUFBA, Salvador, pp. 244–297.

Hatje, V., Bruland, K.W., Flegal, A.R., 2014. Determination of rare earth elements after pre-concentration using NOBIAS-chelate PA-1 ® resin : method development and application in the San Francisco Bay plume. Mar. Chem. 160, 34–41.

Hatje, V., Bruland, K.W., Flegal, A.R., 2016. Increases in anthropogenic gadolinium anomalies and rare earth element concentrations in San Francisco Bay over a 20 year record. Environ. Sci. Technol. 50.

Hatje, V., Attisano, K.K., De Souza, M.F.L., Mazzilli, B., De Oliveira, J., Mora de, T.A., Burnett, W.C., 2017. Applications of radon and radium isotopes to determine submarine groundwater discharge and flushing times in Todos os Santos Bay, Brazil. J. Environ. Radioact. 178–179, 136–146. https://doi.org/10.1016/j.jenvrad.2017.08.004. Available at:.

Hoyle, J., Elderfield, H., Gledhill, A., Greaves, M., 1984. The behaviour of the rare earth elements during mixing of river and sea waters. Geochim. Cosmochim. Acta 48, 143–149. Available at: http://linkinghub.elsevier.com/retrieve/pii/0016703784903569.

Joffe, P., Thomsen, H.S., Meusel, M., 1998. Pharmacokinetics of gadodiamide injection in patients with severe renal insufficiency and patients undergoing hemodialysis or continuous ambulatory peritoneal dialysis. Acad. Radiol. 5, 491–502.

Johannesson, K., Cortés, A., Leal, J., 2005. Geochemistry of rare earth elements in groundwaters from a rhyolite aquifer, central méxico. Rare Earth Elements in Groundwater Flow Systems. Springer, Netherlands, pp. 187–222. Available at: http://link.springer.com/chapter/10.1007/1-4020-3234-X_8.

Johannesson, K.H., Palmore, C.D., Fackrell, J., Prouty, N.G., Swarzenski, P.W., Chevis, D.A., Telfeyan, K., White, C.D., Burdige, D.J., 2017. Rare earth element behavior during groundwater – seawater mixing along the Kona Coast of Hawaii. Geochim. Cosmochim. Acta 198, 229–258. https://doi.org/10.1016/j.gca.2016.11.009. Available at:.

Kim, I., Kim, G., 2011. Large fluxes of rare earth elements through submarine groundwater discharge (SGD) from a volcanic island, Jeju, Korea. Mar. Chem. 127, 12–19. Available at: http://linkinghub.elsevier.com/retrieve/pii/S0304420311000831 (Accessed June 26, 2013).

Kim, I., Kim, G., 2014. Submarine groundwater discharge as a main source of rare earth elements in coastal waters. Mar. Chem. 160, 11–17. Available at: http://linkinghub.elsevier.com/retrieve/pii/S0304420314000048.

Kulaksiz, S., Bau, M., 2007. Contrasting behaviour of anthropogenic gadolinium and natural rare earth elements in estuaries and the gadolinium input into the North Sea. Earth Planet. Sci. Lett. 260, 361–371.

Kulaksiz, S., Bau, M., 2011. Rare earth elements in the Rhine River, Germany: first case of anthropogenic lanthanum as a dissolved microcontaminant in the hydrosphere. Environ. Int. 37, 973–979.

Lawrence, M.G., Jupiter, S.D., Kamber, B.S., 2006. Aquatic geochemistry of the rare earth elements and yttrium in the Pioneer River catchment, Australia. Mar. Freshw. Res. 57, 725. Available at: http://www.publish.csiro.au/?paper=MF05229.

Lawrence, M.G., Kamber, B.S., 2006. The behaviour of the rare earth elements during estuarine mixing-revisited. Mar. Chem. 100, 147–161.

Lawrence, M.G., Keller, J., Poussade, Y., 2010. Removal of magnetic resonance imaging

contrast agents through advanced water treatment plants. Water Sci. Technol. 61, 685–692.
Lawrence, M.G., Ort, C., Keller, J., 2009. Detection of anthropogenic gadolinium in treated wastewater in South East Queensland, Australia. Water Res. 43, 3534–3540. Available at: http://www.ncbi.nlm.nih.gov/pubmed/19541341 (Accessed September 9, 2014).
Lessa, G.C., Cirano, M., Genz, F., Tanajura, C.A.S., Silva, R.R., 2009. Oceanografia física. In: Hatje, V., Andrade, J. (Eds.), Baía De Todos Os Santos: Aspectos Oceanográficos. Salvador, pp. 67–120.
Lessa, G.C., Dominguez, J.M.L., Bittencourt, A.C.S.P., Brichta, A., 2001. The tides and tidal circulation of todos os Santos Bay, Northeast Brazil : a general characterization. An. Acad. Bras. Cienc. 73, 245–261.
Lessa, G., Dias, K., 2009. Distribuição espacial das litofácies de fundo da Baía de Todos os Santos. Quat. Environ. Geosci. 01, 84–97.
Magnavita, L.P., Davison, I., Kusznir, N.J., 1994. Rifting, erosion, and uplift history of the Recbncavo-. Tectonics 13, 367–388.
Martin, J., Hogdahl, O., Philippot, J., 1976. Rare earth element supply to the ocean. J. Geophys. 81, 3119–3124.
Merschel, G., Bau, M., Baldewein, L., Dantas, E.L., Walde, D., Bühn, B., 2015. Tracing and tracking wastewater-derived substances in freshwater lakes and reservoirs: Anthropogenic gadolinium and geogenic REEs in Lake Paranoá, Brasilia. Comptes Rendus - Geosci. 347, 284–293.
Merschel, G., Bau, M., Dantas, E.L., 2017. Contrasting impact of organic and inorganic nanoparticles and colloids on the behavior of particle-reactive elements in tropical estuaries: an experimental study. Geochim. Cosmochim. Acta 197, 1–13.
Moffett, J.W., 1990. Microbially mediated cerium oxidation in sea water. Nature 345, 421–423. https://doi.org/10.1038/345421a0.
Moore, W.S., 2010. The effect of submarine groundwater discharge on the ocean. Ann. Rev. Mar. Sci. 2, 58–88.
Morteani, G., Möller, P., Fuganti, A., Paces, T., 2006. Input and fate of anthropogenic estrogens and gadolinium in surface water and sewage plants in the hydrological basin of Prague (Czech Republic). Environ. Geochem. Health 28, 257–264.
Nakajima, T., Sugimoto, R., Tominaga, O., Takeuchi, M., Honda, H., Shoji, J., Taniguchi, M., 2018. Fresh and Recirculated Submarine Groundwater Discharge Evaluated by Geochemical Tracers and a Seepage Meter at Two Sites in the Seto Inland Sea, Japan. Hydrology 5, 61. https://doi.org/10.3390/hydrology5040061.
Nozaki, Y., Lerche, D., Alibo, D.S., Snidvongs, A., 2000. The estuarine geochemistry of rare earth elements and indium in the Chao Phraya River. Thailand. 64, 3983–3994.
Ogata, T., Terakado, Y., 2006. Rare earth element abundances in some seawaters and related river waters from the Osaka Bay area, Japan: significance of anthropogenic Gd. Geochem. J. 40, 463–474.
Osborne, A.H., Haley, B.A., Hathorne, E.C., Plancherel, Y., Frank, M., 2014. Rare earth element distribution in Caribbean seawater: continental inputs versus lateral transport of distinct REE compositions in subsurface water masses. Mar. Chem. 177, 172–183.
Pedreira, R.M.A., Pahnke, K., Böning, P., Hatje, V., 2018. Tracking hospital effluent-derived gadolinium in Atlantic coastal waters off Brazil. Water Res. 145, 62–72. Available at: https://linkinghub.elsevier.com/retrieve/pii/S0043135418306262.
Rabiet, M., Brissaud, F., Seidel, J.L., Pistre, S., 2009. Positive gadolinium anomalies in wastewater treatment plant effluents and aquatic environment in the Hérault watershed (South France). Chemosphere 75, 1057–1064. https://doi.org/10.1016/j.chemosphere.2009.01.036.
Rempfer, J., Stocker, T.F., Joos, F., Dutay, J., Siddall, M., 2011. Modelling Nd-isotopes with a coarse resolution ocean circulation model : sensitivities to model parameters and source / sink distributions. Geochim. Cosmochim. Acta 75, 5927–5950. https://doi.org/10.1016/j.gca.2011.07.044. Available at:.
Rousseau, T.C.C., Sonke, J.E., Chmeleff, J., van Beek, P., Souhaut, M., Boaventura, G., Seyler, P., Jeandel, C., 2015. Rapid neodymium release to marine waters from lithogenic sediments in the Amazon estuary. Nat. Commun. 6, 7592. https://doi.org/10.1038/ncomms8592. Available at:.
Schijf, J., Christy, I.J., 2018. Effect of Mg and Ca on the stability of the MRI contrast agent Gd – DTPA in seawater. Front. Mar. Sci. 5, 1–17.
Schumann-Giampieri, G., Krestin, G., 1991. Phamacokinetics of Gd-DTPA in patients with chronic renal failure. Invest. Radiol. 26, 975–979.
Sholkovitz, E., Elderfield, H., Szymczak, R., Casey, K., 1999. Island weathering: river sources of rare earth elements to the Western Pacific Ocean. Mar. Chem. 68, 39–57. Available at: http://linkinghub.elsevier.com/retrieve/pii/S030442039900064X.
Sholkovitz, E., Boyle, E., Price, N., 1983. The removal of dissolved humic acid during estuarine mixing. Estuar. Coast. Shelf Sci. 16, 431–440. Available at: http://www.sciencedirect.com/science/article/pii/027277148390104X.
Sholkovitz, E.R., 1992. Chemical fractionation of rare earth elements: fractionation between colloidal and solution phases of filtered river water. Earth Planet. Sci. Lett. 114, 77–84.
Sholkovitz, E.R., 1995. The aquatic chemistry of rare earth elements in rivers and estuaries. Aquat. Geochemistry 1, 1–34.
Sholkovitz, E.R., 1993. The geochemistry of rare earth elements in the Amazon River estuary. Geochim. Cosmochim. Acta 57, 2181–2190.
Sholkovitz, E.R., Copland, D., 1981. The coagulation, solubility and adsorption properties of Fe, Mn, Cu, Ni, Cd, Co and humic acids in a river water. Geochim. Cosmochim. Acta 45, 181–189.
Sholkovitz, E.R., Landing, W.M., Lewis, B.L., 1994. Ocean particle chemistry: the fractionation of rare earth elements between suspended particles and seawater. Geochim. Cosmochim. Acta 58, 1567–1579.
Sholkovitz, E., Szymczak, R., 2000. The estuarine chemistry of rare earth elements: comparison of the Amazon, fly, Sepik and the Gulf of Papua systems. Earth Planet. Sci. Lett. 179, 299–309.
Song, H., Shin, W.-J., Ryu, J.-S., Shin, H.S., Chung, H., Lee, K.-S., 2017. Anthropogenic rare earth elements and their spatial distributions in the Han River, South Korea. Chemosphere 172, 155–165. Available at: http://linkinghub.elsevier.com/retrieve/pii/S0045653516318781.
Tachikawa, K., Athias, V., Jeandel, C., 2003. Neodymium budget in the modern ocean and paleo-oceanographic implications. J. Geophys. Res. 108, 3254. https://doi.org/10.1029/1999JC000285. Available at:.
Taniguchi, M., Ishitobi, T., Shimada, J., 2006. Dynamics of submarine groundwater discharge and freshwater-seawater interface. J. Geophys. Res. 111, C01008. https://doi.org/10.1029/2005JC002924.
Taniguchi, M., Burnett, W.C., Dulaiova, H., Siringan, F., Foronda, J., Wattayakorn, G., Rungsupa, S., Kontar, E.A., Ishitobi, T., 2008. Groundwater Discharge as an Important Land-Sea Pathway into Manila Bay, Philippines. J. Coast. Res. 1, 15–24. https://doi.org/10.2112/06-0636.1.
Tepe, N., Romero, M., Bau, M., 2014. High-technology metals as emerging contaminants: strong increase of anthropogenic gadolinium levels in tap water of Berlin, Germany, from 2009 to 2012. Appl. Geochem. 45, 191–197. Available at: http://linkinghub.elsevier.com/retrieve/pii/S0883292714000791 (Accessed August 6, 2014).
Vidal, O., Goffé, G., Arndt, N., 2013. Metals for a low-carbon society. Nat. Geosci. 6, 894–896.
Wang, Z.L., Liu, C.Q., 2008. Geochemistry of rare earth elements in the dissolved, acid-soluble and residual phases in surface waters of the Changjiang Estuary. J. Oceanogr. 64, 407–416.
Zheng, X.Y., Plancherel, Y., Saito, M.A., Scott, P.M., Henderson, G.M., 2016. Rare earth elements (REEs) in the tropical South Atlantic and quantitative deconvolution of their non-conservative behavior. Geochim. Cosmochim. Acta 177, 217–237.
Zhu, Y., Hoshino, M., Yamada, H., Itoh, A., Haraguchi, H., 2004. Gadolinium anomaly in the distributions of rare earth elements observed for coastal seawater and river waters around Nagoya city. Bull. Chem. Soc. Jpn. 77, 1835–1842.

SUPPLEMENTARY MATERIAL

Numerical Procedures

- PAAS normalization

Due to the well-known Oddo-Harkins effect, even–odd variation in the natural abundance of isotopes, the REE patterns in environmental samples are generally normalized to shales (Piper and Bau, 2013). The Post Archean Australian Shale (PAAS) (McLennan, 1989) is widely used as a normalizing agent to evidence the fractionation of REE relative to the source also allowing ease of comparison between studies. Because of these reasons, PAAS has been chosen as the main normalizing agent for the REE abundances in this study.

It is a usual approach to calculate the expected shale-normalized concentration of a REE and compare this theoretical value with the one measured in order to quantify anomalous concentrations in relation to its neighboring REE (De Baar et al., 1985; Moller et al., 2002; Lawrence et al., 2009; Hissler et al., 2015; Tepe and Bau, 2016). There are a few different methods for calculating the theoretical shale-normalized concentration of REE. The third order polynomial fit method is based on modeling the shape of the REE pattern and is advantageous because it allows estimating the normalized concentration without assuming that the element should behave as a light, medium or heavy rare earth, which is especially useful when comparing waters with diverse salinities. In order to avoid possible interferences in the estimated concentration, it is important to exclude known anomalous REE, such as Ce and Eu, from the calculation (Lawrence and Kamber, 2006; Kulaksız and Bau, 2007; Lawrence et al., 2009). As Gd is an ambiguous element, sometimes being considered MREE and others HREE, its anomaly (Gd/Gd*) was calculated using the third order polynomial fit method with nine elements (Pr, Nd, Sm, Tb, Dy, Ho, Er, Tm, Yb) (Moller

et al., 2002). In the case of Ce, anomalies were quantified using the following equation (McLennan, 1989):

$Ce/Ce^* = Ce_{SN} / (La_{SN} \times Pr_{SN})^{0.5}$

Where $_{SN}$ stands for shale-normalized value of the REE concentration, and * denotes the interpolated concentration.

For both Ce and Gd, if the resulting ratio (Ce/Ce* or Gd/Gd*) equals 1, it means there is no anomaly, once the observed value is equal to the predicted. However, if the ratio is above 1, it indicates an excess of the element, i.e. positive anomaly, while ratios below a unit indicate a relative depletion of the element, i.e. negative anomalies.

Table S1. Concentrations (pmol kg^{-1}) and recoveries of REEs obtained for SAFe (n = 4) and GSC (n = 4) GEOTRACES reference samples*.

	GSC			SAFe		
	This work	Hatje et al., 2016	Accuracy (%)	This work	Behrens et al., 2016	Accuracy (%)
La	18.0 ± 0.5	16.4 ± 0.48	109	65 ± 3	65.3 ± 2.05	100
Ce	15.1 ± 0.2	14.0 ± 0.11	108	3.7 ± 0.2	3.8 ± 1.35	97
Pr	3.4 ± 0.1	3.06 ± 0.03	112	10.6 ± 0.2	10.3 ± 0.35	103
Nd	14.1 ± 0.4	13.8 ± 0.13	102	46.8 ± 1.1	45.9 ± 1.45	102
Sm	2.7 ± 0.1	3,16 ± 0.08	85	9.1 ± 0.2	9.0 ± 0.20	101
Eu	0.67 ± 0.02	0,62 ± 0.005	108	2.45 ± 0.04	2.4 ± 0.05	102
Gd	3.9 ± 0.2	3.32 ± 0.02	117	13.1 ± 0.3	12.7 ± 0.85	103
Tb	0.58 ± 0.02	0.54 ± 0.004	108	2.04 ± 0.03	2.0 ± 0.05	102
Dy	4.23 ± 0.04	3.76 ± 0.01	113	15.6 ± 0.6	14.7 ± 0.25	106
Ho	1.11 ± 0.03	1.11 ± 0.01	100	3.8 ± 0.1	3.7 ± 0.05	102
Er	3.49 ± 0.05	3.39 ± 0.02	103	12.9 ± 0.7	12.7 ± 0.15	101
Tm	0.52 ± 0.02	0.46 ± 0.005	114	2.0 ± 0.1	1.9 ± 0.05	106
Yb	3.1 ± 0.2	2.85 ± 0.02	110	14.1 ± 0.8	13.4 ± 0.25	105
Lu	0.56 ± 0.02	0.46 ± 0.003	122	2.6 ± 0.1	2.4 ± 0.15	108

*GEOTRACES reference samples: SAFE (North Pacific 3000m) and GSC (Santa Barbara Costal water).

Table S2. Parameters for surface water stations along the continuum between Paraguaçu Estuary through Todos os Santos Bay to the continental shelf of Salvador, Bahia, Brazil.

Station	Latitude	Longitude	T (ºC)	Salinity	pH	Turbidity (NTU)	DO (mg L^{-1})	Ce/Ce*	Gd/Gd*	ΣREE	HREE/LREE	ΣLREE	ΣHREE
P0								0.59		540		484	56
P1	12°42'38.5" S	38°56'08.1" W	25.5	1.35	8.18	9.8	8.2	0.63	1.6	707	0.10	639	68
P2	12°43'10.0" S	38°55'57.9" W	25.7	5.29	7.74	5.1	8.9	0.69	1.4	348	0.16	299	49
P3	12°43'19.8" S	38°55'49.4" W	26.1	9.68	8.25	2.4	9.3	0.64	1.5	264	0.17	225	40
P4	12°43'51.4" S	38°55'08.5" W	26.3	15.15	8.03	1.8	8.9	0.56	1.5	256	0.22	212	44
P5	12°44'23.8" S	38°54'39.0" W	26.3	20.55	7.98	0.5	7.9	0.46	1.5	242	0.23	198	44
P6	12°45'05.0" S	38°53'54.7" W	26.2	24.78	7.95	1.4	7.2	0.5	1.2	264	0.24	213	51
P7	12°47'31.4" S	38°51'35.9" W	26.3	27.26	7.79	<0.3	7.0	0.49	1.3	303	0.21	250	53
P8	12°49'24.5" S	38°51'32.0" W	26.0	27.76	7.55	1.7	6.9	0.47	1.1	286	0.21	233	53
P9	12°50'45.6" S	38°49'44.3" W	26.1	28.87	7.85	1.6	6.8	0.43	1.2	268	0.24	214	53
B1	13°01'22.7" S	38°34'24.3" W	25.6	33.40	8.00	<0.3	7.3	0.79	1.4	256	0.12	228	28
B2	12°57'11.9" S	38°33'25.9" W	25.9	32.93	8.06	<0.3	6.9	0.56	1.3	159	0.21	132	27
B3	12°53'39.2" S	38°34'52.8" W	25.7	32.55	8.16	<0.3	7.0	0.51	1.1	172	0.21	139	33
B4	12°47'19.0" S	38°29'39.5" W	26.7	32.52	8.21	<0.3	7.4	0.63	1.2	106	0.29	81	25
B5	12°48'23.6" S	38°32'55.3" W	26.3	32.06	8.30	<0.3	7.1	0.42	1.3	148	0.28	113	35

B6	12°50'03.0" S	38°37'34.4" W	26.2	30.92	8.15	<0.3	7.2	0.35	1.2	201	0.24	159	42
B7	12°49'21.4" S	38°38'51.4" W	26.5	30.42	8.31	<0.3	7.4	0.38	1.1	213	0.26	166	48
B8	12°45'32.1" S	38°40'24.9" W	26.5	29.73	8.36	<0.3	7.4	0.39	1.1	233	0.25	180	53
B9	12°38'55.2" S	38°40'20.5" W	27.5	28.63	8.27	2.1	7.1	0.38	1.1	264	0.25	200	64
B10	12°43'00.2" S	38°41'42.1" W	27.3	29.69	8.34	2.1	7.1	0.33	1.2	231	0.29	172	59
B11	12°47'21.3" S	38°43'07.6" W	26.6	28.92	8.42	0.9	7.6	0.4	1.1	246	0.23	192	53
B12	12°50'03.3" S	38°47'22.4" W	26.4	29.33	8.36	1.2	7.3	0.35	1.2	235	0.27	183	52
B13	12°53'11.7" S	38°42'22.4" W	27.0	30.89	8.40	0.8	7.3	0.39	1.3	216	0.24	170	47

DO = dissolved oxygen; $Ce/Ce^* = Ce_{SN} / (La_{SN} \times Pr_{SN})^{0.5}$; $HREE/LREE = Yb_{SN}/Nd_{SN}$; ΣREE (La, Ce, Pr, Nd, Sm, Eu, Gd, Tb, Dy, Ho, Er, Tm, Yb and Lu); ΣHREE (Tb, Dy, Ho, Er, Tm, Yb and Lu); ΣLREE(La, Ce, Pr, Nd, Sm, Eu and Gd).

Table S3. Parameters in surface waters collected hourly during a 12h period at station TS (12°55'14.4"S, 38°30'37.9"W, Todos os Santos Bay, Bahia, Brazil).

Sample	Local time	T (ºC)	Salinity	pH	Turbidity (NTU)	DO (mg L^{-1})	Ce/Ce*	Gd/Gd*	ΣREE	ΣLREE	ΣHREE	HREE/LREE
T1	9:00	24.6	33.53	7.67	9.9	7.9	0.97	1.3	658	614	44	0.06
T2	10:00	24.9	33.41	8.60	14.8	7.6	0.83	1.6	262	235	27	0.11
T3	11:00	25.2	33.31	8.64	11.9	7.6	0.80	1.5	203	179	24	0.13
T4	12:00	25.6	33.34	8.65	4.2	7.5	0.77	1.6	177	154	23	0.16
T5	13:00	25.9	33.28	8.72	2.1	8.6	0.86	1.5	163	141	23	0.17
T6	14:00	26.0	33.26	8.72	0.6	8.3	0.76	2.0	152	132	21	0.16
T7	15:00	26.0	33.30	8.72	0.5	8.3	0.64	2.3	70	54	16.1	0.36
T8	16:00	25.7	33.45	8.71	<0.3	7.9	0.62	1.8	72	55	16.6	0.34
T9	17:00	25.5	33.60	8.71	<0.3	7.8	0.57	1.4	75	59	16.6	0.29
T10	18:00	25.9	33.52	8.66	<0.3	7.9	0.59	1.4	110	89	21	0.19
T11	19:00	25.8	33.40	8.73	<0.3	8.2	0.55	2.3	79	63	16.1	0.25
T12	20:00	25.5	33.45	8.72	<0.3	8.2	0.59	2.1	75	59	16.2	0.30
T13	21:00	25.3	33.48	8.70	0.3	7.4	0.65	1.8	74	58	15.9	0.28

$Ce/Ce^* = Ce_{SN} / (La_{SN} \times Pr_{SN})^{0.5}$; $HREE/LREE = Yb_{SN}/Nd_{SN}$; ΣREE (La, Ce, Pr, Nd, Sm, Eu, Gd, Tb, Dy, Ho, Er, Tm, Yb and Lu); ΣHREE (Tb, Dy, Ho, Er, Tm, Yb and Lu); ΣLREE(La, Ce, Pr, Nd, Sm, Eu and Gd).

Table S4. Percentage of removal for each rare earth element in Paraguaçu Estuary samples compared to P1 (S=1.35).

	La	Ce	Pr	Nd	Sm	Eu	Gd	Tb	Dy	Ho	Er	Tm	Yb	Lu	Salinity
P1	0%	0%	0%	0%	0%	0%	0%	0%	0%	0%	0%	0%	0%	0%	1.35
P2	57%	52%	55%	53%	50%	49%	46%	40%	30%	37%	23%	31%	23%	32%	5.29
P3	62%	67%	71%	64%	66%	62%	59%	53%	44%	46%	38%	42%	40%	42%	9.68
P4	63%	70%	69%	68%	66%	64%	56%	51%	41%	38%	29%	32%	30%	33%	15.15
P5	61%	76%	72%	70%	68%	64%	59%	53%	41%	36%	30%	30%	29%	32%	20.55
P6	59%	72%	70%	68%	67%	63%	60%	47%	30%	31%	15%	24%	21%	30%	24.78
P7	50%	68%	66%	61%	64%	57%	57%	46%	25%	27%	14%	21%	19%	26%	27.26
P8	52%	71%	69%	63%	66%	59%	60%	47%	25%	25%	12%	22%	21%	27%	27.76
P9	56%	75%	69%	66%	66%	61%	60%	45%	27%	24%	9%	18%	18%	27%	28.87

The percentage of removal (%REE_{Px}) was calculated as indicated below:

$$\%REE_{Px} = \left(1 - \frac{[REE_{Px}]}{[REE_{P1}]}\right) \times 100\%$$

Where REE_{Px}= the concentration of REE at the station x of the estuary; and REE_{P1}= the concentration of REE at the station P1 of the estuary.

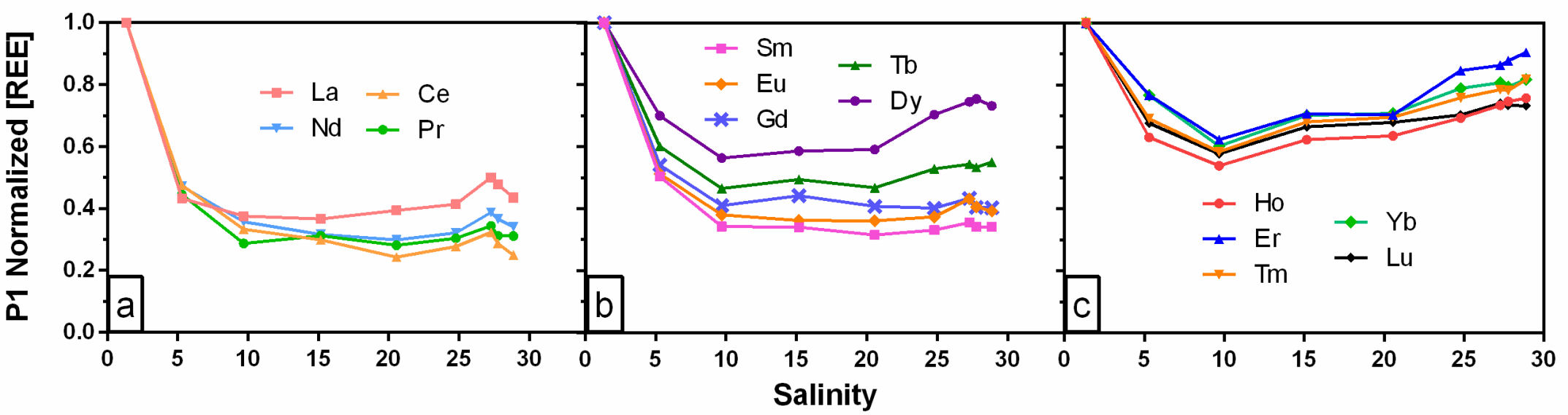

Figure S1 – Concentrations of light (a), medium (b), and heavy (c) REE normalized to the REE concentrations of the freshwater endmember (station P1) versus salinity.

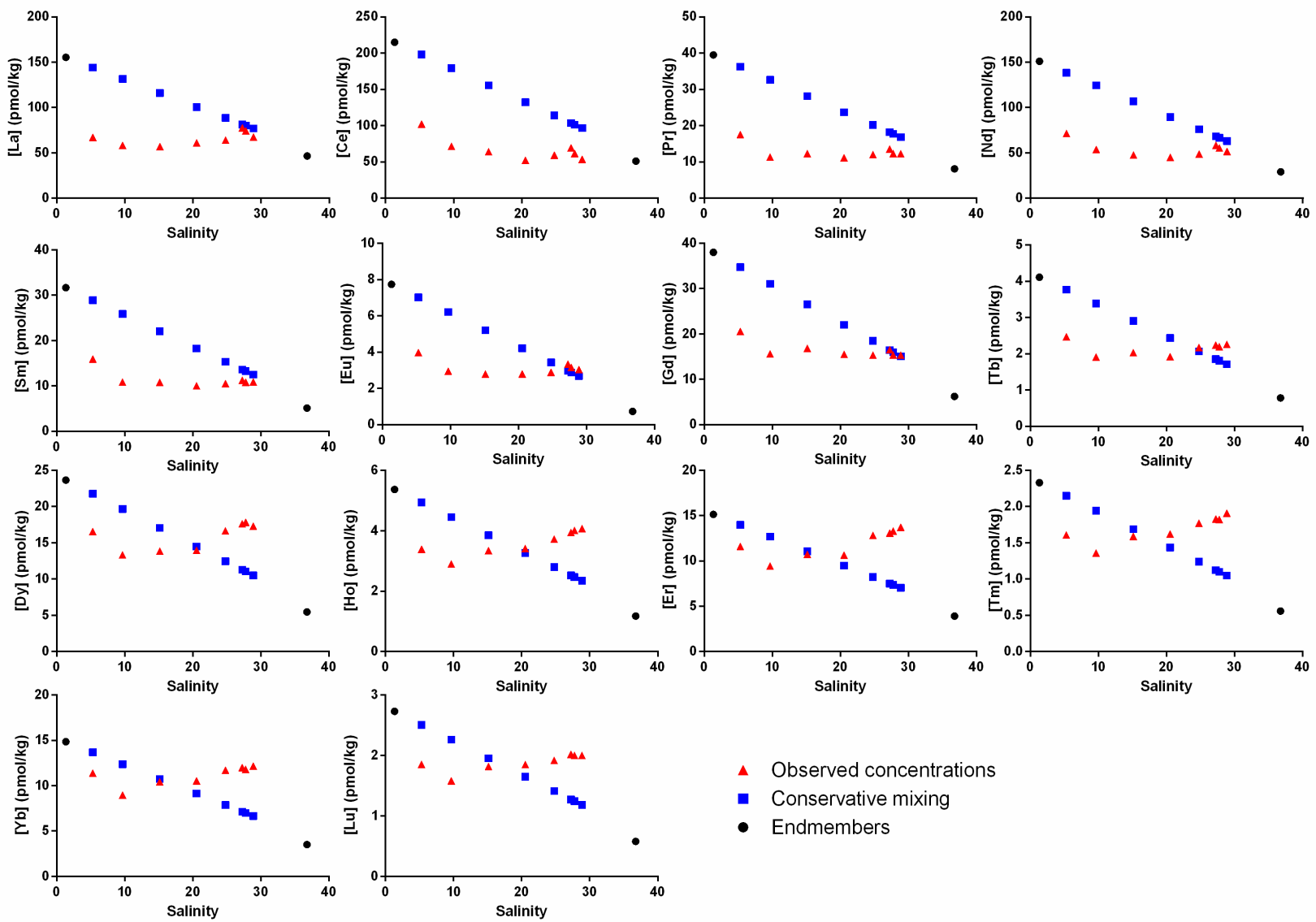

Figure S2 – Dissolved REE concentrations (red triangles) observed through the salinity gradient in the Paraguaçu estuary. Theoretical REE concentrations (blue squares) obtained for conservative mixing and river (P1) and marine (E02S; Pedreira et al. 2018) endmembers (black dots) are also plotted.

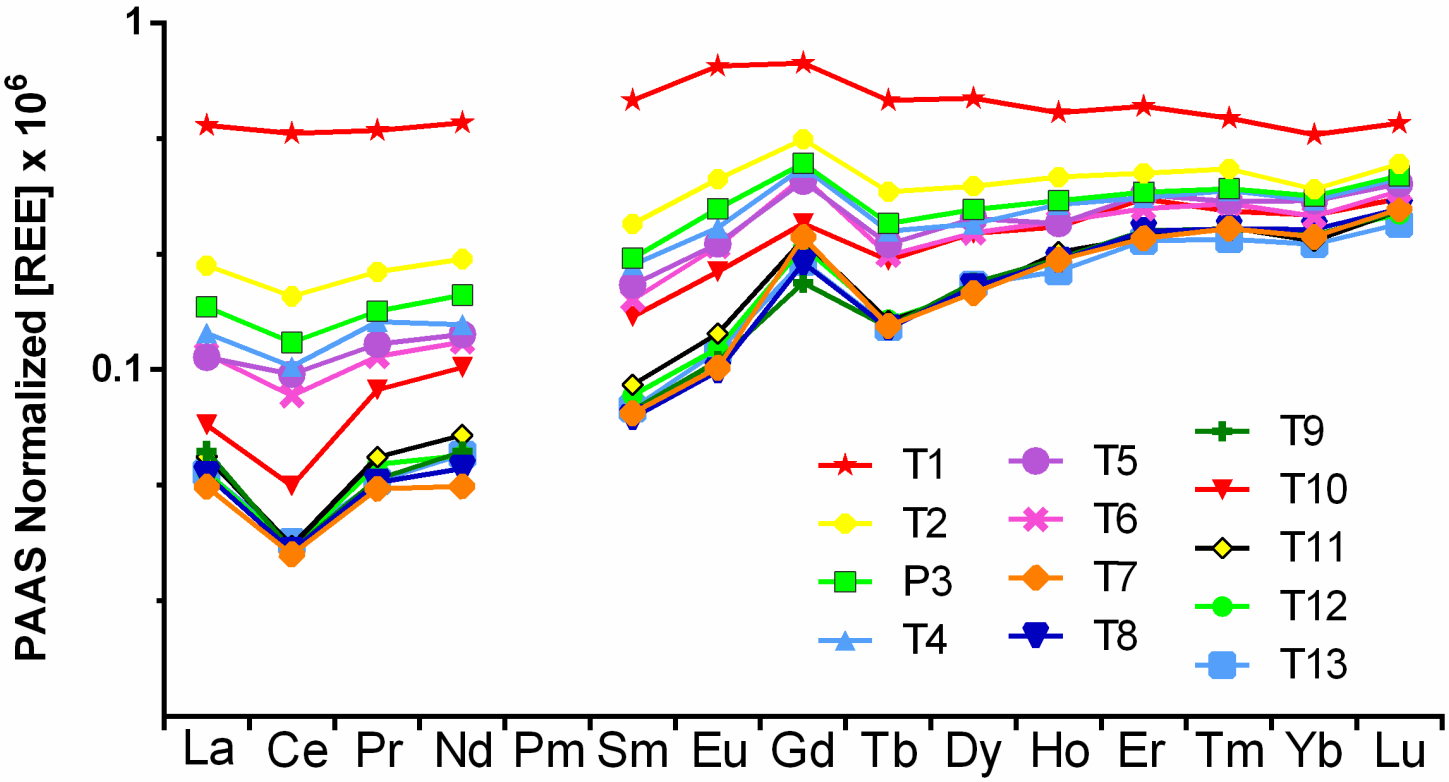

Figure S3 – PAAS-normalized REE patterns in surface water samples collected hourly during a 12h period at station TS (12°55'14.4"S, 38°30'37.9"W, Todos os Santos Bay, Bahia, Brazil). The tide was low at T1 and high at T7, reaching low again about 30 min after T13.

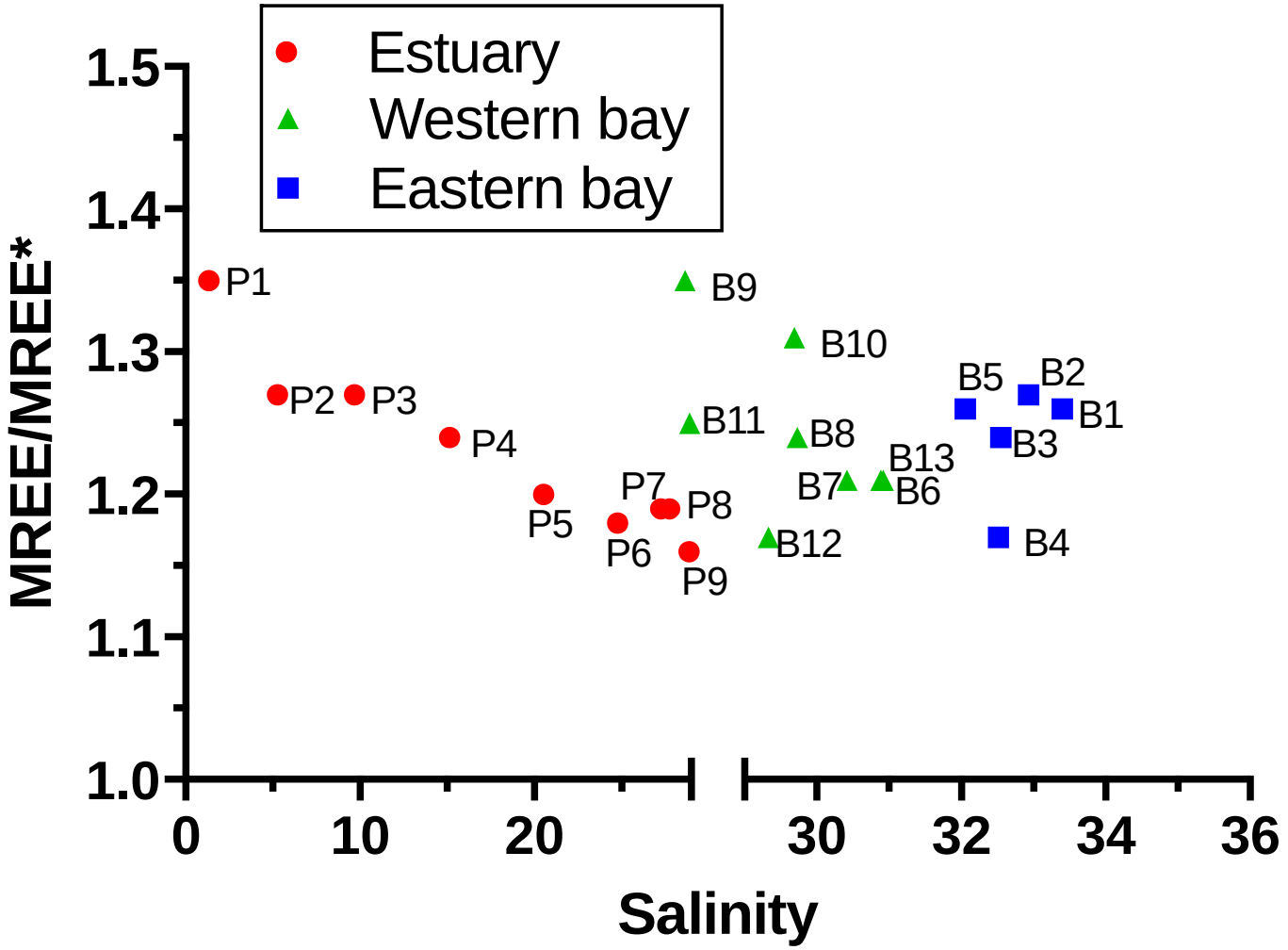

Figure S4 –MREE/MREE* through the salinity gradient across the Paraguaçu estuary and Todos os Santos Bay. where MREE/MREE* is the ratio between the average of Gd_{SN} and Dy_{SN} and the average of Yb_{SN} and Nd_{SN}.

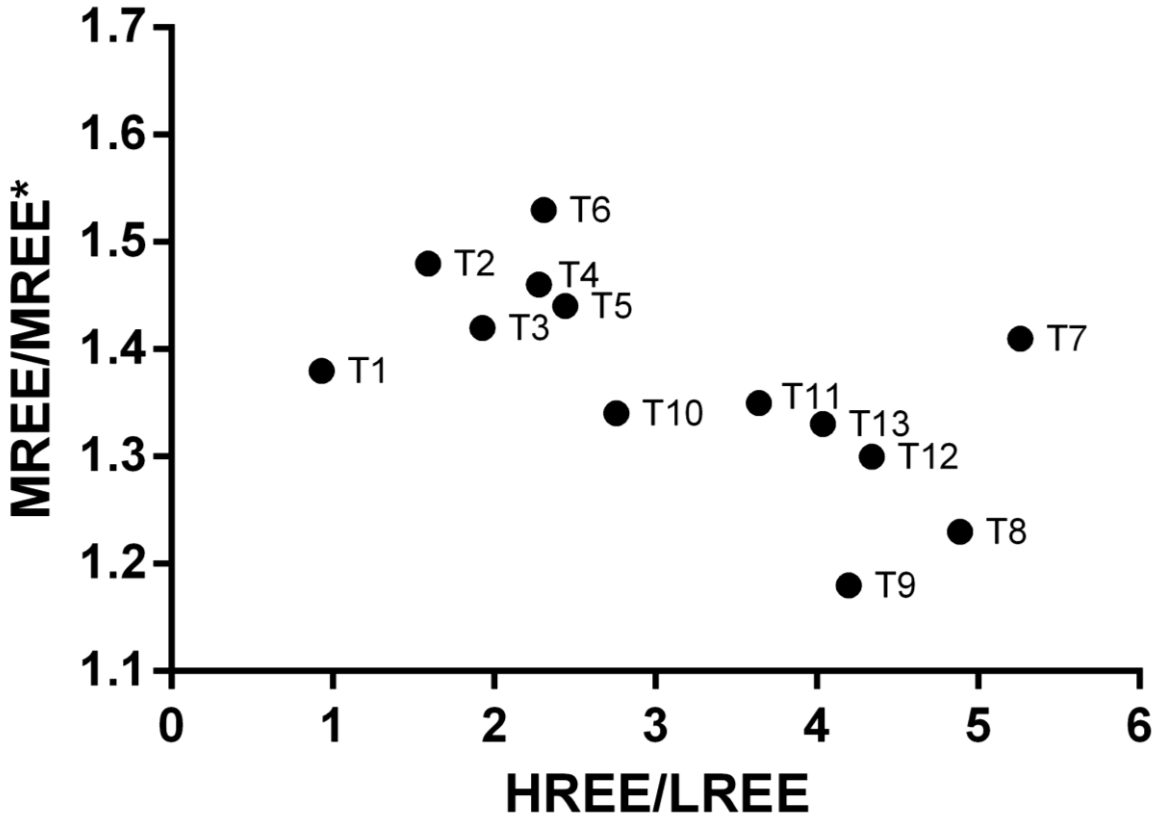

Figure S5 – HREE/LREE versus MREE/MREE* for the temporal series. Where HREE/LREE is represented by Yb_{SN}/Nd_{SN} and MREE/MREE* is the ratio between the average of Gd_{SN} and Dy_{SN} and the average of Yb_{SN} and Nd_{SN}. The tide was low at T1 and high at T7, reaching low again about 30min after T13. Between each sampling there is 1h difference, completing a 12h cycle.

REFERENCES

De Baar H. J. W., Brewer P. G. and Bacon M. P. (1985) Anomalies in rare earth distributions in seawater: Gd and Tb. *Geochim. Cosmochim. Acta* **49**, 1961–1969. Available at: http://linkinghub.elsevier.com/retrieve/pii/0016703785900900.

Hissler C., Hostache R., Franc J., Pfister L. and Stille P. (2015) Anthropogenic rare earth element fluxes into floodplains: Coupling between geochemical monitoring and hydrodynamic sediment transport modelling. *Comptes Rendus Geosci.* **347**, 294–303.

Kulaksiz S. and Bau M. (2007) Contrasting behaviour of anthropogenic gadolinium and natural rare earth elements in estuaries and the gadolinium input into the North Sea. *Earth Planet. Sci. Lett.* **260**, 361–371.

Lawrence M. G. and Kamber B. S. (2006) The behaviour of the rare earth elements during estuarine mixing-revisited. *Mar. Chem.* **100**, 147–161.

Lawrence M. G., Ort C. and Keller J. (2009) Detection of anthropogenic gadolinium in treated wastewater in South East Queensland, Australia. *Water Res.* **43**, 3534–40. Available at: http://www.ncbi.nlm.nih.gov/pubmed/19541341 [Accessed September 9, 2014].

McLennan S. M. (1989) Rare earth elements in sedimentary rocks: influence of provenance and sedimentary processes. In *Geochemistry and Mineralogy of Rare Earth Elements. Reviews in Mineralogy* (eds. B. Lipin and G. McKay). pp. 169–200.

Moller P., Paces T., Dulski P. and Morteani G. (2002) Anthropogenic Gd in Surface Water, Drainage System and the Water Supply of the City of Prague, Czech republic. *Env. Sci Technol* **36**, 2387–2394.

Pedreira R. M. A., Pahnke K., Böning P. and Hatje V. (2018) Tracking hospital effluent-derived gadolinium in Atlantic coastal waters off Brazil. *Water Res.* **145**, 62–72. Available at: https://linkinghub.elsevier.com/retrieve/pii/S0043135418306262.

Piper D. Z. and Bau M. (2013) Normalized Rare Earth Elements in Water , Sediments , and Wine : Identifying Sources and Environmental Redox Conditions. *Am. J. Anal. Chem.* **2013**, 69–83.

Tepe N. and Bau M. (2016) Behavior of rare earth elements and yttrium during simulation of arctic estuarine mixing between glacial-fed river waters and seawater and the impact of inorganic (nano-) particles. *Chem. Geol.* **438**, 134–145. Available at: http://dx.doi.org/10.1016/j.chemgeo.2016.06.001.

Capítulo 3:

Neodymium isotopes across Antarctic and South and Central western Atlantic

Neodymium isotopes across Antarctic and South and Central western Atlantic

INTRODUCTION

The Rare earth elements (REE) are, according to the classification of the International Union of Pure and Applied Chemistry (IUPAC), a group of 17 chemical elements, of which 15 belong to the lanthanide group in the periodic table. Due to their characteristics and fractionation capacity, REE become good geochemical tracers of natural and even anthropogenic processes, allowing inferences on complex processes that other tracer elements do not (e.g. Hatje et al., 2014). Examples are: the composition of source areas (e.g. Mercadier et al., 2011; Shynu et al., 2013); particle adsorption and desorption/dissolution (e.g. Chaillou et al., 2006; Haley et al., 2004; Lacan & Jeandel, 2005; Rousseau et al., 2015); redox conditions (e.g. Liu et al., 2019); ocean circulation patterns and water masses (e.g. Garcia-Solsona et al., 2014; Molina-Kescher et al., 2014; Sotto Alibo & Nozaki, 2004; Wu et al., 2022; Zheng et al., 2016); reconstruction of paleo conditions (e.g. Copard et al., 2012; Hu et al., 2016; Liu et al., 2019); as well as, identifying contaminations from mining, industrial, and domestic/hospital activities (e.g. Bau & Dulski, 1996; Hatje et al., 2014, 2016; Johannesson et al., 2017; Kulaksiz & Bau, 2013; Mirlean et al., 2020; Romero et al., 2010; Shynu et al., 2013; Sousa et al., 2022).

Among the REE, neodymium (Nd) is particularly interesting, once its isotopic composition, expressed as εNd[4], has been applied for decades as a tracer for water circulation,

[4] εNd is defined by equation:

$$\varepsilon\mathrm{Nd} = \left[\frac{\left({}^{143}\mathrm{Nd}/{}^{144}\mathrm{Nd}\right)_{Amostra}}{\left({}^{143}\mathrm{Nd}/{}^{144}\mathrm{Nd}\right)_{CHUR}} - 1\right] \times 10000$$

where $({}^{143}\mathrm{Nd}/{}^{144}\mathrm{Nd})_{CHUR}$=0.512638 and refers to the Chondritic Uniform Reservoir as an estimate of the bulk Earth (Wasserburg et al., 1981).

provenance, and past and present mixing (e.g. Behrens et al., 2018; Frank, 2002; Fröllje et al., 2016; Grasse et al., 2017; Grenier et al., 2013; Hu et al., 2016; Jeandel, 1993; Lambelet et al., 2016; Piepgras & Wasserburg, 1987; Wu et al., 2022). The radiogenic ^{143}Nd is produced by decay of ^{147}Sm ($t_{1/2}$=1.06 10^{11} yr). During the melting in Earth's mantle, fractionation of parent and daughter isotopes occurs, resulting in significant radiogenic isotope differences between rocks of different age and lithology, which results in variations in the ratio of $^{143}Nd/^{144}Nd$ in natural rocks. The dissolved Nd present in seawater is originated from lithogenic sources and the εNd of seawater varies systematically as a result of the processes (e.g. inputs from terrestrial runoff, submarine groundwater, Boundary Exchange) occurring through the circulation path as the water interacts with sources with different isotopic signatures (e.g. Fröllje et al., 2016; Johannesson et al., 2017; Lacan & Jeandel, 2001, 2005). These facts are key for the applications of εNd in water masses studies (Lacan & Jeandel, 2001; Rempfer et al., 2011).

The residence time estimated for Nd in the ocean is shorter than the Global Overturning Circulation, which implies that though deep currents transport Nd, they don't homogenize it (Arsouze et al., 2009; Lacan et al., 2012; Rempfer et al., 2011; Siddall et al., 2008; Tachikawa et al., 1999, 2003). In fact, there are registered observations of εNd values in seawater ranging from -26.6 in the Baffin Bay to +4.3 in the Panama basin (Grasse et al., 2017; Lacan et al., 2012). Also, in deep open ocean, away from the margins, the mixing of water masses is the main cause for changes in εNd, allowing the Nd isotopic composition to be applied as a quasi-conservative circulation tracer (Lambelet et al., 2016; Tachikawa et al., 2017; Wu et al., 2022). At the open ocean, εNd presents relative homogeneity in the water column, but gradual increase from the deep North Atlantic to the deep North Pacific Waters (Lacan et al., 2012). Meanwhile, the dissolved Nd concentrations of major ocean basins present a nutrient-

like profile, which is relatively depleted at surface and enriched in deep waters, presenting an increase in concentrations with the Global Overturning Circulation (Lacan et al., 2012).

The decoupling of Nd concentrations and εNd is named “Nd Paradox”, and it implied that there is a source of Nd that is not being considered in its biogeochemical cycle (Johannesson & Burdige, 2007; Lacan & Jeandel, 2001, 2005; Tachikawa et al., 2003; R. Wang et al., 2022).

One proposed solution for this paradox is the Boundary Exchange (BE) (Gu et al., 2019; Lacan & Jeandel, 2001; Rempfer et al., 2011; Siddall et al., 2008; Tachikawa et al., 2003). This process involves an exchange of elements in the sediment/rock and seawater interface, causing a significant variation in isotopic composition, followed by local removal of the element, maintaining the concentration approximately invariable. The BE is supposed to be relevant at continental margins and could include a series of processes such as submarine groundwater inputs, benthic flux, and dissolution of sediments (Jeandel, 2016). Some studies estimate that the BE could be the main source of Nd to the ocean (Arsouze et al., 2009; Rempfer et al., 2011; Tachikawa et al., 2003), responsible for supplying around 90% of Nd, compared to 6% and 4% of fluvial and atmospheric inputs, respectively (Rempfer et al., 2011). More recent works highlight that the impacts of BE are dependent of factors such as mineralogical composition and the isotopic difference between sediment/rock and seawater (Adebayo et al., 2022; Huang et al., 2023). However, the BE flux is not well constrained yet but it is needed to understand the ocean Nd budget and improve its application as tracer of ocean circulation.

The Atlantic is an important region to study ocean circulation due to the formation of the North Atlantic Deep Water (NADW) and, in the south, its positioning between the northward flowing Antarctic Intermediate Water (AAIW) and Antarctic Bottom Water (AABW) from the Antarctic (Talley, 2013). Due to diverse Nd sources (e.g., river input, oceanic volcanism, marginal sediments, atmospheric input) and unique circulation patterns, the South Atlantic is

crucial for studying modern and paleoceanographic global overturning circulation, as well as the Nd biogeochemical cycle and its influencing factors. The South Atlantic is much less studied than the North, resulting in an imbalance in available εNd data (Lacan et al., 2012; Tachikawa et al., 2017). The shortage of seawater εNd values limits its use as a tracer. To address this, our work presents dissolved Nd isotopic ratios from the Northwest Atlantic to the Antarctic Peninsula (from 15°N to 65°S), covering the exportation region of AABW from the Antarctic, the mixing zone of the main water masses in the Atlantic sector of the global overturning circulation, as well as 3 continent-ocean transects at the western Atlantic Ocean.

STUDY AREA

- Oceanographic setting

Antarctic

This study encompasses a large area, going from western North Atlantic to Antarctic waters (fig. 1). In the Antarctic the sampled areas include the Powell Basin and the Gerlache and the Bransfield Straits in the Northern Antarctic Peninsula (fig. 1). They are characterized by strong alongshore hydrographic gradients caused by the input of cold waters from the Weddell Sea continental shelf (tip of Antarctic Peninsula), warm modified Circumpolar Deep Water and surface waters, predominantly coming from the Bellingshausen Sea through southwestern passages (Damini et al., 2022; Dotto et al., 2016; Sangrà et al., 2017; Zhou et al., 2002). The Bransfield Strait shows rapid and dynamic circulation and can be divided in western (~1000m deep), central (~2000m deep), and eastern (~2500m deep) basins (e.g. Monteiro et al., 2023). Meanwhile, the Gerlache Strait has a deep basin with limited connection (surface to 350m) with the Bellingshausen Sea and a 700m deep sill connecting to the Western Basin of the Bransfield Strait (Parra et al., 2020). The topographic restrictions in the studied areas cause changes in ocean circulation, allowing the occurrence of upwelling

of modified CDW in the western basin of Bransfield and the Gerlache Straits (Parra et al., 2020; Venables et al., 2017). The interaction of ocean circulation and topography forms mesoscale eddies in the eastern Bransfield Basin (Damini et al., 2023; X. Wang et al., 2022).

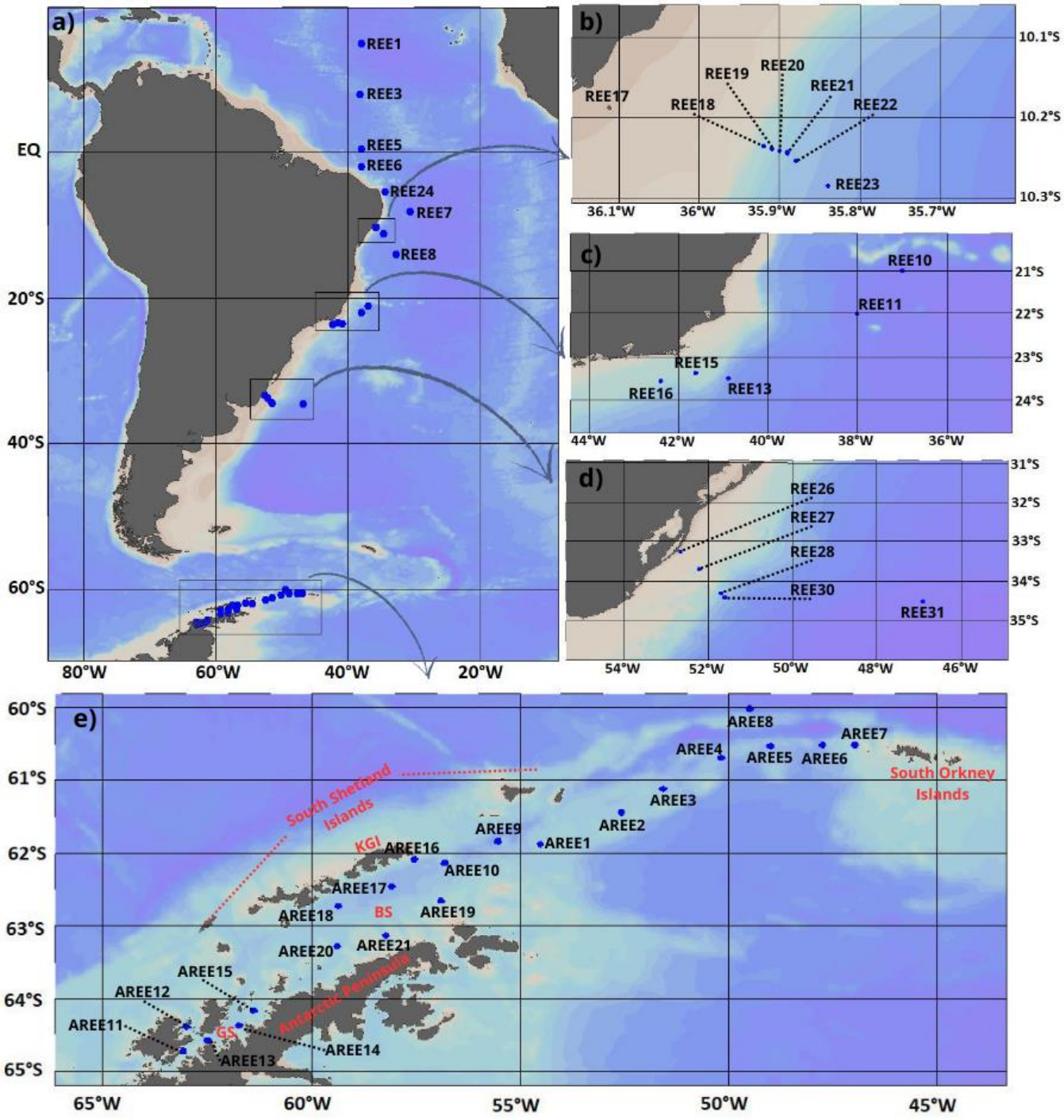

Figure 1 - Sampling stations (blue dots) across the South and Central Western Atlantic and the Antarctic Ocean. a) Shows Atlantic stations including: b)stations at the coast of Alagoas

State, c) stations at the coast of Rio de Janeiro State, and d) stations at the coast between Brasil and Uruguay. e) shows stations at the Antarctic region, where some features are identified in red: South Shetland Islands; South Orkney Islands; KGI: King George Island; BS: Bransfield Strait; and GS: Gerlache Strait.

At upper layers, the area is influenced by local surface waters and modified Circumpolar Deep Water (Sangrà et al., 2017; Zhou et al., 2002). At intermediate layers, the western basin of Bransfield Strait is characterized by the modified Circumpolar Deep Water, while central and eastern basis are mainly composed by Dense Shelf Water (Barlett et al., 2018; Damini et al., 2022; Dotto et al., 2016; X. Wang et al., 2022). The deep water of the Strait is mainly formed by High-salinity Shelf Water (HSSW) and Low-salinity Shelf Water (LSSW), allowing its use as a proxy for thermohaline variations of a key source component of AABW (Dotto et al., 2016; Kerr et al., 2018). Studies have pointed that these deep waters are experiencing long-term freshening and lightening, even though they present a high degree of interannual variability in thermohaline proprieties, likely caused by different proportions of source water mass mixing each year (Damini et al., 2022; Dotto et al., 2016; Hellmer et al., 2011; Schmidtko et al., 2014).

Atlantic

At surface, many currents influence the composition of seawater in the sampled areas. From tropical North Atlantic (15°N) to the equator, samples were collected away from the margins and under the influence of equatorial surface currents and countercurrents. Considering its position, the fluvial input from the Amazon and Orinoco Rivers, as well as the influence of eolian transported aerosols from the Saharan desert, might also be relevant to the samples collect in this area.

From equator southwards, samples were collected closer to the continental margin and influenced by the northward North Brazil current and the southward Brazil current flowing along the South American continental shelf. Both currents are formed around 17°S in July and 13°S in November by the bifurcation of the South Equatorial current coming from the eastern side of the South Atlantic. Along the Brazilian coast, notable geographic features include: i) major rivers such as São Francisco (10°S; discharge: 1200 $m^3 s^{-1}$; Paiva & Schettini, 2021) and Doce Rivers (19.6°S; discharge: 985 m^3/s; Lyra & Rigo, 2019); ii) the Vitória-Trindade Ridge (20°S), a west-east line of submerged magmatic (alkaline basalt) mounts and banks along the Vitória-Trindade Fracture Zone (Rego et al., 2021), and iii) the Cabo Frio upwelling system (23°S), driven by north-northeast winds and coastal geomorphology, promoting the seasonal upwelling of the South Atlantic Central Water (SACW), which intensifies during summer (Valentin, 2001). The La Plata River (35°S; discharge: 22000 $m^3 s^{-1}$; Stewart et al., 2022) also significantly influences the area with its large freshwater input.

The studied region contains the main Atlantic Meridional Overturning Circulation (AMOC) water masses, including the southward flowing North Atlantic Deep Water and the northward flowing Antarctic Intermediate Water (AAIW) and Antarctic Bottom Water (AABW). The vertical profiles of the sampling stations contain different water masses that vary with depth and latitude. The Tropical Water (TW) is observed at the top layers (down to 100m) of the stations down to 23°S. The North Atlantic Central Water (NACW) or the South Atlantic Central Water (SACW) are observed at intermediate depths (~200 to ~600m) at each hemisphere. The SACW is formed by varieties of Subtropical Mode Water, mainly from the central and eastern regions of South Atlantic and from the boundaries of the South Atlantic Subtropical Front (Souza et al., 2018). Underneath SACW (~600 to over 1200m), flows the northward Antarctic Intermediate Water (AAIW), formed by the denser flow entering the Atlantic through

the Drake Passage (Talley et al., 2011). Below that, at ~1200 to 3500m flowing southward there is the North Atlantic Deep Water (NADW), formed at the North Atlantic and the convective sources are the Denmark Strait Overflow Water (DSOW), the Iceland Scotland Overflow Water (ISOW), the Labrador Sea Water (LSW), and the Mediterranean Water (MW) (Ferreira & Kerr, 2017; Talley et al., 2011). The NADW is not the exclusive water mass flowing at this depth range. The Circumpolar Deep Water enters the South Atlantic from the Southern Ocean and flows northward at around 2500m deep (Talley et al., 2011). The Antarctic Bottom Water (AABW), formed by deep convection at the continental slope at the Weddel Sea, is observed at the abyssal layer, still its northward flow and modification is constrained by the bottom topography (Talley et al., 2011).

MATERIAL AND METHODS

- ### Sampling Campaign

Forty-five full depth (up to 6000m deep) water profiles (Figure 1; Table S1) were sampled between November 2017 and March 2020 distributed between 15N to 65S in the Atlantic and Southern Oceans during the PIRATA XVII/GEOTRACES GApr10 cruise and PIRATA XVIII (on board of the R/V Vital de Oliveira during the austral summer), SAMBAR 2019 (on board of the R/V Alpha Crucis during austral winter), and PROVOCCAR/GEOTRACES GApr15 (on board of the R/V Almirante Maximiano during austral summer). Seawater samples were collected using Niskin bottles mounted on a 24-bottle CTD-equipped rosette. Samples were filtered in-line with a trace-metal clean system that included a peristaltic pump (Masterflex Cole Parmer Instrument Company, USA) and Teflon tubing coupled to pre-cleaned (0.1M HCl) capsule filters (0.2mm Supor Acropak® with Fluorodyne II membrane). Before each sampling, the tubing and capsule filters were also rinsed with at least 4L of local water. Samples collected for the determination of Nd isotopic composition were stored in pre-

cleaned sampling plastic bags (10L). Samples were acidified to pH 1.8 with HCl (suprapur®, Merck or bi-distilled) and stored in at least two plastic bags at ambient temperature. All bags used for sampling were pre-cleaned with detergent bath (Extran®, Merck, Germany), followed by a weeklong bath in a 6 N HCl solution (reagent grade) and another in 6N HNO_3 solution. The cleaning steps followed the protocols for trace metal-clean sampling of the GEOTRACES program (Cutter et al., 2017).

- Sample treatment

The preconcentration and analyses of Nd isotopic composition followed the method described in Rousseau et al. (2015). The pH of the 10L samples was adjusted to 3.7±0.4 using ammonium hydroxide (Suprapur, Merck) and then they were pre-concentrated in two C18 SepPak cartridges loaded with a strong REE complexant Bis(2-ethylhexyl) phosphate 95% (Alfa Aesar). This step was performed in the lab for all Atlantic samples. For the Antarctic samples, the pre-concentration was performed onboard, and the pH was adjusted directly to 3.7±0.4 using HCl (bi-distilled). In the laboratory, the analytes were eluted from the C18 cartridges using 6N HCl, then evaporated, and redissolved in 1M HCl. The sample was then loaded on a cation-exchange column (0.6 cm in diameter, 4.8 cm in height) packed with Biorad AG50W-X8 (200-400 mesh) resin and washed with HCl and HNO_3 solutions in order to remove the remaining matrix. The REE were eluted using 6 N HCl, the solution was evaporated, redissolved in 0.2 N HCl, and loaded in an anion-exchange column (0.4cm in diameter, 4cm in height) packed with Ln-Spec resin. The neodymium was then separated and recovered using 0.2N HCl solution. This final solution was evaporated again, redissolved in 1.5mL of 2M HCl, and loaded on a rhenium filament for later isotopic analysis by thermal ionization mass spectrometry (TIMS) in static mode (ThermoFinnigan mass spectrometer MAT 261, Observatoire Midi-Pyrénées, Toulouse). Repeated analysis of the Rennés

standard gave a 143Nd/144Nd ratio of 0.511966±0.000006 (n=48) in agreement with the recommended value of 0.511973.

RESULTS AND DISCUSSION

ANTARCTIC

The εNd profiles for all sampling stations are shown in figure 2. The data relative to each sample is presented in table S1. The εNd ranged from about -3.3 (AREE12.1, Gerlache Strait, Antarctica) to -20.0 (REE13.1, Coast of Rio de Janeiro, Brazil). In general, the Antarctic samples presented a more radiogenic Nd isotopic composition of seawater than the Atlantic ones. The εNd profile section showed a gradual decrease in εNd values from Antarctic to Atlantic waters, with the more radiogenic signals at the Gerlache Strait. These lower εNd values obtained are consistent with what has been previously reported on seafloor surface and core sediments in the region (Roy et al., 2007; Simões Pereira et al., 2018; R. Wang et al., 2022). The Nd values on sediments reflect the geological composition and origin of these sediments. Regions influenced by the erosion of young basaltic soils and/or volcanic emissions usually present a more radiogenic Nd composition. The South Shetland Islands present younger sediments enriched in Smectite, formed either by hydrothermal alteration, submarine weathering, or the interaction of hot volcanic matter with ice, and which, usually, present more radiogenic εNd values than other clay minerals (Bayon et al., 2015; Beny et al., 2020; Hillenbrand et al., 2003; R. Wang et al., 2022).

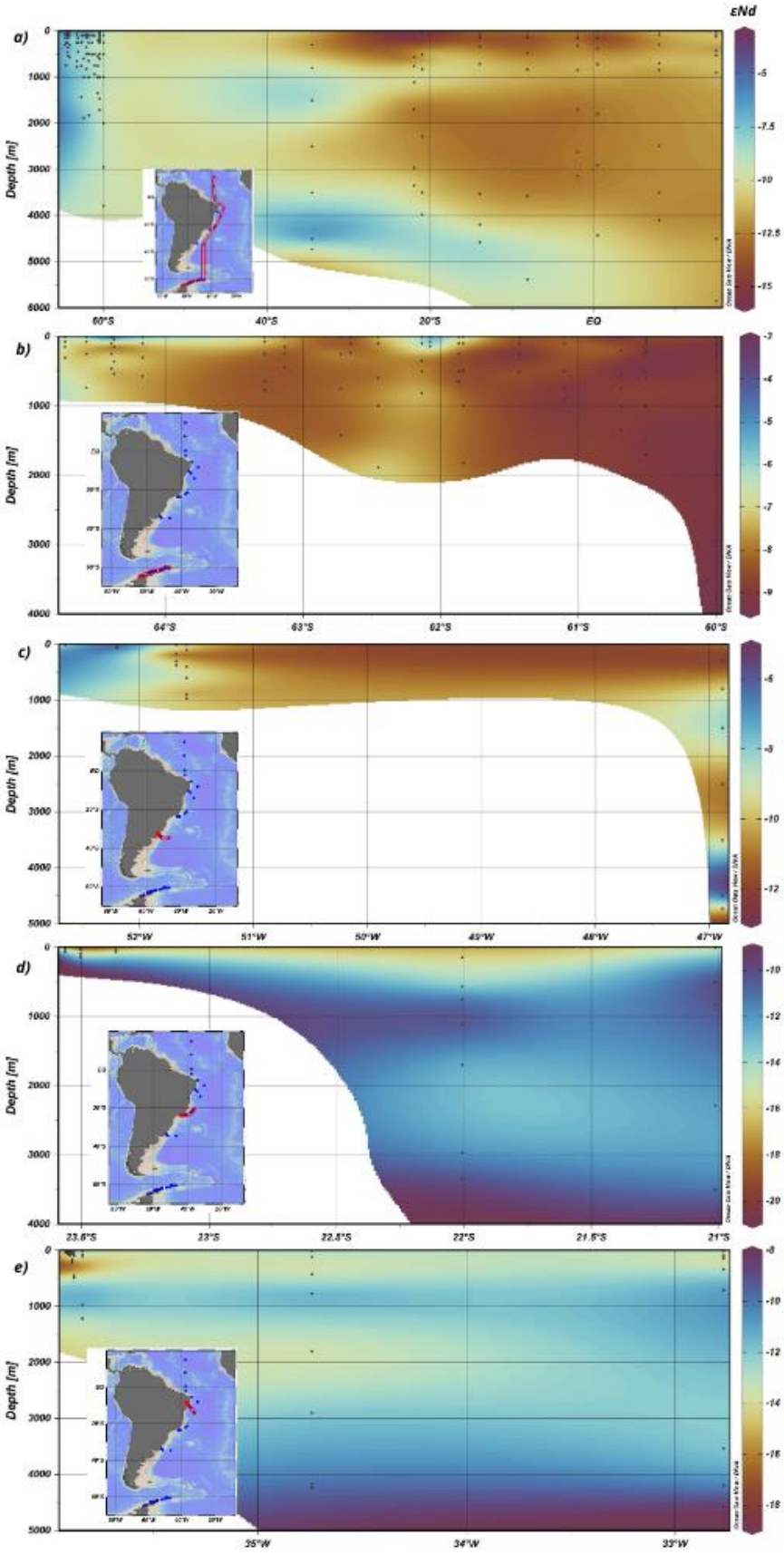

Figure 2 - Vertical sections displaying εNd distributions across regions: a) Antarctic and Atlantic stations, where the x-axis represents latitude; b) Antarctic stations, where the x-axis

represents latitude; c) Atlantic stations around 34°S: transect close to La Plata River, where the x-axis represents longitude; d) Atlantic stations around 23°S: transect close do Rio de Janeiro Coast, where the x-axis represents latitude; e) Atlantic stations around 10°S: transect close to Alagoas Coast, where the x-axis represents longitude.

Stichel et al. (2012) also observed more radiogenic Nd values in a surface seawater at the vicinity of King George Island (εNd=-4.0). This result was accompanied by higher REE concentrations for the region, indicating external inputs of these elements from the basaltic rocks, but not enough to explain the variation in the Nd composition, implying the occurrence of a BE process (Stichel et al., 2012). Similarly, R. Wang et al. (2022) identified the occurrence of BE along the Pacific margin of West Antarctica, where the εNd values increased due to the partial dissolution of radiogenic sediments, followed by re-scavenging onto Fe-Mn oxyhydroxides, shifting the Nd signature of the porewaters without significant increases in Nd concentrations.

In our study, the εNd values observed in the Antarctic Peninsula are too high to have been originated only from the mixing of water masses in the region. Even considering the water masses influenced by the Antarctic Circumpolar Current (ACC εNd= ~-8; Stichel et al., 2012). Therefore, an external source of Nd must be influencing the region. The exact extend and nature of this external source cannot be established by εNd data only. Still, the εNd of marine sediments previously reported in the Bransfield Strait was 2.2, while in the Antarctic Peninsula it varied from-5.4 to 5.7 (Blanchet, 2021). Considering this information, the Nd signatures obtained and the previously reported BE occurrence in the area (Stichel et al., 2012), BE processes are likely the cause of the change in Nd isotopic composition. Nevertheless, it is also important to stress that the samples presenting higher εNd values in Gerlache Strait were the subsurficial ones, which presented lower salinity in the stations

($\varepsilon Nd_{AREE11.1}$= -5.9±0.1, $S_{AREE11.1}$= 33.58; $\varepsilon Nd_{AREE12.1}$= -3.3±0.1, $S_{AREE12.1}$= 33.43; $\varepsilon Nd_{AREE12.2}$= -5.8±0.3, $S_{AREE12.2}$= 34.24; $\varepsilon Nd_{AREE13.1}$= -5.9±0.3, $S_{AREE13.1}$= 33.66; $\varepsilon Nd_{AREE14.1}$= -5.2±0.4, $S_{AREE12.1}$=33.68; $\varepsilon Nd_{AREE15.1}$= -5.6±0.1 $S_{AREE15.1}$=33.50). Similarly, REE16 presented lower salinity and more radiogenic εNd in the vicinity to King George Island. These results indicate that ice melting may also play an important role influencing the Nd signature in the area, either by carrying more terrigenous sediments into the seawater or by the input of freshwater with different Nd composition. Unfortunately, to properly address these hypotheses, data on REE concentrations (still to be determined) is needed.

The impact of this external influence in the Nd signature at the Bransfield and Gerlache Straits appears to be more locally limited to areas closer to the islands. The εNd decreased to around -8.0 at stations more distant to the islands, especially the ones in the Weddel sea, which reached εNd= -9.4±0.1 at the bottom of station AREE8 (table S1). Interestingly, the samples collected at the canyons in the Bransfield Strait didn't seem to be as influenced by similar processes causing εNd as the ones collected in Gerlache Strait and King George Island. The circulation in the area might be one fact that helps keep the more radiogenic Nd close to the South Shetland Islands. In fact, the mCDW flows northward in the surface around the South Shetland Islands, while the DSW flows southward near the Antarctic Peninsula and at the bottom of the Bransfield strait (Santos-Andrade et al., 2023). As the mCDW samples presented more radiogenic values (~ -6.5) than the DSW ones (~ -8.0), it seems that the Nd originated from the external source is being carried northwestward. However, the stations AREE2 to AREE8, outside of Bransfield and Gerlache Straits in the transect from the South Shetland Islands to the South Orkney Islands, present the least radiogenic Nd values from the Antarctic stations, extending from εNd= -8.2±0.2 (AREE3; Tab. S1) to εNd= -9.5±0.2 (AREE5; Tab S1). The vertical profiles of these stations showed low εNd variability. Only surface samples from stations AREE1 and AREE6 presented slightly more radiogenic Nd

isotopic signatures compared to the vertical profile. There was also a subtle tendency to reduction in radiogenicity towards stations AREE5 and AREE8, possibly caused by the distancing from the islands in both sides. In general, these results are in accordance to Stichel et al. (2012) observations that the BE processes occurring in the King George Island and influencing Nd composition were limited to the area and not powerful enough to significantly influence the waters from the Drake Passage.

ATLANTIC

In the Atlantic, the deepest profile around 34°S (REE31; depth 4740m; Table S1) showed two main regions with higher εNd values (fig. 2), one at 800m (AAIW; $\varepsilon Nd_{REE31.4}$= -8.3±0.3) and the other one at 4500m deep (around 240m from the bottom; AABW; $\varepsilon Nd_{REE31.7}$= -6.2±0.2). According to the literature, the observed Nd signature is in accordance to the expected value for AAIW (εNd =-8.0 to -8.7; Jeandel, 1993; Wu et al., 2022). The sample at the bottom ($\varepsilon Nd_{REE31.8}$= -9.9±0.1) actually presents a Nd signature close to what is expected for AABW (εNd =-8.0 to -9.6; Jeandel, 1993; Stichel et al., 2012; Wu et al., 2022), but the one above (REE31.7) presents a εNd signal a lot more radiogenic than expected. These results indicate the presence of an external source of radiogenic Nd close to the bottom. One possible hypothesis is the presence of volcanic activity/hydrothermal sources in the region that might be adding new and consequently more radiogenic material to this layer. Another possibility is the presence of a nepheloid layer, which is characterized by its high particle concentrations that can act as a source of Nd (Stichel et al., 2015). In fact, nepheloid layers are produced by resuspension of bottom sediments, usually on continental margins or from ridges and seamounts, caused by the shear stress from currents, internal waves, and seawater dynamics in general and can eventually spread away from the source (McCave, 2009; Tian et al., 2022). Besides, the marine sediments from Argentina's continental shelf

are more radiogenic (εNd from -4.0 to -0,1; Blanchet, 2021) than the observed in the southern Brazilian shelf (εNd from -7.5 to -17.1; Blanchet, 2021) and if resuspended could potentially cause a punctual increase in εNd of less radiogenic water masses. The observed isotopic composition could be a direct result from the addition of external Nd or could be resulting from an exchanging process (BE). To better constrain the process, data on REE concentrations is needed and will be determined.

It is important to notice that the transect close to the Plata River discharge (~34°S) showed higher variability and more radiogenic εNd (-5 to -12) in a small area. This difference was expected, considering the region is both influenced by the submarine groundwater discharge from the Albardão area (Attisano et al., 2008, 2013) and the freshwater inputs originated from the proximity to the La Plata River. In fact, during sampling the stations REE26 and REE27 showed very high amount of suspended material, to the point of clogging the filter. These are also the stations with lower salinity in the area, indicating they are the most influenced by freshwater input. The samples more influenced by the freshwater showed εNd ranging from -7.1±0.2 to -8.7±0.2. These results are within expectation since the La Plata River receives material eroded from basalts and sedimentary rocks of the Paraná basin which εNd varies from −10.7 to -6.0 (Blanchet, 2021; Mantovanelli et al., 2018). Still, sample REE27.2 presented εNd of -5.1±0.1, which is a lot higher than the subsurficial and bottom samples from the same station. This result might reflect the impact of the submarine groundwater discharge or the heterogeneity of the riverine sources, once the Paraguay River that also contributes to the La Plata River runs through areas of generally more radiogenic and variable Nd signatures (0.60 to -6.6; Comin-Chiaramonti et al., 2015).

Figure 3 shows that as latitude changes southward, a higher variability of εNd is observed in the water column of the Atlantic stations. Also, a trend towards less radiogenic values is observed in the tropical South Atlantic region when compared to the North Atlantic and

subtropical South Atlantic stations. This trend seems to be especially intense in surface samples of shallower stations on the continental shelf, possibly due to the influence of the South American continent. In fact, similar trend has been previously reported for near surface waters from the equator to ~35°S by Wu et al. (2022), with εNd ranging from ~-18 to ~-11.5. The authors hypnotized that this trend could be caused by the influence of the South American craton (εNd=~ -17 to -8) from terrigenous detritus or benthic fluxes of submarine groundwater, or from eolian dust carried by the trade winds from the African continent (εNd=~ -19 to -8). They did not detail or test these hypotheses; however, the data of the 3 continent-ocean transects presented in this work has the potential to help elucidate this.

In the two transects from the continent to the ocean in the Brazilian coast the Nd signal in seawaters up to 250m varied from -18.6±0.2 to -13.1±0.2 for Alagoas (~10°S) and -20±0.1 to -13.1±0.4 for Rio de Janeiro (~23°S) with the predominant water masses being TW and SACW. In the case of the Alagoas transect, the decrease in εNd values seems to be a consequence of the proximity to the Western Pernambuco-Alagoas Domain (εNd=-40.79 to -8.00; da Cruz et al., 2014) and its influence in the coastal stations. In the case of Rio de Janeiro, there is also a resurgence process occurring in the region, which takes the SACW to the surface. The Rio de Janeiro area is also composed by a few different geological groups with variable Nd isotopic signatures from the sedimentary rocks of the Paraná basin (εNd=-7.7 to -6.0), coastal domains from the Ribeira belt (εNd=-10.9 to -6.5), Paraiba do Sul and Embú domains from the Ribeira belt (εNd=-19.3 to -15.0), and the rocks from older pre-Cambrian domains of the Ribeira belt and the Luis Alves craton (εNd=-36.0 to -19.5) (Mantovanelli et al., 2018). Therefore, the gradual decrease in radiogenicity with the proximity to the coast observed for the samples in the Rio de Janeiro transect also seem to indicate an influence of the geological constitution of the region, especially in subsurficial samples from REE10 to REE16.

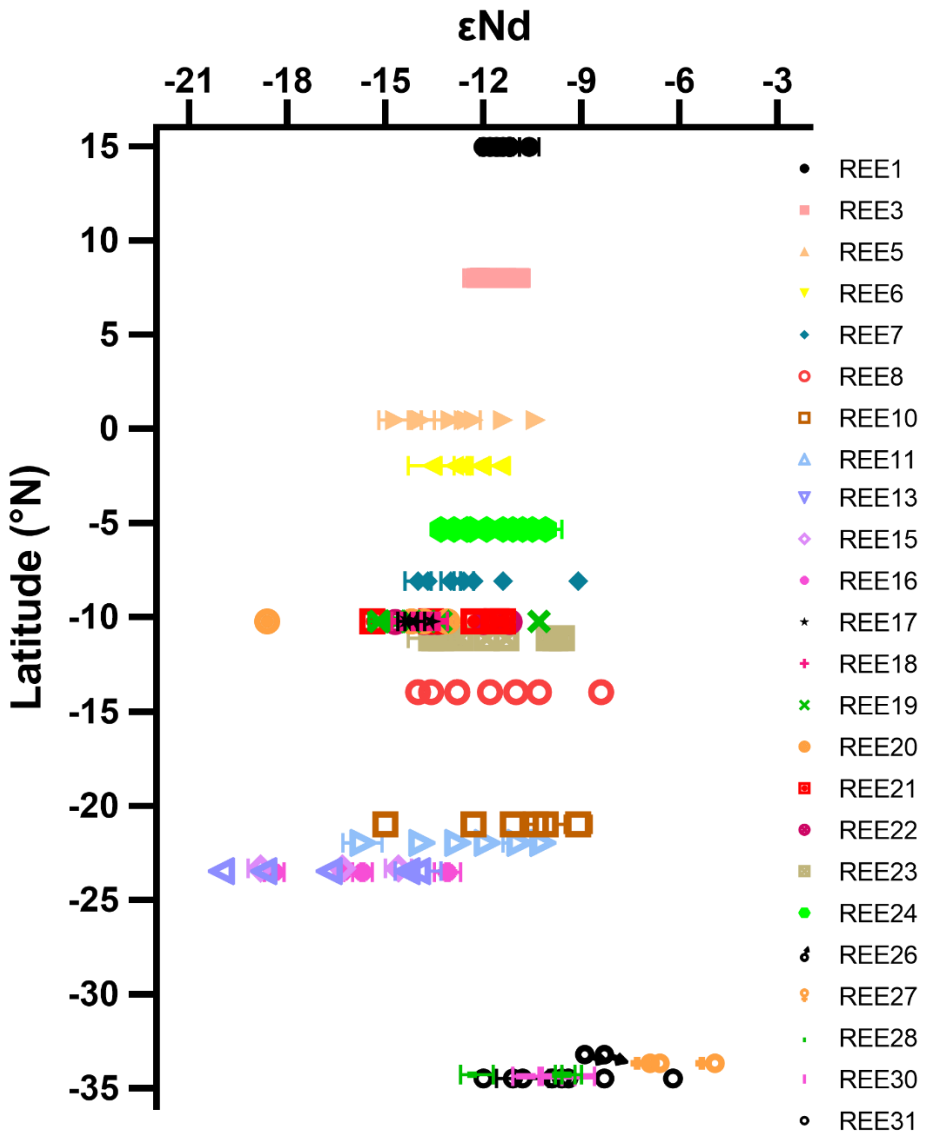

Figure 3 - Plot of εNd vs. Latitude (°N) for all depths of the Atlantic stations.

For the more oceanic waters, the Vitória-Trindade Ridge region (~20°S) doesn't appear to have significantly affected the isotopic composition of Nd in the seawater. Comparing samples from the same water mass, such as the bottom samples, both AABW, it is not possible to state that there was a significant change in signal before (REE10.8; εNd= -9.1±0.4) and after (REE8.8; εNd= -8.4±0.2) crossing this ridge region. The lower part of the NADW, which flows southward, showed a slightly less radiogenic signal after passing through

the ridge (REE10.7; εNd= -11.1±0.2), when compared to the REE8.7 sample (εNd= -10.3±0.2) before it. This is the opposite of what was expected, as the ridge is formed by oceanic basalts which in theory would be adding a higher Nd isotopic signal. This result may be more related to other influences in the region, since the distance between stations REE10 (~21°S) and REE8 (~14°S) is large. Even so, the results observed in this study are in agreement with what was previously reported by Wu et al. (2022), indicating negligible influence of the Vitória-Trindade Ridge on the isotopic composition of water masses at the Western South Atlantic Ocean.

At the northern hemisphere, samples REE3.1 and REE3.2, respectively at 7 and 80m deep, showed salinity values slightly lower than the surface samples from stations REE1 and REE5, possibly indicating that the influence of the Amazon River plume is reaching station REE3. Unfortunately, the reported εNd data for the amazon plume water (-13.9 to -10.6; Rousseau et al., 2015; Xu et al., 2023) is within the range of the seawater at the region, so no significant variation was observed between REE1 and REE3 surface and subsurface samples. There was a decrease in εNd values at similar depths of station REE5, but that trend persists for the stations southward, possibly influenced by equatorial surface currents.

The NADW became more radiogenic southward (fig. 4), especially the lower NADW, reaching εNd as low as -10.3±0.2 (REE8.7; ~14°S) in the tropical Atlantic and -10.8±0.8 (REE31.5; ~34°S) in the subtropical Atlantic. The opposite trend was observed in AAIW, ranging from -12.2±0.3 (REE31.4; ~34°S) to -8.3±0.3 (REE8.7; ~7°N). These trends are probably due to the combination of the facts that each of these water masses comes from a different region and presents a different signature at the time of formation, more radiogenic for AAIW (εNd=~−8.7; Jeandel, 1993) and less radiogenic for NADW (εNd=~−13.3; Lambelet et al., 2016). A water mass will slowly influence the isotopic composition of the other directly in contact with it along the circulation by means of conservative mixing, with a tendency

towards homogenization that is just never achieved. In fact, conservative mixing was previously reported as the main responsible for changes in Nd isotopic composition in the deeper layers of the Atlantic Ocean (Wu et al., 2022).

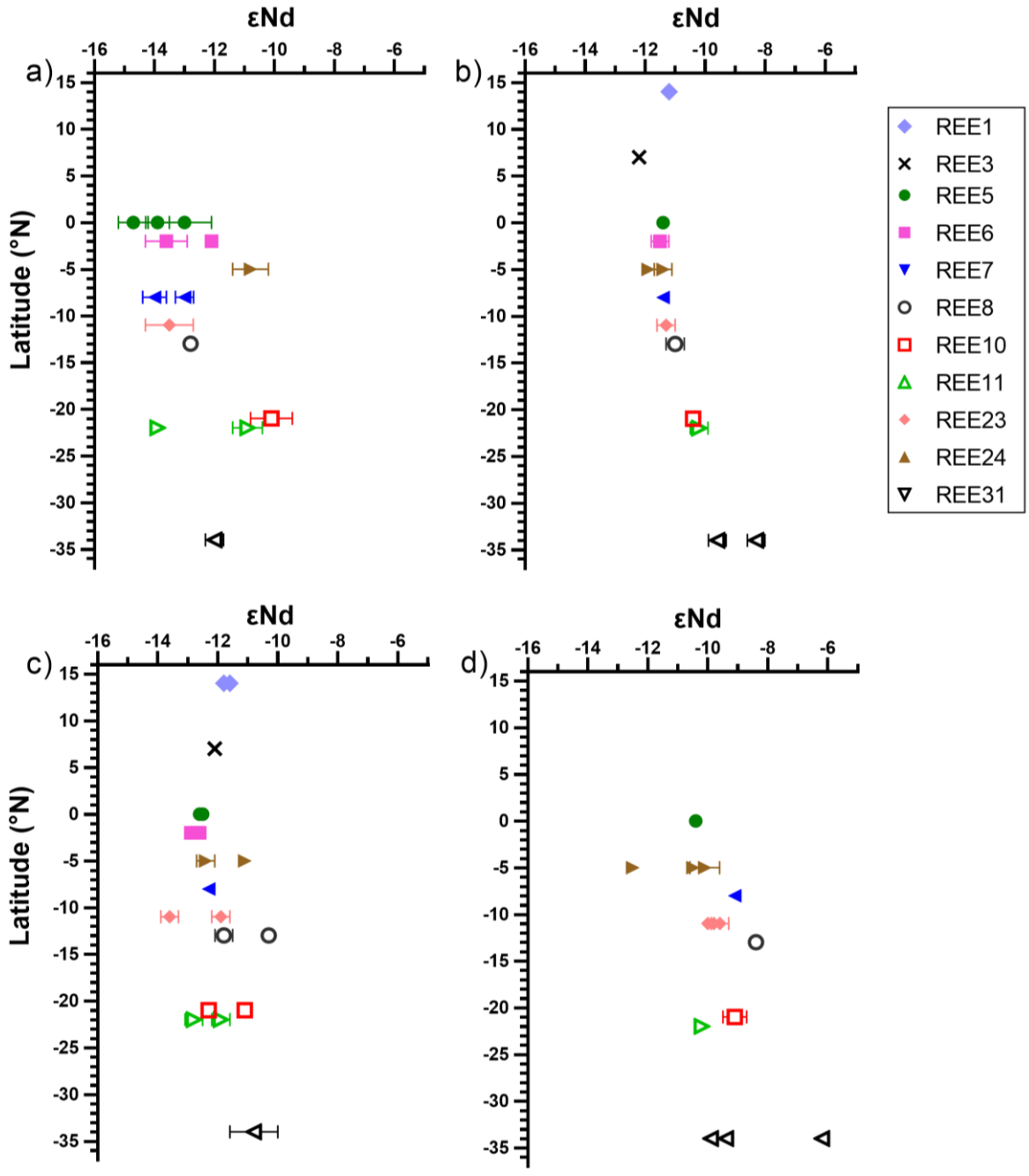

Figure 4 - Plot εNd vs. Latitude (°N) selected by water masses in deep Atlantic stations: a) samples of SACW; b) samples of AAIW; c) samples of NADW; d) samples of AABW. This plot doesn't include shelf stations.

Although the AABW also exhibited some variability in Nd composition in the Atlantic (εNd=-12.5±0.2 to -6.2±0.2), there was no clear tendency. The lack of a clear tendency in the Nd composition variation through this water mass pathway might be due a complex set of interactions with various sources, such as sediment remobilization at the margins and bottom of the ocean, hydrothermal sources, as well as interaction with NADW. Similarly, the SACW also didn't show any specific pattern of changes in Nd composition. In fact, the SACW goes through a recirculation process along its path and the number of samples and the geographical restriction of sampling is not enough in the present work was insufficient to identify the changes caused by this process.

The NACW was only observed in two stations (REE1 and REE3) and showed similar Nd results in both. Even so, this water mass presented considerable variability within each vertical profile (NACW εNd_{REE1}= -12.0±0.2 to -10.6±0.3 and εNd_{REE3}= -12,1±0.3 to -10,9±0.3).

CONCLUSIONS

The Nd isotopic composition of seawater in the Antarctic Peninsula seems to be influenced by the proximity to islands, becoming more radiogenic as the water masses move through the islands, suggesting the occurrence of BE. Still this change in isotopic composition is limited and as the water masses move away from the islands, the εNd decreases.

In the Atlantic, all three continent-ocean transects (at ~34°S, ~23°S, and ~10°S) showed variations in Nd signatures tending towards the geological composition of each continental area. This trend was also the likely responsible by a general decreasing tendency in εNd from the northernmost stations southward.

The Vitoria-Trindade Ridge didn't cause a perceptible variation in Nd isotopic composition. Meanwhile, the Amazon plume signal was detected by the reduction in salinity of samples,

but didn't cause noticeable changes in εNd, once the Nd added by the plume presented similar composition to the seawater.

The NADW showed higher εNd southward, while AAIW became less radiogenic as it moved northwards. This tendency is probably due to conservative mixing of these water masses. While AABW and SACW presented higher variability with no clear tendency.

The data presented in this study cannot lead to conclusions regarding the actual sources of the changes in Nd signatures, however, it can point areas of special interest for future studies on the topic, where Nd behaves in an unexpected way, as well as indicate hypothesis of possible sources of external Nd to these areas. Further calculations using more data is necessary to actually test the hypothesis raised in the present work.

REFERENCES

Adebayo, S. B., Cui, M., Williams, T. J., Martin, E., & Johannesson, K. H. (2022). Evolution of rare earth element and εNd compositions of Gulf of Mexico seawater during interaction with Mississippi River sediment. *Geochimica et Cosmochimica Acta*, *335*, 231–242. https://doi.org/10.1016/j.gca.2022.08.024

Alibo, D. S., & Nozaki, Y. (2004). Dissolved rare earth elements in the eastern Indian Ocean: Chemical tracers of the water masses. *Deep-Sea Research Part I: Oceanographic Research Papers*, *51*(4), 559–576. https://doi.org/10.1016/j.dsr.2003.11.004

Arsouze, T., Dutay, J.-C., Lacan, F., & Jeandel, C. (2009). Reconstructing the Nd oceanic cycle using a coupled dynamical-biogeochemical model. In *Biogeosciences* (Vol. 6). www.biogeosciences.net/6/2829/2009/

Attisano, K. K., Luis, ;, Hax, F., Idel, N. ;, Bigliardi, C., Caroline, M. ;, Machado, S., Márcio, ;, Milani, R., Zarzur, S., & Ferreira De Andrade, C. F. (2008). EVIDENCES OF CONTINENTAL GROUNDWATER INPUTS TO THE SHELF ZONE IN ALBARDÃO, RS, BRAZIL. In *BRAZILIAN JOURNAL OF OCEANOGRAPHY* (Vol. 56, Issue 3).

Attisano, K. K., Santos, I. R., Ferreira De Andrade, C. F., Lopes De Paiva, M., Cristina, I., Milani, B., Felipe, L., & Niencheski, H. (2013). SUBMARINE GROUNDWATER DISCHARGE REVEALED BY RADIUM ISOTOPES (Ra-223 and Ra-224) NEAR A PALEOCHANNEL ON THE SOUTHERN BRAZILIAN CONTINENTAL SHELF. In *BRAZILIAN JOURNAL OF OCEANOGRAPHY* (Vol. 61, Issue 3).

Barlett, E. M. R., Tosonotto, G. V., Piola, A. R., Sierra, M. E., & Mata, M. M. (2018). On the temporal variability of intermediate and deep waters in the Western Basin of the Bransfield Strait. *Deep-Sea Research Part II: Topical Studies in Oceanography*, *149*, 31–46. https://doi.org/10.1016/j.dsr2.2017.12.010

Bau, M., & Dulski, P. (1996). Anthropogenic origin of positive gadolinium anomalies in river waters. *Earth and Planetary Science Letters*, *143*, 245–255.

Bayon, G., Toucanne, S., Skonieczny, C., André, L., Bermell, S., Cheron, S., Dennielou, B., Etoubleau, J., Freslon, N., Gauchery, T., Germain, Y., Jorry, S. J., Ménot, G., Monin, L., Ponzevera, E., Rouget, M. L., Tachikawa, K., & Barrat, J. A. (2015). Rare earth elements and neodymium isotopes in world river sediments revisited. *Geochimica et Cosmochimica Acta*, *170*, 17–38. https://doi.org/10.1016/j.gca.2015.08.001

Behrens, M. K., Pahnke, K., Schnetger, B., & Brumsack, H. J. (2018). Sources and processes affecting the distribution of dissolved Nd isotopes and concentrations in the West Pacific. *Geochimica et Cosmochimica Acta*, *222*, 508–534. https://doi.org/10.1016/j.gca.2017.11.008

Beny, F., Bout-Roumazeilles, V., Davies, G. R., Waelbroeck, C., Bory, A., Tribovillard, N., Delattre, M., & Abraham, R. (2020). Radiogenic isotopic and clay mineralogical signatures of terrigenous particles as water-mass tracers: New insights into South Atlantic deep circulation during the last termination. *Quaternary Science Reviews*, *228*. https://doi.org/10.1016/j.quascirev.2019.106089

Blanchet, C. L. (2021). A global database of radiogenic Nd and Sr isotopes in marine and terrestrial samples (V. 3.0). . *GFZ Data Services*.

Chaillou, G., Anschutz, P., Lavaux, G., & Blanc, G. (2006). Rare earth elements in the modern sediments of the Bay of Biscay (France). *Marine Chemistry*, *100*(1–2), 39–52. https://doi.org/10.1016/j.marchem.2005.09.007

Comin-Chiaramonti, P., Gomes, C. B., De Min, A., Ernesto, M., & Gasparon, M. (2015). Magmatism along the high Paraguay River at the border of Brazil and Paraguay: A review and new constraints on emplacement ages. In *Journal of South American Earth Sciences* (Vol. 58, pp. 72–81). Elsevier Ltd. https://doi.org/10.1016/j.jsames.2014.12.010

Copard, K., Colin, C., Henderson, G. M., Scholten, J., Douville, E., Sicre, M. A., & Frank, N. (2012). Late Holocene intermediate water variability in the northeastern Atlantic as recorded by deep-sea corals. *Earth and Planetary Science Letters*, *313–314*(1), 34–44. https://doi.org/10.1016/j.epsl.2011.09.047

Cutter, G., Casciotti, K., Croot, P., Geibert, W., Geochemistry, M., Heimbürger, L.-E., & Lohan, M. (2017). *Sampling and Sample-handling Protocols for GEOTRACES Cruises*.

da Cruz, R. F., Pimentel, M. M., De Accioly, A. C. A., & Rodrigues, J. B. (2014). Geological and isotopic characteristics of granites from the western pernambuco-alagoas domain: Implications for the crustal evolution of the neoproterozoic borborema province. *Brazilian Journal of Geology*, *44*(4), 627–652. https://doi.org/10.5327/Z2317488920140004008

Damini, B. Y., Costa, R. R., Dotto, T. S., Mendes, C. R. B., Torres-Lasso, J. C., Azaneu, M. do V. C., Mata, M. M., & Kerr, R. (2023). Antarctica Slope Front bifurcation eddy: A stationary feature influencing CO2 dynamics in the northern Antarctic Peninsula. *Progress in Oceanography*, *212*. https://doi.org/10.1016/j.pocean.2023.102985

Damini, B. Y., Kerr, R., Dotto, T. S., & Mata, M. M. (2022). Long-term changes on the Bransfield Strait deep water masses: Variability, drivers and connections with the northwestern Weddell Sea. *Deep-Sea Research Part I: Oceanographic Research Papers*, *179*. https://doi.org/10.1016/j.dsr.2021.103667

Dotto, T. S., Kerr, R., Mata, M. M., & Garcia, C. A. E. (2016). Multidecadal freshening and lightening in the deep waters of the Bransfield Strait, Antarctica. *Journal of Geophysical Research: Oceans*, *121*(6), 3741–3756. https://doi.org/10.1002/2015JC011228

Ferreira, M. L. de C., & Kerr, R. (2017). Source water distribution and quantification of North Atlantic Deep Water and Antarctic Bottom Water in the Atlantic Ocean. *Progress in Oceanography*, *153*, 66–83. https://doi.org/10.1016/j.pocean.2017.04.003

Frank, M. (2002). Radiogenic isotopes: Tracers of past ocean circulation and erosional input. *Reviews of Geophysics*, *40*(1), 1-1-1–38. https://doi.org/10.1029/2000RG000094

Fröllje, H., Pahnke, K., Schnetger, B., Brumsack, H. J., Dulai, H., & Fitzsimmons, J. N. (2016). Hawaiian imprint on dissolved Nd and Ra isotopes and rare earth elements in the central North Pacific: Local survey and seasonal variability. *Geochimica et Cosmochimica Acta*, *189*, 110–131. https://doi.org/10.1016/j.gca.2016.06.001

Garcia-Solsona, E., Jeandel, C., Labatut, M., Lacan, F., Vance, D., Chavagnac, V., & Pradoux, C. (2014). Rare earth elements and Nd isotopes tracing water mass mixing and particle-seawater interactions in the SE Atlantic. *Geochimica et Cosmochimica Acta*, *125*, 351–372. https://doi.org/10.1016/j.gca.2013.10.009

Grasse, P., Bosse, L., Hathorne, E. C., Böning, P., Pahnke, K., & Frank, M. (2017). Short-term variability of dissolved rare earth elements and neodymium isotopes in the entire water column of the Panama Basin. *Earth and Planetary Science Letters*, *475*, 242–253. https://doi.org/10.1016/j.epsl.2017.07.022

Grenier, M., Jeandel, C., Lacan, F., Vance, D., Venchiarutti, C., Cros, A., & Cravatte, S. (2013). From the subtropics to the central equatorial Pacific Ocean: Neodymium isotopic composition and rare earth element concentration variations. *Journal of Geophysical Research: Oceans*, *118*(2), 592–618. https://doi.org/10.1029/2012JC008239

Gu, S., Liu, Z., Jahn, A., Rempfer, J., Zhang, J., & Joos, F. (2019). Modeling Neodymium Isotopes in the Ocean Component of the Community Earth System Model (CESM1). *Journal of Advances in Modeling Earth Systems*, *11*(3), 624–640. https://doi.org/10.1029/2018MS001538

Haley, B. A., Klinkhammer, G. P., & McManus, J. (2004). Rare earth elements in pore waters of marine sediments. *Geochimica et Cosmochimica Acta*, *68*(6), 1265–1279. https://doi.org/10.1016/j.gca.2003.09.012

Hatje, V., Bruland, K. W., & Flegal, A. R. (2014). Determination of rare earth elements after pre-concentration using NOBIAS-chelate PA-1®resin: Method development and application in the San Francisco Bay plume. *Marine Chemistry*, *160*, 34–41. https://doi.org/10.1016/j.marchem.2014.01.006

Hatje, V., Bruland, K. W., & Flegal, A. R. (2016). Increases in Anthropogenic Gadolinium Anomalies and Rare Earth Element Concentrations in San Francisco Bay over a 20 Year Record. *Environmental Science and Technology*, *50*(8), 4159–4168. https://doi.org/10.1021/acs.est.5b04322

Hellmer, H. H., Huhn, O., Gomis, D., & Timmermann, R. (2011). On the freshening of the northwestern Weddell Sea continental shelf. *Ocean Science*, *7*(3), 305–316. https://doi.org/10.5194/os-7-305-2011

Hillenbrand, C.-D., Grobe, H., Diekmann, B., Kuhn, G., & Fütterer, D. K. (2003). Distribution of clay minerals and proxies for productivity in surface sediments of the Bellingshausen and Amundsen seas (West Antarctica) – Relation to modern environmental conditions. *Marine Geology*, *193*(3–4), 253–271. https://doi.org/10.1016/S0025-3227(02)00659-X

Hu, R., Piotrowski, A. M., Bostock, H. C., Crowhurst, S., & Rennie, V. (2016). Variability of neodymium isotopes associated with planktonic foraminifera in the Pacific Ocean during the Holocene and Last Glacial Maximum. *Earth and Planetary Science Letters*, *447*, 130–138. https://doi.org/10.1016/j.epsl.2016.05.011

Huang, Y., Colin, C., Liu, Z., Douville, E., Dapoigny, A., Haurine, F., Wu, Q., & Tien-Shun Lin, A. (2023). Impacts of nepheloid layers and mineralogical compositions of oceanic margin sediments on REE concentrations and Nd isotopic compositions of seawater. *Geochimica et Cosmochimica Acta*, *359*, 57–70. https://doi.org/10.1016/j.gca.2023.08.026

Jeandel, C. (1993). Concentration and isotopic composition of Nd in the South Atlantic Ocean. *Earth and Planetary Science Letters*, *117*, 581–591.

Jeandel, C. (2016). Overview of the mechanisms that could explain the “Boundary Exchange” at the land-ocean contact. In *Philosophical Transactions of the Royal Society A: Mathematical,*

Physical and Engineering Sciences (Vol. 374, Issue 2081). Royal Society of London. https://doi.org/10.1098/rsta.2015.0287

Johannesson, K. H., & Burdige, D. J. (2007). Balancing the global oceanic neodymium budget: Evaluating the role of groundwater. *Earth and Planetary Science Letters*, *253*(1–2), 129–142. https://doi.org/10.1016/j.epsl.2006.10.021

Johannesson, K. H., Palmore, C. D., Fackrell, J., Prouty, N. G., Swarzenski, P. W., Chevis, D. A., Telfeyan, K., White, C. D., & Burdige, D. J. (2017). Rare earth element behavior during groundwater–seawater mixing along the Kona Coast of Hawaii. *Geochimica et Cosmochimica Acta*, *198*, 229–258. https://doi.org/10.1016/j.gca.2016.11.009

Kerr, R., Dotto, T. S., Mata, M. M., & Hellmer, H. H. (2018). Three decades of deep water mass investigation in the Weddell Sea (1984–2014): Temporal variability and changes. *Deep-Sea Research Part II: Topical Studies in Oceanography*, *149*, 70–83. https://doi.org/10.1016/j.dsr2.2017.12.002

Kulaksiz, S., & Bau, M. (2013). Anthropogenic dissolved and colloid/nanoparticle-bound samarium, lanthanum and gadolinium in the Rhine River and the impending destruction of the natural rare earth element distribution in rivers. *Earth and Planetary Science Letters*, *362*, 43–50. https://doi.org/10.1016/j.epsl.2012.11.033

Lacan, F., & Jeandel, C. (2001). Tracing Papua New Guinea imprint on the central Equatorial Paci¢c Ocean using neodymium isotopic compositions and Rare Earth Element patterns. *Earth and Planetary Science Letters*, *186*, 497–512. www.elsevier.com/locate/epsl

Lacan, F., & Jeandel, C. (2005). Neodymium isotopes as a new tool for quantifying exchange fluxes at the continent-ocean interface. *Earth and Planetary Science Letters*, *232*(3–4), 245–257. https://doi.org/10.1016/j.epsl.2005.01.004

Lacan, F., Tachikawa, K., & Jeandel, C. (2012). Neodymium isotopic composition of the oceans: A compilation of seawater data. *Chemical Geology*, *300–301*, 177–184. https://doi.org/10.1016/j.chemgeo.2012.01.019

Lambelet, M., van de Flierdt, T., Crocket, K., Rehkämper, M., Kreissig, K., Coles, B., Rijkenberg, M. J. A., Gerringa, L. J. A., de Baar, H. J. W., & Steinfeldt, R. (2016). Neodymium isotopic composition and concentration in the western North Atlantic Ocean: Results from the GEOTRACES GA02 section. *Geochimica et Cosmochimica Acta*, *177*, 1–29. https://doi.org/10.1016/j.gca.2015.12.019

Liu, X. M., Hardisty, D. S., Lyons, T. W., & Swart, P. K. (2019). Evaluating the fidelity of the cerium paleoredox tracer during variable carbonate diagenesis on the Great Bahamas Bank. *Geochimica et Cosmochimica Acta*, *248*, 25–42. https://doi.org/10.1016/j.gca.2018.12.028

Lyra, B. U., & Rigo, D. (2019). Deforestation impact on discharge regime in the Doce River Basin. *Ambiente e Agua - An Interdisciplinary Journal of Applied Science*, *14*(4), 1. https://doi.org/10.4136/ambi-agua.2370

Mantovanelli, S. S., Tassinari, C. C. G., De Mahiques, M. M., Jovane, L., & Bongiolo, E. (2018). Characterization of nd radiogenic isotope signatures in sediments from the southwestern Atlantic margin. *Frontiers in Earth Science*, *6*. https://doi.org/10.3389/feart.2018.00074

McCave, I. N. (2009). Nepheloid Layers. In J. H. Steele (Ed.), *Encyclopedia of Ocean Sciences* (2nd ed.). Academic Press.

Mercadier, J., Cuney, M., Lach, P., Boiron, M. C., Bonhoure, J., Richard, A., Leisen, M., & Kister, P. (2011). Origin of uranium deposits revealed by their rare earth element signature. *Terra Nova*, *23*(4), 264–269. https://doi.org/10.1111/j.1365-3121.2011.01008.x

Mirlean, N., Calliari, L., & Johannesson, K. (2020). Dredging in an estuary causes contamination by fluid mud on a tourist ocean beach. Evidence via REE ratios. *Marine Pollution Bulletin*, *159*. https://doi.org/10.1016/j.marpolbul.2020.111495

Molina-Kescher, M., Frank, M., & Hathorne, E. (2014). South Pacific dissolved Nd isotope compositions and rare earth element distributions: Water mass mixing versus biogeochemical cycling. *Geochimica et Cosmochimica Acta*, *127*, 171–189. https://doi.org/10.1016/j.gca.2013.11.038

Monteiro, T., Henley, S. F., Pollery, R. C. G., Mendes, C. R. B., Mata, M., Tavano, V. M., Garcia, C. A. E., & Kerr, R. (2023). Spatiotemporal variability of dissolved inorganic macronutrients along the northern Antarctic Peninsula (1996–2019). *Limnology and Oceanography*, *68*(10), 2305–2326. https://doi.org/10.1002/lno.12424

Paiva, B. P., & Schettini, C. A. F. (2021). Circulation and transport processes in a tidally forced salt-wedge estuary: The São Francisco river estuary, Northeast Brazil. *Regional Studies in Marine Science*, *41*. https://doi.org/10.1016/j.rsma.2020.101602

Parra, R. R. T., Laurido, A. L. C., & Sánchez, J. D. I. (2020). Hydrographic conditions during two austral summer situations (2015 and 2017) in the Gerlache and Bismarck straits, northern Antarctic Peninsula. *Deep-Sea Research Part I: Oceanographic Research Papers*, *161*. https://doi.org/10.1016/j.dsr.2020.103278

Piepgras, D. J., & Wasserburg, G. J. (1987). Rare earth element transport in the western North Atlantic inferred from Nd isotopic observations. *Geochimica et Cosmochimica Acta*, *51*, 1257–1271.

Rego, C. A. Q., Quaresma, G. de O. A., Santos, A. C. dos, Mohriak, W. U., Jesus, J. V. M. de, & Rodrigues, S. W. de O. (2021). Davis Bank geodynamic context, South Atlantic Ocean: Insights into the Vitória-Trindade Ridge evolution. *Journal of South American Earth Sciences*, *112*. https://doi.org/10.1016/j.jsames.2021.103620

Rempfer, J., Stocker, T. F., Joos, F., Dutay, J. C., & Siddall, M. (2011). Modelling Nd-isotopes with a coarse resolution ocean circulation model: Sensitivities to model parameters and source/sink distributions. *Geochimica et Cosmochimica Acta*, *75*(20), 5927–5950. https://doi.org/10.1016/j.gca.2011.07.044

Romero, F. M., Prol-Ledesma, R. M., Canet, C., Alvares, L. N., & Pérez-Vázquez, R. (2010). Acid drainage at the inactive Santa Lucia mine, western Cuba: Natural attenuation of arsenic, barium and lead, and geochemical behavior of rare earth elements. *Applied Geochemistry*, *25*(5), 716–727. https://doi.org/10.1016/j.apgeochem.2010.02.004

Rousseau, T. C. C., Sonke, J. E., Chmeleff, J., Van Beek, P., Souhaut, M., Boaventura, G., Seyler, P., & Jeandel, C. (2015). Rapid neodymium release to marine waters from lithogenic sediments in the Amazon estuary. *Nature Communications*, *6*. https://doi.org/10.1038/ncomms8592

Roy, M., van de Flierdt, T., Hemming, S. R., & Goldstein, S. L. (2007). 40Ar/39Ar ages of hornblende grains and bulk Sm/Nd isotopes of circum-Antarctic glacio-marine sediments: Implications for sediment provenance in the southern ocean. *Chemical Geology*, *244*(3–4), 507–519. https://doi.org/10.1016/j.chemgeo.2007.07.017

Sangrà, P., Stegner, A., Hernández-Arencibia, M., Marrero-Díaz, Á., Salinas, C., Aguiar-González, B., Henríquez-Pastene, C., & Mouriño-Carballido, B. (2017). The Bransfield Gravity Current. *Deep-Sea Research Part I: Oceanographic Research Papers*, *119*, 1–15. https://doi.org/10.1016/j.dsr.2016.11.003

Santos-Andrade, M., Kerr, R., Orselli, I. B. M., Monteiro, T., Mata, M. M., & Goyet, C. (2023). Drivers of Marine CO2-Carbonate Chemistry in the Northern Antarctic Peninsula. *Global Biogeochemical Cycles*, *37*(3). https://doi.org/10.1029/2022GB007518

Schmidtko, S., Heywood, K. J., Thompson, A. F., & Aoki, S. (2014). Multidecadal warming of Antarctic waters. *Science*, *346*(6214), 1227–1231. https://doi.org/10.1126/science.1256117

Shynu, R., Rao, V. P., Parthiban, G., Balakrishnan, S., Narvekar, T., & Kessarkar, P. M. (2013). REE in suspended particulate matter and sediment of the Zuari estuary and adjacent shelf,

western India: Influence of mining and estuarine turbidity. *Marine Geology*, *346*, 326–342. https://doi.org/10.1016/j.margeo.2013.10.004
Siddall, M., Khatiwala, S., van de Flierdt, T., Jones, K., Goldstein, S. L., Hemming, S., & Anderson, R. F. (2008). Towards explaining the Nd paradox using reversible scavenging in an ocean general circulation model. *Earth and Planetary Science Letters*, *274*(3–4), 448–461. https://doi.org/10.1016/j.epsl.2008.07.044
Simões Pereira, P., van de Flierdt, T., Hemming, S. R., Hammond, S. J., Kuhn, G., Brachfeld, S., Doherty, C., & Hillenbrand, C. D. (2018). Geochemical fingerprints of glacially eroded bedrock from West Antarctica: Detrital thermochronology, radiogenic isotope systematics and trace element geochemistry in Late Holocene glacial-marine sediments. *Earth-Science Reviews*, *182*, 204–232. https://doi.org/10.1016/j.earscirev.2018.04.011
Sousa, T. A., Venancio, I. M., Marques, E. D., Figueiredo, T. S., Nascimento, R. A., Smoak, J. M., Albuquerque, A. L. S., Valeriano, C. M., & Silva-Filho, E. V. (2022). REE Anomalies Changes in Bottom Sediments Applied in the Western Equatorial Atlantic Since the Last Interglacial. *Frontiers in Marine Science*, *9*. https://doi.org/10.3389/fmars.2022.846976
Souza, A. G. Q. de, Kerr, R., & Azevedo, J. L. L. de. (2018). On the influence of Subtropical Mode Water on the South Atlantic Ocean. *Journal of Marine Systems*, *185*, 13–24. https://doi.org/10.1016/j.jmarsys.2018.04.006
Stewart, N. R., Denevan, W. M., Oteiza, D., & Oliveira, W. F. (2022, September 25). *Río de la Plata*. Encyclopaedia Britannica. https://www.britannica.com/place/Rio-de-la-Plata
Stichel, T., Frank, M., Rickli, J., & Haley, B. A. (2012). The hafnium and neodymium isotope composition of seawater in the Atlantic sector of the Southern Ocean. *Earth and Planetary Science Letters*, *317–318*, 282–294. https://doi.org/10.1016/j.epsl.2011.11.025
Stichel, T., Hartman, A. E., Duggan, B., Goldstein, S. L., Scher, H., & Pahnke, K. (2015). Separating biogeochemical cycling of neodymium from water mass mixing in the Eastern North Atlantic. *Earth and Planetary Science Letters*, *412*, 245–260. https://doi.org/10.1016/j.epsl.2014.12.008
Tachikawa, K., Arsouze, T., Bayon, G., Bory, A., Colin, C., Dutay, J. C., Frank, N., Giraud, X., Gourlan, A. T., Jeandel, C., Lacan, F., Meynadier, L., Montagna, P., Piotrowski, A. M., Plancherel, Y., Pucéat, E., Roy-Barman, M., & Waelbroeck, C. (2017). The large-scale evolution of neodymium isotopic composition in the global modern and Holocene ocean revealed from seawater and archive data. *Chemical Geology*, *457*, 131–148. https://doi.org/10.1016/j.chemgeo.2017.03.018
Tachikawa, K., Athias, V., & Jeandel, C. (2003). Neodymium budget in the modern ocean and paleo-oceanographic implications. *Journal of Geophysical Research: Oceans*, *108*(8). https://doi.org/10.1029/1999jc000285
Tachikawa, K., Jeandel, C., & Roy-Barman, M. (1999). A new approach to the Nd residence time in the ocean: the role of atmospheric inputs. In *Earth and Planetary Science Letters* (Vol. 170). www.elsevier.com/locate/epsl
Talley, L. D. (2013). Closure of the global overturning circulation through the Indian, Pacific, and southern oceans. *Oceanography*, *26*(1), 80–97. https://doi.org/10.5670/oceanog.2013.07
Talley, L. D., Pickard, G. L., Emery, W. J., & Swift, J. H. (2011). *Descriptive Physical Oceanography* (6th ed.). Elsevier. https://doi.org/10.1016/C2009-0-24322-4
Tian, Z., Liu, Y., Zhang, X., Zhang, Y., & Zhang, M. (2022). Formation Mechanisms and Characteristics of the Marine Nepheloid Layer: A Review. In *Water (Switzerland)* (Vol. 14, Issue 5). MDPI. https://doi.org/10.3390/w14050678
Valentin, J. L. (2001). The Cabo Frio Upwelling System, Brazil. In U. Seeliger & B. Kjerfve (Eds.), *Ecologial Studies* (Vol. 144, pp. 97–105). Springer.
Venables, H. J., Meredith, M. P., & Brearley, J. A. (2017). Modification of deep waters in Marguerite Bay, western Antarctic Peninsula, caused by topographic overflows. *Deep-Sea*

Research Part II: Topical Studies in Oceanography, *139*, 9–17. https://doi.org/10.1016/j.dsr2.2016.09.005

Wang, R., Williams, T. J., Hillenbrand, C. D., Ehrmann, W., Larkin, C. S., Hutchings, A. M., & Piotrowski, A. M. (2022). Boundary processes and neodymium cycling along the Pacific margin of West Antarctica. *Geochimica et Cosmochimica Acta*, *327*, 1–20. https://doi.org/10.1016/j.gca.2022.04.012

Wang, X., Moffat, C., Dinniman, M. S., Klinck, J. M., Sutherland, D. A., & Aguiar-González, B. (2022). Variability and Dynamics of Along-Shore Exchange on the West Antarctic Peninsula (WAP) Continental Shelf. *Journal of Geophysical Research: Oceans*, *127*(2). https://doi.org/10.1029/2021JC017645

Wasserburg, G. J., Jacobsen, S. B., DePaolo, D. J., McCulloch, M. T., & Wen, T. (1981). Precise determination of Sm/Nd ratios, Sm and Nd isotopic abundances in standard solutions*. *Geochimica et Cosmochimica Acta*, *45*, 2311–2323.

Wu, Y., Pena, L. D., Anderson, R. F., Hartman, A. E., Bolge, L. L., Basak, C., Kim, J., Rijkenberg, M. J. A., de Baar, H. J. W., & Goldstein, S. L. (2022). Assessing neodymium isotopes as an ocean circulation tracer in the Southwest Atlantic. *Earth and Planetary Science Letters*, *599*. https://doi.org/10.1016/j.epsl.2022.117846

Xu, A., Hathorne, E., Laukert, G., & Frank, M. (2023). Overlooked riverine contributions of dissolved neodymium and hafnium to the Amazon estuary and oceans. *Nature Communications*, *14*(1). https://doi.org/10.1038/s41467-023-39922-3

Zheng, X. Y., Plancherel, Y., Saito, M. A., Scott, P. M., & Henderson, G. M. (2016). Rare earth elements (REEs) in the tropical South Atlantic and quantitative deconvolution of their non-conservative behavior. *Geochimica et Cosmochimica Acta*, *177*, 217–237. https://doi.org/10.1016/j.gca.2016.01.018

Zhou, M., Niiler, P. P., & Hu, J.-H. (2002). Surface currents in the Bransfield and Gerlache Straits, Antarctica. In *Deep-Sea Research I* (Vol. 49).

Table S1 -Sample, cruise, station, date, location, depth, temperature, salinity, oxygen, date of sampling and εNd; TW: Tropical Water; SACW: South Atlantic Central Water; AAIW: Antarctic Intermediate Water; NADW: North Atlantic Deep Water; AABW: Antarctic Bottom Water; SW: Surface Water; mCDW: modified Circumpolar Deep Water; DSW: Dense Shelf Water; LSSW: Low Salinity Shelf Water; HSSW: High Salinity Shelf Water.

Sample	Cruise	Station	Date	Latitude	Longitude	Depth (m)	Max. Depth (m)	Temp. (°C)	Salinity	Oxygen (ml/L)	Water masses	εNd	Std (εNd)
REE1.1	PIRATA 2017	REE1	2017-Nov	14°56'26.40"N	38°02'44.40"W	8	5897	26,95	36,2180	4,40	TW	-11,4	0,3
REE1.2			2017-Nov	14°56'26.40"N	38°02'44.40"W	82		22,41	36,7970	4,35	TW	-11,2	0,3
REE1.3			2017-Nov	14°56'26.40"N	38°02'44.40"W	132		16,90	36,3000	2,85	NACW	-10,6	0,3
REE1.4			2017-Nov	14°56'26.40"N	38°02'44.40"W	420		10,01	35,1000	1,91	NACW	-12,0	0,2
REE1.5			2017-Nov	14°56'26.40"N	38°02'44.40"W	525		9,10	35,0120	1,88	NACW	-11,2	0,3
REE1.6			2017-Nov	14°56'26.40"N	38°02'44.40"W	900		6,25	34,8190	2,60	AAIW	-11,2	0,2
REE1.7			2017-Nov	14°56'26.40"N	38°02'44.40"W	4501		2,35	34,8680	5,37	NADW	-11,8	0,3
REE1.8			2017-Nov	14°56'26.40"N	38°02'44.40"W	5845		2,35	34,8510	5,46	NADW	-11,6	0,2
REE 3.1	PIRATA 2017	REE3	2017-Nov	07°59'13.80"N	38°01'44.40"W	7	4221	27,93	35,8960	4,39	TW	-11,3	0,2
REE 3.2			2017-Nov	07°59'13.80"N	38°01'44.40"W	80		17,44	35,8680	2,75	TW	-11,5	0,2
REE 3.3			2017-Nov	07°59'13.80"N	38°01'44.40"W	300		8,90	34,8130	2,68	NACW	-12,1	0,3
REE 3.4			2017-Nov	07°59'13.80"N	38°01'44.40"W	700		6,19	34,6460	2,44	NACW	-10,9	0,3
REE 3.5			2017-Nov	07°59'13.80"N	38°01'44.40"W	850		5,53	34,6390	2,81	NACW	-11,9	0,3
REE 3.6			2017-Nov	07°59'13.80"N	38°01'44.40"W	2490		3,04	34,9370	5,57	AAIW	-12,2	0,3
REE 3.7			2017-Nov	07°59'13.80"N	38°01'44.40"W	3500		2,46	34,8940	5,58	NADW	-12,1	0,1
REE 3.8			2017-Nov	07°59'13.80"N	38°01'44.40"W	4100		2,12	34,8600	5,50	NADW	-12,1	0,5
REE5.1	PIRATA 2017	REE5	2017-Nov	00°02'41.76"N	38°00'05.64"W	7	4448	27,16	36,1970	4,36	TW	-12,3	0,2
REE5.2			2017-Nov	00°02'41.76"N	38°00'05.64"W	135		21,07	36,5260	4,10	SACW	-14,7	0,5
REE5.3			2017-Nov	00°02'41.76"N	38°00'05.64"W	148		16,86	35,8430	3,63	SACW	-13,9	0,4
REE5.4			2017-Nov	00°02'41.76"N	38°00'05.64"W	376		9,48	34,8390	3,17	SACW	-13,0	0,9
REE5.5			2017-Nov	00°02'41.76"N	38°00'05.64"W	721		5,36	34,5070	3,21	AAIW	-11,4	0,2
REE5.6			2017-Nov	00°02'41.76"N	38°00'05.64"W	1780		3,78	35,0000		NADW	-12,6	0,2
REE5.7			2017-Nov	00°02'41.76"N	38°00'05.64"W	2901		2,80	34,9220	5,63	NADW	-12,5	0,2
REE5.8			2017-Nov	00°02'41.76"N	38°00'05.64"W	4431		1,11	34,7480	4,99	AABW	-10,4	0,2

Sample	Cruise	Station	Date	Latitude	Longitude	Depth (m)	Max. Depth (m)	Temp. (°C)	Salinity	Oxygen (ml/L)	Water masses	εNd	Std (εNd)
REE6.1	PIRATA 2017	REE6	2017-Nov	01°59'17.28"S	38°00'15.00"W	7	3166	27,18	36,3470	4,40	TW	-12,9	0,4
REE6.2			2017-Nov	01°59'17.28"S	38°00'15.00"W	127		24,15	36,8480	4,36	TW	-12,1	0,3
REE6.3			2017-Nov	01°59'17.28"S	38°00'15.00"W	156		17,25	35,9070	3,17	SACW	-13,6	0,7
REE6.4			2017-Nov	01°59'17.28"S	38°00'15.00"W	317		8,90	34,7300	3,80	SACW	-12,1	0,2
REE6.5			2017-Nov	01°59'17.28"S	38°00'15.00"W	850		4,76	34,5040	3,49	AAIW	-11,5	0,3
REE6.6			2017-Nov	01°59'17.28"S	38°00'15.00"W	1700		4,11	34,9680	5,26	NADW	-12,9	0,2
REE6.7			2017-Nov	01°59'17.28"S	38°00'15.00"W	2616		2,59	34,9100	5,68	NADW	-12,7	0,2
REE6.8			2017-Nov	01°59'17.28"S	38°00'15.00"W	3146		2,88	34,9280	5,65	NADW	-12,6	0,1
REE7.1	PIRATA 2017	REE7	2017-Dec	08°00'38.16"S	30°37'36.72"W	6	5402	27,25	36,5090	4,34	TW	-12,6	0,3
REE7.2			2017-Dec	08°00'38.16"S	30°37'36.72"W	113		23,77	36,7160	4,23	TW	-13,7	0,2
REE7.3			2017-Dec	08°00'38.16"S	30°37'36.72"W	152		18,49	36,0920	3,06	SACW	-14,0	0,4
REE7.4			2017-Dec	08°00'38.16"S	30°37'36.72"W	375		9,15	34,7990	2,37	SACW	-	-
REE7.5			2017-Dec	08°00'38.16"S	30°37'36.72"W	473		8,03	34,6990	1,92	SACW	-13,0	0,3
REE7.6			2017-Dec	08°00'38.16"S	30°37'36.72"W	833		4,60	34,4550	3,46	AAIW	-11,4	0,2
REE7.7			2017-Dec	08°00'38.16"S	30°37'36.72"W	3579		2,42	34,8930	5,58	NADW	-12,3	0,2
REE7.8			2017-Dec	08°00'38.16"S	30°37'36.72"W	5384		0,67	34,6920	4,83	AABW	-9,1	0,2
REE8.1	PIRATA 2017	REE8	2017-Dec	13°59'18.60"S	32°46'13.80"W	7	4593	27,64	36,9970	4,39	TW	-12,8	0,1
REE8.2			2017-Dec	13°59'18.60"S	32°46'13.80"W	89		24,96	37,2900	4,71	TW	-13,6	0,2
REE8.3			2017-Dec	13°59'18.60"S	32°46'13.80"W	143		23,36	37,1760	4,51	TW	-14,0	0,2
REE8.4			2017-Dec	13°59'18.60"S	32°46'13.80"W	340		11,46	35,0280	3,27	SACW	-12,8	0,2
REE8.5			2017-Dec	13°59'18.60"S	32°46'13.80"W	708		4,55	34,3760	4,24	AAIW	-11,0	0,3
REE8.6			2017-Dec	13°59'18.60"S	32°46'13.80"W	3538		2,47	34,8900	5,57	NADW	-11,8	0,3
REE8.7			2017-Dec	13°59'18.60"S	32°46'13.80"W	4198		1,38	34,7730	5,11	NADW	-10,3	0,2
REE8.8			2017-Dec	13°59'18.60"S	32°46'13.80"W	4573		0,52	34,6830	4,83	AABW	-8,4	0,2
REE10.1	PIRATA 2017	REE10	2018-Jan	21° 00'05.34"S	36°59'50.88"W	6	3996	27,24	37,2230	4,50	TW	-15,0	0,2
REE10.2			2018-Jan	21° 00'05.34"S	36°59'50.88"W	130		22,97	37,1070	4,54	TW	-	-
REE10.3			2018-Jan	21° 00'05.34"S	36°59'50.88"W	510		9,39	34,7350	4,12	SACW	-10,1	0,7

Sample	Cruise	Station	Date	Latitude	Longitude	Depth (m)	Max. Depth (m)	Temp. (°C)	Salinity	Oxygen (ml/L)	Water masses	εNd	Std (εNd)
REE10.4	PIRATA 2017	REE10	2018-Jan	21° 00'05.34"S	36°59'50.88"W	620	3996	7,44	34,5530	3,83	SACW	-	-
REE10.5			2018-Jan	21° 00'05.34"S	36°59'50.88"W	839		4,64	34,3860	4,15	AAIW	-10,4	0,2
REE10.6			2018-Jan	21° 00'05.34"S	36°59'50.88"W	2289		3,09	34,9310	5,50	NADW	-12,3	0,2
REE10.7			2018-Jan	21° 00'05.34"S	36°59'50.88"W	3497		1,85	34,8300	5,28	NADW	-11,1	0,2
REE10.8			2018-Jan	21° 00'05.34"S	36°59'50.88"W	3982		0,51	34,6900	4,81	AABW	-9,1	0,4
REE11.1	PIRATA 2017	REE11	2018-Jan	22°00'02.76"S	38°30'01.68"W	6	3360	26,95	37,0170	4,47	TW		
REE11.2			2018-Jan	22°00'02.76"S	38°30'01.68"W	150		21,61	36,8040	4,65	TW	-15,7	0,6
REE11.3			2018-Jan	22°00'02.76"S	38°30'01.68"W	569		9,08	34,6960	4,28	SACW	-13,9	0,2
REE11.4			2018-Jan	22°00'02.76"S	38°30'01.68"W	756		5,50	34,3720	4,49	SACW	-10,9	0,5
REE11.5			2018-Jan	22°00'02.76"S	38°30'01.68"W	1110		3,50	34,4960	4,12	AAIW	-10,2	0,3
REE11.6			2018-Jan	22°00'02.76"S	38°30'01.68"W	1698		3,86	34,9250	5,16	NADW	-12,8	0,3
REE11.7			2018-Jan	22°00'02.76"S	38°30'01.68"W	2968		2,54	34,8990	5,51	NADW	-11,9	0,3
REE11.8			2018-Jan	22°00'02.76"S	38°30'01.68"W	3347		1,30	34,7760	5,10	AABW	-10,2	0,1
REE13.1	PIRATA 2017	REE13	2018-Jan	23°03'1.80"S	40°53'58.80"W	5	146	25,50	36,9240	4,59	TW	-20,0	0,1
REE13.2			2018-Jan	23°03'1.80"S	40°53'58.80"W	25		24,92	37,0830	4,66	TW	-18,7	0,3
REE13.3			2018-Jan	23°03'1.80"S	40°53'58.80"W	35		23,98	37,2050	4,75	TW	-16,7	0,3
REE13.4			2018-Jan	23°03'1.80"S	40°53'58.80"W	95		21,91	36,9000	4,56	TW	-14,0	0,7
REE13.5			2018-Jan	23°03'1.80"S	40°53'58.80"W	145		19,23	36,3010	4,44	SACW	-14,3	0,3
REE15.1	PIRATA 2017	REE15	2018-Jan	23°02'11.40"S	41°38'04.20"W	7	83	23,93	35,9400	4,84	TW	-18,8	0,4
REE15.2			2018-Jan	23°02'11.40"S	41°38'04.20"W	49		19,66	36,3900	4,45	SACW	-16,3	0,2
REE15.3			2018-Jan	23°02'11.40"S	41°38'04.20"W	65		15,74	35,5950	3,93	SACW	-14,6	0,4
REE15.4			2018-Jan	23°02'11.40"S	41°38'04.20"W	75		14,73	35,5160	3,90	SACW	-	-
REE16.1	PIRATA 2017	REE16	2018-Jan	23°03'23.40"S	42°25'09.60"W	7	75	20,46	36,1340	4,81	SACW	-18,4	0,3
REE16.2			2018-Jan	23°03'23.40"S	42°25'09.60"W	21		18,08	35,9650	5,15	SACW	-16,3	0,2
REE16.3			2018-Jan	23°03'23.40"S	42°25'09.60"W	32		16,30	35,7650	4,20	SACW	-15,7	0,3
REE16.4			2018-Jan	23°03'23.40"S	42°25'09.60"W	68		13,70	35,3110	4,40	SACW	-13,1	0,4

Sample	Cruise	Station	Date	Latitude	Longitude	Depth (m)	Max. Depth (m)	Temp. (°C)	Salinity	Oxygen (ml/L)	Water masses	εNd	Std (εNd)
REE17.1	PIRATA 2018	REE17	2018-Sep	10°14'10.20"S	35°55'23.40"W	10	52	26,50	37,1650	4,04	TW	-13,6	0,1
REE17.2			2018-Sep	10°14'10.20"S	35°55'23.40"W	20		26,32	37,3060	4,03	TW	-14,3	0,2
REE17.3			2018-Sep	10°14'10.20"S	35°55'23.40"W	30		26,25	37,2550	4,05	TW	-14,1	0,3
REE17.4			2018-Sep	10°14'10.20"S	35°55'23.40"W	40		26,09	37,2990	4,06	TW	-14,3	0,3
REE18.1	PIRATA 2018	REE18	2018-Sep	10°14'21.00"S	35°54'43.50"W	10	80	26,36	37,1730	4,02	TW	-13,4	0,3
REE18.2			2018-Sep	10°14'21.00"S	35°54'43.50"W	45		25,88	37,2870	4,03	TW	-13,9	0,3
REE18.3			2018-Sep	10°14'21.00"S	35°54'43.50"W	60		23,63	37,0550	4,01	TW	-13,8	0,3
REE18.4			2018-Sep	10°14'21.00"S	35°54'43.50"W	70		23,63	37,0540	4,01	TW	-14,5	0,3
REE19.1	PIRATA 2018	REE19	2018-Sep	10°14'32.76"S	35°53'58.80"W	10	100	26,40	37,1550	4,03	TW	-13,3	0,1
REE19.2			2018-Sep	10°14'32.76"S	35°53'58.80"W	25		26,23	37,2420	4,03	TW	-14,2	0,2
REE19.3			2018-Sep	10°14'32.76"S	35°53'58.80"W	45		25,89	37,3010	4,07	TW	-10,3	0,1
REE19.4			2018-Sep	10°14'32.76"S	35°53'58.80"W	60		23,54	37,0400	3,99	TW	-15,2	0,3
REE19.5			2018-Sep	10°14'32.76"S	35°53'58.80"W	80		23,21	37,0020	3,94	TW	-15,2	0,3
REE19.6			2018-Sep	10°14'32.76"S	35°53'58.80"W	90		23,03	36,9740	3,93	TW	-14,7	0,3
REE20.1	PIRATA 2018	REE20	2018-Sep	10°14'39.78"S	35°53'34.68"W	10	240	26,33	37,1670	4,05	TW	-14,2	0,2
REE20.3			2018-Sep	10°14'39.78"S	35°53'34.68"W	60		25,76	37,3050	4,07	TW	-14,2	0,2
REE20.2			2018-Sep	10°14'39.78"S	35°53'34.68"W	159		17,88	36,0100	3,94	SACW	-13,1	0,3
REE20.4			2018-Sep	10°14'39.78"S	35°53'34.68"W	189		16,76	35,8000	3,91	SACW	-13,8	0,6
REE20.5			2018-Sep	10°14'39.78"S	35°53'34.68"W	219		16,23	35,7100	3,91	SACW	-18,6	0,2
REE20.6			2018-Sep	10°14'39.78"S	35°53'34.68"W	229		16,25	35,7160	3,91	SACW		
REE21.1	PIRATA 2018	REE21	2018-Sep	10°15'15.48"S	35°52'42.72"W	10	500	26,27	37,1820	4,05	TW	-11,6	0,2
REE21.2			2018-Sep	10°15'15.48"S	35°52'42.72"W	58		25,89	37,3300	4,05	TW	-11,6	0,3
REE21.3			2018-Sep	10°15'15.48"S	35°52'42.72"W	95		23,08	36,9810	3,94	TW	-11,4	0,3
REE21.4			2018-Sep	10°15'15.48"S	35°52'42.72"W	275		14,68	35,4420	3,92	SACW	-	-
REE21.5			2018-Sep	10°15'15.48"S	35°52'42.72"W	450		9,12	34,7330	3,69	SACW	-15,4	0,3
REE21.6			2018-Sep	10°15'15.48"S	35°52'42.72"W	480		8,61	34,6740	3,70	SACW	-12,3	0,3
REE21.7			2018-Sep	10°15'15.48"S	35°52'42.72"W	490		8,53	34,6660	3,69	SACW	-13,6	0,1

Sample	Cruise	Station	Date	Latitude	Longitude	Depth (m)	Max. Depth (m)	Temp. (°C)	Salinity	Oxygen (ml/L)	Water masses	εNd	Std (εNd)
REE22.1	PIRATA 2018	REE22	2018-Sep	10°17'04.80"S	35°50'39.00"W	10	1230	26,24	37,1340	4,07	TW	-13,4	0,3
REE22.2			2018-Sep	10°17'04.80"S	35°50'39.00"W	70		25,27	37,2730	4,05	TW	-13,8	0,2
REE22.3			2018-Sep	10°17'04.80"S	35°50'39.00"W	110		22,83	36,9620	3,88	TW	-14,7	0,2
REE22.4			2018-Sep	10°17'04.80"S	35°50'39.00"W	360		11,25	34,9760	3,84	SACW	-	-
REE22.5			2018-Sep	10°17'04.80"S	35°50'39.00"W	970		4,00	34,4760	3,59	AAIW	-11,2	0,3
REE22.6			2018-Sep	10°17'04.80"S	35°50'39.00"W	1126		3,94	34,5900	3,58	AAIW	-	-
REE22.7			2018-Sep	10°17'04.80"S	35°50'39.00"W	1210		4,07	34,6730	3,62	AAIW	-12,0	0,2
REE22.8			2018-Sep	10°17'04.80"S	35°50'39.00"W	1220		4,07	34,6730	3,62	AAIW	-13,6	1,0
REE23.1	PIRATA 2018	REE23	2018-Oct	11°7'40.80"S	34°44'06.60"W	7	4342	26,46	36,6470	4,05	TW	-12,7	0,3
REE23.2			2018-Oct	11°7'40.80"S	34°44'06.60"W	118		25,27	37,2350	4,06	TW	-13,3	0,3
REE23.3			2018-Oct	11°7'40.80"S	34°44'06.60"W	148		22,76	36,8670	3,92	TW	-	-
REE23.4			2018-Oct	11°7'40.80"S	34°44'06.60"W	425		8,34	34,7340	1,89	SACW	-13,5	0,8
REE23.5			2018-Oct	11°7'40.80"S	34°44'06.60"W	772		4,35	34,4320	3,51	AAIW	-11,3	0,3
REE23.6			2018-Oct	11°7'40.80"S	34°44'06.60"W	1800		3,86	34,9720	4,82	NADW	-13,6	0,3
REE23.7			2018-Oct	11°7'40.80"S	34°44'06.60"W	2900		2,92	34,9330	4,91	NADW	-11,9	0,3
REE23.8			2018-Oct	11°7'40.80"S	34°44'06.60"W	4164		1,10	34,7580	4,45	AABW	-10,0	0,1
REE23.9			2018-Oct	11°7'40.80"S	34°44'06.60"W	4219		1,09	34,7560	4,45	AABW	-9,6	0,3
REE23.10			2018-Oct	11°7'40.80"S	34°44'06.60"W	4232		1,09	34,7561	4,44	AABW	-9,8	0,1
REE24.1	PIRATA 2018	REE24	2018-Oct	05°21'43.20"S	35°25'09.00"W	7	4475	26,77	36,3481	4,02	TW	-12,9	0,3
REE24.2			2018-Oct	05°21'43.20"S	35°25'09.00"W	90		26,02	36,4809	3,97	TW	-13,3	0,2
REE24.3			2018-Oct	05°21'43.20"S	35°25'09.00"W	397		7,71	34,6475	2,62	SACW	-10,8	0,6
REE24.4			2018-Oct	05°21'43.20"S	35°25'09.00"W	822		4,69	34,4761	3,03	AAIW	-11,9	0,2
REE24.5			2018-Oct	05°21'43.20"S	35°25'09.00"W	1300		4,53	34,8976	3,98	AAIW	-11,4	0,3
REE24.6			2018-Oct	05°21'43.20"S	35°25'09.00"W	2500		2,94	34,9330	4,90	NADW	-12,4	0,3
REE24.7			2018-Oct	05°21'43.20"S	35°25'09.00"W	3598		2,52	34,9106	5,06	NADW	-11,1	0,2
REE24.8			2018-Oct	05°21'43.20"S	35°25'09.00"W	4396		1,08	34,7530	4,45	AABW	-10,1	0,5
REE24.9			2018-Oct	05°21'43.20"S	35°25'09.00"W	4457		1,02	34,7461	4,43	AABW	-12,5	0,2
REE24.10			2018-Oct	05°21'43.20"S	35°25'09.00"W	4465		1,02	34,7460	4,43	AABW	-10,5	0,2

Sample	Cruise	Station	Date	Latitude	Longitude	Depth (m)	Max. Depth (m)	Temp. (°C)	Salinity	Oxygen (ml/L)	Water masses	εNd	Std (εNd)
REE26.1	SAMBAR 2019	REE26	2019-Jun	33°15'00.27"S	52°38'51.84"W	3	13	16,90	29,5664	5,23	SW	-8,7	0,2
REE26.2			2019-Jun	33°15'00.27"S	52°38'51.84"W	12		16,82	29,6205	5,16	SW	-8,1	0,2
REE27.1	SAMBAR 2019	REE27	2019-Jun	33°42'35.04"S	52°12'04.32"W	3	73	15,86	27,7086	5,38	SW	-7,1	0,2
REE27.2			2019-Jun	33°42'35.04"S	52°12'04.32"W	50		19,90	34,6130	3,84	SW	-5,1	0,1
REE27.3			2019-Jun	33°42'35.04"S	52°12'04.32"W	68		20,33	34,9373	3,82	SW	-6,8	0,2
REE28.1	SAMBAR 2019	REE28	2019-Jun	34°18'44.10"S	51°40'32.88"W	5	380	21,14	35,3909	4,67	SW	-9,6	0,2
REE28.2			2019-Jun	34°18'44.10"S	51°40'32.88"W	180		15,36	35,5684	4,23	SACW	-12,2	0,5
REE28.3			2019-Jun	34°18'44.10"S	51°40'32.88"W	300		11,74	35,0499	4,33	SACW	-9,5	0,3
REE28.4			2019-Jun	34°18'44.10"S	51°40'32.88"W	375		9,01	34,6959	4,37	SACW	-9,3	0,3
REE30.1	SAMBAR 2019	REE30	2019-Jun	34°24'22.02"S	51°35'05.82"W	3	975	20,82	35,2169	4,77	SW	-9,7	0,2
REE30.2			2019-Jun	34°24'22.02"S	51°35'05.82"W	100		20,51	36,2841	3,83	SW	-9,1	0,2
REE30.3			2019-Jun	34°24'22.02"S	51°35'05.82"W	400		7,26	34,4959	4,55	SACW	-9,9	0,3
REE30.4			2019-Jun	34°24'22.02"S	51°35'05.82"W	600		4,82	34,2929	4,82	AAIW	-8,9	0,3
REE30.5			2019-Jun	34°24'22.02"S	51°35'05.82"W	900		3,44	34,3435	4,36	AAIW	-10,7	0,4
REE30.6			2019-Jun	34°24'22.02"S	51°35'05.82"W	970		3,38	34,3562	4,31	AAIW	-9,4	0,2
REE31.1	SAMBAR 2019	REE31	2019-Jun	34°30'00.00"S	46°53'38.40"W	3	4740	19,53	36,1800	4,84	SW	-11,1	0,3
REE31.2			2019-Jun	34°30'00.00"S	46°53'38.40"W	300		15,45	35,7065	4,64	SACW	-12,0	0,3
REE31.3			2019-Jun	34°30'00.00"S	46°53'38.40"W	800		5,57	34,3086	5,00	AAIW	-9,6	0,3
REE31.4			2019-Jun	34°30'00.00"S	46°53'38.40"W	1500		2,49	34,5084	3,92	AAIW	-8,3	0,3
REE31.5			2019-Jun	34°30'00.00"S	46°53'38.40"W	2500		3,17	34,9043	5,09	NADW	-10,8	0,8
REE31.6			2019-Jun	34°30'00.00"S	46°53'38.40"W	3500		1,45	34,7512	4,59	AABW	-9,4	0,2
REE31.7			2019-Jun	34°30'00.00"S	46°53'38.40"W	4500		0,27	34,6643	4,69	AABW	-6,2	0,2
REE31.8			2019-Jun	34°30'00.00"S	46°53'38.40"W	4730		0,26	34,6613	4,67	AABW	-9,9	0,1

Sample	Cruise	Station	Date	Latitude	Longitude	Depth (m)	Max. Depth (m)	Temp. (°C)	Salinity	Oxygen (ml/L)	Water masses	εNd	Std (εNd)
AREE1.1	PROVOCCAR 2020	AREE1	2020-Feb	61°52'14.23"S	54°31'08.22"W	5	631	0,90	34,2542	8,03	mCDW	-7,3	0,3
AREE1.2			2020-Feb	61°52'14.23"S	54°31'08.22"W	100		0,07	34,3981	7,52	mCDW	-8,3	0,1
AREE1.3			2020-Feb	61°52'14.23"S	54°31'08.22"W	250		-0,46	34,4673	6,98	LSSW	-8,3	0,2
AREE1.4			2020-Feb	61°52'14.23"S	54°31'08.22"W	500		-0,50	34,4917	6,82	LSSW	-8,9	0,2
AREE1.5			2020-Feb	61°52'14.23"S	54°31'08.22"W	649		-0,48	34,5203	6,56	LSSW	-8,6	0,2
AREE2.1	PROVOCCAR 2020	AREE2	2020-Feb	61°25'51.24"S	52°34'15.78"W	5	509	0,10	34,1285	8,13	-	-8,5	0,1
AREE2.2			2020-Feb	61°25'51.24"S	52°34'15.78"W	100		-0,31	34,3202	7,62	-	-8,4	0,2
AREE2.3			2020-Feb	61°25'51.24"S	52°34'15.78"W	250		-0,52	34,4888	6,57	-	-9,1	0,2
AREE2.4			2020-Feb	61°25'51.24"S	52°34'15.78"W	508		-0,40	34,5536	6,18	-	-8,4	0,2
AREE3.1	PROVOCCAR 2020	AREE3	2020-Feb	61°06'26.70"S	51°33'38.70"W	5	960	0,26	33,9044	8,26	-	-8,3	0,3
AREE3.2			2020-Feb	61°06'26.70"S	51°33'38.70"W	101		-0,49	34,3962	7,11	-	-8,2	0,2
AREE3.3			2020-Feb	61°06'26.70"S	51°33'38.70"W	251		-0,54	34,5051	6,57	-	-	-
AREE3.4			2020-Feb	61°06'26.70"S	51°33'38.70"W	502		-0,35	34,5625	6,10	-	-8,5	0,3
AREE3.5			2020-Feb	61°06'26.70"S	51°33'38.70"W	749		-0,01	34,6200	5,65	-	-9,0	0,3
AREE3.6			2020-Feb	61°06'26.70"S	51°33'38.70"W	940		-0,04	34,6302	5,62	-	-9,1	0,3
AREE4.1	PROVOCCAR 2020	AREE4	2020-Feb	60°41'24.42"S	50°10'58.91"W	5	1447	1,54	33,9383	8,29	-	-9,2	0,2
AREE4.2			2020-Feb	60°41'24.42"S	50°10'58.91"W	205		-0,87	34,4882	6,74	-	-8,3	0,5
AREE4.3			2020-Feb	60°41'24.42"S	50°10'58.91"W	550		0,21	34,6341	5,44	-	-9,2	0,1
AREE4.4			2020-Feb	60°41'24.42"S	50°10'58.91"W	750		0,07	34,6413	5,51	-	-8,8	0,2
AREE4.5			2020-Feb	60°41'24.42"S	50°10'58.91"W	999		0,04	34,6514	5,48	-	-8,9	0,1
AREE4.6			2020-Feb	60°41'24.42"S	50°10'58.91"W	1348		-0,13	34,6488	5,60	-	-8,9	0,2
AREE5.1	PROVOCCAR 2020	AREE5	2020-Feb	60°31'10.59"S	48°59'50.94"W	5	1468	1,76	34,0163	8,27	-	-	-
AREE5.2			2020-Feb	60°31'10.59"S	48°59'50.94"W	149		-0,95	34,4140	7,34	-	-9,1	0,2
AREE5.3			2020-Feb	60°31'10.59"S	48°59'50.94"W	250		-0,55	34,5308	6,13	-	-9,1	0,2
AREE5.4			2020-Feb	60°31'10.59"S	48°59'50.94"W	500		0,48	34,6661	5,14	-	-9,5	0,2
AREE5.5			2020-Feb	60°31'10.59"S	48°59'50.94"W	1000		0,18	34,6670	5,27	-	-9,0	0,1
AREE5.6			2020-Feb	60°31'10.59"S	48°59'50.94"W	1473		-0,15	34,6508	5,62	-	-9,2	0,2

Sample	Cruise	Station	Date	Latitude	Longitude	Depth (m)	Max. Depth (m)	Temp. (°C)	Salinity	Oxygen (ml/L)	Water masses	εNd	Std (εNd)
AREE6.1	PROVOCCAR 2020	AREE6	2020-Feb	60°30'36.60"S	47°44'46.80"W	7	1690	1,94	33,8694	8,24	-	-8,4	0,2
AREE6.2			2020-Feb	60°30'36.60"S	47°44'46.80"W	101		-0,29	34,3367	7,51	-	-8,6	0,1
AREE6.3			2020-Feb	60°30'36.60"S	47°44'46.80"W	198		-0,56	34,4883	6,53	-	-9,3	0,2
AREE6.4			2020-Feb	60°30'36.60"S	47°44'46.80"W	604		0,53	34,6748	5,11	-	-8,8	0,1
AREE6.5			2020-Feb	60°30'36.60"S	47°44'46.80"W	999		0,25	34,6700	5,19	-	-8,8	0,2
AREE6.6			2020-Feb	60°30'36.60"S	47°44'46.80"W	1706		0,10	34,6653	5,32	-	-9,0	0,2
AREE7.1	PROVOCCAR 2020	AREE7	2020-Feb	60°30'33.87"S	46°58'29.22"W	5	219	1,17	33,7378	8,29	-	-8,5	0,1
AREE7.2			2020-Feb	60°30'33.87"S	46°58'29.22"W	50		0,54	33,8427	8,14	-	-8,8	0,2
AREE7.3			2020-Feb	60°30'33.87"S	46°58'29.22"W	100		-0,52	34,0710	7,67	-	-	-
AREE7.4			2020-Feb	60°30'33.87"S	46°58'29.22"W	215		-0,45	34,4411	6,25	-	-8,5	0,3
AREE8.1	PROVOCCAR 2020	AREE8	2020-Feb	60°00'17.82"S	49°29'24.72"W	5	3750	2,34	34,2118	8,00	mCDW	-8,7	0,1
AREE8.2			2020-Feb	60°00'17.82"S	49°29'24.72"W	100		-0,13	34,4258	7,47	LSSW	-9,1	0,2
AREE8.3			2020-Feb	60°00'17.82"S	49°29'24.72"W	250		-0,55	34,5048	6,51	LSSW	-9,1	0,1
AREE8.4			2020-Feb	60°00'17.82"S	49°29'24.72"W	502		0,12	34,6169	5,49	CDW	-9,0	0,3
AREE8.5			2020-Feb	60°00'17.82"S	49°29'24.72"W	1000		0,18	34,6524	5,37	CDW	-9,0	0,1
AREE8.6			2020-Feb	60°00'17.82"S	49°29'24.72"W	2000		-0,02	34,6550	5,51	HSSW	-9,2	0,3
AREE8.7			2020-Feb	60°00'17.82"S	49°29'24.72"W	2950		-0,08	34,6564	5,58	HSSW	-9,2	0,1
AREE8.8			2020-Feb	60°00'17.82"S	49°29'24.72"W	3782		-0,19	34,6497	5,75	HSSW	-9,4	0,1
AREE11.1	PROVOCCAR 2020	AREE11	2020-Feb	64°43'37.17"S	63°04'31.74"W	5	299	1,01	33,5813	7,19	mCDW	-5,9	0,1
AREE11.2			2020-Feb	64°43'37.17"S	63°04'31.74"W	75		0,65	34,1915	5,68	mCDW	-6,8	0,1
AREE11.3			2020-Feb	64°43'37.17"S	63°04'31.74"W	150		0,73	34,3891	5,07	mCDW	-6,6	0,2
AREE11.4			2020-Feb	64°43'37.17"S	63°04'31.74"W	305		0,57	34,5110	4,92	mCDW	-7,0	0,2
AREE12.1	PROVOCCAR 2020	AREE12	2020-Feb	64°23'24.27"S	62°59'59.10"W	5	459	1,28	33,4272	7,05	mCDW	-3,3	0,1
AREE12.2			2020-Feb	64°23'24.27"S	62°59'59.10"W	100		0,46	34,2448	5,74	mCDW	-5,8	0,3
AREE12.3			2020-Feb	64°23'24.27"S	62°59'59.10"W	250		0,98	34,5917	4,57	mCDW	-7,0	0,1
AREE12.4			2020-Feb	64°23'24.27"S	62°59'59.10"W	463		1,44	34,6904	4,06	mCDW	-7,2	0,3

Sample	Cruise	Station	Date	Latitude	Longitude	Depth (m)	Max. Depth (m)	Temp. (°C)	Salinity	Oxygen (ml/L)	Water masses	εNd	Std (εNd)
AREE13.1	PROVOCCAR 2020	AREE13	2020-Feb	64°34'20.88"S	62°29'57.60"W	5	734	1,32	33,6568	7,26	mCDW	-5,9	0,3
AREE13.2			2020-Feb	64°34'20.88"S	62°29'57.60"W	74		0,62	34,2511	5,50	mCDW	-6,9	0,2
AREE13.3			2020-Feb	64°34'20.88"S	62°29'57.60"W	250		-0,23	34,4834	5,69	DSW	-7,5	0,3
AREE13.4			2020-Feb	64°34'20.88"S	62°29'57.60"W	741		-0,51	34,5333	5,87	DSW	-6,7	0,2
AREE14.1	PROVOCCAR 2020	AREEE14	2020-Mar	64°22'14.64"S	61°44'09.48"W	5	546	1,23	33,6834	7,08	mCDW	-5,2	0,4
AREE14.2			2020-Mar	64°22'14.64"S	61°44'09.48"W	48		0,57	34,1351	5,94	mCDW	-6,2	0,1
AREE14.3			2020-Mar	64°22'14.64"S	61°44'09.48"W	148		-0,12	34,3957	6,26	DSW	-9,0	0,3
AREE14.4			2020-Mar	64°22'14.64"S	61°44'09.48"W	363		-0,27	34,5057	5,72	DSW	-6,8	0,3
AREE14.5			2020-Mar	64°22'14.64"S	61°44'09.48"W	538		-0,48	34,5294	5,86	DSW	-7,6	0,2
AREE15.1	PROVOCCAR 2020	AREE15	2020-Mar	64°09'49.26"S	61°23'51.36"W	5	583	1,46	33,5025	7,36	mCDW	-5,6	0,3
AREE15.2			2020-Mar	64°09'49.26"S	61°23'51.36"W	100		0,05	34,3122	6,35	mCDW	-6,9	0,1
AREE15.3			2020-Mar	64°09'49.26"S	61°23'51.36"W	300		-0,07	34,5106	5,54	DSW	-7,4	0,3
AREE15.4			2020-Mar	64°09'49.26"S	61°23'51.36"W	572		-0,41	34,5268	5,76	DSW	-7,5	0,1
AREE18.1	PROVOCCAR 2020	AREE18	2020-Mar	62°43'31.68"S	59°21'57.60"W	5	1444	1,34	34,1274	7,56	mCDW	-8,0	0,4
AREE18.2			2020-Mar	62°43'31.68"S	59°21'57.60"W	250		-0,64	34,5069	6,31	DSW	-7,2	0,2
AREE18.3			2020-Mar	62°43'31.68"S	59°21'57.60"W	750		-0,93	34,5545	6,08	DSW	-8,1	0,2
AREE18.4			2020-Mar	62°43'31.68"S	59°21'57.60"W	1428		-1,46	34,5535	6,57	DSW	-8,2	0,5
AREE17.1	PROVOCCAR 2020	AREE17	2020-Mar	62°27'21.72"S	58°04'35.88"W	5	1885	2,29	34,1828	7,52	mCDW	-7,0	0,2
AREE17.2			2020-Mar	62°27'21.72"S	58°04'35.88"W	100		-0,47	34,4189	6,74	DSW	-7,5	0,2
AREE17.3			2020-Mar	62°27'21.72"S	58°04'35.88"W	600		-1,01	34,5484	6,22	DSW	-8,1	0,2
AREE17.4			2020-Mar	62°27'21.72"S	58°04'35.88"W	1000		-1,35	34,5509	6,54	DSW	-7,7	0,2
AREE17.5			2020-Mar	62°27'21.72"S	58°04'35.88"W	1885		-1,50	34,5613	6,57	DSW	-7,1	0,3
AREE10.1	PROVOCCAR 2020	AREE10	2020-Feb	62°08'18.33"S	56°48'42.00"W	5	817	2,28	34,1471	7,56	mCDW	-6,9	0,2
AREE10.2			2020-Feb	62°08'18.33"S	56°48'42.00"W	99		0,08	34,3713	6,74	mCDW	-7,1	0,2
AREE10.3			2020-Feb	62°08'18.33"S	56°48'42.00"W	350		-0,72	34,5272	6,19	DSW	-8,0	0,3
AREE10.4			2020-Feb	62°08'18.33"S	56°48'42.00"W	500		-0,94	34,5310	6,28	DSW	-7,6	0,3
AREE10.5			2020-Feb	62°08'18.33"S	56°48'42.00"W	820		-1,26	34,5491	6,43	DSW	-7,3	0,2

Sample	Cruise	Station	Date	Latitude	Longitude	Depth (m)	Max. Depth (m)	Temp. (°C)	Salinity	Oxygen (ml/L)	Water masses	εNd	Std (εNd)
AREE9.1	PROVOCCAR 2020	AREE19	2020-Feb	61°50'22.41"S	55°31'15.06"W	5	1842	-0,82	34,5242	6,17	DSW	-6,2	0,2
AREE9.2			2020-Feb	61°50'22.41"S	55°31'15.06"W	100		-0,82	34,5242	6,17	DSW	-6,3	0,2
AREE9.3			2020-Feb	61°50'22.41"S	55°31'15.06"W	499		-0,82	34,5242	6,17	DSW	-8,1	0,2
AREE9.4			2020-Feb	61°50'22.41"S	55°31'15.06"W	999		-0,89	34,5435	6,08	DSW	-8,1	0,1
AREE9.5			2020-Feb	61°50'22.41"S	55°31'15.06"W	1826		-0,88	34,5528	4,47	DSW	-8,1	0,2
AREE16.1	PROVOCCAR 2020	AREE16	2020-Mar	62°04'47.46"S	57°31'55.26"W	5	145	1,76	34,1134	7,42	mCDW	-4,8	0,2
AREE16.2			2020-Mar	62°04'47.46"S	57°31'55.26"W	75		1,16	34,2215	6,94	mCDW	-5,1	0,2
AREE16.3			2020-Mar	62°04'47.46"S	57°31'55.26"W	143		0,89	34,2855	6,59	mCDW	-5,7	0,2
AREE19.1	PROVOCCAR 2020	AREE19	2020-Mar	62°39'21.42"S	56°53'13.26"W	5	240	-0,43	34,1164	7,57	DSW	-8,8	0,2
AREE19.2			2020-Mar	62°39'21.42"S	56°53'13.26"W	100		-1,19	34,3683	6,94	DSW	-8,4	0,2
AREE19.3			2020-Mar	62°39'21.42"S	56°53'13.26"W	235		-1,23	34,4214	6,69	DSW	-8,7	0,2
AREE20.1	PROVOCCAR 2020	AREE20	2020-Mar	63°16'42.66"S	59°23'09.96"W	5	786	0,71	34,1936	7,51	mCDW	-7,4	0,1
AREE20.2			2020-Mar	63°16'42.66"S	59°23'09.96"W	75		-0,08	34,2803	7,26	mCDW	-6,9	0,4
AREE20.3			2020-Mar	63°16'42.66"S	59°23'09.96"W	250		-0,92	34,4440	6,56	DSW	-8,1	0,2
AREE20.4			2020-Mar	63°16'42.66"S	59°23'09.96"W	650		-0,84	34,5455	6,00	DSW	-8,4	0,2
AREE20.5			2020-Mar	63°16'42.66"S	59°23'09.96"W	778		-0,96	34,5427	6,13	DSW	-8,4	0,2
AREE21.1	PROVOCCAR 2020	AREE21	2020-Mar	63°08'01.14"S	58°12'53.52"W	5	451	0,15	34,2608	7,46	mCDW	-7,7	0,2
AREE21.2			2020-Mar	63°08'01.14"S	58°12'53.52"W	150		-0,80	34,3722	6,92	DSW	-7,9	0,2
AREE21.3			2020-Mar	63°08'01.14"S	58°12'53.52"W	250		-0,96	34,4425	6,52	DSW	-8,5	0,2
AREE21.4			2020-Mar	63°08'01.14"S	58°12'53.52"W	450		-0,88	34,5080	6,15	DSW	-8,4	0,2

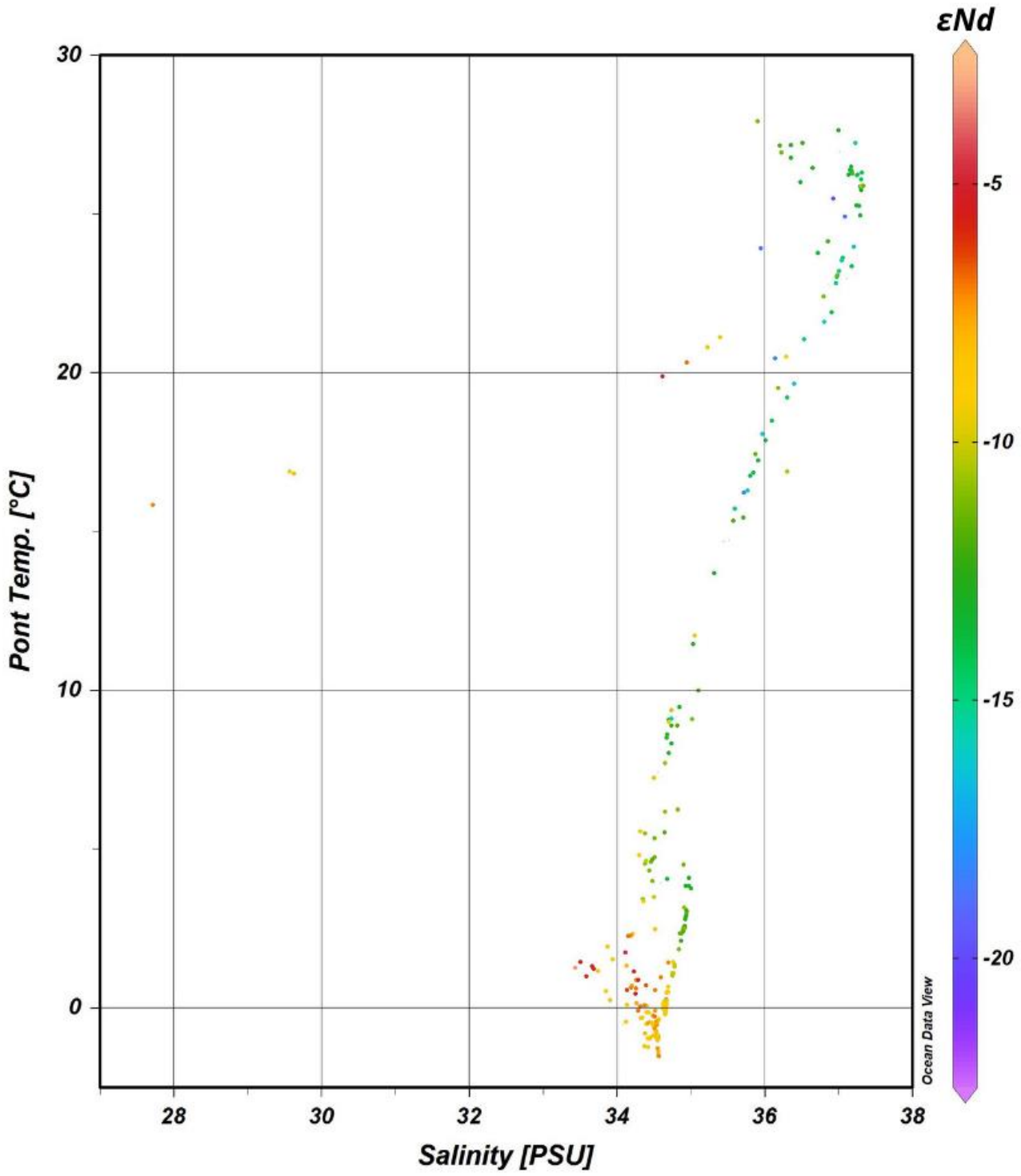

Figure S1 Potential temperature-salinity diagram of all samples from Antarctic and Atlantic stations. The color scale represents the εNd value of each sample.

Capítulo 4:

Pollutants in the South Atlantic Ocean: Sources, Knowledge Gaps and Perspectives for the Decade of Ocean Science

frontiers in Marine Science

REVIEW
published: 25 March 2021
doi: 10.3389/fmars.2021.644569

Pollutants in the South Atlantic Ocean: Sources, Knowledge Gaps and Perspectives for the Decade of Ocean Science

Vanessa Hatje[1,2], Raiza L. B. Andrade[1,2], Carina Costa de Oliveira[3], Andrei Polejack[4,5] and Thandiwe Gxaba[6]*

[1] Centro Interdisciplinar de Energia e Ambiente (CIEnAm), Universidade Federal da Bahia, Salvador, Brazil, [2] Instituto de Química, Universidade Federal da Bahia, Salvador, Brazil, [3] Grupo de Estudos em Direito, Recursos Naturais e Sustentabilidade (GERN), Faculdade de Direito, Universidade de Brasília, Brasília, Brazil, [4] Sasakawa Global Ocean Institute, World Maritime University, Malmö, Sweden, [5] Ministério da Ciência, Tecnologia e Inovações, Brasília, Brazil, [6] Benguela Current Convention (BCC), Swakopmund, Namibia

The current manuscript presents the main issues related to the "Clean Ocean" outcome that arose from the Regional South Atlantic (SA) Planning Workshop for the UN Decade of Ocean Science and five Brazilian Regional Planning Workshops. An interdisciplinary and *trans*-sectoral group constituted by the academia, non-governmental agencies, the private sector, decision-makers, the navy, and local communities discussed the main anthropogenic drivers compromising the current environmental status of the SA and its ecological services, and debated the main research gaps, priorities and needs for improving technical and structural capacities in order to roadmap the Brazilian actions for the Decade of Ocean Science. The aim of this review is to contribute to a social solution-driven understanding of the ocean ecosystems, to create conditions to promote sustainable development and to secure a clean, healthy ocean. We are proposing a list of actions to be implemented by the Decade of Ocean Science that will have the pivotal role to promote technical and scientific capacity development, increase research infrastructure and institutional frameworks, develop national public policies aimed at reducing the input of pollutants and management of impacts, and warranting food security and ecosystem health. The earlier the actions in controlling pollutants are implemented, along with the identification of key sources and prevention of crossing of thresholds will help to avert worst-case scenarios, reducing the socio-economic disparities of impacts across nations and social groups and supporting the sustainable development of a pollutant-free ocean.

Keywords: UN Decade of Ocean Science, pollution, anthropogenic impacts, SGD 14, research gaps, capacity building, South Atlantic, contaminant sources

OPEN ACCESS

Edited by:
Mario Barletta, Independent Researcher, Recife, Brazil

Reviewed by:
Begoña Jiménez, Consejo Superior de Investigaciones Científicas (CSIC), Spain
Stephen John Montague Blaber, Consejo Superior de Investigaciones Científicas (CSIC), Spain

****Correspondence:***
Vanessa Hatje
vhatje@ufba.br

Specialty section:
This article was submitted to Marine Pollution, a section of the journal Frontiers in Marine Science

Received: *21 December 2020*
Accepted: *18 February 2021*
Published: *25 March 2021*

Citation:
Hatje V, Andrade RLB, Oliveira CC, Polejack A and Gxaba T (2021) Pollutants in the South Atlantic Ocean: Sources, Knowledge Gaps and Perspectives for the Decade of Ocean Science. Front. Mar. Sci. 8:644569. doi: 10.3389/fmars.2021.644569

INTRODUCTION

The ocean is vast, highly dynamic, and harbors a large reservoir of unique diversity. It sustains life and provides numerous ecosystem services including food provision (e.g., food security), climate regulation (e.g., carbon sequestration and temperature regulation), habitats services, cultural services (e.g., recreation and aesthetic experience), and biogeochemical cycling of nutrients,

connecting the coastal, surface and benthic realms of the ocean (e.g., nutrient regeneration), promoting the sequestration of carbon (Hattam et al., 2015).

The quality and resilience of ocean ecosystems, nevertheless, are in peril from climate change and increased anthropogenic threats as thresholds are passed (Steffen et al., 2007; Selkoe et al., 2015). The provision of goods and services for 7.8 billion people is causing local and global environmental changes including habitat loss, pollution, harmful algal blooms (HABs), the introduction of invasive species, and climate change, causing cumulative and synergic effects that have deleterious consequences. By the year 2050 human population will likely be nearly 10 billion, a 30% increase over current population estimates (UN, 2019). The demands for food, fuel, water, and sanitation will only continue to rise. In order to guarantee food security for populations, the use of fertilizers will have to increase in developing countries. At the same time, urbanization and lack of sewage treatment will lead to an escalation in nutrient discharge to surface waters. Thus, by 2050 the HABs risk is expected to spread in developing countries of South America and Africa (Glibert, 2020). There is no doubt that ocean degradation, pollution, and human health are inextricably linked, causing adverse health and social consequences for even remote human populations (Knap et al., 2002; Weihe et al., 2016). However, the impacts of ocean pollution on human health are only beginning to be understood.

Globally, the ocean is being treated as a waste sink, mostly due to human erroneous propensity to view dilution as the solution to pollution (Knowlton, 2004). While high-income countries treat ∼70% of the municipal and industrial wastewater, in low-income countries only 8% undergoes any treatment, which leads to an estimation that over 80% of all wastewater is globally discharged without any treatment (WWAP, 2017) and may end up in the ocean. Human developments in terms of agriculture, industries, and technologies have been at the price of degrading the marine environments, especially near land-based sources. In that sense, trace metals (e.g., lead – Pb, zinc – Pb, copper – Cu, and mercury – Hg) are used in many industrial processes that, inappropriately discarded, have led to contamination of the coastal and open ocean ecosystems. Similarly, the development of the organic chemistry promoted the synthesis of a diverse group of new substances including plasticizers, pesticides, brominated and organophosphate flame retardants, among others. Many of those substances and their by-products have proved to have a wide range of hazardous side effects. For instance, the resultant contaminant toxicity (e.g., methyl mercury; persistent organic pollutants), microbial pollution (e.g., cholera and antimicrobial resistance), and natural toxins (e.g., from HABs) can cause illness and death by exposure through seafood consumption or via contact with seawater (Depledge and Bird, 2009; Weihe et al., 2016; Bell et al., 2017; Miranda et al., 2021). Integrated impacts of pollutants may be further exacerbated by negative feedback loops, like microplastics carrying pathogenic bacteria, antimicrobial resistance genes, and endocrine−disrupting chemicals entering the food web (Fleming et al., 2019).

The ocean plays a key role in the achievement of the 2030 Agenda for the Sustainable Development, in particular through the Sustainable Development Goal (SGD) 14 – Life below water (Le Blanc et al., 2017). The urgent need to foster and apply ocean science in supporting the shift of society onto a sustainable and resilient path caused the United Nations (UN) to proclaim the Decade of Ocean Science for Sustainable Development (hereafter the Decade) from 2021 to 2030 (IOC-UNESCO, 2020b). The main objectives of the Decade are to produce interdisciplinary science to provide social solution-driven understanding of the ocean ecosystems, stop degradation, and create conditions to promote sustainable development (Ryabinin et al., 2019). The UN expect to achieve a major change in the knowledge and management of the ocean by adopting a Global System Approach, generating seven interrelated societal outcomes (**Table 1**). Outcome 1 is a "Clean Ocean," where sources of pollution are identified and reduced or removed in an efficient manner. The concept of a "Clean Ocean" arose during the 1st Global Planning Meeting of the Decade and was defined as an ocean where inputs of all contaminants and pollutants are minimized and do not have adverse effects on physical, chemical and biological processes, ecosystem functions and services.

Despite the efforts of the international community in large research projects such as GEOTRACES[1], IMBER[2], and SOLAS[3] that vastly expanded the amount of available data, the knowledge of the ocean systems is still limited and unevenly distributed. The South Atlantic (SA) Ocean, region between

[1]http://www.geotraces.org/

[2]http://imber.info/about/what-is-imber/

[3]https://www.solas-int.org

TABLE 1 | The societal outcomes for the UN Decade of Ocean Science for Sustainable Development.

Societal outcome	
Clean ocean	A clean ocean whereby sources of pollution are identified, quantified and reduced and pollutants removed from the ocean
Health and resilient ocean	A healthy and resilient ocean whereby marine ecosystems are mapped and protected, multiple impacts, including climate change, are measured and reduced, and provision of ocean ecosystem services is maintained
Predicted ocean	A predicted ocean whereby society has the capacity to understand current and future ocean conditions, forecast their change and impact on human wellbeing and livelihoods
Safe ocean	A safe ocean whereby human communities are protected from ocean hazards and where the safety of operations at sea and on the coast is ensured
Sustainably ocean	A sustainably harvested and productive ocean ensuring the provision of food supply and alternative livelihoods
Transparent and accessible ocean	A transparent and accessible ocean whereby all nations, stakeholders and citizens have access to ocean data and information, technologies and have the capacities to inform their decisions
Inspiring and engaging ocean	An inspiring and engaging ocean where society understands and values the ocean in relation to human wellbeing and sustainable development.

the Equator and the Southern Ocean at 60°S is, for instance, less researched than the Northern Atlantic and the Pacific. This may be due to discrepancies in infrastructure and scientific and institutional capabilities. For example, the measurements for the elements Hg and Pb, important contaminants oceanwide (Boyle et al., 2014; Lamborg et al., 2014b; Hatje et al., 2018; Anderson, 2020), are less abundant in the South Atlantic. Consequently, there is a lack of data and hence knowledge to understand natural processes, to mitigate marine adverse impacts, to inform policy makers, and to support South Atlantic Ocean governance.

National ocean science research in the SA region, in many cases, are still modest and incremental. Partly because access to research vessels and large equipment is limited, costly, and complex to afford and maintain. Although the number of Atlantic researchers is similar in the South (731) and the North Atlantic (807) (IOC-UNESCO, 2017), scientific publications are much lower in the South (Inniss et al., 2017) and have a weak level of international collaboration, as seen by the low share of international co-authored articles (IOC-UNESCO, 2020a). Despite large coastlines in the region (e.g., Brazil and South Africa), and the diversity of ecosystems therein (mangroves, seagrasses, coral reefs, islands, major rivers, bays, and estuaries), marine and ocean research institutes are few. In addition, a large number of traditional coastal communities have a strong reliance on marine-based-diets that are safe for human consumption (Foltz et al., 2019), especially in low-income countries. Marine research capabilities, nevertheless, are limited and thus constrain the efficiency in fostering transnational, interdisciplinary research to contribute to environmental protection and informed decision making. From a social, a political, and a legal perspective, the main national and regional gaps are: the absence of instruments to ensure the implementation of modern conservation initiatives; the lack of regulation of shipping and other activities based on an integrated approach; the absence of environmental monitoring and reporting mechanisms; and the scarcity of legally binding instruments to guarantee biodiversity conservation.

The current approach adopted to regulate marine resources and issues, such as pollution in Brazil, is sectoral, disregard scientific data, and does not consider the connectivity of ecosystems along the continuum continent-ocean. The recent oil spill that occurred in early September 2019, which affected more than 3.000 km of the South Atlantic Ocean and around 1.000 Brazilian beaches (Lourenço et al., 2020; Soares et al., 2020), is a vivid example of management difficulties to address large environmental accidents. Several institutional and procedural limits complicated the management of this disaster. For example, the legal provisions that require the activation of the National Contingency Plan (Law n° 9.966/2000) were not implemented and the establishment of a competent federal group to deal with the disaster at the national level took too long, was inefficient, and is yet to deliver environmental and social solution-driven outputs. There was a lack of national coordination between the different federal, state and municipal administrative bodies. On the contrary, the civil society and non-governmental agencies made an outstanding contribution to remove oil from mangroves, beaches, and reefs along the coast during the consecutive months after the oil reached the coast. This oil spill clearly exemplifies the need for regional organization in the SA to build up an institutional framework in order to provide competent actions and necessary preventive and remediation tools for addressing environmental disasters and for chronic pollution in the region.

The important existing collaborative initiatives within the Atlantic Ocean scientific community (e.g., AtlantOS, see deYoung et al., 2019) as well as existing regional science, innovation and technology policy frameworks (e.g., Galway and Belém Statements, BRICs, and South-South Framework for Scientific and Technical Cooperation in the South and Tropical Atlantic and Southern Oceans) and various other *trans*-Atlantic cooperation mechanisms are a good start (Polejack and Barros-Platiau, 2020). These initiatives provide an interesting background for the South Atlantic region to move forward building on current international cooperation that will impact the Decade's implementation. Further, the Regional South Atlantic Planning Workshop for the UN Decade of Ocean Science, November 2019 (IOC-UNESCO, 2020b) triggered a series of actions in Brazil toward the implementation of the Decade. Brazil was the first IOC Member State to create a national committee to oversee the Decade's local implementation. Since then, Brazil hosted five internal workshops from which a National Science and Implementation Plan for the Decade will be designed, considering the peculiarities of each national region. All workshop discussions were framed around the societal outcomes of the Decade (**Table 1**).

In this context, the aims of this article are: (i) to map the main anthropogenic drivers (sources and types of pollutants) potentially impacting the environmental status of the South Atlantic and its ecosystems services and functions; (ii) to identify research gaps; (iii) to identify capacity building priorities, and (iv) research infrastructure and institutional frameworks in order to implement relevant actions and effective developments to achieve the 'Clean Ocean' by 2030. This work presents a compilation of information gathered from the Regional South Atlantic Planning Workshop for the UN Decade of Ocean Science, the five Brazilian regional workshops and the authors' own views considering the areas within and beyond national jurisdiction of the South Atlantic States. Focus will be given to the challenge that ocean pollution represents in the southwest Atlantic, in particular the Brazilian scenario, in face of the ambitions presented by the Decade of Ocean Science for a 'Clean Ocean.' The current status of capabilities, infrastructures, and expertise of other countries besides Brazil has not been raised because data is still scarce and fragmented (IOC-UNESCO, 2017). This is not meant to be a complete review on pollution, but rather a snapshot of the complex confluence of factors at the nexus of ocean pollution under a scenario of rapid climate changes in a specific oceanic region to highlight the diversity therein and further be used as a case study for the Decade's implementation. We understand that a regional scientific and technological coordination is needed to exchange

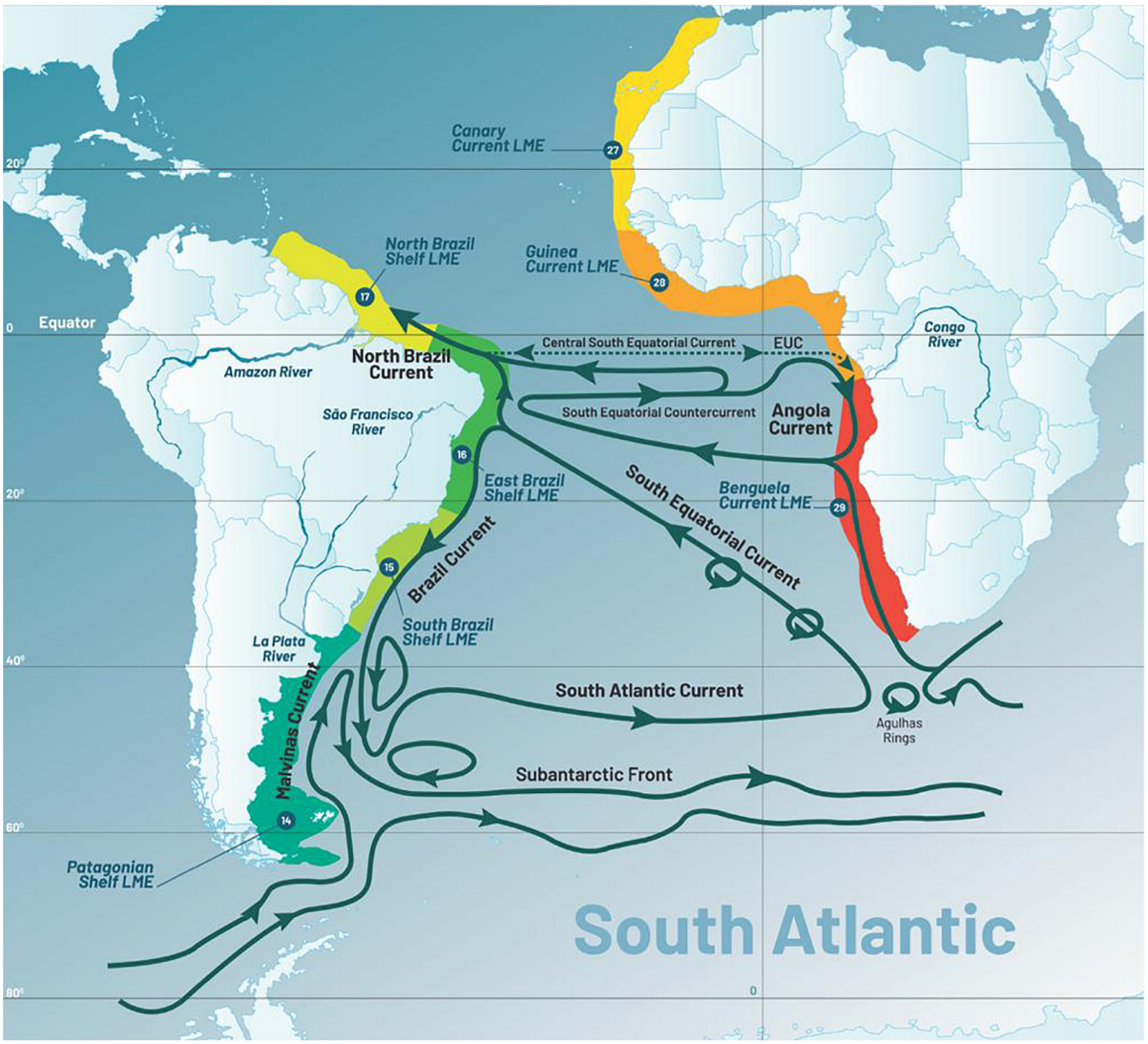

FIGURE 1 | Environmental settings of the South Atlantic Ocean, showing surface circulation schematics, large rivers, and the Large Marine Ecosystems (LMEs) present in the region. Adapted from Talley et al. (2011).

information and provide paths for enhancing capacities to deal with pollution management.

CONTEXT – THE SOUTH ATLANTIC REGION

Environmental Settings

Southwestern Atlantic is limited to the north by the Amazon River plume and to the south by the Malvinas current (i.e., the northward flow component of the South Atlantic subpolar gyre) (**Figure 1**). The South Atlantic coastal regions differ in ecosystems, species composition, and fisheries importance/activities, mostly by changes in water temperature, the influence of continental inputs of water and nutrients (e.g., Prata, São Francisco, and Amazon rivers), and local circulation. Mangroves, seagrass meadows, coral reefs, sandy beaches, estuaries, bays, and deltas are important systems in the tropical and subtropical areas providing numerous ecosystem services (Barbier et al., 2011; Pascual et al., 2017; Díaz et al., 2018). Unique biodiversity with high levels of endemism is found in rhodolith beds (Calegario et al., 2020; Carvalho et al., 2020), in the coral reefs of Abrolhos (Leão et al., 2003; Mazzei et al., 2017), and in the coralline-algae Rocas Atoll, the only atoll in the SA (Gherardi and Bosence, 2001; Amado-Filho et al., 2016). The western Atlantic is also composed by four Large Marine Ecosystems (LMEs), three of which are in the Brazilian coastline (North, East, and South Brazil Shelf LMEs) and a southern LME in Argentina, the Patagonian Shelf LME (**Figure 1**).

The eastern side of the SA presents a large area of high productivity and important fisheries zones under the influence of the Benguela Upwelling System. The African coast shows

high levels of diversity both in the tropical region (intersecting the cold upwelling oceanic waters) and further south, where the coastline has lower habitat diversity (Castilho et al., 2013). Along the eastern shoreline, the SA is bordered by the countries on the western coastline of the African continent, which constitute the three LMEs in that region, namely, the Canary LME which comprises seven countries (Cabo Verde, Gambia, Guinea-Bissau, Guinea, Morocco, Senegal, and Mauritania), the Guinea Current LME with 16 countries and the Benguela Current LME (BCLME). The BCLME includes the coastlines and exclusive economic zones (EEZs) of Angola, Namibia, and South Africa (**Figure 1**).

At the Eastern SA, the Benguela and Agulhas systems interact, playing a key role in the establishment of the oceanic teleconnection. The warm and more saline waters from Agulhas Current, originated in the Indian Ocean, travel northward and reach the northern hemisphere, feeding the global meridional overturning circulation (MOC) by becoming denser and composing the North Atlantic Deep Water (Talley et al., 2011). On the southwestern Atlantic Ocean, the Brazil–Malvinas Confluence is an area of strong mesoscale variability and important exchange of heat and freshwater between the subtropical Atlantic Ocean and the northern branch of the Antarctic Circumpolar Current (Talley et al., 2011). The section of the Atlantic that bridges South and North is also remarkable for understanding the Earth system. A specific example is the Tropical Atlantic sea surface temperature dipole, a cross-equatorial sea surface temperature pattern that appears dominant on decadal timescales and is one of the key features in the Tropical Atlantic Ocean. Its variability has a direct impact on climate (through the displacement of the Intertropical Convergence Zone northwards or southwards) and on continental regions, such as northeastern Brazil and the neighboring Western Africa (Sahel) region, as well as on the formation of cyclones in the North Atlantic (Wainer et al., 2020).

Regarding the institutional framework for environmental protection, it is worth mentioning the importance of marine protected areas. Except for Brazil, Gabon, and South Africa, the percentages of nationally protected marine areas in countries at SA borders are much lower than the world's average of ∼11% (**Table 2**). However, the fact that those areas are officially protected does not necessarily mean that they are properly managed due to the control and monitoring limits of each country.

Socio-Economic Aspects

Brazil, Uruguay, and Argentina are at the southwestern Atlantic Coast, whereas Gabon, Congo, Democratic Republic of Congo, Angola, Namibia, Sao Tome and Principe, and South Africa are on the eastern SA. The population density of these countries is quite variable (**Table 2**) and mostly lives at the coast. As such, a large percentage of the population is vulnerable to any increase both in intensity as in the frequency of extreme events

TABLE 2 | Socio-economic data for South Atlantic bordering countries (World Bank, 2020).

Country	GDP per capita (US$, 2019)	Population (Million, 2019)	Nationally protected marine areas (% of territorial waters, 2018)	People using at least basic drinking water services (% of population, 2017)	People using at least basic sanitation services (% of population, 2016)	Mortality rate attributed to unsafe sanitation and lack of hygiene (per 1,00,000 population, 2016)	CO_2 emissions (metric tons per capita, 2016)	Poverty headcount ration at $1.90 a day[7] (% of population, 2018)
Angola	2, 973.60	31.8	0.0	55.8	48.6	48.8	1.2	51.8
Argentina	10, 006.10	44.9	3.8	99.1[1]	94.3	0.4	4.6	1.3
Brazil	8, 717.20	211.0	26.6	98.2	87.4	1.0	2.2	4.4
Congo	2, 011.10	5.4	3.2	73.2	20.4	59.8	0.7	38.2[2]
Dem. Rep. of Congo	545.20	86.8	0.2	43.2	19.5	38.7	– –	77.2[3]
Gabon	7, 667.40	2.2	28.8	85.8	47.4	20.6	2.6	3.4[4]
Namibia	4, 957.50	2.5	1.7	82.5	34.2	18.3	1.8	13.8[5]
Sao Tome and Principe	1, 994.90	0.2	0.0	84.3	42.8	11.4	0.6	35.6[4]
South Africa	6, 001.40	58.6	12.1	92.7	74.8	13.7	8.5	18.7[6]
Uruguay	16, 190.10	3.5	0.7	99.4	96.4	0.4	2.0	0.1
World	11, 428.60	7, 591.93	11.4	89.6	72.5	11.8	– –	9.2[4]

[1] *Data from 2016;*
[2] *data from 2011;*
[3] *data from 2012;*
[4] *data from 2017;*
[5] *data from 2015;*
[6] *data from 2014;*
[7] *data for purchasing power parity (PPP) from 2011.*

(e.g., heat waves, heavy rainstorms, and hurricanes) resulting from global changes (e.g., temperature and sea-level rise) with significant ecological, economic, and social consequences. These threats place a disproportionate burden on the least developed countries and developing countries in the region due to the lack of proper land-use planning and effective readiness systems.

The region is socio-economically diverse (World Bank, 2020), but has similar characteristics including a low to modest economic development, with a large percentage of the population relying on informal economies, low education level, inadequate access to tap water and sanitation, as well as insufficient legal apparatus to mitigate and/or reduce the input of contaminants, and limited environmental protection. The Gross Domestic Product (GDP) per capita varies widely among the countries (**Table 2**). In 2019, Uruguay had the highest GDP per capita (US$ 16,190.10) and the Democratic Republic of Congo had the lowest (US$ 545.20) (**Table 2**), being the country with the highest rates of extreme poverty, reaching more than 3/4 of the population.

In general, oil and gas exploitation, as well as mining, are relevant activities for the economies of countries on both sides of the South Atlantic. Brazil is a world-class producer of oil, natural gas and mineral resources. The total production of oil and natural gas was ∼3,120 million barrels/day and 139 million m^3/day, respectively, in January 2020 (ANP, 2020). Offshore platforms accounted for 97 and 81% of the national oil and gas production, respectively. Historically, mining is also a relevant activity in the coastal zone and the territorial sea of Brazil (Lima, 2019). Most of the continental shelf of the SA is still unexplored and at present, deep-sea mining is not economically viable compared to traditional mining practices.

For the countries on the American border, agricultural production is also very important, with Brazil, Argentina, and Uruguay presenting strong economic dependence on agribusiness. However, on the African border, with the exception of South Africa, agricultural production is mostly for subsistence.

There are 4 megacities on the countries boarding the South Atlantic that significantly impact the coastal zones: São Paulo and Rio de Janeiro, in Brazil; Buenos Aires, in Argentina; and Kinshasa, in Democratic Republic of Congo (Cirelli and Ojeda, 2008; Rocha et al., 2009, 2010; Wagener et al., 2010; Avigliano et al., 2015; Fries et al., 2019; Mata et al., 2020). Though São Paulo and Kinshasa are not coastal cities, they are both connected to the Atlantic through fluvial systems (e.g., Congo River).

All in all, countries bordering the SA share similar socio-economic challenges. They lack scientific capacities both in ocean research infrastructure as well as in human capital. Marine research capacities, ranging from expertise, well-equipped laboratories to research vessels and other instruments, are not well distributed along the region. For the Decade of Ocean Science to be successful, it will need to tackle this unbalanced set of scientific capabilities and search for ways to even the basic production of knowledge in the SA. We advocate that beneficial international cooperation will be deeply needed to unveil the vast ocean unknowns necessary for improved management of the anthropogenic drivers challenging the resilience of the ocean.

ANTHROPOGENIC DRIVERS THAT THREATENS THE OCEAN

Land-Based and Ocean Sources of Pollutants

During the Regional SA Workshop, the 'Clean Ocean' working group, constituted by participants of all relevant stakeholders (i.e., academia, non-governmental agencies, private sector, decision-makers at different governmental levels, the navy, and local communities), identified a list of pressing issues and pollutants for the Science Action and Implementation Plan for the Ocean Decade (IOC-UNESCO, 2020b). This list was later extended with the specific contributions gathered during the 5 Brazilian regional workshops and further with the input of the authors of this manuscript to compile the main anthropogenic activities and pollutants for the Brazilian coastal waters and the SA ocean in general. Ocean pollution is a complex mixture of anthropogenic chemicals and biological material, and changes in physical conditions (e.g., turbidity, sound, and light). **Table 3** summarizes the main continental and oceanic anthropogenic drivers in the SA Ocean and the associated pollutants types, whereas **Figure 2** also lists potential resulting impacts in biota and on the ecosystem services (i.e., seafood provision, climate mitigation, fisheries, recreational and aesthetic values, and genetic resources), that are the conduit between nature and good quality of life.

Figure 2 illustrates how a large range of pollutants enters the coastal waters from multiple sources, most of which are land-based (∼80%; UNESCO, 2020), such as surficial runoff, industrial discharges, agricultural and mining activities, and poor waste management, while other are ocean-based, primarily shipping, commercial and recreational fishing, oil exploration, mining, and atmospheric deposition. For instance, agriculture discharges nutrients and pesticides, harbor and shipping activities cause the introduction of invasive species and release of fossil fuel gases; animal wastes, runoff, and atmospheric deposition in the downwind plumes from major cities are important sources of nitrogen and may lead to harmful algal blooms (HABs), while urban settlements release a load of different pollutants including, nutrients, metals, pharmaceuticals, among others. Noise and light pollution have also become a growing global concern due to their damaging effects on aquatic species. These kinds of pollution are caused by urbanization and industrialization of coastal zones, recreational boating, seismic and drilling operations at sea (Depledge et al., 2010; Bugnot et al., 2019). They can cause ecological shifts in natural communities, cognitive impairment and affect the underwater behavior of organisms (Buxton et al., 2017; Leduc et al., 2021). Pollution is more severe in coastal environments (e.g., mangroves, bays, and estuaries) due to proximity to land-based sources. The inputs

TABLE 3 | Pressing anthropogenic drivers and associated pollutants for the coastal ecosystems and the South Atlantic Ocean.

Source	Activity	Receiving waters	Main pollutants
Terrestrial	Domestic sewage, sewer outflows, and sewage spills	Rivers, estuaries, and groundwaters	Pathogens, biohazard (parasitic organisms), metals, endocrine disruptors, pharmaceutical and personal care products residues (PPCPs), plastics, plasticizers, antimicrobial resistance, nutrients, HABs, persistent organic pollutants (POPs), brominated and organophosphate flame retardants, perfluoroalkyl and polyfluoroalkyl substances (PFASs), polycyclic aromatic hydrocarbons (PAH)
	Mining (industrial and artisanal)	Rivers, atmosphere, and groundwaters	Metals (Hg, Cu, Pb, Zn, etc.)
	Submarine sewage outfalls	Ocean	Pathogens, biohazard (parasitic organisms), metals, endocrine disruptors, pharmaceutical and personal care products residues (PPCPs), plastics, plasticizers, antimicrobial resistance, nutrients, HABs, persistent organic pollutants (POPs), brominated and organophosphate flame retardants, perfluoroalkyl and polyfluoroalkyl substances (PFASs), polycyclic aromatic hydrocarbons (PAH)
	Industries	Rivers, estuaries, and groundwaters	Organic pollutants (polychlorinated and polybrominated biphenyls, organochlorine pesticides, PAH, PFASs, etc.), metals, plastics, CO_2, heat, light, sound
	Agriculture	Rivers, estuaries, and groundwaters	Nutrients, POPs (e.g., pesticides), PAH, and metals
	Harbors/ports	Coastal areas	CO_2, antifouling paints (metals), organometals, plastics, and PAH
	Aquaculture	Estuaries, rivers	Nutrients, metals, antibiotics, HABs, and antimicrobial resistance
	Fossil fuel combustion	Estuaries, rivers	CO_2, metals (Hg is particularly important for coal burning), and organic contaminants (PAH), polycyclic aromatic sulfur heterocycles (PASHs)
	Tourism	Coastal zone	Invasive species, solid waste, sound, and light
	Nuclear plants	Coastal zone, atmosphere	Radionuclides and heat
	Damming	Rivers	Erosion, remobilization of contaminants
	Run off	Coastal zone	Metals, diverse group of organic compounds, nutrients, PPCPs, brominated and organophosphate flame retardants
Oceanic	Oil rigs	Ocean	Noise, light, invasive species, metals, PAH, and PASHs
	Fisheries	Ocean	Plastics, light
	Aquaculture	Ocean	Nutrients, metals, antibiotics, exotic species, plastics
	Shipping	Ocean	Noise, light, invasive species, fossil fuel exhausts, metals (e.g., Zn and Cu)
	Seismic surveys	Ocean	Noise, light, and invasive species
	Fossil fuel combustion	Ocean	CO_2, metals, and organic contaminants (e.g., PAH and PASHs)
	Tourism	Ocean	Noise, light, invasive species, and plastics
	Bottom trawling	Coastal areas	Turbidity, erosion and remobilization of contaminants
	Dredging	Coastal areas	Physical disturbance of the seafloor, turbidity, and contaminants remobilization
	Mining	Deep sea and coastal	Noise, metals, physical disturbance of the seafloor, and turbidity
Atmospheric*	Mining	Ocean, continental	Hg
	Fossil fuel combustion	Ocean, continental	CO_2, metals, PAH, and PASHs,

**Anthropogenic activities based mostly on land but cause contamination in open, remote environments.*

of pollutants in the environment (**Table 3**) can cause local problems at various levels of biological organization (from cells to communities), compromising ecosystem functions and services, and producing risks at small spatial scale, or causing large-scale impacts (CO_2 pollution), which pose risks at the regional or global level (e.g., climate change). Diffuse emissions, such as agriculture and road runoff are especially difficult to handle, because they are characterized by strong seasonal variation and poorly traceable origins due to the many possible sources (Houtman, 2010).

The SA region is expected to present an upward trend in land-based pollution sources as a result of increasing urbanization and industrialization in the coastal zone and the lack of comprehensive regulation, appropriated enforcement, and mostly abatement. In recent years in Brazil, for instance, there has been a dismantling of the environmental regulatory authorities that suffered a drastic reduction in investments and loosening of existing legislation that protects important ecosystems and human health (Abessa et al., 2019; Araújo, 2020).

The Main Problems

There are several commonalities regarding the main problems associated with the high demographics and amount of waste per capita of the diverse coastal zones of the SA and possible solutions to address regional challenges. While in the North Atlantic pollutants derive mostly from industrial activities and burning of fossil fuels by developed economies, the

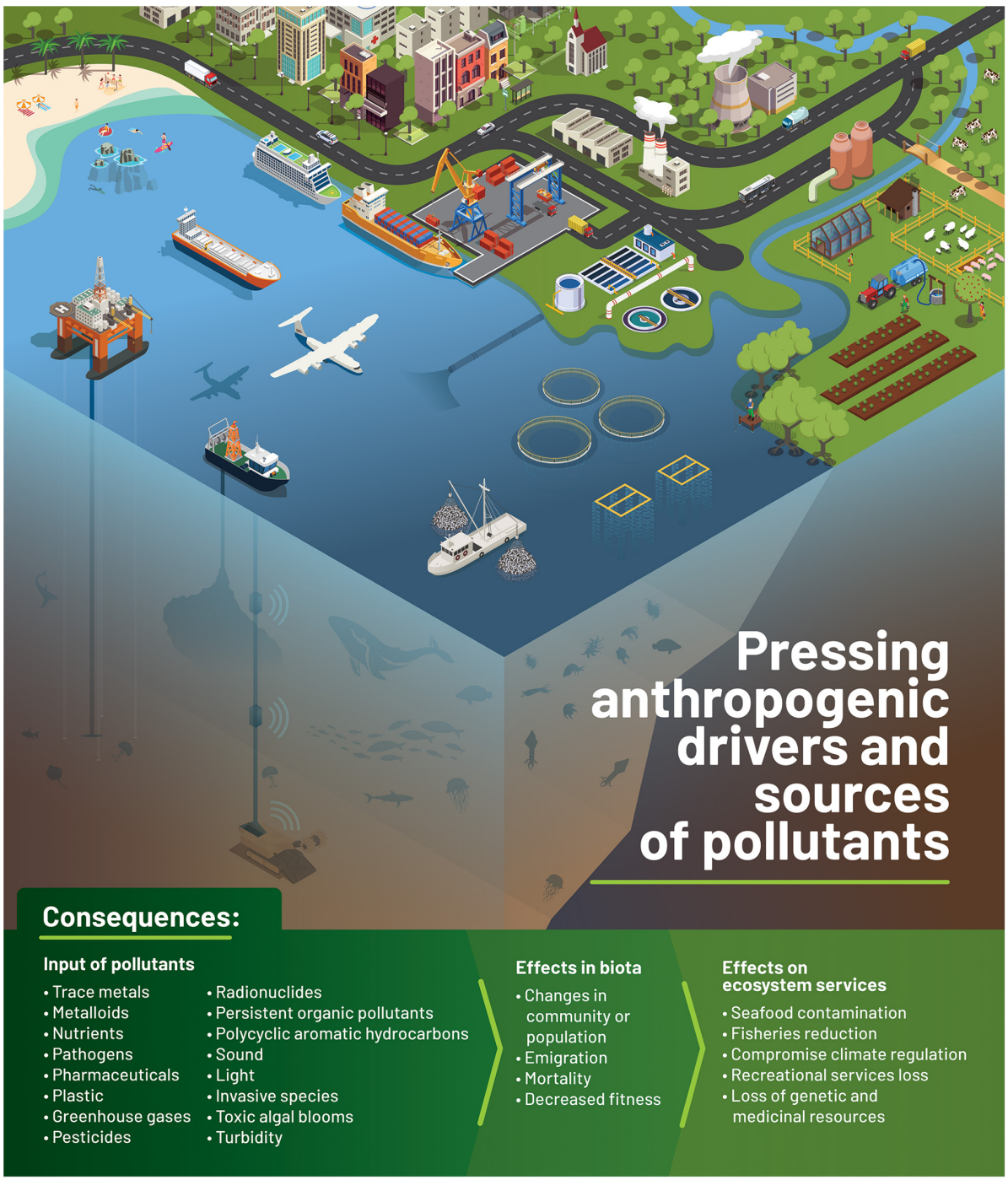

FIGURE 2 | Anthropogenic impact drivers, pollutants and negative impacts on the ocean.

foremost source of pollution identified in the SA workshop for the Decade of Ocean Science was the lack of adequate sewage systems and wastewater treatment plants (**Table 2**; WWAP, 2017). The untreated sewage discharged in the aquatic systems contains high loads of organic matter that may cause deoxygenation and increase dead zones, altering biogeochemical cycles and marine biodiversity (Breitburg et al., 2018). Sewage also presents a myriad of toxic pollutants, some carrying human pathogens and some others contaminating the food chains in detrimental ways to ecosystems and human well-being (Iwamoto et al., 2010; Bradley et al., 2017; Nilsen et al., 2019). These have a disproportionately greater impact

on the traditional communities' economic security and health, mostly because marine resources (fish and shellfish) tend to play a fundamental role in providing food and financial resources (de Souza et al., 2011; World Bank, 2020; Miranda et al., 2021). Coastal economic activities, such as fisheries, aquaculture, and tourism are also acutely dependent on the ocean environmental quality and the increasing environmental status changes. Despite the known interactions between the ocean and human well-being, more interdisciplinary research is needed to uncover the uncertainties related to how each group of pollutants affects local human populations, ecosystem functions and services.

Untreated sewage, sewer overflows, wastewater treatment plant effluents, ocean submarine outfalls, and land runoff are vehicles of diseases and parasites (e.g., typhoid and cholera) that cause gastrointestinal illness as well as life-threatening diseases in humans on both sides of the SA (**Table 2**), with death numbers attributed to unsafe water and lack of sanitation in the African border being generally higher than world's average. It may also cause eutrophication in rivers, bays, and coastal waters. Besides, there is also increasing concern about the spread of antibiotic-resistant pathogens (Gullberg et al., 2011). Since they don't degrade in the environment, bacteria reproduce and can amplify antibiotic resistance genes and pass them through the microbial community and, thus, can represent a critical environmental and human health risk (Pruden et al., 2006). The introduction from land-based allochthonous bacteria carrying resistance genes may account for the acquisition of antimicrobial resistance by indigenous pathogens such as *Vibrio* (Landrigan et al., 2020). Developing countries around the SA lack infrastructure for waste and water treatment and to recycle waste to prevent epidemics. For example, the sewage network in Brazil collects only ∼61% of the sewage generated in urban areas, but only ∼50% of the sewage is treated (SNS, 2018). The focus of management efforts on reducing visible impacts such as solid waste generation can divert attention from the impacts of untreated domestic effluents (e.g., diseases, toxicity, eutrophication, and biodiversity loss).

On the other hand, the impacts of plastic pollution, the second major pollutant identified in the regional debate, capture attention from stakeholders through emotional images of entangled biota and voluminous material in beaches. Many marine biota taxa are deeply impacted by plastic pollution, not only through entanglement but also ingestion and bioaccumulation that cause life-threatening complications (Vegter et al., 2014). The share of plastics in municipal solid waste increased from less than 1% in 1960 to more than 10% by 2005 in middle-and high-income countries (Jambeck et al., 2015) and correlate strongly with gross national income per capita (Wilson, 2015). Once they are stable, durable, and resistant to degradation, they persist for decades in the marine environment and travel considerable long distances, resulting in a rapid and substantial increase in plastic debris in all ocean basins (Barnes et al., 2009). Plastics and fibers can be a major vector for the dispersal of fouling organisms including hazardous microbes, vectors for human disease (Zettler et al., 2013). Typically, about 500 items of anthropogenic debris strand on SA shores per linear kilometer per year (Barnes and Milner, 2005). In fact, Brazil and South Africa are among the top 20 countries responsible for ∼80% of the land-based plastics that end up in the ocean (Jambeck et al., 2015). Recently, the first global review using a holistic approach to assess the ecological, social, and economic impacts of marine plastic pollution suggested that all ecosystem services are impacted to some extent by the presence of plastics (Beaumont et al., 2019). The need for strong actions to prevent plastic pollution's worst consequences on marine life and in the health of the ocean has long been cautioned (Van Rensburg et al., 2020). Improving waste management infrastructure of plastics and other pollutants along with changes in consumption habits are paramount and need concerted implementation actions of scientists, the private sector, governments, and the civil society.

A detailed assessment of all sources will be crucial to identify and prioritize the resolution of problems associated with all potential pollutants (e.g., plastics, CO_2, domestic sewage, nutrients, metals, technology critical elements, pesticides, exotic species, noise, etc. **Table 3** and **Figure 2**). Although we lack pollutant source inventories, several contaminants, such as metals, are already well understood in terms of sources, sinks, fate and toxicity (Iwamoto et al., 2010; Abdel-Shafy and Mansour, 2016; Gworek et al., 2016; Bradley et al., 2017) and evidence exist to warrant a reduction of inputs if political actions are motivated (e.g., Clean Air Act Amendments, Minamata and Stockholm Conventions). At the same time, new groups of yet unregulated contaminants, the so-called emerging contaminants (e.g., plasticizers, personal care products, pharmaceuticals, rare earth elements, and platinum-group elements), have attracted attention and their continuous introduction in surficial waters may lead to still unknown adverse effects. The synergetic and cumulative effects, added to the impacts of global changes (e.g., changing water temperature, deoxygenation, acidification, sea level rise, extreme events, and coastal erosion), can bring even more complexity to the system, changing both the environmental conditions (e.g., anoxia) and the state of ecosystems, causing, for instance, loss of habitats and associated services. Global environmental changes superimposed upon the effects of local pressures can maximize the remobilization of pollutants accumulated in soils and sediments, which are long-term archives of contaminants (UNEP, 2019; Lacerda et al., 2020), leading to an increase in pollutant fluxes into the ocean. It is then expected an enhanced of contaminants' bioaccumulation in coastal food webs (Emmerton et al., 2013; Miranda et al., 2021), and loss of ecosystem services which may translate into food insecurity and impacts on cultural integrity, health, and wellbeing (Newton et al., 2020). Ocean acidification, associated with global changes, may also modify the speciation of metals in seawater, which can alter their bioavailability and therefore toxicity (Millero et al., 2009).

The anthropogenic pressures change the dynamics of ecosystem functions, affecting their natural resilience as well as eventual impacts on human welfare such as food safety, public health, and decrease fisheries and aquaculture revenues. Preventing degradation, setting measurable pollution reduction goals, and implementing environment-friendly management

practices provide a road map for involving scholars, private sector, non-profits organizations, citizens, and government agencies to form the basis for the ambitious Decade of Ocean Science agenda on "Clean Ocean" and climate mitigation.

RESEARCH KNOWLEDGE GAPS AND PRIORITIES

Consideration of the full scope of human and ecosystem risks from pollutants requires a comprehensive evaluation of single and combined impacts on ocean and coastal ecosystems. The SA, however, still is one of the least studied systems, where baselines for most contaminants do not exist. South Atlantic bordering African countries present limited and uneven information of contaminants in coastal systems compared to the western Atlantic coast, hampering the identification of sources and temporal trends (GESAMP, 2018). A detailed assessment of the contaminants' distribution and their temporal dynamics is then urgent to inform prioritization of actions and strengthening the governance regimes in search for solutions within the SA region. A good start is to consider that whereas we lack pollutant source inventories, several pollutants, such as metals and persistent organic pollutants (POPs), are well known, and evidence exist to warrant emissions reduction at short-time scales.

The reduction and elimination of pollution sources rely on the accurate measurement of contaminants in the environment. In order to address pollutant's knowledge gaps, it is necessary first to debate technical aspects, establish and implement clear quality assurance and quality control procedures to make all data comparable and in accordance with the best available international practices (Hatje et al., 2013). Documentation of quality assurance and quality control (QA/QC) data facilitates related capacity development and the use of best practices. The database to be generated must comply with the FAIR data principles (Wilkinson et al., 2016) to promote its maximum use by all stakeholders.

Future strategic research planning should include:

- Inventory of sources of the main impact drivers (e.g., mining, fisheries, tourism, aquaculture, industries, maritime transportation, etc.) considering their synergic interactions.
- Sampling, sample treatment, and quality assurance protocols. A series of protocols and standards for sampling, processing, and data reporting will need to be developed or adapted from existent material which will then be applied to the whole region in order to support the construction of a regional database according to internationally accepted quality standards.
- Baselines of target macro and micro contaminants (e.g., plastics, nutrients, trace metals, organic contaminants, radionuclides, nanomaterial, CO_2, invasive species, among others) aiming to identify hotspots areas that need immediate attention, and/or remediation and restoration.
- Life cycle assessment as a tool to evaluate environmental impacts of pollutants (e.g., plastics) on the basis of multiple impact categories (e.g., climate change, acidification, eutrophication, solid waste generation, human and ecological toxicity, energy and water use, etc.) that occur along the supply chain of products (Hauschild et al., 2013).
- Design of a strategic environmental assessment and long-term monitoring, which is critical to track trends, identify hot spots, and to evaluate the effectiveness of interventions. It is important to apply the ecosystem approach, considering the connection between ecosystems, its functions and services, the position of humans within these systems, and the participation of all stakeholders (Atkins et al., 2011).
- Development of environmental quality indicators for different ecosystems. There is no single indicator that shows when ecosystem tipping points are reached and the resilience of marine ecosystems can no longer be maintained (Hattam et al., 2015). A suite of specific indicators will have to be developed or adapted to inform policy and evaluate progress not only of water quality or pollution but also to track degradation of ecological services and functions, considering their temporal variability and tailored to local and regional particularities.
- Risk assessments. Human risks relative to the ocean are typically associated with (a) consumption of pathogen-contaminated or chemically contaminated seafood; (b) spread of human pathogens (e.g., cholera) via the release of untreated sewage into coastal waters; (c) exposure to toxins from harmful algae; and (d) effects of weather and climate on the rates and means of transmission and severity of infectious diseases (Sandiffer et al., 2004). We need to understand the human and environmental risks of ongoing and future types of single and multiple pollutants, including the atmosphere global pollution transport and its exposure pathways. Attention should be given to emerging contaminants, such as the technology critical contaminants (e.g., rare earth elements, platinum group of elements, and nanoproducts) (Cobelo-García et al., 2015), newly registered pesticides, pharmaceuticals, personal care products, and fire retardants (Houtman, 2010; Nilsen et al., 2019). Since 2019, nearly 500 new pesticides have been approved in Brazil, accelerating the trend of previous years and introducing new contaminants, possibly impacting environmental quality and food safety, at an unprecedented rate (Braga et al., 2020). The majority of these chemicals have not been tested for safety or toxicity and even less is known about their potential synergic effects.
- Development and improvement of models to predict and assess long-term trends and risks of pollutants and propose preventive solutions;
- Evaluation of trade-offs of interventions, restoration and replacement of practices and substances. Trade-off analysis is an important aspect in assessment studies of pollution and its effects on ecosystem services and it is a key issue in decision making and in the analysis of alternative pathways that lead to future sustainable land use (Rounsevell et al., 2012). Points to be considered are i. population and individual risks and the cost of risk reduction by using cost

per life saved as a criterion and ii. cost-effectiveness as a justification for remediation.
- Determination of the caring capacity for ecological and biological significant areas to sustain human impacts and economic development (e.g., Abrolhos reef system, and mangrove belt of Amazonia and the Amazon reef system).
- Strengthening governance regimes to encourage more sustainable production and consumption practices under national, regional and international legal frameworks.
- Integrated management of the coastal zone, marine space, and areas beyond national jurisdiction through precise principles, rules, obligations and instruments.
- Consider the knowledge of traditional communities and indigenous peoples when building databases and discussing management decisions.
- Promote ecosystem conservation and restoration of coastal vegetated systems (wetlands) to help improve water quality, reducing pollutants (e.g., pathogen and nutrient concentration) and promoting ecological functions.

Altogether, these measures will augment the science capacity and make it fit to minimize total environmental impacts of pollutants, informing sustainable development and addressing human and environmental short- and long-term risks from all forms of pollution.

THE WAYS TO SEEK SOLUTIONS

The long-term changes in the ocean or the seriousness of the impacts of ocean degradation on human and ecosystem health are hard for the public and decision-makers to grasp, as they challenge the eyesight and short-term thinking. The consequence may be the establishment of irreversible outcomes, beyond the resilience of ecosystems. To date, response to early warnings has been limited to only timid measures to reduce pollutant emissions. The overarching aim of the Decade with regard to a 'Clean Ocean' is to severely reduce the input of pollutants and hence limit anthropogenic impacts, leading to very low acceptable levels of plastics, noise, light, chemical, and microbial contaminants in coastal and open waters. This result, nevertheless, needs bold, urgent, and efficient measures. The longer we take to act, the costlier and more challenging the measures to revert the degradation cycle will become. We need to remember that modifications in the distribution of contaminants, such as Hg and Pb may set large-scale changes that reverberate for decades or centuries, once contaminants will be trapped and circulated along with the meridional overturning circulation (Boyle et al., 2014; Lamborg et al., 2014a). Future research on the interface between ocean and human health should focus on how to better manage interacting pollutants and other stressors in the long-run, as well as exposures to actual contaminants while capturing the potential for co—benefits available through intelligent management (Deprietri and McPhearson, 2017). This will demand collaborations by individuals and institutions working across sectors, and responsible economic development administered through environmental sustainability and social inclusion to ensure that the voice of those most affected by ocean pollution is heard (e.g., traditional and indigenous communities) (Fleming et al., 2019). In this respect, a greater focus on truly transdisciplinary research and training will be especially valuable. From a legal perspective, there is a lack of effective instruments of compliance and management of the marine environment that integrate the coastal zone and adjacent areas, in particular in Brazil (Spolidorio, 2018). There is also a need to better define additional criteria and standards to measure ocean resilience in service of legal measures (Tanaka, 2004; Long et al., 2015; Silva and Moraes, 2020).

The research capabilities and expertise required to achieve the 'Clean Ocean' we want, as for the 2030 agenda, are very heterogeneous across the SA region and rely on the implementation of better research infrastructure, capacity building, and mechanisms of transfer of marine technology. The solutions developed should lead to cost-effective prevention, monitoring, and mitigation actions. As such, we need coordinated efforts to promote regional and national capacity building solutions for technical and institutional capabilities, research funding, and regional coordination to support the ambitious goals of the Decade.

Regional Scientific Capabilities

The SA marine scientific facilities and research infrastructure are neither mapped nor easily assessed. Brazil and South Africa are among the countries in the region with the best infrastructure in terms of platforms to perform ocean sciences and on-land based measurements of organic and inorganic pollutants and to apply nuclear and isotopic techniques in environmental studies. Recent changes in the Brazilian administration policies for universities have jeopardized the hiring of technicians and lab assistants. As a consequence, complex instruments, in many cases, rely on the work of graduate students even in the Brazilian largest universities. That creates a huge problem in the continuity of the activities, dependence on student flows, and the need for continuous training. The number of laboratories currently capable of performing trace level measurements of organic contaminants and metals in seawater is extremely low (less than half a dozen, being optimistic). In fact, many laboratories lack the basic equipment and capability to measure macronutrients in seawaters. Certainly, there is no need for equipping labs for all sorts of chemical and physical measurements, but reference laboratories across the region are needed to work as analytical and capacity building hubs, to serve the whole community. The connection of reference laboratories to a regional network will enhance the technical and operational capabilities of reference laboratories in the identification of pollution, control, mitigation, and management of sources. Reference laboratories will also benefit from the expertise and knowledge acquired by the other laboratories in the network.

Research Funding

The list of the necessary actions identified here can only be carried out if continuous support is provided. Current funding for ocean sciences is largely inadequate and variable over time,

undermining the capability of ocean sciences to support the sustainable provision of ocean services (IOC-UNESCO, 2020a). Long-term research funding is rare everywhere. In Brazil, for instance, one of the very few exceptions is the Long-Term Ecological Research Program (PELD[4]). The implementation of such programs, which include long time series of data on ecosystems and their associated biota, are crucial to produce knowledge, create expertise, research capabilities, and infrastructure. Besides, they are critical to allow temporal evaluation of phase-out of contaminants, remediation, and restoration measurements and provide information for the sustainable use of the ocean, securing that its ecosystem services and functions are preserved. The amount of total expenditure for research in Brazil (1.3% of the GDP), although substantiality higher than other SA bordering countries like South Africa (0.8%), Argentina (0.5%), and Namibia (0.3%), is much smaller than the investments of industrialized nations [e.g., United States (2.8%), China (2.2%), United Kingdom (1.7%), and Germany (3.0%)] (World Bank, 2020). Moreover, the current Brazilian Government has devaluated science and the role it can have in advising public policy. Cuts for science research budget in the past few years have led to a drop in investments from a peak of about US$2.6 billion in 2014 to less than one-third of this value in 2020 (Tollefson, 2020). Additional funding is the only way to bolster efforts to better understand, evaluate, and manage the ocean and coastal ecosystems.

Capacity Development

Discussions during the Decade's SA planning workshop, plus results from the Brazilian regional workshops have identified not only sources and types of pollution, but also diverse capacity building needs. These are listed below.

- Chemical and data analyses of nutrients, microplastics, petroleum hydrocarbons (PAHs), legacy (POPs listed in Stockholm Convention) and emerging contaminants (e.g., pharmaceuticals, novel flame retardants, personal care products, pesticides, nanomaterials, and technology critical elements);
- Public and private decision-making regarding pollutants and strengthening of the science-policy interface;
- Ecosystem and human health risk assessments;
- Mitigation of pollution and restoration of marine ecosystems/habitats;
- Prevention, preparedness and response to environmental disasters. The need for such action can be illustrated by the delayed and lack of coordination actions for the recent accidents of a mining dam's burst (Gomes et al., 2017; Hatje et al., 2017) and the oil spill in 2019 (Lourenço et al., 2020) that led to substantial negative environmental, social and economic impacts;
- Cross-sectors integration between public and private organizations and across disciplines;
- Evaluation of socio-economic impacts.

[4]http://cnpq.br/apresentacao-peld

As alluded to earlier, capacity development is one of the core areas that need to be fostered in the SA region. This includes building up programs targeted to produce the necessary knowledge to properly manage ocean pollution in the region, involving not only academia but also government officials, and the industry. In addition, there is a need to foster an effective technology transfer mechanism so countries in the region will grant access and co-develop marine technologies that are fit for the purpose. The current international standards for data acquisition and quality assurance and control post a further need for enhancement in the regional science capacity. Technology and knowledge transfer will also need to be more effective and inclusive than the currently available mechanisms, such as the IOC guidelines, that have not yet fulfilled their goals (Harden-Davies, 2016; Salpin et al., 2018).

National Institutional Regulatory Frameworks

National institutional frameworks, designed to regulate the management of the coastal zone and the marine space in an integrated way, are also key to improve environmental protection and conservation. In general, countries in the SA region possess sectoral and uncoordinated instruments to combat pollution, disregarding the synergic effects and cumulative impacts of different activities, and the ecosystem connectivity along the continuum continent-ocean. In this sense, there is a need to establish procedural and substantial norms to prevent, to remediate, and to repair environmental impacts. The polluter-pays principle (Adshead, 2018) needs to be strengthened, resulting in better economic instruments, such as tax incentives to adopt the use of best-suited technologies to avoid pollution or produce preventive labels/certifications to encourage sustainability. Countries should also invest in public and private collaborations to develop their marine spatial planning and water quality monitoring programs. Finally, actions need to be taken even in face of great scientific uncertainties. Therefore, the precautionary principle should be further applied and instruments such as adaptive licensing need to ensure effective pollution protection for the marine environment (de Sadeleer, 2009; Krämer and Orlando, 2018; Oliveira et al., 2019).

The development of a coordinated act or bill could provide such integration between different sectors and ocean activities. Developing a sole legislation would contribute to the harmonization of procedural and substantial rules applicable to the marine environment and to the coastal zone. In the case of federal states such as Brazil, where the federation, states, and municipalities have different competences to legislate and to manage the marine environment, a comprehensive norm would clarify and better distribute the competences of each entity to manage the impacts of pollution. This scenario would bring more clarity and legal certainty to stakeholders on their rights and obligations. Moreover, this integration would strengthen the management of cumulative impacts of different sources of pollution, based on a more precise connection between the public bodies (which are responsible for the allocation of budget) and

the environmental agencies. By better designing the national institutional frameworks to deal with the impacts of different types of pollution within the areas under national jurisdiction, South Atlantic countries will be more prepared to consolidate a regional coordination on this issue.

Regional Coordination

Ocean pollution is largely based on non-point sources. Thus, relies on regional and international collaborations to tackle the issue. These collaborations should include deliberations about sampling monitoring designs, thresholds, and management of decision-making, particularly because of the links to human food security and other potential impacts on ecosystem services. Some level of regional institutional coordination will be required to bring together all the States from the region as well as big business with a key role in the sustainability governance (Blasiak et al., 2018) to deal with marine pollution, fostering cross-ocean basin assessments and mitigation actions.

There are international and regional treaties and organizations that already address the impacts caused by some pollutants like mercury (Minamata Convention), hazardous wastes (e.g., plastics) (Basel Convention) and persistent organic pollutants (Stockholm Convention) to protect human health and the environment. Other types of pollution are regulated by treaties related to shipping, mining and fishing (Montego Bay Convention, MARPOL Convention, Regulations of the International Seabed Authority). In the context of the Southwestern Atlantic, there is a binational commission ratified by Argentina and Uruguay (Comisión Técnica Mixta del Frente Marítimo) and created by the Tratado del Río de la Plata y su Frente Marítimo (November, 1973) that deals with continental pollution inputs to the ocean. SA countries need to work together even in the lack of a broader intergovernmental framework regulating marine pollution. In this regard, science diplomacy might play an interesting role to unveil all the possible exchanges that science and international relations may have in dealing with cross-border and global concerns and interests (Flink and Rüffin, 2019).

A well-coordinated science diplomacy effort among the countries in the region could help to address marine pollution issues dealing with national policies and international cooperation. This coordination should be certainly informed by scientific evidence taken up to policy making and finally to diplomacy. Negotiations will need to face multiple challenges such as balancing national interests, in particular industry's interests, with regional concern over pollution (Berkman, 2019). Another challenge will be to agree on leveled actions which are mostly State-led policies to combat marine litter. Thus, informal scientific peer-to-peer cooperation needs to be formalized through adequate international instruments. Researchers and civil society need to organize the debate and present the available evidence, so countries are pressured to act collectively. As evidenced during the current COVID-19 pandemic, in which States adopted diverse national plans of actions, despite the available scientific evidence, many times contributing to spread and intensify the crisis. On one hand, diversity of actions was caused by the high scientific uncertainties with regard to this new virus, and on the other, due to political statements and actions overruling the available scientific evidence and generating insecurity. Thus, a regional bidding commitment should level and inform national policies on the best course of action, resulted from a negotiation informed by science and in balance with national interests and regional concern. One interesting example, designed under the auspices of the International Seabed Authority for mining activities, is the development of the Regional Environmental Management Plans (REMPs). They are part of an environmental policy by establishing standards and guidelines for the region to determine thresholds to mining exploitation. This type of instrument is an example of what a solid institutional framework can provide for the region (Domingos and Barros-Platiau, 2021).

The Decade of Ocean Science calls for long-term commitment and investments to promote continuous funding for science, relevant and effective institutional and human capacities to deal with the complexities involved in stopping the degradation of the ocean ecosystems services and functions, and aggravating impacts associated with climate change. Finally, we will only be successful if we integrate the social, economic, and natural sciences in the search for solutions and in the development of public policies aimed at reducing the input of pollutants and warranting food security, in addition to, of course, the restoration of degraded ecosystems.

CONCLUSION

Like many scientific advances, our better understanding of the ocean and reversal of its degradation cycle will evolve not only through research and development of innovative solutions in individual institutions but mostly through collaborations between national and international groups of stakeholders, including scientists, traditional communities, indigenous peoples and the private sector who could contribute with their experience, time, and other resources. The planning for the Decade is a voluntary pact that sought to build momentum by allowing countries to better define priorities for the Ocean Decade. The actions to be implemented by the Decade of Ocean Sciences have the potentially pivotal role to:

(1) Advance the knowledge on the fate of pollutants to prevent the contamination of the environmental resources and associated human health and ecosystems impacts;
(2) Develop cost-effective technologies and solutions to prevent, monitor (marine ecosystems and biota), mitigate and remediate polluted ecosystems in an integrated manner for protecting human health and marine ecosystems. Prevention of pollution from land-based and ocean sources is critical;
(3) Development and improvement of models to predict and assess long-term trends and risks of pollutants and propose preventive solutions;
(4) Promote technical and scientific capacity development and technology transfers reducing regional inequalities;

(5) Improve on-land scientific facilities and ocean research infrastructure;
(6) Advance regulatory science based on the latest scientific evidence to develop national public policies aimed at reducing the input of pollutants, better management of solid residues (e.g., plastics), and warranting food security and ecosystem health;
(7) Facilitate national and international cooperation in marine research and regional institutional frameworks;
(8) Improve risk assessment to facilitate risk management and data communication of regulatory relevance;
(9) Foster interdisciplinary and *trans*-sectoral collaborations between marine, terrestrial, and social scientists, as well as public health researchers, promoting social inclusion, to ensure that those least able to influence the process but often most affected (e.g., traditional communities and indigenous peoples) are heard when addressing the local and global challenges of human-ocean interactions.

The earlier the actions in controlling pollutants are implemented, identifying key sources and preventing the crossing of thresholds, there will be higher chances of averting worst-case scenarios and reducing the economic and social costs having disparate impacts across nations and social groups. Ensuring that the most vulnerable and unpowered are properly protected from pollution and its consequences requires the early establishment of agreements, protections, and policies that will minimize social inequality and secure a clean, healthy ocean. Finally, controlling land-source pollutants will help to attain multiple Sustainable Development Goals (SDG), besides the preservation of life below water (SGD14), contributing to the improvement of human health and well-being (SDG 3), clean water and sanitation (SDG 6), the end of hunger (SDG 2) and responsible consumption (SGD 12).

AUTHOR CONTRIBUTIONS

VH conceived the manuscript and wrote the first draft. All authors contributed to the writing of the manuscript and gave final approval for publication.

FUNDING

This study was financially supported by CNPq (441264/2017-4). The authors were sponsored by CAPES (RA), CNPq (VH, 304823/2018-0 and CCO, 309985/2018-8), the Swedish Agency for Marine and Water Management, the German Ministry of Transport and Digital Infrastructure (through the Land-to-Ocean Leadership Program), and Ministério da Ciência, Tecnologia e Inovações (MCTI) (AP). AP received support by the MISSION ATLANTIC project funded by the European Union's Horizon 2020 Research and Innovation Program (No. 862428).

ACKNOWLEDGMENTS

The authors would like to acknowledge IOC-UNESCO, MCTI, and the Brazilian Navy for coordinating the South Atlantic Regional Decade Workshop.

REFERENCES

Abdel-Shafy, H. I., and Mansour, M. S. M. (2016). A review on polycyclic aromatic hydrocarbons: source, environmental impact, effect on human health and remediation. *Egypt. J. Pet.* 25, 107–123. doi: 10.1016/j.ejpe.2015.03.011

Abessa, D., Famá, A., and Buruaem, L. (2019). The systematic dismantling of Brazilian environmental laws risks losses on all fronts. *Nat. Ecol. Evol.* 3, 510–511. doi: 10.1038/s41559-019-0855-9

Adshead, J. (2018). The application and development of the polluter-pays principle across jurisdictions in liability for marine oil pollution: the tales of the erika and the prestige. *J. Environ. Law* 30, 425–451.

Amado-Filho, G. M., Moura, R. L., Bastos, A. C., Francini-Filho, R. B., Pereira-Filho, G. H., Bahia, R. G., et al. (2016). Mesophotic ecosystems of the unique South Atlantic atoll are composed by rhodolith beds and scattered consolidated reefs. *Mar. Biodivers.* 46, 933–936. doi: 10.1007/s12526-015-0441-6

Anderson, R. (2020). GEOTRACES: accelerating research on the marine biogeochemical cycles oftrace elements and their isotopes robert. *Ann. Rev. Mar. Sci.* 12, 49–85.

ANP (2020). *Boletin da Produção de Petróleo e Gás Natural*. Rio de Janeiro: ANP.

Araújo, S. M. (2020). Environmental policy in the bolsonaro government: the response of environmentalists in the legislative arena. *Braz. Polit. Sci. Rev.* 14, 1–20. doi: 10.1590/1981-3821202000020005

Atkins, J. P., Gregory, A. J., Burdon, D., and Elliott, M. (2011). Managing the marine environment: is the DPSIR framework holistic enough?. *Syst. Res. Behav. Sci.* 28, 497–508.

Avigliano, E., Schenone, N. F., Volpedo, A. V., Goessler, W., and Fernández Cirelli, A. (2015). Heavy metals and trace elements in muscle of silverside (Odontesthes bonariensis) and water from different environments (Argentina): aquatic pollution and consumption effect approach. *Sci. Total Environ.* 506–507, 102–108. doi: 10.1016/j.scitotenv.2014.10.119

Barbier, E. B., Hacker, S. D., Kennedy, C., Koch, E., Stier, A., and Silliman, B. R. (2011). The value of estuarine and coastal ecosystem services. *Ecol. Monogr.* 81, 169–193.

Barnes, D. K. A., Galgani, F., Thompson, R. C., and Barlaz, M. (2009). Accumulation and fragmentation of plastic debris in global environments. *Philos. Trans. R. Soc. B Biol. Sci.* 364, 1985–1998. doi: 10.1098/rstb.2008.0205

Barnes, D. K. A., and Milner, P. (2005). Drifting plastic and its consequences for sessile organism dispersal in the Atlantic Ocean. *Mar. Biol.* 146, 815–825. doi: 10.1007/s00227-004-1474-8

Beaumont, N. J., Aanesen, M., Austen, M. C., Börger, T., Clark, J. R., Cole, M., et al. (2019). Global ecological, social and economic impacts of marine plastic. *Mar. Pollut. Bull.* 142, 189–195. doi: 10.1016/j.marpolbul.2019.03.022

Bell, L., Evers, D., Johnson, S., Regan, K., DiGangi, J., Federico, J., et al. (2017). *Mercury in Women of Child-Bearing Age in 25 Countries*. Available online at: http://ipen.org/sites/default/files/documents/updateNov14_mercury-women-report-v1_6.pdf (accessed February 25, 2020).

Berkman, P. A. (2019). Evolution of science diplomacy and its local-global applications. *Eur. Foreign Aff. Rev.* 24, 63–80.

Blasiak, R., Jouffray, J. B., Wabnitz, C. C. C., Sundström, E., and Osterblom, H. (2018). Corporate control and global governance of marine genetic resources. *Sci. Adv.* 4, 1–7. doi: 10.1126/sciadv.aar5237

Boyle, E., Lee, J., Echegoyen, Y., Noble, A., Moos, S., Carrasco, G., et al. (2014). Anthropogenic lead emissions in the ocean: the evolving global experiment. *Oceanography* 27, 69–75.

Bradley, M., Barst, B., and Basu, N. (2017). A review of mercury bioavailability in humans and fish. *Int. J. Environ. Res. Public Health* 14:169. doi: 10.3390/ijerph14020169

Braga, A. R. C., de Rosso, V. V., Harayashiki, C. A. Y., Jimenez, P. C., and Castro, ÍB. (2020). Global health risks from pesticide use in Brazil. *Nat. Food* 1, 312–314. doi: 10.1038/s43016-020-0100-3

Breitburg, D., Levin, L. A., Oschlies, A., Grégoire, M., Chavez, F. P., Conley, D. J., et al. (2018). Declining oxygen in the global ocean and coastal waters. *Science* 359:eaam7240. doi: 10.1126/science.aam7240

Bugnot, A. B., Hose, G. C., Walsh, C. J., Floerl, O., French, K., Dafforn, K. A., et al. (2019). Urban impacts across realms: Making the case for inter-realm monitoring and management. *Sci. Total Environ.* 648, 711–719. doi: 10.1016/j.scitotenv.2018.08.134

Buxton, R. T., Mckenna, M. F., Mennitt, D., Fristrup, K., Crooks, K., Angeloni, L., et al. (2017). Noise pollution is pervasive in U.S. protected areas. *Science* 356, 531–533.

Calegario, G., Freitas, L., Appolinario, L. R., Venas, T., Arruda, T., Otsuki, K., et al. (2020). Conserved rhodolith microbiomes across environmental gradients of the Great Amazon Reef. *Sci. Total Environ.* 5:143411. doi: 10.1016/j.scitotenv.2020.143411

Carvalho, V., Assis, J., Serrão, E., Nunes, J., Batista, A., Batista, M., et al. (2020). Environmental drivers of rhodolith beds and epiphytes community along the South Western Atlantic Coast. *Mar. Environ. Res.* 154:104827.

Castilho, R., Grant, W. S., and Almada, V. M. (2013). Biogeography and phylogeography of the Atlantic. *Front. Biogeogr.* 5, 5–7. doi: 10.21425/f5fbg17059

Cirelli, A. F., and Ojeda, C. (2008). Wastewater management in Greater Buenos Aires, Argentina. *Desalination* 218, 52–61. doi: 10.1016/j.desal.2006.10.040

Cobelo-García, A., Filella, M., Croot, P., Frazzoli, C., Du Laing, G., Ospina-Alvarez, N., et al. (2015). COST action TD1407: network on technology-critical elements (NOTICE)—from environmental processes to human health threats. *Environ. Sci. Pollut. Res.* 22, 15188–15194. doi: 10.1007/s11356-015-5221-0

de Sadeleer, N. (2009). The precautionary principle as a device for greater environmental protection: lessons from EC courts. *RECIEL* 18, 3–10.

de Souza, M. M., Windmöller, C. C., and Hatje, V. (2011). Shellfish from Todos os Santos Bay, Bahia, Brazil: treat or threat?. *Mar. Pollut. Bull.* 62, 2254–2263. doi: 10.1016/j.marpolbul.2011.07.010

Depledge, M. H., and Bird, W. J. (2009). The blue gym: health and wellbeing from our coasts. *Mar. Pollut. Bull.* 58, 947–948. doi: 10.1016/j.marpolbul.2009.04.019

Depledge, M. H., Godard-Codding, C. A. J., and Bowen, R. E. (2010). Light pollution in the sea. *Mar. Pollut. Bull.* 60, 1383–1385. doi: 10.1016/j.marpolbul.2010.08.002

Deprietri, Y., and McPhearson, T. (2017). "Integrating the grey, green, and blue in cities: nature-based solutions for climate change adaptation and risk reduction," in *Nature-Based Solutions to Climate Change Adaptation in Urban Areas*, ed. N. Kubisch (Cham: Springer), 91–109.

deYoung, B., Visbeck, M., Filho, M. C. A., Baringer, M. O., Black, C. A., Buch, E., et al. (2019). An integrated all-Atlantic ocean observing system in 2030. *Front. Mar. Sci.* 6:428. doi: 10.3389/fmars.2019.00428

Díaz, S., Pascual, U., Stenseke, M., Martín-López, B., Watson, R. T., Molnár, Z., et al. (2018). Assessing nature's contributions to people. *Science* 359, 270–272. doi: 10.1126/science.aap8826

Domingos, N., and Barros-Platiau, A. (2021). "Deep-seabed mining and ocean governance: deciphering multilateral rule-making at the International Seabed Authority," in *A Função Do Direito na Gestão Sustentável dos Recursos Minerais Marinhos*, ed. C. Oliveira (Rio de Janeiro: Processo).

Emmerton, C. A., Graydon, J. A., Gareis, J. A. L., St. Louis, V. L., Lesack, L. F. W., Banack, J. K. A., et al. (2013). Mercury export to the Arctic Ocean from the Mackenzie River, Canada. *Environ. Sci. Technol.* 47, 7644–7654. doi: 10.1021/es400715r

Fleming, L. E., Maycock, B., White, M. P., and Depledge, M. H. (2019). Fostering human health through ocean sustainability in the 21st century. *People Nat.* 1, 276–283. doi: 10.1002/pan3.10038

Flink, T., and Rüffin, N. (2019). "The current state of the art of science diplomacy," in *Handbook on Science and Public Policy*, eds D. Simon, J. S. Kuhlmann, J. Stamm, and W. Canzler (Cheltenham: Edgar Elgar Publishing), 104–121.

Foltz, G. R., Brandt, P., Richter, I., Rodriguez-fonseca, B., Hernandez, F., Dengler, M., et al. (2019). The tropical atlantic observing system. *Front. Mar. Sci.* 6:206. doi: 10.3389/fmars.2019.00206

Fries, A. S., Coimbra, J. P., Nemazie, D. A., Summers, R. M., Azevedo, J. P. S., Filoso, S., et al. (2019). Guanabara Bay ecosystem health report card: science, management, and governance implications. *Reg. Stud. Mar. Sci.* 25:100474. doi: 10.1016/j.rsma.2018.100474

GESAMP (2018). "Global trends in pollution of coastal ecosystems," in *IMO/FAO/UNESCO-IOC/UNIDO/WMO/IAEA/UN/UNEP/UNDP/ISA Joint Group of Experts on the Scientific Aspects of Marine Environmental Protection*, eds A. C. Ruiz-Fernández and J. A. Sanchez-Cabeza, Rep. Stud. GESAMP No. 106, 101.

Gherardi, D. F. M., and Bosence, D. W. J. (2001). Composition and community structure of the coralline algal reefs from Atol das Rocas, South Atlantic, Brazil. *Coral Reefs* 19, 205–219. doi: 10.1007/s003380000100

Glibert, P. M. (2020). Harmful algae at the complex nexus of eutrophication and climate change. *Harmful Algae* 91:101583. doi: 10.1016/j.hal.2019.03.001

Gomes, L. E., de, O., Correa, L. B., Sá, F., Neto, R. R., and Bernardino, A. F. (2017). The impacts of the Samarco mine tailing spill on the Rio Doce estuary, Eastern Brazil. *Mar. Pollut. Bull.* 120, 28–36. doi: 10.1016/j.marpolbul.2017.04.056

Gullberg, E., Cao, S., Berg, O. G., Ilbäck, C., Sandegren, L., Hughes, D., et al. (2011). Selection of resistant bacteria at very low antibiotic concentrations. *PLoS Pathog.* 7:e1002158. doi: 10.1371/journal.ppat.1002158

Gworek, B., Bemowska-Kałabun, O., Kijeńska, M., and Wrzosek-Jakubowska, J. (2016). Mercury in marine and oceanic waters—a review. *Water Air Soil Pollut.* 227:371. doi: 10.1007/s11270-016-3060-3

Harden-Davies, H. (2016). Marine science and technology transfer: can the intergovernmental oceanographic commission advance governance of biodiversity beyond national jurisdiction? *Mar. Policy* 74, 260–267. doi: 10.1016/j.marpol.2016.10.003

Hatje, V., da Costa, M. F., and da Cunha, L. C. (2013). Oceanografia e Química: unindo conhecimentos em prol dos oceanos e da sociedade. *Quim. Nova* 36, 1236–1241.

Hatje, V., Lamborg, C., and Boyle, E. (2018). Trace-metal contaminants: human footprint on the Ocean. *Elements* 14, 403–408.

Hatje, V., Pedreira, R. M. A., De Rezende, C. E., Schettini, C. A. F., De Souza, G. C., Marin, D. C., et al. (2017). The environmental impacts of one of the largest tailing dam failures worldwide. *Sci. Rep.* 7:10706. doi: 10.1038/s41598-017-11143-x

Hattam, C., Atkins, J., Beaumont, N., Borger, T., Bohnke-Henrichs, Burdon, D., et al. (2015). Marine ecosystem services: linking indicators to their classificatio. *Ecol. Indic.* 49, 61–65.

Hauschild, M. Z., Goedkoop, M., Guinée, J., Heijungs, R., Huijbregts, M., Jolliet, O., et al. (2013). Identifying best existing practice for characterization modeling in life cycle impact assessment. *Int. J. Life Cycle Assess.* 18, 683–697. doi: 10.1007/s11367-012-0489-5

Houtman, C. J. (2010). Emerging contaminants in surface waters and their relevance for the production of drinking water in Europe. *J. Integr. Environ. Sci.* 7, 271–295. doi: 10.1080/1943815X.2010.511648

Inniss, L. A. S., Ajawin, A. Y., Alcala, A. C., Bernal, P., and Calumpong, H. P. (2017). *The First Global Integrated Marine Assessment*. Cambridge, MA: Cambridge University Press.

IOC-UNESCO (2017). *Global Ocean Science Report: The Current Status of Ocean Science Around the Worls*. Paris: UNESCO Publishing.

IOC-UNESCO (2020a). *Global Ocean Science Report 2020- Charting capacity for Ocean Sustainability*. Paris: UNESCO Publishing.

IOC-UNESCO (2020b). *Summary Report of the Regional Planning Workshop for the South Atlantic*. Paris: UNESCO Publishing.

Iwamoto, M., Ayers, T., Mahon, B. E., and Swerdlow, D. L. (2010). Epidemiology of seafood-associated infections in the United States. *Clin. Microbiol. Rev.* 23, 399–411. doi: 10.1128/CMR.00059-09

Jambeck, J., Geyer, R., Wilcox, C., Siegler, T. R., Perryman, M., Andrady, A., et al. (2015). Plastic waste inputs from land into the ocean. *Science* 347, 768–771.

Knap, A., Dewailly, É, Furgal, C., Galvin, J., Baden, D., Bowen, R. E., et al. (2002). Indicators of ocean health and human health: developing a research and monitoring framework. *Environ. Health Perspect.* 110, 839–845. doi: 10.1289/ehp.02110839

Knowlton, N. (2004). Ocean health and human health. *Environ. Health Perspect.* 112:262.

Krämer, L., and Orlando, E. (2018). *Principles of Environmental Law*. Cheltenham: Edward Elgar Publishing Ltd.

Lacerda, L. D., De Marins, R. V., and Dias, F. J. S. (2020). An arctic paradox: response of fluvial Hg inputs and bioavailability to global climate change in an extreme coastal environment. *Front. Earth Sci.* 8:93. doi: 10.3389/feart.2020.00093

Lamborg, C., Bowman, K., Hammerschmidt, C., Gilmour, C., Munson, K., Selin, N., et al. (2014a). Mercury in the Anthropocene Ocean. *Oceanography* 27, 76–87. doi: 10.5670/oceanog.2014.11

Lamborg, C., Hammerschimidt, C., Bowman, K., Swarr, G., Munson, K., Ohnemus, D., et al. (2014b). A global ocean inventory of anthropogenic mercury based on water column measurements. *Nature* 512, 65–68. doi: 10.1038/nature13563

Landrigan, P. J., Stegeman, J. J., Fleming, L. E., Allemand, D., Anderson, D. M., Backer, L. C., et al. (2020). Human health and ocean pollution. *Ann. Glob. Heal.* 86, 1–64.

Le Blanc, D., Freire, C., and Vierros, M. (2017). "Mapping the linkages between oceans and other sustainable development goals: a preliminary exploration," in *Proceedings of the UNITED NATIONS Department of Economic and Social Affairs Working Paper no 149*, ed. N. United (Berlin: Elsevier).

Leão, Z. M. A. N., Kikuchi, R. K. P., and Testa, V. (2003). ""Corals and coral reefs of Brazil," in *Latin American Coral Reefs*, ed. J. Cortes (Berlin: Elsevier), 9–52.

Leduc, A. O. H. C., Nunes, C. C., De Araújo, C. B., Quadros, L. S., Gabrielle, S., Barros, F., et al. (2021). Land-based noise pollution impairs reef fish behavior: a case study with a Brazilian carnival. *Biol. Conserv.* 253:108910.

Lima, R. (2019). *O Licenciamento Ambiental Como Instrumento Para Uma Gestão Integrada Dos Recursos Minerais No Espaço Marinho Brasileiro*. Brasília: Universidade de Brasília.

Long, R., Charles, A., and Stephenson, R. (2015). Key principles of marine ecosystem-based management. *Mar. Policy* 57, 53–60.

Lourenço, R. A., Combi, T., da Rosa, M. A., Sasaki, S. T., Zanardi-Lamardo, E., and Yogui, G. T. (2020). Mysterious oil spill along Brazil's northeast and southeast seaboard (2019–2020): trying to find answers and filling data gaps. *Mar. Pollut. Bull.* 156:111219. doi: 10.1016/j.marpolbul.2020.111219

Mata, H. K., Al Salah, D. M. M., Ngweme, G. N., Konde, J. N., Mulaji, C. K., Kiyombo, G. M., et al. (2020). Toxic metal concentration and ecotoxicity test of sediments from dense populated areas of Congo River, Kinshasa, Democratic Republic of the Congo. *Environ. Chem. Ecotoxicol.* 2, 83–90. doi: 10.1016/j.enceco.2020.07.001

Mazzei, E. F., Bertoncini, A. A., Pinheiro, H. T., Machado, L. F., Vilar, C. C., Guabiroba, H. C., et al. (2017). Newly discovered reefs in the southern Abrolhos Bank, Brazil: anthropogenic impacts and urgent conservation needs. *Mar. Pollut. Bull.* 114, 123–133. doi: 10.1016/j.marpolbul.2016.08.059

Millero, F., Woosley, R., DiTrolio, B., and Waters, J. (2009). Effect of ocean acidification on the speciation of metals in Seawater. *Oceanography* 22, 72–85. doi: 10.5670/oceanog.2009.98

Miranda, D. A., Benskin, J. P., Awad, R., Lepoint, G., Leonel, J., and Hatje, V. (2021). Bioaccumulation of Per- and polyfluoroalkyl substances (PFASs) in a tropical estuarine food web. *Sci. Total Environ.* 754:142146. doi: 10.1016/j.scitotenv.2020.142146

Newton, A., Icely, J., Cristina, S., Perillo, G. M. E., Turner, R. E., Ashan, D., et al. (2020). Anthropogenic, direct pressures on coastal wetlands. *Front. Ecol. Evol.* 8:144. doi: 10.3389/fevo.2020.00144

Nilsen, E., Smalling, K. L., Ahrens, L., Gros, M., Miglioranza, K. S. B., Picó, Y., et al. (2019). Critical review: grand challenges in assessing the adverse effects of contaminants of emerging concern on aquatic food webs. *Environ. Toxicol. Chem.* 38, 46–60. doi: 10.1002/etc.4290

Oliveira, C., Moraes, G., and Ferreira, F. (2019). *A Interpretação do Princípio da Precaução Pelos tribunais: Análise Nacional, Comparada e Internacional*. São Paulo: Pontes Editores.

Pascual, U., Balvanera, P., Díaz, S., Pataki, G., Roth, E., Stenseke, M., et al. (2017). Valuing nature's contributions to people: the IPBES approach. *Curr. Opin. Environ. Sustain.* 26–27, 7–16. doi: 10.1016/j.cosust.2016.12.006

Polejack, A., and Barros-Platiau, A. (2020). "A Ciência Oceânica como ferramenta de Cooperação e Diplomacia no Atlântico Andrei," in *Conservação dos Recursos Vivos em Áreas Além da Jurisdição Nacional*, eds A. Barros-Platiau and C. de Oliveira (Rio de Janeiro: Lumen Juris), 45–65.

Pruden, A., Pei, R., Storteboom, and Carlson, K. (2006). Antibiotic resistance genes as emerging contaminants: studies in Northern Colorado". *Environ. Sci. Technol.* 40, 7445–7450. doi: 10.1021/es0680156

Rocha, P. S., Azab, E., Schmidt, B., Storch, V., Hollert, H., and Braunbeck, T. (2010). Changes in toxicity and dioxin-like activity of sediments from the Tietc River (São Paulo, Brazil). *Ecotoxicol. Environ. Saf.* 73, 550–558. doi: 10.1016/j.ecoenv.2009.12.017

Rocha, P. S., Luvizotto, G. L., Kosmehl, T., Böttcher, M., Storch, V., Braunbeck, T., et al. (2009). Sediment genotoxicity in the Tietê River (São Paulo, Brazil): in vitro comet assay versus in situ micronucleus assay studies. *Ecotoxicol. Environ. Saf.* 72, 1842–1848. doi: 10.1016/j.ecoenv.2009.04.013

Rounsevell, M. D. A., Pedroli, B., Erb, K. H., Gramberger, M., Busck, A. G., Haberl, H., et al. (2012). Challenges for land system science. *Land Use Policy* 29, 899–910. doi: 10.1016/j.landusepol.2012.01.007

Ryabinin, V., Barbière, J., Haugan, P., Kullenberg, G., Smith, N., McLean, C., et al. (2019). The UN decade of ocean science for sustainable development. *Front. Mar. Sci.* 6:470. doi: 10.3389/fmars.2019.00470

Salpin, C., Onwuasoanya, V., Bourrel, M., and Swaddling, A. (2018). Marine scientific research in Pacific Small Island Developing States. *Mar. Policy* 95, 363–371. doi: 10.1016/j.marpol.2016.07.019

Sandiffer, P., Holland, A., Rowles, T., and Scott, G. (2004). The oceans and human health. *Environ. Heal.* 18, 454–456.

Selkoe, K. A., Blenckner, T., Caldwell, M. R., Crowder, L. B., Erickson, A. L., Essington, T. E., et al. (2015). Principles for managing marine ecosystems prone to tipping points. *Ecosyst. Heal. Sustain.* 1, 1–18. doi: 10.1890/EHS14-0024.1

Silva, A., and Moraes, G. (2020). "Definição do dano ambiental por poluição nas águas do continente ao mar: parâmetros administrativos como critério de tolerabilidade dos ecossistemas," in *Io ambiente marinho, sustentabilidade e Direito*, ed. C. Ovileira (Rio de Janeiro: Lumen Juris).

SNS (2018). *24º Diagnóstico dos Serviços de Água e Esgoto*. Brasilia: SNS.

Soares, M., de, O., Teixeira, C. E. P., Bezerra, L. E. A., Paiva, S. V., Tavares, T. C. L., et al. (2020). Oil spill in South Atlantic (Brazil): environmental and governmental disaster. *Mar. Policy* 115:103879. doi: 10.1016/j.marpol.2020.103879

Spolidorio, P. (2018). *As Contribuições do Direito Francês à Gestão Ecossistêmica Das Águas Na Zona Costeira Brasileira: O Uso do Plano de Bacia Hidrográfica Como Instrumento Jurídico de Integração*. Brasília: Universidade de Brasília.

Steffen, W., Crutzen, J., and McNeill, J. R. (2007). The Anthropocene: are humans now overwhelming the great forces of Nature? *Ambio* 36, 614–621.

Talley, L. D., Pickard, G. L., Emery, W. J., and Swift, J. H. (2011). "Atlantic Ocean," in *Descriptive Physical Oceanography*, ed. G. L Pickard (Amsterdam: Elsevier Ltd), 245–301.

Tanaka, Y. (2004). Zonal and integrated management approaches to ocean governance: reflections on a dual approach in international Law of the Sea. *Mar. Policy* 19, 483–514.

Tollefson, J. (2020). Brazilian lawmakers in showdown to double science budget. *Nature*. doi: 10.1038/d41586-020-02433-y [Epub ahead of print].

UN (2019). *World Population Prospects 2019: Highlights*. New York, NY: UN.

UNEP (2019). *Global Mercury Assessment*. Geneva: UNEP.

UNESCO (2020). *Facts and figures on marine pollution*. Available online at: http://www.unesco.org/new/en/natural-sciences/ioc-oceans/focus-areas/rio-20-ocean/blueprint-for-the-future-we-want/marine-pollution/facts-and-figures-on-marine-pollution/ (accessed December 18, 2020).

Van Rensburg, M. L., Nkomo, S. L., and Dube, T. (2020). The 'plastic waste era'; social perceptions towards single-use plastic consumption and impacts on the marine environment in Durban, South Africa. *Appl. Geogr.* 114:102132. doi: 10.1016/j.apgeog.2019.102132

Vegter, A. C., Barletta, M., Beck, C., Borrero, J., Burton, H., Campbell, M. L., et al. (2014). Global research priorities to mitigate plastic pollution impacts on marine wildlife. *Endanger. Species Res.* 25, 225–247. doi: 10.3354/esr00623

Wagener, A., Hamacher, C., Farias, C., Godoy, J. M., and Sco, A. (2010). Evaluation of tools to identify hydrocarbon sources in recent and historical sediments of a tropical bay. 121, 67–79. doi: 10.1016/j.marchem.2010.03.005

Wainer, I., Prado, L. F., Khodri, M., and Otto-Bliesner, B. (2020). The South Atlantic sub-tropical dipole mode since the last deglaciation and changes in rainfall. *Clim. Dyn.* 56, 109–122. doi: 10.1007/s00382-020-05468-z

Weihe, P., Debes, F., Halling, J., Petersen, M. S., Muckle, G., Odland, J. Ø, et al. (2016). Health effects associated with measured levels of contaminants in the Arctic. *Int. J. Circumpolar Health* 75, 1–20. doi: 10.3402/ijch.v75.33805

Wilkinson, M., Dumontier, M., and Aalbersberg, I. (2016). The FAIR Guiding Principles for scientific data management and stewardship. *Sci. Data* 3, 1–9.

Wilson, D. (2015). *Global Waste Management Outlook*. Nairobi: United Nations Environment Programme.

World Bank (2020). *World Development Indicators*. Washington, DC: The World Bank Group.

WWAP (2017). *Wastewater: the Untapped Resource*. Paris: WWAP.

Zettler, E., Mincer, T., and Amaral-Zettler, L. (2013). Life in the "Plastisphere": microbial communities on plastic marine debris. *Environ. Sci. Technol.* 47:7137.

Disclaimer: This paper reflects only the authors' views. The Ministério da Ciência, Tecnologia e Inovações is not liable for any use that may be made of the information it contains.

Conflict of Interest: The authors declare that the research was conducted in the absence of any commercial or financial relationships that could be construed as a potential conflict of interest.

2. CONCLUSÃO

Os Terras Raras são um grupo de elementos de aplicabilidade vasta, desde aplicações tecnológicas, médicas, agropecuárias até aplicações como traçadores de processos geoquímicos tanto em ambientes terrestres quando marinhos. O aumento do seu emprego em atividades antrópicas levou ao surgimento de preocupações com relação aos possíveis impactos desse tipo de contaminação (vide capítulo 1). Para avaliar de forma mais adequada os impactos das atividades humanas envolvendo esses elementos, bem como para obter melhores resultados em sua utilização como traçadores, a compreensão não apenas das fontes e sumidouros, mas também dos processos envolvidos no seu ciclo biogeoquímico é essencial. Nesse contexto, o capítulo 1 do presente trabalho envolveu a realização de uma ampla revisão bibliográfica indicando o estado do saber científico sobre os REE, bem como apontando as lacunas de conhecimento que ainda precisamos preencher para garantir tanto o seu uso de forma sustentável nas diversas atividades antrópicas, como sua melhor aplicabilidade como traçador em estudos geoquímicos.

Com o propósito de contribuir com o preenchimento das lacunas de conhecimento no ciclo biogeoquímico dos REE, os capítulos 2 e 3 da presente tese foram dedicados a estudos de caso. No capítulo 2, o foco foi o estudo dos padrões de distrubuição e fracionamento dos REE no contínuo continente-oceano. Nesse trabalho a investigação destacou como os factores ambientais, como os gradientes de salinidade, os ciclos das marés, a circulação das águas e a origem geológica, bem como os factores antropogénicos, afetam as concentrações e o fracionamento dos REE nas águas costeiras da Baía de Todos os Santos, Bahia. Por conter tantos fatores de influência como o aporte de diversos rios, estruturas geológicas com caracteristicas distintas, aporte de água subterrânea, conexão aberta para o oceano (com uma plataforma continental estreita), a Baía de Todos os Santos se mostrou um ambiente de estudo bastante propício para investigações de processos na interface continente-oceano.

No estuário do Paraguaçu, a inesperada observação de anomalias de gadolínio demonstrou que o impacto das aplicações antropogênicas dos REE pode atingir regiões mais distantes do que o esperado e isso precisa ser levado em consideração no planejamento de políticas públicas. Além disso, o estudo também expôs a importância das interações água-partículas ao longo do gradiente de salinidade, evidenciando que em diferentes zonas de salinidade, ocorrem diferentes processos com intensidades variadas.

Há uma intensa remoção dos REE na zona de baixa salinidade, seguida por uma liberação menos intensa desses elementos em salinidades de média a alta. Esses processos também não ocorrem na mesma intensidade para todos os REE, seguindo um gradiente que causa fracionamento. Isso gera as diferenças de padrão normalizado desses elementos em águas naturais marinhas, que apresentam concentrações mais baixas e enriquecidos em REE pesados, quando comparadas a águas de rios e lagos. Esses aspectos levantaram a necessidade de novos estudos combinando a análise das concentrações dos REE nas frações dissolvida, particulada e coloidal para avançar ainda mais no entendendimento dos processos controladores da distribuição desses elementos nesses compartimentos.

Outro ponto importante nesse estudo foi a combinação de dados de ^{224}Ra com os dados de REE para melhor compreensão dos impactos do ciclo de maré e de água subterrânea nas distribuições de REE. Isso expôs a importância da realização de estudos com multiplos parâmetros para compreensão de processos ambientais, já que muitas vezes esses processos são complexos e precisam de mais de um traçador para serem devidademente compreendidos.

No capítulo 3 desta tese, buscou-se ampliar a área de estudo com o enfoque em compreender processos que afetam de forma mais ampla o oceano, especialmente o BE. Nos oceanos Antártico e Atlântico, as composições isotópicas do Nd ofereceram informações sobre a influência das características geológicas e dos movimentos das massas d'água em processos que podem controlar a distribuição dos REE. Na Península Antártica a composição isotópica do Nd variou com a proximidade das ilhas Shetland do Sul, sugerindo a ocorrência de BE, porém com influencia limitada, não havendo indícios de mudança significativa no εNd na região do Drake.

No Atlântico, os diversos transectos continente-oceano evidenciaram a influência da composição geológica do continente na assinatura isotópica das águas adjacentes. Ainda assim, não foi possivel observar variações significativas no εNd na região influenciada pela pluma do rio Amazonas e nem em amostras de água que haviam cruzado a cadeia Vitória-Trindade.

Os processos de mistura de massas d'água também se mostraram importantes, sendo a provável causa o aumento da radiogenicidade do Nd da Água Profunda do Atlântico Norte a medida que ela se move para sul, enquanto a Água Intermediária Antártica se torna menos radiogênica a medida que se move para norte. O estudo não conseguiu revelar tendências claras na Água de Fundo Antártica e nem na Água Central do Atlântico Sul,

possivelmente devido a influência de outros fatores que dificilmente podem ser apontados apenas com os dados da composição isotópica de Nd.

Esse capítulo identificou diversas regiões de interesse para aprofundamento na investigação dos processos que controlam a distribuição dos REE no Atlântico Oeste e na Antártica. Embora avanços significativos tenham sido feitos neste trabalho, os dados de concentrações de REE não puderam ser gerados devido a limitações analíticas atuais relacionadas ao equipamento disponível, mesmo associado ao método usando diluição isotópica. Esses dados são de grande importância para uma compreensão mais completa e, portanto, esses aspectos serão deixados para investigação em trabalhos futuros, como um pós-doutorado. Futuras pesquisas poderão preencher essas lacunas e contribuir ainda mais para o avanço da área

Por fim, o capítulo 4 deste trabalho permitiu a identificação das principais fontes de contaminação para o oceano Atlântico Sul, bem como quais as lacunas de conhecimento que ainda precisamos preencher visando o desenvolvimento sustentável, propondo algumas áreas de investimento na busca para alcançar a meta do “Oceano Limpo” apresentada pela Década da Ciência Oceânica para o Desenvolvimento Sustentável.

Para além dos aspectos ambientais, as questões socio-econômicas também tiveram que ser levadas em consideração nesse estudo. Apesar da heterogeneidade da região, a falta de saneamento básico se mostrou um problema comum à diversos países, demonstrando que a busca por soluções de forma conjunta pode ser chave para avanços mais rápidos nas questões sócioambientais do Atlântico Sul. Além disso, o Atlântico Sul se mostrou heterogêneo nas produções científicas sobre poluentes, tendo mais estudos na borda americana que na africana e, geral, menos estudos que outras regiões do mundo. Assim, a colaboração estratégica entre grupos de pesquisa nacionais e internacionais, incluindo cientistas, povos e comunidades tradicionais, setor privado e governo poderia promover uma aceleração na compreensão do oceano e ações no sentido de reverter o processo de degradação já em curso. Ao concentrarem-se na prevenção da poluição, no desenvolvimento tecnológico e na investigação interdisciplinar, estes esforços podem mitigar os impactos negativos dos poluentes e garantir um ambiente oceânico mais saudável.

De uma forma geral, este trabalho permitiu identificar lacunas de conhecimento no que diz respeito aos REE, tanto nos aspectos de distribuições naturais e aplicações como traçadores, como em aplicações antrópicas e sustentabilidade. Algumas questões relacionados à distribuição natural dos REE e seu uso como traçadores geoquímicos foram

mais profundamente tratados, porém ainda existem muitas perguntas a serem respondidas e se torna imprescindível o investimento em novos estudos para esclarecer o mecanismo por detrás do BE, entender como ocorre o fracionamento dos elementos durante a dissolução e precipitação mineral, além da relação com processos bióticos, e assim quantificar os fluxos desses elementos para o oceano. Dessa forma, será possível compreender melhor a biogeoquímica dos oceanos e prever seu comportamento, especialmente em meio a atividades antrópicas e mudanças climáticas. Para tal, iniciativas de colaboração nacional e internacional se fazem essenciais, pois permitem a troca de conhecimento através de treinamentos, estabelecimento de metodologias e protocolos em comum, compartilhamento de tecnologia etc. O presente trabalho é o resultado de colaborações entre vários grupos de pesquisa. Esse tipo de iniciativa causa a multiplicação de pessoas trabalhando e produzindo resultados com qualidade equiparada, aumentando a dimensão dos trabalhos que podem ser realizados, por exemplo: trabalhando com mais traçadores e matrizes para ter uma visão mais completa dos processos. Tudo isso em conjunto tem o potencial de gerar um aumento na velocidade de obtenção de respostas as questões e isso será determinante para o futuro que seremos capazes de construir num contexto de aceleração de impactos antropópicos e mudanças climáticas.